Vol. 63 September, 1959 No. 9

THE JOURNAL OF PHYSICAL CHEMISTRY

(Registered in U. S. Patent Office)

CONTENTS

Notes

THE JOURNAL OF PHYSICAL CHEMISTRY

(Registered in U. S. Patent Office)

Published monthly by the American Chemical Society at 20th and Northampton Sts., Easton, Pa.

Second-class mail privileges authorized at Easton, Pa. This publication is authorized to be mailed at the special rates of postage prescribed by Section 131.122.

The *Journal of Physical Chemistry* is devoted to the publication of selected symposia in the broad field of physical chemistry and to other contributed papers.

Manuscripts originating in the British Isles, Europe and Africa should be sent to F. C. Tompkins, The Faraday Society, 6 Gray's Inn Square, London W. C. 1, England.

Manuscripts originating elsewhere should be sent to W. Albert Noyes, Jr., Department of Chemistry, University of Rochester, Rochester 20, N. Y.

Correspondence regarding accepted copy, proofs and reprints should be directed to Assistant Editor, Allen D. Bliss, Department of Chemistry, Simmons College, 300 the Fenway, Boston 15, Mass.

Business Office: Alden H. Emery, Executive Secretary, American Chemical Society, 1155 Sixteenth St., N. W., Washington 6, D. C.

Advertising Office: Reinhold Publishing Corporation, 430 Park Avenue, New York 22, N. Y.

Articles must be submitted in duplicate, typed and double spaced. They should have at the beginning a brief Abstract, in no case exceeding 300 words. Original drawings should accompany the manuscript. Lettering at the sides of graphs (black on white or blue) may be pencilled in and will be typeset. Figures and tables should be held to a minimum consistent with adequate presentation of information. Photographs will not be printed on glossy paper except by special arrangement. All footnotes and references to the literature should be numbered consecutively and placed in the manuscript at the proper places. Initials of authors referred to in citations should be given. Nomenclature should conform to that used in *Chemical Abstracts*, mathematical characters marked for italic, Greek letters carefully made or annotated, and subscripts and superscripts clearly shown. Articles should be written as briefly as possible consistent with clarity and should avoid historical background unnecessary for specialists.

Notes describe fragmentary or incomplete studies but do not otherwise differ fundamentally from articles and are subjected to the same editorial appraisals as are articles. In their preparation particular attention should be paid to brevity and conciseness. Material included in Notes must be definitive and may not be republished subsequently.

Communications to the Editor are designed to afford prompt preliminary publication of observations or discoveries whose value to science is so great that immediate publication is imperative. The appearance of related work from other laboratories is in itself not considered sufficient justification for the publication of a Communication, which must in addition meet special requirements of timeliness and significance. Their total length may in no case exceed 500 words or their equivalent. They differ from Articles and Notes in that their subject matter may be republished.

Symposium papers should be sent in all cases to Secretaries of Divisions sponsoring the symposium, who will be responsible for their transmittal to the Editor. The Secretary of the Division by agreement with the Editor will specify a time after which symposium papers cannot be accepted. The Editor reserves the right to refuse to publish symposium articles, for valid scientific reasons. Each symposium paper may not exceed four printed pages (about sixteen double spaced typewritten pages) in length except by prior arrangement with the Editor.

Remittances and orders for subscriptions and for single copies, notices of changes of address and new professional connections, and claims for missing numbers should be sent to the American Chemical Society, 1155 Sixteenth St., N. W., Washington 6, D. C. Changes of address for the *Journal of Physical Chemistry* must be received on or before the 30th of the preceding month.

Claims for missing numbers will not be allowed (1) if received more than sixty days from date of issue (because of delivery hazards, no claims can be honored from subscribers in Central Europe, Asia, or Pacific Islands other than Hawaii), (2) if loss was due to failure of notice of change of address to be received before the date specified in the preceding paragraph, or (3) if the reason for the claim is "missing from files."

Subscription Rates (1959): members of American Chemical Society, $8.00 for 1 year; to non-members, $16.00 for 1 year. Postage free to countries in the Pan American Union; Canada, $0.40; all other countries, $1.20. Single copies, current volume, $1.35; foreign postage, $0.15; Canadian postage $0.05. Back volumes (Vol. 56–59) $15.00 per volume; (starting with Vol. 60) $18.00 per volume; foreign postage, per volume $1.20, Canadian, $0.15; Pan-American Union, $0.25. Single copies: back issues, $1.75; for current year, $1.35; postage, single copies: foreign, $0.15; Canadian, $0.05; Pan American Union, $0.05.

THE JOURNAL OF PHYSICAL CHEMISTRY

(Registered in U. S. Patent Office) (© Copyright, 1959, by the American Chemical Society)

VOLUME 63 OCTOBER 1, 1959 NUMBER 9

THE ENTROPIES OF DILUTION OF STRONG ELECTROLYTES

BY ROBERT H. WOOD[1]

Contribution from the Department of Chemistry of the University of California, and the University of Delaware, Newark, Delaware

Received October 7, 1958

The partial molal entropies of dilution of some 1-1 and 2-1 electrolytes have been correlated using a single parameter for each ion. In the case of the negative ions this parameter is very nearly the reciprocal of the ionic radius. For most of the compounds which do not fit the correlation very well, there is other evidence for the abnormal behavior of solutions of these compounds. More data are needed to see whether this correlation is valid for other types of electrolytes.

Introduction

At the concentrations above 0.1 m the deviations of the relative partial molal entropies of dilution of strong electrolytes from the values predicted by the Debye–Hückel equation[2] are quite large. This investigation was undertaken to find a correlation of entropies of dilution with some other parameter. It was hoped that such a correlation would shed some light on the reasons for the deviations from the predicted behavior.

Calculations.—The integral heats of dilution have been taken from the data of the National Bureau of Standards.[3] The relative partial molal heat contents of the salts ($\bar{L}_2$) were computed from the slopes of a graph of the relative heat content *vs.* the square root of the concentration in moles per kg. of water. The relative non-ideal partial molal free energies and entropies were computed from the activity coefficients[4] and $\bar{L}_2$ by means of the equations

$$\bar{F}^E = RT \ln (\gamma\pm)^\nu$$

and

$$T\bar{S}^E = \bar{L}_2 - \bar{F}^E$$

where $\bar{F}^E$ and $\bar{S}^E$ are the excess (*i.e.*, non-ideal) relative partial molal free energy and entropy. The total number of ions that form when the salt is dissolved in water is given by ν and $\gamma\pm$ is the mean molal activity coefficient.

The data are given in Tables I, II, and III. Because of the difficulty in measuring the slope of a curve and because of the inaccuracy in some of the data the values of some salts may be in error by 30 calories or more.

TABLE I

$\bar{L}_2$ FOR 1-1 ELECTROLYTES 25°

Molality	0.1	0.2	0.5	1.0	1.5	2.0	3.0
HCl	206	278	437	648	868	1065	1376
HBr	177	233	344	528	689	874	1110
HI	142	179	248	413	607	637	578
HNO_3	133	245	151	138	130	155	310
LiOH	212	302	418	580	710	811	
LiCl	182	242	356	490	622	747	998
LiBr	153	220	320	467	599	732	964
$LiNO_3$	160	199	259	313	345	378	
NaOH	134	155	102	7	− 43	− 75	− 37
NaF	148	190	255	263	255		
NaCl	103	86	− 14	− 196	− 335	− 452	− 623
NaBr	91	75	− 28	− 238	− 435	− 575	− 724
NaI	101	95	− 13	− 247	− 481	− 634	− 896
$NaNO_3$	3	−111	− 371	− 644	−1055	−1712	−1717
$NaClO_3$	27						
$NaClO_4$	−125						
NaSCN	45	− 2	− 182	− 430	− 727	− 922	−1248
KOH	178	206	235	275	342	396	518
KF	147	173	191	222	243	262	311
KCl	95	90	− 20	− 183		− 446	
KBr	63	39	− 98	− 333	− 533	− 664	− 913
KI	39	− 15	− 187	− 450	− 715	− 964	−1310
$KClO_3$	−135	−266	−1175				
RbCl	68	62	111				
RbBr	57	25					
$RbNO_3$	−154	−376	− 780	−1292			
CsCl	43	− 33	− 397	− 506			
CsBr	24						
$CsNO_3$	−179	−369	− 850	−1233			

(1) Department of Chemistry, University of Delaware, Newark, Delaware. The author wishes to express his appreciation to E. I. du Pont de Nemours & Company for a summer faculty fellowship.

(2) P. Debye and E. Hückel, *Phys. Z.*, **24**, 185 (1923); P. Gross and O. Halpern, *ibid.*, **26**, 403 (1925); N. Bjerrum, *Z. physik. Chem.*, **119**, 145 (1926).

(3) National Bureau of Standards Circular 500 "Selected Values of Chemical Thermodynamic Properties," Washington, D. C., 1952.

(4) R. A. Robinson and R. H. Stokes, "Electrolyte Solutions," Academic Press, New York, N. Y., 1955.

TABLE II

$T\bar{S}^E$ FOR 1-1 ELECTROLYTE

Molality	0.1 Expt.	0.1 Calcd.	0.2 Expt.	0.2 Calcd.	0.5 Expt.	0.5 Calcd.	1.0 Expt.	1.0 Calcd.	1.5 Expt.	1.5 Calcd.	2.0 Expt.	2.0 Calcd.	3.0 Expt.	3.0 Calcd.
HCl	475	463	592	577	765	720	899	820	996	914	1055	926	1051	918
HBr	432	441	522	539	622	637	692	674		703		699		597
HI[a]	378	405	431	478	452	504	458	438	457	361	277	253	− 250	80
HNO_3	410	427	478	510	539	573	521	561	468	539	428	469	422	349
LiOH[a]	535	499	719	639	988	856	1278	1061	1463	1264	1597	1351		1447
LiCl	460	467	571	584	714	736	794	849	829	956	842	976	828	980
LiBr	422	445	534	546	654	653	727	702	727	744	715	719	616	659
$LiNO_3$	441	428	537	517	637	589	665	589	633	580	591	519		411
NaOH[a]	449	421	531	506	542	565	467	547	395	518	332	444	249	318
NaF	464	450	594	555	798	672	920	735		792		777		732
NaCl	384	389	450	451	440	445	302	334	163	211	25	70	− 226	− 148
NaBr	381	367	430	414	398	363	207	188	− 18	− 2	−205	−188	− 478	− 468
NaI[a]	383	331	433	353	369	229	116	− 48	−173	−344	−399	−604	− 854	− 987
$NaNO_3$[a]	324	350	304	384	201	299	68	75	−250	−166	−841	−387	− 736	− 717
$NaClO_3$[a]	333	307		311		139		−209		−576		−885		−1338
$NaClO_4$[a]	176	300		299		112		−255		−645		−969		−1442
NaSCN	328	329	337	349	213	221	− 30	− 62	−352	−365	−574	−629	−1006	−1018
KOH[a]	464	432	531	524	603	605	607	717	585	621	535	569	425	473
KF	468	461	550	573	664	712	740	806	761	894	756	901	462	887
KCl	403	400	482	469	490	485	415	405		313	210	195		8
KBr	369	378	423	432	398	403	239	259	71	101	− 46	− 63	− 300	− 313
KI	336	342	350	371	277	269	70	23	−181	−240	−431	−478	− 804	− 830
$KClO_3$[a]	129	318	188	330	−507	178		−138		−472		−761		−1182
RbCl	386	391	468	455	429	453		348		231		95		− 117
RbBr	376	369	437	417		371		202		19		−163		− 437
$RbNO_3$[a]	210	352	117	388	− 38	307	−294	89		−144		−362		− 686
CsCl[a]	373	387	399	448	195	437	214	320		190		45		− 179
CsBr	357	365		410		355		174		− 21		−213		− 449
$CsNO_3$[a]	186	348	131	381	− 96	291	−210	61		−185		−412		− 748

[a] Salts which do not fit the correlation very well ("abnormal salts").

TABLE III

$\bar{L}_2$ AND $T\bar{S}^E$ FOR 2-1 AND 1-2 ELECTROLYTES AT 0.1 MOLAL, 25°

	$\bar{L}_2$	$T\bar{S}^E$ Expt.	$T\bar{S}^E$ Calcd.[a]
$MgCl_2$	640	1770	1786
$MgBr_2$	573	1675	1679
$Mg(NO_3)_2$	471	1621	1596
$CaCl_2$	586	1753	1744
$CaBr_2$	507	1628	1637
$Ca(NO_3)_2$	169	1454	1554
$SrCl_2$	536	1728	1717
$SrBr_2$	459	1599	1610
$Sr(NO_3)_2$	25	1335	1527
$BaCl_2$	522	1752	1744
$BaBr_2$	445	1630	1637
$Ba(NO_3)_2$	−588	919	1554
Li_2SO_4	630	1980	
Na_2SO_4	310	1749	
K_2SO_4	217	1672	
Rb_2SO_4	189	1604	
Cs_2SO_4	74	1469	

[a] Calculated from $T\bar{S}^E = 1640 + 3500\,(P_- + P_+ - 1.45)$ for the 2-1 electrolytes.

Correlations.—When the $T\bar{S}^E$ values given in Table II are plotted *vs.* the square root of the molality the curves for most electrolytes fall into a somewhat irregular family of curves. Although the curves often cross over one or two neighboring curves they seldom deviate by more than this. Because HI, NaI, $NaNO_3$, CsCl and $CsNO_3$ deviate sharply from the normal pattern, these compounds were not expected to fit any correlation and were not used in finding a correlation.

If the $T\bar{S}^E$ for the "normal" compounds at a concentration of 0.5 molal are plotted *vs.* the sum of the reciprocals of the Goldschmidt ionic radii,[5] the points can be fairly well represented by a series of parallel lines with a separate line for each cation. However, the hydroxide ion and fluoride ion are a constant distance above the line. The acids can be put on the plot by assuming an arbitrary radius for the hydrogen ion ($1/R = 1.59$). In order to put the complex anions on the plot an estimate of their radii was required. A plot of the cube of the ionic radius[6] *vs.* the partial molal volume at infinite dilution was used. The partial molal volumes were taken from Owen and Brinkley[6] except for the values for ClO_4^- (51 cm.^{3}/mole) and SCN^- (42 cm.^{3}/mole) which were estimated from the densities of aqueous $HClO_4$ at 25°, and of aqueous NaSCN and LiSCN at 18°.[7]

The radii calculated by this method were 2.25 Å. for the thiocyanate ion, 2.33 Å. for the chlorate ion, 2.39 Å. for the perchlorate ion, and 2.04 Å. for the nitrate ion.

The actual values of the radius are certainly not accurate and in fact it is difficult to define the

(5) V. M. Goldschmidt, *Ber.*, **60**, 1263 (1927).

(6) B. B. Owen and R. S. Brinkley, *Chem. Revs.*, **29**, 461 (1942).

(7) "International Critical Tables," McGraw-Hill Book Co., Inc., New York, N. Y., Vol. 3, p. 91.

"radius" of a complex ion. However, this method does give a measure of relative size which is sufficient for the purposes of this correlation.

In order to put the points on the same straight line, the parameters $(1/R)$ for the positive ions, the hydroxide ion and the fluoride ion must be adjusted. We will designate the adjusted values by P_+ for positive ions and P_- for negative ions. In this adjustment the parameter for the potassium ion was kept constant. A single parameter for each ion was found adequate to correlate the data in the concentration range 0.1 to 3.0 molal. In order to improve the correlation even more, the parameters of all of the ions were adjusted so that the sum of the deviations of all compounds of an ion was equal to zero.

In this adjustment the data for LiOH, $NaClO_4$ and $NaClO_3$ were not used because these salts showed marked deviations from the correlation. The data for NaOH and KOH were used to find P_- for OH^- even though these salts do not fit the correlation too well.

All of the negative ions were adjusted first and then using the new values of P_- the positive ions were adjusted. The new values were plotted against $T\bar{S}^E$ at each concentration, and a new line was drawn through these points. Since the new lines were somewhat different from the old lines the parameters of the ions were adjusted to the new lines in the same manner as before. Table II gives the values of $T\bar{S}^E$ calculated from the adjusted parameters. Table IV gives the average deviations of $T\bar{S}^E$ for the electrolytes used in this correlation from the calculated values at each concentration.

The standard $T\bar{S}^E$ curves at several concentrations are given in Table V, while the values of P and $1/R$ for each ion are given in Table VI.

If $\bar{L}_2$ instead of $T\bar{S}^E$ is plotted *vs.* the sum of $1/R$ for the two ions the correlation still exists although it is not nearly as good.[8] Other functions of the radius either gave curved lines for the cations or correlations which were not as good.

TABLE IV

TEST OF EFFECTIVENESS OF CORRELATION

	Concentration, m						
	0.1	0.2	0.5	1.0	1.5	2.0	3.0
Normal electrolytes[a]							
Av. $T\bar{S}^E$	404	485	536	512	372	326	57
Av. dev. from av.	37	63	144	266	396	451	619
Av. dev. from correlation	10	18	29	50	59	60	97
Abnormal electrolytes							
Av. dev. from correlation	70	97	144	151	118	179	120

[a] The "normal electrolytes" are all electrolytes in Table II except the "abnormal electrolytes" which are III, LiOH, NaOH, NaI, $NaNO_3$, $NaClO_3$, $NaClO_4$, KOH, $KClO_3$, $RbNO_3$, CsCl and $CsNO_3$.

Discussion

I. Frank and Robinson[9] have discussed the relative partial molal entropy of the water in solutions of strong electrolytes, in terms of what happens to the hydration spheres of the ions. The same factors affect the relative partial molal entropies of dilution of the salts.

Since this correlation uses one parameter for each ion, any specific interactions between a pair of ions may result in deviations from the normal entropy of dilution curves. The 1–1 electrolytes that show marked deviations from the normal behavior are $NaNO_3$, $RbNO_3$, $CsNO_3$, LiOH, NaOH, KOH, HI, NaI, CsCl, $NaClO_4$ and $NaClO_3$.

II. For all of these compounds except HI, NaI and $NaClO_4$ there is some other evidence for abnormal behavior. This abnormal behavior has often been attributed to "ion pairing" where "ion pairing" is used to indicate compound formation, Bjerrum type ion trapping,[10] and "localized hydrolysis." The evidence for abnormal behavior is given below.

On the basis of conductivity measurements on $NaNO_3$, KNO_3, $KClO_3$, $KClO_4$ and CsCl, Davies and others have postulated that these compounds form ion pairs and have calculated the dissociation constants for the ion pairs.[11–14] Although the ion pair dissociation constants reported by these authors are open to questions, the conductivities of the salts ($NaNO_3$, KNO_3, $KClO_3$, $KClO_4$ and CsCl) are significantly lower than expected from a consideration of the conductivities of some other salts: *i.e.*, HCl, LiCl, NaCl, KCl, KBr, KSCN and $LiNO_3$.

From the activity coefficients of the alkali metal

TABLE V

NORMAL $T\bar{S}^E$ CURVES

$T\bar{S}^E = A + B(P_+ + P_- - 1.30)$

Concn.	A, cal.	B, cal.
0.1	405	713
0.2	478	1217
0.5	504	2667
1.0	438	4720
1.5	361	6830
2.0	253	8310
3.0	80	10360

TABLE VI

THE RECIPROCAL OF THE RADIUS AND THE CORRELATION PARAMETERS FOR VARIOUS IONS

Ion	$1/R$	P_-	Ion	$1/R$	P_+
OH^-	0.76	0.590	H^+	..	0.836
F^-	.75	.630	Li^+	1.28	.842
Cl^-	.55	.545	Na^+	1.02	.733
Br^-	.51	.514	K^+	0.75	.748
I^-	.45	.464	Rb^+	.67	.736
NO_3^-	(.49)[a]	.490	Cs^+	.61	.73
ClO_3^-	(.43)	.43	Mg^{++}		.947
ClO_4^-	(.42)	.42	Ca^{++}		.935
SCN^-	(.44)	.461	Sr^{++}		.927
			Ba^{++}		.935

[a] Values in parentheses are estimated from the partial molal volumes of the ions.

(8) For a correlation of $\bar{L}_2$ for sodium and potassium salts at concentrations below 0.1 molal see T. F. Young and M. B. Smith, THIS JOURNAL, **58**, 716 (1954).

(9) H. S. Frank and A. L. Robinson, *J. Chem. Phys.*, **8**, 933 (1940).

(10) N. Bjerrum, *K. danske vidensk. Selsk.* **7**, No. 9 (1926): Selected Papers p. 108, Einar Munkesgaard (Copenhagen, 1949).

(11) C. W. Davies, *Trans. Faraday Soc.*, **23**, 354 (1927).

(12) R. A. Robinson and C. W. Davies, *J. Chem. Soc.*, 574 (1937).

(13) J. H. Jones, *J. Am. Chem. Soc.*, **67**, 855 (1945).

(14) E. C. Righellato and C. W. Davies, *Trans. Faraday Soc.*, **26**, 592 (1930).

nitrates, Robinson and Harned conclude that the nitrates of rubidium and cesium form ion pairs.[15]

Although sodium and potassium hydroxide have been used in finding this correlation, their entropy of dilution curves bend down more than expected at the higher concentrations. In order to explain the "reversed order" of the activity coefficients of the hydroxide and fluorides, Robinson and Harned[15] have postulated a "localized hydrolysis" of these compounds. Gimblett and Monk and others[16] also have concluded that LiOH and NaOH behave abnormally. The fluorides of sodium and potassium do not show any "localized hydrolysis" effect.

The negative deviations of $CsNO_3$, $RbNO_3$, $KClO_3$, $NaClO_4$ mean that if ion pairing is to be used as an explanation, the entropy change for the reaction

$$M^+ + X^- \longrightarrow MX(aq)$$

must be negative for these salts. Several methods have been proposed for estimating the entropy of complex ion formation.[17-19] Although these methods disagree in detail, all of them indicate that the entropy of formation of complexes of the type MX where M and X are univalent should be slightly negative for complexes involving the larger cations and ions. It is just these compounds which show the largest deviations from the predicted behavior.

(15) R. A. Robinson and H. S. Harned, *Chem. Revs.*, **28**, 419 (1941).
(16) F. G. R. Gimblett and C. B. Monk, *Trans. Faraday Soc.*, **50**, 965 (1954).
(17) W. M. Latimer and W. L. Jolly, *J. Am. Chem. Soc.*, **75**, 1548 (1953).
(18) J. Cobble, *J. Chem. Phys.*, **21**, 1447 (1953).
(19) G. H. Nancollas, *Disc. Faraday Soc.*, **24**, 108 (1957).

Although a failure to fit the correlation can be interpreted in terms of ion pairing, it must be pointed out that this is not the only interpretation. Thus all electrolytes in concentration solution may be ion paired to some extent and deviations from our correlation may mean that either the degree of ion pairing is anomalous or the entropy of formation of an ion pair is anomalous. Likewise, there may be some salts which fit our correlation only because the entropy of formation of ion pairs is small. In this case an abnormal degree of ion pairing would not noticeably affect the entropy of dilution.

2-1 and 1-2 Electrolytes.—Using the previously established values of P_- for the chloride and bromide ions, values of P_+ for magnesium, calcium, strontium and barium ions can be established by the procedure that was used in the case of the 1–1 electrolytes. The values of P_+ are given in Table VI. The experimental and calculated values of TS^E are given in Table III while the equation relating P_+, P_- and TS^E is $TS^E = 1640 + 3500 \cdot (P_- + P_+ - 1.45)$. The average deviation of the calculated values is 10 cal. Except for $Mg(NO_3)_2$, the nitrates do not fit the correlation. Other evidence for the abnormality of the nitrates of Ba, Sr and Ca is given in reference 13.

Very few data are available for 1–2 electrolytes (see Table III). These data does not seem to fit a correlation.

Acknowledgments.—The author is indebted to Professor Robert E. Connick and Professor Leo Brewer for many helpful discussions in connection with this work.

A PRECISION ADSORPTION APPARATUS FOR THE STUDY OF THE INTERACTIONS BETWEEN GAS ATOMS AND SURFACES[1]

BY G. CONSTABARIS,[2] J. H. SINGLETON AND G. D. HALSEY, JR.

Department of Chemistry, University of Washington, Seattle 5, Wash.

Received November 24, 1958

A precision apparatus for the study of the interactions between gas atoms and surfaces of low specific area is described. A low temperature adiabatic calorimeter is used as the sample cryostat and the precise techniques of gas thermometry are used for pressure measurement. The gas is metered into the system with an accurate gas transfer apparatus. Data for the measurement of known volumes, and of the apparent volume of a vessel containing a low specific area, highly graphitized carbon black, are given. These measurements, made with different rare gases at various temperatures, indicate a precision of between 1 and 2 parts per 10,000. The apparent volume data are converted to the usual quantity of adsorbed volume to give room temperature adsorption isotherms at coverages of less than 2% of the monolayer.

Introduction

The interaction of rare gas atoms with high area powders, in the temperature region above the critical point of the rare gas, has been investigated[3-5] because in this region, although the experiments are more difficult, the theoretical analysis of the data is not subject to the approximations that have marred the treatment of adsorption in the conventional range of temperatures. If in a conventional gas transfer apparatus, a quantity of powder with a surface area of about 3000 m.^{2} is used as a sample, the accuracy is sufficient to achieve sensible results at surface concentrations so small that, effectively, the gas atoms are interacting with the surface, without interacting with each other.[4] At lower temperatures or higher pressures, the experiments can be extended to the range in which pairwise interactions between the rare gas atoms are important.

(1) This research was supported in part by the United States Air Force through the Air Force Office of Scientific Research of the Air Research and Development Command under contract No. AF 18-(600)-987.
(2) Presented in partial fulfillment of the requirements for the degree of Doctor of Philosophy. General Electric Fellow, 1955–1956.
(3) W. A. Steele and G. D. Halsey, Jr., *J. Chem. Phys.*, **22**, 979 (1954).
(4) W. A. Steele and G. D. Halsey, Jr., THIS JOURNAL, **59**, 57 (1955).
(5) M. P. Freeman and G. D. Halsey, Jr., *ibid.*, **59**, 181 (1955).

The results can be analyzed to give an apparent area and interaction energy at an apparent distance of closest approach. However, because the available high-area solids are poorly defined with respect to both structure and surface purity, these parameters have only qualitative significance. It seemed desirable to extend the measurements to well-defined low-surface-area solids, in particular, the graphitized carbon black P33(2700°). In order to do this it was necessary to design and construct an apparatus with approximately tenfold greater accuracy than the conventional gas transfer system.

Apparatus

A. Temperature Control and Measurement.— It is necessary to use a cryostat that will hold a temperature to better than 0.01° for extended periods at any point between room temperature and one somewhat below the boiling point of nitrogen. Several cryostats with these properties have been described.[6-8] The one adopted here is based on the low temperature adiabatic calorimeter. A description of a modern design of this instrument has been given by Morrison and Los[9] and our cryostat is essentially an automatically-controlled version of theirs.

The cryostat is shown in Fig. 1. The massive copper bulb 7, which contains the powder, is evacuated at 150° outside the cryostat, filled to atmospheric pressure with C.P. argon, and soldered into position at the tubing connector 14. This connector leads to the manometric system through the gas inlet tube 19. (A spare inlet tube is shown in the figure.) The cryostat components are then assembled. The electrical leads which enter the radiation shields run through the spiral grooves on the outside of the side section 8 and are tied to the inner binding post 5. The shield heaters completely cover the outer surfaces. Above the shields the wires are tied in a bundle which is led through the grease-filled trough of the heat interchanger 15 and the evacuation tube 18 to the tapered plug 27, where it is split. The individual wires exit through grooves on 27, and are tied to the main binding post 26 where connections are made to the external circuits. The positions of the temperature controlling thermopiles are indicated by the arrows between the shields and the bulb. The junctions are held in place with small clips, from which they are insulated with one thickness of rice cigarette paper.

The internal wiring is shown in Fig. 2 (which omits a series of thermocouples spaced at known distances of about 7 cm. along the inlet tube). The wires that enter the cryostat are 32 swg. double rayon wrapped copper. The heater wires are similarly insulated 32 swg. constantan. (These wires were supplied by the Concordia Electric Wire and Cable Co., Ltd., Long Eaton, Nr. Nottingham, Eng.) The difference thermocouple junctions are soft-soldered together. Those of the controlling thermopiles are arc welded under a thin mica sandwich; the residual e.m.f. between the sets of junctions was found to be less than 0.1 microvolt when the sets were thermally equilibrated in a water triple point cell.

The separate groups of wires of Fig. 2 are connected to various external circuits. The thermometer resistance is measured potentiometrically[10] in an all copper circuit in which, on current reversal, thermal e.m.f.s larger than 0.2 microvolt are not observed. The circuit contains a Tinsley 4363A Vernier potentiometer and a Leeds and Northrup Type HS galvanometer with a 2 m. scale distance. The

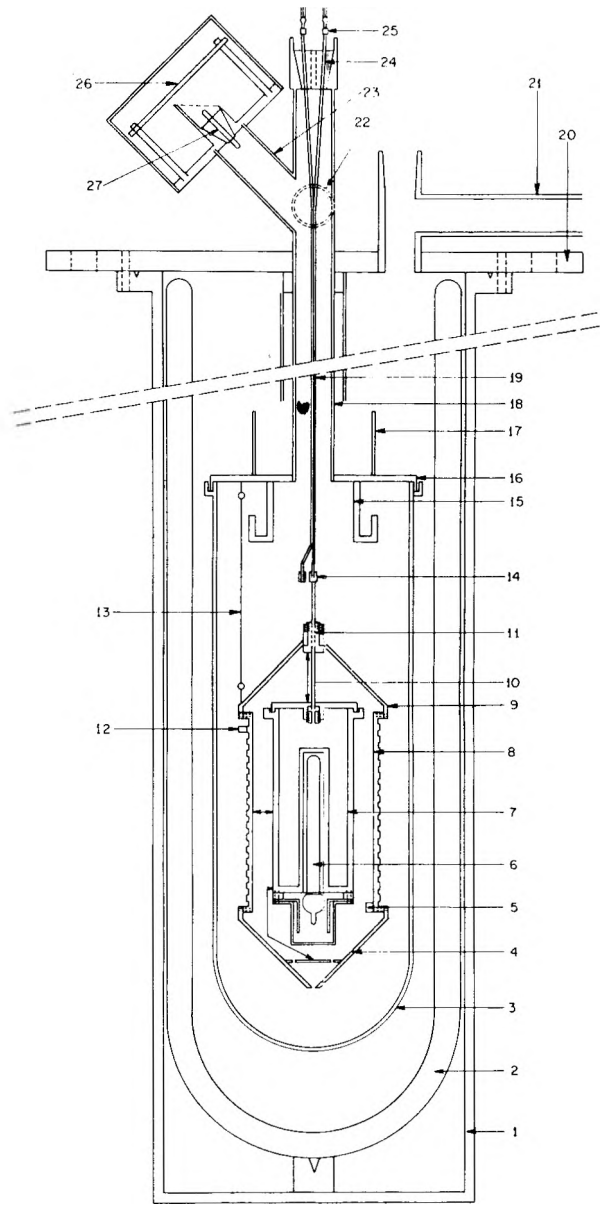

Fig. 1.—The cryostat: 1, brass outer can (6″ × 28″); 2, glass dewar; 3, brass inner can; 4, bottom radiation shield; 5, inner binding post; 6, Pt resistance thermometer; 7, copper sample bulb; 8, side radiation shield; 9, top radiation shield; 10, German silver inlet tube; 11, copper stud; 12, outer binding post; 13, Nylon guy line; 14, brass connector; 15, copper heat interchanger; 16, Wood's metal gutter; 17, water well; 18, German silver evacuation tube; 19, German silver gas inlet tube; 20, brass cryostat top; 21, refrigerant filling tube; 22, evacuation tube; 23, wire bundle exit tube; 24, brass taper plug; 25, brass connector; 26, external binding post; 27, brass taper plug.

lead wires from the difference thermocouples and controlling thermopiles are thrown onto the galvanometer with a set of Tinsley Series A copper selector switches. The lead wires of the thermopiles can be removed from this circuit and placed in an automatic controller circuit. The individual heaters draw current from a 500 ohm Helipot connected across an Automatic Electric 3 amp., 24 v. d.c., battery eliminator. In series with each heater are a two range (0–100 ma., 0–250 ma.) milliammeter, and a three position switch which selects off, high and low current. In the last position a variable resistance (0–100 ohm) is put in series with the heater. The heater circuit is fused at 250 ma.

If the temperature of the shields is allowed to oscillate

(6) R. B. Scott and F. G. Brickwedde, *J. Research Natl. Bur. Standards*, **6**, 401 (1931).

(7) J. A. Morrison and D. M. Young, *Rev. Sci. Instr.*, **25**, 518 (1954).

(8) J. C. Southard and R. J. Milner, *J. Am. Chem. Soc.*, **55**, 4386 (1933).

(9) J. A. Morrison and J. M. Los, *Disc. Faraday Soc.*, **8**, 321 (1950).

(10) J. A. Hall in "Temperature, Its Measurement and Control in Science and Industry," Vol. II, Reinhold Publ. Corp., New York, N. Y., 1955, p. 113.

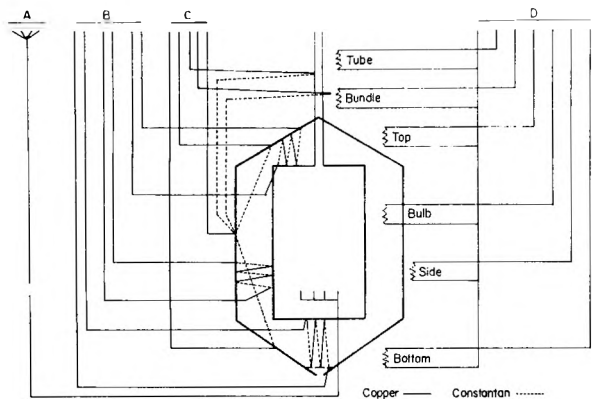

Fig. 2.—Internal wiring of the cryostat. Heater resistances in ohms; tube-85, bundle-25, top-100, side-140, bottom-120, bulb-80: A, resistance thermometers; B, controlling thermopiles; C, difference-thermocouples; D, heaters.

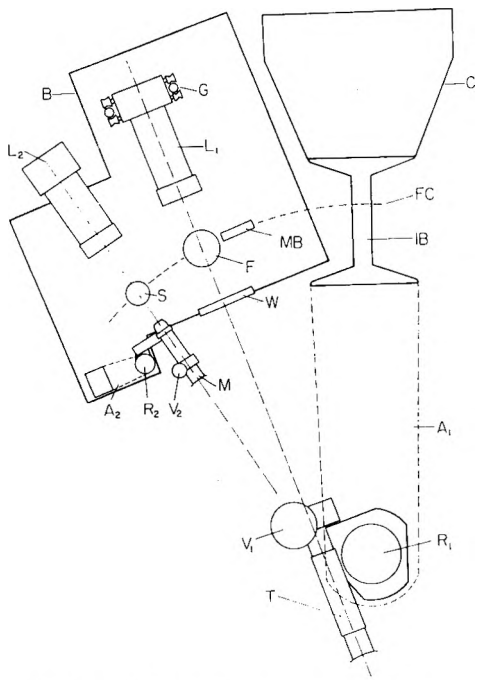

Fig. 3.—Plan of the manometer system.

symmetrically about some temperature, that of the bulb will oscillate about the same temperature, but the extremely high thermal inertia of the system greatly chokes the amplitude of the oscillation at the bulb. Therefore the problem of maintaining the temperature of the bulb to 0.001° is reduced to the simpler problem of keeping temperature of the shields oscillating about the bulb temperature with an amplitude of, say, 0.01°. These facts make the control of the cryostat fairly simple, although it is somewhat complicated by the poor thermal conductivity between the three shields, which necessitates individual control for each shield component. The inlet tube, wire bundle, shield assembly and bulb are brought to the same temperature by use of the heaters and the two groups of thermocouples. The power to the inlet tube and wire bundle is then adjusted to maintain these components slightly above cryostat temperature. The controlling thermopiles are monitored, and the power to the shield heaters is adjusted alternately to high and low manually to give the desired temperature control. When temperature control has been obtained manually the thermopiles are switched into the automatic controller. In this, a motor driven (2 r.p.m.) thermal e.m.f.-free rotary switch is synchronized with a mechanical interlock relay switch. The former throws the thermopiles, in turn, onto a Type HS galvanometer, the light from which actuates a flip-flop phototube relay. This relay in turn actuates the selected interlock relay which puts the heater series resistance in and out of the heater circuit. The controller thus simulates manual control. The details of this device may be found elsewhere.[11]

B. Pressure Measurement.—The nature of the experimental data which are sought demands exacting methods for the determination of the pressure. The amount of gas that interacts with the powder is obtained as the difference of two large quantities: the amount of gas in the sample bulb under conditions of negligible interaction, and the amount present when conditions permit measurable interaction. These quantities are obtained directly from the pressure. Ordinarily, in a volumetric apparatus the pressure is assumed to be correct to ± 0.1 mm., an error which would make our results almost meaningless in the high temperature region. Accordingly, a number of methods for the precision measurement of the pressure were examined, but only a modification of the one based on the sophisticated techniques of Beattie and his co-workers,[12] developed for use in constant volume gas thermometry, was found to be adaptable to accurate gas–solid interaction studies. The manometric system to be described, coupled with a novel gas transfer system, is believed to be accurate to within ±0.005 mm.; as the gas transfer system used permits a wide variety of accurate pressure multiplications to 50–75 cm. it would therefore be concluded that in the pressure range of 7 to 50 cm. the pressure determinations are accurate to ±1 part in 100,000. However, other effects, which are described below, reduce the accuracy by two.

A plan of the manometric system is shown in Fig. 3. The I-beam which supports the cryostat also supports the cathetometer by means of the arms A_1. The telescope T is collared to the shaft R_1, a two inch diameter steel rod which rotates about vertical on ball bearings. T travels vertically 2 cm. on a micrometer screw attached to the vernier head V_1, which can be read to 0.002 mm. The focal cylinder of T, which has a radius of 40 cm., is shown as the dashed circle FC. In this cylinder are mounted a Carpenter stainless steel meter bar MB, (Gaertner serial no. 109au, certified), the free leg F, and the short, or fixed, leg S of the constant volume mercury manometer. These rest on the $^1/_4$" steel base plate B. B is securely bolted to studs anchored in cement-filled concrete blocks which form a pedestal for the manometer. The frame which supports the manometer is bolted to B.

The meniscus in F is illuminated by the lamp L_1, made and mounted according to the specifications of Collins and Blaisdell,[13] which moves vertically in the guides G. L_2 is a similar lamp in a fixed position. M is a short depth of field microscope which is used to zero the mercury level in the short leg. The cross hairs of M are moved with the vernier head V_2, which can be read to 0.0002 mm. M is clamped to the stainless steel shaft R_2 which rotates on ball bearings in the support arms A_2. In order to use L_2 for observation with both M and T the positions are chosen so that the three optical axes of T, M and L_2 coincide and go through the center of S. The illumination for the meter bar is provided by a small spotlight which rides on the collar of T.

The right side of Fig. 4, which is a sketch of the complete system, depicts the manometric part in elevation. S and F are connected through a stainless steel, Teflon packed valve V (Autoclave Engineering Cat No. 1-A-A-1, $^1/_4$"), which is connected to the glass tubing with standard tapers sealed with a small ring of wax which does not come into contact with the mercury. The traps T_1, T_2 and T_3 protect the

(11) G. Constabaris, Thesis, University of Washington, 1957.

(12) J. A. Beattie, D. D. Jacobus, J. M. Gaines, Jr., M. Benedict and B. E. Blaisdell, *Proc. Am. Acad. Soc.*, **74**, 327 (1941).

(13) S. C. Collins and B. E. Blaisdell, *Rev. Sci. Instr.*, **7**, 213 (1937).

manometer legs from contamination. The mercury originates in the reservoir R which is connected either to vacuum or to 5 lb. air pressure. Clamp C_1, over a short length of rubber tubing, fixes the amount of mercury in the manometers and a similar clamp C_2 allows this amount to be adjusted slightly for zeroing the manometer. The free leg is connected to the high vacuum line and the short leg to the gas transfer system and the cryostat.

The manometer is enclosed in a thermostated housing indicated by the dotted line in Fig. 4, the temperature of which is controlled to $\pm 0.04°$ by an ether vapor pressure regulator. With this control the error in estimating the mercury density imposes an error less than 1 part per 50,000 on the pressure. The housing temperature is kept about 1° above the temperature of the room, which is maintained at $\pm 0.4°$ with the use of a three-ton air conditioning unit.

Because the design of the short leg is the most critical factor in the precise measurement of volume and pressure in the apparatus, it is considered here in some detail. As the diameter of the short leg varies three factors, two competing against the other, affect the accuracy in such a way that maximum accuracy is obtained at a certain diameter. The volume of the apparatus above the meniscus in the short leg is part of the external dead space volume and the first two diameter dependent factors are concerned with this volume. The first of these is the mis-set of the mercury at the zero level; the second is the variation of the covolume of the meniscus from determination to determination. The error in the estimation of these volumes increases with increasing diameter. The third factor is the error in the estimation of the capillary depression of the meniscus, which becomes less with increasing diameter. The over-all effect of increasing the diameter of the short leg is to increase the accuracy of the pressure determination and to decrease the accuracy of the estimation of the external dead space volume.

The capillary depression and meniscus covolume can be obtained from the radius and height of the meniscus with the use of tables prepared by Blaisdell,[14] which have been confirmed experimentally by Kistemaker.[15] If it is assumed that a volume of 50 cc. above the short leg is measured at a pressure of 50 cm. which has an error of 0.01 mm., and that the meniscus height in the short leg can be read to 0.05 mm., the tables can be used to estimate the volume and pressure errors for different sizes of tubing. With a mis-set of 0.01 mm., in a 25 mm. short leg the volume error (including the covolume error) is one part in 5,000, whereas the pressure error is less than one part in 50,000. With a tube of 15 mm. diameter the pressure error is two parts in 50,000 and the volume error is also two parts in 50,000. Tubing of about this size has accordingly been used for the short leg. These considerations do not apply to the free leg for if it is of large diameter the capillary depression and the constancy of radius are of no importance.

The form of the short leg is shown in Fig. 4. The top is slightly convex inward; the lowest point of this may be brought into extremely sharp focus in the ocular of the microscope. The mercury meniscus, when viewed within 0.02 cm. of this point, is also in sharp focus. By use of the movable cross-hairs the mercury meniscus can be brought to the same position with respect to the low point. After the level is set the microscope is swung away and the meniscus level and height are read on the cathetometer telescope. This type of short leg has reduced the volume in this part of the system to about 0.5 cc.

The covolume is obtained from the meniscus height using Kistemaker's equation,[15] and the depression by interpolation into his tables. Although the covolume values cannot be checked here, those for the depression can be when both legs of the manometer are evacuated. The depression was measured between runs over a four month period. Representative observed values and tabulated values are given in mm. by the following pairs, in which the observed value is listed first: 0.173–0.171, 0.198–0.194, 0.180–0.194, 0.207–0.196. It is evident that the reliability of the correction is such that it limits the accuracy of the pressure determination to about ± 0.005 mm. The reduction of the observed pressure to the absolute value is carried out by taking into account the density of mercury in the manometer, the acceleration due to gravity at the University, and the temperature dependence of the length of the meter bar.

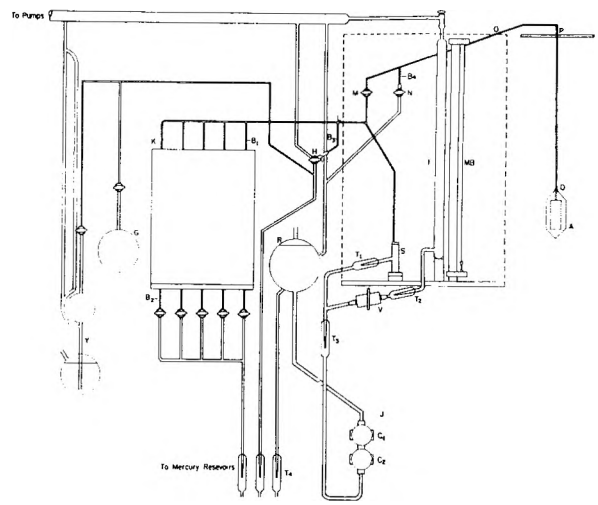

Fig. 4.—Gas transfer, external dead space volume, and manometer.

C. Gas Transfer System.—The conventional gas transfer system, which consists of a transfer buret and manometer, has inherent errors[16] which preclude its use in this work. These errors arise from the type of manometer that must be used, the relatively poor temperature control that is obtained for the water jacket of the buret, the lack of precise definition of the gas volume transferred through the buret stopcock, and the cumulative error due to successive gas doses. The gas transfer system, depicted in the left portion of Fig. 4, effectively reduces these errors to within the desired range.

The ice mantle K contains five mercury pipets with volumes between the calibration marks B_1 and B_4 of 10, 20, 40, 60 and 160 ml., respectively. Thus, combinations of these give volumes at 10-ml. intervals between 0 and 310 ml. The direct connection between the pipets and the short leg makes the system unimanometric: both gas dose and run pressures are measured on the same precise manometer. At times during a run a large fraction of the gas is in the pipets. This does not introduce an appreciable error into the estimation of the amount of gas inside the sample bulb for the temperature measurement and control of an ice mantle are virtually free of experimental error.

After the system is evacuated the mercury is run up to the mark B_4, and M and N are closed. The pipets that have the desired volume are emptied and the gas from G pumped into the system through the Toepler pump Y. The mercury is raised to B_3 and H is closed. (This arrangement for stopcocks M and N is used so that sharp cut-off volumes, as well as adequate evacuation rates, are obtained.) The pressure, the known volumes below M, and the equation of state for the gas, give the total amount of gas introduced into the system. In the pressure–temperature range used the pipet volumes are such that the gas dosage is done only once for a run.

The cryostat is set on temperature and the gas is introduced into the sample bulb through M. Gas is thereafter transferred in and out of the bulb by filling and emptying various pipet combinations. For pressure multiplication M is closed and the appropriate pipets are filled.

D. Calibration.—We are primarily interested in measuring the apparent volume of a sample bulb which contains a large surface. The apparent volume is defined as

$$V_a = n_b RT/P$$

(14) B. E. Blaisdell, *J. Math. Phys.*, **19**, 186 (1940).

(15) J. Kistemaker, *Physica*, **11**, 270 (1945).

(16) W. V. Lobenstein and V. E. Deitz, *J. Chem. Phys.*, **15**, 687 (1947).

where n_b is the number of moles of gas inside the sample bulb, P the pressure, T the temperature and R the gas constant. Thus, the experiments are simply the gasometric determination of volumes. The fraction of the gas outside the bulb is given by a sum of V/T terms multiplied by the pressure, each term corresponding to a volume element with its particular temperature. Therefore, the absolute error in the determination of the volumes of these elements must be within the desired error in V_a. Further, if the volume is large, the temperature must be known with a corresponding accuracy, and conversely, if the temperature cannot be precisely determined, the volume must be kept low.

The pipets were calibrated *in situ* by weighing the mercury, at the ice point, delivered from between the calibration marks B_1 and B_2. The mercury delivery for each pipet was done in triplicate, the three weights not differing by more than 10 mg. in the worst case. The volumes are pressure dependent but only for the two largest pipets does this need to be taken into account.

The volumes of the different sections of the pressure transmitting lines were gasometrically determined by expansion of gas from one pipet to another. After this has been done with two pipets the volumes of the other pipets can be determined in a similar manner. This procedure is a critical test of the apparatus for it gives a direct comparison of a gasometric volume with one obtained from contained mercury.

Numerous measurements were made to establish the volumes of the several parts of the external region. The results of two series of these are reported here in order to indicate some of the quantitative features of the measurements. In the first, the total external volume up to Q, (Fig. 4), was determined using a variety of pressures and pipet combinations. The results, given in Table I, were obtained with reagent grade helium. Each series denotes a different gas dose. The results indicate a maximum deviation of 0.006 ml.

TABLE I

DETERMINATION OF THE TOTAL EXTERNAL DEAD SPACE VOLUME (HELIUM)

Series	Pipet	Pressure, cm.	Temp., °K. Room	Manometer	Mantle	Volume, ml.
I	V_{10}	66.5655	296.7	297.37	273.148	...
	V_{20}	36.7437	296.3	297.37	273.148	2.662
	V_{40}	19.6021	296.0	297.31	273.148	2.664
	V_{80}	10.0551	296.3	297.34	273.148	2.664
II	V_{20}	60.1566	296.1	297.36	273.148	...
	V_{40}	32.0984	296.4	297.33	273.148	2.667
	V_{80}	16.4592	296.3	297.28	273.148	2.662
	V_{160}	8.3999	296.1	297.28	273.148	2.661
III	V_{10}	39.6739	296.1	297.27	273.150	...
	V_{20}	21.1944	296.2	297.21	273.150	2.667
	V_{40}	11.6931	296.0	297.27	273.150	2.670
					Av.	2.664

The results of the second set of experiments, in which neon was used, are given in Table II, and in this case are reported as gasometric determination of pipet volumes as compared to contained mercury volumes. The comparison shows that the agreement is to within 2 parts per 10,000. It is usually assumed that the dead space volume in a conventional volumetric apparatus can be measured to within 1%,[16] although with care this can be lowered to perhaps 0.2%. The present apparatus evidently has permitted an increase in this accuracy by an order of magnitude, or greater.

If it is assumed that the temperature gradient in the gas inlet tube is linear between the thermocouples spaced along the tube, the amount of gas inside the tube can be obtained as a sum of simple integrals. The error introduced by this assumption was estimated in the following way. A known amount of helium was put into the external volume (capped at Q). The bottom of the inlet tube was connected by a thermal shunt to a liquid nitrogen pool, the temperature distribution varied with the tube heater, and the pressure at each distribution measured. From this and the known volumes exterior to the tube the amount of gas inside the tube was obtained. Results obtained this way compared to those given by the temperature distribution to within 1.5%; the contribution of this error to the error in V_a varies with the temperature, but the maximum contribution of this to the results given in the next section is 2 parts per 10,000.

TABLE II

GASOMETRIC MEASUREMENT OF THE PIPET VOLUMES COMPARED TO THE MERCURY WEIGHT CALIBRATIONS (NEON)

Hg vol., ml.	Gasometric vol., ml.	Diff. parts per 10 thousand
20.174	20.170	−2
80.440	80.428	−2
160.036	160.026	−0.6
240.475	240.482	0.3

The platinum resistance thermometer was calibrated by measuring resistances at the triple point of water, the oxygen point, and at two intermediate temperatures which were ascertained with an NBS certified resistance thermometer. All auxiliary thermometers were periodically standardized against the latter thermometer.

Apparent Volume of a Bulb Containing a Graphitized Carbon Black

Some experimental results for V_a with a low area black are given in this section. The black used is designated as P33(2700°) which was first prepared and studied by Polley, Schaeffer and Smith.[17] This carbon is ideal for the study of gas surface interactions because of the nearly homogeneous nature of its surface. It has a BET area of about 13 m.²/g.; as 29.90 g. were put in the sample bulb the total area used was approximately 400 m.².

TABLE III

APPARENT VOLUME AT THE ICE POINT—He, Ne, A, Kr

Helium Series	Pressure, cm.	V_a, ml./g.	Argon Series	Pressure, cm.	V_a, ml./g
2	59.5640	1.5272	2	50.1300	1.5771
1	45.4973	1.5267	1	43.7279	1.5768
2	32.5526	1.5273	2	41.7479	1.5763
1	27.9804	1.5273	1	34.0572	1.5766
1	17.0491	1.5272	2	27.7748	1.5763
	Av.	1.5271	3	23.4819	1.5766
	Av. dev.	1.3×10^{-4}		Av.	1.5766
				Av. dev.	1.9×10^{-4}

Neon Series	Pressure, cm.	V_a, ml./g.	Krypton (one series) Pressure, cm.	V_a, ml./g.
2	59.5547	1.5296	56.3062	1.6785
3	46.7634	1.5297	47.2855	1.6795
3	46.7737	1.5298	40.6876	1.6781
1	32.8069	1.5297	35.7830	1.6805
2	32.5717	1.5294	32.0056	1.6784
3	22.9744	1.5296	28.8785	1.6799
2	22.3460	1.5294	24.1419	1.6804
3	12.6357	1.5298	19.3613	1.6792
3	9.0940	1.5304	15.3541	1.6782
3	6.8699	1.5294	11.7451	1.6802
3	6.2908	1.5306	Av.	1.6793
	Av.	1.5298	Av. dev.	4.7×10^{-4}
	Av. dev.	1.3×10^{-4}		

The first measurements to be reported were car-

(17) M. H. Polley, W. D. Schaeffer and W. R. Smith, THIS JOURNAL, **57**, 469 (1953).

ried out at the ice point with reagent grade He, Ne, A and Kr, which were obtained from Air Reduction Sales Co. The values for V_a are given in Table III. Although the error in a determination is not equally probable at different pressures the formal average deviation is listed in the table and indicates a reproducibility to within 0.02%, except in the case of krypton.

TABLE IV

APPARENT VOLUME WITH ARGON AT VARIOUS TEMPERATURES

Pressure, cm.	Temp., °K.	V_a, ml./g.	Pressure, cm.	Temp., °K.	V_a, ml./g.
58.4424	174.092	1.8663	55.2028	214.769	1.6511
43.8205	174.104	1.8681	42.2052	214.771	1.6514
26.3278	174.105	1.8703	34.2058	214.769	1.6514
			28.7528	214.768	1.6514
71.0537	197.299	1.7127	21.7751	214.768	1.6514
57.3243	197.332	1.7132	17.5302	214.766	1.6516
52.3364	197.300	1.7133			
50.3726	197.299	1.7131	62.2372	237.279	1.6097
36.3430	197.299	1.7138	62.2308	237.283	1.6095
33.8933	197.300	1.7138	46.1898	237.288	1.6093
23.3050	197.299	1.7144	36.8406	237.287	1.6093
			28.1370	237.288	1.6093
			21.4299	237.287	1.6094
			9.7994	237.286	1.6094

These results may be put into the more familiar terms of the volume adsorbed at STP, V_{STP}. If the internal dead space volume is V_{DS}, then by the definition of the apparent volume

$$V_{STP} = (273.15P)(V_a - V_{DS})/(76.000T)$$

As a first approximation the dead space volume may be taken to be the apparent volume of the bulb determined with He at the ice point. The appropriate gas imperfection correction is applied to the gas in V_{DS}. The data in Table III are converted in this way to the conventional isotherm and are plotted in Fig. 5 as the fraction of a filled monolayer, θ, *vs.* the pressure. To convert V_{STP} to θ the specific area of the sample and the collision diameters of the rare gas atoms were used.

Similar data for the apparent volume with argon at different temperatures are given in Table IV. At temperatures above which the apparatus can resolve no pressure dependence for V_a (*viz.*, 215°K.), the worst deviation from average is 3 parts in 10,000. At the two lower temperatures given in the table

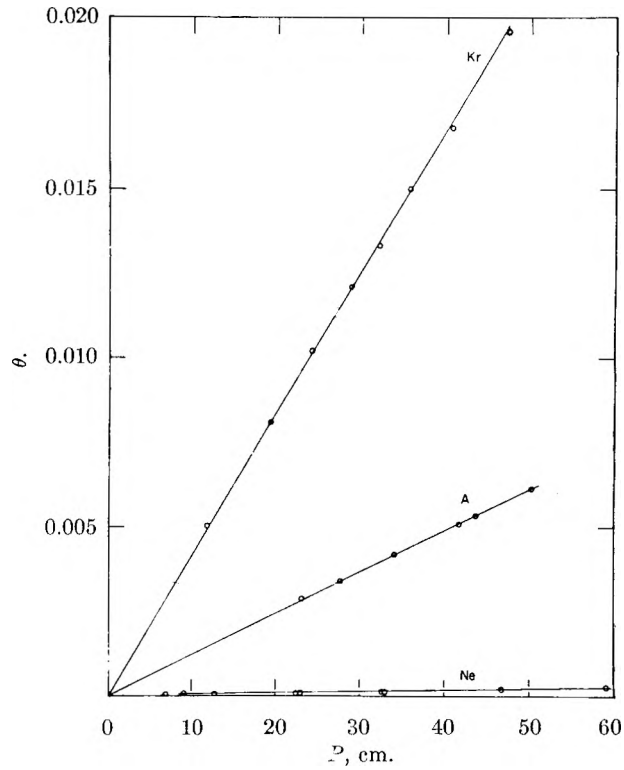

Fig. 5.—Adsorption isotherms with P33(2700°) at the ice point. Fraction of a filled monolayer, θ, with pressure, cm. Hg.

the pressure dependency has become observable. In the case of the 197°K. run, which was done in three series, the maximum deviation from a straight line plot of V_a *vs.* P is about 2 parts per 10,000.

These data, extrapolated to zero pressure, have been analyzed by the method of Steele and Halsey[3] elsewhere, for both a hard sphere model[18] and for the softer 9-3 potential model.[19]

Acknowledgment.—We wish to thank Dr. W. R. Smith of Godfrey L. Cabot, Inc., Cambridge, Mass. for supplying us with an unusually large sample of the P33(2700°). We are indebted to Dr. J. A. Morrison of the National Research Council, Ottawa, Canada, and Professor J. G. Aston, Pennsylvania State University, for much essential advice.

(18) G. Constabaris and G. D. Halsey, Jr., *J. Chem. Phys.*, **27**, 1433 (1957).

(19) Mark P. Freeman, THIS JOURNAL, **62**, 723 (1958).

PHASE RELATIONSHIPS IN MIXTURES OF THE SIMPLE POLYPHENYLS AND CONDENSED RING AROMATICS. A SURVEY OF ORGANIC REACTOR COOLANT MIXTURES

BY V. H. TROUTNER

Reactor and Fuels Research and Development Operation, Hanford Laboratories Operation, Richland, Washington

Received December 8, 1958

Solid–liquid–vapor phase diagrams are determined and discussed for the binary, ternary, quaternary and quinary mixtures of biphenyl, *o*-terphenyl, *m*-terphenyl, naphthalene and phenanthrene. The suitability of these mixtures as reactor coolants is discussed.

In recent years, considerable interest has been shown in the possible use of an organic material as a coolant for nuclear reactors. Organic materials offer the advantages over aqueous systems of operation at high temperatures (up to 400°) with relatively low pressures and virtually no corrosion problems. It was the purpose of this work to investigate the possible organic compounds and mixtures which might be used as a reactor coolant and to select the most promising system based on certain physical criteria. Restrictions imposed by reactor considerations narrowed the possible coolants down to five most promising compounds and their mixtures. The restrictions imposed were, (a) that the organic material must have good pyrolytic and radiolytic stability, (b) it should have a low melting point and high boiling point, and (c) it should be relatively non-toxic and safe to handle. The stability conditions are best met by the simple polyphenyls and condensed ring aromatics.[1] The presence of aliphatic side chain substitutions reduces the stability markedly and these substituted compounds were not considered in this study. Imposing the arbitrary limitation that compounds to be considered must have a melting point of 100° or less, and eliminating benzene because of the hazardous nature and low boiling point, the materials to be studied were limited to the five shown in Table I.

TABLE I

ORGANIC COOLANT MATERIALS

Compound	M.p., °C.	B.p., °C.
Biphenyl	69	254
o-Terphenyl	56	336
m-Terphenyl	87	371
Naphthalene	80	217
Phenanthrene	100	340

It is clearly desirable that a coolant material be liquid at room temperature, 25°. All five of the compounds included in this study are solid at 25°. Based on theoretical considerations, French and Epstein[2] have shown that mixtures of these compounds are possible which melt below 25°. However, there is an important additional requirement which must be met if low melting mixtures are considered. The composition of the vapor phase in equilibrium with the liquid mixture must be of such a composition that when condensed it is also liquid. This requirement was mentioned by Bowen and Groot[3] in their theoretical treatment of some of the binary and ternary mixtures.

An optimum coolant mixture may be defined by the criteria: (1) it must have good pyrolytic and radiolytic stability; (2) it must be liquid at 25°; (3) it must have a high boiling point; (4) the vapor in equilibrium with the mixture must be of such a composition that it is liquid when condensed at 25°.

Strictly speaking, this set of criteria defines a "25° optimum mixture." In general, optimum mixtures may be referred to other base temperatures.

The objectives of this study were, (a) to examine the solid–liquid–vapor phase relationships of all mixtures of the compounds biphenyl, *o*-terphenyl, *m*-terphenyl, naphthalene and phenanthrene, (b) to compare the experimentally determined phase diagrams with those based on theoretical considerations and (c) to determine the temperatures and compositions of optimum coolant mixtures.

Summary and Conclusions

Melting point diagrams were determined for all the binary and ternary mixtures of biphenyl, *o*-terphenyl, *m*-terphenyl, naphthalene and phenanthrene. Wide ranges of solid solubility were found and consequently they differed significantly from the calculated theoretical diagrams of French and Epstein[2] which were based on ideality and the assumption that the solid phases are in every case the pure components. Boiling point and vapor composition diagrams were calculated for all of these mixtures. Some experimental melting point data were obtained for the quaternary and quinary mixtures.

It was shown that no combination of the five compounds formed optimum mixtures which melted below 35°.

Experimental

The organic materials used in this investigation were of the highest purity obtainable. They had a capillary melting point range of one degree centigrade or less, and were nominally 99 + % pure.

The melting point diagrams were determined using mixtures which were weighed out to give incremental mole per cent. compositions. Five mole per cent. intervals were used for the binary systems and 10 mole % intervals were used for the ternary systems. These mixtures were sealed in

(1) R. O. Bolt and J. G. Carroll, "Organics as Reactor Moderator-Coolants: Some Aspects of Their Thermal and Radiation Stabilities," Proceedings of the International Conference on the Peaceful Uses of Atomic Energy, Geneva, August, 1955, Vol. 7, p. 546.

(2) N. E. French and L. F. Epstein, "Preliminary Considerations of Phase Relations in Systems of Diphenyl with Terphenyls and Other Aromatic Hydrocarbons," Knolls Atomic Power Laboratory, KAPL-M-NEF-1, October, 1956.

(3) H. C. Bowen and C. Groot, "Boiling Points, Vapor Compositions and Freezing Points for Some Aromatic Hydrocarbon Mixtures," Hanford Atomic Products Operation, HW-48427, February, 1957.

glass ampoules and placed in a constant temperature bath, whose temperature was increased in steps of one degree every two hours. The temperatures at which melting began and at which they were completely melted were recorded. The procedure of cooling melted mixtures until the first crystals were observed could not be used because of the strong tendency of these systems to supercool. Some vapor composition data were obtained experimentally with an Othmer equilibrium still[4] which had additional heaters for use at high temperatures. The equilibrium liquid and vapor samples were analyzed by gas chromatography.

Discussion

Vapor Composition.—Only a limited amount of experimental vapor composition data was obtained because of difficulties encountered in the operation of the equilibrium still at high temperatures (300° and above). These data were used to calculate the activity coefficients of the components in the various mixtures as defined by

$$\gamma = \frac{P_t N_v}{P_v N_l}$$

where

γ = activity coefficient of the given component
P_t = total pressure (1 atm. in this case)
N_v = mole fraction of the given component in the vapor
N_l = mole fraction of the given component in the liquid
P_v = vapor pressure of the given component at the b.p. of the mixture

P_v was calculated using the following vapor pressure equations where P_v is in atmospheres and t is in centigrade degrees

Biphenyl:

$$\log P = 4.576 - \frac{2213.3}{t + 230}$$

Naphthalene:

$$\log P = 4.394 - \frac{1962.4}{t + 230}$$

o-Terphenyl:

$$\log P = 4.7338 - \frac{2680.1}{t + 230}$$

m-Terphenyl:

$$\log P = 4.7337 - \frac{2848.2}{t + 230}$$

Phenanthrene:

$$\log P = 26.6669 - \frac{4743.3}{T} - 6.7893 \log T$$

$$T = t + 273.13$$

These vapor equations are those used by Bowen and Groot.[3]

The experimental vapor composition and boiling point data are given in Table II along with the calculated activity coefficients.

The activity coefficients appeared to be randomly scattered about unity and those determined from runs of high reliability (runs in which no experimental troubles occurred) were very close to unity. It was decided, therefore, to assume activity coefficients of one and to use the foregoing vapor pressure equations and Raoult's law to calculate all the desired vapor compositions and boiling points. Accordingly

$$P_p = N_l P_v = N_v P_t$$

$$\text{or } \log N_v = \log N_l + \log P_v, \text{ when } P_t = 1 \text{ atm.}$$

where P_p = partial pressure of the given component.

(4) D. F. Othmer, *Anal. Chem.*, **20**, 763 (1948).

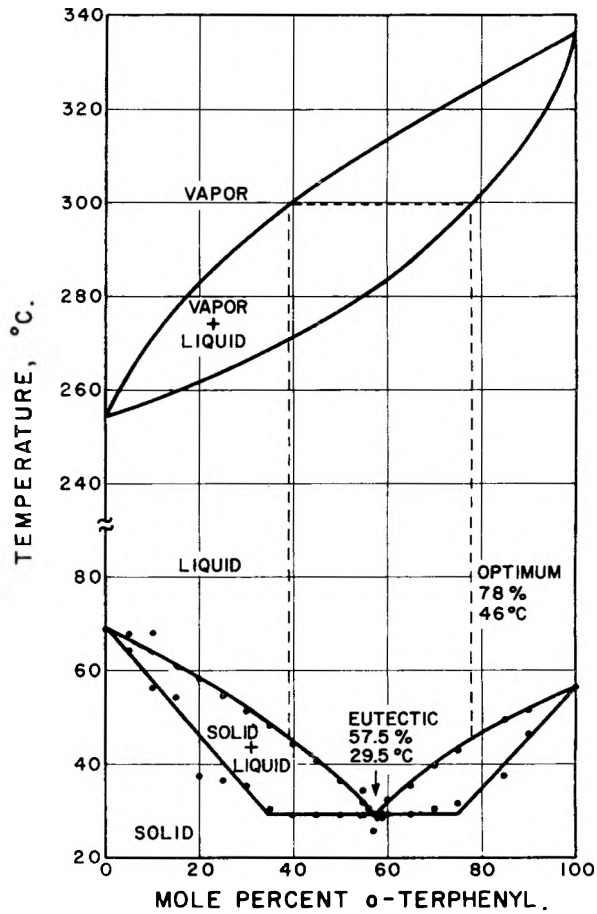

Fig. 1.—*o*-Terphenyl: biphenyl.

TABLE II

VAPOR COMPOSITION DATA

Mixture composition	B.p., °C.	N_v	N_l	P_v, atm.	γ
Biphenyl	261	0.961	0.779	1.17	1.05
o-Terphenyl	261	.039	.221	0.188	0.94
Biphenyl	269	.925	.675	1.38	0.99
o-Terphenyl	269	.075	.325	0.231	1.00
Biphenyl	278	.845	.496	1.66	1.03
o-Terphenyl	278	.155	.504	0.287	1.07
Phenanthrene	337	.502	.493	0.957	1.06
o-Terphenyl	337	.498	.507	1.016	0.97
m-Terphenyl	352	.352	.541	0.692	0.94
o-Terphenyl	352	.648	.459	1.346	1.05
m-Terphenyl	301	.087	.376	0.235	0.99
o-Terphenyl	301	.191	.332	0.486	1.19
Biphenyl	301	.722	.292	2.561	0.97
Phenanthrene	346	.401	.321	1.127	1.14[a]
o-Terphenyl	346	.411	.319	1.205	1.07[a]
m-Terphenyl	346	.189	.370	0.616	0.83[a]
m-Terphenyl	316	.086	.240	0.329	1.09[b]
o-Terphenyl	316	.171	.227	0.669	1.13[b]
Biphenyl	316	.451	.169	3.334	0.80[b]
Phenanthrene	316	.292	.364	0.641	1.25[b]

[a] Non-equilibrium caused by heater failure. [b] Non-equilibrium caused by leaky fittings.

Binary Systems.—A typical binary diagram is shown in Fig. 1. The lowest melting optimum mixture is shown by the dotted line. It contains 78 mole % *o*-terphenyl and 22 mole % biphenyl and melts at 45.5°. The vapor in equilibrium with this mixture contains 39 mole % *o*-terphenyl and 61 mole % biphenyl. The condensed vapor will

TABLE III

BINARY SYSTEMS

Mixture	Eutectic: Mole % of 1st Component	Eutectic: m.p., °C.	Optimum: Mole % of 1st Component	Optimum: m.p., °C.	Solid solubility regions (mole % of 1st component)	Source
o-Terphenyl:biphenyl	57.5	29.5°	78.0	46	0–35, 75–100	This work.[5] Figure 1
	(61.0)	(22.8)				Nakayato and Gercke[6]
	(59.8)	(27.5)				Anderson[7]
o-Terphenyl:naphthalene	63.0	31.5	88.5	52	–16, 76–100	This work[5]
o-Terphenyl:phenanthrene	70 0	39.0	67.5	43	–30, 85–100	This work[5]
o-Terphenyl:*m*-terphenyl	75.0	39.0	69.0	49	–63, 82–100	This work[5]
Biphenyl:naphthalene	55 0	39.5	66.0	50	–30, 70–100	This work[5]
	(56)	(39.4)				Washburn and Read[8]
	(60)	(38.0)				Mason, *et al.*[9]
	(55)	(39.5)				Lee and Warner[10]
m-Terphenyl:biphenyl	35.5	45.5	57.0	64.5	–22, 52–100	This work[5]
	(45 0)	(41.5)				Anderson[7]
m-Terphenyl:naphthalene	41.0	49.5	76.0	75	–10, 55–100	This work[5]
Phenanthrene:naphthalene	43.0	52.0	65 5	74	–27, 61–100	This work[5]
	(45.8)	(47 5)				Rudolfi[11]
	(42.7)	(51.0)				Kravchenko[12]
	(45 0)	(48 0)				Miolati[13]
	(41.8)	(54.0)				Klochko-Zhovnir[14]
Phenanthrene:*m*-terphenyl	50.0	56.5	41.0	64.5	–38, 65–100	This work[5]
Phenanthrene:biphenyl	30.0	58.5	47.0	64.5	0–100	This work[5]

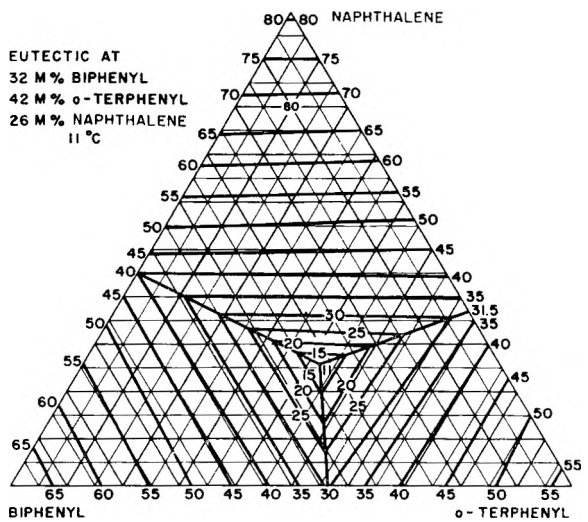

Fig. 2.—Biphenyl:*o*-terphenyl:naphthalene melting point diagram.

begin to freeze at 45.5°. Although mixtures exist which melt at lower temperatures, their condensed vapors begin to freeze at higher temperatures.

The binary data are summarized in Table III along with the existing values available in the literature. As shown in the table, there are no binary optimum mixtures near 25°. The lowest melting optimum mixture consists of *o*-terphenyl and phenanthrene with a melting point of 43°.

The complete set of phase diagrams for the ten binary systems are available in ref. 5.

Ternary Systems.—A typical set of phase diagrams for a ternary mixture is shown in Figs. 2 to 5. The melting point diagram, Fig. 2, is plotted as isothermal contours.

The vapor freezing point diagram, Fig. 3, was calculated using the previously listed vapor pressure equations. The vapor composition with a given freezing point was taken from the melting point diagram. The vapor pressure equations were then used to calculate the composition of the liquid mixture which has this vapor composition. The isotherms on the vapor freezing point diagram thus show the composition of the mixture whose condensed vapors begin to freeze at the temperature of the isotherm.

The optimum mixture diagram, Fig. 4, was obtained by combining the melting point and vapor freezing point diagrams. The isotherms outline the regions of composition which are common to both. For example the area bounded by the 40° isotherm indicates all the ternary mixtures of biphenyl, *o*-terphenyl and naphthalene which are liquid at 40° or less and whose condensed vapors are also liquid at 40°. Notice in this system there are no mixtures which meet these conditions at 30° or less.

The boiling point diagram, Fig. 5, was calculated from the vapor pressure equations.

A summary of the ternary data is given in Table IV. A complete set of phase diagrams for the ten ternary systems is available in ref. 5.

The only previously reported ternary eutectic was by de Halas,[15] who reports a eutectic at 33.2 mole % biphenyl, 49.0 mole % *o*-terphenyl and 17.8

(5) V. H. Troutner, "Phase Relationships in Mixtures of the Simple Polyphenyls and Condensed Ring Aromatics," Hanford Atomic Products Operation, HW-57431, 1958, Available from the Office of Technical Service, U. S. Dept. of Commerce, Washington 25, D. C.

(6) S. Nakayato and R. H. J. Gercke, "Organic In-Pile Loop, NAA-18," Atomics International, NAA-SR-1592, 1956.

(7) K. Anderson, "Engineering Properties of Diphenyl," Argonne National Laboratory, ANL-5121, August, 1953.

(8) E. W. Washburn and J. W. Read, *Proc. Nat. Acad. Sci.*, **1**, 191, (1915).

(9) C. M. Mason, B. W. Rosen and R. M. Swift, *J. Chem. Educ.*, **18**, 473 (1941).

(10) H. H. Lee and J. C. Warner, *J. Am. Chem. Soc.*, **57**, 318 (1935).

(11) E. Rudolfi, *Z. physik. Chem.*, **66**, 705 (1909).

(12) V. M. Kravchenko, *Ukrain., Khim. Zhur.*, **18**, 473 (1952).

(13) A. Miolati, *Z. physik. Chem.*, **9**, 649 (1892).

(14) Yu. F. Klochko-Zhovnir, *Zhur. Priklad. Khim.*, **22**, 848 (1949).

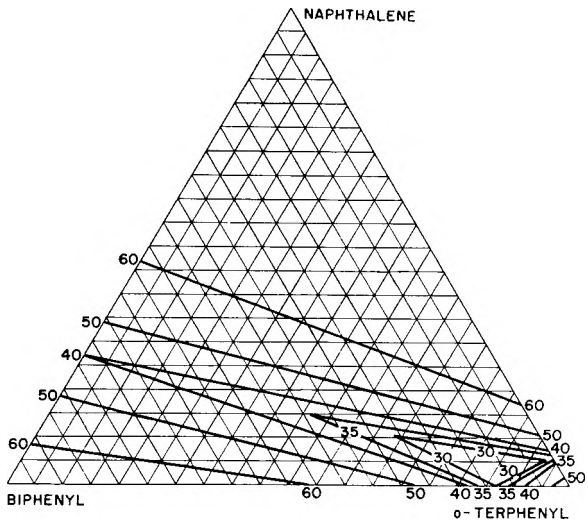

Fig. 3.—Biphenyl:*o*-terphenyl:naphthalene vapor freezing point diagram.

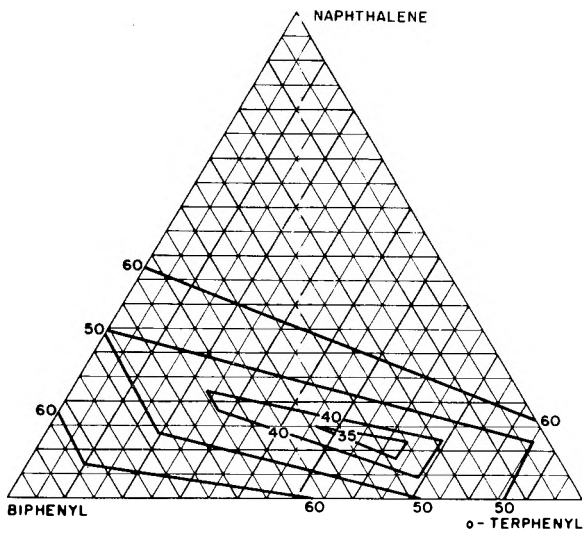

Fig. 4.—Biphenyl:*o*-terphenyl:naphthalene optimum mixture diagram.

TABLE IV

TERNARY SYSTEMS

Eutectic composition, mole %	Eutectic, m.p., °C.	Lowest optimum m.p., °C.
o-Terphenyl, 42:naphthalene, 26:biphenyl, 32	11	35
o-Terphenyl, 59:naphthalene, 30:*m*-terphenyl, 11	20	45
o-Terphenyl, 49:biphenyl, 37:*m*-terphenyl, 15	23	40
o-Terphenyl, 49:biphenyl, 32:phenanthrene, 19	23	35
o-Terphenyl, 50:phenanthrene, 20:naphthalene, 30	24	40
o-Terphenyl, 59.5:phenanthrene, 23.5:*m*-terphenyl, 17	28	35
Biphenyl, 40.5:naphthalene, 35:phenanthrene, 24.5	31	45
Biphenyl, 42:naphthalene, 39:*m*-terphenyl, 19	32	40
Phenanthrene, 31:*m*-terphenyl, 27.5:naphthalene, 41.5	37	55
Phenanthrene, 29:*m*-terphenyl, 26:biphenyl, 45	38	50

[a] The optimum melting point isotherms were determined to the nearest 5°. For example, a lowest optimum melting point of 35° indicates that there is no 30° optimum although an optimum mixture may occur between these temperatures.

TABLE V

CALCULATED QUATERNARY AND QUINARY EUTECTICS

Composition, mole %	Calcd. m.p., °C.	Exptl. m.p. range, °C.
Biphenyl, 25.6:*o*-terphenyl, 40.8:*m*-terphenyl, 17.3:naphthalene, 16.3	2	6.5–30
Biphenyl, 26.0:*o*-terphenyl, 40.9:*m*-terphenyl, 17.7:phenanthrene, 15.4	3	8.5–26
Biphenyl, 26.3:*o*-terphenyl, 41.2:naphthalene, 16.9:phenanthrene, 15.6	3.5	12 –15
o-Terphenyl, 44.4:*m*-terphenyl, 19.8:naphthalene, 18.7:phenanthrene, 20.3	7	17.2–32
Biphenyl, 33.3:*m*-terphenyl, 23.6:naphthalene, 22.8:phenanthrene, 20.3	14	22.4–33
Biphenyl, 22.5:*o*-terphenyl, 35.9:*m*-terphenyl, 14.8:naphthalene, 13.8:phenanthrene, 13.0	−3.5	3.8–20.5

(15) D. R. de Halas, "Irradiation of the Biphenyl, *ortho*-, *meta*-Terphenyl Eutectic," Hanford Atomic Products Operation, HW-54994, February, 1958.

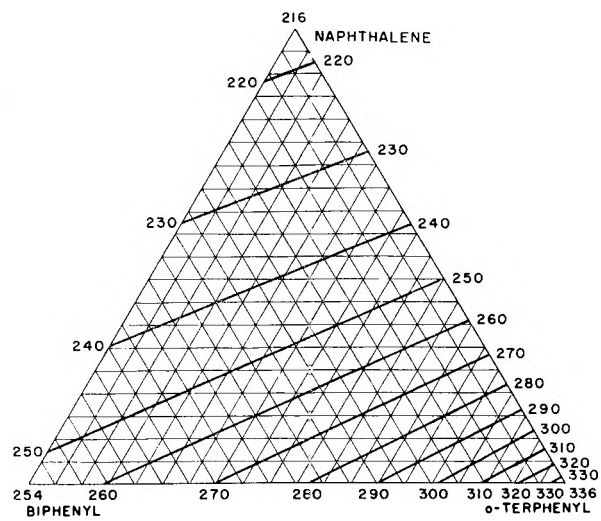

Fig. 5.—Biphenyl:*o*-terphenyl:naphthalene boiling point diagram.

mole % *m*-terphenyl with a pour point of about −15°. The eutectic composition is in fair agreement with the present determination. The low pour point is a result of supercooling and the use of commercial grade compounds.

There are no optimum mixtures which melt near 25°. The lowest melting optimum mixtures melt at about 35°.

Quaternary and Quinary Systems.—The quaternary and quinary eutectic compositions and melting points were calculated using the ideal solution equations of French and Epstein.[2] These values are given in Table V along with the experimentally determined melting points of these mixtures. The observed melting points were much higher than the calculated values, and the wide melting point range indicates that these mixtures are not the true eutectic compositions. A few additional melting points were determined and these are listed in Table VI.

No estimate was made of the true eutectic or optimum compositions from the experimental data.

TABLE VI

QUATERNARY AND QUINARY MELTING POINT DATA

Composition, mole %					M.p., °C.
Biphenyl	*o*-terphenyl	*m*-terphenyl	naphthalene		
20	20	20	40		33.5°
20	20	40	20		50.5
20	40	20	20		32.9
40	20	20	20		28.4
Biphenyl	*o*-terphenyl	*m*-terphenyl	phenanthrene		
20	20	20	40		49.5
20	20	40	20		51.6
20	40	20	20		32.9
40	20	20	20		30.9
Biphenyl	*o*-terphenyl	naphthalene	phenanthrene		
20	20	20	40		50.5
20	20	40	20		35.6
20	40	20	20		[a]
40	20	20	20		32.9
o-Terphenyl	*m*-terphenyl	naphthalene	phenanthrene		
20	20	20	40		48.5
20	20	40	20		34.5
20	40	20	20		53.6
40	20	20	20		32.9
Biphenyl	*m*-terphenyl	naphthalene	phenanthrene		
20	20	20	40		48.5
20	20	40	20		35.6
20	40	20	20		52.9
40	20	20	20		32.9
Biphenyl	*o*-terphenyl	*m*-terphenyl	naphthalene	phenanthrene	
20	20	20	20	20	30.9

[a] Did not solidify as a result of supercooling or a very low melting point.

However, it is possible to consider these systems qualitatively. Although the actual eutectic melting points are probably higher than the calculated values, it is quite probable that they are about 25° or less. It is very doubtful, however, that any of these systems have optimum compositions which melt at 25° or less. All the quaternary and quinary systems contain either biphenyl or naphthalene, or both. These compounds have low boiling points and, consequently, the vapor phase is markedly enriched in them which raises the vapor freezing point considerably above the melting point of the original mixture.

Acknowledgments.—The author wishes to acknowledge the valuable discussion and assistance given by H. C. Bowen and C. Groot. The author would also like to thank Mr. Frances De Mers for providing the gas chromatographic analyses, and Mrs. Pauline Stewart for her assistance in weighing out the sample mixtures.

EQUILIBRIA IN THE REACTION OF BARIUM WITH CALCIUM CHLORIDE[1]

BY DAVID T. PETERSON AND J. A. HINKEBEIN

Contribution No. 685 from the Institute for Atomic Research and Department of Chemistry, Iowa State College, Ames, Iowa.
(1) Work was performed in the Ames Physical Chemistry Laboratory of the U. S. Atomic Energy Commission

Received December 15, 1958

The reaction of barium with calcium chloride in the liquid state was investigated by quenching and analyzing equilibrated samples and by thermal analysis. The reaction appeared to obey the law of mass action over a large part of the salt composition range. The equilibrium constant at 900° was 116 and at 950° was 87. The solubility of metal in the salt phase varied with composition in a manner which indicated that this solubility was controlled by the composition of the liquid metal phase. The solubility of metal chloride in the liquid metal decreased from the solubility in calcium metal to a minimum at 10 mole % barium and then increased to the value for barium.

Introduction

The use of metallothermic processes for the preparation of reactive metals has stimulated interest in metal–metal halide equilibria. The phase systems formed by a number of metals with their halide salts have been investigated but only a few reactions of a

metal with another metal halide have been studied. A system of this type can be specified by an equilibrium constant if the salt and metal phases are insoluble in each other, and the activity of each component in its respective phase is known as a function of concentration. However, if the phases are soluble in each other to a significant extent, the solubility must also be known as a function of concentration. The reaction of barium with calcium chloride was investigated at 950 and 900° by determining the composition of the two liquid phases. The Ca–$CaCl_2$ and Ba–$BaCl_2$ binary systems were known to exhibit appreciable mutual solubility of the liquid phases. The Ba–$BaCl_2$–$CaCl_2$ ternary system permitted the determination of the solubility of metal in the liquid salt phase and of salt in the liquid metal at various compositions. The law of mass action was applied to this reaction, using mole fractions of total barium and calcium in each phase to determine whether it would accurately express the completeness of the reaction.

Experimental Methods

Materials.—Anhydrous calcium chloride was prepared by dehydrating J. T. Baker Analyzed hydrated calcium chloride (99.95%) by heating it slowly to 140° for two days and fusing in a platinum boat by heating to 850° for 8–10 hours under pure dry HCl. The maximum calcium oxide content as determined by titration with acid was 0.006%. The m.p. of this material determined by thermal analysis was 770°.

Anhydrous barium chloride was prepared by drying J. T. Baker Analyzed barium chloride (99.85%) at 140°for two days and fusing in a platinum boat at 1000° under pure dry HCl. The product was neutral to phenolphthalein. The m.p. was 962° and the transformation temperature was 926°.

Calcium metal, prepared by alumothermic reduction of calcium oxide, was purified by vacuum distillation. The purified product contained 0.002% Al, 0.005% Fe, 0.005% N_2, 0.003% manganese and 0.03% magnesium as the principal impurities. No analyses for carbon, oxygen or hydrogen were available. The m.p. was 836°.

Barium in the form of cast sticks was purified by double distillation under reduced pressure. The product contained 0.0073% N_2, 0.0035% C, 0.0023% Fe and 0.008% Mn as the principal impurities. The m.p. of this Ba was 729°, which is significantly higher than most reported values. The higher m.p. probably was due to lower oxygen contamination resulting from handling the barium under an argon atmosphere.

Methods.—The tie-lines of the isothermal sections were determined by equilibrating mixtures of either calcium chloride and barium or barium chloride and calcium at 900 or 950° and quenching into cold water. The mixtures were heated in type 304 stainless steel capsules which were 6″ long, $^7/_{16}$″ inside diameter, and had a 0.035″ wall. Stainless steel was quite resistant to attack by these mixtures and no evidence of corrosion was observed. The mixtures after heating were analyzed for iron, chromium and nickel. No increase in the content of these elements was observed. The capsules were charged in a glove box under purified argon and sealed by arc welding in the same glove box. The capsules were held at temperature for 2 hours with intermittent shaking and were held an additional hour to allow separation of the phases before quenching. The attainment of equilibrium under these conditions was verified by reaching the same equilibrium point starting with either barium and calcium chloride or calcium and barium chloride. Holding the samples at temperature for up to 24 hours, or heating to a higher temperature and cooling to the desired temperature, did not change the observed compositions. The capsule was opened in a glove box after slitting the walls with a silicon carbide cutoff wheel. Each phase was sampled and the samples placed in weighing bottles in the glove box.

The salt phase was analyzed by determining the chloride content by precipitating and weighing as AgCl and by titrating the alkalinity to measure the amount of free metal. The barium and calcium contents were calculated from the chloride analysis and free metal content. The high accuracy of the chloride analysis permitted a more accurate determination of the calcium and barium content than was achieved by flame photometry or by separation and gravimetric determination of the calcium and barium. The amount of chloride in the metal phase was determined by precipitating and weighing as silver chloride. The calcium and barium were precipitated together by adding sulfuric acid to an aqueous solution and diluting with absolute methanol to a final concentration of 90% methanol by volume. The calcium and barium contents were calculated from the weight of the total sulfate precipitate and the chloride analysis. Since the reactants were weighed accurately and no material was lost from the sealed capsule, the analytical results were checked by a material balance.

Thermal analyses were made on samples enclosed in type 304 stainless steel capsules 2.5″ long and $^7/_8$″ in diameter with $^3/_{16}$″ diameter thermocouple well. These capsules were filled under argon in a glove box and sealed by arc welding. A differential thermal analysis method was used in which the sample temperature and the difference between the sample and the furnace temperature was recorded with a recording potentiometer. The thermocouples were standardized with a U. S. Bureau of Standards aluminum sample and a coulometer-grade silver sample. At both temperatures the thermocouple agreed within 0.5° with the table for chromel–alumel thermocouples in the N.B.S. Circular 561.

Results and Discussion

The Ba–$BaCl_2$ and Ca–$CaCl_2$ binary systems were checked by thermal analysis and analysis of quenched equilibrium mixtures. The data on the Ba–$BaCl_2$ system agreed very well with the phase system reported by Schäfer and Niklas.[2] The monotectic was at 15 mole % Ba and 890°, the consolute temperature was 1017° and the eutectic temperature 710°. The monotectic and eutectic temperatures of the Ca–$CaCl_2$ system agreed with those reported by Cubicciotti and Thurmond.[3] The monotectic was at 99.5 mole % Ca and 820°, and the eutectic at 2 mole % Ca and 768°. The solubilities of each phase in the other at 900 and 950°, determined by analysis of quenched samples, are reported in Tables I and II. The observed solubility of calcium in calcium chloride was much lower than that reported by Cubicciotti and Thurmond. Water, calcium oxide or other impurities could result in high values for this solubility. Several samples, which were prepared from calcium chloride containing traces of water, gave solubilities as high as 20 mole %. Thermal analysis results agreed with the lower solubility values as the monotectic arrest was observed in a 5 mole % calcium sample. The Ca–$CaCl_2$ system differs from the Ba–$BaCl_2$ system in the lower solubilities, at the monotectic and eutectic temperatures, and in the much smaller increase of the solubility of each phase in the other with increasing temperature.

The phase equilibrium data at 950° are shown in Fig. 1 as an isothermal section of the ternary phase diagram. The diagram was plotted as a square figure to avoid the unequal ordinate dimensions of a truncated triangle. The solubility of metal in the salt phase decreased rapidly as the mole fraction of total barium in the salt decreased to 0.90. This solubility was nearly independent of the salt phase composition over the remainder of the composition

(2) H. Schäfer and A. Niklas, *Angew. Chem.*, **64**, 610 (1952).

(3) D. D. Cubicciotti and C. D. Thurmond, *J. Am. Chem. Soc.*, **71**, 2149 (1949).

TABLE I

EQUILIBRIUM COMPOSITIONS

Temp., °C.	Salt phase N_{Ba}	Salt phase N_{Metal}	Metal phase N_{Ba}	Metal phase N_{MCl_2}	Concn. quotient[a]
950	1.000	0.198[b]	1.000	0.120[b]	...
	0.990	.278[c]	0.856	.082	17
	.983	.145	.588	.027	40.5
	.964	.105	.335	.016	53
	.895	.041	.096	.0071	80
	.885	.042	.070	.0067	102
	.841	.039	.056	.0068	89
	.613	.045	.019	.021	82
	.454	.030	.010	.009	82
	.201	.040	...	.012	...
	0	.042	0	.0156	...
900	1.000	0.160[b]	1.000	0.052	...
	0.920	.0326	0.081	.0056	130
	.905	.0329	.081	.0036	108
	.896	.0314	.063	.0038	128
	.887	.0393	.063	.0042	117
	.884	.0369	.063	.0038	113
	.849	.0276	.044	.0044	122
	.789	.0615	.038	.0048	94.7
	.763	.0358	.027	.0050	116
	0	.0380	0	.0102	...

[a] Concentration quotient = $(N_{Ba}^{Salt})(1 - N_{Ba}^{Meta})/(1 - N_{Ba}^{Salt})(N_{Ba}^{Metal})$. [b] Determined by thermal analysis. [c] Incomplete separation of metal phase.

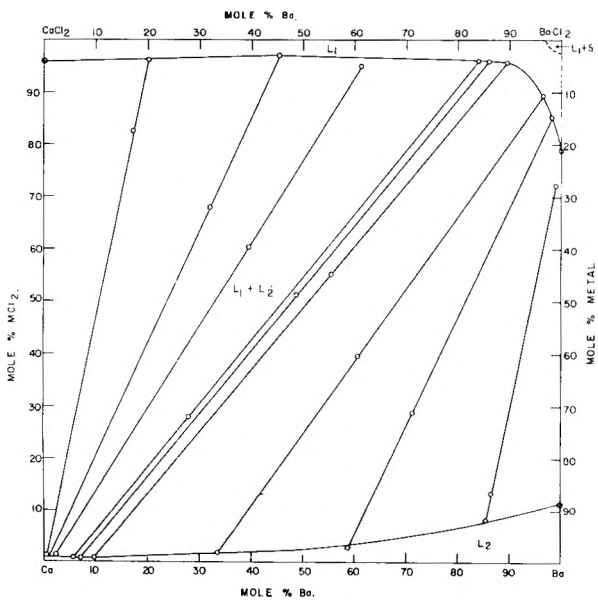

Fig. 1.—Isothermal section of the Ba–$CaCl_2$–$BaCl_2$ system at 950°.

range. The solubility of salt in the metal phase decreased as the metal phase composition varied from pure calcium to 10 mole % barium and increased smoothly with further increase in barium concentration.

In Table I are given the compositions of the equilibrium phases at 950°. Since the metal phase contained dissolved salt and the salt phase contained dissolved metal, the compositions were expressed by the mole fractions of total calcium and total barium and the mole fraction of the metal or metal chloride in solution. Chemical analysis of quenched samples cannot differentiate between calcium in the salt phase which was present as calcium chloride and calcium which was present as dissolved calcium metal. At the present time the nature of these solutions is not well understood and the value of making such a distinction has not been established. The concentration quotients calculated using the mole fraction of total barium and calcium are given in the last column of this table. The values are reasonably constant up to barium contents above 0.9 in the salt phase. At 900° the composition range was restricted by the boundary of a three phase (liquid metal, liquid salt and solid $BaCl_2$) field at high barium contents. This was a result of the monotectic temperature being raised to a maximum of 914° in the ternary system. The concentration quotients did not change with composition over the limited composition range which was studied.

The activity coefficient quotient was assumed to be unity because of the similarity of the component metals and of the component salts. Calcium and barium are reported by Sheldon[4] to form a complete series of solid solutions and should form nearly ideal liquid solutions. The $CaCl_2$–$BaCl_2$ system is reported by Bukhalova[5] to have a eutectic at 595° and 37 mole % barium chloride and a compound, $CaCl_2$–$BaCl_2$, melting at 629°.

The free energy for the reaction

$$Ba_{(L)} + CaCl_{2(L)} \rightleftharpoons BaCl_{2(L)} + Ca_{(L)}$$

was calculated for each temperature, assuming that the concentration quotients were equilibrium constants. At 900°, the equilibrium constant was 116 and the free energy change −11.1 kcal. Using only the data up to 0.90 mole fraction of barium in the salt phase, the averaged equilibrium constant at 950° was 87.0 and the free energy change was −10.8 kcal. The enthalpy of reaction calculated from these two equilibrium constants was −16.5 kcal. These results are compared with values calculated from compiled thermodynamic data in Table II.

TABLE II

THERMODYNAMIC DATA FOR THE REACTION OF BARIUM WITH CALCIUM CHLORIDE

Source	ΔF 900°	ΔF 950°	ΔH
This investigation	−11.1	−10.8	−16.5
Brewer[6]	− 8.4	− 8.2	−16.7
Villa[7]	−13.0	−13.1	
Ostertag[8]		−12.5	(At 1000°)

The uncertainty of the compiled thermodynamic data makes an evaluation of the assumptions used in calculating the free energy from the experimental data impossible.

This reaction has been investigated at 1000° by Ostertag[8] using a similar method of equilibrating the mixtures. The average equilibrium constant was

(4) E. Sheldon, "Exploration of the Phase Diagram of the Calcium–Barium Alloy System," unpublished Ph.D. Thesis, Syracuse University Library, Syracuse, N. Y., 1949.

(5) G. Bukhalova and A. Bergman, *J. Gen. Chem. U.S.S.R.*, **21**, 1723 (1951).

(6) L. Brewer, L. Bromley, P. Gilles and N. Lofgren, "The Thermodynamic Properties of the Halides," L. L. Quill Ed.: "The Chemistry and Metallurgy of Miscellaneous Materials," McGraw–Hill Book Co., Inc., New York, N. Y., 1950, p. 76–192.

(7) H. Villa, *Soc. Chem. Ind.*, **69**, Supp. I, S 9 (1950).

(8) H. Ostertag, *Compt. rend.*, **246**, 1052 (1958).

larger than that obtained by extrapolating our data to 1000°. No explanation of this difference is obvious from the description of the procedure. Since the accuracy of the equilibrium constant depends on the determination of small amounts of barium and calcium in the presence of large amounts of the other, a small systematic error in the analytical method used in either investigation could be responsible.

The solubility of metal in the salt phase shows an interesting dependence on composition. The amount of dissolved metal does not vary in proportion to the amount of each component of the salt, as would be expected if the solubility were governed by the solvent properties of the salt. A solubility curve which agrees quite well with the observed solubilities can be calculated by assuming that the solvent properties of the salt do not change with composition and each metal dissolves independently in the salt. Then $N_{(Ca,°S)} = k_1 \cdot N_{(Ca,M)}$ where $N_{(Ca,°S)}$ is the mole fraction of calcium metal dissolved in the salt phase, $N_{(Ca,M)}$ is the mole fraction of total calcium in the metal phase and k_1 is the mole fraction of calcium dissolved in pure calcium chloride. A similar expression was used to calculate the amount of dissolved barium metal. The calculated solubilities at 950° were somewhat higher than the observed values. Assuming that each metal interacts only with its own ion, a solubility expression $N_{(Ca,°S)} = k_1 \cdot N_{(Ca,M)} \cdot N_{(Ca,S)}$ where $N_{(Ca,S)}$ is the mole fraction of total calcium in the salt, can be formulated. This leads to calculated solubilities which are low and do not agree as well as the first expression. A very close fit can be obtained by postulating that calcium interacts less with barium ions than with calcium ions. However, this introduces an empirical parameter and the significance of the better fit is questionable considering the approximation made by assuming the activity of each metal was directly proportional to the total mole fraction in the metal phase.

THE HEAT OF VAPORIZATION AND SOLUTION OF A BINARY MIXTURE OF FLUOROCARBONS[1]

By E. F. Neilson and David White

Contribution of the Cryogenic Laboratory, Department of Chemistry, The Ohio State University, Columbus, Ohio

Received December 22, 1958

A new method is discussed for the determination of integral heats of solutions for a completely miscible binary system. The method involves the use of a conventional low temperature calorimeter from which a mixture of known composition is completely vaporized. The results for the binary mixture chlorodifluoromethane–dichlorodifluoromethane over a wide composition range are given. The method appears quite satisfactory for systems exhibiting relatively small integral heats of solution.

The heat of vaporization of a pure substance is a well defined quantity. For binary mixtures, this quantity depends on the conditions under which the vaporization takes place, and in fact five such quantities can be defined.[2] Four of these can be related to one another, provided additional thermodynamic information is available.

From the experimental standpoint, the determination of the heat of vaporization of a binary system has required special types of calorimeters,[3] and possibly for this reason very little work has been reported on this subject. A method employing a conventional low temperature calorimeter is reported here. The quantity measured is related to the integral heat of vaporization at constant temperature and composition, and can be used to determine the heat of solution of the binary liquid mixture provided the thermodynamic properties of the pure components are known.

The heat of vaporization and solution over a wide composition range, of a liquid mixture consisting of chlorodifluoromethane (Freon-22) and dichlorodifluoromethane (Freon-12), is reported here. These liquids are completely miscible at the temperature at which the experiments were performed.

(1) This work was supported by the General Electric Company, Schenectady, New York.

(2) V. Fischer, *Ann. Physik.*, [5] **17**, 209 (1933).

(3) L. I. Dana, *Proc. Amer. Acad.*, **60**, 241 (1925).

Theory.—Consider the reversible vaporization of a binary mixture at constant temperature T from the calorimeter shown schematically in Fig. 1. Assume initially the calorimeter is completely filled with 1 mole solution containing n_1 moles of component 1 and n_2 moles of component 2, and then completely vaporized. During the vaporization, the valve at the top of the calorimeter is adjusted so as to maintain constant temperature during the run. The material escaping the calorimeter (outside the adiabatic shield) is continuously removed to the gas storage system. Let P_i be the initial pressure in the calorimeter, and P_f the final pressure, when the last drop of liquid is vaporized.

For an infinitesimal amount of material vaporized from the calorimeter we can write

$$dE + P\,dV = DQ$$

where DQ is the amount of heat added to the calorimeter

$$\text{or } dH = DQ + V\,dp$$

where V is the volume of the calorimeter, equal to the initial molar volume of the liquid solution V_{ls}. Integrating the above expression between the initial and final state ($P_i \rightarrow P_f$) we have

$$H_{gs}(T, P_k, n_{k(1)}, n_{k(2)}) - H_{ls}(T, P_i, n_1, n_2) = Q + V_{ls}(P_f - P_i)$$

where Q is the amount of heat added to the calorim-

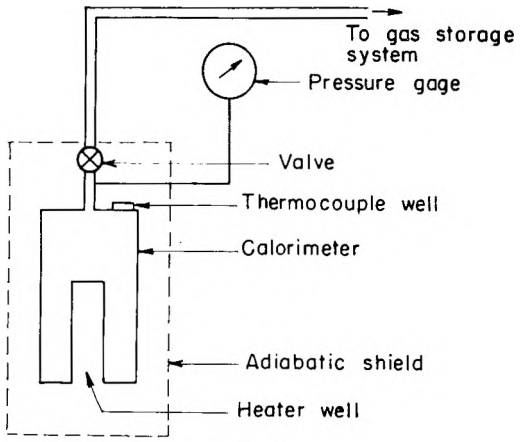

Fig. 1.

eter to vaporize *completely* the liquid solution; $H_{ls}(T, P_i, n_1, n_2)$, the heat content of the liquid solution at temperature T, pressure P_i and composition n_1, n_2. Since the composition of the gas changes continuously as the vaporization takes place $H_{gs}(T, P_k, n_{k(1)}, n_{k(2)})$ represents the heat content of a large number of infinitesimal amounts of gas, making up 1 mole, at temperature T but at different pressures P_k and compositions, $n_{k(1)}$, $n_{k(2)}$; k refers to the increment of material vaporized from the calorimeter.

To achieve a real final state for the gas, let us mix these infinitesimal portions of gas removed from the calorimeter to some common pressure $\tilde{P}$. The final composition of the gas will be n_1, n_2, the initial composition of the liquid solution. If the liquid solution is assumed incompressible, then

$$H_{gs}(T, \tilde{P}, n_1, n_2) - H_{ls}(T, \tilde{P}, n_1, n_2) = Q + V_{ls}(P_f - P_i) - \left(V_{ls} - T\frac{\partial V_{ls}}{\partial T}\right)(\tilde{P} - P_i) + \Delta H'_{mix} = \Delta H_{vs} \quad (1)$$

where $\Delta H'_{mix}$ is the change in enthalpy of mixing these infinitesimal portions of gas at different pressures and composition, and ΔH_{vs} can be called the heat of vaporization of the binary mixture at temperature T, and pressure $\tilde{P}$. If $\tilde{P}$ is defined as

$$\tilde{P} = \frac{\int_0^n P\, dn}{n_1 + n_2}$$

where n is the total no. of moles in the calorimeter at any given instant, then to a good approximation, the only important contributions to $\Delta H'_{mix}$ arise from the non-ideality of the gas. If the equation of state of the pure gases or gaseous mixtures can be represented by the equation

$$PV = n(RT + BP)$$

then as an upper limit for $\Delta H'_{mix}$ we can write

$$\Delta H'_{mix} < -\tilde{P}\, n_1 n_2 \left(1 - T\frac{d}{dT}\right)(B_{11} - 2B_{12} + B_{22})$$

where the right-hand side corresponds to the heat of mixing of n_1 moles of pure component 1 and n_2 moles of pure component 2. B_{11} and B_{22} are the second virial coefficients for pure component 1 and 2, respectively, and B_{12}, the virial coefficient for the interaction of components 1 and 2. It is evident from equation 1 that if

$$B_{12} = \frac{B_{11} + B_{22}}{2} \quad (2)$$

(which is the case for similar gases) and $(\tilde{P} - P_i)$, $(P_f - P_i)$ are small, to a good approximation, the heat of vaporization of a binary liquid solution at constant temperature, pressure and composition is simply Q, the heat required to vaporize completely the solution.

In order to obtain the integral heat of solution at temperature T, pressure $\tilde{P}$ and composition n_1, n_2 from the heat of vaporization for the binary mixture, it is necessary to combine this quantity with the heats of vaporization of the pure components. If ΔH_{v1} is the heat of vaporization of pure component 1 at temperature T and equilibrium pressure P_1, and ΔH_{v2} the same for pure component 2 at temperature T and equilibrium pressure P_2, then it can be shown easily that the integral heat of solution at temperature T, pressure $\tilde{P}$ and composition n_1, n_2 is

$$\Delta H_s(T, \tilde{P}, n_1, n_2) = \{n_1\Delta H_{v1} + n_2\Delta H_{v2} - Q\} + \left\{n_1\left(B_{11} - T\frac{dB_{11}}{dT}\right)(\tilde{P} - P_1) + n_2\left(B_{22} - T\frac{dB_{22}}{dT}\right)(\tilde{P} - P_2) - \tilde{P}n_1n_2\left(1 - T\frac{d}{dT}\right)(B_{11} - 2B_{12} + B_{22})\right\} - \left\{n_1\left(V_{L1} - T\frac{\partial V_{L1}}{\partial T}\right)(\tilde{P} - P_1) + n_2\left(V_{L2} - T\frac{\partial V_{L2}}{\partial T}\right)(\tilde{P} - P_2) - \left(V_{LS} - T\frac{\partial V_{LS}}{\partial T}\right)(\tilde{P} - P_i)\right\} - \Delta H'_{mix} - V_{LS}(P_f - P_i) \quad (3)$$

provided the liquids are incompressible. V_{L1} and V_{L2} are the molar volumes of pure liquids 1 and 2.

Again if eq. 2 is valid and $(\tilde{P} - P_i)$, $(\tilde{P} - P_1)$, $(\tilde{P} - P_2)$ and $(P_f - P_i)$ are small, to a good approximation

$$\Delta H_s(T, \tilde{P}, n_1, n_2) = \{n_1\Delta H_{v1} + n_2\Delta H_{v2} - Q\} + \left\{n_1\left(B_{11} - T\frac{dB_{11}}{dT}\right)(\tilde{P} - P_1) + n_2\left(B_{22} - T\frac{dB_{22}}{dT}\right)(\tilde{P} - P_2)\right\} \quad (4)$$

Apparatus and Materials

The calorimeter employed in these experiments was previously described by Rifkin, Kerr and Johnston.[4] The temperature of the calorimeter was measured by means of a calibrated[5] copper–constantan thermocouple located at the top of the calorimeter. During the vaporization experiments the temperature was maintained constant to ±0.06°. Because of the location of the thermocouple, the temperature of the gas flowing out of the calorimeter was in effect maintained constant. All the experiments were performed at 222.00°K.

The fluorocarbons, Freon-12 and Freon-22, were supplied through the courtesy of the General Electric Research Laboratories at Schenectady, New York. They were high purity samples from General Chemical Division of Allied Chemical and Dye Corporation at Morristown, New York. From a calorimetric determination of the melting points of these fluorocarbons, the purity of both materials was estimated to be at least 99.98 mole %.

Experimental

The experimental results are shown in Table I. Approximately 0.6 mole was vaporized from the calorimeter in each run.

The heats of vaporization of the pure components

(4) E. B. Rifkin, E. C. Kerr and H. L. Johnston, *J. Am. Chem. Soc.*, **75**, 785 (1953).

(5) T. Rubin, H. L. Johnston and H. Altman, *ibid.*, **73**, 3401 (1951).

TABLE I

HEAT OF VAPORIZATION AND SOLUTION OF A BINARY MIXTURE OF FREON 12 AND FREON 22 AT 222.00°K.

Composition, mole % F-22	$\bar{P}$, atm.	ΔH_{vs}, cal. mole^{-1}	ΔH_s, cal. mole^{-1}
100.00	0.602	4934.3	0.0
	0.602	4937.1	
84.03	0.603	4873.4	76.2
	0.603	4870.3	
71.08	0.478	4865.4	103.1
	0.478	4860.9	
59.98	0.471	4858.2	110.3
	0.471	4863.6	
42.93	0.454	4867.0	117.6
	0.454	4864.4	
31.69	0.438	4902.5	98.3
	0.438	4902.7	
	0.438	4901.7	
19.95	0.418	4927.5	84.7
	0.418	4923.8	
10.00	0.394	4968.1	51.9
	0.394	4968.4	
0.00	0.363	5029.7	0.0
	0.363	5031.6	

are in good agreement with the results of previous investigations.[5,6]

A plot of the integral heat of solution as a function of composition is shown in Fig. 2.

The heat of vaporization at any given composition, shown in Table I, was measured at least twice to determine the effect of variation of rate of energy input on the reproducibility. For finite flow rates one cannot expect the vaporization to be truly reversible. It is evident from the data that the error arising from such an effect is small. It is estimated that the uncertainty in the heat of vaporization is ±2–3 cal., the largest error arising from the heat leak correction, due to a difference in temperature between the calorimeter and its surroundings during vaporization. The experiment can no doubt be improved by the use of an automatic controlled adiabatic calorimeter.

The integral heats of solution given in Table I were computed from the average values of the heats of vaporization. The uncertainty in the heat of solution includes not only the uncertainty in the heats of vaporization, but also the uncertainty in the non-ideality of the gaseous pure components and solution. The total uncertainty of the heat of solution is estimated at ±3–4 cal. This is indicated in Fig. 2.

It should be pointed out that the heats of solution given in Table I are not at a common pressure. Since the pressure ($\bar{P}$) is low, correction of the data to a common pressure results in changes of only a few tenths of a calorie. This is considerably smaller than the over-all uncertainty in the heat of solution given above, and has therefore been neglected.

(6) E. F. Neilson and David White, *ibid.*, **79**, 5618 (1957).

(7) Thermodynamic Properties of Freon-12, E. I. du Pont de Nemours and Company, Wilmington 98, Delaware, 1956.

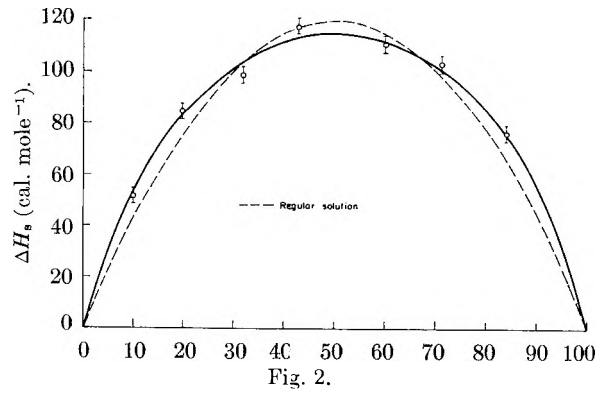

Fig. 2.

Discussion of Results

A preliminary investigation[8] of the phase equilibria in the binary system Freon-12–Freon-22 indicates that it exhibits positive deviations from ideality. Furthermore, the results indicate the existence of a minimum boiling azeotrope. This is in accord with the above heats of solution. Since the heat of solution is positive, positive deviations from Raoult's law are to be expected. The magnitude of the heat of solution can give rise to an azeotrope.

For a regular solution,[9] the integral heat of solution is given by the relationship

$$\Delta H_s = uN_1N_2$$

where u is a constant and N_1, N_2 the mole fraction of component 1 and 2, respectively. In Fig. 2, the continuous curve is the one which best fits the data. The broken curve corresponds to a regular solution with a value of u = 480 cal. It is evident from Fig. 2 that the behavior of the solution only approximates that of a regular solution. This is to be expected since the molar volumes of the pure components are quite different. The molar volumes of Freon-12 and Freon-22 at 222.00°K. are 78.22 and 60.10 cc., respectively. The change of volume on mixing, however, is small. At 222.00°K. for a solution containing 31.69 mole % Freon-22, the change in volume on mixing is 0.502 cc. It may therefore still be possible, to a good approximation, to treat the binary system Freon-12–Freon-22 as a regular solution. Unfortunately a precise investigation of the phase equilibria with which to make a comparison is not available, but is presently under way in this Laboratory.

Acknowledgment.—The authors wish to express their thanks to J. W. Farnham for his assistance in carrying out some of the experiments.

(8) T. E. Etherington, General Electric Research Laboratories, Schenectady, New York.

(9) E. A. Guggenheim, "Mixtures," Oxford University Press, 1952, p. 80.

HIGH ENERGY γ-IRRADIATION OF VINYL MONOMERS. I. RADIATION POLYMERIZATION OF ACRYLONITRILE[1]

BY JETT C. ARTHUR, JR., ROBERT J. DEMINT AND ROBERT A. PITTMAN

Contribution from Southern Regional Research Laboratory, New Orleans, Louisiana[2]

Received December 27, 1958

Acrylonitrile monomer, in the presence of water and N,N-dimethylformamide, was exposed to high energy γ-radiation from cobalt-60 and high dose rates ranging from 1.21 to 5.44 × 10^{20} e.v./l./min. Increasing radiation dosage, ranging to 2.3 × 10^{24} e.v./l. increased the intrinsic viscosities of the polymers rapidly and then, at higher dosages, decreased their intrinsic viscosities exponentially. After an inhibition period, which was shorter the higher the dose rate, the rate of polymerization of acrylonitrile monomer was proportional to the dose rate. In contrast to polymer formation in the presence of water, the polymers formed in N,N-dimethylformamide were completely soluble in the solvent. This may indicate that polymers formed in the presence of water have a higher molecular weight and are more highly crosslinked than those formed in N,N-dimethylformamide.

Polymerization of acrylonitrile, dissolved in water, induced by the action of radium γ-rays and 50 and 220 kilovolt X-rays, has been reported by Collinson and Dainton.[3] The kinetics of the polymerization were studied over the concentration range of 0.036 to 0.75 *M* of acrylonitrile. Two radium sources of 400 and 232.5 millicurie strength, screened by the equivalent of 0.5 mm. of platinum, were used. At the radiation intensities available to these investigators, it was found that the kinetics of the polymerization reactions were more sensitive to changing modifications of radiation intensity, reactant concentration and radical distribution than are the kinetics of reactions which are complete in a single stage.

The polymerization of acrylonitrile, induced by nuclear radiation, at much higher radiation intensities, energy of γ-rays and concentration of acrylonitrile would be of practical interest in the possible preparation of graft polymers with cotton cellulose, to yield fibers having new and unique properties. Exploratory work of this possibility has indicated that graft polymers of acrylonitrile and cotton cellulose may be formed at low concentrations of acrylonitrile.[4]

The effects of radiation dose rate and dosage of cobalt-60 γ-rays on the polymerization of acrylonitrile monomer in the presence of water are given in this report.

Experimental

Radiation Source.—In June 1957, 994 curies of cobalt-60 were obtained from the Oak Ridge National Laboratory in the form of 57 metallic pieces of cobalt about 1 cm. in diameter and 1 mm. thick, weighing about 40 g. The cobalt is contained in the wall of a hollow brass cylinder at positions calculated to give a uniform radiation field along the center axis of the cylinder. The radiation assembly is similar to that of Ghormley and Hochanadel.[6]

Ferrous–ferric dosimetry in 0.5 *N* H_2SO_4[6] indicated dose rates, depending on the relative position of the source and the sample to be irradiated, ranging up to about 5.5 × 10^{20} e.v./l./min.

Polymer Formation.—Samples of acrylonitrile monomer were placed in glass vials which were sealed and then placed into a desired position relative to the radiation source at room temperature, 25–30°. After a designated time interval, at ambient conditions, the irradiated samples were removed, and the polymers formed were isolated. The polymers formed in the aqueous solutions precipitated, were filtered onto tared crucibles, thoroughly washed with water to remove monomer, air dried at 50°, and weighed. Polymers formed in N,N-dimethylformamide were precipitated by the addition of water and isolated, as described. The percentage of conversion of monomer to polymer was calculated by dividing the weight of isolated polymer by the weight of monomer exposed to the radiation.[7]

Methods. Intrinsic Viscosity.—The viscosities of the polymers in N,N-dimethylformamide solvent, the solutions being clarified by centrifuging at 25,000 times gravity for 15 min., were determined at 25° using Ostwald viscosimeters. The reduced viscosities were plotted against concentration (g./dl.) and extrapolated to zero concentration to obtain the intrinsic viscosities (dl./g.). The slopes of the linear plots were measured, as an indication of solvent–polymer interaction.[8]

Solubles.—The polymeric solubles in N,N-dimethylformamide were determined by suspending a weighed quantity of polymer in the solvent (about 0.5 g. in 100 ml.). After a period of equilibration at 25°, followed by centrifuging at 25,000 times gravity, an aliquot of the solution was evaporated to remove the solvent, and the fraction of polymer dissolved was weighed.

Light Scattering Molecular Weight.—Weight-average molecular weights were determined using the Brice–Phoenix light scattering photometer and differential refractometer.[9] Readings were taken at 436 mμ from 90° measurements, with no corrections, on triplicates at four concentrations of polymer dissolved in N,N-dimethylformamide ranging from about 0.1 to 0.9 g./100 ml.[10] The solutions were clarified by centrifuging at 25,000 times gravity for 15 min.

The refractive index increment for the system was determined to be 0.0826.

Materials.—Acrylonitrile monomer and other chemicals used in these studies were reagent grade materials. The acrylonitrile monomer was saturated with water. The solubility of acrylonitrile in water at 25° is 7.4%; the solubility of water in acrylonitrile at 25° is 3.4%.[11]

(1) Presented at the 14th Southwest Regional Meeting of the American Chemical Society, San Antonio, Texas, December 4–6, 1958.

(2) One of the laboratories of the Southern Utilization Research and Development Division, Agricultural Research Service, United States Department of Agriculture.

(3) E. Collinson and F. S. Dainton, *Disc. Faraday Soc.*, **12**, 212 (1952).

(4) S. A. Goldblith, *et al.*, unpublished data. Work being done at the Massachusetts Institute of Technology under contract with the Agricultural Research Service, United States Department of Agriculture.

(5) J. A. Ghormley and C. J. Hochanadel, *Rev. Sci. Instr.*, **22**, 473 (1951).

(6) R. H. Schuler and A. O. Allen, *J. Chem. Phys.*, **24**, 56 (1956).

(7) D. J. Angier and W. F. Watson, *J. Polymer Sci.*, **20**, 235 (1956).

(8) H. Mark and A. V. Tobolsky, "Physical Chemistry of High Polymeric Systems," (High Polymers Vol. II) Interscience Publishers, Inc., New York, N. Y., 1950, pp. 287–304.

(9) Trade names are given as part of the exact experimental conditions and not as an endorsement of the products over those of other manufacturers.

(10) B. A. Brice, M. Halwer and R. Speiser, *J. Opt. Soc. Am.*, **40**, 768 (1950).

(11) H. S. Davis, in "Encyclopedia of Chemical Technology," eds. R. E. Kirk and D. F. Othmer, The Interscience Encyclopedia, Inc., New York, N. Y., 1947, Vol. I, pp. 184–189.

Experimental Results

The effects of radiation dosage and monomer to water ratio on polymerization, solubles and intrinsic viscosity of acrylonitrile are shown in Table I. It was observed that: (1) increasing dosage increased the percentage of conversion of monomer to polyacrylonitrile; (2) increasing dosage increased the intrinsic viscosity of the polyacrylonitrile; except at the higher dosages, after an increase, a decrease in intrinsic viscosity was noted, (3) increasing dosage increased the slope of the reduced viscosity *versus* concentration plots, agreeing fairly well with Huggins relation,[12] except at the higher dosages, after an increase, a decrease in slope was noted; (4) the lower the ratio of acrylonitrile to water, the more rapid the initial conversion of monomer to polymer; (5) the higher the ratio of acrylonitrile to water, the greater was the decrease in polymeric solubles at the higher dosages.

TABLE I

EFFECT OF RADIATION DOSAGE AND MONOMER TO WATER RATIO ON POLYMERIZATION, SOLUBILITY AND INTRINSIC VISCOSITY OF POLYACRYLONITRILE DOSE RATE = 5.44×10^{20} E.V./L./MIN.

Dosage $\times 10^{21}$, e.v./l.[a]	Conversion, %	Solubles in DMF,[b] %	Intrinsic viscosity in DMF,[b] dl./g.	Slope K[c] (dl./g.)^2
Acrylonitrile:water, 1:25				
5.2	2	100	1.34	0.35
10	10	100	3.44	3.13
16	40	100	3.09	4.88
26	71	100	3.18	4.70
39	82	100	3.26	4.78
52	85	100	2.60	..
260	96	..	2.43	..
590	96	..	..	..
Acrylonitrile:water, 1:12				
5.2	1	100	1.72	0.46
10	4	100	2.20	1.33
16	7	100	3.65	5.33
26	42	100	5.42	9.79
39	84	100	5.38	13.3
52	93	100	5.81	22.0
250	95	..	2.35	1.94
540	98	..	2.50	1.00
Acrylonitrile:water, 1:4				
5.2	1	100	2.17	0.83
10	3	100	2.55	1.62
16	11	100	4.75	9.20
26	46	41	12.8	..
39	92	41	6.00	4.44
52	93	36	5.85	3.02
240	96	45	3.90	..
500	97	39	2.60	..
Acrylonitrile:water, 29:1				
33	13	100	7.00	..
78	95	16	..	..
98	95	..	..	..
130	95	14	..	..
150	96	15	..	..
250	96	20	2.64	..
620	94	18	0.80	..
2300	88	10	..	..

[a] E.v./l. = electron volts per liter. [b] DMF = N,N-dimethylformamide. [c] K = slope of reduced viscosity *vs.* concentration plots.

(12) P. J. Flory, "Principles of Polymer Chemistry," Cornell Univ. Press, Ithaca, New York, N. Y., 1953, p. 310.

The effect of dose rate and dosage on the rate of polymerization of acrylonitrile monomer is shown in Table II. After an inhibition period, which was shorter the higher the dose rate, the rate of polymerization of acrylonitrile monomer was proportional to the dose rate. The inhibition period may be due to the presence of oxygen or other impurities or may be due to the initial formation of water-soluble, shorter-chained polymers. Collinson and Dainton,[3] working with solutions of acrylonitrile, also found that the rate of polymerization was dependent on radiation dose rate and that an initial inhibition period was observed even with highly purified materials. At high dosages, a decrease in percentage of conversion of monomer to polyacrylonitrile was observed. This decrease may be due to a partial depolymerization of the polyacrylonitrile and to formation of water-soluble fractions.

TABLE II

EFFECT OF DOSE RATE AND DOSAGE ON POLYMERIZATION OF ACRYLONITRILE MONOMER

	Dose rate, 1.21×10^{20}, e.v./l./min.		Dose rate, 2.33×10^{20}, e.v./l./min.		Dose rate, 5.44×10^{20}, e.v./l./min.	
Time, hr.	Dosage, $\times 10^{21}$, e.v./l.	Conversion, %	Dosage, $\times 10^{21}$, e.v./l.	Conversion, %	Dosage, $\times 10^{21}$, e.v./l.	Conversion, %
1	..	..	..	..	33	8
2	..	..	..	..	65	94
2.4	..	..	34	4	79	95
3	22	8	62	28	96	95
4	29	21	56	70	131	95
7.6	55	80	106	88	246	96
19.4	141	89	271	90	634	94
69.5	504	84	972	86	2270	88

Light scattering molecular weights of the polymers were proportional to radiation dosage, ranging from about 400,000 for polymers produced at dosages of 26×10^{21} e.v./l. to about 2,000,000 for polymers produced at dosages of 500×10^{21} e.v./l.

TABLE III

POLYMERIZATION OF ACRYLONITRILE IN N,N-DIMETHYLFORMAMIDE SOLVENT

(Acrylonitrile:DMF, 1:9; dose rate = 5.44×10^{20} e.v./l./min.)

Dosage, $\times 10^{21}$, e.v./l.	Conversion, %	Solubility in DMF,[a] %	Reduced viscosity, dl./g.	Color in soln.
10	3.6	100	0.14	Very light yellow
26	11	100	.27	Light yellow
52	22	100	.34	Yellow
210	66	100	.45	Amber
1400	100	100	.47	Dark amber

[a] DMF = N,N-dimethylformamide.

The polymerization of acrylonitrile in N,N-dimethylformamide solvent is shown in Table III. The initial conversion of monomer to polymer was proportional to the radiation dosage. The reduced viscosity indicated polymer formation. In contrast to polymer formation in the presence of water at the higher acrylonitrile–water ratios, the polymers

formed in N,N-dimethylformamide were completely soluble in the solvent. This may indicate that polymers formed in the presence of water have a higher molecular weight and are more highly crosslinked.

THE POTENTIAL OF THE SEMICONDUCTOR–SOLUTION INTERFACE IN THE ABSENCE OF NET CURRENT FLOW: GERMANIUM

BY B. LOVREČEK[1] AND J. O'M. BOCKRIS

John Harrison Laboratory of Chemistry, University of Pennsylvania, Philadelphia 4, Pennsylvania

Received December 29, 1958

The potential at the interface between n- and p-type Ge electrodes of crystal orientations 110 and 111 has been measured in highly pure aqueous solutions of GeO_2, of *p*H 0–14. The potential was affected by stirring and by impurities in the low *p*H range. Over certain ranges of *p*H, $\partial e/\partial p\mathrm{H} \simeq 2.303RT/F$. GeO_2 and H_2 concentrations have no definite effect. O_2 tends to increase the range in which $\partial e/\partial pH = 2.303RT/F$. No essential difference was observed between n- and p-type samples, or those of different crystal orientation. Calculation of the mixed potential indicates only a small deviation from a thermodynamically reversible potential. Calculation of potential–*p*H relations for various reactions involving Ge suggests a significant error in the previously accepted values. The observed results correspond to those of the reaction $Ge + H_2O \rightleftharpoons GeO + 2H^+ + 2e_0^-$, the germanous oxide appearing in two forms, depending on *p*H and age of the electrode. The recorded phenomena are consistent with this mechanism.

Introduction

The properties of the semiconductor–solution interface (sc.–s.i.) merits an increasing interest. Thus, it has numerous technological implications: *e.g.*, in etching, electropolishing, electrodeposition of semiconductors, and the preparation of p-n junctions by deposition of metals such as In onto the semiconductor. The fundamental electrochemical processes which underly these technological possibilities are as yet almost completely unexplored.[2–5]

Fundamental investigations of the sc.–s.i. are needed, not only because of their usefulness to technology, but also because the electrode kinetics of processes at the sc.–s.i. involve aspects novel to this field, *e.g.*, the presence of two types of electron flow. Moreover, electrochemical measurements offer certain advantages in elucidation of the structure of the surface region in semiconductors compared with measurements made for this purpose with the semiconductor in contact with a gas (g). Thus: (i) The surface of sc.'s cannot be cleaned by methods successfully used for the preparation of the surfaces of metals; but they may be electrodissolved into highly decontaminated solutions. In general, "preparation" of a "clean" surface for a sc. is more easily achieved in solution than in contact with the gas phase. (ii) A larger range of potentials (and their free energy levels) can be achieved for the sc.–s.i. than for the sc.–g. interface. Hence, the possibility of determining the energy of surface states is increased. (iii) By controlled specific adsorption of ions from solution, a greater variation in the potential distribution at the sc.–s.i. is possible than at the sc.–g. interface.

The study of the kinetics and mechanism of processes at the sc.–s.i. interface has as its object the elucidation of the path and rate-determining step of the electrode reaction. However, before a detailed study of this may be made, it is necessary to ascertain what is the over-all reaction at the sc.–s.i., in a given system, *i.e.*, the process given by the thermodynamics of the electrode-solution interface at equilibrium. A study of this subject for the interface Ge(n- and p-type, single crystals)–aqueous solution is herewith recorded. No previous experimental study of the thermodynamics of this type of system has been published (but *cf.* Nichols and Cooper[6]).

Experimental

(i) **General.**—Preliminary work carried out with solutions of Analytical Purity showed a considerable instability of potential. Decontamination of the solution from parasitic oxidation–reduction systems showed not only an increase in stability, but also a substantial change in values of $\partial e/\partial p\mathrm{H}$ in acid solutions. Consequently, precautions were taken throughout the work to achieve relatively clean conditions of solution and electrode surface. The cell and connecting glass parts were made of As-free Pyrex. Only glass was used in the cell and purification trains except for a very short connection of gas cylinder to the train by means of Tygon. Purified helium could be introduced into all parts of the apparatus and was used to eliminate oxygen therefrom. It also was used to impel solutions from one part of the system to another.

(ii) **Cell and Temperature Conditions.**—The cell contained arrangements whereby four electrodes and a glass reference electrode could be introduced into the solution. The cell, together with certain parts of the purification trains, were maintained in a darkened air thermostat maintained at 25±1°.

(iii) **Electrodes.**—The electrodes were single crystals supplied by the Philco Corporation in the form of discs, diameter c. 1 cm. and thickness 0.5 mm. They were defined by the designation "n" or "p"; the specific resistivity; and the crystal face.

Because it was desired to carry out the measurements on a specific crystal face, the electrode could not be heated into the form of a sphere.[7] Sealing into glass is also difficult because of the danger of deformation and introduction of unintentional impurities.

The preparation of the electrodes was carried out by: (i) washing in cellosolve; (ii) washing in distilled water; (iii) treatment for one minute in C.P.-4; (iv) washing in distilled water; (v) soldering electrical connections of tinned copper wire onto back of electrode; (vi) repetition of washing in cellosolve and distilled water; (vii) covering solder and

(1) On leave of absence from the Chemistry Department of the Technical Faculty, University of Zagreb, Zagreb, Yugoslavia.

(2) W. H. Brattain and C. G. B. Garrett, *Phys. Rev.*, **94**, 750 (1954); *Bell Syst. Techn. J.*, **34**, 129 (1955).

(3) D. R. Turner, *J. Electrochem. Soc.*, **103**, 252 (1956).

(4) H. Gerischer and F. Beck, *Z. physik. Chem. N. F.*, **13**, 389 (1957).

(5) M. Green, Chapter V in "Modern Aspects of Electrochemistry," II, J. O'M. Bockris, Ed., Butterworth's, London, 1959.

(6) M. L. Nichols and S. R. Cooper, *Ind. Eng. Chem., Anal. Ed.*, **7**, 350 (1935).

(7) J. O'M. Bockris, B. E. Conway and W. Mehl, *J. Sci. Instr.*, **33**, 400 (1956).

surrounding area with polystyrene coating; (viii) electrodes were then pulled against the ground end of a glass tube by means of the connecting wire. The lower part of this tube then was filled with molten paraffin.[8]

(iv) **Purification of Materials.**—H_2SO_4 (A. R.) was distilled in a low pressure of purified He. K_2SO_4 (A. R.) was twice recrystallized in an atmosphere of purified He. KOH (A. R.) was dissolved in conductance water and subject to electrolysis, using pure Hg as a cathode. The K amalgam formed was transferred directly and without contact with air to a decomposition vessel. Herein, it was allowed to dissolve to form pure KOH. GeO_2 was made up by dissolving the spectroscopically pure material (Vieille Montagne) in conductance water. Helium was purified by passage through Hopcalite, soda lime, active Cu powder at 200°,[9] SiO_2 gel (2 tubes), three traps maintained at liquid N_2 temperatures, two of which contained activated charcoal; and finally through a fritted disc in conductance water.

(v) **Electrical.**—A conventional tube potentiometer was used for the potential measurements and a second for the *p*H measurements. A saturated calomel electrode was used as a reference (potentials recorded in this paper refer to the standard H_2 scale).

(vi) **Procedure.**—After cleaning in chromic–sulfuric acid and washing with distilled water, the cell was placed in position and connected by means of glass bridges to the other parts of the apparatus. The glass electrode was introduced into one of the electrode holders in the main compartment of the cell; others were closed by means of ground glass plugs. The cell was left in contact with distilled water overnight. The pre-electrolysis compartment (Fig. 1) was filled with 0.1 *N* K_2SO_4 solution by means of He pressure, and pre-electrolysis was commenced. (The cathode for the pre-electrolysis was a Ge plate.) Pre-electrolysis was carried out for more than 12 hours with c.d. of 10 ma. cm.$^{-2}$, the atmosphere being purified He. The cell was emptied by means of purified He and Ge electrodes introduced. The cell was washed with conductance water and the solution introduced, the electrodes washed, the solution rejected, further solution introduced, and the GeO_2 solution added to the required concentration.

The potential of the Ge electrode was followed by readings every few minutes until constant (1–2 mv. in 10 minutes). *p*H was changed by addition of H_2SO_4 (from the redistilled H_2SO_4), or by purified KOH, the amount needed being read directly from the glass electrode.

Results

(i) **Nature of Potential Measured.**—Introduction of stirring with He causes the electrode potential under zero net current flow (e) to become more positive. Passage of current densities of the order of 10 microamp. caused changes of electrode potential of the order of about 0.1 volt. The potential was sluggish in returning to the equilibrium value after polarization. Hence, the interface under examination is likely to represent a mixed potential.[10]

(ii) **Evaluation of Results, Accuracy.**—The evaluation of the potential of Ge electrode on the standard H_2 scale was carried out as follows. Let E be the measured potential between the Ge and calomel electrode. Then

$$e_{Ge} - e_{sat\ cal} = E - \Sigma \text{ l.j.p.}$$

the liquid junction potentials being those across the tap between the main compartment and that of the reference electrode, and between the calomel electrode and the electrolyte in the reference electrode compartment (see Fig. 2). These were calculated

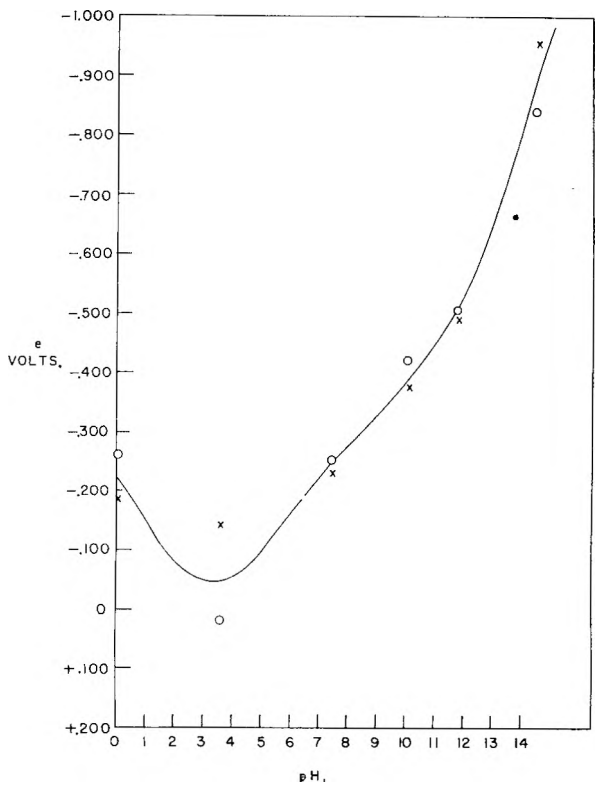

Fig. 1.—Approximate experimental e–*p*H relation for solution of 0.02 mole l.$^{-1}$ GeO_2, produced without special purification, but deoxygenated with He: (x = n-type electrodes, 110 face, resistivity, 2.4–2.5 ohms cm.; ○ = p-type electrode, 110 face, resistivity 1.8–1.9 ohms cm.).

TABLE I

THERMODYNAMIC VALUES USED IN CALCULATION OF EQUILIBRIA INVOLVING GE

	$\Delta H°$, kcal. mole^{-1}	$\Delta F°$, kcal. mole^{-1}	$S°$, cal. mole^{-1} deg.$^{-1}$
GeO_2 soluble, hexag.	−128.5[a]	−114.2	12[b]
GeO_2 insoluble, tetr.		−118.29[c]	
GeO black, solid	− 59.5[c]	− 52.5	11.5[c]
GeO brown, hydrous		− 52.1[f]	
GeO yellow, hydrous		− 44.9[f]	
Ge^{2+}		10.67[g]	
H_2GeO_3, aq.		−169.02[h]	
$HGeO_3^-$, aq.		−157.41[i]	
GeO_3^{2-}, aq.		−140.06[i]	
Ge solid	0.0	0.0	10.14[b]
O_2 gascous	0.0	0.0	49.003[b]
H_2O liquid	68.317[b]	− 56.690[b]	16.716[b]

[a] Jolly, Jolly and Latimer (ref. 14, 20). [b] Latimer (ref. 17). [c] Using Muller's value for solubility of GeO_2 tetr. in water, 0.0045 g./l. (ref. 23). [d] Using Jolly's value (ref. 14) for heat of reaction $GeO(s) + 1/2O_2 = GeO_2$, $\Delta H = -69$ kcal. mole^{-1}. [e] Jolly (ref. 14). [f] Using the potential measurements of GeO/GeO_2 electrodes by Jolly (ref. 14) or Jolly and Latimer (ref. 21). [g] Using the solubility measurement of GeO by Jolly (ref. 14). [h] Using the solubility measurement of GeO_2 sol. in water, 4.47 g./l. by Pugh (ref. 12). [i] Using dissociation constants for H_2GeO_3 determined by Pugh (ref. 24).

(8) It is important that the insulating paraffin covers all parts of the back of the electrode which could be in contact with air. Thus, if this is not done, minute current paths develop between the front and back of the electrode. These currents cause the sc. to function as a mixed electrode (with respect to the soldered Cu wire, and oxygenated solution) and its potential becomes unstable (this mechanism was established by observing the effect of introducing controlled leaks). The sensitivity of the electrode to these leaks suggests a relatively low exchange c.d. for the reaction at the sc.–s.i. To allow for the possibility of solution contact with the paraffin, this was boiled in 1 *N* KOH, water, 1 *N* H_2SO_4 and water for several days before use.

(9) F. R. Meyer and G. Ronge, *Z. angew. Chem.*, **52**, 637 (1939).

(10) J. O'M. Bockris and J. F. Herringshow, *Disc. Faraday Soc.*, **43**, No. 1. 328 (1947).

TABLE II

POTENTIALS CALCULATED USING THE THERMODYNAMIC DATA FROM TABLE I

1.	$Ge \rightleftarrows Ge^{2+} + 2e_0^-$	a.[a] $e = 0.231 + 0.0295 \log (Ge^{2+})$
		b. $e = 0\ 097 - 0.0591\ pH$
2.	$Ge + 3H_2O \rightleftarrows H_2GeO_3 + 4H^+ + 4e_0^-$	$e = 0.011 - 0.0591\ pH + 0.0148 \log (H_2GeO_3)$
3.	$Ge + 3H_2O \rightleftarrows HGeO_3^- + 5H^+ + 4e_0^-$	$e = 0.137 - 0.0738\ pH + 0.0148 \log (HGeO_3^-)$
4.	$Ge + 3H_2O \rightleftarrows GeO_3^{2-} + 6H^+ + 4e_0^-$	$e = 0.325 - 0.0886\ pH + 0\ 0148 \log (GeO_3^{2-})$
5.	$Ge + H_2O \rightleftarrows GeO_{brown} + 2H^+ + 2e_0^-$	$e = 0.100 - 0.0591\ pH$
6.	$Ge + H_2O \rightleftarrows GeO_{yellow} + 2H^+ + 2e_0^-$	$e = 0.256 - 0.0591\ pH$
7.	$Ge + 2H_2O \rightleftarrows GeO_{2hex.} + 4H^+ + 4e_0^-$	$e = -0.009 - 0.0591\ pH$
8.	$Ge + 2H_2O \rightleftarrows GeO_{2tetr.} + 4H^+ + 4e_0^-$	$e = -0\ 053 - 0.0591\ pH$
9.	$Ge^{2+} + 3H_2O \rightleftarrows H_2GeO_3 + 4H^+ + 2e_0^-$	a. $= -0.209 - 0.1182\ pH + 0.0295 \log \frac{(H_2GeO_3)}{(Ge^{2+})}$
		b. $e = -0.074 - 0.0591\ pH + 0.0295 \log (H_2GeO_3)$
10.	$Ge^{2+} + 3H_2O \rightleftarrows HGeO_3^- + 5H^+ + 2e_0^-$	a. $e = 0.043 - 0.1477\ pH + 0.0295 \log \frac{(HGeO_3^-)}{(Ge^{2+})}$
		b. $e = 0.178 - 0.0886\ pH + 0.0295 \log (HGeO_3^-)$
11.	$Ge^{2+} + 3H_2O \rightleftarrows GeO_3^{2-} + 6H^+ + 2e_0^-$	a. $e = 0\ 420 - 0.1773\ pH + 0\ 0295 \log \frac{(GeO_3^{2})}{(Ge^{2+})}$
		b. $e = 0.555 - 0.1182\ pH + 0.0295 \log (GeO_3^{2-})$
12.	$Ge^{2+} + 2H_2O \rightleftarrows GeO_{2hex} + 4H^+ + 2e_0^-$	a. $e = -0.249 - 0.1182\ pH - 0.0295 (\log Ge^{2+})$
		b. $e = -0.114 - 0.0591\ pH$
13.	$Ge^{2+} + 2H_2O \rightleftarrows GeO_{2tetr.} + 4H^+ + 2e_0^-$	a. $e = -0.338 - 0.1182\ pH - 0.0295 \log (Ge^{2+})$
		b. $e = -0\ 203 - 0.0591\ pH$
14.	$GeO_{brown} + H_2O \rightleftarrows GeO_{2hex} + 2H^+ + 2e_0^-$	$e = -0.117 - 0.0591\ pH$
15.	$GeO_{brown} + H_2O \rightleftarrows GeO_{2tetr.} + 2H^+ + 2e_0^-$	$e = -0.206 - 0.0591\ pH$
16.	$GeO_{yellow} + H_2O \rightleftarrows GeO_{2hex.} + 2H^+ + 2e_0^-$	$e = -0.273 - 0.0591\ pH$
17.	$GeO_{yellow} + H_2O \rightleftarrows GeO_{2tetr.} + 2H^+ + 2e_0^-$	$e = -0\ 362 - 0.0591\ pH$
18.	$GeO_{brown} + 2H_2O \rightleftarrows H_2GeO_3 + 2H^+ + 2e_0^-$	$e = -0.077 - 0.0591\ pH + 0.0295 \log (H_2GeO_3)$
19.	$GeO_{brown} + 2H_2O \rightleftarrows HGeO_3^- + 3H^+ + 2e_0^-$	$e = 0.175 - 0\ 0886\ pH + 0.0295 \log (HGeO_3^-)$
20.	$GeO_{brown} + 2H_2O \rightleftarrows GeO_3^{2-} + 4H^+ + 2e_0^-$	$e = 0\ 552 - 0.1182\ pH + 0.0295 \log (GeO_3^{2-})$
21.	$GeO_{yellow} + 2H_2O \rightleftarrows H_2GeO_3 + 2H^+ + 2e_0^-$	$e = -0.233 - 0.0591\ pH + 0.0295 \log (H_2GeO_3)$
22.	$GeO_{yellow} + 2H_2O \rightleftarrows HGeO_3^- + 3H^+ + 2e_0^-$	$e = 0\ 019 - 0.0886\ pH + 0\ 0295 \log (HGeO_3^-)$
23.	$GeO_{yellow} + 2H_2O \rightleftarrows GeO_3^{2-} + 4H^+ + 2e_0^-$	$e = 0.395 - 0.1182\ pH + 0\ 0295 \log (GeO^{2-})$

[a] Taking: $GeO_{brown} + 2H^+ = Ge^{2+} + H_2O$ with known equilibrium constant,[14] $K = 3 \times 10^{-5}$, $\log Ge^{2+} = -4.53 - 2\ pH$.

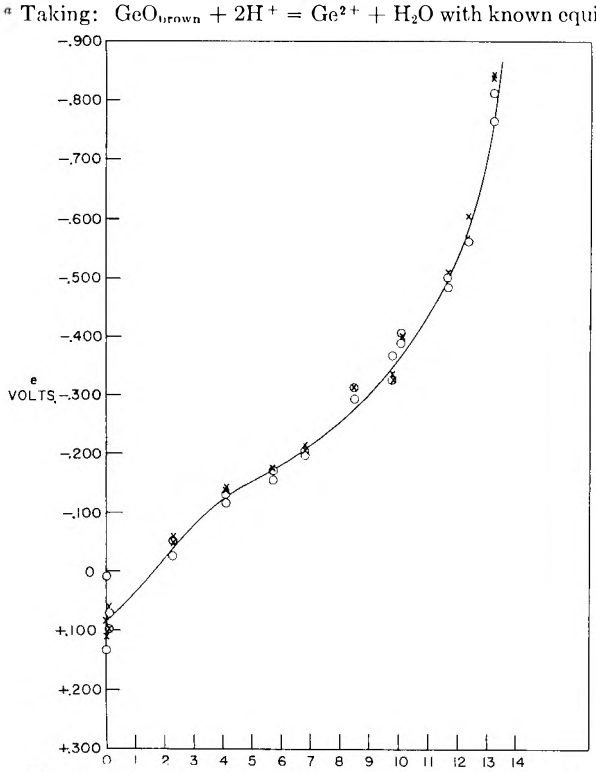

Fig. 2.—Experimental e–pH relation for a highly purified solution of 0.0036 mole $l.^{-1}$ GeO_2: (x = n-type electrodes, 110 face, resistivity, 2.4–2.5 ohms cm.; O = p-type electrode, 110 face, resistivity 1.8–1.9 ohms cm.).

by means of the Henderson equation[11] and the results recalculated for the standard H_2 scale assuming a value of 0.242 v. for the saturated calomel electrode at 25°.

The reproducibility of the measurements was c. ±10 mv. In solutions of extreme pH regions, the reproducibility decreased to ±30 mv. In solutions which had not been carefully decontaminated, the reproducibility was much less.

Observations were repeated some four to eight times in identical systems.

(iii) **Impurity Effects.**—In reagents of analytical purity, the results differed very considerably in the acid region from those obtained in solutions which had been decontaminated as described in section Experimental (iv). At pH 0, values were about 150 mv. more negative in the ordinary (*i.e.*, contaminated), than in the purified, solutions.

(iv) **Time Effects.**—After establishment of a new solution composition, the electrode potential reached a constant value after times of the order of one hour.

(v) **pH Effects.**—The relation of e to pH in 0.0036 mole $l.^{-1}$ GeO_2 is shown in Figs. 1 and 2. At pH's near to 0 and 10, about eight concordant measurements were carried out.

(vi) **GeO_2 Effects.**—A comprehensive investigation of the effect of GeO_2 concentration is difficult because of the low solubility of GeO_2 (*i.e.*, 0.04 mole

(11) P. Henderson, *Z. physik. Chem.*, **59**, 118 (1907); **63**, 325 (1908).

l.$^{-1}$)[12,13] in low pH ranges. Measurements made at 0.0036 mole l.$^{-1}$, 0.036 mole l.$^{-1}$, and by direct addition of GeO_2 solution to the cell, showed no significant change of potential.

(vii) **O_2 Effect.**—Replacement of the He atmosphere with O_2 caused the e–pH relation at constant GeO_2 composition to tend to linearity over most of the pH range with $\partial e/\partial p\mathrm{H} = 0.057$ at 25°.

(viii) **H_2 Effect.**—Replacement of a He by an H_2 atmosphere did not affect the potential.

(ix) **Effect of Type of Ge.**—The n-type electrodes had a mean value of 5 mv. more negative than that of the p-type electrodes over the pH range 0–13.5.

(x) **Effect of Crystal Face.**—The measurements recorded above were carried out on Ge single crystals of face 110. Measurements were also carried out on crystals of face 111 having the same resistivity as that for the 110 crystals. The pH range was 2.5–12. The difference between the results on the 111 face and those on the 110 face was less than the experimental uncertainty (see Results, ii).

Discussion

(i) **Mixed Potential.**—In order to interpret the fact that the electrode potential is sensitive to stirring effects, it is necessary to assume that at least one other reaction occurs at a significant rate at the electrode–solution interface, in addition to the reaction which, having a relatively high i_0 value, determines the potential. As will be shown in detail below, this latter reaction is probably

$$Ge + H_2O \rightleftharpoons GeO + 2H^+ + 2e_0^- \qquad (5, 6, \text{Table II})$$

The electrode potential would remain constant with agitation at a given pH were it not for a slight solubility of GeO.[14] Not enough GeO is hence present on the surface for the equilibrium to be maintained without the partaking of another electrode reaction, the kinetic function of which is either: (i) to utilize the excess electrons which would be produced at the electrode by the above reaction proceeding from left to right; (ii) direct formation of GeO by means of dissolved O_2 or the reaction of H_2GeO_3 with Ge, etc.

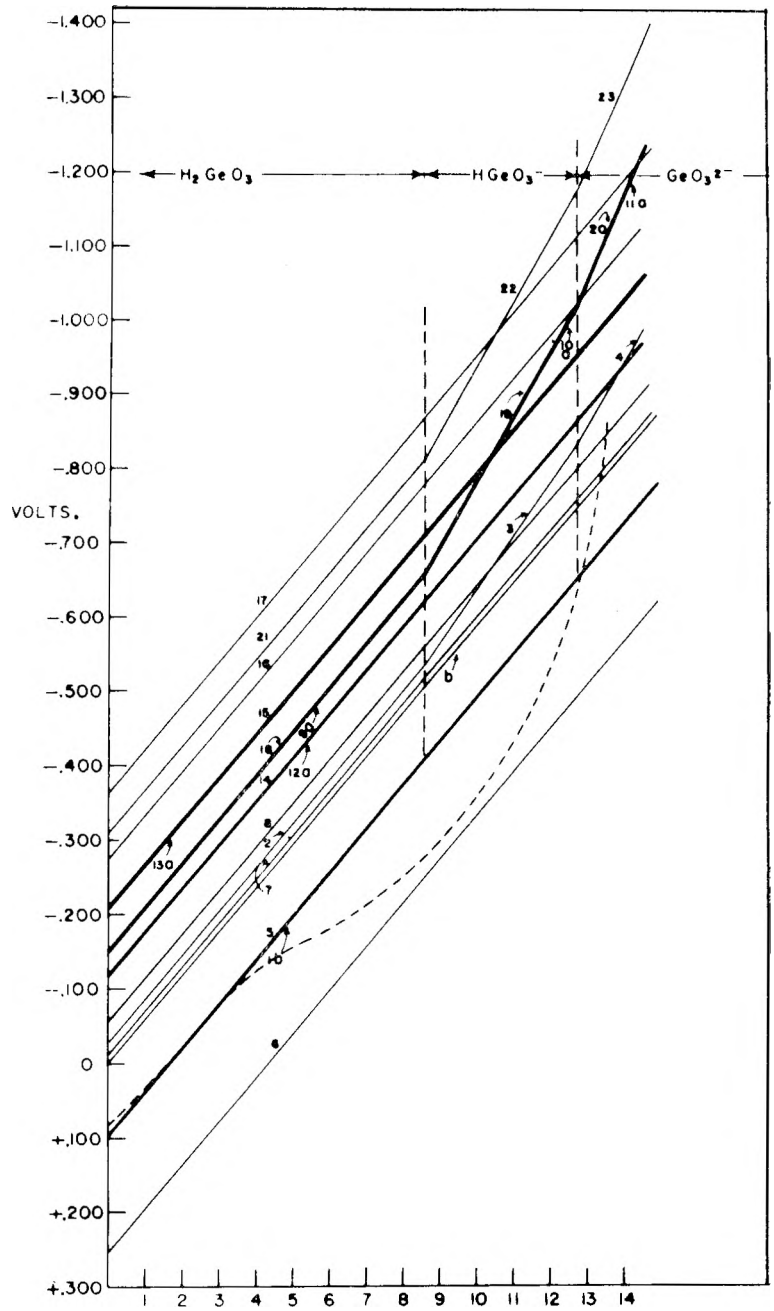

Fig. 3.—Values of e as a function of pH for various electrode equilibria involving Ge calculated from thermodynamic data of Table I. For key to reaction numbers, see Table II: GeO_2 concentration taken as 0.0036 mole l.$^{-1}$; dotted curve, experimental values.

The most likely reaction concerned in (i) is the cathodic hydrogen evolution reaction, which could take place in equilibrium with H_2 at a pressure well below the atmospheric pressure (*vide infra*). The stirring effect would arise both because increased agitation would remove into the bulk of the solution both H_2 produced at the interface and GeO dissolved thereat.

Thus, it is possible to show theoretically that the effect of the corrosion of the Ge electrode upon the observed potential is such that this differs negli-

(12) W. Pugh, *J. Chem. Soc.*, 1537 (1929).

(13) N. De Zoubov, E. Deltombe and M. Pourbaix, "Comportement électrochimique du germanium. Diagramme d'équilibre tension—pH du systeme Ge–H_2O a 25°," Report technique No. 27 CEBELCOR, 1955.

(14) W. L. Jolly, "Some Problems in the Chemistry of Germanium" (thesis), Radiation Laboratory University of California, 1952, United States Atomic Energy Commission UCRL-1638, Technical Information Service, Oak Ridge, Tennessee.

gibly from that of the thermodynamically reversible potential 5 (Table II) under similar conditions. Thus, the rate of corrosion[2] of n-type Ge at a *p*H of 13[2] is not more than about 2×10^{-6} amp. cm.$^{-2}$. Assuming that this c.d. represents the order of magnitude of the corrosion rate in all solutions measured in the present work, it is possible to calculate the reversible H_2 potential corresponding to this rate of dissolution from equations for corrosion rates as a function of the reversible hydrogen potential (Bockris)[15] (*i.e.*, the cathodic partial current is that of the hydrogen evolution reaction; and the anodic current is that of 5).

This value, which corresponds to a pressure of H_2 of about 10^{-10} atm. at *p*H 3, is then substituted into the equation for the mixed potential, assuming that the reaction involving Ge is 5. Using the parameters: $(i_0)_H = 10^{-8}$ amp. cm.$^{-2}$;[16] $(i_0)_{Ge} = 2 \times 10^{-6}$ amp. cm.$^{-2}$ (extrapolated from Turner[3]), it is possible to calculate the mixed potential. The resulting mixed potential at *p*H 3 is some 17 mv. more positive than is the thermodynamic value of reaction 5 (see Table II). The agreement between this forecast deviation from the thermodynamically calculated and observed value is satisfactory, and it may be concluded that the mixed potential set-up by the low corrosion rate present changed the electrode potential from its thermodynamic value by not more than 20 mv.

(ii) **Thermodynamics of Electrode Reactions involving Ge.**—The potentials corresponding to certain electrode equilibria involving Ge have been calculated from thermodynamic data by conventional means. The data selected for the calculation are shown in Table I, and the equilibria and corresponding calculated potential in Table II. The calculated potentials as a function of *p*H are shown graphically in Fig. 3 for the GeO_2 concentration most frequently used in this work (0.0036 mole l.$^{-1}$). The dotted line indicates the position of the experimental potentials relative to their theoretical values.

The calculated potentials of Table II disagree with those published by Zoubov, Deltombe and Pourbaix,[18] the magnitude of the discrepancy amounting to 0.1–0.3 v. This discrepancy appears to arise from the choice by these authors of the value of −141 kcal. mole^{-1} quoted by Latimer[17] for the heat of formation of GeO_2. This quoted value, however, appears to be considerably discrepant from the values of Becker and Roth,[18] −128.1 kcal. mole^{-1}, Hahn and Juza,[19] −128.6 kcal. mole^{-1}, of Jolly,[14] and Jolly and Latimer,[20] −129.2 kcal. mole^{-1}. The weighted mean chosen by Jolly and Latimer[20] of −128.5 kcal. mole^{-1} was used for the calculations of Table II.

A comparison of the observed values of the potential with the thermodynamic values of Fig. 4 indicates that only the thermodynamic equilibria 5 and 6 (Table II) give potentials in the range of those observed experimentally for the *p*H range 0–13. A similar agreement with the observed results could also be obtained with equilibrium 1 (Table II), but Ge^{2+} ions in contact with water form GeO and consequently the equilibrium, 1, becomes essentially 5 and 6, *i.e.*

$$Ge + H_2O \rightleftharpoons GeO_{brown} + 2H^+ + 2e_0^- \quad (5)$$

$$Ge + H_2O \rightleftharpoons GeO_{yellow} + 2H^+ + 2e_0^- \quad (6)$$

(iii) **Other Observations.**—The marked effect of impurities on the results in solution of low *p*H is presumably associated with the complexing of the divalent Ge, so that its concentration is reduced. Such complexing has been described and may take place with one of the impurities present.[13]

Time effects probably are connected with equilibration between the two forms of GeO. This is known to be slow.[14,21,22]

*p*H effects are well in accord with the interpretation that the reactions 5 and 6 are the main equilibria. Thus, over the range *p*H 0–4, $\partial e/\partial p\mathrm{H}$ −0.05 and this is consistent with the primacy of the brown form of GeO, (*i.e.*, reaction 5 (see below)). At *p*H above 4, the *e*–*p*H relation undergoes an inflection and again attains a section over the *p*H range 6–12 in which the slope is in accordance with the theory for reaction 6 of Table II. This is in accord with the observation that the yellow form is stable in solutions of middle *p*H range but transforms to the brown form upon addition of H_2SO_4.[23]

At *p*H > 12.5, the potential departs in the negative direction from values which correspond to the reactions 5 and 6. In accord with this, Everest and Terrey[22] have referred to a change in color of GeO at "high" *p*H's. The *e*–*p*H range after the sharp change in slope is insufficient in *p*H range to enable a definite conclusion concerning the relevant oxide equilibrium to be made. However, the possible reaction must be one involving GeO_3^{2-} ions which have been shown to predominate in the high *p*H range.[24] This fact, and the numerical values of the thermodynamically calculated lines in Fig. 3, leave reaction 4 (of Table II) as the likely potential-determining equilibrium at *p*H values greater than 13.

The absence of GeO_2 and H_2 concentration effects is in accord with the reaction equilibrium suggested for the *p*H range 0–12.5 (Table II).

The tendency of the *e*–*p*H relation to become linear over most of the *p*H range in the presence of excess O_2 may be interpreted by the basis that the O_2 will cause the electrodes' behavior to approximate more to that of an electrode involving GeO in the yellow form. Thus, a possible mechanism would be that O_2 forms GeO_2 with the GeO film on the electrode and that the more soluble GeO_2 dissolves, thus giving rise to the formation of a fresh (and therefore[22] yellow) GeO film. This explanation would involve the assumption of rapid dissolution of GeO_2 because otherwise the electrode GeO–GeO_2 would be set up.[14,17]

The fact that n-type electrodes have a mean value over most of the *p*H range of some 5 mv. more negative than that of the p-type electrodes appears

(15) J. O'M. Bockris, "Modern Aspects of Electrochemistry," I, Butterworth's, London, 1954, eqn., 281, p. 256, eq. 280, p. 255.

(16) Report to the Philco Corporation No. H-2056 (June, 1957).

(17) W. M. Latimer, "Oxidation Potentials," second edition, Prentice–Hall, Inc., New York, 1952.

(18) G. Becker and W. A. Roth, *Z. physik. Chem.*, **A161**, 69 (1932).

(19) H. Hahn and R. Juza, *Z. anorg. allgem. Chem.*, **244**, 120 (1940).

(20) W. L. Jolly and W. M. Latimer, *J. Am. Chem. Soc.*, **74**, 5757 (1952).

(21) W. L. Jolly and W. M. Latimer, *ibid.*, **74**, 5751 (1952).

(22) A. Everest and H. Terrey, *J. Chem. Soc.*, 2282 (1950).

(23) J. H. Muller, *Proc. Am. Phil. Soc.*, **65**, 193 (1926).

(24) W. Pugh, *ibid.*, 1994 (1929).

to be inconsistent with the thermodynamic expectation that n and p-type electrodes should give rise to the same reversible potentials if exposed to the same soluble conditions.[5] However, the small difference observed is exactly what would be expected if the hydrogen evolution reaction is the cathodic reaction of a mixed potential set up at the Ge–solution interface (*cf.*, Discussion, (i)). At n- and p-type Ge electrodes *in pure solutions*, the $(i_0)_H$ is lower for the n-type material by about one power of ten.[16] This change affects the mixed potential in the direction of the experimentally found difference.

Acknowledgments.—The authors wish to express their thanks to the Philco Corporation for financial assistance during the course of this work; and to Dr. P. Schmidt, Philco, for discussion thereof.

ACID–BASE INTERACTION IN THE ADSORPTION OF OLEFINS ON ALUMINUM KAOLINITE

By J. J. Jurinak and D. H. Volman

Department of Soils and Plan Nutrition and Department of Chemistry, University of California, Davis, California

Received January 5, 1959

The interaction of *n*-butane, *trans*-butene-2, 1-chloroethylene and *trans*-1,2-dichloroethylene with Na-, Ca- and Al-saturated kaolinite was investigated using adsorption and desorption techniques. Al-kaolinite was observed to chemisorb both butene-2 and 1-chloroethylene. The data support the contention that adsorbed aluminum is the site of surface acidity. Varying the degassing temperature of Al-kaolinite from 25 to 315° indicated an intimate relation between surface acidity and the moisture associated with the clay surface. Calculations suggest that the interaction with *trans*-butene-2 involves an acid-catalyzed polymerization.

Introduction

During the course of studies involving the adsorption of various organic vapors on dehydrated clay systems it was noted that under certain conditions olefinic compounds exhibited reactivity toward the clay systems when compared with saturated hydrocarbon vapors. This study was initiated to investigate the nature of this apparent interaction of olefin vapor using homoionic kaolinite as the adsorbing surface.

Experimental Methods

The clay mineral used was kaolinite, A.P.I. No. 2, Birch Pit, Macon, Georgia. Homoionic samples were prepared by saturating the clay with a chloride solution of the appropriate cation. The clay was subsequently washed with water and dried in air at 60°. The sample was crushed and the 0.5–1.0 mm. aggregate fraction was retained. This material is taken as the standard initial state for the water loss experiments described later.

The adsorption apparatus was the same as described previously.[1] The solid sample was degassed for 16 hours at 120° and 10^{-5} mm. adsorbates used were *n*-butane, 1-chloroethylene, *trans*-1,2-dichloroethylene and *trans*-butene-2.

Surface areas of the clay samples were determined by application of the BET equation[2] to the experimental data. Uncertainties involved in assigning molecular areas to the various adsorbates made comparisons between the calculated surface areas an unsatisfactory criterion for evaluating reactivity. The adsorption experiments were therefore followed by desorption experiments in order to evaluate chemisorption. After an adsorption isotherm had been completed, the samples were degassed at 23–24° for 24 hours. A final pressure of 10^{-5} mm. and constant weight was reached in all cases. The gain in weight of the clay sample after this cycle of treatment was attributed to chemisorption. This criterion for chemisorption has been recently used in studies of the adsorption of pyridine and trimethylamine on silica–alumina catalysts[3] and of butylamine on attapulgite clay.[4]

Results and Discussion

Figure 1 shows the adsorption of *n*-butane at 0° by the homoionic kaolinite surfaces. As expected the adsorbed cation has little effect on the adsorption of the saturated hydrocarbon. Assuming an average molecular area of 44.0 Å. for butane,[5] the surface area obtained is 21.8 $m.^2/g.$ The total variation between the samples is about 10%. Desorption at room temperature rapidly removed all adsorbed *n*-butane from the samples.

The adsorption of *trans*-butene at 0°, Fig. 2, clearly indicates a strong specificity of the aluminum saturated surface for the butene molecule. The Na^+ and Ca^{++} saturated samples have a calculated area of 21.5 $m.^2/g.$, in good agreement with the results obtained by *n*-butane adsorption, while the aluminum system exhibits an area of 47.0 $m.^2/g.$ The area of the *trans*-butene molecule used in the above calculations was 40.0 $Å.^2$. This value was obtained by adsorbing both *n*-butane and *trans*-butene on a reference charcoal at 0.0°. The surface area obtained with *n*-butane was used to calculate a molecular area of *trans*-butene which would yield the same surface area.

The specificity of the Al-kaolinite for *trans*-butene is clearly shown in Fig. 3. This figure illustrates the method used to determine chemisorption. In 1.5 hours all of the physically adsorbed *n*-butane is removed from the surface while the desorption of *trans*-butene proceeds rapidly at first and then much more slowly to constant weight. The adsorbate retained after 24 hours of desorption is the defined chemisorbed portion. This curve is similar to the desorption rate curve of trimethylamine adsorbed on synthetic acid silica–alumina catalyst.[3] The Al-kaolinite chemisorbed 0.13 mmole of *trans*-butene per gram of clay. No *trans*-butene was retained by either the Na- or Ca-saturated clay. It was observed that a pink-purple color developed in the bu-

(1) F. A. Beetleheim, C. Sterling and D. H. Volman, *J. Polymer Sci.*, **22**, 303 (1956).

(2) S. Brunauer, P. H. Emmett and E. Teller, *J. Am. Chem. Soc.*, **60**, 309 (1938).

(3) R. L. Richardson and S. W. Benson, This Journal, **61**, 405 (1957).

(4) J. J. Chessick and A. C. Zettlemoyer, *ibid.*, **62**, 1217 (1958).

(5) S. J. Gregg and R. Stock, *Trans. Faraday Soc.*, **53**, 1355 (1957).

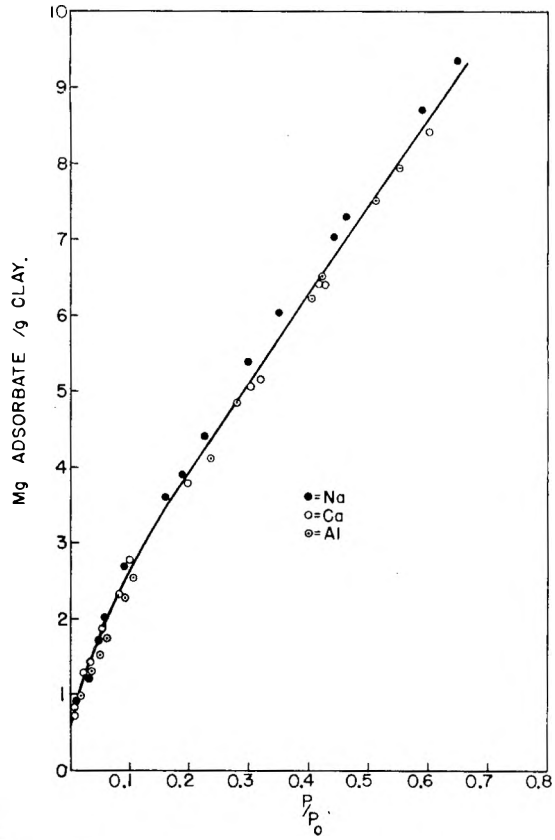

Fig. 1.—Adsorption of *n*-butane at 0.0° by homoionic kaolinite.

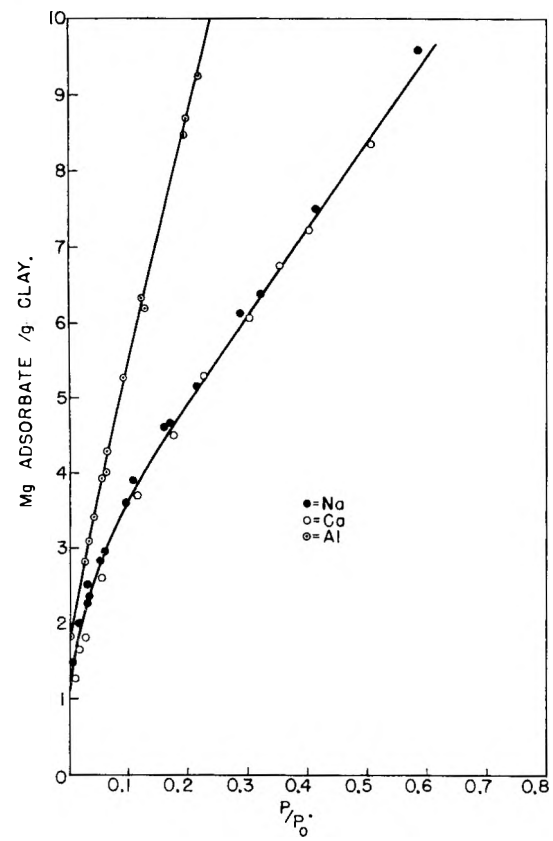

Fig. 2.—Adsorption of *trans*-butene-2 at 0.0° by homoionic kaolinite.

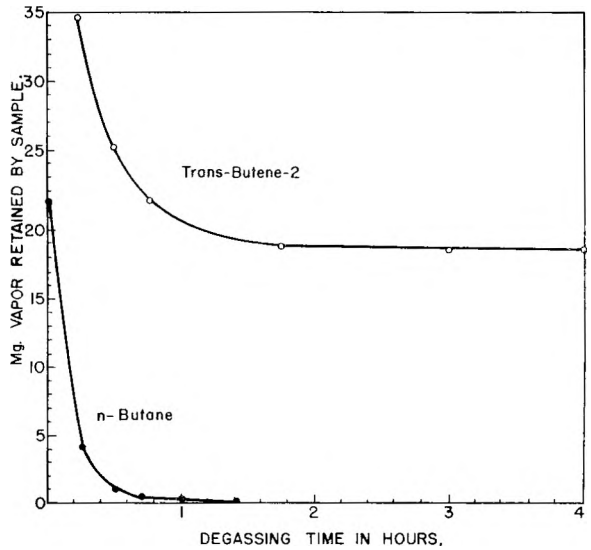

Fig. 3.—Desorption of *n*-butane and *trans*-butene-2 at room temperature from Al kaolinite degassed at 120°.

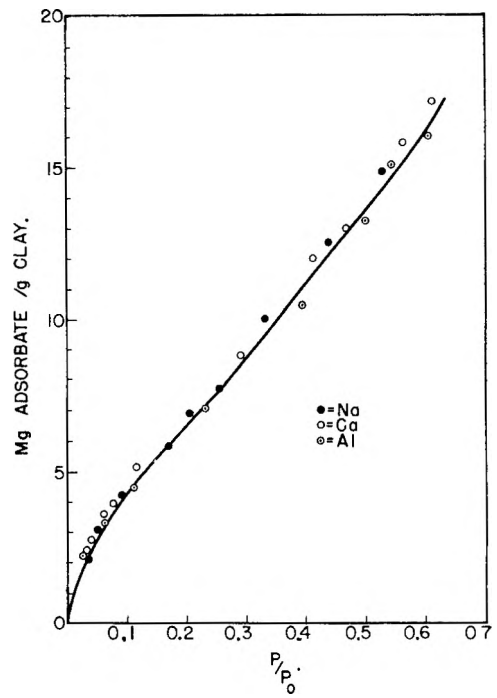

Fig. 4.—Adsorption of *trans*-1,2-dichloroethylene at 28.4° by homoionic kaolinite.

tene–clay system upon exposure to air after the desorption period.

The interaction of *trans*-butene with Al-kaolinite can be explained in terms of an acid–base mechanism with adsorbed aluminum considered to be the center of surface acidity. It is recognized, however, that adsorbed protons would not be entirely absent in this system. The formation of an acid site is ascribed to the tendency of adsorbed aluminum to attract electrons to its incomplete p orbital. The tendency to acquire electrons is independent of whether the adsorbed aluminum exists as the tri (⩾ Al) or di (> Al-OH) valent adsorbed form, which are the two ionic species considered important in this study.[6] The base reacting with the acid site is

(6) R. K. Schofield and W. A. Taylor, *J. Chem. Soc.*, 4445 (1954).

considered to be any adsorbate molecule capable of supplying electrons. In this study, the olefin molecule because of the high electron density about the double bond serves as the base.

The possibility exists that *trans*-butene reacted not with an adsorbed form of aluminum but with precipitated $Al(OH)_3$ which may have been formed during the saturation and washing of the Al-kaolinite. This possibility was eliminated when no interaction could be detected between commercially prepared $Al_2O_3 \cdot nH_2O$ and *trans*-butene. X-Ray diffraction showed the $Al_2O_3 \cdot nH_2O$ to be mainly gibbsitic material.

To test the validity of the surface acid–base approach further, two additional olefins with varying basicities were studied. The adsorption of *trans*-1,-2-dichloroethylene, considerably less basic than *trans*-butene, by various kaolinite systems is shown in Fig. 4. Both the adsorption and desorption data indicated no chemisorption on the clay surfaces. These results, however, do not invalidate the acid–base mechanism for they could indicate that the acidity of the Al-kaolinite is insufficient to obtain chemisorption with the weakly basic dichloroethylene molecule.

Figure 5 shows the adsorption of 1-chloroethylene which should exhibit greater basic tendencies than dichloroethylene. The adsorption data fails to indicate any reaction with the Al system. The desorption data, however, indicated a weak but definite interaction of 1-chloroethylene with Al-kaolinite. The amount of adsorbate retained after desorption was 0.01 mmole per gram of Al-kaolinite. No interaction was noted in the Na or Ca systems. These data support the contention that an acid–base mechanism is operative in the adsorption of olefins by Al-kaolinite.

All preceding data have failed to take into account the effect, if any, of water molecules associated with the system. The literature[7,8] reveals that water molecules play a decisive role in determining the surface acidity and resultant activity of cracking catalysts. Since Al-kaolinite can be visualized as related to the artificial silica–alumina catalytic surfaces, an experiment was conducted to investigate the effect of moisture on the interaction of *trans*-butene with Al-kaolinite. The clay was degassed at various temperatures for 16 hours under a vacuum of 10^{-5} mm. The sample was exposed to *trans*-butene vapor for 2.5 hours at 0.0°, then desorbed as described. The amount of *trans*-butene chemisorbed is plotted against per cent. moisture weight lost from standard initial state in Fig. 6. These data show that water must be intimately associated with the surface reaction of olefins. The curve indicates that there is a critical amount of water above and below which surface activity decreases.

To show that the variation of degassing temperature did not effect the surface area of the sample, *n*-butane was adsorbed at 0.0° on samples degassed at 33, 120 and 315°. The calculated surface areas of Al-kaolinite were 20.2, 20.2 and 20.6 $m.^2/g.$, respectively. Therefore, the reaction is independent of surface area. The same experiment was repeated using 1-chloroethylene and only 2 degassing temperatures. The results, Fig. 6 indicate that the same mechanism is involved in the adsorption of both olefins.

An explanation of the data shown in Fig. 6 is that the adsorbed aluminum preferentially acquires its electrons from the oxygen atom of the water, coordinating the hydroxyl group about the adsorbed

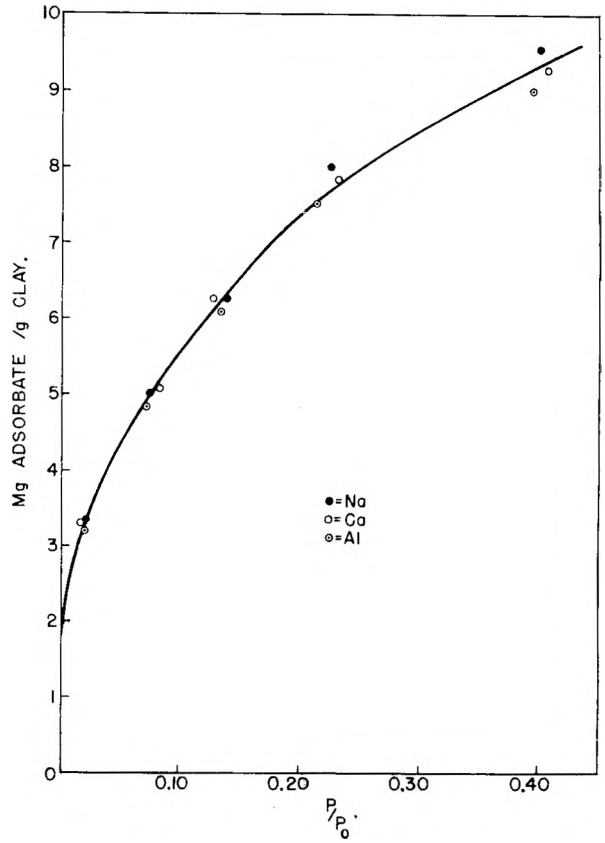

Fig. 5.—Adsorption of 1-chloroethylene at 0.0° by homoionic kaolinite.

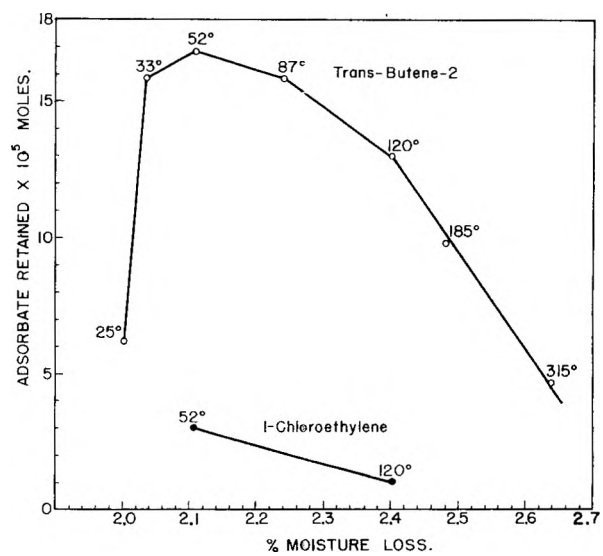

Fig. 6.—Effect of moisture loss on the amount of *trans*-butene-2, and 1-chloroethylene chemisorbed on Al-kaolinite degassed at various temperatures (centigrade).

(7) S. G. Hindin, G. A. Mills and A. G. Oblad, *J. Am. Chem. Soc.*, **73**, 278 (1951).

(8) R. C. Hansford, P. G. Waldo, L. C. Drake and R. E. Honig, *Ind. Eng. Chem.*, **44**, 1108 (1952).

aluminum and placing the remaining hydrogen atom in a state where it can easily be removed. The presence of water, hence, converts the original Lewis acid sites to a Brönsted acid site which can easily donate protons to the olefin molecule giving rise to a carbonium ion complex. This process is schematically shown below using the tri-valent form of adsorbed aluminum. At the high degassing tem-

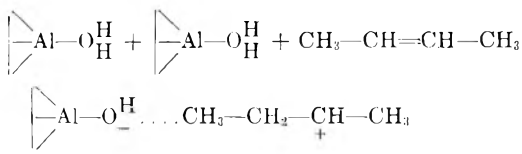

peratures, the loss of moisture decreases the proton donating ability of the acid sites, whereas, at the low degassing temperature, the excess water either acts as a base in competition with the olefin or reduces the surface acidity by hydration of the site.

Additional information concerning the reaction of *trans*-butene with Al-kaolinite may be gained by calculating the amount of surface covered by the chemisorbed butene. The area covered varies from 40.5 m.²/g. on clay degassed at 52° to 11.2 m.²/g. on clay degassed at 315° as compared to the total area determined by *n*-butane of 20.3 m.²/g. Indeed, the chemisorbed butene of Al-kaolinite degassed at 120°, Fig. 3, is calculated to cover 31 m.²/g. which accounts for the discrepancy of 27 m.²/g. which occurs between the *n*-butane area, 20.2 m.²/g., and *trans*-butene area, 47.0 m.²/g. The magnitude of the above data preclude the possibility of the reaction being limited to simple chemisorption on surface sites, particularly on kaolinite where most of the cation exchange occurs only on edges. The reaction may be credited to an acid-catalyzed polymerization of butene. The initiation of the polymerization is the extraction of the proton by *trans*-butene from the acid site forming a carbonium ion. Subsequently, another olefin molecule may add to the positive organic fragment attached to the surface, similar to the manner in which the proton added to the first olefin molecule.[9]

(9) F. C. Whitmore, *ibid.*, **26**, 94 (1934).

MULTISEGMENT ADSORPTION OF LONG CHAIN POLYMERS ON CARBON BLACK

BY JESSE S. BINFORD, JR.,[1] AND ALBERT M. GESSLER

Department of Chemistry, University of Texas, Austin, Texas and Chemicals Research Division, Esso Research and Engineering Co., Linden, New Jersey

Received January 5, 1959

The effects of unsaturation and molecular weight of polymeric hydrocarbons on the properties of adsorption on a carbon black are measured. Polymers are dispersed in an organic solvent and mixed with the carbon black until equilibrium is reached. The extent of adsorption is correlated with the concentration of adsorbate in the supernatant liquid. Solvent effects and adsorption rates are discussed briefly. It is found that the adsorption isotherms are not affected by saturation of the olefinic polymer but are strongly dependent on the chain length. The weight of polymer in a monolayer calculated from a Langmuir plot is relatively independent of either unsaturation or molecular weight. An attempt has been made to calculate $\langle\nu\rangle$ from the Frisch–Simha–Eirich multisegment adsorption isotherm.

A. Introduction

Carbon black is a mixture of high molecular weight compounds containing principally carbon, with several per cent. oxygen and 0.5% hydrogen by weight.[2] In this study a typical channel black is used (MPC, Kosmobile 66). It has a large surface area, approximately 100 m.²/g. It exists in the form of essentially spherical particles, which, on the average, are 25–30 mμ in diameter. About one in every twenty carbon atoms is on the surface, and this partly accounts for the high surface activity of carbon black. The oxygen is linked to the carbon atoms in ordinary covalent bonds forming such groups as carbonyl, carbinol and carboxyl.[3]

Butyl rubber is a high molecular weight copolymer of isobutylene with a few per cent. isoprene. It is soluble in a variety of organic solvents such as carbon tetrachloride, hexane and benzene. Like natural rubber, its mechanical properties are greatly improved by adding up to 50% carbon black with thorough mixing.

Both physical and chemical bonds are believed to exist in rubber-carbon mixtures. In the case of a chemical bond, the point of attack on the long chain Butyl rubber molecule would most likely be at the double bond. Heats of adsorption of vapors on carbon blacks at 100° have been shown to be changed by the existence of double bonds in the adsorbate and by the extent and type of surface of the adsorbent.[4]

If the bonding is physical, the attractive forces are of the non-specific van der Waals type. In this case one would expect the complete carbon-black surface to be available for interaction and not just that portion containing chemically bound oxygen.

B. Adsorption Equilibria

1. **Experimental Method.**—Our experimental procedure is similar to the method used by Kraus and Dugone.[5] The polymer to be studied is dispersed in an organic solvent at a known concentration (approximately 5 g./l.). Aliquots of 25.0 cc. are pipetted into a series of sample bottles and

(1) Department of Chemistry, College of the Pacific, Stockton, Calif.

(2) W. D. Schaeffer, W. R. Smith and M. H. Polley, *Ind. Eng. Chem.*, **45**, 1721 (1953).

(3)(a) M. L. Studebaker, E. W. D. Huffman, A. C. Wolfe and L. G. Nabors, *ibid.*, **48**, 162 (1956); (b) A. M. Gessler and R. L. Zapp, *Rubber Age*, **74**, 243 (1953).

(4) W. D. Schaeffer, M. H. Polley and W. R. Smith, THIS JOURNAL, **54**, 227 (1950).

(5) G. Kraus and J. Dugone, *Ind. Eng. Chem.*, **47**, 1809 (1955).

weighed amounts of the carbon black, from 0.1 to 10 g., are added. The bottles are shaken gently at room temperature until equilibrium conditions are attained. From each bottle a 10.0-cc. aliquot is filtered and placed in an aluminum weighing dish. The organic solvent is driven off on a steam-bath and the last traces are removed by heating the dish several hours *in vacuo* at 40°. The amount of polymer is determined by weighing, and the amount adsorbed by the carbon black can then be calculated.

Data are correlated by plotting x/m, where x is the grams of polymer adsorbed and m is the grams of carbon black, *versus* c, the final concentration of polymer in the supernatant liquid expressed in g./liter. x/m is directly proportional to θ, the fraction of the surface covered by polymer.

Adsorption of macromolecules on carbon black is of the monomolecular layer type according to Jenckel and Rumbach.[6] Thus one would expect x/m to approach some limiting value for large values of c.

The polymer samples used in this study are described in the following table. Per cent. unsaturation is expressed on the basis of mole per cent. isoprene.

TABLE I

Polymer	Mol. wt.	% Unsaturation	Designation
Enjay Butyl 325	325,000	1.88	B "325"
Enjay Butyl 035	325,000	0.89	B "035"
Special Butyl	18,000	1.64	B 18000
Special Butyl	8,800	2.29	B 8800
Polyisobutylene	14,000	0.05	PIB 14000
Polyisobutylene	8,300	.08	PIB 8300
Polyisobutylene	5,100	.08	PIB 5100

2. **Solvent Effects.**—Two solvents are used in this study, carbon tetrachloride and hexane. Adsorption does not occur in carbon tetrachloride at any concentration of the polymer. Either carbon tetrachloride molecules are adsorbed preferentially to the surface or the interaction between the solvent and polymer is such that the latter no longer has any attraction for the surface.

The possibility of preferential adsorption of carbon tetrachloride was tested in the following manner. An attempt was made to adsorb CCl_4 on the carbon black surface from hexane solutions containing between 0.2 and 5 volume % CCl_4. After agitation for one day, the supernatant liquid was analyzed for CCl_4 by measuring the intensity of the infrared band at 12.65 μ. It was found that no CCl_4 was adsorbed to the carbon black. Thus CCl_4 molecules do not compete with the polymer for adsorption sites. It was calculated that a monomolecular layer of CCl_4 on the amount of carbon black used would have totally depleted a 0.5 volume % CCl_4 solution.

When hexane is used as solvent, adsorption occurs at all concentrations.

3. **Rates of Adsorption.**—Figure 1 shows the rates of adsorption of two unsaturated polymers and the saturated polymers. Adsorption is shown to be complete within several hours except in the case of the very high molecular weight polymer. In this case adsorption approaches completion at the end of one day of agitation.

4. **Adsorption Isotherms.**—Figure 2 shows adsorption isotherms for the series of polymers having different molecular weights and degrees of unsaturation. In all cases, the solvent is hexane and the adsorbent is Kosmobile 66.

The B "325" and "035" samples follow the same adsorption curve which reaches apparent saturation at a fairly low concentration. The degree of unsaturation in the polymer molecule is seen to have no effect on its adsorption isotherm at room temperature. This is seen to hold true for lower molecular weight polymers also. Thus B 8800 and PIB 8300 follow very similar paths as do B 18000 and PIB 14000. One would expect a difference if the double bonds were in any way responsible for the adsorption.

However, the effect of molecular weight on the isotherm is significant. The sharp rise in surface coverage at low concentrations disappears for low molecular weight polymers and the resemblance to the Langmuir isotherm becomes more noticeable.

5. **Extraction.**—It is a well-known fact that a certain fraction of the rubber in a mixture with carbon black is not extractable, *i.e.*, continued refluxing with an ordinarily good solvent in a Soxhlet extractor is incapable of separating this fraction of the polymer from the black. This same phenomenon was observed in these experiments with the only two polymers for which it was sought. The carbon blacks were allowed to adsorb approximately one-third the maximum amount of polymer. The per cents. of this amount removed after 24 hours extraction with hexane were 39% for B 8800 and 3% for B "325." This suggests that a certain fraction of the polymer has very great difficulty in being desorbed from the surface once it has been adsorbed and that the difficulty increases as the chain length increases.

(6) E. Jenckel and B. Rumbach, *Z. Elektrochem.*, **55**, 612 (1951).

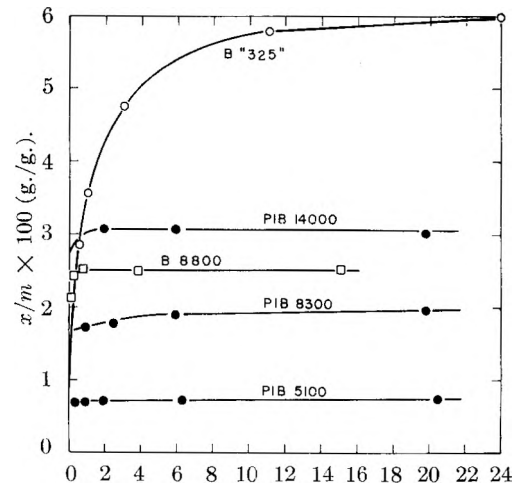

Fig. 1.—Rates of adsorption.

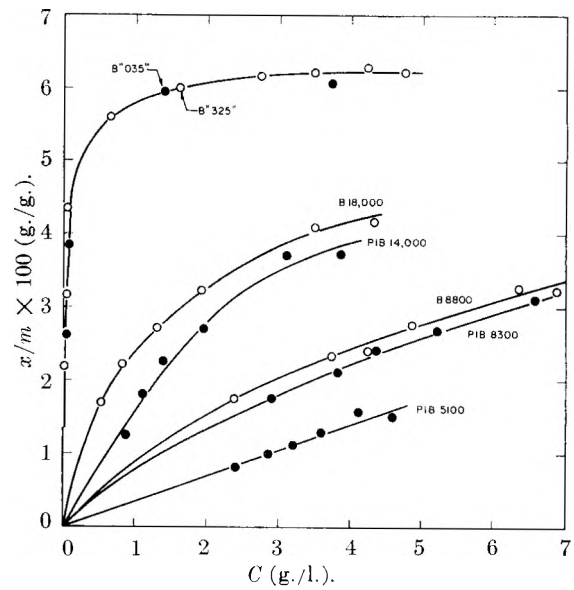

Fig. 2.—Adsorption isotherms.

C. Theoretical Treatment

The manner in which the polymer molecule is adsorbed can be visualized in two ways. Either the attachment is at a single point and the major portion of the molecule lies in the solution or the polymer adsorbs in segments and a large fraction of the molecule lies close to the surface. That the latter case seems the more likely of the two possibilities is seen from the following considerations. Let m/x be plotted against $1/c$ for B "325" and "035" and the polyisobutylenes (Fig. 3). It is seen that $(x/m)_{max}$ is very nearly the same for all polymers

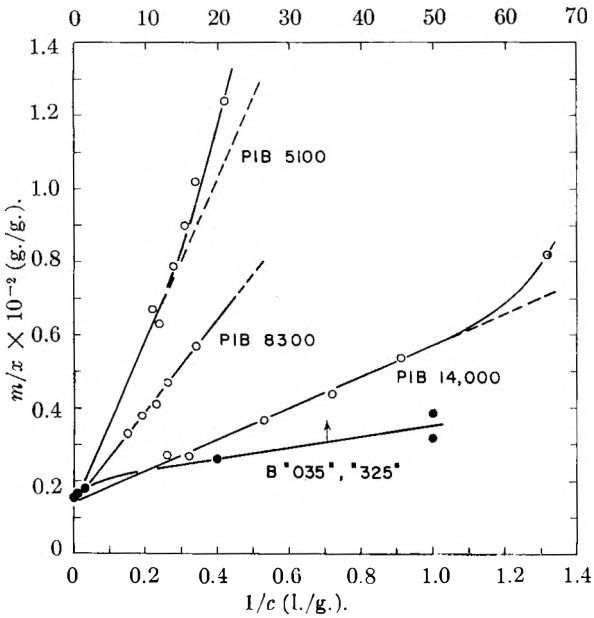

Fig. 3.—Langmuir plots.

with the possible exception of PIB 5100. In this case the extrapolation to high concentrations is questionable. These numbers may be compared with the number of surface carbon atoms per gram of Kosmobile 66 black. For simplicity the black is considered to be composed entirely of carbon and the particles are considered spherical. From the specific gravity[7] 1.85 and the diameter, 25–30 mμ, the number of surface atoms per gram is calculated to be between 3.1×10^{21} and 2.5×10^{21}. Table II shows the comparison of this number with the maximum number of CH_2 groups adsorbed per gram of carbon black.

TABLE II

Polymer	$(x/m)_{max}$, g./g.	No. CH_2 groups per g.
B "325"	6.2×10^{-2}	2.7×10^{21}
PIB 14000	7.2×10^{-2}	3.1×10^{21}
PIB 8300	7.7×10^{-2}	3.3×10^{21}
PIB 5100	7.7×10^{-2} (?)	3.3×10^{21} (?)

These facts lead one to believe that in all cases, except perhaps PIB 5100, the polymers lie flat on the surface of the carbon black. This interpretation must be qualified by the fact that the data are adequately represented by the Freundlich isotherm and $(x/m)_{max}$ may not correspond to complete coverage of the surface.

Jenckel and Rumbach[6] treat macromolecular adsorption as Langmuir chemisorption. Frisch, Simha and Eirich[8-10] point out that the rise in adsorption with increasing concentration is greater for macromolecules than would be expected for Langmuir adsorption. These authors derive an adsorption isotherm based on a statistical analysis of multisegment attachment of the adsorbed polymer. They point out that their treatment would not apply to carbon black since this adsorbent has such a large internal surface area.

However the recent work of Kraus and Dugone[5] indicates that Butyl rubber molecules do not penetrate the pores of the carbon black. The two principal blacks, channel and furnace, differ widely in the extent of internal surface area. Schaeffer, Polley and Smith[4] show by comparison of electron microscope and low temperature nitrogen adsorption measurements that furnace blacks have practically no internal surface while some channel blacks have even more internal surface than external. Kraus and Dugone plot the saturation adsorption of Butyl rubber per gram of various carbon blacks *versus* electron microscope external surface area per gram. The relationship is linear, with furnace and channel blacks falling on the same straight line. Thus Kraus and Dugone conclude that polymer adsorption is external only and that the Frisch, Simha and Eirich derivation should be applicable. The data in Table II show that if this is true for the very high molecular weight polymers, it is true also for the low ones which have the same $(x/m)_{max}$ values.

The F.-S.-E. isotherm[9,10] can be written in the form

$$[\theta \exp(2K_1\theta)/(1 - \theta)]\langle\nu\rangle = KC$$

where $\langle\nu\rangle$ = average number of segments deposited per chain. This expression, of course, does not yield a linear relation between θ^{-1} and C^{-1} as expected for Langmuir adsorption. That the data for B "325" and "035" in Fig. 3 deviate from linearity in the prescribed way is shown by the fact that θ^{-1} *versus* C^{-1} has negative curvature for θ close to unity. Values of $\langle\nu\rangle$ were calculated for all polymers from a log-log plot of $\theta/(1-\theta)$ *versus* C. Values close to one were found for all polymers except those with the highest molecular weight. For mol. wt. = 325,000, a value of 2.6 was found for $\langle\nu\rangle$. This, of course, is not reasonable unless the adsorbing segment is somewhere between 18,000 and 325,000 in molecular weight. In a similar study[5] Kraus and Dugone obtained $\langle\nu\rangle = 2.2$ for a very long polymer chain. It should be pointed out that our value of $\langle\nu\rangle = 2.6$ was determined between $\theta = 0.5$ and $\theta = 0.9$, and that more reliable results would be expected for smaller values of θ.

D. Summary

Irreversible polymer adsorption by carbon black has been observed at room temperature and unsaturation is seen to play a minor role in this interaction. The length of the polymer chain, however, is quite significant. From $(x/m)_{max}$ values it is concluded that both short and long polymers lie flat on the *external* surface of the carbon black. Calculated values of $\langle\nu\rangle$ from the Frisch–Simha–Eirich isotherm are all 2.6 and below, but these values may be unreliable for surface coverages as large as those used here.

The authors would like to express their great appreciation to Dr. Larry Eby, Enjay Company, Inc., for supplying us with the special Butyl samples and the polyisobutylene.

(7) E. M. Dannenberg and B. B. S. T. Boonstra, *Ind. Eng. Chem.*, **47**, 339 (1955).

(8) L. H. Frisch, R. Simha and F. R. Eirich, *J. Chem. Phys.*, **21**, 365 (1953).

(9) L. H. Frisch and R. Simha, THIS JOURNAL, **58**, 507 (1954).

(10) R. Simha, L. H. Frisch and F. R. Eirich, *ibid.*, **57**, 584 (1953).

THE EFFECT OF MOLECULAR INTERACTIONS ON N.M.R. REFERENCE COMPOUNDS

BY EDWIN D. BECKER

National Institutes of Health, Bethesda, Maryland

Received January 8, 1959

A study has been made of the effect of molecular interactions on the proton magnetic resonance (p.m.r.) frequencies of cyclohexane and tetramethylsilane, two compounds that are frequently used as internal references for p.m.r. investigations. In most of the cases studied the resonance frequencies of these compounds shifted 1–4 c.p.s. (at 40 mc.p.s.) when the composition of solutions containing the compounds was varied over a wide concentration range. The presence of hydrogen bonding molecules did not cause appreciably larger interaction effects than were found for hydrocarbon–CCl_4 solutions, but benzene at high concentration caused interaction shifts of 15–17 c.p.s.

Nuclear magnetic resonance, especially proton resonance (p.m.r.), is being used increasingly to distinguish between similar structural features in complex molecules[1] and to study weak molecular interactions, particularly hydrogen bonding.[2] Since these phenomena sometimes result in p.m.r. frequency shifts of only a few parts in 10^8, the frequency of the proton of interest must be measured accurately with respect to a proton in a reference molecule that is either dissolved in the same solution as the molecule of interest (an "internal reference") or placed in a separate capillary or coaxial tube (an "external reference"). The relative merits of the two types of reference have been discussed extensively by Bothner-By and Glick[3] and by Zimmerman and Foster.[4] The physical separation of an external reference is desirable in preventing interaction between the sample and reference substances, but its use requires that a correction be made for the effect of the bulk magnetic susceptibility of the sample. Bothner-By and Glick[3] made the susceptibility correction by replacing the theoretical "shape factor" for a solution in a cylinder, $2\pi/3$, by an empirical factor averaging about 25% larger, but varying from system to system. Stephen[5] has shown theoretically that the presence of an electrically or magnetically anisotropic molecule in a solution can cause molecular interactions that will affect the n.m.r. frequencies of other molecules, even though they are isotropic. He attributes the apparent departures in shape factor reported by Bothner-By and Glick[3] to the effect of such interactions.

Recently tetramethylsilane has been proposed as an internal reference and has been shown to offer several distinct advantages, including magnetic and electric isotropy,[6] which might be expected to reduce but not necessarily eliminate interactions that would alter its p.m.r. frequency. The present work is designed to evaluate the effects of molecular interactions on two p.m.r. reference compounds, tetramethylsilane and cyclohexane. Particular attention is given to systems containing hydrogen bonding molecules. The formation of a hydrogen bond generally causes a pronounced change in the p.m.r. frequency of the bonded proton and might also influence the frequency of an internal reference compound.

Experimental

The experiments were conducted with a Varian V-4300-2 high resolution n.m.r. spectrometer operating at 40 mc./sec., and a Varian 12" magnet with field trimmer and flux stabilizer. Frequency differences were measured by the side-band superposition technique.[7] Each reported value is the average of three independent measurements and is accurate to about ± 0.4 c.p.s. All studies were made with solutions in precision concentric tubes,[4] with either benzene or dioxane in the annulus as an external reference.

Measurements were made at room temperature, $28 \pm 2°$. Chemicals were high purity reagent grades which were further purified by appropriate standard procedures.[8a,b] Tetramethylsilane (Dow–Corning) was supplied by Dr. C. M. Huggins of the General Electric Company and was vacuum distilled by him. The compound showed no spurious p.m.r. lines. The solutions were prepared by weighing all components except the tetramethylsilane. The total volume of the former components was made up to 10 ml. in a volumetric flask and 0.5 ml. of tetramethylsilane was added to the solution just before use.[9] This procedure minimized evaporation of the volatile tetramethylsilane and ensured that all solutions contained identical volume fractions ($\sim$ 0.05) of tetramethylsilane. The susceptibility correction for tetramethylsilane was thereby held constant for all experiments and did not affect the determination of frequency shifts. No attempt was made to degas the samples. The presence of atmospheric oxygen in the solutions is likely to cause only a small alteration of the p.m.r. frequency ($\sim$ 0.5 c.p.s.),[10] which will be approximately the same for all the solutions studied herein.

Results and Discussion

Each set of experiments consisted of the measurement of p.m.r. frequencies as a function of the mole fraction of one of the components in a binary, ternary or quaternary solution. The systems studied are listed in the second column of Table I. Several of these particular combinations of substances were chosen so that the volume magnetic susceptibility of the solutions remained constant as the relative concentrations of two of the components were varied. The magnetic susceptibility

(1) See, for example, (a) R. U. Lemieux, R. K. Kullnig, H. J. Bernstein and W. G. Schneider, *J. Am. Chem. Soc.*, **79**, 1005 (1957); (b) J. N. Shoolery and M. T. Rogers, *ibid.*, **80**, 5121 (1958).

(2) See, for example, (a) C. M. Huggins, G. C. Pimentel and J. N. Shoolery, THIS JOURNAL, **60**, 1311 (1956); (b) A. D. Cohen and C. Reid, *J. Chem. Phys.*, **25**, 790 (1956); (c) L. W. Reeves and W. G. Schneider, *Canadian J. Chem.*, **35**, 251 (1957); (d) E. D. Becker, U. Liddel and J. N. Shoolery, *J. Mol. Spectroscopy*, **2**, 1 (1958); (e) C. M. Huggins and D. R. Carpenter, THIS JOURNAL, **63**, 238 (1959).

(3) A. A. Bothner-By and R. E. Glick, *J. Chem. Phys.*, **26**, 1647 (1957).

(4) J. R. Zimmerman and M. R. Foster, THIS JOURNAL, **61**, 282 (1957).

(5) M. J. Stephen, *Molecular Physics*, **1**, 223 (1958).

(6) G. V. D. Tiers, THIS JOURNAL, **62**, 1151 (1958).

(7) J. T. Arnold and M. E. Packard, *J. Chem. Phys.*, **19**, 1608 (1951).

(8) (a) A. Weissberger, *et al.*, "Organic Solvents," Interscience Publ., New York, N. Y., 1955. (b) L. F. Fieser, "Experiments in Organic Chemistry," D. C. Heath Co., New York, N. Y., 1941.

(9) Tetramethylsilane was stored below room temperature and its volume measured at approximately 15°.

(10) D. F. Evans, *Chemistry and Industry*, 526 (1958).

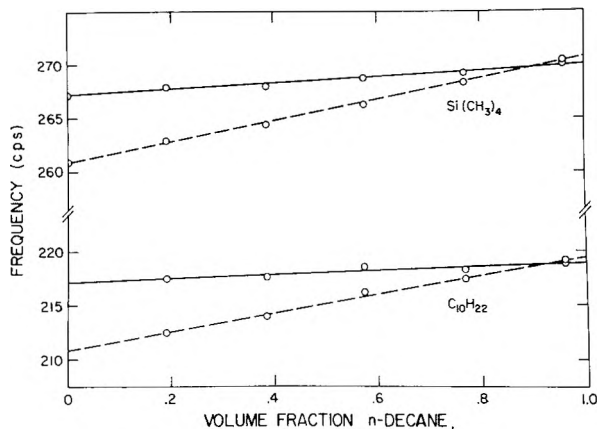

Fig. 1.—P.m.r. frequencies of tetramethylsilane and *n*-decane, measured with respect to benzene as an external reference: – – – –, observed data; ————, corrected for bulk magnetic susceptibility changes.

data used in this work are given in Table II. Since there are wide discrepancies among many

TABLE I

FREQUENCY SHIFTS OF P.M.R. REFERENCE COMPOUNDS

Expt.		Compounds[a]	Frequency shift[b] Obsd.	Cor.[c]
A	1	1-Butanol	....	...
	2	Cyclohexane	....	...
	3	Tetramethylsilane	−1.3	−1.3
B	1	Cyclohexanol	....	...
	2	Carbon tetrachloride	....	...
	3	Tetramethylsilane	1.8	1.8
C	1	Methanol	....	...
	2	Carbon tetrachloride	....	...
	3	Cyclohexane	16.8	3.0
	4	Tetramethylsilane	17.4	3.6
D	1	2,2,4-Trimethylpentane	11.3	3.8
	2	Carbon tetrachloride	....	...
	3	Tetramethylsilane	11.5	3.7
E	1	*n*-Decane	8.2	1.5
	2	Carbon tetrachloride	....	...
	3	Tetramethylsilane	9.2	2.5
F	1	Benzene	17.7	18.3
	2	Cyclohexane	16.4	16.9
	3	Tetramethylsilane	14.7	15.3
G	1	Chloroform	−19.9	−9.1
	2	Cyclohexane	−12.2	−1.9

[a] Solutions contained components 1 and 2 at volume fractions v_1, v_2 of 0 to ~ 0.95, and components 3 and 4 at v_3, $v_4 \approx 0.05$. [b] Shift in resonance frequency (c.p.s.) as v_1 increases from 0 to 1.0. A positive number indicates a shift to higher field (greater number of c.p.s. from benzene) with increasing v_1. [c] Frequency shift corrected for change in magnetic susceptibility of solution. Correction made using theoretical shape factor $2\pi/3$. For details of calculation see references 2c, 3 and 4.

published susceptibility data, we attempted wherever possible to select compounds for which two or more literature values are in agreement.[11] Venkateswarlu and Sriraman[12] have shown for a number of hydrogen bonding systems that the magnetic susceptibility per gram (specific susceptibility) is not dependent on the extent of hydrogen bonding. The specific susceptibility of such a solution can therefore be calculated in the usual way, as the weighted arithmetic mean of the specific susceptibilities of the components. The departures from additivity in density found by Venkateswarlu and Sriraman[12] are not large enough to be significant in the present work.

(11) An error in susceptibility of 0.012×10^{-6} c.g.s. units is equivalent to an n.m.r. frequency change of 1.0 c.p.s

(12) K. Venkateswarlu and S. Sriraman, *Bull. Chem. Soc. Japan*, **31**, 211 (1958).

TABLE II

VOLUME MAGNETIC SUSCEPTIBILITIES

Compound	K × 10⁶ (c.g.s. units) Used in this work	Other values
Benzene	0.617[a]	0.617,[b] 0.617,[c] 0.616[d]
Cyclohexane	.611[d]	.631[e]
1-Butanol	.611[d]	
n-Decane	.613[d]	.614[a]
2,2,4-Trimethylpentane	.596[d]	
Cyclohexanol	.694[d]	
Carbon tetrachloride	.692[b]	.691[g]
Chloroform	.740[d]	.731[e]
Methanol	.530[d]	.529[f]

[a] V. C. G. Trew, *Trans. Faraday Soc.*, **49**, 604 (1953). [b] C. M. French and V. C. G. Trew, *ibid.*, **41**, 439 (1945). [c] C. M. French, *ibid.*, **43**, 356 (1947). [d] S. Broersma, *J. Chem. Phys.*, **17**, 873 (1949). [e] Value used in references 2c. [f] D. B. Woodbridge, *Phys. Rev.*, **48**, 672 (1935).

Plots of typical data are given in Fig. 1. The frequencies are expressed relative to benzene as an external reference. A summary of the results is presented in Table I. In each experiment the proportions of components 1 and 2 were varied over wide ranges, while components 3 and 4 were present in small and constant volume fractions. The figures in the table give the total frequency shift of the line due to the indicated component as the mole fraction N_1 of component 1 is varied from 0 to 1. (It was necessary to make a small extrapolation to obtain results at $N_1 = 0$ and 1.0.) A positive number indicates a shift toward higher field (greater number of c.p.s. from benzene) with increasing N_1.

Experiments A, B and C demonstrate the behavior of the tetramethylsilane resonance in solutions containing varying proportions of a hydrogen bonding molecule and a relatively inert, non-polar molecule. The shifts of 1–3 c.p.s. probably arise from variations in the molecular interactions between tetramethylsilane and its changing environment. The shift in C, which includes a substantial susceptibility correction, is not noticeably different from A and B, where no correction was needed.

In experiments D and E (with only non-polar molecules) the frequency shifts of both tetramethylsilane and the hydrocarbon are not significantly different from those in A-C, where alcohols were present. All three molecules present in D are isotropic or nearly isotropic and would be expected theoretically[5] to undergo little or no magnetic interaction. The observed 4 c.p.s. shift might be due to perturbations not included in Stephen's treatment or possibly to errors in susceptibility measurement or isomeric composition of the hydrocarbon.

The large shifts observed in F, where practically no susceptibility correction is needed, must be

attributed to the effect of molecular interactions, probably arising from the large magnetic anisotropy of benzene.[4,13] It is noteworthy that the tetramethylsilane and cyclohexane frequencies shift nearly as much as that of benzene. Although Tiers[6] has commented on the discrepancies to be found in aromatic systems, his figures do not indicate the extent of the interaction effect or the degree to which tetramethylsilane must be regarded as suspect when used as an internal reference in solutions containing aromatic components in high concentration.

In G our experimental result on the frequency shift of chloroform, which is probably self-associated through weak hydrogen bonds, is in excellent agreement with that of Reeves and Schneider.[2] The corrected shift of 9 c.p.s. differs from the reported 11 c.p.s.[2] because of a different choice of susceptibility data. The 2 c.p.s. shift of the cyclohexane frequency is in accord with the results of A-E.

The origin of the small frequency shifts (1–4 c.p.s.) observed in most of these experiments is far from clear. Although the treatment by Stephen[5] suggests some of the types of interaction that can cause such effects, the theory is not sufficiently refined to permit a meaningful calculation of the magnitude of these small shifts.

When the data of Bothner-By and Glick[3,13] are analyzed in terms of frequency shifts not accounted for by the classical susceptibility correction, rather than in terms of an empirical shape factor, it is seen that the only shifts significantly larger than those found in the present work are for aromatic systems and for molecules containing highly polarizable iodine atoms (CHI_3 and CH_2I_2). In both instances interactions are predicted to be large and can be accounted for in order of magnitude.[5] In the present study there is apparently no dependence of interaction shift on susceptibility change. Thus there seems to be little or no justification for using an arbitrarily averaged empirical factor in externally referenced systems.

With regard to internal references, the present study shows that the strong perturbations involved in hydrogen bonding do not exert a measurable influence on the resonance frequency of an "inert" reference compound such as cyclohexane or tetramethylsilane. This behavior is in marked contrast to the frequency shift of the hydrogen bonded proton, which frequently amounts to 200 c.p.s. or more (at 40 mc.p.s.) for a moderately strong hydrogen bond.[2] In the study of such strong bonds a 2–3 c.p.s. shift of the reference frequency is likely to be negligible; but with weak hydrogen bonds, where the total shift may be less than 10 c.p.s.,[14] it is apparent that measurements made with an internal reference can be seriously in error. It is clear, too, from our results that an internal reference should be avoided whenever possible in a system containing aromatics at high concentration.

Acknowledgment.—We would like to thank Mr. Robert B. Bradley for collaborating in this investigation.

(13) A. A. Bothner-By and R. E. Glick, *J. Chem. Phys.*, **26**, 1651 (1957).

(14) *Cf.* experiment G and references 2c,e.

PHENOMENOLOGICAL THEORY OF ION SOLVATION. EFFECTIVE RADII OF HYDRATED IONS

BY E. R. NIGHTINGALE, JR.

Department of Chemistry, University of Nebraska, Lincoln 8, Nebraska

Received January 10, 1959

The empirical correction to Stokes' law proposed by Robinson and Stokes has been extended for small ions to provide a concordant set of radii for the hydrated ions. Ions with a crystal ionic radius of about 2 Å. exhibit a minimum hydrated radius of 3.3 Å. corresponding to the maximum in the equivalent conductance. The internal consistency of the set of radii is demonstrated by correlation with the temperature coefficient of equivalent conductance, the viscosity *B*-coefficient and the partial molar ionic entropy. Except for the small monatomic ions with the minimum hydrated radius, the hydrated ionic radius at 25° is demonstrated to be a linear function of the viscosity *B*-coefficient. The significance of this relation is discussed in terms of the structural modification rendered by the ions to water.

Introduction

The interpretation of ionic processes in solution, particularly in water, has been the subject of many discussions. The recent monographs by Harned and Owen,[1] and Robinson and Stokes[2] summarize well the present status of the field. One of the most difficult problems encountered in studying electrolyte solutions is that concerning the nature of the ion–solvent interaction, and the interpretation of thermodynamic and transport processes in terms of appropriate parameters such as the effective radii of solvated ions. Much of the difficulty arises because the applicability of a single model to represent the various phemonena has never been demonstrated and, in fact, is not to be expected, for solvation as measured by irreversible transport phenomena is quite different from that inferred from thermodynamic measurements. Thermodynamic interpretations require *a priori* a suitable theory of ionic interaction and solvation. Hence it is probable that transport processes can provide the most appropriate information concerning the ion–solvent interaction since these processes supply information concerning the nature of the kinetic entities. The present discussion concerns the derivation of a consistent set of radii

(1) H. S. Harned and B. B. Owen, "Physical Chemistry of Electrolyte Solutions," Reinhold Publ. Corp., 3rd ed., New York, N. Y., 1957.

(2) R. A. Robinson and R. H. Stokes, "Electrolyte Solutions," Academic Press, Inc., New York, N. Y., 1955.

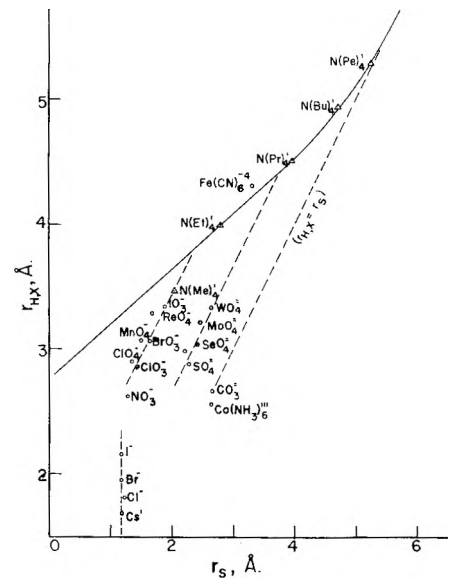

Fig. 1.—Calibration curve for determining corrections to Stokes' law radii: solid line, effective hydrated radius r_H *vs.* Stokes radius r_s; broken lines, crystal radius r_x *vs.* Stokes radius.

for the hydrated ions and the correlation of this set with viscosity parameters and partial molar ionic entropies.

Derivation of the Model.—The transport processes of conductance and diffusion are unique in providing ionic parameters directly from experimental measurements. By means of the relations of G. G. Stokes and of Stokes and Einstein, the radius, r_s, of migrating or diffusing species may be calculated using equation 1, where z is the

$$r_s = 0.820z/\lambda^0\eta^0 = 0.732 \times 10^{-8}T/D^0\eta^0 \qquad (1)$$

absolute charge of the ion, λ^0 is the limiting ionic equivalent conductance, η° is the viscosity of the solvent, T is the absolute temperature and D° is the limiting ionic diffusion coefficient. However, Stokes' law radii, calculated from limiting equivalent conductances, are often inappropriately small because water is not a continuous medium and the radii of the hydrated ions usually are not sufficiently large compared with that of the water molecules for the conditions of viscous flow to be fulfilled. In order to measure effectively the deviations from Stokes' law for small ions, it is desirable to establish a calibration procedure based upon ions whose radii in solution are known, and consequently, upon the crystal radii of ions which are unhydrated. Recently, Robinson and Stokes[3] have proposed such a correction to Stokes' law to represent the size of the solvated ions in water. By assuming that the large tetraalkylammonium ions possess a sufficiently small surface charge density to be unhydrated, a calibration curve is prepared by plotting r_x/r_s *vs.* r_s where r_x is the crystal ionic radius and r_s is the Stokes radius of the tetraalkylammonium ions. From this curve, the corrected or effective hydrated radius may be determined for those species with a Stokes radius greater than about 2.5 Å. However, since r_x/r_s diverges as r_s goes to zero, the determination by extrapolation of the effective hydrated radius for those species with a Stokes radius less than 2.5 Å. is highly uncertain.

The present procedure assumes that all of the tetraalkylammonium ions except the tetramethylammonium ion are unhydrated. In order to compensate for the inapplicability of the Robinson–Stokes procedure for small ions, the effective or hydrated radius, r_H, of an ion is defined by a calibration curve which possesses a finite limit as r_s goes to zero. The calibration curve is prepared by plotting r_x (ordinate) *vs.* r_s (abcissa) for the tetraalkylammonium ions, and using this curve, the deviations from the Stokes' law radius and the necessary corrections thereto may be evaluated. These modifications to the Robinson–Stokes treatment are essential to the definition of the effective hydrated radii for ions with a maximum equivalent conductance (minimum Stokes radius). If the calibration curve is properly established, the "corrected" radius for any hydrated ion is given by the ordinate value corresponding to the Stokes radius for that ion.

Figure 1 illustrates the calibration curve prepared by plotting the crystal radius against the Stokes radius for all the tetraalkylammonium ions except the tetramethylammonium ion. While the question of extrapolating this curve to small values of the Stokes radius still remains, it is reasonable to assume that the curve cannot exhibit a minimum, and it is difficult to avoid the implication that the ordinate intercept approaches the diameter of a water molecule, 2.76 Å., as r_s goes to zero. In this work, the value 2.69 Å. has arbitrarily been chosen as the limiting value for r_H, although the exact magnitude is not critical in as much as Stokes radii less than 1.1 Å. are not observed except for the hydrogen and hydroxyl ions. Using the calibration curve thus established, the Stokes radii of 0.28 Å. for the hydrogen ion and 0.46 Å. for the hydroxyl ion correspond, perhaps fortuitously, to hydrated radii of 2.82 and 3.00 Å., respectively.

Several features of the calibation curve in Fig. 1 are significant. For ions with a Stokes radius greater than 5.2 Å., the Stokes radius is equal to the crystal radius, verifying the Stokes relation for large ions. The deviations of the tetraethyl-, tetra-*n*-propyl- and tetra-*n*-butylammonium ions from this relation are indicative of the inapplicability of Stokes' law for ions whose crystal radius is not large compared with that of the solvent molecules. If the ions upon which this calibration curve is based are unhydrated, the curve should be unique and independent of temperature. As shall be discussed in a later section, the product of the viscosity of the solvent by the limiting equivalent conductance for all the tetraalkylammonium ions except the tetramethylammonium ion is a constant (Walden's rule), and the temperature independence of the calibration curve is verified experimentally. From these relations, it is clear that the assumption by Robinson and Stokes that the tetramethylammonium ion is unhydrated is incorrect, for the calibration curve cannot exhibit an inflection. An inflection in this curve would contradict the experimental relation between

(3) Ref. 2, p. 118 ff.

TABLE I

COMPARISON OF CRYSTAL, STOKES AND HYDRATED RADII AT 25°

Ion	r_X, Å.[a]	r_S, Å.	r_H, Å.
$(Me)_4N^+$	3.47[b]	2.05	3.67
$(Et)_4N^+$	4.00[b]	2.82	4.00
$(n\text{-}Pr)_4N^+$	4.52[b]	3.94	4.52
$(n\text{-}Bu)_4N^+$	4.94[b]	4.72	4.94
$(n\text{-}Pe)_4N^+$	5.29[b]	5.26	5.29
H^+	...	(0.28)	(2.82)
Li^+	0.60	2.38	3.82
Na^+	0.95	1.84	3.58
K^+	1.33	1.25	3.31
Rb^+	1.48	1.18	3.29
Cs^+	1.69	1.19	3.29
Ag^+	1.26	1.48	3.41
Tl^+	1.44	1.23	3.30
NH_4^+	1.48	1.25	3.31
Be^{+2}	0.31	4.09	4.59
Mg^{+2}	.65	3.47	4.28
Ca^{+2}	.99	3.10	4.12
Sr^{+2}	1.13	3.10	4.12
Ba^{+2}	1.35	2.90	4.04
Ra^{+2}	1.52[c]	2.76	3.98
Mn^{+2}	0.80	3.68	4.38
Fe^{+2}	.75	3.44	4.28
Co^{+2}	.72	3.35	4.23
Ni^{+2}	.70	2.92	4.04
Cu^{+2}	.72[d]	3.25	4.19
Zn^{+2}	.74	3.49	4.30
Cd^{+2}	.97	3.41	4.26
Pb^{+2}	1.32[c]	2.83	4.01
Al^{+3}	0.50	4.39	4.75
Cr^{+3}	.64	4.12	4.61
Fe^{+3}	.60	4.06	4.57
La^{+3}	1.15	3.96	4.52
Ce^{+3}	1.1[e]	3.96	4.52
Tm^{+3}	0.9	4.22	4.65
$Co(NH_3)_6^{+3}$	2.55[e]	2.71	3.96
OH^-	1.76	(0.46)	(3.00)
F^-	1.36	1.66	3.52
Cl^-	1.81	1.21	3.32
Br^-	1.95	1.18	3.30
I^-	2.16	1.19	3.31
NO_3^-	2.64[f]	1.29	3.35
ClO_3^-	2.88[f]	1.42	3.41
BrO_3^-	3.08[f]	1.65	3.51
IO_3^-	3.30[f]	2.22	3.74
ClO_4^-	2.92[f]	1.35	3.38
IO_4^-	3.19[f]	1.68	3.52
MnO_4^-	3.09[f]	1.50	3.45
ReO_4^-	3.30[f]	1.66	3.52
CO_3^{-2}	2.66[f]	2.66	3.94
SO_4^{-2}	2.90[f]	2.30	3.79
SeO_4^{-2}	3.05[f]	2.43	3.84
MoO_4^{-2}	3.23[f]	2.47	3.85
CrO_4^{-2}	3.00[f]	2.22	3.75
WO_4^{-2}	3.35[f]	2.65	3.93
$Fe(CN)_6^{-4}$	4.35	3.32	4.22

[a] L. Pauling, "Nature of the Chemical Bond," Cornell University Press, 2nd. ed., Ithaca, N. Y., 1948. [b] Ref. 2, p. 120. [c] V. M. Goldschmidt, *Ber.*, 60, 1263 (1927). [d] F. Basolo and R. G. Pearson, "Mechanisms of Inorganic Reactions," John Wiley and Sons, New York, N. Y., 1958, p. 66. [e] Estimated. [f] M–O covalent radius + 1.4 Å. (see ref. *a*). Many of the crystallographic M–O radii are available in the literature.

the equivalent conductance of an ion and the crystal ionic radius. Having established the calibration curve on the basis of the crystal radii of the tetraalkyl ammonium ions, the ordinate in Fig. 1 now becomes the effective radius of any ion in solution, hydrated or not, with a given Stokes radius.[4]

For comparison, the crystal ionic radius of a number of ions has also been plotted in Fig. 1 as a function of the Stokes radius at 25°. The Stokes radius for oxygenated anions of a given charge type is a linear function of the crystal radius. For a given crystal radius, the divalent oxy-anions exhibit a larger Stokes radius than univalent ions of the same size indicative of the more extensive hydration of the divalent ions. Consequently, the correction necessary to obtain the proper hydrated radius for univalent ions is less than for those of higher charge type. The monatomic ions exhibit a minimum Stokes radius of about 1.1 Å. corresponding to the maximum observed when the limiting equivalent conductance is plotted as a function of the crystal radius. Table I compares the crystal, Stokes and hydrated radii for a number of ions.

In Fig. 2, the hydrated radius for some of the uni-, di- and trivalent ions at 25° is plotted as a function of the crystal ionic radius. The most striking feature of this plot is the minimum at r_H = 3.3 Å. for univalent ions corresponding to the maximum in the limiting equivalent conductance. Traditionally, these ions, K^+, Rb^+, Cs^+, Cl^-, Br^- and I^-, etc., have often been considered to be unhydrated. The present evidence demonstrates that these ions are hydrated but that the extent of their hydration is minimal.[5] The broad minimum for univalent ions in Fig. 2 is interpreted to indicate that hydration in the first layer about an ion may occur over a wide range of ion sizes or surface charge densities. If one assumes a simple ion–dipole interaction between an ion and the first layer of water molecules about the ion, and further assumes that an ion is hydrated when the energy of the ion–dipole interaction exceeds the heat of vaporization per molecule of water at 25°, then a univalent ion will be hydrated when the ion–dipole distance is less than about 3.7 Å. corresponding to a crystal ionic radius of 2.3 Å. or less. This approximation predicts that the iodide and smaller ions will be hydrated while the nitrate and larger ions will be unhydrated in the sense of formal ion–solvent bond formation. As the surface charge density increases with decreasing crystal radius hydration may occur in the second and subsequent

(4) Recent studies by H. S. Frank and W. Y. Wen (private communication) on the apparent partial molal heat capacity of the tetraethanolammonium ion indicate that the tetraalkylammonium ions are not entirely free from solvent interaction. If the former species more nearly represents the "ideal solute," a small shift in the ordinate axis in Fig. 1 may be indicated.

(5) Several recent investigations provide evidence for the hydration of the halide and large alkali metal ions. See J. B. Hasted, D. M. Ritson and C. H. Collie, *J. Chem. Phy.*, **16**, 1 (1948); F. E. Harris and C. T. O'Konski, THIS JOURNAL, **61**, 310 (1957); O. Ya. Samoilov, *Disc. Faraday Soc.*, **24**, 141 (1957); M. Smith and M. C. R. Symons, *ibid.*, **24**, 206 (1957).

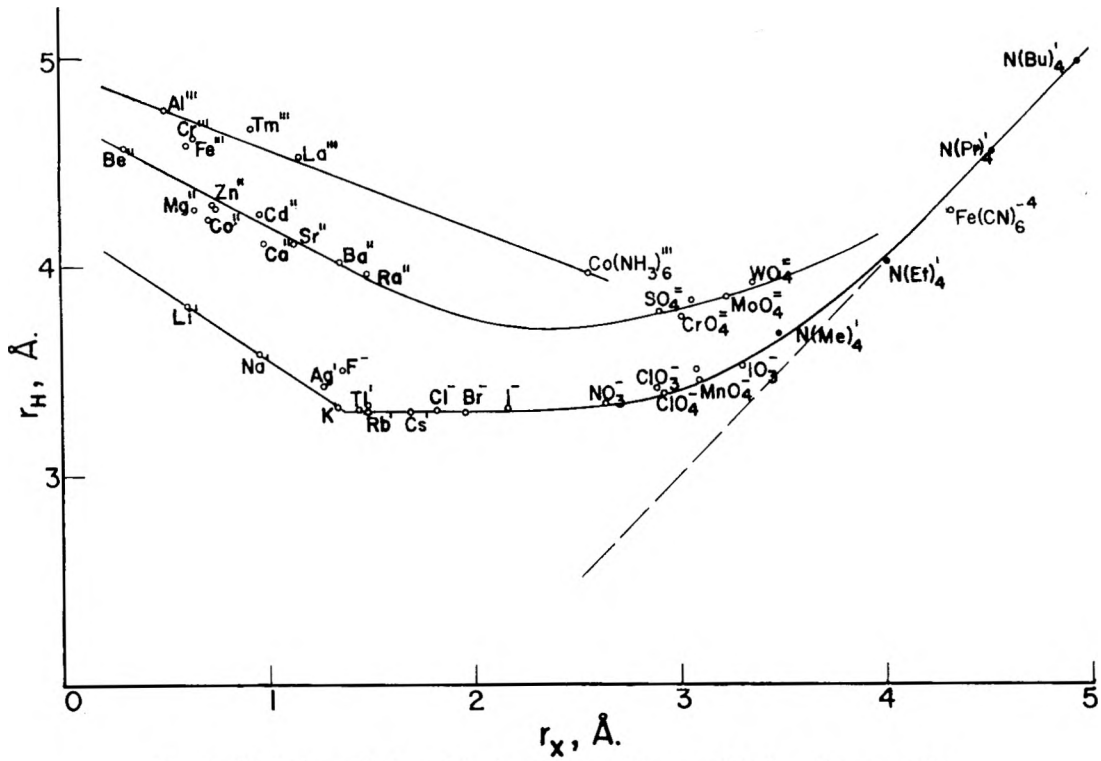

Fig. 2.—Variation of hydrated ionic radius r_H with crystal ionic radius r_x, at 25°.

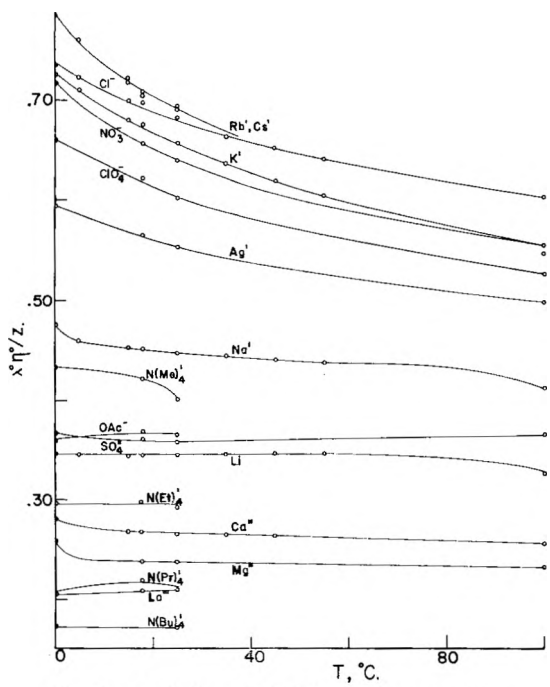

Fig. 3.—Variation of $\lambda°\eta°/z$ with temperature.

layers about the ion, and the hydrated radius of the ion increases.

Discussion

Temperature Coefficient of Limiting Equivalent Conductance.—In constructing the calibration curve in Fig. 1, the extrapolation procedure introduced uncertainty into the determination of the effective radius of those ions with Stokes radius between 1.1 and 2.5 Å. The best evidence for the correctness of the present procedure comes from the temperature coefficient of the limiting equivalent conductance. Figure 3 illustrates the product $\lambda°\eta°/z$ as a function of the temperature. Those ions for which $\lambda°\eta°/z$ is less than about 42 obey Walden's rule. This behavior indicates that the viscosity dependence required by Stokes' law is of the correct form even though the Stokes radius must be corrected because the ions are not sufficiently large compared with the size of the water molecules for the conditions of viscous flow in a continuous medium to be fulfilled. Because Walden's rule accounts for the variation of equivalent conductance with viscosity, the Stokes and hydrated radii of these ions are independent of temperature.

Walden's rule is not obeyed for the small ions for which $\lambda°\eta°/z$ is greater than 45, and the Stokes radius for these ions increases with temperature. Qualitatively, this suggests that these ions which possess a minimum hydration at low temperatures tend to become more highly hydrated as the structure of water is destroyed by the increase in thermal energy at the higher temperatures. Two ions, the sodium ion and the tetramethylammonium ion, lie in the intermediate region $42 < \lambda°\eta°/z < 45$ in which the deviations from Walden's rule begin to occur. These two ions are interpreted as being approximately equal in their effective hydrated radius (Table I) and intermediate in size between those ions which are too small to obey Walden's rule and those ions for which the rule is followed. Thus the behavior of the highly hydrated sodium ion and the slightly hydrated tetramethylammonium ion, whose crystal radii lie on either side of the minimum in Fig. 2, infers that the extrapolation procedure used in Fig. 1 is of the correct form.

The temperature dependence of the hydrated radii for small ions requires that the portion of the curve in Fig. 2 for univalent ions with hydrated radius less than 3.7 Å. must not be temperature independent and is defined only at a single temperature (25°).

Viscosity *B*-Coefficient.—The significance of the present set of hydrated radii, other than as a measure of the relative sizes of the ions as determined by transport processes, is best illustrated by their relation to the *B*-coefficient in the Jones–Dole equation[6] for the viscosity of strong electrolytes. The *B*-coefficient is a measure of the order or disorder introduced by the ions into their cospheres, although no satisfactory theoretical treatment has yet been given. A positive *B*-coefficient indicates that the ions tend to order the solvent structure and increase the viscosity of the solution, while a negative *B*-coefficient indicates disordering and a decrease of viscosity. The partitioning of the *B*-coefficients into their ionic components was first proposed by Cox and Wolfenden[7] and recently has been reexamined by Gurney[8] and Kaminsky.[9] Gurney defined the *B*-coefficient of the potassium ion as equal to that of the chloride ion at 25° based upon the fact that the ratio $(\lambda^\circ\eta^\circ)_{18^\circ}/(\lambda^\circ\eta^\circ)_{0^\circ}$ for the two ions is equal. From the relations in Fig. 3, it is apparent that this assignment still is to be considered tentative, for above 18°, a more satisfactory partitioning based solely on the conductance relations would relate the chloride and the rubidium or even cesium ions. A definitive assignment must await a satisfactory theory for the *B*-coefficient.

In Fig. 4, the viscosity *B*-coefficient for a number of ions at 25° is plotted as a function of the hydrated radius. Except for the monatomic ions with negative *B*-coefficients, it is observed that for each class of ions (M^{+a}, XO_3^-, XO_4^{-b}, etc.), the viscosity *B*-coefficient is a linear function of the hydrated radius. Consequently, with the single exception of the monatomic ions with negative *B*-coefficients, the hydrated radius measures the region about an ion in which the solvent is more or less ordered than in bulk water. While not shown in Fig. 4, the tetraethylammonium ion lies exactly on and the tetrabutylammonium ion lies close to the line for the XO_4^{-b} ions. This behavior infers that the *B*-coefficients for all tetrahedral ions are a single function of the effective hydrated radius of these ions. It should be emphasized that tetrahedral ions such as the tetraalkylammonium cations and the tetraoxygenated anions are not spherically symmetrical with respect to the surface charge density. The separate functions exhibited in Fig. 4 for the hydrated monatomic ions and the tetrahedral ions necessarily are attributed to the charge assymmetry of the tetrahedral ions, although the effect of tetrahedral ions such as the perchlorate ion fitting into the water lattice[10] more appropriately than do the spherically symmetrical monatomic ions should not be discounted.

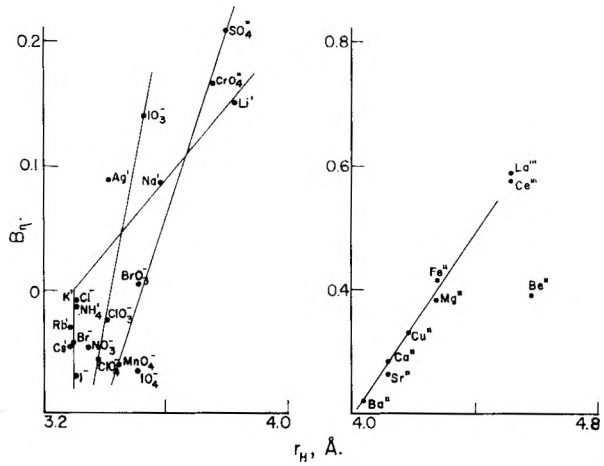

Fig. 4.—Variation of hydrated radius r_H with viscosity ionic *B*-coefficient at 25°.

The significance of the relation between the *B*-coefficient and the hydrated radius is well supported by the recent discussions of Frank and Wen[11] and Podolsky.[12] In considering the nature of ion–solvent interactions in aqueous solution, Frank and Wen have proposed a model to represent the structural modification of the solvent produced by an ion in water. Three regions about the ion are proposed: (a) an innermost region A in which the water molecules are firmly bound to the ion and immobilized by the electric field of the ion; (b) an intermediate zone B in which the water molecules are less organized than in bulk water; and (c) an outer region C in which the normal structure of water prevails. This model is particularly well adapted to the present discussion of the viscosity *B*-parameter. A positive *B*-coefficient for a hydrated ion appears to measure the effective radius of Frank's A-region in which the water is highly ordered about the ion. Presumably, a finite but small B-zone still exists about the hydrated ion. In any event, the effect of this zone of disorder is negligibly small compared with that of the ordered solvent immediately surrounding the ion. Negative *B*-coefficients indicate that the B-zone encroaches upon the A-region to the extent that, for the larger ions, virtually no A-region exists because of the weak electric field about such ions. For large unhydrated ions, the positive *B*-coefficient reflects a viscosity increment which arises in the same manner as for non-polar solutes where the increase in the ice-like structure is proportional to the size of the non-polar region.[11]

In considering the nature of transport processes in electrolyte solutions, Podolsky[12] has plotted, in a figure analogous to our Fig. 2, the ionic *B*-coefficient *versus* the crystal radius. It is demonstrated that the width of the "U-shaped curve for the univalent ions is of the same order as the diameter of the water molecules" supporting "the classical view that large ions—migrate as the naked ion, while the small ions—move with a single layer of

(6) G. Jones and M. Dole, *J. Am. Chem. Soc.*, **51**, 2950 (1929).

(7) W. M. Cox and J. H. Wolfenden, *Proc. Roy. Soc. (London)*, **A145**, 475 (1934).

(8) R. W. Gurney, "Ionic Processes in Solution," McGraw-Hill Book Co., Inc., New York, N. Y., 1953, p. 160 ff.

(9) M. Kaminsky, *Z. Naturforsch*, **12a**, 424 (1957).

(10) Th. G. Kujumzelis, *Z. physik*, **110**, 742 (1938).

(11) H. S. Frank and W. Y. Wen, *Trans. Faraday Soc.*, **24**, 133 (1957).

(12) R. J. Podolsky, *J. Am. Chem. Soc.*, **80**, 4442 (1958).

electrostatically bound water molecules".[13] If the distance between equilibrium positions of the solute particles in the solution lattice is independent of the activation energy for transition of the particles, the mode of transport for hydrated and unhydrated ions is approximately the same, and it is not necessary to envision the same transport mechanism for ions with widely varying (crystal) radii.

The relation between the viscosity B-coefficient and the hydrated ionic radius should not be confused with the Einstein relation[14] which predicts that the increase in the viscosity of the solution is proportional to the volume fraction of the solute particles. This relation was derived for unhydrated solute species in a continuous medium and is not applicable to ions whose size is not large compared with that of the solvent molecules. The volume fraction calculated for a one molar solution of ions with a crystal radius of about 5 Å. is small as compared, using the Bingham relation,[15] with the B-coefficient for such ions.

Except for the iodide ion, negative B-coefficients appear to be peculiar to water and to temperatures less than about 40°. Referring to Fig. 2, only monatomic ions with the minimum hydrated radius (3.3–3.4 Å.) exhibit negative B-coefficients in water at 25°. Only ions whose effective radius in water is small can loosen or disrupt locally the pseudo-tetrahedral structure of water in the cosphere about the ion and decrease the viscosity of the solution. The recent data by Kaminsky on the temperature coefficient of ionic B-coefficients[7] yields evidence concerning the extent of the ion–solvent interaction. Unfortunately however, Kaminsky also defined the ionic B-coefficients by assuming that the values for the potassium and chloride ions are equal at all temperatures. This procedure was improperly justified by the similarity of the equivalent conductances for these two ions in the temperature range considered. As indicated above, the divergence of λ° for the potassium ion from that of the chloride ion at temperatures above 18° is too large for this assumption to be rigorous. Nevertheless, Kaminsky's data indicates that the B-coefficient increases with temperature for those ions which may be characterized by (1) a negative B-coefficient at 25°, or (2) a Stokes radius which is temperature dependent ($\lambda^0\eta^0/z > 45$), or (3) a minimal hydrated radius with r_H less than about 3.5 Å. at 25°. Qualitatively the increase in the B-coefficient correlates with the decrease in $\lambda^0\eta^0$ with temperature, and is further evidence for a more extensive hydration of these ions as the structure of water is destroyed with increasing temperature.

For some of the highly hydrated ions such as Li^+, Be^{+2} and Ce^{+3}, whose crystal radii are small, the B-coefficients decrease with temperature over the range 15 to 42.5°. This behavior appears to infer that the relative magnitude of ordering of the solvent about the ion decreases with increasing thermal energy as does the ordering of the water structure itself.

Kaminsky has cited the similarity between the temperature coefficients of the viscosity B-coefficient, the apparent molal heat capacity and the apparent molal volume as evidence for the appropriateness of his assignment of ionic B-coefficients. However, the uncertainty in the partitioning of the molecular values is sufficient to render uncertain any conclusions concerning the magnitude of dB/dT. If, as indicated in Fig. 3, the effective hydrated radius of the potassium ion increases with temperature more than does that for the chloride ion, the decrease in the B-coefficient for the highly hydrated cations with increasing temperature is less than that given by Kaminsky and the increase in the B-coefficient for the slightly hydrated anions becomes greater. It may be noted that a more satisfactory relation is obtained between the B-coefficient and the partial molal volume, both of which entail the electrostricted volume of the water molecules about the ion, if a less negative temperature coefficient is assigned to the hydrated cations. The assignment of ionic B-coefficients at 25° is strengthened considerably by the relation with the partial molar ionic entropy (*vide infra*), but entropy data at temperatures different from 25° are not at present available to test these relations further.

Partial Molar Entropy of Hydrated Ions.—When a strong electrolyte is dissolved in water, the sum of the partial molar entropies for the ions of the salt in solution, $\bar{S}^0_{aq}$, is given by

$$\bar{S}^0_{aq} = \bar{S}^0_{ref} + \Delta S_{soln} \qquad (2)$$

where $\bar{S}_{ref}$ is the absolute partial molar entropy for the solute in its reference state (*i.e.*, the Third Law entropy for crystalline salts) and ΔS_{soln} is the experimentally measured change in the entropy which results from dissolving 1 mole of solute in its reference state into 1000 g. of solvent. The partitioning of $\bar{S}^0_{aq}$ into its ionic components has been the subject of numerous discussions.[16] Gurney[8] has recently demonstrated a linear relation between the viscosity B-coefficient and the partial molar entropy for monatomic ions. This relation has been the basis for his selection of the value -5.5 e.u. as the absolute partial molar entropy of the hydrated hydrogen ion at 25°. While the evidence for this value is convincing, the acceptance of this value[17,18] is still subject to experimental confirmation. By virtue of the relation between the viscosity B-coefficient and the partial molar ionic entropy, the hydrated radii for the various classes of ions in Fig. 4 are also a linear function of the partial molar ionic entropy.

The Gurney relation correlates a single class of ions, the monatomic ions, but requires separate functions for the various classes. The present discussion and the relations demonstrated in Fig. 4 suggest that the various classes of ions may be represented by a single function if allowance is made for differences in the reference state of the pure solutes and also for configurational contributions to the ionic entropy. In order to compensate for

(13) The more appropriate interpretation is that the difference between the effective hydrated radius r_H and the crystal radius r_x for small and large ions is of the order of the diameter of a water molecule. See Table I.

(14) A. Einstein, *Ann. physik. Lpz.*, **19**, 289 (1906); **34**, 591 (1911).

(15) E. C. Bingham, THIS JOURNAL, **45**, 885 (1941).

(16) Ref. 2, p. 66 ff; ref. 8, p. 172 ff; and references cited therein.

(17) K. H. Laidler, *Can. J. Chem.*, **34**, 1107 (1956).

(18) L. G. Hepler, THIS JOURNAL, **61**, 1426 (1957).

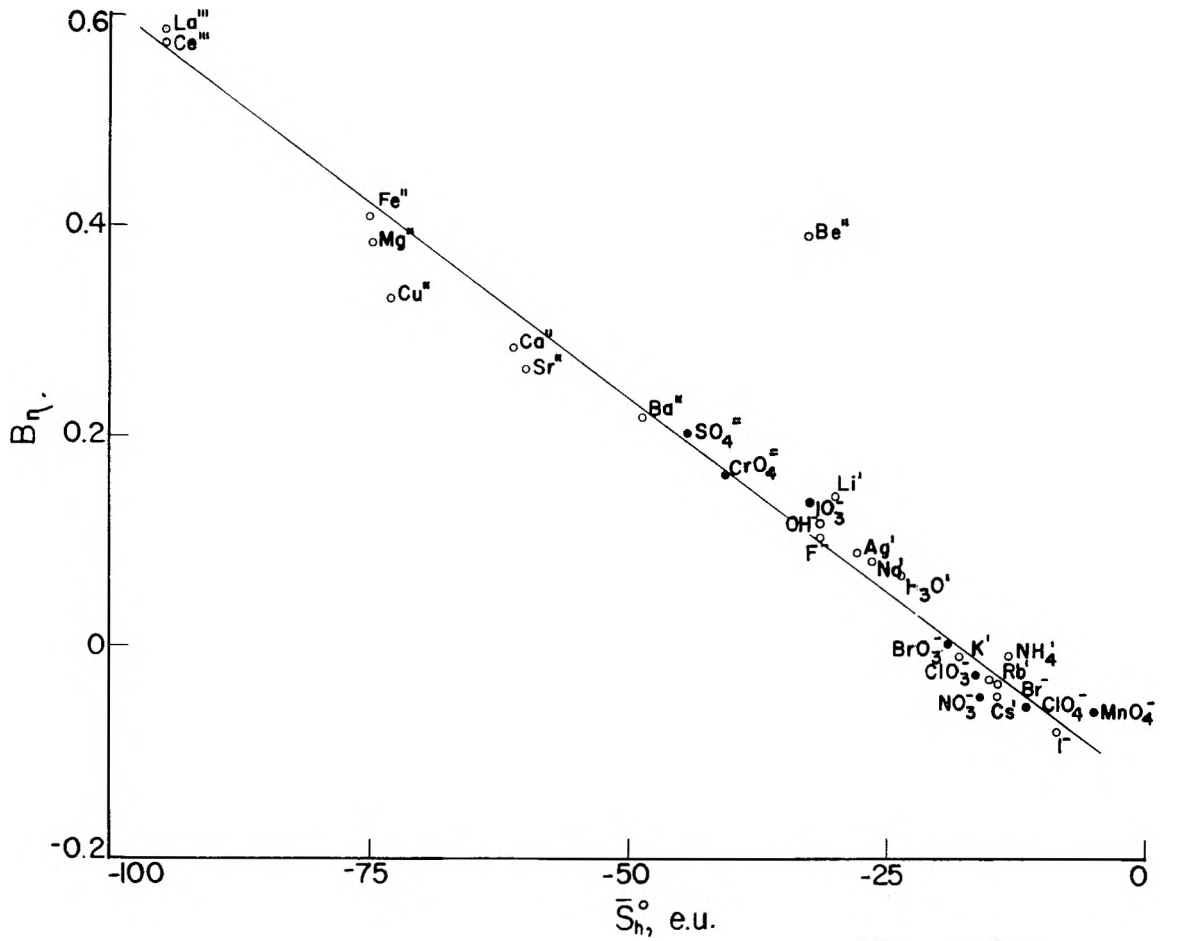

Fig. 5.—Variation of viscosity ionic B-coefficient with partial molar entropy of hydration, $\bar{S}^0_h$, at 25°. $(\bar{S}^0_{H^+})_{aq} = -5.5$ e.u.

these differences, it is desirable to compute the entropy of hydration, $\bar{S}^0_h$ for the aqueous ions relative to that for the ions in the hypothetical ideal gas state, and

$$\bar{S}^0_h = \bar{S}^0_{aq} - \bar{S}^0_g \qquad (3)$$

where $\bar{S}^0_g$ is the sum of the translational and rotational entropies of the gaseous ions as may be calculated from the Sackur–Tetrode equation and the rotational partition function respectively.[19] The partial molar entropies of hydration, relative to $(\bar{S}^0_{H^+})_{aq} = -5.5$ e.u. in the hypothetical molal solution, have been calculated for the solvation of the gaseous ions at 25° at a standard state pressure corresponding to a concentration of one mole per liter. These values are plotted as a function of the viscosity ionic B-coefficients in Fig. 5. This figure demonstrates that if the partial molar entropies of the XO_3^- and XO_4^{-b} ions are corrected for their loss in rotational entropy, the partial molar ionic entropy of hydration can be represented by a single linear function of the viscosity B-coefficient for all ions.[20] In this procedure, the polyatomic ions are assumed to lose all of their rotational entropy, and no allowance is made for libration of the ion in its solvent cage. In view of the previous considerations concerning the minimal hydration of polyatomic ions, a more rigorous treatment might allow for a small librational contribution. In as much as the viscosity B-coefficient is a measure of the order introduced by the ion into the solvent, and since positive B-coefficients measure the effective size of the hydrated ion, it appears appropriate that the B-coefficient should be related to the mass-compensated entropy of hydration rather than the absolute ionic entropy in solution.

(19) J. W. Mayer and M. G. Mayer, "Statistical Mechanics," John Wiley and Sons, New York, N. Y., 1940.

(20) A (non-linear) relation between the Bingham fluidity increment Δ, where $\Delta = -BC/\eta^0$, and the entropy of vaporization was first demonstrated by H. S. Frank and M. W. Evans, *J. Chem. Phys.*, **13**, 507 (1945).

NUCLEAR MAGNETIC SHIELDING OF PROTONS IN AMIDES AND THE MAGNETIC ANISOTROPY OF THE C=O BOND

BY P. T. NARASIMHAN AND MAX T. ROGERS

Kedzie Chemical Laboratory, Michigan State University, East Lansing, Michigan

Received January 14, 1959

The magnetic shielding of nuclei due to distant chemical groups may be calculated from a knowledge of the magnetic anisotropy of the bonds in these groups. The reverse procedure, namely, the calculation of the magnetic anisotropy of bonds from n.m.r. (nuclear magnetic resonance) shielding constants seems to offer some hope and has been employed here to estimate the magnetic anisotropy of the C=O bond from the available data on formamide and dimethylformamide. The internal chemical shift between the two protons which are *cis* and *trans* with respect to the C=O bond in acetamide and similarly the shift between the two N-methyl groups in dimethylacetamide have also been calculated.

I. Introduction

The magnetic shielding of a nucleus in a molecule due to the neighboring electron cloud has been the subject of several important theoretical investigations in recent years.[1-8] Using second-order perturbation theory Ramsey[1] has derived an equation for the shielding tensor in terms of the ground and excited state wave functions of the molecule in which the nucleus is present. The variational method has also been employed by several authors[3-5,8] and many of them have limited themselves to the case of the proton shielding in the hydrogen molecule. However, when one considers larger molecules the application of the complete perturbation theory or the variational procedure is a very difficult task indeed. Further, such an approach is not likely to be fruitful at the present state of our knowledge concerning molecular wave functions. Thus it appears desirable to make the following approximations. We consider the electron cloud immediately surrounding the nucleus in question as contributing a shielding $\underset{\sim}{\sigma}_l$, where the subscript l denotes the local shielding. Other distant charge distributions in the molecule may then be thought of as contributing $\underset{\sim}{\sigma}_d$ to the total shielding of the nucleus. Thus we may write

$$\underset{\sim}{\sigma} = \underset{\sim}{\sigma}_l + \underset{\sim}{\sigma}_d \qquad (1)$$

where $\underset{\sim}{\sigma}$ is the net shielding of the nucleus in the molecule.

The reason for this separation of the total shielding into local and distant ones is that it is easier to estimate $\underset{\sim}{\sigma}_d$ from a knowledge of the magnetic anisotropy of the distant groups. It is then necessary to carry out the perturbation or variational calculations for the region nearest to the nucleus only. In this manner we can simplify an otherwise almost intractable problem. Stephen[8] has recently made use of this procedure and has calculated the shielding constants of protons in methane, ethylene and acetylene. The variational procedure was used in his calculations for estimating $\underset{\sim}{\sigma}_l$. However, in the present work we shall not be concerned with the details for calculating $\underset{\sim}{\sigma}_l$, but since our interest is in the magnetic anisotropy ($\Delta\chi$) of bonds we shall consider in greater detail the quantity $\underset{\sim}{\sigma}_d$, this being directly related to $\Delta\chi$.

The expression for $\underset{\sim}{\sigma}_d$ in terms of the magnetic anisotropy of distant groups can be derived from the general equation for the shielding tensor on the basis of both perturbation and variational methods as has been demonstrated recently by McConnell[7] and Stephen.[8] In a classical sense, the externally applied uniform magnetic field may be thought of as inducing magnetic dipoles in these distant groups and the secondary field at the nucleus due to these dipoles as contributing to $\underset{\sim}{\sigma}_d$. For purposes of calculation we may approximate these induced dipoles by point dipoles or ideal dipoles when the distances between the nucleus and these groups are large. In high resolution n.m.r. spectroscopy, with which we are presently concerned, the samples are usually in the form of liquids or gases and the molecule containing the nucleus under consideration is assuming different orientations in the magnetic field due to molecular motions. The secondary field from the induced dipoles is thus averaged out and in order to observe a finite shielding $\underset{\sim}{\sigma}_d \neq 0$ the distant groups must be magnetically anisotropic and the molecular geometry and motions be such that these factors do not enable the condition $\underset{\sim}{\sigma}_d = 0$ to be realized.

Since the magnitude of the shielding contribution from distant groups depends on their magnetic anisotropy and molecular geometry (including changes in this) the question naturally arises whether one can obtain any information concerning the anisotropy from the experimental shielding data. In order to answer this question we have considered the n.m.r. shielding of protons which are *cis* and *trans* to the carbonyl oxygen atom in amides, and using the available anisotropy data,[9,10] we have been able to estimate the anisotropy of the C=O bond. From the data thus obtained calculations have been made of the difference in the shielding of the *cis*- and *trans*-protons in acetamide and dimethylacetamide. The results are encouraging and may serve to show the usefulness of this approach. However, before proceeding further, we shall consider the rather classical problem of the secondary field due to an induced dipole and thus

(1) N. F. Ramsey, "Nuclear Moments," John Wiley and Sons, Inc., New York, N. Y., 1953. "Molecular Beams," Clarendon Press, Oxford, 1956.

(2) H. M. McConnell, *Ann. Rev. Phys. Chem.*, **8**, 105 (1957).

(3) J. F. Hornig and J. O. Hirschfelder, *J. Chem. Phys.*, **23**, 474 (1955).

(4) T. P. Das and R. Bersohn, *Phys. Rev.*, **104**, 849 (1956).

(5) B. R. McGarvey, *J. Chem. Phys.*, **27**, 68 (1957).

(6) J. A. Pople, *Proc. Roy. Soc. (London)*, **A239**, 541, 550 (1957).

(7) H. M. McConnell, *J. Chem. Phys.*, **27**, 226 (1957).

(8) M. J. Stephen, *Proc. Roy. Soc. (London)*, **A243**, 264 (1957).

(9) J. Tillieu and J. Guy, *J. Chem. Phys.*, **24**, 1117 (1956). See also J. Tillieu, *Ann. Phys.*, **2**, 471, 631 (1957).

(10) J. Baudet, J. Tillieu and J. Guy, *Compt. rend.*, **244**, 2920 (1957).

derive a general expression for $\underset{\sim}{\sigma}_d$ along purely classical lines in terms of the magnetic anisotropy of a bond when this bond is farther away from the nucleus whose shielding is being examined.

II. Magnetic Shielding from an Anisotropic Bond

Let us now consider the shielding of the nucleus N due to an anisotropic bond A–B formed between two atoms A and B. We choose a point P somewhere along the bond as the location of the induced dipole due to the external uniform magnetic field $\vec{H}_0$ which is taken to be applied along A–B (z-axis). With P as the origin of cartesian coördinates, and denoting the radius vector between P and N by R, we can write the secondary field at N due to the ideal dipole at P as [11]

$$\vec{H}_N = -\boldsymbol{T}\vec{\mu} \tag{2}$$

where the tensor $\boldsymbol{T}$ written in dyadic form is (boldface type indicates the tensor)

$$\boldsymbol{T} = \frac{1}{R^3}\left(\mathbf{1} - 3\frac{\vec{R}..\vec{R}}{R^2}\right) \tag{3}$$

In equation 3, $\mathbf{1}$ is the unit dyad and $\vec{R}..\vec{R}$ is the dyad for the radius vector. Now, the components of the magnetic moment $\vec{\mu}$ are

$$\left.\begin{aligned}\mu_x &= \chi^b_{xx}H_x\\ \mu_y &= \chi^b_{yy}H_y\\ \mu_z &= \chi^b_{zz}H_z\end{aligned}\right\} \tag{4}$$

where χ^b_{xx}, χ^b_{yy} and χ^b_{zz} are the principal magnetic susceptibilities of the bond A–B. The magnetic field $\vec{H}_N$ at the nucleus N is related to the externally applied uniform magnetic field $\vec{H}_0$ by the shielding tensor σ_N as follows

$$\vec{H}_N = \vec{H}_0 - \sigma_N\vec{H}_0 \tag{5}$$

and hence we may write $\underset{\sim}{\sigma}_d$ as

$$\underset{\sim}{\sigma}_d = 1/3\,\frac{\boldsymbol{T}\vec{\mu}}{\vec{H}_0} \tag{6}$$

where the factor $^1/_3$ has been introduced in order to average the shielding due to molecular motions in liquids and gases. In the case of an axially symmetric bond, that is one with $\chi_{zz} \neq \chi_{yy} = \chi_{xx}$ it is easily seen that

$$\underset{\sim}{\sigma}_d = \frac{\Delta\chi}{3L_0R^3}(1 - 3\cos^2\theta_z) \tag{7}$$

where θ_z is the angle between the z-axis and the radius vector $\vec{R}$. In equation 7 $\Delta\chi$ is the molar anisotropy, namely, $\chi_{zz} - \chi_{yy} = \chi_{zz} - \chi_{xx}$ and L_0 is the Avogadro number. Equation 7 has been used by McConnell[7] in discussing proton shifts in benzene and methyl halides. For a bond with $\chi_{zz} \neq \chi_{yy} \neq \chi_{xx}$ the following expression holds good provided the y-axis (or x-axis) can be chosen such that R lies in the z–y (or z–x) plane. Thus (for R lying in the z–y plane) we have

$$\underset{\sim}{\sigma}_d = \frac{1}{3L_0R^3}(2\Delta\chi_1 - \Delta\chi_2 - \Delta\chi_1 \times 3\cos^2\theta_z) \tag{8}$$

where $\Delta\chi_1 = \chi_{zz} - \chi_{yy}$ and $\Delta\chi_2 = \chi_{zz} - \chi_{xx}$. If the radius vector does not lie in any of the three principal planes then general expression (9) has to be used.

$$\underset{\sim}{\sigma}_d = \frac{1}{3L_0R^3}(1 - 3\cos^2\theta_x)\chi_{xx} + (1 - 3\cos^2\theta_y)\chi_{yy} + (1 - 3\cos^2\theta_z)\chi_{zz} \tag{9}$$

In some cases the values of θ and/or R may change with internal molecular motions and here one must use appropriate average values (see Appendix) in the expressions $(1 - 3\cos^2\theta)_{av}$ or $[(1-3\cos^2\theta/R^3)]_{av}$ as the case may be.

III. Proton Shielding in Formamide and Dimethylformamide

The high resolution proton resonance spectrum of formamide with N^{14} has been obtained recently by Piette, Ray and Ogg[12] using a double resonance technique and by Schneider[13] with N^{15}. The proton resonance spectrum of dimethylformamide was obtained earlier by Phillips[14] and Gutowsky and Holm.[15] The evidence for restricted rotation around the C–N bond in these amides at low temperatures is conclusive and the two sites marked A and B (see Fig. 1) are magnetically non-equivalent. Since the high resolution spectra at low temperatures show that the rate of rotation around the C–N bond is so slow as to give two distinct resonance lines for the A and B type protons we may be justified in considering the planar structure for these molecules with the groups "frozen" in this position. Taking then, for example, the case of formamide (I) it is easy to show that the difference in the shielding values of the two types of protons marked A and B is a result of the difference between $\underset{\sim}{\sigma}_d{}^A$ and $\underset{\sim}{\sigma}_d{}^B$, since on account of local symmetry the $\underset{\sim}{\sigma}_l$ values of these protons will be identical. It is assumed that the effect of distant groups, such as the carbonyl group, on $\underset{\sim}{\sigma}_l$ for protons A and B is equal. Denoting the net shielding of these two types of protons by $\underset{\sim}{\sigma}^A$ and $\underset{\sim}{\sigma}^B$, we have

$$\underset{\sim}{\sigma}^A - \underset{\sim}{\sigma}^B = \underset{\sim}{\sigma}_d{}^A - \underset{\sim}{\sigma}_d{}^B \tag{10}$$

Thus we have identified the observed shielding difference of these protons with the difference in the shielding contributions to these nuclei from the distant groups, namely C=O and C–H bonds (Fig. 1)

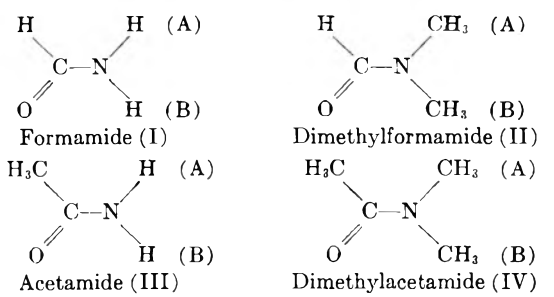

Fig. 1.—Structures of amides with magnetically non-equivalent sites marked A and B.

(11) C. J. F. Bottcher, "Theory of Dielectric Polarization," Elsevier Publishing Co., New York, N. Y., 1952.

(12) L. H. Piette, J. D. Ray and R. A. Ogg, *J. Mol. Spectroscopy*, **2**, 66 (1958).

(13) W. G. Schneider (private communication).

(14) W. D. Phillips, *J. Chem. Phys.*, **23**, 1363 (1955).

(15) H. S. Gutowsky and C. H. Holm, *ibid.*, **25**, 1228 (1956).

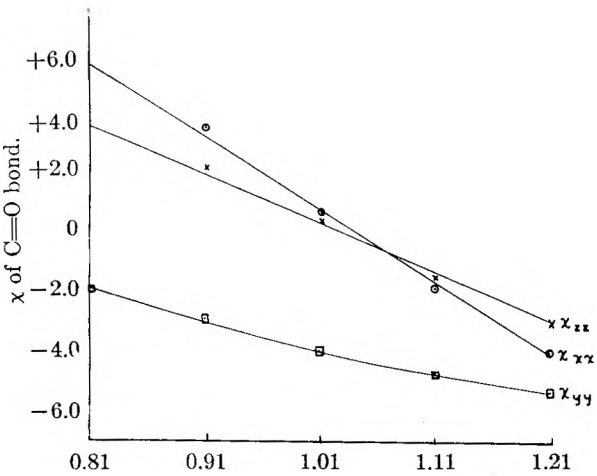

Fig. 1.

From the known geometry of these molecules it is possible to calculate this difference in shielding, that is, the internal chemical shift between A and B protons, by using the expressions given earlier for the shielding due to anisotropic bonds. (We have neglected here the contribution to σ_d from steric, electrostatic and similar factors. To a certain extent these are included in the molecular geometry as well as the bond anisotropy.) Thus, we have in the case of formamide

$$\sigma^A - \sigma^B = \frac{1}{3L_0}\left\{\left[\frac{(2\Delta\chi_1 - \Delta\chi_2 - \Delta\chi_1 3\cos^2\theta_{OA})}{R^3_{OA}} + \Delta\chi_{CH}\frac{(1 - 3\cos^2\theta_{HA})}{R^3_{HA}}\right] - \left[\frac{(2\Delta\chi_1 - \Delta\chi_2 - \Delta\chi_1 3\cos^2\theta_{OB})}{R^3_{OB}} + \Delta\chi_{CH}\frac{(1 - 3\cos^2\theta_{HB})}{R^3_{HB}}\right]\right\} \quad (11)$$

The subscripts A, B, refer to the nuclei and O and H refer to the locations of the point dipoles of the C=O and C–H bonds. The molecule is taken to be in the z–y plane (z-axis along the bonds) and $\Delta\chi_1$ and $\Delta\chi_2$ refer to the C=O bond and are defined following equation 8. In the case of the C–H σ-bond we have $\chi_{zz} \neq \chi_{yy} = \chi_{xx}$ and hence we have used equation 7 while for the C=O bond, which involves a π-bond, equation 8 has been used in deriving expression 11.

For the evaluation of the internal shift between the protons of the two N-methyl groups in dimethylformamide equation 11 is not applicable since the rotation of these methyl groups around their respective N–C bonds causes the angles and distances between the C=O dipole, and similarly the C–H dipole of the CHO group, and these methyl protons to vary. We must therefore make use of the general expression (equation 9) and also use suitable averages. Thus for dimethylformamide (II) the following expression holds good

$$\sigma^A - \sigma^B = \frac{1}{3L_0}\{(T^0_{Ax} - T^0_{Bx})\chi_{xx}^{C=O} + (T^0_{Ay} - T^0_{By})\chi_{yy}^{C=O} + (T^0_{Az} - T^0_{Bz})\chi_{zz}^{C=O} + [(T_{Ax}{}^H - T_{Bx}{}^H) + (T_{Ay}{}^H - T_{By}{}^H)]\chi_{xx}^{C-H} + (T_{Az}{}^H - T_{Bz}{}^H)\chi_{zz}^{C-H}\} \quad (12)$$

where, for example

$$T^0_{Az} = \left(\frac{1 - 3\cos^2\theta_{OA}}{R^3_{OA}}\right)_{av} \quad (13)$$

and

$$T'_{Az}{}^H = \left(\frac{1 - 3\cos^2\theta_{HA}}{R^3_{HA}}\right)_{av} \quad (14)$$

$\chi_{zz}^{C=O}$ refers to the C=O bond and χ_{zz}^{C-H} to the C–H bond. Details of the method of evaluating the average values (equations similar to 13) are given in the Appendix.

It will be seen from equation 11 that from a knowledge of the values of $\Delta\chi_1$, $\Delta\chi_2$ and $\Delta\chi_{C-H}$ one can calculate the internal chemical shift between the A and B protons in formamide. Similarly we can make use of equation 12 for dimethylformamide provided the principal susceptibilities of the C=O and C–H bonds are known. Tillieu and Guy[9] have calculated the principal susceptibilities of the C–H bond for various states of hybridization of carbon using both Slater and Coulson–Duncanson wave functions while Baudet, *et al.*,[10] have calculated similar values for the C=O σ-bond. However, theoretical calculations are not available at present for the C=O bond and hence an *a priori* calculation or the internal chemical shift is unfortunately not possible. But this situation forces us to consider the question raised earlier in this paper, namely, whether it is possible to obtain any information regarding the magnetic anisotropy of bonds from the experimental shielding data. In fact, the magnetic anisotropy of the C=O bond in these amides can be calculated from the observed data on internal chemical shift between the A and B type protons in formamide and dimethylformamide by making use of the available experimental data on magnetic susceptibilities of these compounds[16] as well as the theoretically derived bond susceptibilities.[9] The results thus obtained on the C=O bond have been employed in the calculation of the internal chemical shift of A and B type protons in acetamide (III) and dimethylacetamide (IV). Of course, one has to make the assumption that the electronic structure, and hence the principal susceptibilities of the C=O bond in these molecules, are not appreciably different. To a certain extent, this assumption may be justified on the basis of the additivity of bond susceptibilities in these molecules.

IV. Results

Tables I and II show the results of the calculations on the magnetic anisotropy of the C=O bond in formamide and dimethylformamide. In the calculations pertaining to Table I $\Delta\sigma$ was taken to be negative for both formamide and dimethylformamide while the sign of $\Delta\sigma$ was taken to be positive in the calculations pertaining to Table II. There is an uncertainty in the sign of $\Delta\sigma$ owing to the fact that it has not been possible to decide experimentally at which one of these sites the proton is more shielded than the other. The possibility of $\Delta\sigma$ being positive for one molecule, say formamide, and negative for the other can be ruled out on the basis of the extremely large magnitudes of the calculated susceptibility and anisotropy values (*e.g.*, $\Delta\chi_1$ =

(16) P. W. Selwood, "Magnetochemistry," Interscience Publishers, New York, N. Y., 1956.

-20.994×10^{-6}; $\Delta\chi_2 = -92.278 \times 10^{-6}$) for the C=O bond.

The data given in Tables I and II were obtained as follows. Equations similar to (11) and (12) were set up for the two compounds and solved in terms of one of the principal susceptibilities. The average susceptibility, χ_{av}, of the C=O bond in these compounds can be obtained from the experimental molar susceptibility data[16] and the available bond susceptibility data. Since

$$\chi_{av} = \frac{1}{3}(\chi_{xx} + \chi_{yy} + \chi_{zz}) \qquad (15)$$

the three principal susceptibilities of the C=O bond are easily evaluated.

TABLE I

PRINCIPAL SUSCEPTIBILITIES OF THE C=O BOND DERIVED FROM N.M.R. INTERNAL CHEMICAL SHIFT DATA ON FORMAMIDE AND DIMETHYLFORMAMIDE ($\Delta\sigma$ NEGATIVE)

Location of the C=O dipole from carbon Å.	Value of $\Delta\chi_{CH}$ ($\times 10^6$)	Magnetic anisotropy of the C=O bond ($\times 10^6$) $\Delta\chi_1$	$\Delta\chi_2$	Principal susceptibilities of the C=O bond ($\times 10^6$) χ_{xx}	χ_{yy}	χ_{zz}
0.81	+0.26	+5.508	+9.724	−5.987	−1.771	+3.737
	+ .49	+5.771	+10.033	−6.105	−1.843	+3.928
0.91	+ .26	+5.004	+6.024	−3.688	−2.668	+2.336
	+ .49	+5.305	+6.200	−3.705	−2.810	+2.495
1.01	+ .26	+4.184	+1.492	−0.940	−3.632	+0.552
	+ .49	+4.370	+1.360	−0.790	−3.800	+0.570
1.11	+ .26	+3.257	−2.822	+1.627	−4.452	−1.195
	+ .49	+3.389	−3.194	+1.919	−4.664	−1.275
1.21	+ .26	+2.448	−6.315	+3.686	−5.077	+2.629
	+ .49	+2.532	−6.879	+4.090	−5.321	−2.789

TABLE II

PRINCIPAL SUSCEPTIBILITIES OF THE C=O BOND DERIVED FROM N.M.R. INTERNAL CHEMICAL SHIFT DATA ON FORMAMIDE AND DIMETHYLFORMAMIDE ($\Delta\sigma$ POSITIVE)

Location of the C=O dipole from carbon (Å.)	Value of $\Delta\chi_{CH}$ ($\times 10^6$)	Magnetic anisotropy of the C=O bond ($\times 10^6$) $\Delta\chi_1$	$\Delta\chi_2$	Principal susceptibilities of the C=O bond ($\times 10^6$) χ_{xx}	χ_{yy}	χ_{zz}
0.81	+0.26	−5.118	−8.223	+2.436	−0.669	−5.787
	+ .49	−5.381	−8.533	+2.555	− .597	−5.978
0.91	+ .26	−5.003	−6.022	+1.007	− .012	−5.015
	+ .49	−5.305	−6.200	+1.025	+ .130	−5.175
1.01	+ .26	−4.184	−1.491	−1.741	+ .952	−3.232
	+ .49	−4.370	−1.360	−1.890	+1.120	−3.250
1.11	+ .26	−3.251	+2.846	−4.317	+1.774	−1.477
	+ .49	−3.383	+3.212	−4.609	+1.986	−1.397
1.21	+ .26	−2.448	+6.314	−6.365	+2.397	−0.051
	+ .49	−2.532	+6.879	−6.770	+2.641	+0.109

The internal chemical shift data were taken from the work of Piette, Ray and Ogg,[12] Schneider,[13] and Gutowsky and Holm.[15] It is interesting to note that before the results of Schneider on liquid formamide (with N^{15}) were available to us we extrapolated the data of Piette, *et al.*, on aqueous solutions of formamide by the equation

$$\Delta\sigma = \sigma^A - \sigma^B = \Delta\sigma_\infty(1 - C) + CK \qquad (16)$$

where C is the concentration of water and K is a constant. The value of $\Delta\sigma_\infty = \pm 2.2 \times 10^{-7}$ thus obtained may be compared with the value of $\pm 2.23 \times 10^{-7}$ obtained by Schneider on the pure liquid. In the present calculations the value of $\Delta\sigma = \pm 2.2 \times 10^{-7}$ has been used. The various bond lengths and angles used here have been taken from Wheland.[17]

Table III presents the results of calculations on the internal chemical shift between the A and B type protons in acetamide (using an equation similar to 11) and dimethylacetamide (using an equation similar to 12). The χ values have been taken from Tables I and II. In these compounds the secondary field due to the C–C bond of the $C-CH_3$ group alone was taken into account while those from the three C–H bonds in this methyl group were neglected because of the larger distance. It may be pointed out here that for a given sign of $\Delta\sigma$ the calculated internal chemical shift values in these two molecules are not affected by the choice in the location of the C=O dipole as long as one takes consistent sets from Table I or Table II.

TABLE III

THE INTERNAL CHEMICAL SHIFT OF A AND B TYPE PROTONS IN ACETAMIDE AND DIMETHYLACETAMIDE (SEE FIG. 1)

Compound	$\Delta\chi_{CH}$ ($\times 10^6$)[a]	$\Delta\sigma$ (calcd.) ($\times 10^7$) χ values from Table I	χ values from Table II	$\Delta\sigma$ (obsd.) ($\times 10^7$)
Acetamide	+0.26	−1.63	+3.10	[b]
	+ .49	−1.78	+3.24	
Dimethyl-acetamide	+ .26	−1.43	+2.31	±2.21
	+ .49	−1.53	+2.41	

[a] The $\Delta\chi_{CH}$ values refer to those used in formamide and dimethylformamide calculations (see Tables I and II).
[b] Value not available.

Discussion

An examination of Tables I and II shows the dependence of the $\Delta\chi$ and χ values on various parameters such as the location of the C=O dipole and the $\Delta\chi$ value of the C–H bond. While the latter is due to an uncertainty in the theoretical calculations on the principal susceptibilities of the C–H bond using different wave functions (see ref. 9) the former arises from a very serious difficulty in the present method itself. We shall now discuss this matter in greater detail. It was mentioned earlier that for mathematical simplicity we idealize the induced dipoles by point dipoles and in fact such an idealization is valid when we consider the field due to these dipoles at very large distances. For actual calculations it is customary to locate this dipole somewhere along the bond by making use of certain assumptions. One such assumption is to locate the dipole at the electrical center of gravity of the electron distribution constituting the bond. Unfortunately the task of locating the dipole in this manner is not as trivial as it appears at first sight. From theoretical studies on dipole moments of bonds[18] it is well-known that the location of the center of gravity of a charge distribution in a bond is dependent among other things, on two important factors, namely, the hybridization and ionic character of the bond. At present these two quantities are not as accurately known as one would desire and hence the location of the dipole in this manner is subject to some error.

(17) G. W. Wheland, "Resonance in Organic Chemistry," John Wiley and Sons, Inc., New York, N. Y., 1955.
(18) C. A. Coulson, "Valence," The Clarendon Press, Oxford, 1952.

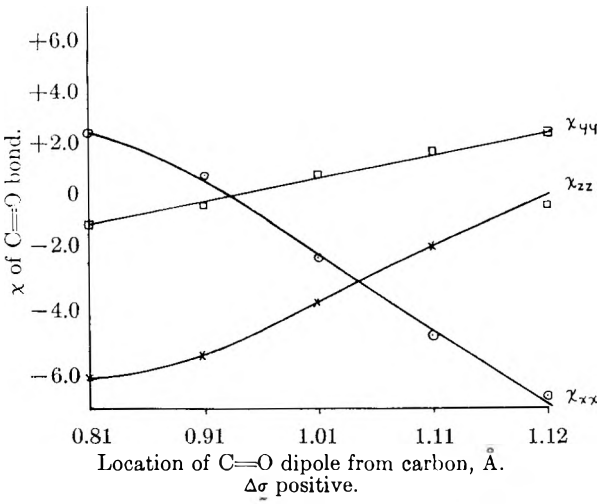

Figs. 2(a) and 2(b).—Dependence of the calculated principal susceptibility values on the location of the carbonyl dipole.

In the case of a purely covalent bond one can, perhaps without serious error, place the dipole along the bond at a distance corresponding to the covalent radii of the two atoms forming the bond. In fact in the present calculations this assumption has been made for the C–H bond. But in the case of more polar bonds the electrical center of gravity is likely to shift toward the more electronegative atom while the exact location of this point is not easily determined. In the present case of the C=O bond, the oxygen atom being much more electronegative than carbon, the center of gravity is likely to be very near the oxygen atom and hence calculations have been made with the C=O dipole at different locations near the oxygen as well as on the oxygen itself. Owing to this uncertainty in the location of the induced dipole the anisotropy and susceptibility values differ widely although it must be mentioned that the values themselves are of reasonable order of magnitude. We shall return to the question of locating the dipole and choosing the probable susceptibility values a little later.

In Figs. 2a and 2b the calculated values of χ_{xx}, χ_{yy} and χ_{zz} for the C=O bond are plotted against the distance between the dipole and the carbon atom. The two figures have been obtained using two different signs for $\Delta\sigma$. We shall now discuss the probable sign of $\Delta\sigma$ in these molecules from the point of view of the present calculations and certain theoretical considerations. It has been shown recently by Pople[6] that the C=O bond in aldehydes makes a large paramagnetic contribution in the 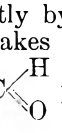 plane. An explanation of this is based on the concentration of the π-bonding orbital on the oxygen atom. Such a situation leads to an electron deficiency on the $2p\pi$ atomic orbital of carbon and large paramagnetic contributions in the 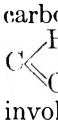 plane may then arise from transitions which involve the transfer of the C–O σ-electrons to the antibonding π-orbitals. A similar argument can be extended to the case of the C=O bond in these amides. According to Table I the χ_{zz} and χ_{yy} values (Z-Y is the molecular plane) become diamagnetic as the dipole is moved towards oxygen while according to Table II χ_{yy} (and probably χ_{zz} also) becomes paramagnetic as the dipole is shifted toward oxygen. This trend in the latter case is in good agreement with the theoretical considerations mentioned above and hence we may conclude that $\Delta\sigma$ is positive in these molecules. Further the calculated $\Delta\sigma$ value in dimethylacetamide appears to be in better agreement with experiment when one uses χ values from Table II.

The principal susceptibility of the C=O bond in urea in the direction perpendicular to the plane of the molecule (*i.e.*, the value of χ_{xx}) can be approximately calculated from the available molar anisotropy data[19] and from the bond principal susceptibility data.[9,10] The value thus obtained for χ_{xx} is -9.7×10^{-6}. It is therefore very likely that the C=O bond in these amides is also characterized by such a large diamagnetic susceptibility value for χ_{xx}. According to Table I such a value for χ_{xx} is possible only when the dipole is located farther away from the oxygen atom. This situation is certainly contradictory to simple electronegativity concepts. On the other hand, the results of Table II are in better agreement with the large diamagnetic value of χ_{xx} particularly since this corresponds to the dipole being located nearer to the oxygen atom. Regarding the question of locating the dipole we may therefore conclude that no serious error will result by assuming the dipole to be located on the oxygen atom itself. In this case then the most probable values of anisotropy and susceptibility are: $\Delta\chi_1 \sim -2.5 \times 10^{-6}$; $\Delta\chi_2 \sim +6.6 \times 10^{-6}$; $\chi_{xx} \sim -6.6 \times 10^{-6}$; $\chi_{yy} \sim +2.5 \times 10^{-6}$; $\chi_{zz} \sim 0$. One must of course bear in mind the approximate nature of these values. It is indeed rather unfortunate that no direct experimental measurement of these quantities is possible at present. Also, if the electronic center of gravity of the C=O bond in these molecules could be located more precisely by other methods it might then be possible to limit the choice in the χ values more satisfactorily. However, these drawbacks may be overcome in the near future.

From Table III the internal chemical shift for acetamide is found to be $\sim +3.2 \times 10^{-7}$ ($\Delta\sigma$ taken to be positive). Experimental internal shift data for acetamide are not available at present and it will be interesting to compare this value when data on this compound are forthcoming. In the present treatment we have considered the induced dipole effect to be the only factor in the shielding by distant groups and have neglected electronegativity effects. Also, the theoretical values of $\Delta\sigma$ refer to the A and B type protons as being "frozen-in" while experimental values are obtained under conditions of exchange between A and B. Of course it is possible to determine the value of $\Delta\sigma$ under conditions of extremely slow exchange, as for example, by working at low temperatures and the value thus obtained should be compared with the theoretical results. Further,

(19) K. Lonsdale, *Proc. Roy. Soc.* (*London*), **A177**, 272 (1941).

on the experimental side the measurements of internal chemical shifts might be affected by association in the liquid state. Such association shifts have been observed in the case of formamide by Piette and co-workers. It will therefore be desirable to obtain internal chemical shift data on these compounds by dissolving them in inert solvents and extrapolating the data to infinite dilution and also working at low temperatures. It is probable that better agreement might then result by following the procedure outlined in the present paper for calculating the internal chemical shifts.

Acknowledgments.—Our thanks are due to Dr. W. G. Schneider for communicating the results of his measurements on formamide with N^{15} prior to publication. We also wish to thank the staff of the computer (MISTIC) laboratory of Michigan State University for their valuable coöperation. This research was supported in part by the Atomic Energy Commission through contract AT-(11-1)-151.

Appendix

When a given nucleus is involved in internal molecular motions the average shielding of that nucleus due to a point dipole must be used in equation 9 (above). The components $T_\epsilon = (1 - 3\cos^2\theta_\epsilon/R^3)_{av}$ (where $\epsilon = x, y, z$) were evaluated numerically in the following manner.

Case 1: $\xi < (90^0 - \eta)$ (see Fig. 3).—Let us consider the case of a nucleus N which is free to rotate around the axis A–B, this axis being taken to be in the Z–Y plane. With the point dipole placed at O, the quantities of interest to us now are the radius vector R and θ_z. Since AN ($=r_1$) and AB are chosen to be at right angles to each other we can express α(the angle between NA and AO, *i.e.*, r_1 and r_2) in terms of β and ϕ(ϕ is the angle of rotation of r_1 in its plane). Thus it can be shown that

$$\cos\alpha = \sin\beta\cos\phi \qquad (1A)$$

and hence we can express R as

$$R = (r_1^2 + r_2^2 - 2r_1r_2\sin\beta\cos\phi)^{1/2} \qquad (2A)$$

Now we have also

$$\cos\theta_z = (R^2 + r_3^2 - r_4^2)/2Rr_3 \qquad (3A)$$

and hence we can write

$$T_z = \left(\frac{1 - 3\cos^2\theta_z}{R^3}\right)_{av} = \left\{R^{-3}\left[1 - 3\left(\frac{R^2 + r_3^2 - r_4^2}{2Rr_3}\right)^2\right]\right\}_{av} \qquad (4A)$$

Since ϕ varies for 0 to 2π we can find the average value by integrating the left-hand side of equation 4A after substituting equation 2A for R and dividing finally by 2π. Thus after rearranging we obtain

$$T_z = \frac{1}{2\pi}\left\{J_B - \frac{3}{4r_3^2}[(r_3^2 - r_4^2)^2 J_C + 2(r_3^2 - r_4^2)J_B + J_A]\right\} \qquad (5A)$$

where

$$J_A = \int_0^{2\pi}(a + b\cos\phi)^{-1/2}\,d\phi \qquad (6A)$$

$$J_B = \int_0^{2\pi}(a + b\cos\phi)^{-3/2}\,d\phi \qquad (7A)$$

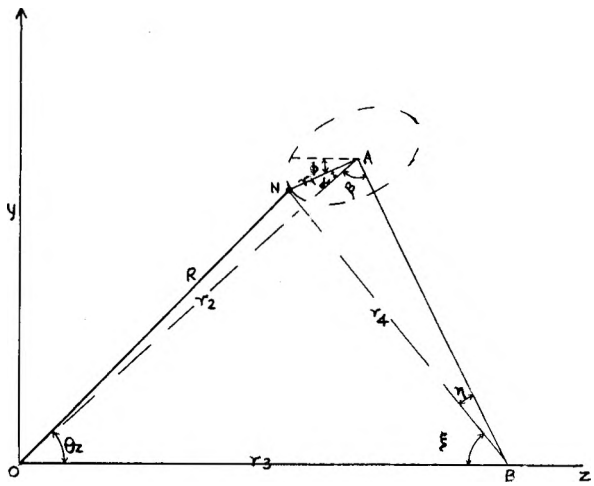

Fig. 3.—Evaluation of T_ϵ average values. Case 1: $\xi < (90° - \eta)$. The dipole is located at O and the nucleus N is free to rotate around the axis A–B.

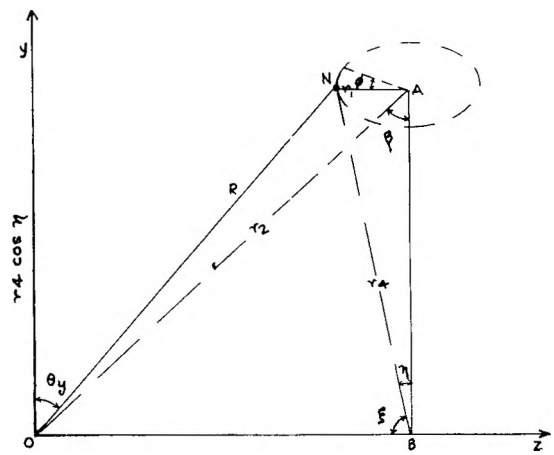

Fig. 4.—Evaluation of T_ϵ average values. Case 2: $\xi = (90° - \eta)$. The dipole is located at O and the nucleus N is free to rotate around the axis A–B.

and

$$J_C = \int_0^{2\pi}(a + b\cos\phi)^{-5/2}\,d\phi \qquad (8A)$$

with $a = r_1^2 + r_2^2$ and $b = -2r_1r_2\sin\beta$.

In order to evaluate T_y in this case we may proceed as follows. Extend the line AB (Fig. 3) until it intersects the Y-axis at a point, say P. As in the case of T_z we may now consider OP as r_3, NP as r_4 and OA and NA as r_2 and r_1, respectively. However, β is now the angle between PA and r_2. Cos θ_y can be expressed as in 3A and T_y can be obtained in a similar manner (4A).

Case 2: $\xi = (90° - \eta)$ (see Fig. 4).—In this instance we can evaluate T_z as in case 1 but T_y is given by

$$T_y = \left(\frac{1 - 3\cos^2\theta_y}{R^3}\right)_{av} = \frac{1}{2\pi}[J_B - 3r_4^2]\cos^2\eta\, J_C \qquad (9A)$$

Equation 9A is obtained by a method similar to that used in the derivation of (4A). J_B and J_C are as defined in equations 7A and 8A.

Case 3: $T_x = [1-3\cos^2\theta_x/R^3]_{av}$. (see Fig. 5).—We now consider the case (Fig. 5) in which the

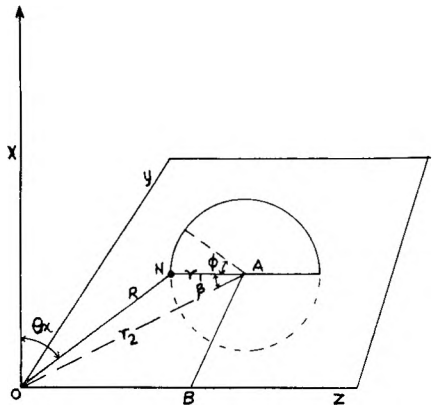

Fig. 5.—Case 3: evaluation of T_x average values. The dipole is located at O and the nucleus N is free to rotate around the axis A–B which lies in the Z–Y plane.

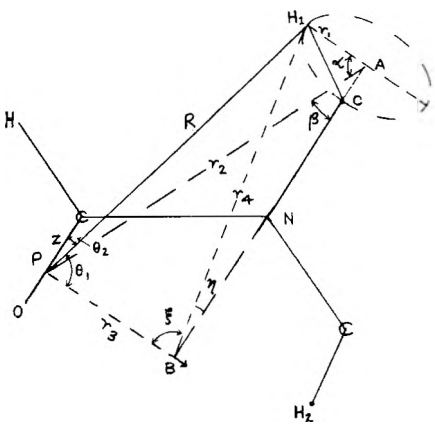

Fig. 6.—Illustration of the details of calculating T_x average values for proton H_1 in dimethylacetamide. The carbonyl dipole is located at P.

X-axis is chosen perpendicular to the axis AB of the rotating nucleus. Then the plane described by the rotating nucleus is perpendicular to the Z–Y plane. Now, using the relation

$$\cos^2\theta_x = (r_1 \sin\phi/R)^2 \qquad (10A)$$

and substituting equation 2A for R in (10A) and proceeding as before we find

$$T_x = \frac{1}{2\pi}\left\{3r_1^2/b^2 \times J_A + \frac{1 - 6r_1^2a}{b^2} J_B + 3r_1^2\left(\frac{a^2}{b_2} - 1\right) J_C\right\} \qquad (11A)$$

Again J_A, J_B and J_C are as defined in equations 6A, 7A and 8A.

The above three cases are sufficient to deal with the averages required for the compounds treated here. As an illustration let us consider dimethylformamide (Fig. 6). For the present we shall confine our attention to only one of the protons of the N–CH_3 group (proton 1).

The secondary field at proton 1 due to the C=O dipole at P is required. The Z-axis is chosen along the bond and the X-axis is perpendicular to the plane of the molecule (*i.e.*, Z and Y in the plane of the paper). An examination of Fig. 6 shows that T_z can be obtained in a manner similar to T_y of equation 9A. Similarly T_y can be obtained by the use of an expression similar to T_z of equation 4A while T_x can be obtained from equation 11A. The procedure can be similarly applied for proton (2) but in each case the Z-axis is chosen along the bond (here C=O, for example) and X-axis perpendicular to the plane of the molecule.

The evaluation of the integrals in equations 6A, 7A and 8A is necessary for the calculation of T_x, T_y and T_z in these cases. These integrals are of the elliptic type and cannot be evaluated in a closed form. In the present work we have evaluated these integrals by numerical integration using the high speed electronic digital computer, MISTIC at Michigan State University. The program used enables one to obtain J_A, J_B and J_C for the corresponding values of a and b which are punched on a data tape. In the computer 179 ϕ's are generated (0 to 2π are initially supplied) for the interval 0–2π and the corresponding functions, say $(a + b\cos\phi)^{-1/2}$ are computed and stored. The integration is then performed by taking seven functions successively and evaluating the integrals for each set (six intervals) by using a sixth degree polynomial approximation. The integral is then obtained by adding the 30 values thus obtained. As an example, we have given below the values of J_A, J_B and J_C obtained for some typical values of a and b. The values of T_{Ax}°, T_{Ay}° and T_{Az}° for this case (dimethylacetamide–dipole on oxygen, *i.e.*, 1.21 Å. from carbon) have also been given.

a	b	J_A	J_B
+16.0838 $\times 10^{-8}$	−2.4208 $\times 10^{-8}$	1.5734358 $\times 10^{8}$	9.95241128 $\times 10^{22}$
J_C	T_{Ax}°	T_{Ay}°	T_{Az}°
6.36724915 $\times 10^{37}$	+1.4274 $\times 10^{22}$	+1.1355 $\times 10^{22}$	−2.5629 $\times 10^{22}$

Finally it may be pointed out here that the internal chemical shift values calculated by using equation 11 become almost identical with those obtained from (12) when $a>>b$.

ON THE TEMPERATURE DEPENDENCE OF THE PURE QUADRUPOLE SPECTRUM OF SOLID 1,2-DICHLOROETHANE

BY J. L. RAGLE

Department of Chemistry, University of Massachusetts, Amherst, Mass.

Received January 15, 1959

Experimental observations on solid 1,2-dichloroethane are discussed. One finds that in the temperature range 20 to 238°K. the Cl^{35} quadrupole resonance frequency changes by 13% (from 34.4 to 29.9 mc.p.s.), while the line width passes through a maximum at approximately 155°K. A shift of 16% is to be expected for rapid uniform motion about the chlorine–chlorine axis, neglecting all other motion. It is proposed that the observed effects are due to an abrupt onset of reorientational motion at a frequency greater than approximately 10^8 sec.$^{-1}$, the nuclear Larmour frequency.

Measurements by diverse experimental methods have led many workers to suggest that an extensive degree of reorientational freedom is available to dichloroethane molecules in the solid between approximately 170°K. and the melting point at 238°K.[1-6]

It is supposed that the reorientational motion takes place predominantly about an axis passing nearly through the chlorine atoms on opposite ends of the molecule,[7,8] and nuclear magnetic resonance studies suggest that the mean frequency of this motion exceeds 4×10^4 sec.$^{-1}$ at 177°K.[4] More recent measurements by Linder[5] of proton spin-lattice relaxation times at 30 mc.p.s. indicate that the mechanism responsible for relaxation is a thermally activated motion against a hindering potential of 1.5 kcal. mole^{-1}, and is not the same as the mechanism responsible for proton line narrowing. This note presents a discussion of the effect of 1-dimensional reorientation about the chlorine–chlorine axis on the pure quadrupole spectrum of dichloroethane, together with experimental observations of frequency and line width in the temperature range 77 to 238°K. (Fig. 1 and Table I).[9]

A nucleus with spin I = 1 or greater (units of $h/2\pi$) may interact with the molecular electronic charge distribution in such a way as to cause partial splitting of the nuclear spin degeneracy. The theory of this effect has been thoroughly discussed in the literature,[10,11] and will not be presented here. The Hamiltonian for the interaction may be written as

$$\mathcal{H} = \sum_{k=-2}^{2} (-1)^k Q_k^{(2)} \nabla E_{-k} \qquad (1)$$

where the quantities $Q_k^{(2)}$ and ∇E_{-k} designate, respectively, the five components of the nuclear quadrupole moment and the electric field gradient in irreducible tensor form. The quantities ∇E_{-k} involve, as parameters, angular variables which give the relative orientations of the principal axes of the field gradient tensor with respect to a space-fixed coördinate system. The natural molecular motions in the crystal modulate these parameters and thus effect both a temperature dependence of the line frequency and a mechanism whereby energy transport into and out of the spin system is facilitated. Using the expressions given by Pound[10] for the above quantities, and assuming spin 3/2 and axial symmetry in the static molecule, we obtain the following expression by direct solution of the secular equation

$$\omega = \omega_0/2[\langle(3\cos^2\theta - 1)\rangle^2 + 12\langle\sin\theta\cos\theta\exp(i\phi)\rangle \times \langle\sin\theta\cos\theta\exp(-i\phi)\rangle + 3\langle\sin^2\theta\exp(2i\phi)\rangle \times \langle\sin^2\theta\exp(-2i\phi)\rangle]^{1/2} \qquad (2)$$

In this expression ω_0 is the angular frequency of the quadrupole line for the (hypothetical) static molecule, ω is the frequency of the quadrupole line for the moving molecule θ and ϕ are the colatitude and azimuth, respectively, of the chlorine–chlorine internuclear axis with respect to the carbon–chlorine bond axis, and the averages are to be taken over the motion of the molecule. If we neglect all motion except the reorientation about the chlorine–chlorine axis and further assume uniform rotation at a frequency much greater than the Larmour frequency of the nuclei ($\omega_0 = 2.164 \times 10^8$ sec.$^{-1}$), equation 2 simplifies to

$$\omega = \omega_0/2\,|3\cos^2\theta - 1| \qquad (3)$$

In the rigorous computation of averages of the

TABLE I

TEMPERATURE DEPENDENCE OF LINE WIDTH IN SOLID DICHLOROETHANE

Temp., °K.	Isotopic mass no.	Line width, Mc.p.s.
77	35	4.7[a]
77	37	3.9[a]
135	37	20.1
141	37	18.6
147	35	23
150	35	30
154	35	35
179	35	22
195	35	21
195	37	13.6
215	35	10.8
225	35	10.3
232	35	10.7
233	37	8.7

[a] These data were taken with regenerative recording spectrometer.

(1) K. S. Pitzer, *J. Am. Chem. Soc.*, **62**, 331 (1940).
(2) I. Ichishima and S. Mizushima, *J. Chem. Phys.*, **18**, 1420 (1950).
(3) C. P. Smythe, "Dielectric Behavior and Structure," McGraw-Hill Book Co., Inc., New York, N. Y., 1955, p. 133 ff.
(4) H. S. Gutowsky and G. E. Pake, *J. Chem. Phys.*, **18**, 162 (1950).
(5) S. Linder, *ibid.*, **26**, 900 (1957).
(6) H. W. Dodgen and J. L. Ragle, *ibid.*, **25**, 376 (1956).
(7) T. B. Reed and W. N. Lipscomb, *Acta Cryst.*, **6**, 45 (1953).
(8) M. E. Milford and W. N. Lipscomb, *ibid.*, **4**, 369 (1951).
(9) J. L. Ragle, unpublished Ph.D. thesis, State College of Washington, 1957.
(10) R. V. Pound, *Phys. Rev.*, **79**, 685 (1950).
(11) T. P. Das and E. L. Hahn, "Nuclear Quadrupole Resonance Spectroscopy," Academic Press, Inc., New York, N. Y., 1958.

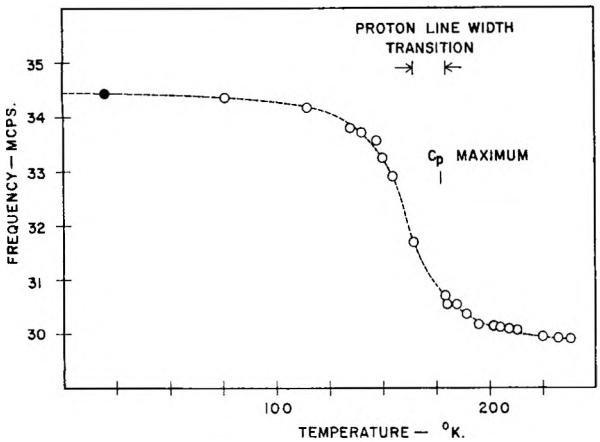

Fig. 1.—Dependence of Cl^{35} quadrupole frequency on temperature for dichloroethane. The point at 20°K. is taken from the data of Livingston (*J. Chem. Phys.*, **20**, 1170 (1952)).

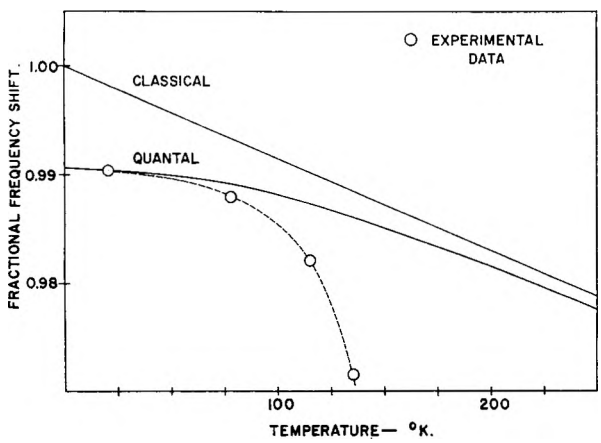

Fig. 2.—Theoretical curves for 1-dimensional harmonic oscillator representation of dichloroethane.

angle factors over the molecular motion it is necessary to proceed in two steps. These quantities must first be averaged over the motion for each energy level accessible to the molecule. After this process has been carried out, the result must be averaged over the distribution-in-energy of the molecules in the assembly. That this is so is seen from the following argument: At any reasonably high temperature (say between 77 and 238°K.) transitions between molecular torsional states occur very often on a nuclear time scale, but seldom in comparison to the torsional frequency. Thus a given nucleus experiences the average over torsional levels of the average field gradient associated with each torsional state. A detailed calculation of these averages for an assembly of quantum-mechanical harmonic oscillators is easily carried through, and agrees with the results of Bayer's paper,[12] except that the contribution of the zero-point motion is included explicitly (see Fig. 2). The shift due to zero-point motion alone may be computed from the expressions

$$\begin{aligned} &\langle \exp(\pm i\phi) \rangle = \exp(-1/4a^2) \\ &\langle \exp(\pm 2i\phi) \rangle = \exp(-1/a^2) \qquad (4) \\ &a = 2\pi/h(k_f I)^{1/2} \qquad (5) \end{aligned}$$

where k_f is the restoring force constant and I is the moment of inertia about the chlorine–chlorine axis. Calculations indicate that the zero-point motion may cause sizable effects and hence that one is not justified in using quadrupole frequencies extrapolated to absolute zero as characteristic of a chemical bond without some caution, especially where small shifts from molecule to molecule are concerned.

For the case of a rotator hindered by a sinusoidal potential,[13] the problem is considerably more involved. One may assume for algebraic convenience that the hindering potential possesses two minima per 2π radians. It is convenient to focus one's attention on the random jumping between minima and to neglect the torsional averaging which is superimposed on this process. Since the azimuthal angle ϕ takes on the values 0, π randomly in time, the terms in $\exp(\pm 2i\phi)$ in equation 2 contain no time dependence and average to unity for all temperatures. Time dependent processes for $\Delta m = \pm 2$ also contribute nothing to spin-lattice relaxation on this model. Rewriting equation 2 with $\theta = 19° 16'$ gives

$$\omega = \omega_0/2\,[2.863 + 1.137 \langle \cos \phi \rangle^2]^{1/2} \qquad (6)$$

and the problem of explaining the anomalous temperature dependence of the quadrupole frequency in dichloroethane reduces to the calculation of $\langle \cos \phi \rangle$. This quantity may be calculated by random variable theory.[14] The result of this calculation is

$$\langle \cos \phi \rangle = 2/\pi \tan^{-1} \frac{\omega_0}{2\lambda} \qquad (7)$$

where λ is the mean rate of jumping between minima. This result follows from the assumption that all jumping motions with frequency greater than a quantity of the order of ω_0 average the angle function to zero. It is customary in nuclear magnetic resonance studies to assume that λ varies as predicted by rate theory

$$\lambda = P \exp(-V_0/RT) \qquad (8)$$

where P is a frequency factor of the order of the rate of collision with the barrier, and V_0 is a molar activation energy of the order of the barrier height. However, as is well known,[15,16] this assumption is only true when one is near the bottom of the barrier thermally speaking. Figure 3 shows the form of equation 6 with $V_0 = 2.5$ kcal. mole^{-1} and $P = 10^{11}$ sec.$^{-1}$ Lowering V_0 and P makes the curve shallower in appearance. Aside from the fact that this result does not fit the experimental data particularly well, it contradicts the observations of Gutowsky and Pake[4] that proton line narrowing occurs at approximately the same temperature as the shift in quadrupole frequency. It is the present writer's opinion that no physically reasonable combination of V_0 and P in equation 8 can make thermal activation of jumping occur sufficiently rapidly to bring the proton line width transition and the quadrupole frequency shift into coincidence.

(12) H. Bayer, *Z. physik*, **130**, 227 (1951).

(13) K. S. Pitzer, "Quantum Chemistry," Prentice-Hall, Inc., New York, N. Y., 1953, p. 240.

(14) J. G. Powles and H. S. Gutowsky, *J. Chem. Phys.*, **23**, 1692 (1955).

(15) T. P. Das, *ibid.*, **27**, 763 (1957).

(16) S. Chandrasekhar, *Rev. Mod. Phys.*, **15**, 1 (1943).

(For the values of V_0 and P given above, proton line narrowing should occur at less than 100°K. on this model. The mid-point of the experimentally observed transition is roughly 177°K.)

Ayant[17] has given a discussion of the effect of hindered rotation on the thermal relaxation time of the quadrupole spin system. Briefly, one relates the probability of transitions $\Delta m = \pm 1, \pm 2$ to the spectral density of the random thermal motions.[18] One then calculates the spectral density function from the theory of random processes and the correlation function of the azimuthal variable ϕ. The correlation function depends formally on the number of minima in the potential function but the calculated relaxation times appear to be fairly insensitive to this quantity. One may estimate crudely the effect of hindered rotation on the line width through the uncertainty principle in the usual way. For two minima the result is

$$\Delta\omega = 3\pi\omega_0^2 \cos^2\theta \sin^2\theta \frac{2\lambda}{(2\lambda)^2 + \omega_0^2} \qquad (9)$$

Qualitatively, the maximum value of $\Delta\omega$ occurs at that temperature for which the average jump rate is comparable in magnitude to the nuclear precession frequency. Thus the crude line width data presented in Table I support Linder's conclusion that the same motion does not effect relaxation of the proton and chlorine spins on the one hand and proton line narrowing on the other.

Due to the low intensity and extreme breadth of the Cl^{35} spectral line in this material at temperatures above 77°K., it was necessary to make the majority of the frequency and line-width measurements using a Zeeman-modulated superregenerative recording spectrometer. Use of the line width data obtained in this way for quantitative purpose would of course be unsatisfactory, but it appears that the line reaches its maximum breadth between the proton T_1 minimum at 125°K. and the λ point near 177°K.[1] It is not clear from these measurements what part of the line width is due to lifetime broadening and what part is due to other factors, such as static inhomogeneity in the field gradient or magnetic interactions. Furthermore, the maximum in the observed line width near 155°K. might reasonably be interpreted as due to production of disorder by the incipient molecular motion rather than a T_1 mechanism. Observation of the Cl^{37} line width as a function of temperature was attempted in order to shed some light on this matter, but the low signal intensity unfortunately precluded such measurements in the temperature region of interest. Further measurements on quadrupole spin-lattice relaxation in this material by pulse techniques are being made.

The measured quadrupole frequency decreases abruptly with increasing temperature, as shown in Fig. 1, and takes on the value 29.92 mc.p.s. at 238°K. From equation 3, one may estimate a high temperature limiting value of 28.9 mc.p.s. This value assumes an extrapolated value of 68.90 mc.p.s. for the quadrupole coupling constant at 0°K. In order that equation 3 be applicable, the reorientational frequency must be considerably greater than 10^8 sec.$^{-1}$. From the observed line width of 10 kc.p.s. at the melting point, one may estimate a reorientational frequency of 10^{11} sec.$^{-1}$, or one reorientation in approximately ten to one hundred torsional oscillations. Preliminary attempts to observe infrared spectra of solid films in this temperature region were unsuccessful.

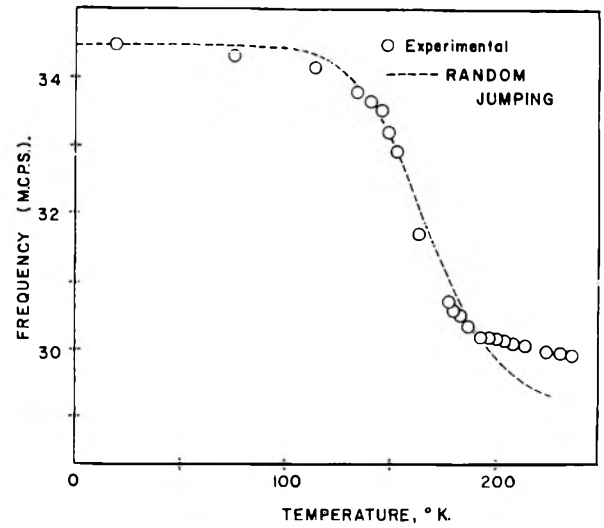

Fig. 3.—Comparison of experimental data on dichloroethane with the model represented by eq. 7 in the text.

Calculation of the frequency shift using equation 3 neglects contributions due to zero-point motion, changes in the asymmetry parameter with temperature, other modes of motion, and changes in the crystalline field contribution to the coupling constant. To correct for the zero-point torsion, it is necessary to know restoring force constants for the molecule in the crystalline site. Choosing a reasonable value for the force constant restoring displacements about the long axis of the molecule, one obtains a contribution of 0.4 mc.p.s. from this source. Temperature dependent deviations of the field gradient from axial symmetry will also result in a correction to the calculated frequency shift. If the asymmetry parameter is greater at high temperatures, as seems physically reasonable, the contribution from this source will have the same sign as the zero-point correction. It is probable that the lattice contribution to the coupling constant is inversely proportional to the molar volume, thus producing a correction of opposite sign to those factors discussed above. Since it is known[7,8] that the unit cell undergoes an expansion of roughly 18 cubic angstroms in this temperature region, the agreement between measured and calculated frequencies must be regarded as somewhat fortuitous.

The author would like to acknowledge stimulating discussion with Richard Bersohn of Cornell University about the possible physical interpretation of the experimental data presented above.

(17) Y. Ayant, *Ann. Physik*, **10**, 487 (1955).
(18) A. Abragam and R. V. Pound, *Phys. Rev.*, **92**, 943 (1953).

HEAT OF ADSORPTION OF PARAHYDROGEN AND ORTHODEUTERIUM ON GRAPHON

BY E. L. PACE AND A. R. SIEBERT

Morley Chemical Laboratory, Western Reserve University, Cleveland, Ohio

Received January 15, 1959

An experimental investigation of the differential and isosteric heats of adsorption for parahydrogen and orthodeuterium adsorbed on graphon has been carried out in the neighborhood of the normal boiling points of the gases by the use of conventional low temperature calorimetric procedures. Assuming the interaction of an isolated molecule of the gas with a surface having the structure and parameters of graphite, good agreement is obtained between the computed and experimental values of the heat of adsorption at low coverages. The larger heat of adsorption of deuterium as compared to that of hydrogen is reasonably explained by the difference in the zero point energies associated with the degree of freedom perpendicular to the adsorbent surface.

Introduction

The present investigation is one of a series which is being carried out which involves the adsorption of low boiling gases on Graphon. The interest in the two isotopic species of hydrogen arises from the fact that the relative masses should enter significantly into the energetics of the adsorption process. Qualitative confirmation of this fact has come from studies with hydrogen and deuterium[1,2] adsorbed on carbon surfaces which report the stronger adsorption of deuterium. It is the purpose of the present investigation to reach some semi-quantitative conclusions on this matter.

The use of the forms of hydrogen and deuterium stable at low temperature is governed by the necessity of minimizing the uncertainty in the heat of adsorption coming from conversion effects on the adsorbent surface. The choice of Graphon as an adsorbent is based on evidence[3] that it is a material closely approaching the characteristics of true graphite while retaining a surface area large enough to make calorimetric adsorption studies possible. Recent work by Graham[4] has confirmed this fact by showing that Graphon has a very small percentage of non-uniform sites.

Experimental

The adsorbent used in the investigation was a 31.3-g. portion of a sample received from Godfrey L. Cabot, Inc. Laboratories. X-Ray data provided with the sample specified a c value of 6.96 Å. as compared to 6.70 Å. for true graphite. The BET area with nitrogen was 85.9 $m.^2 g.^{-1}$. The sample of Graphon was activated by heating at 220° for five days and simultaneous evacuation until a pressure less than 10^{-6} mm. was obtained.

The hydrogen was obtained from the Ohio Chemical Company, Cleveland, Ohio. The purity was stated to be 99.5%. Deuterium of 99.5% purity was purchased from the Stuart Oxygen Company, San Francisco, California. Each of the gases was passed through a trap immersed in liquid nitrogen to remove traces of water.

Prior to their use in the absorption experiments, the hydrogen and deuterium were converted to approximately 95% parahydrogen and orthodeuterium by contact with activated charcoal in successive baths of liquid nitrogen and liquid helium.

The calorimetric apparatus and experimental procedure for determining heats of adsorption and adsorption isotherms have been previously described.[5,6]

Even though the hydrogen and deuterium were largely converted to the stable low temperature forms, the measurement of the heat of adsorption was complicated by the presence of small scale heat effects from ortho–para conversion associated with changes in temperature of the calorimeter during the measurement. Including the uncertainty in the conversion process, the error in the experimental values is estimated as being not more than ±20 cal. per mole. The heats of adsorption as a function of coverage were measured calorimetrically at average temperatures of 20.4°K. for parahydrogen and 23.5°K. for orthodeuterium.

Equilibrium pressures in the neighborhood of the boiling points were obtained either as a function of coverage at two temperatures or at several essentially constant coverages over a range of temperatures. It was possible to derive values of the isosteric heat of adsorption from conventional methods employing these data either in plots of ln p *vs.* $1/T$ or in the integrated form of the Clausius–Clapeyron equation.

Results and Discussion

The results of measurements are presented in Fig. 1 for parahydrogen and Fig. 2 for orthodeuterium. The calorimetrically determined differential heats of adsorption are represented by open circles while the isosteric heats of adsorption determined from equilibrium pressure data are represented by solid or half-solid circles. Since the isosteric heat of adsorption is identified thermodynamically with the differential heat of adsorption, the values obtained by the two different experimental methods appear to be internally consistent with this fact.

The shape of the curves is of interest. By analogy with the case for argon adsorbed on Graphon,[7] the sharp break in the curve can be reasonably interpreted as the result of the completion of the first layer and incipient occupation of second and third layer sites by molecules of the adsorbed gas. We wish to remark here without further amplification at this time since the matter will be discussed in a later paper that the break in the curve corresponds to a coverage which gives approximately the BET area with nitrogen if liquid packing of the hydrogen and deuterium on the surface is assumed. A considerable difference exists between this value and the values of 169.3 and 174.3 $m.^2 g.^{-1}$ for hydrogen and deuterium, respectively, obtained by the use of isotherm data with molecular areas from liquid packing in conventional BET plots.

The curves are also capable of interpretation with respect to (1) order of magnitude of the observed

(1) R. M. Barrer and E. K. Rideal, *Proc. Roy. Soc.* (*London*), **A149**, 231 (1935).

(2) W. van Dingener and A. van Itterbeck, *Physica*, **6**, 49 (1939).

(3) W. D. Schaeffer, W. R. Smith and M. H. Polley, *Ind. Eng. Chem.*, **45**, 1721 (1953).

(4) D. Graham, THIS JOURNAL, **61**, 1310 (1957).

(5) E. L. Pace, L. Pierce and K. S. Dennis, *Rev. Sci. Instr.*, **26**, 20 (1955).

(6) E. L. Pace, E. L. Heric and K. S. Dennis, *J. Chem. Phys.*, **21**, 1225 (1953).

(7) E. L. Pace, *ibid.*, **27**, 1341 (1957).

heat of adsorption at low coverages and (2) the fact that orthodeuterium has a higher heat of adsorption at low coverages than parahydrogen.

Since Graphon has been shown to have a small percentage of non-uniform sites, it is reasonable to assume that if one selects an experimental value of the heat of adsorption at low coverage, say $\theta \lesssim 0.2$, such a value should correspond approximately to the energy of an isolated molecule on the surface. At surface coverages of the magnitude specified above, the surface heterogeneity has been largely eliminated and interaction between adjacent molecules has not yet become significant. Values which we have determined from the graphs in this manner are 910 cal. mole^{-1} for parahydrogen and 950 cal. mole^{-1} for orthodeuterium.

The preceding experimental values can be compared with those obtained theoretically for an isolated molecule on the surface of the Graphon, assuming the graphon to have the parameters and structure of true graphite. Computations of this type have been carried out by a number of investigators.[7-11] In the usual procedure, the two parameters of the Lennard-Jones (6-12) potential are fixed by the use of the Kirkwood–Müller formula[12] for the attractive energy per molecule-carbon atom pair and an assumed equilibrium spacing for a molecule-carbon atom pair. In this case, the equilibrium spacing has been taken as the average of the liquid-packed diameter of the adsorbed molecule and the interplanar spacing of graphite. Diamagnetic susceptibilities and polarizabilities for use in the Kirkwood–Müller formula are taken from the work by Barrer.[9]

The molecule of hydrogen was assumed to approach the surface along the normal perpendicular to the center of a carbon hexagon in the surface. In order to establish the shape of the potential curve, the value of the potential energy was established at a succession of points along the path of approach. At each such point, the attractive energy was summed over the nearest 250 carbon atoms and integrated over the remainder while the repulsive energy was summed over the nearest 67 carbon atoms. The foregoing procedure established a potential energy minimum of 0.0709×10^{-12} ergs molecule^{-1} or 1020 cal. mole^{-1} at an equilibrium distance above the surface of 2.95 Å. Since hydrogen and deuterium have identical force fields the preceding two parameters which characterize the potential energy curve are the same for both molecules.

The zero point energy ϵ_0 was evaluated from the expression

$$\epsilon_0 = \frac{1}{2}\hbar(f/m)^{1/2}$$

in which the force constant f was evaluated as 2400 dynes cm.$^{-1}$ from the curvature of the potential energy curve in the region near the minimum. The zero point energies thus computed were 140 cal. mole^{-1} for deuterium and 200 cal. mole^{-1} for hydrogen.

Therefore, the energy of the zero level is 820 cal. mole^{-1} for hydrogen and 880 cal. mole^{-1} for deuterium. Because of the small mass of the molecules, the energy spacing between levels is large relative to RT at the temperature of the measure-

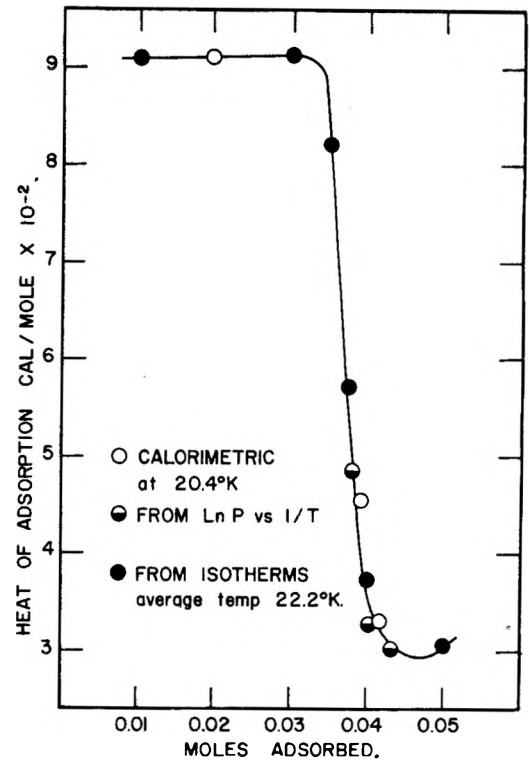

Fig. 1.—Heat of adsorption of hydrogen on Graphon.

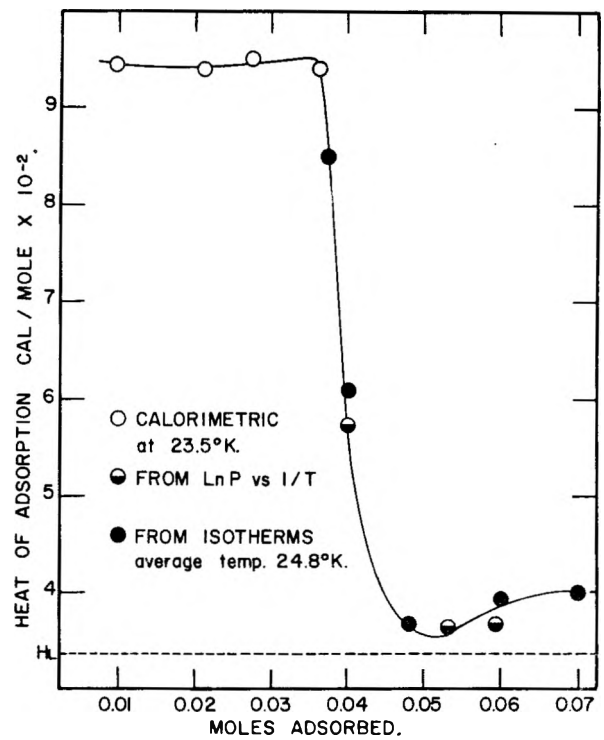

Fig. 2.—Heat of adsorption of deuterium on Graphon.

(8) W. J. C. Orr, *Trans. Faraday Soc.*, **35**, 1247 (1939).
(9) R. M. Barrer, *Proc. Roy. Soc.* (*London*), **A161**, 476 (1937).
(10) D. M. Young, *Trans. Faraday Soc.*, **48**, 548 (1952).
(11) A. D. Crowell and D. M. Young, *ibid.*, **49**, 1080 (1953).
(12) A. Müller, *Proc. Roy. Soc.* (*London*), **A154**, 624 (1936).

ments. As a result, the occupancy of the levels is essentially restricted to the zero level. Considering that uncertainties of the order of 10% exist in this type of calculation, further refinement of the calculation does not appear justified. Comparison of the observed heats of adsorption at low coverage with the computed energy of the zero level shows differences of the expected order of magnitude.

Of greater interest, however, is the fact that the computed difference in zero point energies of 60 cal. $mole^{-1}$ is in good agreement with the observed difference of 40 cal. $mole^{-1}$. Therefore, it appears reasonable to conclude that the difference in the experimental heats of adsorption which has been observed between parahydrogen and orthodeuterium is largely a mass effect associated with the zero point energy for the motion of the adsorbed molecule in the degree of freedom perpendicular to the surface.

Acknowledgment.—We are indebted to Dr. W. D. Schaeffer of Godfrey L. Cabot Inc., Boston, Massachusetts for graciously providing us with the sample of Graphon and the relevant X-ray data and to Mr. Robert Shepard and the National Carbon Company, Cleveland, Ohio, for the liquid helium used in the ortho–para conversion of the hydrogen and deuterium. The research work has been supported by the Atomic Energy Commission under Contract No. AT(30-1)-824.

CATALYTIC ISOMERIZATION OF CYCLOPROPANE

BY RICHARD M. ROBERTS

Contribution from the Shell Development Co., Emeryville, Calif.

Received January 26, 1959

Catalytic isomerization of cyclopropane was found to occur rapidly on acidic solids. At 135° and 22 sec. contact time in a flowing system, phosphotungstic acid, silicotungstic acid, silica–alumina, boria–alumina, activated bentonite, silica–zirconia–alumina, phosphomolybdic acid, silicomolybdic acid were active catalysts, while silica–magnesia, alumina gel, silica gel and activated carbon were inactive. On silica–zirconia–alumina the activation energy of isomerization was 19 kcal./mole. Side reactions at high conversion on this catalyst were dimerization, disproportionation and hydrogen transfer. Anthracene or acridine adsorbed on silica–zirconia-alumina inhibited the isomerization, and there was evidence of preferential adsorption of these compounds on catalytic sites.

Catalytic isomerization of cyclopropane to propylene is known to occur on platinum,[1] alumina[1,2] and platinum supported on alumina.[2] The purpose of the present article is to show that acidic solids are particularly good catalysts for this isomerization. The reaction was found to proceed at convenient rates in the temperature range 100 to 150° and is among the fastest hydrocarbon reactions catalyzed by acidic surfaces.

Experimental Details

Reaction System.—The experiments were carried out by flowing cyclopropane at atmospheric pressure and a known rate over a fixed bed of solid catalyst. The reaction chamber was a cylindrical copper tube, 1.3 cm. i.d., with a preheating section, a catalyst section 6.5 to 7.5 cm. in length, and a central thermocouple well. The reactor was maintained at constant temperature by a surrounding bath of boiling liquid. Catalyst was placed in the reactor, which was then brought to the desired temperature and purged with dry nitrogen. At the beginning of an isomerization experiment the gas flow was switched from nitrogen to cyclopropane by means of a valve at the inlet of the reactor. Products were collected over successive time intervals, measured volumetrically and analyzed.

Reagents.—Cyclopropane "for anesthesia" from Ohio Chemical and Manufacturing Company was employed; mass spectrometric analysis showed the presence of 1% propane. Anthracene and acridine, Eastman Kodak Company highest grade, were employed without further purification.

Analysis.—The products were analyzed for cyclopropane and propylene by infrared spectrophotometry. The absorption was measured at two wave lengths, 10.35 μ for propylene and 11.9 μ for cyclopropane, at 150 mm. pressure in a 10 cm. cell. The presence of propane was checked if necessary at 13.3 μ and 500 mm. pressure. Closures of analyses of products by this method were slightly low in some cases, probably because of side reactions (see below).

Catalysts.—Each of the following solid materials was heated for four hours at 150° before being placed in the reactor.

Phosphotungstic acid, $H_7PW_{12}O_{42}.6H_2O$, 14–60 mesh.

Silica–alumina I, 25% Al_2O_3, 75% SiO_2, 6–14 mesh, calcined 6 hours at 565°, surface area 480 $m.^2/g.$

Silica–alumina II, Chicago Chemical Company cracking catalyst. 3 × 3 mm. pellets, calcined for 3 hours at 550°, surface area 456 $m.^2/g.$, about 12% Al_2O_3.

Silicotungstic acid, $H_4SiW_{12}O_{40}.7H_2O$, 14–60 mesh.

Activated bentonite, Filtrol Corporation Grade D cracking catalyst. 4 × 4 mm. pellets, calcined for 3 hours at 550°, surface area 240 $m.^2/g.$

Silica–zirconia–alumina, Universal Oil Products Company Type B cracking catalyst, 87.0% SiO_2, 9.1% ZrO_2, 2.6% Al_2O_3, 3 × 3 mm. pellets, calcined for 15 hours at 450 to 500°, surface area 409 $m.^2/g.$

Phosphomolybdic acid, state of hydration was unknown, 60–150 mesh.

Silica–alumina III (used), American Cyanamid Company cracking catalyst, removed from a commercial fluid cracking unit, 4 × 4 mm. pellets, calcined at 550°, surface area 75 $m.^2/g.$, about 12% Al_2O_3.

Boria–alumina, 15.6% B_2O_3 supported on Alcoa H-40 alumina gel, surface area 360 $m.^2/g.$

Silicomolybdic acid, state of hydration was unknown, 60–150 mesh.

Silica–magnesia, 29% MgO, 4 × 4 mm. pellets, calcined at 550°, surface area 290 $m.^2/g.$

Alumina gel, Alcoa H-40 alumina gel, 6% SiO_2, surface area 340 $m.^2/g.$

Silica gel, a special laboratory preparation, containing 0.001% Al, 6–14 mesh, calcined for 6 hours at 565°, surface area 737 $m.^2/g.$

Activated carbon, Union Carbide and Carbon Chemicals Corporation, Columbia activated carbon, grade S.

(1) V. N. Ipatieff and W. Huhn, *Ber.*, **36**, 2014 (1903). Catalysis on iron also seems indicated by a report of isomerization on iron turnings at 100° (V. N. Ipatieff, *ibid.*, **35**, 1063 (1902)). However, the temperature of this experiment is given elsewhere (V. N. Ipatieff, *J. Russ. Phys. Chem. Soc.*, **34**, 322 (1902), and "Catalytic Reactions at High Pressures and Temperatures," The Macmillan Co., New York, N. Y., p. 154) as 600°, at which temperature homogeneous isomerization would be rapid. It therefore appears doubtful that iron is a catalyst.

(2) B. Brown, Ph.D. Thesis, University of Washington, Seattle, 1953; Dissertation Abstracts, **13**, 999 (1953); University Microfilm Publication No. 6404.

TABLE I

CATALYTIC ISOMERIZATION OF CYCLOPROPANE AT 135°, ATMOSPHERIC PRESSURE

Catalyst	Catalyst bulk density, g./cc.	Space velocity, moles cyclopropane/l. catalyst/hr.	Process period, min.	% Cyclopropane charged: Unconverted	Converted to propylene	Retained by catalyst[a]
Phosphotungstic acid	2.21	4.6	15	3.3	86.7	10.0
			30	2.6	85.5	11.9
			45	2.3	85.3	12.4
			60	2.4	85.0	12.6
Silicotungstic acid	2.14	4.9	15	6.3	44.3	49.4
			30	5.1	46.1	48.8
			45	4.0	48.5	47.5
			60	3.4	50.7	45.9
Silica-alumina I	0.445	5.0	11	15.9	53.3	30.8
			29	12.6	70.6	16.8
			45	10.7	77.0	12.3
			53	9.9	78.9	11.2
Silica-alumina II	0.800	5.2	14	6.5	48.5	45.0
			32	9.2	63.3	27.5
			40	9.7	66.2	24.1
			56	10.1	69.9	20.0
Boria-alumina	0.850	5.3	11	21.3	22.9	55.8
			28	38.0	19.9	42.1
			43	46.0	17.4	36.6
			58	50.4	16.1	33.5
Silica-zirconia-alumina	0.766	5.3	10	33.0	37.5	29.5
			20	47.5	33.7	18.8
			30	54.8	31.3	13.9
			60	64.0	28.6	7.4
Activated montmorillonite	0.815	5.4	17	48.0	34.8	17.2
			33	49.5	37.6	12.9
			41	49.4	39.1	11.5
			57	48.8	41.5	9.7
Phosphomolybdic acid	1.51	5.2	15	64.6	27.6	7.8
			30	71.5	21.7	6.8
			45	75.4	19.2	5.4
			60	77.9	17.6	4.5
Silicomolybdic acid	1.34	5.1	15	80.8	16.8	2.4
			30	84.7	13.0	2.3
			45	86.5	11.3	2.2
			60	88.0	10.1	1.9
Silica-alumina III (used)	0.647	5.1	14	94.8	5.2	
			30	92.0	8.0	
			46	91.9	8.1	
			54	91.8	8.0	0.2
Silica-magnesia	0.796	5.5	15	91.1	0.9	8.0
			30	94.1	.9	5.0
			45	95.1	.9	4.0
			60	95.5	.9	3.6
Alumina	0.701	5.2	61	99.8	0.0	0.2
Silica gel	...	4.5[b]	15	100	0.0	..
Activated carbon	0.528	5.3	60	77.5	0.0	22.5

[a] By difference between input and output. [b] 147°.

Results and Discussion

The equilibrium in the isomerization reaction, cyclopropane(g) = propylene(g), lies far to the right. At 25°, log K for the reaction is estimated to be +7.36.[3] The equilibrium constant increases with increasing temperature, and log K is between 9 and 10 in the temperature range of the present experiments, 100 to 150°.

Absence of catalysis on the reactor surface was shown by passing cyclopropane through the empty reactor at 147° and 70 sec. contact time; the conversion was less than 1%.

The results of isomerization experiments with a

(3) The free energy of formation of cyclopropane was taken as +24.99 kcal./mole, *cf.* J. W. Linnett, *J. Chem. Phys.*, **6**, 701 (1938), and J. W. Knowlton and F. D. Rossini, *J. Research Natl. Bur. Standards*, **43**, 113 (1949). The free energy of propylene was taken from "Selected Values of Properties of Hydrocarbons," Nat. Bur. Standards Circular C 461, U. S. Government Printing Office, Washington, 1947, p. 384.

number of solids are given in Table I. These experiments were all carried out at 135° and a space velocity of about 5 moles of cyclopropane per liter catalyst per hour, corresponding to a contact time of 22 seconds. The activity of the more active catalysts was not constant, and in four cases actually increased with time, despite a gradual increase in amount of material adsorbed by the catalyst.

A large fraction of the cyclopropane was retained by some of the solids studied. In the case of activated carbon, where no propylene was detected in the gas product, the material retained was probably physically adsorbed cyclopropane. In other cases, when retention accompanied isomerization activity, the adsorbed material may have been largely chemisorbed cyclopropane or polymeric products.

Alumina, silica and silica–magnesia are only weakly acidic,[4] and had no activity for isomerization of cyclopropane. Activated carbon appeared to have no isomerization activity (see above).

The remaining materials were acidic solids and all displayed more or less activity. Silica–alumina III (used), which contained about 12% Al_2O_3, had a low surface area as a result of use in a commercial catalytic cracking unit and was a comparatively poor catalyst for cyclopropane isomerization.

The activity of the four unsupported heteropolyacids was remarkable. Phosphotungstic acid was the most active catalyst tested. The surface areas of the heteropolyacids were not measured. However, a sample of phosphotungstic acid similar to that tested was found by krypton adsorption to have a surface area of 4.5 m.²/g. The surface areas of all four heteropoly acids are probably low, as compared with the other solids studied, and they may therefore have much higher isomerization activities per unit surface area than the other catalysts.

Cyclopropane isomerization on silica–zirconia–alumina was measured at several space velocities at each of the temperatures 100, 112, 124 and 135°. An Arrhenius plot of the space velocities required for 20% conversion to propylene, at 1 hour process period, gave an activation energy of 19 kcal./mole. This value is to be compared with 65 kcal./mole for the homogeneous uncatalyzed reaction in the temperature range 440 to 520°.[5] Data obtained at 135° over a range of space velocities were tested for kinetics in which the isomerization rate was proportional to one of the following quantities: (1) $p_{\text{cyclopropane}}$, (2) $p^2_{\text{cyclopropane}}$, (3) $p_{\text{cyclopropane}}/p_{\text{propylene}}$. The data certainly did not conform to (1), and did not agree fully with either (2) or (3), although one would expect propylene to inhibit the reaction.

The material retained by the catalysts was probably largely propylene and polymers of propylene, and it is doubtful that a steady-state activity would ever have been reached with any of the catalysts studied, because of gradual accumulation of polymers. An experiment was made to determine some of the side reaction products formed by one catalyst, silica–zirconia–alumina. A large charge of fresh catalyst (165 g.) was calcined for four hours at 550° and was placed in a conventional steel reaction tube surrounded by a manually controlled electric heater. The cyclopropane flow was 2.9 moles per liter catalyst per hour, and the initial temperature was 120°; the temperature rose steadily during the one-hour run, because of poor heat transfer from the catalyst bed, finally reaching 144°. The products emerging from the reactor were collected and were subjected to low temperature distillation; the C_3 fraction was analyzed by infrared methods, and the higher boiling fraction by mass spectrometry, with the results shown in Table II. Removal of the material adsorbed on the catalyst was not attempted. Judging from Table II, the most important side reaction was dimerization of propylene. Hydrogen transfer and disproportionation also occurred, as shown by the presence of paraffins and of C_6 and C_7 hydrocarbons.

TABLE II

BY-PRODUCTS OF CYCLOPROPANE ISOMERIZATION ON SILICA–ZIRCONIA–ALUMINA CATALYST

Atmospheric pressure, 120 to 144°, 2.9 moles/l. hr.

Product	Mole %	
Propylene	53.9	[a]
Cyclopropane	44.9	[a]
Higher Boiling	1.2	[a]

	Mole % of H.B.	
Pentenes	10	[b]
n-Pentane	2	[b]
Hexenes	Remainder	[b]
Hexanes	3 to 10	[b]
Benzene	0.02	[b]
Heptenes	1 to 2	[b]
Heptanes	0.5 to 5	[b]

[a] Low temperature distillation and infrared analysis of the C_3 fraction. [b] Mass spectrometric analysis.

Isomerization of cyclopropane on silica–zirconia–alumina catalyst was inhibited by anthracene or acridine adsorbed on the catalyst. A sample of catalyst (11.5 g.) was placed in a glass vessel separated by a sintered glass partition from a chamber containing solid anthracene. The apparatus was sealed off under high vacuum and was heated in an oven at 150° for 9 hours, with frequent shaking to redistribute the catalyst pellets. The cooled anthracene-treated catalyst, containing 4.8% C, was placed in the cyclopropane isomerization reactor, and an experiment was made at 112° and a space velocity of 5.6 moles of cyclopropane per liter catalyst per hour. A similar experiment was made with acridine-treated catalyst, containing 5.7% C, prepared by incubating the catalyst with acridine vapor for 9 hours at 105°. The interior of the treated catalyst pellets in both cases appeared uniform.

In experiments at 112°, atmospheric pressure, and a space velocity of 5.7 moles of cyclopropane per liter-hr., with the catalysts containing anthra-

(4) H. A. Benesi, *J. Am. Chem. Soc.*, **78**, 5490 (1954). The alumina gel tested contained 6% SiO_2. If the silica were present as "copolymer," the catalytic activity might be expected to be higher than that of pure alumina. However, activity is known to increase much less rapidly on addition of silica to alumina than *vice versa*; see V. C. F. Holm and R. W. Blue, *Ind. Eng. Chem.*, **43**, 496 (1951); V. C. F. Holm, G. C. Bailey and A. Clark, Am. Chem. Soc., Div. of Petroleum Chem., Preprints of General Papers, Vol. 2, No. 1, March, 1957, page 334.

(5) E. S. Corner and R. N. Pease, *J. Am. Chem. Soc.*, **67**, 2071 (1945); *cf.* also R. H. Lindquist and G. K. Rollefson, *J. Chem. Phys.*, **24**, 729 (1956).

cene or acridine the formation of propylene from cyclopropane was reduced to about the same extent, to 22 and 18%, respectively, of the value found with fresh catalyst. Retention of material on the catalyst was slightly increased by the presence of anthracene and slightly decreased by acridine, at the end of 30 minutes. Assuming an area of 70 Å.^{2} for the anthracene or acridine molecule, the quantities of these substances adsorbed amounted to 30 and 38%, respectively, of the B.E.T. nitrogen surface area. Actually, the entire nitrogen surface area is probably not accessible to these large molecules, resulting in a non-uniform distribution on the catalyst surface. At all events, the isomerization experiments show that the activity is reduced to a greater extent than would be expected from random coverage of the surface, pointing to specificity of poisoning by anthracene and acridine. Because of the basic character of these molecules, adsorption may have occurred preferentially on the acidic regions of the catalyst surface.

It is not surprising that solid acids catalyze the isomerization of cyclopropane. Cyclopropane is absorbed with cleavage by sulfuric or perchloric acids at room temperature to form propyl esters.[6] Further, it has long been known that ring cleavage of alkyl cyclopropanes by halogen acids to form alkyl halides obeys the Markovnikov Rule, in that the ring is broken between the most and least substituted carbon atoms.[7] Terpenoids containing the cyclopropane ring, such as carane, are also attacked by acids, with opening of the cyclopropane ring.[8] A molecular orbital treatment of the cyclopropane molecule shows that the orbitals forming the carbon–carbon bonds in the cyclopropane ring may be regarded as hybrids making an angle of 22° with the line joining adjacent carbon atoms.[9] The greater p character of these orbitals as compared with sp^3 hybrids gives rise in substituted cyclopropanes to conjugative effects with an adjacent carbon–carbon double bond or benzene ring.[10] It therefore seems reasonable that the greater p character would also facilitate proton attack at a ring carbon atom. Cyclopropane isomerization in the present case may be imagined to occur by way of a carbonium ion intermediate

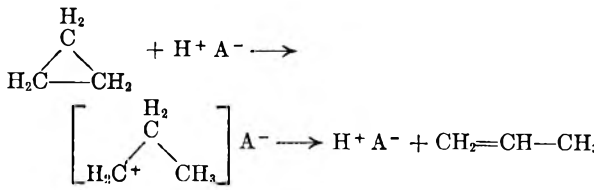

where H^+A^- represents the solid acid catalyst.

It is worthy of remark that cyclopropane isomerization is among the fastest hydrocarbon reactions catalyzed by acidic solids. It proceeds at a rate comparable to those of several reactions of olefins. Polymerization of propylene has been shown to occur at easily measurable rates on silica–alumina catalyst in the temperature range 150 to 200°.[11] *cis–trans* isomerization and double bond shift isomerization are particularly fast reactions of olefins.[12] For example, isomerization of 1-butene to 2-butenes was found to proceed at 110° on the same silica–zirconia–alumina catalyst employed in the cyclopropane isomerization experiments described above; at a space velocity of 16 moles per liter-hr. the conversion to 2-butene was 59% of the equilibrium value during the first half-hour of the experiment.

The author is indebted to O. Johnson and L. B. Ryland for providing several catalysts, to J. R. Douglass, L. W. Smith and the late S. E. Reaume for experimental assistance, and to B. S. Greensfelder and H. H. Voge for many helpful discussions.

(6) C. D. Lawrence and C. F. H. Tipper, *J. Chem. Soc.*, 713 (1955).
(7) R. A. Raphael, in "The Chemistry of Carbon Compounds," E. H. Robb, Editor, Elsevier Publishing Co., Amsterdam and N. Y., 1953, Vol. IIA, p. 26.
(8) P. de Mayo, *Perfumery and Essential Oil Rec.*, **49**, 238 (1958).
(9) C. A. Coulson and W. E. Moffitt, *Phil. Mag.*, **40**, 1 (1949).
(10) L. L. Ingraham, "Steric Effects in Organic Chemistry," edited by M. S. Newman, John Wiley and Sons, New York, N. Y., 1956, p. 518.
(11) O. Johnson, THIS JOURNAL, **59**, 827 (1955).
(12) H. H. Voge, G. M. Good and B. S. Greensfelder, *Ind. Eng. Chem.*, **38**, 1034 (1946); H. N. Dunning, *ibid.*, **45**, 551 (1953).

CALCULATED BOND CHARACTERS IN OXAMIDE AND OTHER AMIDES

BY E. L. WAGNER

Contribution from the Department of Chemistry, State College of Washington, Pullman, Washington

Received January 27, 1959

The bond characters, bond lengths and stretching force constants for the bonds in the amide groups of oxamide and several other amides have been calculated by the usual simple L.C.A.O. molecular orbital treatment. The results obtained are in fair agreement with the experimental values. Significant improvement of the agreement could not be obtained by using different sets of values for the Coulomb integrals than those normally employed. Molecular diagrams showing the bond orders, electron distributions and free valences of formamide, oxamide, carbamic acid, acrylamide, urea, oxamic acid, fumaric acid diamide, *meso*-oxalic acid diamide and benzamide are presented which are in qualitative agreement with the known and predicted properties and chemical behaviors.

Infrared spectra[1] and X-ray crystallographic data[2] on solid oxamide, $(CONH_2)_2$, indicate that, as in other amides, the CO and CN bonds possess hybrid characters not readily describable as ordinary double or single bonds, respectively. Also, it is now known that amides are not satisfactorily described in terms of ionic and covalent resonance forms since the dipole moments[3] and the para-

(1) T. A. Scott and E. L. Wagner, *J. Chem. Phys.*, **30**, 465 (1959).
(2) E. M. Ayerst and J. R. C. Duke, *Acta Cryst.*, **7**, 588 (1954).
(3) R. G. Bates and M. E. Hobbs, *J. Am. Chem. Soc.*, **73**, 2151 (1951).

chors[4] can be accounted for without any contributions of the ionic forms at all.

In order to obtain a description of the bonding involved in oxamide for comparison with that in other simple amides and with the X-ray and spectrographic results, the bond orders and electronic charge distributions were obtained from a simple L.C.A.O. molecular orbital treatment without overlap for this eight π-electron system as well as for formamide, $HCONH_2$; oxamic acid, $HOOCCONH_2$; *meso*-oxalic acid diamide, $O{:}C(CONH_2)_2$; fumaric acid diamide, $(:CHCONH_2)_2$; carbamic acid, $HOCONH_2$; benzamide, $C_6H_5CONH_2$; acrylamide, $CH_2{:}CHCONH_2$; and urea, NH_2CONH_2. The calculated bond orders obtained are very similar in all of these compounds and the bond distances estimated from existing bond order–bond length curves for the CO and CN bonds[5] agree with each other to within 0.03 Å. and with the measured values to within 0.06 Å. when the usual relations for the Coulomb and exchange integrals are used.[6] Similar estimations of the CN and CO stretching force constants[7] give values which agree with each other to within 5 and 6%, respectively, and are of the order of magnitude expected for amides.

In the first calculations the set of Coulomb and exchange integral values suggested by Orgel, *et al.*,[6] were used. These are

$$\alpha(C) = \alpha + 0.1\delta X \qquad \beta(CC) = \beta$$
$$\alpha(O) = \alpha + 2\beta \qquad \beta(CO) = 1.4\beta$$
$$\alpha(N) = \alpha + 2\beta \qquad \beta(CN) = 1.2\beta$$

where α is the Coulomb integral of a benzene-type carbon atom, β is the exchange integral of the carbon–carbon bond in benzene, and $\delta X = \Sigma[\alpha(X) - \alpha]$ where the sum is over the atoms attached to the carbon atom concerned. This latter term takes into account the effect of electronegative atoms on the Coulomb integral of an adjacent carbon atom. In the case of oxamide it increases the calculated CO, CN and CC bond orders by 1 to 3%, increases the calculated charge on the carbon atoms by about 10%, and decreases the charge on the oxygen and nitrogen atoms by 2 to 4%. The roots of the sixth-order secular equation for oxamide obtained using the above values for the Coulomb and exchange integrals are

$$E_1 = \alpha + 3.5851\beta$$
$$E_2 = \alpha + 2.9646\beta$$
$$E_3 = \alpha + 2\beta$$
$$E_4 = \alpha + 2\beta$$
$$E_5 = \alpha - 0.1451\beta$$
$$E_6 = \alpha - 1.5246\beta$$

These roots give the energies of the different molecular orbitals, and since β in negative, the most stable orbital corresponds to E_1, the next most stable to E_2, etc. The system possesses eight pi-electrons and in the ground state these completely fill the first four bonding molecular orbitals. The total pi-electron energy is then $8\alpha + 21.0994\beta$.

On the other hand, if the structure of oxamide is truly represented by the structural formula

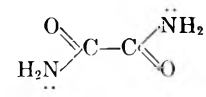

with localized pi-electrons, an equivalent molecular orbital treatment gives as the total pi-electron energy in the ground state the value $8\alpha + 19.2905\beta$. The delocalization energy for oxamide is then 1.8089β or about 36 kcal. per mole.

From the calculated values of the coefficients appropriate to the filled molecular orbitals, the bond orders, N, and the charges on the atoms, q, can be obtained.[8] For oxamide these are

$$N(C{=}O) = 1.6872$$
$$N(C{=}N) = 1.5890$$
$$N(C{=}C) = 1.2101$$
$$q(C) = 0.6398$$
$$q(O) = 1.6312$$
$$q(N) = 1.7291$$

These bond orders correspond to bond lengths of 1.233–1.287,[9] 1.357 and 1.495 Å., respectively, as compared with the X-ray values of 1.243, 1.315 and 1.542 Å. The agreement here between the calculated and observed bond lengths is within 0.05 Å. which is often as good as the older X-ray data. The force constants estimated for these bond orders are: for the CN bond stretch, 7.8–8.6 md./Å.; for the CO stretch, 9.6–11.0 md./Å.; and for the CC bond stretch, 5.4 md./Å. These are all reasonable values.

A similar molecular orbital treatment for formhydroxamic acid[10] as well as our own equivalent treatments for formamide, oxamide acid, *meso*-oxalic acid diamide, fumaric acid diamide, carbamic acid, benzamide, acrylamide and urea gave the bond orders listed in Table I together with the estimated bond lengths shown.

The observed CN and CO bond distances for formamide are 1.300 and 1.255 Å., and for urea they are 1.37 and 1.26 Å., respectively. The general agreement between the bond order values and the force constants for the CO and CN bonds in these different compounds indicates the similarity of the electronic structures in the different amide groups, however, it is apparent that the nature of the X atom influences the bonding in the amide group to a certain extent.

The molecular diagrams of these molecules are shown in Fig. 1, where as usual the bond orders are written on the bonds, the charges in electronic units are written under the atoms, and the carbon atom free valences at the ends of the arrows.

The most arbitrary part of this simple treatment as illustrated with oxamide is in the empirical assignment of values to the Coulomb and exchange integrals of the heteroatoms in terms of those for a carbon atom and a carbon–carbon bond. Although it is known that within the framework of the molec-

(4) R. P. Shukla and R. P. Bhatnager, *J. Indian Chem. Soc.*, **32**, 611 (1955).

(5) E. G. Cox and G. A. Jeffrey, *Proc. Roy. Soc. (London)*, **A207**, 110 (1951).

(6) L. E. Orgel, T. L. Cottrell, W. Dick and L. E. Sutton, *Trans. Faraday Soc.*, **47**, 113 (1951).

(7) B. Pullman and A. Pullman "Les Theories Electroniques de la Chimie Organique," Masson et Cie, Editeurs, Paris, 1952, p. 386.

(8) C. A. Coulson, *Proc. Roy. Soc. (London)*, **A169**, 413 (1939).

(9) The CO bond order–bond length data have a much wider range of values than the corresponding curves for the CN and CC bonds so that only an estimated range of values can be given for the CO bond lengths.

(10) W. J. Orville-Thomas and A. E. Parsons, *J. Molecular Spect.*, **2** 203 (1958).

TABLE I

CALCULATED BOND ORDERS AND BOND LENGTHS IN VARIOUS AMINES, X-CONH$_2$

Molecule	CN Bonds: Order	CN Bonds: Length, Å.	CO Bonds: Order	CO Bonds: Length, Å.	CX Bonds: Order	CX Bonds: Length, Å.	Delocal. energy, β
Formamide	1.597	1.357	1.696	1.232–1.285	1.0		0.7951
Oxamic acid	1.591	1.358	1.689	1.232–1.286	1.246	1.491	1.7723
Oxamide	1.589	1.359	1.687	1.233–1.287	1.210	1.49	1.8089
meso-Oxalic acid diamide	1.588	1.359	1.686	1.234–1.288	1.219	1.496	2.0370
Formhydroxamic acid[7]	1.57	1.362	1.69	1.232–1.286			
Fumaric acid diamide	1.546	1.367	1.637	1.248–1.298	1.370	1.465	2.4003
Carbamic acid	1.543	1.368	1.633	1.250–1.300	1.449	1.304	1.4812
Benzamide	1.540	1.369	1.630	1.251–1.301	1.386	1.462	3.1924
Acrylamide	1.529	1.371	1.617	1.255–1.304	1.428	1.435	1.2699
Urea	1.520	1.372	1.606	1.258–1.306	1.520	1.372	1.4869

TABLE II

BOND ORDERS AND CHARGE DISTRIBUTIONS IN OXAMIDES AS A FUNCTION OF λ

Quality calcd.	$\lambda = 0$	$\lambda = 1/4$	$\lambda = 1/2$	$\lambda = 1$	$\lambda = 2$	$\lambda = 3$	$\lambda = 4$
N(C=O)	1.7328	1.7320	1.7298	1.7209	1.6872	1.6382	1.5823
N(C=N)	1.6281	1.6275	1.6256	1.6178	1.5890	1.5471	1.4981
N(C=C)	1.2617	1.2608	1.2579	1.2472	1.2101	1.1649	1.1234
q(C)	1.0000	0.9525	0.9053	0.8124	0.6398	0.4936	0.3782
q(O)	1.4236	1.4509	1.4782	1.5318	1.6312	1.7156	1.7820
q(N)	1.5766	1.5967	1.6169	1.6560	1.7291	1.7912	1.8380

ular orbital theory almost any reasonable set of values for the Coulomb and exchange integrals will lead to the same general conclusions,[11] it may be that in any particular case an apparently improved agreement between the estimated and observed bond lengths, force constants, dipole moments, etc., could be obtained by using slightly different values for the Coulomb and exchange integrals. If instead of the set of values used above we use

$$\alpha(C) = \alpha + 0.22\lambda\beta \qquad \beta(CC) = \beta$$
$$\alpha(O) = \alpha + \lambda\beta \qquad \beta(CO) = 1.4\beta$$
$$\alpha(N) = \alpha + \lambda\beta \qquad \beta(CN) = 1.2\beta$$

and recalculate the bond orders and charge distributions in oxamide as a function of the parameter λ, we get the results shown in Table II.

As λ increases all of the bond orders and the charge on the carbon atom decrease while the charges on the oxygen and nitrogen atoms increase. To get the best agreement between the calculated and measured bond distances the CN bond order should be about 1.81, the CO bond order should be 1.65 to 1.88, and the CC bond order about 1.0. Obviously a variation of λ cannot accomplish this.

Coulson[12] has suggested that for nitrogen a value for the Coulomb integral of $\alpha + 1/2\beta$ is a more likely value than $\alpha + 2\beta$. Then using for the Coulomb and exchange integrals the values

$$\alpha(C) = \alpha + (\sigma + \rho)/9\beta \qquad \beta(CC) = \beta$$
$$\alpha(O) = \alpha + \sigma\beta \qquad \beta(CO) = 1.4\beta$$
$$\alpha(N) = \alpha + \rho\beta \qquad \beta(CN) = 1.2\beta$$

and recalculating the bond orders and charges in oxamide as a function of σ for the value $\rho = 1/2$ gives the results listed in Table III.

(11) H. C. Longuet-Higgins and G. W. Wheland, *Ann. Rev. Phys Chem.*, **1**, 133 (1950).

(12) C. A. Coulson, "Valence," Oxford University Press, London, 1952, p. 242.

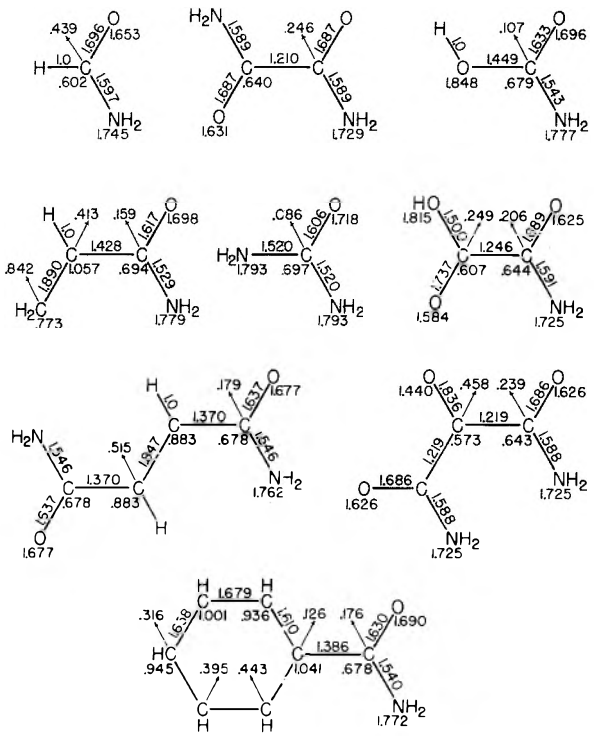

Fig. 1.—Molecular diagrams of some amides.

TABLE III

BOND ORDERS AND CHARGE DISTRIBUTIONS IN OXAMIDES AS A FUNCTION OF σ

Quality calcd.	$\sigma = 0$	$\sigma = 1/2$	$\sigma = 1$	$\sigma = 2$	$\sigma = 3$
N(C=O)	1.8040	1.7298	1.6441	1.4872	1.3744
N(C=N)	1.5302	1.6256	1.7053	1.8077	1.8587
N(C=C)	1.2669	1.2579	1.2591	1.2848	1.3158
q(C)	0.9774	0.9053	0.8645	0.8502	0.8771
q(O)	1.3119	1.4782	1.6139	1.7868	1.8728
q(N)	1.7108	1.6169	1.5217	1.3631	1.2502

Here an increase in σ decreases N(C=O) and increases N(C=N) and N(C=C). The CN and CO bond orders become equal at about $\sigma = 0.8$ where the estimated bond lengths are 1.342 and 1.238–1.290 Å., respectively. When $\rho = 0$ the bond orders are equal at $\sigma = 1/3$ and the estimated bond lengths are 1.340 and 1.234–1.288 Å., respectively. Although the agreement between calculated and observed bond lengths is better here than before the improvement is probably not significant.

We must therefore conclude that varying the values and the ratios of the Coulomb integrals of the nitrogen and oxygen atoms in oxamide cannot give significantly improved bond order values for predicting bond lengths over those obtained using the set of Coulomb and exchange integral values of Orgel, *et al.*[6] The use of their values does, however, give bond orders and charge distributions for the amide groups consistent with the physical and chemical properties of the compounds tested, but, of course, this success cannot be regarded as justifying the unique validity of the parameters used.

THE SORPTION OF ORGANIC VAPORS BY POLYETHYLENE

BY C. E. ROGERS, V. STANNETT AND M. SZWARC

Department of Chemistry, State University College of Forestry at Syracuse University, Syracuse 10, New York

Received January 28, 1959

The sorption behavior of organic vapors in polyethylenes of different degrees of linearity and crystallinity has been treated by assuming that the crystalline portions are impenetrable to the solvent and act therefore as regions of cross-linkage. An expression for the partial molal free energy of dilution and swelling for semi-crystalline polymers has been developed with those assumptions using equations derived previously by Flory. By the use of this expression values of the "intrinsic" Flory–Huggins interaction parameter μ and the average molecular weight between crystallites M_c can be obtained without prior assumptions as to their values. The sorption of thirteen common organic vapors in three polyethylenes of differing crystallinity have been determined over a wide range of vapor activity. The values of M_c for highly branched and for essentially linear polyethylenes are 215 and 100, respectively, at 25°. These values agree well with the values from equilibrium solution swelling and infrared techniques but are smaller than those found by X-ray analysis. The values of μ by this method are generally lower than those found from homogeneous solutions but still follow the same trends predicted by the theories of polymer solutions. Solvent clustering in the polymer has been determined as a function of the volume fractions by the method of Zimm and Lundberg. It appears that the sorption is essentially random mixing of solvent and amorphous polymer up to a critical volume fraction which is dependent on the degree of crystallinity. Subsequent sorption of vapor past this critical volume fraction results in formation primarily of solvent clusters within the polymer matrix.

Introduction

The sorption isotherms of condensable vapors in polymers often can be represented over a substantial range of concentration by expressions based on the lattice theory of solvent–polymer solutions. For example, Long and co-workers[1] have presented data for the sorption of several organic vapors in polyvinyl acetate, a non-crystalline polymer, where the isotherms essentially obey the simplified form of the Flory–Huggins equation[2,3]

$$\ln (P_i/P_i^0) \approx \ln a_i = \ln v_1 + v_2 + \mu v_2^2$$

where v_1 and v_2 are the volume fractions of sorbed vapor and polymer, respectively, and μ is a constant related to interaction free energy of the first-neighbors.

A complication limiting the usefulness of the simple Flory–Huggins equation for predicting solubility isotherms for many polymers is the anomalous behavior caused by the crystalline regions of the polymer. For polyethylene, which has at room temperature a crystalline content of 60% or higher, depending on the amount of chain branching, the simple Flory–Huggins equation does not describe vapor isotherms accurately over the whole range of vapor activity with any one value of μ.[4]

At temperatures well below the polymer melting point we may expect that the crystalline areas of the polymer will be physically inaccessible to the solvent molecules,[5] at least at low solvent concentrations, so that the effective composition should be computed on the basis of the amorphous content. In addition, for the better solvents and swelling agents, it may be expected that the restraining action imposed on the polymer chains by the semi-crystalline network lattice causes the crystallites to act as giant cross-linkages[6] leading to an unfavorable entropy effect which limits the maximum swelling and sorption. Therefore, the usual Flory–Huggins equation for the activity of the solvent would have to be modified to an expression analogous to that derived by Flory and Rehner for the swelling of a cross-linked polymer.[7,8] Such a relationship is easily obtained utilizing expressions derived previously by Flory.

Partial Molal Free Energy of Dilution and Swelling for Semi-crystalline Polymers.—The free energy change ΔF involved in the mixing of pure solvent with the initially pure, semi-crystalline, unstrained polymeric system in which the crystallites are to be considered impenetrable to the solvent, acting therefore as areas of cross-linking, may be considered to consist of two parts: the free

(1) R. J. Kokes, A. R. DiPietro and F. A. Long, *J. Am. Chem. Soc.*, **75**, 6319 (1953).
(2) P. J. Flory, *J. Chem. Phys.*, **10**, 51 (1942).
(3) M. L. Huggins, *ibid.*, **9**, 440 (1941).
(4) I. Sobolev, J. A. Meyer, V. Stannett and M. M. Szwarc, *Ind. Eng. Chem.*, **49**, 441 (1957).
(5) R. B. Richards, *Trans. Faraday Soc.*, **41**, 127 (1945); **42**, 10 (1946).
(6) R. F. Boyer, *J. Appl. Phys.*, **20**, 540 (1949).
(7) P. J. Flory and J. Rehner, *J. Chem. Phys.*, **11**, 512 (1943).
(8) P. J. Flory, *ibid.*, **18**, 108 (1950).

energy of mixing ΔF_M and the elastic free energy ΔF_{el} consequential to the expansion of the network structure.

$$\Delta F = \Delta F_M + \Delta F_{el} \quad (1)$$

The free energy of mixing ΔF_M may be obtained utilizing an expression for the total configurational entropy of a semi-crystalline polymer–solvent mixture which was developed by Flory.[9]

If we assume that the chain polymer consists of x chain segments, each of which is equal in size to a solvent molecule,[10] so that $x = \bar{V}_2/\bar{V}_1$, where $\bar{V}_2$ and $\bar{V}_1$ are the molar volumes of polymer and solvent, respectively, a simplified form of the total configurational entropy S_c derived by Flory is

$$S_c = k\{-n_1 \ln [n_1/(n_1 + \lambda x n_2)] - n_2 \ln [n_2/(n_1 + \lambda x n_2)] + [n_2(x-1) - m(L-1)] \ln [(z-1)/e] + m \ln v_2 + m \ln [(x - L + 1)/x]\} \quad (2)$$

where

n_1 = no. of solvent molecules
n_2 = no. of polymer molecules
m = total no. of crystalline sequences
L = av. length of crystallite in no. of segments
λ = fraction of polymer in the amorphous state
v_2 = volume fraction of polymer

To calculate the configurational entropy of mixing partially disorientated polymer and solvent, we may conceive that the formation of the solution occurs in two steps: disorientation of the pure, perfectly ordered polymer to the semi-crystalline order and mixing of the partially disorientated polymer with solvent. The separate entropy changes are obtained as follows: the entropy of disorientation ΔS_d is given by equation 2 with $n_1 = 0$

$$\Delta S_d = (S_c)_{n_1=0} = k\{-n_2 \ln [n_2/\lambda x n_2] + [n_2(x-1) - m(L-1)] \ln [(z-1)/e] + m \ln [(x - L + 1)/x]\} \quad (3)$$

The entropy of mixing partially disorientated polymer and solvent may be obtained by subtracting equation 3 from equation 2.

$$\Delta S_M^* = S_c - \Delta S_d$$

$$\Delta S_M^* = -k\{n_1 \ln [n_1/(n_1 + \lambda x n_2)] + n_2 \ln [\lambda x n_2/(n_1 + \lambda x n_2)] + m \ln [x n_2/(n_1 + x n_2)]\} \quad (4)$$

To avoid the paradox of an infinite entropy as $\lambda \to 0$, it is necessary to modify equation 4 by replacing n_2, the total number of polymer molecules by λn_2, the number of amorphous "molecules" as the factor to the second term.[11] Also, since the entropy of mixing of solvent with amorphous polymer is independent of the total number of crystalline sequences, m, the term involving m may be eliminated.[11] Equation 4 may then be rewritten as

$$\Delta S_M^* = -k[n_1 \ln v_{1a} + \lambda n_2 \ln v_{2a}] \quad (5)$$

where

$v_{1a} = n_1/(n_1 + \lambda x n_2)$ = vol. fraction of solvent in amorphous polymer

$v_{2a} = \lambda x n_2/(n_1 + \lambda x n_2)$ = vol. fraction of amorphous polymer segments

An asterisk is appended to the symbol, ΔS_M^*, to indicate that it represents only the configurational entropy computed by considering the external arrangement of the molecules and their segments without regard for the internal situations of the latter. It may be noted that all of the above expressions, equations 2 through 5, reduce to the corresponding expressions given previously by Flory[10] for the case of completely amorphous polymers when $\lambda = 1$ and $m = 0$.

In analogy with the case of a totally amorphous polymer,[10] the heat of mixing ΔH_M may be considered proportional to the product of the number of solvent molecules and the volume fraction of *available* polymer, that is

$$\Delta H_M = kT\mu n_1 v_{2a} \quad (6)$$

where μ is the usual Flory–Huggins interaction constant.

An expression for ΔF_M may be obtained from equations 5 and 6 by setting $n_{2a} = 0$ to account for the absence of individual polymer molecules in the network structure and assuming $\Delta S_M^* = \Delta S_M$, the total entropy change on mixing.

$$\Delta F_M = \Delta H_M - T\Delta S_M = kT[n_1 \ln v_{1a} + \mu n_1 v_{2a}] \quad (7)$$

By analogy with the deformation of rubber, we may assume that no heat change takes place during the swelling process other than the heat of mixing. That being the case, the elastic free energy ΔF_{el} for an isotropic network with f-functional junctions (cross-links) is given by Flory[8] as

$$\Delta F_{el} = \frac{kT\nu_e}{2}\left(3\alpha^2 - 3 - \frac{4}{f}\ln \alpha^3\right) \quad (8)$$

where α is the linear deformation factor and ν_e is the effective number of chains in the network.

The condition of isotropy may or may not be fulfilled depending on the nature of the crystalline polymer network and especially on any orientation of the individual crystallites in the polymer. However, for low degrees of swelling, it may be assumed that approximate isotropic swelling deformation occurs. The chemical potential of solvent in the swollen gel is

$$\Delta\bar{F}_1 = N\left(\frac{\partial \Delta F_M}{\partial n_1}\right)_{n_2,T,P} + N\left(\frac{\partial \Delta F_{el}}{\partial \alpha}\right)_{n_2,T,P}\left(\frac{\partial \alpha}{\partial n_1}\right)_{n_2,T,P} \quad (9)$$

with

$$\alpha^3 = v/v_0 \quad (10)$$

where

N = Avogadro's number
v_0 = volume of relaxed amorphous network
v = volume of swollen amorphous network
$v_0/v = v_{2a}$

Assuming that mixing occurs without significant change in the total volume of the system

$$\alpha^3 = 1/v_{2a} = (v_0 + n_1 V_1/N)/v_0 \quad (11)$$

so that

$$(\partial\alpha/\partial n_1)_{n_2,T,P} = \bar{V}_1/3\alpha^2 v_0 N \quad (12)$$

where $\bar{V}_1$ = molar volume of the solvent. Differentiating equations 7 and 8 and expressing ν_e in moles

(9) P. J. Flory, *J. Chem. Phys.*, **17**, 223 (1949).
(10) P. J. Flory, "Principles of Polymer Chemistry," Cornell University Press, Ithaca, N. Y., 1953.
(11) H. L. Frisch, private communication.

$$\Delta\bar{F}_1 = RT\left[\ln v_{1a} + v_{2a} + \mu v_{2a}^2 + \bar{V}_1(\nu_e/v_0)\left(v_{2a}^{1/3} - \frac{2v_{2a}}{f}\right)\right] \quad (13)$$

When the crystallites are considered as cross-links then the functionality, f, is equal to twice the number of chains ϕ in the cross-section of a crystallite,[12] *i.e.*, $f = 2\phi$. Also from the theory of rubber elasticity[11]

$$\frac{\bar{V}_1\nu_e}{v_0} = \bar{V}_1\rho_a(\bar{M}_c^{-1} - \bar{M}_n^{-1})$$

where

ρ_a = density of unswollen amorphous regions
$\bar{M}_c$ = mol. wt. of cross-linked chain
$\bar{M}_n$ = primary mol. wt. of amorphous polymer

Substituting these expressions into equation 13

$$\Delta\bar{F}_1 = RT\left[\ln v_{1a} + v_{2a} + \mu v_{2a}^2 + \bar{V}_1\rho_a\left(\frac{1}{\bar{M}_c} - \frac{2}{\bar{M}_n}\right)\left(v_{2a}^{1/3} - \frac{v_{2a}}{\phi}\right)\right] \quad (14)$$

For polymers with moderate to high degrees of crystallinity $\bar{M}_a > \bar{M}_c$ and $\phi > v_{2a}$, so that equation 14 reduces to

$$\Delta\bar{F}_1 = RT\left[\ln v_{1a} + v_{2a} + \mu v_{2a}^2 + \frac{\rho_a\bar{V}_1}{\bar{M}_c}v_{2a}^{1/3}\right] \quad (15)$$

Since the pure solvent has been chosen as the standard state, $a_1 = \rho_1/\rho_1^0$, to the approximation that the vapor may be regarded as an ideal gas.

If experimental data is available over a range of vapor activity, equation 15 may be used to simultaneously determine μ and $\bar{M}_c$ without any further or prior assumptions as to their values.

$$\chi = \mu + \frac{\rho_a\bar{V}_1}{\bar{M}_c}v_{2a}^{-5/3} \quad (16)$$

where χ is equal to $[\ln(a_1/v_{1a}) - v_{2a}]/v_{2a}^2$ and is the value of μ calculated for the system disregarding the effect of the crystalline "cross-links." Then, if data is available for a range of solvent activities, one may graph χ *versus* $v_{2a}^{-5/3}$; when $\bar{M}_c$ is constant, the resulting plot will be linear with a slope given by $\rho_a V_1/\bar{M}_c$ and an intercept ($v_{2a}^{-5/3} = 0$) equal to μ. If $\bar{M}_c$ increases with solvent activity and assuming μ to be independent of concentration, the plot will be concave to the $v_{2a}^{-5/3}$ axis. If $\bar{M}_c$ is infinite ($\bar{M}_c = \bar{M}_a$), then a plot of χ *versus* either $v_{2a}^{-5/3}$ or a_1 will have zero slope and $\mu = \chi$ for all values of $v_{2a}^{-5/3}$ or a_1.

It is not to be expected that the value of μ as calculated above will *necessarily* be identical with that calculated from data obtained from homogeneous solutions of solvent and polymer. The relative number of solvent–solvent, polymer–polymer and solvent–polymer contacts is very different in the case of initially sorbed vapor as opposed to the saturated solution; the magnitudes of the heat and entropy contributions will possibly be quite different in the two instances. In addition, it should also be realized that the above expressions are subject to the inaccuracies and limitations inherent in the theories of polymer solutions and rubber-like elasticity. The reasons for non-conformity of solvent–polymer systems to the behavior predicted by statistical expressions based on the lattice theory and the theory of rubber elasticity have been adequately discussed by other authors[10,13] and need not be reiterated in this paper.

(12) More exactly $f = 2\phi \times p'$ where p' is the probability of a chain eaving the crystallite enters a second crystallite. For moderate or high degrees of crystallinity $p' \approx 1$.

Experimental

The equilibrium sorption isotherms were measured by means of a quartz helix microbalance of the type described by Prager and Long.[14] This basic apparatus was modified slightly in design to allow the portion of the glass tube containing the film sample suspended on the helix to be surrounded by a constant temperature bath so that measurements at below room temperature could be made.

The organic solvents and vapors used in this study were of commercial reagent grade. The liquid hydrocarbons were dried over sodium wire and distilled under vacuum directly into a solvent trap which was connected through a stopcock with the spring-sample tube. The distillate was thoroughly degassed and the vapor admitted into the spring-sample tube until the desired pressure was obtained. The alkyl chlorides were dried over anhydrous calcium chloride and distilled in a like manner. The methyl bromide and isobutylene (obtained from the Matheson Company, their purities being 99.4 and 99.0%, respectively) were frozen out under vacuum by a liquid nitrogen trap, then thawed and allowed to pass into the system.

The following polyethylene films were used

Sample[a]	Thickness, mm.	Density (25°)[b]	% Amorphous[c] 0°	25°
Du Pont (I)	0.533	0.919	38	42
Du Pont (II)	.051	.922	36	40
Ziegler	.041	.938	29	32
Phillips (Marlex 100)	.056	.954	23	25

[a] The Du Pont samples were made by the high-pressure process. [b] The densities of the film samples were determined in a density gradient column by the Dow Chemical Company. [c] The per cent. crystallinities were determined directly by X-ray diffraction by H. W. Starkweather, Jr., of du Pont de Nemours, Inc.

The film sample was washed carefully with toluene and/or acetone to remove grease and other impurities from the film surface. The sample was then secured onto the helix spring and evacuated at least 48 hours at less than 10^{-4} mm. pressure before the weight of the degassed sample was determined. The equilibrium pressure and the weight gain of the sample were measured after no further increase in the extension of the spring was observed over a 12-hour period. The volume fractions were calculated from the experimentally determined weight fractions assuming that solvent and polymer volumes were additive on mixing and that sorption occurred only in the amorphous regions of the polymer. The density of the amorphous regions in the semi-crystalline matrix was taken as 0.83 g./cc.

Results and Discussion

Effect of Solvent Type and Temperature on the Interaction Parameter.—The values of χ for methyl bromide and *n*-hexane at 0° and three polyethylenes of different crystallinities are shown as a function of vapor activity a_1 in Fig. 1. It will be noticed that χ increases with the vapor activity a_1 for all three polyethylenes in the case of *n*-hexane, a relatively good solvent. As a result of this constant increase, no one value of χ will adequately serve to define the sorption over the activity range. For methyl bromide, however, χ is essentially constant. This is perhaps not surprising, since methyl bromide has a high cohesive energy density and is not a good solvent or swelling

(13) J. H. Hildebrand and R. L. Scott, "The Solubility of Nonelectrolytes," 3rd Edition, Reinhold Publ. Corp., New York, N. Y., 1950.

(14) S. Prager and F. A. Long, *J. Am. Chem. Soc.*, **73**, 4072 (1951).

agent for polyethylene. Because the degree of swelling is small at all solvent activities, the effect of crystallites as cross-links is negligible and consequently the "effective" M_c is infinite. Since the actual M_c will be shown to be a relatively low finite value, we may say that the partial molal volume of the methyl bromide in solution is essentially zero. This is borne out by the experimental observation that there is little volume change (swelling) during the sorption process. This relatively constant value of $\chi = \mu$ for methyl bromide permits us to represent the sorption isotherms of the different density polyethylenes with a single value of the Flory–Huggins parameter, Fig. 2. This effect of increased crystallinity on solubility confirms the hypothesis that the crystalline regions are essentially impenetrable to the vapor molecules. Correction for the crystalline content results in agreement between the isotherms of different density polyethylenes and *poor* solvents using the same μ values for all polyethylenes. A similar agreement is attained in the case of better solvents when the effect of swelling is considered, but the values of μ vary with the linearity of the polymer as predicted by theory.

Typical plots of χ *versus* $v_{2a}^{-5/3}$ are presented in Figs. 3 through 6. A more detailed account of the vapor sorption isotherms from which these values were calculated will be published elsewhere.[15] The values of μ and M_c calculated from the intercepts and initial slopes by use of equation 16 are listed in Table I. The size and shape as well as the chemical composition of the penetrant molecule appear to determine the thermodynamic interaction with the polymer as expressed by the value of the interaction parameter μ. The more flexible paraffin molecules have the lower μ values attesting to the greater ease and efficiency with which they form penetrant–polymer contacts as opposed to the more rigid aromatics.

The lower values of μ for *n*-hexane in the relatively unbranched polyethylenes, Ziegler and Phillips, as compared with the highly branched Du Pont polyethylene may be partially due to the sensitivity of the χ intercept to experimental errors as the slope $(d\chi/dv_{2a}^{-5/3})$ becomes greater. However, it has been shown[16] that solubility of polymers is highly sensitive to even small degrees of branching in the sense that an isolated branched macromolecule is characterized by a higher degree of local concentration of segments than an isolated linear molecule of the same type in the same solvent. Therefore, there is more segment–segment contact in a branched molecule in solution than in a linear one and the polymer–solvent interaction is decreased. The μ value should then be noticeably lower for a linear molecule than for its branched counterpart.

The interaction parameter μ was originally regarded as a measure of the enthalpy of solution, however it has been suggested[17] that it has the more

(15) C. E. Rogers, V. Stannett and M. Szwarc, to be published.

(16) P. M. Doty, M. Brownstein and W. Schleuer, THIS JOURNAL, **53**, 213 (1949).

(17) P. J. Flory and W. R. Krigbaum, "Annual Review of Physical Chemistry," Vol. 2, Annual Reviews, Inc., Stanford, Calif., 1951, p. 383.

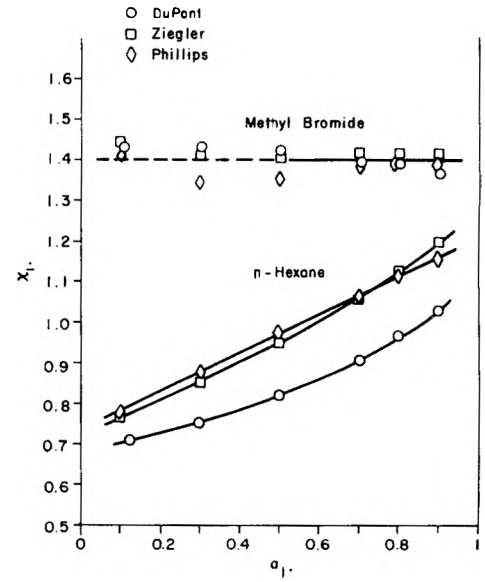

Fig. 1.—Interaction parameter χ_1 *versus* vapor activity; methyl bromide and *n*-hexane vapors in polyethylene, 0°.

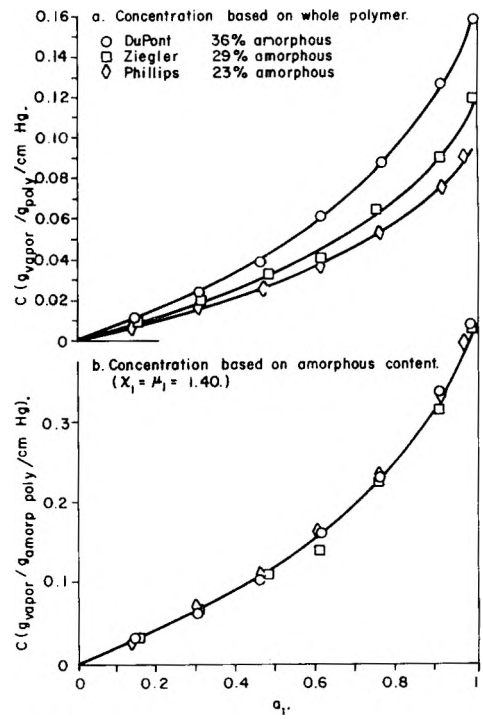

Fig. 2.—Concentration of sorbed vapor *versus* vapor activity; methyl bromide vapor in polyethylene, 0°.

general form

$$\mu v_2^2 = \Delta\bar{F}_1'/RT = \Delta\bar{H}_1/RT - \Delta\bar{S}_1'/R$$

where $\Delta\bar{F}_1'$ is the change in free energy, excluding that due to configurational entropy, when a mole of gas is added to an infinite amount of polymer at concentration v_2. This expression is analogous to the ones presented previously[11,14] separating μ into entropy and heat terms

$$\mu = \mu^S + \mu^H$$

Over a limited range, μ^S will be independent of temperature, while μ^H will be inversely proportional

TABLE I

Sample	Vapor	Temp., °C.	$\bar{V}_1$	δ_1	M	μ	μ^H	μ^S
Du Pont	*n*-Pentane	25	116	7.05	250	0.22	0.18	0.04
	n-Hexane	0	126	...	160	.01	...	...
		25	132	7.30	150	− .063	.11	− .17
		30	132	...	160	− .16	...	...
	n-Heptane	25	147	7.45	220	.096	.075	.21
	n-Octane	25	164	7.55	140	− .31	.056	− .37
	c-Hexane	25	109	8.20	320	.31	.0074	.30
	Benzene	25	89	9.15	230	.50	.20	.30
	Toluene	25	107	8.90	230	.46	.15	.31
	Ethylbenzene	25	123	8.80	210	.41	.14	.27
	p-Xylene	25	124	8.75	160	− .054	.012	− .06
	Chloroform	25	81	9.3	290	.64	.23	.41
	Carbon tetrachloride	25	97	8.6	160	.10	.059	.04
	Methyl bromide	0	55	9.4	∞	1.40	.19	1.2
		30	57	9.4	∞	1.20	.19	1.0
	Ethyl bromide	25	76	8.9	∞	1.02	.11	.91
Ziegler	*n*-Hexane	0	126	7.3	82	−0.56	.1	−0.7
		30	132		100	−0.37		−0.5
	Methyl bromide	0	55	9.4	∞	1.40	.2	1.2
		30	57			1.25		1.1
Phillips	*n*-Hexane	0	126	7.3	83	−0.52	.1	−0.6
		30	132		100	−0.47		−0.6
	Methyl bromide	0	55	9.4	∞	1.40	.2	1.2
		30	57			1.35		1.2

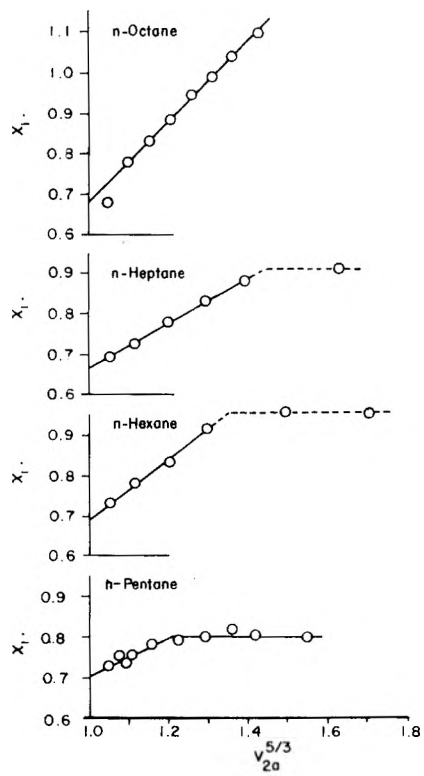

Fig. 3.—Interaction parameter χ_1 *versus* amorphous polymer swelling function $V_{2a}^{-5/3}$ *n*-paraffins in polyethylene, 25°.

to temperature. The data in Table I show that μ does vary as a reciprocal of temperature for *n*-hexane and methyl bromide in Du Pont polyethylene; however a plot of μ *versus* reciprocal temperature is non-linear for *n*-hexane. No calculations of μ^S were attempted from these plots since it was felt that any such calculation would at best give only a poor estimate of μ^S by that method.

The heat term μ^H has been assumed by many investigators to be approximated by the Hildebrand expression[13]

$$\mu^H = V_1(\delta_1 - \delta_2)^2/RT$$

where δ_1 and δ_2 are the square roots of the cohesive energy densities of solvent and polymer, respectively. Then, if μ^S is negligible or does not vary greatly from solvent to solvent, we would expect that μ would pass through a minimum as the absolute difference between the cohesive energy densities of solvent and polymer goes to zero. The values of μ for Du Pont polyethylene at 25° do show a generalized tendency toward this behavior (Fig. 7) with an approximate minimum at $\delta_1 = 8.0 \pm 0.2$; the δ_2 for polyethylene estimated by extrapolation from lower homologous compounds is about 7.9.

Assuming that the above equation gives at least an approximation to μ^H, these values and the corresponding values of μ^S have been calculated and are listed in Table I also. It is apparent that μ^S is proportional to $-\Delta\bar{S}_1$, so that the observed decrease of μ with increase in molecular size ($\bar{V}_1$) may be attributed to an increase in the entropy contribution arising from specific interactions between neighboring solvent molecules and polymer segments in the solution. This assumption is reasonable since the entropy change associated with first neighbor interactions must be proportional to the number of solvent–polymer contacts developed in the solution, just as for the heat change. Therefore, the larger molecules, being capable of more pair contacts per molecule, have the larger entropy of contact formation. As might be expected, the poorer solvents tend to have a

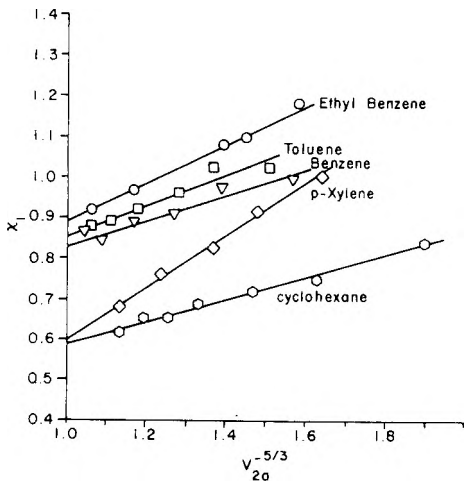

Fig. 4.—Interaction parameter x_1 *versus* amorphous polymer swelling function $V_{2a}^{-5/3}$ aromatic hydrocarbons in polyethylene, 25° (2 mil. DuPont Polyethylene).

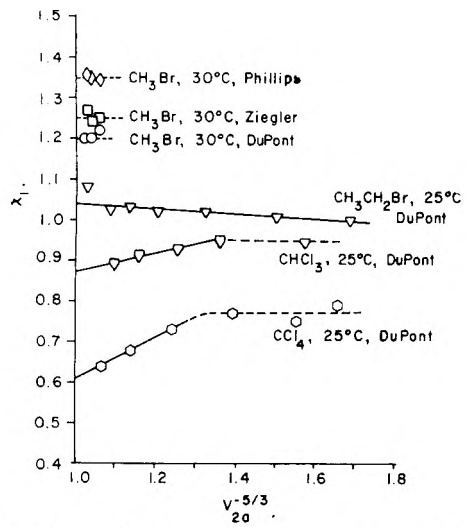

Fig. 5.—Interaction parameter x_1 *versus* amorphous polymer swelling function $V_{2a}^{-5/3}$, halogenated-hydrocarbons in polyethylene, 25 and 30°.

negative entropy of contact formation and the better solvents a positive entropy contribution.

Effect of Solvent Clustering.—A high value of μ ($\mu \gtrsim 0.6$) indicates a positive energy of penetrant–polymer contact formation. Even when the penetrant and polymer are incompatible, some solution or mixing will occur due to a favorable entropy increase; however, penetrant–penetrant and polymer–polymer contacts are preferred to that clustering results. It is supposed that increase of penetrant merely increases the size but not the number of the clusters. The negative entropy of solvent–polymer contact for non-solvents is another indication that the solvent molecules tend to cluster in the polymer–solvent mixture.

A measure of this clustering tendency is afforded by the expressions developed by Zimm and Lundberg[18] based on the statistical mechanics of fluctuations. A relation has been derived between the activity coefficient, $\gamma_1 = a_1/v_1$, and the cluster integral G_{11}

(18) B. H. Zimm and J. L. Lundberg, THIS JOURNAL, **60**, 425 (1956).

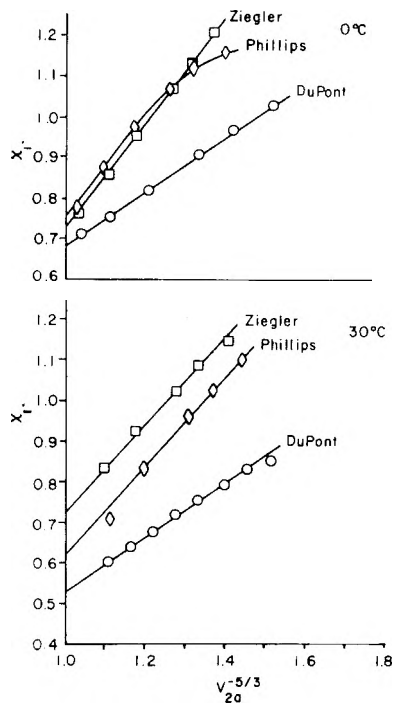

Fig. 6.—Interaction parameter x_1 *versus* amorphous polymer swelling function $V_{2a}^{-5/3}$ *n*-hexane in polyethylene, 0 and 30°.

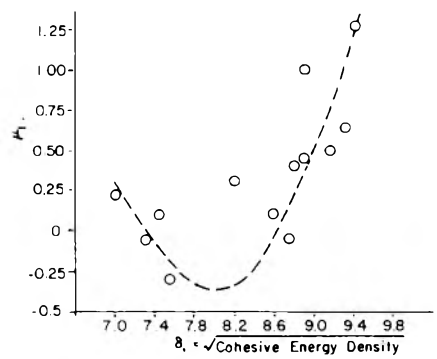

Fig. 7.—Interaction coefficient μ_1 as a function of cohesive energy density, 25°.

$$G_{11}/\phi_1 = -v_2(\partial\gamma_1/\partial a_1)_{P,T} - 1$$

where ϕ_1 is the partial molecular volume of the penetrant in the mixture and v_2 is the volume fraction of polymer. The quantity v_1G_{11}/ϕ_1, is the mean number of penetrant molecules in excess of the mean concentration of penetrant molecules in the neighborhood of a given penetrant molecule; thus, it measures the clustering tendency of the penetrant molecule. For an ideal solution, γ_1 does not vary with concentration, so that G_{11}/ϕ_1 is minus one molecular volume. This means that a particular penetrant molecule excludes its own volume to the other molecules, but otherwise does not affect their distribution.

The clustering functions, G_{11}/ϕ_1, have been calculated for the sorption of vapors at 25° by Du Pont polyethylene and are plotted *versus* vapor volume fraction (v_{1a}) in Fig. 8. As can be seen, a rough correlation exists between the magnitude of μ and the median of the clustering function. Methyl bromide, a non-solvent ($\mu \cong 1.25$), has

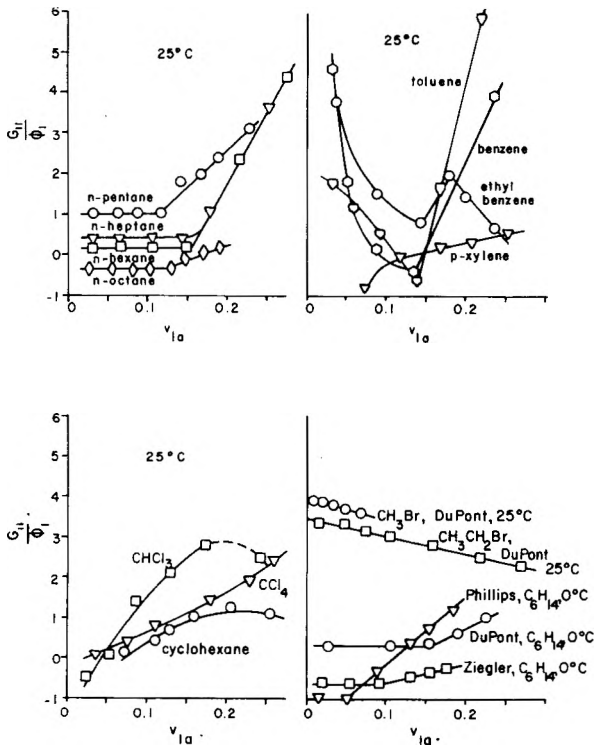

Fig. 8.—Clustering function G_{11}/ϕ_1 *versus* vapor volume fraction at 0 and 25°.

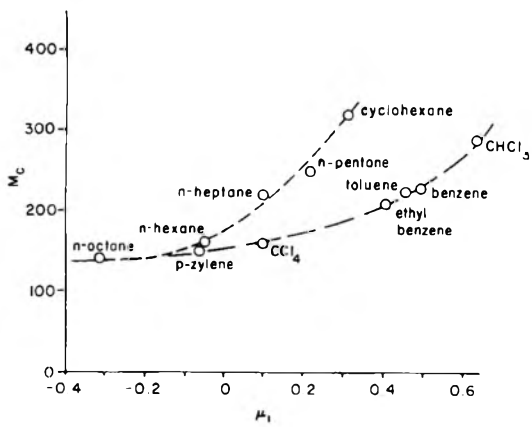

Fig. 9.—Variation of molecular weight between crystallites with the interaction coefficient μ_1 at 25° (2 mil DuPont polyethylene).

a high clustering function ($G_{11}/\phi \sim 3.8$) while *n*-octane, a better solvent ($\mu \cong -0.3$), has a low clustering function ($G_{11}/\phi \sim -0.2$).

The abrupt increase in the clustering of the normal paraffins illustrated in Fig. 8 occurs at approximately the same volume fraction as does the abrupt decrease in slope of χ *versus* $v_{2a}^{-5/3}$ in Fig. 3. As shown in Table II, this critical polymer volume fraction does not change appreciably with temperature but does increase linearly with decrease in the amorphous content of the polymer at a given temperature. It is also apparent that the initial sorption behavior becomes more ideal as the degree of crystallinity increases, as evidenced by the trend of the clustering function to minus values. This may be due to the decrease in branching in the more crystalline polymers. The above phenomena suggests that the sorption of normal paraffins by polyethylene may occur in two successive modes, an initial random mixing up to the point where all available polymer–solvent sites are occupied followed by the formation of solvent clusters.

TABLE II

Sample	Vapor	Temp., °C.	$\bar{V}_1$, cc./m.	$V_{2a}{}^c$
Du Pont	*n*-Hexane	0	126	0.85
Ziegler	*n*-Hexane	0	126	.90
Phillips	*n*-Hexane	0	126	.95
Du Pont	*n*-Pentane	25	116	0.88
	n-Hexane	25	132	.85
	n-Heptane	25	147	.84
	n-Octane	25	164	.87
	Benzene	25	89	.87
	Toluene	25	107	.86
	Ethylbenzene	25	123	.85

The minima exhibited by the clustering functions of the aromatic hydrocarbons occur at approximately the same volume fractions at which the paraffin functions change slope. This indicates a similar relation may apply to the more spherical and rigid ring compounds; however, the plots of χ *versus* $v_{2a}^{-5/3}$ do not show a corresponding change of slope at these volume fractions. The initially high values of the aromatic clustering functions may arise from the fact that due to the rigid symmetrical ring structure the van der Waals forces can initially operate more effectively between adjacent penetrant molecules than between penetrant–polymer. As more vapor is sorbed, the polymer network expands, more penetrant–polymer contact results, and the relative clustering decreases. In comparison, the straight chain paraffins are capable of twisting and bending and so can occupy the available "holes" in the initially unswollen polymer.

Molecular Weight between Crystallites.—The values of the average molecular weight between crystallites, M_c, calculated by equation 16 are listed in Table I. For Du Pont polyethylene at 25°, the variation of M_c with the simultaneously determined value of μ is illustrated in Fig 9. The estimate of M_c is seen to decrease as μ decreases; two generalized curves are indicated, one for saturated hydrocarbons, the other for aromatic and chloro-compounds. This decrease in M_c with μ may be attributed to the greater swelling and solvent powder inherent with solvents of lower μ value. The estimated value of M_c is inversely proportional to the rate of change of a function of free energy, χ, with a function of mass absorbed, $v_{2a}{}^{-5/3}$. It follows that this rate of change will be greater for the better solvents since each molecule of entering vapor then forms penetrant–polymer contacts and has less tendency to form penetrant–penetrant contacts, that is, to cluster. The interaction entropy of a statistical liquid molecule is highest in pure polymer and usually decreases as the concentration of penetrant in polymer increases due to increasing penetrant–penetrant contacts. Thus, the interaction entropy decreases faster with increase in concentration for a poorer solvent

which tends to cluster than for a better (non-clustering) solvent. The variation of M_c with μ would be expected to vanish or go through a minimum as the entropy of interaction goes to zero or becomes positive. This prediction is confirmed by the tendency of the curves in Fig. 9 to converge and level off as μ decreases. This result correlates well with the values of μ^S listed in Table I.

The range of crystallite size for high-pressure process polyethylene (~65% crystalline) determined by X-ray diffraction is usually not greater than 300 Å. and often less than 100 Å.[19] with an average size probably about 140 Å.[20] Ziegler and Phillips polyethylenes have crystallite sizes of about 360 and 400 Å., respectively, in agreement with their higher crystalline content. No great difference is usually found in the three dimensions of the crystallites.

Studies of the infrared spectra[21,22] give a ratio (C/CH_3) equal to about 30 for typical commercial high-pressure process polyethylene. If we assume that the side chains are of the same length as the straight sequences of the main chain then there will be about 16 methylene groups per sequence between branch-points and branch-points and end groups. Assuming that the side chains are predominately butyl[22] or ethyl groups there will be about 25 to 30 methylene groups between branch-points. Then if end groups and/or branch-points are excluded by steric factors from the crystal lattice, the average size of the crystallites would not exceed about 40 Å., which is in line with the lower limit set by the broadening of X-ray diffraction peaks.[22]

From Richards' data[5] for the equilibrium swelling of polyethylene ($\bar{M}_n$ = 14000) in various liquid solvents, we can calculate values of M_c using μ values from the literature. We have assumed the per cent. crystallinity to be about 60% and the activity of the solvent to be unity. Q, as given by Richards, is in units of cc. of solvent sorbed per gram of polymer; Q_a in units of cc. of solvent sorbed per cc. of amorphous polymer, follows as: $Q_a = Q\rho_a/\lambda$, where ρ_a = density of amorphous polymer $\cong$ 0.83, and λ = amorphous fraction $\cong$ 0.4. The volume fraction of amorphous polymer is then

$$v_{2a} = 1/(1 + Q_a)$$

The results, shown in Table III, give an average value of 200 for M_c, which is about 14 methylene units. This corresponds to a crystallite size of about 23 methylene units or 30 Å.

TABLE III

MOLECULAR WEIGHT BETWEEN CRYSTALLITES CALCULATED FROM EQUILIBRIUM SWELLING DATA OF RICHARDS,[5] 25°

Solvent	Q	v_{2a}	μ'	M_c
n-Hexane	0.12	0.80	0.4	184
n-Heptane	.15	.76	.3	190
CCl_4	.19	.72	.28	180
Xylene	.16	.75	.40	230

The average value of M_c for Du Pont polyethylene at 25° as calculated from the data in Table I (from equation 16) is 215 ± 55, corresponding to 15 ± 4 methylene units per amorphous chain segment and about 24 methylene units per crystalline sequence. As mentioned previously, in a branched polyethylene the straight chain sequences are of the order of 16 to 30 methylene units between branch-points.

The agreement between the results on branched polyethylene obtained by sorption, equilibrium swelling and infrared techniques is very satisfactory. The lower values of M_c for Phillips and Ziegler polyethylenes given in Table I reflect the greater crystallinity of these essentially unbranched polyethylenes. The low value of M_c, however, leads to a correspondingly low value for crystallite size, approximately 20 methylene units or 25 Å.

The above values for crystallite size for all three polyethylenes do not agree well with the results of X-ray determinations of crystallite size. It is quite probable that actually the straight chain sequences vary greatly in distribution of lengths so that there will be a corresponding distribution of crystallite sizes. It is possible then that the X-ray tends to overemphasize the fewer large crystallites or perhaps does not differentiate between a large crystallite and a close-packed assembly of many small crystallites. On the other hand, it is also possible that the chain ends and/or branch-points are not excluded from the crystal lattice but cause faults in the crystal structure so that the penetrating solvent is able to easily break up the large crystallites into many smaller crystallites during the sorption and swelling process. Such a process would alter the crystallite size but would not substantially change the over-all per cent. crystallinity.

(19) C. W. Bunn and T. C. Alcock, *Trans. Faraday Soc.*, **41**, 317 (1958).

(20) S. Krimm and A. V. Tobolsky, *J. Polymer Sci.*, **7**, 57 (1951).

(21) R. B. Richards, *J. Applied Chem.*, **1**, 370 (1951).

(22) W. M. D. Bryant and R. C. Voter, *J. Am. Chem. Soc.*, **75**, 6113 (1953).

KINETICS OF THE GAS PHASE DISPROPORTIONATION OF DIMETHOXYBORANE

BY H. S. UCHIDA, H. B. KREIDER, A. MURCHISON AND J. F. MASI

Callery Chemical Company, Callery, Pennsylvania

Received January 29, 1959

A study of the rate of disproportionation of dimethoxyborane in the gas phase has been made by the manometric method. The reaction $3(CH_3O)_2BH \rightleftarrows 2(CH_3O)_3B + {}^1/_2B_2H_6$ is found to be heterogeneous, and in a thoroughly cleaned and dried liter spherical Pyrex glass bulb, at low pressures and moderate temperatures, the rate is proportional to the square of the partial pressure of dimethoxyborane. The rate constants at 40, 60 and 80° are, respectively, 3.91×10^{-7}, 1.69×10^{-6} and 4.97×10^{-6} mm.$^{-1}$ min.$^{-1}$. From these values the activation energy is calculated to be 14.2 kcal. per mole of dimethoxyborane. The effect of a number of different adsorbing surfaces on the rate of disproportionation is considered. On the basis of the experimental results a most probable mechanism is discussed.

Introduction

Previous work on the rate of disproportionation of dimethoxyborane in the gas phase was done by Burg and Schlesinger.[1] Although the reaction was not investigated extensively by them, they did present some helpful experimental results.

1. The stoichiometry for the disproportionation of dimethoxyborane to diborane and methyl borate is

$$6(CH_3O)_2BH \rightleftarrows B_2H_6 + 4(CH_3O)_3B$$

2. The rate of disproportionation is pressure sensitive.

3. The white product, which is formed from the reaction of diborane and methyl alcohol and is analyzed to be a polymer of monomethoxyborane, increases the rate of disproportionation.

The objects of this investigation were to determine the rate constants at different temperatures, the mechanism of the reaction and means of accelerating the disproportionation.

Experimental

Dimethoxyborane.—The dimethoxyborane was prepared by the reaction of diborane and methyl alcohol and was purified in a low temperature Podbielniak column. Active hydrogen analysis revealed the purity of the compound to be greater than 98%. The vapor pressure of pure dimethoxyborane at 0° is 275 mm. and was used as an additional check on purity. Dimethoxyborane does not disproportionate during this measurement if it is made within a half hour's time.

Apparatus and Procedure.—For the static system, the apparatus consisted of a one-liter spherical Pyrex glass bulb with a mercury seal-off, which also served as a manometer. The sample was introduced as a vapor *via* a vacuum line, through the seal-off tube and into the liter bulb, which was immersed in a constant-temperature bath. When the desired initial pressure was obtained, the mercury was admitted into the seal-off and the pressure changes were followed by a cathetometer.

Since the reaction was found to be heterogeneous the reaction bulb was thoroughly cleaned and degassed before starting each run. The bulb was washed before each run with cleaning solution, then distilled water and finally acetone. It was then pumped to dryness and heated with an air–gas flame under high vacuum. When the effect of charcoal was studied, a weighed amount of charcoal was placed in the bulb and then degassed for an extended period of time.

The reactor for the flow system consisted of a 22-mm. Pyrex glass tube, 12 inches long, containing a thermometer and 12.7 g. of charcoal. The flow was regulated by a stopcock and a differential manometer containing mineral oil. Temperature was regulated by means of heating tape. The sample was introduced as a vapor and its pressure was maintained at approximately 275 mm. by evaporating it from a bulb immersed in an ice-bath.

(1) A. Burg and H. Schlesinger, *J. Am. Chem. Soc.*, **55**, 4020 (1933).

Analysis of Sample.—The disproportionated dimethoxyborane was passed through a −131° trap. The methyl borate and dimethoxyborane were fractionated out, and the diborane was expanded into a known volume and its molar quantity obtained by the perfect gas law.

The methyl borate–dimethoxyborane mixture was hydrolyzed with an excess of methanol and the hydrogen evolved was collected with a Toepler pump in a known volume. The hydrogen formed is equivalent to the amount of dimethoxyborane on a one to one basis according to the stoichiometry of the hydrolysis.

$$(CH_3O)_2BH + CH_3OH \longrightarrow (CH_3O)_3B + H_2$$

Results and Discussion

The disproportionation of dimethoxyborane was found to be heterogeneous. This was suspected at an early stage, for reproducible results were obtained only when considerable care was taken in cleaning the reaction bulb. In Fig. 1 the partial pressures of dimethoxyborane both in a clean glass bulb and in a bulb in which the surface area was increased five times by the addition of glass tubes are plotted against time. The curves clearly show the surface dependence of the reaction. Subsequent measurements were confined to the use of a one-liter spherical Pyrex glass bulb.

TABLE I

DATA FOR A TYPICAL DISPROPORTIONATION

Temperature 40°; initial pressure 390.55 mm.

Time, min.	Total pressure, mm.	Partial pressure of $(CH_3O)_2$-BH, mm.	Time, min.	Total pressure, mm.	Partial pressure of $(CH_3O)_2$-BH, mm.
0	390.6	390.6	1465	378.5	318.2
5	390.6	390.6	1535	377.7	313.1
60	389.4	383.3	1595	377.8	313.7
120	389.3	382.7	1694	377.5	311.9
220	388.5	377.9	1920	376.2	304.4
460	386.2	364.1	2035	375.1	297.5
585	384.9	356.6	2110	374.8	296.0
705	394.1	351.5	2205	274.7	295.1
820	383.2	346.4	2260	374.2	292.1
950	381.8	338.0	2800	371.3	274.7
1370	378.9	320.6	2905	370.5	270.1

Three runs were made at 40°, two at 60° and three at 80°. Each run was begun with a different pressure of pure dimethoxyborane. A run consisted of measurement of total pressure and time at frequent intervals up to 25–35% disproportionation. The data for a typical run are given in Table I.

To calculate the partial pressure of dimethoxy-

borane from the total pressure, the expression was used

$$P = 6P_T - 5P^0$$

where

P_T = total pressure
P^0 = initial pressure of dimethoxyborane
P = partial pressure of dimethoxyborane

This relationship was derived from the stoichiometry of the reaction. The gases were assumed to be ideal and there were assumed to be no side reactions. These assumptions were found to be valid up to a certain reaction time for each temperature, since the per cent. disproportionation calculated from the above expression agreed very well with that determined by analysis of the sample. At longer reaction times, deviations occurred due to the decomposition of diborane.

The relationship between the initial pressures and the initial rates of disappearance of dimethoxyborane for the three curves obtained at 40° yielded an average value of 2.19 for the order of the reaction. That the reaction is of order 2 was corroborated by plots of the reciprocal of dimethoxyborane partial pressure *vs.* time; straight lines were obtained in all cases except the experiments at 80°. The deviation from linearity in the latter case is attributed to the thermal decomposition of diborane. Significant amounts of hydrogen were found at the ends of the runs, and after longer periods of time yellow solids were deposited on the walls. This deviation increased with increasing diborane concentration.

The rate constants at 40, 60 and 80° were calculated to be 3.91×10^{-7} $(mm.)^{-1}$ $(min.)^{-1}$, 1.69×10^{-6} $(mm.)^{-1}$ $(min.)^{-1}$ and 4.97×10^{-6} $(mm.)^{-1}$ $(min.)^{-1}$, respectively. These values were obtained by averaging the slopes of the lines obtained from a "second-order plot" (1/concentration *versus* time) for each temperature.

These data were assembled into an Arrhenius plot (Fig. 2) from which rate constants at other temperatures are obtainable by interpolation or extrapolation. From the equation for the line shown $\log k = -3100/T + 3.50$, the rate constants at 25 and 200° were calculated to be 1.26×10^{-7} $(mm.)^{-1}$ $(min.)^{-1}$ and 1.10×10^{-4} $(mm.)^{-1}$ $(min.)^{-1}$, respectively.

The activation energy was calculated to be 14,200 cal. per mole from the slope of the line in Fig. 2. This value is of the right order of magnitude for a bimolecular reaction of measurable rate at room temperature.

It must be emphasized here that these rate constants apply only to the reaction carried out in a

TABLE II

EFFECT OF CHARCOAL ON THE DISPROPORTIONATION

Time (min.)	Amt. B_2H_6 (moles)	Amt. DMB left (moles)	Initial DMB[a] (moles)	Temp., °C.	Disproportionation (%)
Per cent. disproportionation using 1 gram of charcoal					
20	0.000595	0.0138	0.01737	25	20.5
20	.000487	.0140	.01687	25	17.0
20	.000159	.0111	.01462	80	24.0
20	.000159	.0135	.01446	25	6.6
Using 5 g. of charcoal					
20	0.001901	0.00582	0.01722	40	66.2
20	.00213	.00757	.02040	40	62.8
20[b]	.00120	.00110	.01828	40	39.6
Using 10 g. of charcoal[c]					
30	0.001862	0.000444	0.01180	40	94.6

[a] Measured by PVT relationship in known volume at less than 275 mm. pressure. [b] Not all B_2H_6 removed during analysis. [c] Some white solids were present on surface of bulb after run.

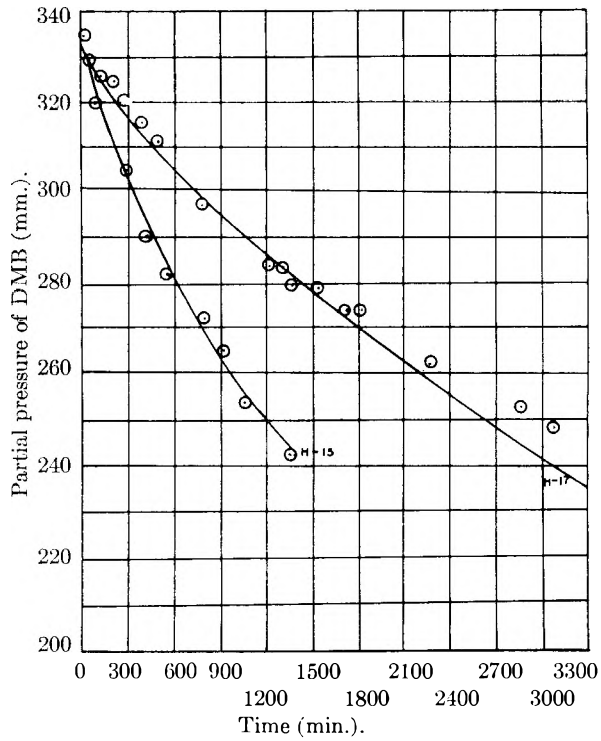

Fig. 1.—Partial pressure of dimethoxyborane *vs.* time at 40°: H-15, glass tube packing; H-17, unpacked bulb.

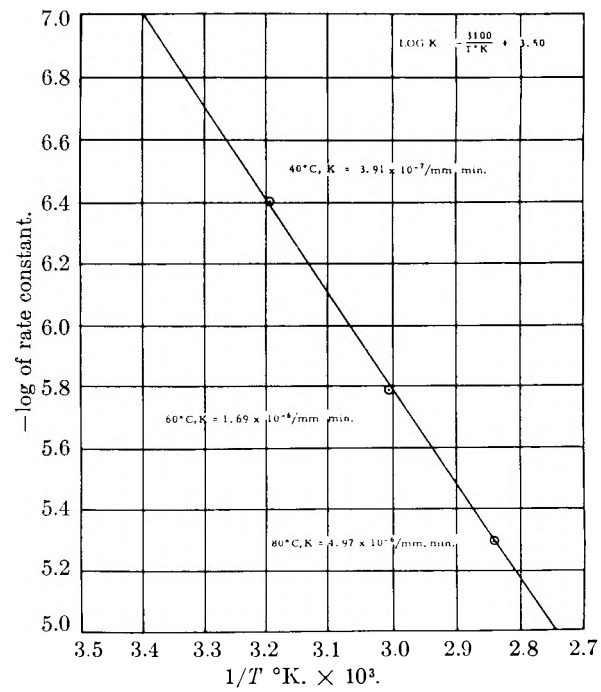

Fig. 2.

one-liter spherical Pyrex glass bulb, since the reaction is heterogeneous.

A partial investigation was made of the effect of several adsorbing surfaces such as charcoal, glass tubes, glass wool, silica gel, magnesium strips and hydrogen reduced copper. Of these, charcoal was much the best catalyst.

In Table II, some of the results obtained from the disproportionation of dimethoxyborane in the presence of charcoal in a static system are shown.

The general conclusions obtained from the charcoal experiments are that the rate appears to be proportional to the amount of charcoal, temperature differences apparently do not affect the rate appreciably, and methyl borate decreases the rate since it is strongly adsorbed. To minimize this undesirable effect a flow system was constructed and the data obtained from it are listed in Table III.

Table III

Disproportionation of $(CH_3O)_2BH$ in a Flow System

Experiment No. 4

Run no.	Time from start of run (min.)	Length of collection of sample (min.)	Temp. of run (°C.)	Residence time (min.)	Disproportionation, %
1	60	20	109	1.06	63.9
2	120	20	109	11.0	64.2
3	180	20	109	1.06	70.3
4	240	20	110	0.87	62.7
5	305	20	106	1.105	60.5
6	325	30	106	0.895	59.5

At 110° and a residence time of approximately one minute, the rate of disproportionation remained near 60% per minute throughout the run. This proved to be the maximum rate obtainable under the conditions studied.

Any proposed mechanism for the disproportionation of dimethoxyborane must account for the observed heterogeneity and the apparent second order. The following is suggested

Step I Adsorption

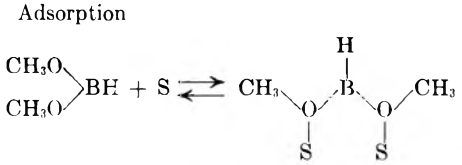

Step II

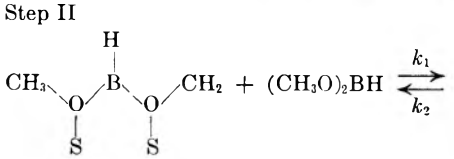

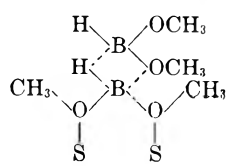

(activated complex)

Step III

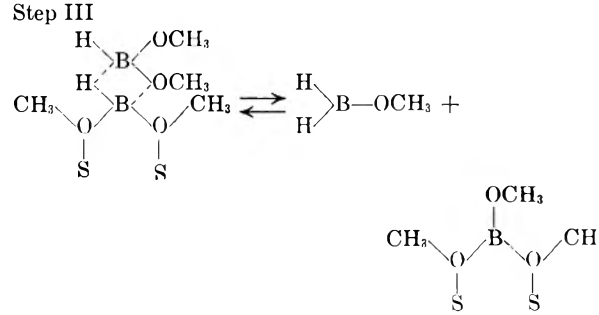

Step IV

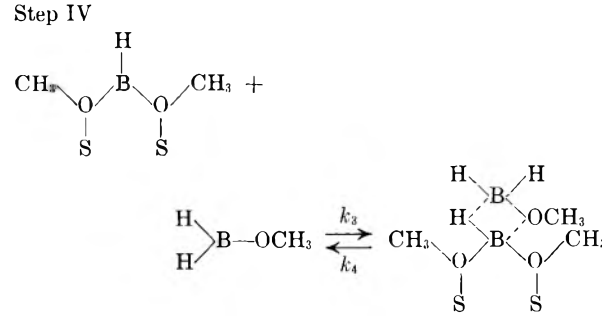

Step V

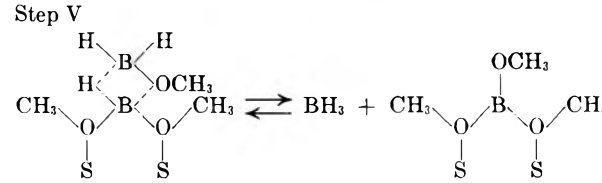

Step VI

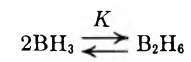

If the bridge-forming step (step II) determines the rate, the reaction will be second order. An equilibrium is denoted in each step to account for the reversibility of the reaction. The presence of the mono-methoxyborane during the reaction was not detected; however, since the polymer of monomethoxyborane was observed by Schlesinger and Burg during the preparation of dimethoxyborane from methyl alcohol and diborane, it is possible that the mono compound is part of the reaction. The assumption that forward reaction 4 is very rapid is supported by the observation made by Schlesinger and Burg and in this Laboratory that the presence of this polymer hastens the reaction rate.

This mechanism postulates that the methyl borate is adsorbed by the surface and thereby decreases the rate of reaction. In the case of charcoal catalyst methyl borate adsorption was observed to reduce the catalyst's effect on the rate of disproportionation over 50%. The mechanism also indicates that the orientation of the dimethoxyborane molecule is important, and suggests that an adsorbent whose active centers are the same distance apart as the oxygen–oxygen distance of the dimethoxyborane molecule and not of methyl borate would increase the over-all rate of disproportionation.

THE EFFECT OF TEMPERATURE ON ION EXCHANGE EQUILIBRIA. II. THE AMMONIUM–HYDROGEN AND THALLOUS–HYDROGEN EXCHANGES

BY O. D. BONNER AND ROBERT R. PRUETT[1,2]

Department of Chemistry, University of South Carolina, Columbia, South Carolina

Received January 30, 1959

Ion-exchange reactions between ammonium and hydrogen and between thallous and hydrogen ion on Dowex-50 resins of 16% DVB content have been studied over the temperature range 0 to 97.5° while maintaining a constant solution ionic strength of approximately 0.1 *M*. The equilibrium constant and the standard free energy, enthalpy and entropy changes have been calculated for each exchange at each temperature. The differential free energy, enthalpy and entropy of exchange for each system is found to vary considerably with resin composition. One possible explanation of this variation is the assumption that the ion exchange resin in the hydrogen form is an acid which is similar in strength but probably slightly weaker than nitric acid.

The ion-exchange process involving the univalent ions A^+, B^+ and a cation-exchange resin may be represented by the metathetical equation

$$A^+ \text{(soln. phase)} + B^+ \text{(resin phase)} = A^+ \text{(resin phase)} + B^+ \text{(soln. phase)} \quad (1)$$

The equilibrium quotient calculated from the concentrations of the ions in the two phases will be dependent not only upon the ions involved in the exchange, the type of exchanger used and the temperature at which the experiment is carried out, but also upon the composition of the phases at equilibrium. The equilibrium constant may be calculated if the exchange is accomplished in aqueous solutions of infinite dilution from the relationship[3,4]

$$\log K_A^B = \int_{X_{B^+}=0}^{X_{B^+}=1} \log k \, dX_{B^+} \quad (2)$$

where K is the thermodynamic equilibrium constant and k is the equilibrium quotient at the resin composition X_{B^+}. A correction for solution phase activity coefficients should be made when solutions of finite concentration are used. It is not always possible to make this correction for equilibria at elevated temperatures as the activity coefficient data are not available. If the solutions are relatively dilute ($\mu = 0.1$ *M*), the correction should be small, however, since it involves a ratio of activity coefficients. The standard free energy change for the above reaction is $\Delta F^\circ = -RT \ln K$. The standard enthalpy and entropy changes ΔH^0 and ΔS^0 may be determined from measurements of the change of the equilibrium constant with temperature. These thermodynamic functions have been reported[5] for the exchange of sodium ion and hydrogen ion and for cupric ion and hydrogen ion on 16% DVB Dowex 50. In this work the ammonium–hydrogen and thallous–hydrogen exchanges on the same resin were studied.

Experimental

Nitric acid, ammonium nitrate and thallous nitrate solutions of an ionic strength of 0.1 *m* were used for these exchanges. The methods of equilibration and temperature control were the same as those for the cupric–hydrogen exchange.[4] The concentration of each ion in each phase was determined experimentally for each of the exchange reactions as follows: Hydrogen ion—concentrations of hydrogen ion were determined volumetrically by titration with standard alkali; ammonium ion—an excess of formaldehyde was added to the solution containing ammonium ion and the liberated hydrogen ion was titrated with standard alkali; thallous ion—thallous ion concentrations were determined volumetrically by titration with standard potassium bromate solution in the presence of hydrochloric acid, methyl orange serving as an indicator.

Discussion and Results

The ion exchange process as represented by equation 1 is in reality the sum of three processes. Ion A^+ is transferred from the dilute aqueous solution to the concentrated resin phase, ion B^+ is transferred from the concentrated resin phase to the dilute aqueous solution, and in the process some water is also usually transferred from one phase to the other as the water content of the fully swollen resin phase is not the same in all ionic forms. If one, however, considers the differential process in which one mole of ion A^+ is exchanged for one mole of ion B^+, the quantities of solution phase and resin phase being so great that there is no resultant change in composition of either phase, then there is no transfer of water from one phase to the other. This process is of further interest in that one may observe the effect of the resin composition on the free energy enthalpy and entropy changes accompanying the exchange reaction.

If one chooses at each temperature the standard state for the aqueous phase to be the usual hypothetical one molal solution, and for the resin phase, the resin having the desired ionic composition at equilibrium, one may then calculate for a resin of composition X_{B^+}, for the differential exchange of ions A^+ and B^+ at temperature T, the thermodynamic quantities

$$\Delta F^* = -2.3003 \, RT \log k \quad (3)$$

$$\Delta H^* = -2.303R \frac{d \log k}{d(1/T)} \quad (4)$$

and

$$\Delta S^* = \frac{\Delta H^* - \Delta F^*}{T} \quad (5)$$

These quantities are related to the corresponding quantities for the exchange represented by equation 1 by the equations

$$\Delta F^0 = \int_{X_{B^+}=0}^{X_{B^+}=1} \Delta F^* \, dX_{B^+} \quad (6)$$

(1) These results were developed under a project sponsored by the United States Atomic Energy Commission.

(2) Part of the work described herein was included in a thesis submitted by Robert R. Pruett to the University of South Carolina in partial fulfillment of the requirements for the degree of Master of Science.

(3) E. Hogfeldt, E. Ekedahl and L. G. Sillen, *Acta Chem. Scand.*, **4**, 1471 (1950).

(4) O. D. Bonner, W. J. Argersinger and A. W. Davidson, *J. Am. Chem. Soc.*, **74**, 1044 (1952).

(5) O. D. Bonner and L. L. Smith, THIS JOURNAL, **61**, 1614 (1957).

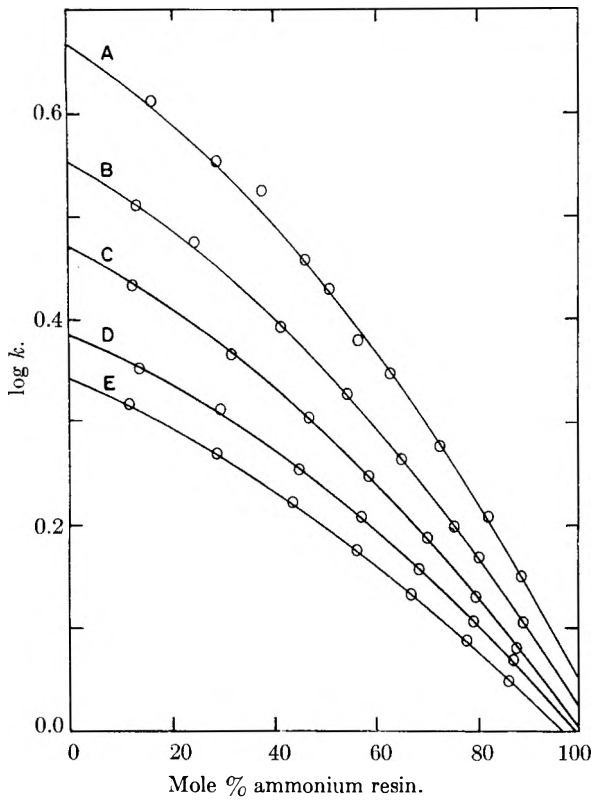

Fig. 1.—Ammonium–hydrogen exchange equilibrium data: A, 0°; B, 25°; C, 50°; D, 77°; E, 97.5°.

$$k = \frac{(X_{NH_4^+})\ \text{resin}\ (m_{H^+})\ \text{soln}}{(X_{H^+})\ \text{resin}\ (m_{NH_4^+})\ \text{soln}}$$

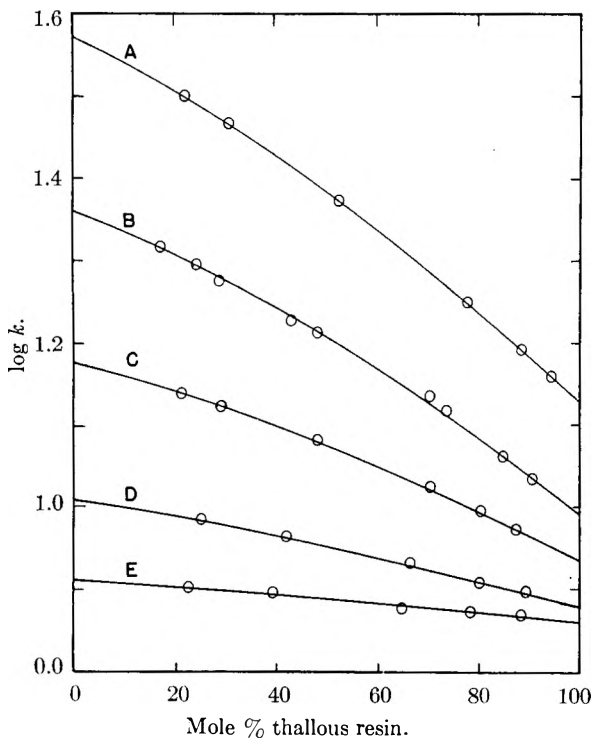

Fig. 2.—Thallous–hydrogen exchange equilibrium data: A, 0°; B, 25°; C, 50°; D, 77°; E, 97.5°.

$$k = \frac{(X_{Tl^+})\ \text{resin}\ (m_{H^+})\ \text{soln}}{(X_{H^+})\ \text{resin}\ (m_{Tl^+})\ \text{soln}}$$

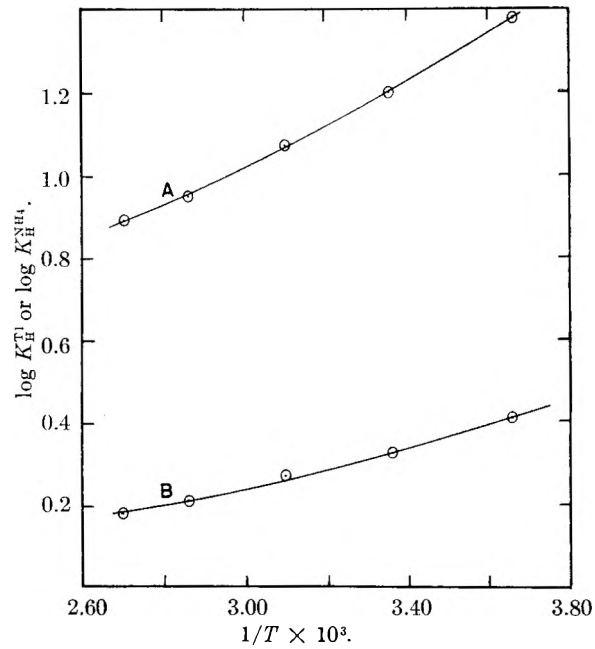

Fig. 3.—Temperature dependence of equilibrium constants: A, thallous–hydrogen exchange B, ammonium–hydrogen exchange.

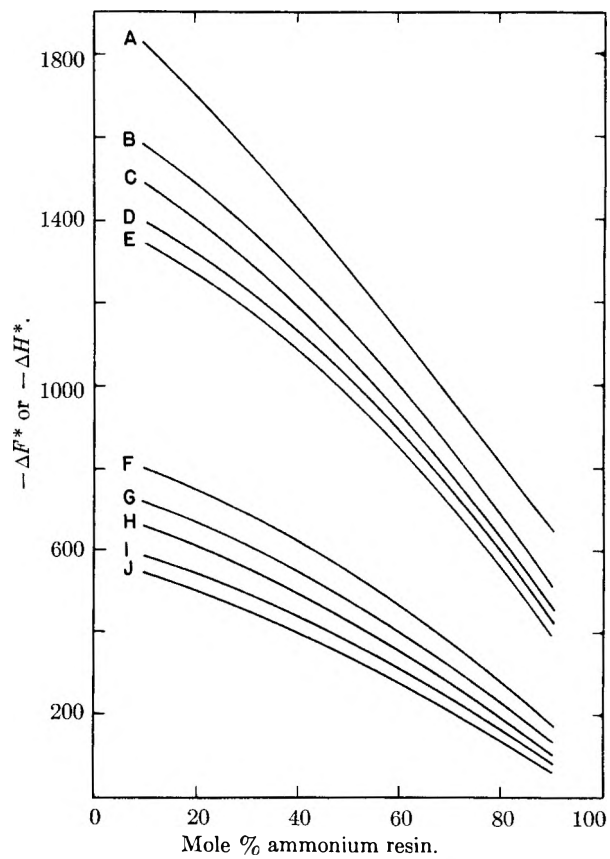

Fig. 4.—Free energy and enthalpy changes for the ammonium–hydrogen exchange: A, ΔH^*, 0°; B, ΔH^*, 25°; C, ΔH^*, 50°; D, ΔH^*, 77°; E, ΔH^*, 97.5°; F, ΔF^*, 0°; G, ΔF^*, 25°; H, ΔF^*, 50°; I, ΔF^*, 77°; J, ΔF^*, 97.5°.

$$\Delta H^0 = \int_{X_{B^+}=0}^{X_{B^+}=1} \Delta H^* \, dX_{B^+} = -2.303R \int_{X_{B^+}=0}^{X_{B^+}=1} \frac{d \log k}{d(1/T)} \, dX_{B^+} \quad (7)$$

$$\Delta S^0 = \int_{X_{B^+}=0}^{X_{B^+}=1} \Delta S^* \, dX_{B^+} \qquad (8)$$

Equilibrium data for the ammonium–hydrogen and thallous–hydrogen systems as a function of temperature are presented in Figs. 1 and 2. Both systems exhibit large variations of k with both temperature and resin composition. In the case of the thallous–hydrogen exchange, k decreases by a factor of four for large hydrogen loadings between 0 and 97.5° and by a factor of two for large thallous loadings over this temperature range. The values of the differential free energy, enthalpy and entropy for these systems (Figs. 4–6) also vary considerably with temperature and resin composition. In both systems the values of these functions become less negative with increasing temperature and decreasing hydrogen ion content of the resin. The values of ΔS^* for the thallous–hydrogen system actually become positive at high temperatures and high thallous loading.

The decrease in the selectivity coefficient with low hydrogen content may be explained by the assumption that all exchange sites are not the same with each ion occupying the sites preferred by it until these sites are used up. This assumption, which would be equally true for an exchange between any pair of ions, is valid if, for example, the sulfonated bridges (DVB rings) have properties different from those of the sulfonated polystyrene rings or if localized concentration differences exist in the resin because of statistical variations in the crosslinkage.[6-9] Since the variation of k with resin loading is greater for exchanges which involve hydrogen ion, it is possible that an additional assumption, that the ion-exchange resin in the hydrogen form is an acid similar in strength but perhaps slightly weaker than nitric acid,[8,10] may be

TABLE I

AMMONIUM–HYDROGEN EXCHANGE DATA ON 16% DVB DOWEX 50

Temp., °C.	$K_H^{NH_4}$	ΔF^0, cal.	ΔH^0, cal.	ΔS^0, e.u.
0	2.58	−511	−1259	−2.73
25	2.13	−449	−1091	−2.15
50	1.87	−402	−1016	−1.90
77	1.66	−353	− 995	−1.72
97.5	1.54	−319	− 912	−1.60

TABLE II

THALLOUS–HYDROGEN EXCHANGE DATA ON 16% DVB DOWEX 50

Temp., °C.	K_H^{Tl}	ΔF^0, cal.	ΔH^0, cal.	ΔS^0, e.u.
0	24.2	−1726	−3107	−5.04
25	15.7	−1636	−2416	−2.62
50	11.8	−1586	−2287	−2.17
77	8.95	−1528	−2090	−1.60
97.5	7.89	−1504	−1898	−1.06

(6) H. F. Walton, *ibid.*, **47**, 371 (1943).

(7) I. H. Spinner, J. A. Ciric and W. F. Graydon, *Canad. J. Chem.*, **32**, 143 (1954).

(8) D. Reichenberg and D. S. McCauley, *J. Chem. Soc.*, 2741 (1955).

(9) G. E. Myers and G. E. Boyd, THIS JOURNAL, **60**, 321 (1956).

(10) The activity coefficients of solutions of nitric and *p*-toluenesulfonic acids tend to support this view. R. A. Robinson and R. H. Stokes, *Trans. Faraday Soc.*, **45**, 612 (1949); O. D. Bonner, G. D. Easterling, D. L. West and V. F. Holland, *J. Am. Chem. Soc.*, **77**, 242 (1955).

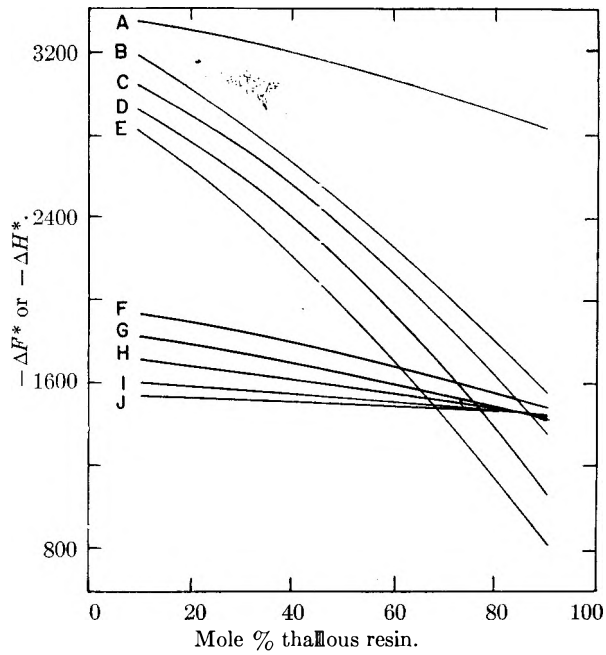

Fig. 5.—Free energy and enthalpy changes for the thallous–hydrogen exchange: A, ΔH^*, 0°; B, ΔH^*, 25°; C, ΔH^*, 50°; D, ΔH^*, 77°; E, ΔH^*, 97.5°; F, ΔF^*, 0°; G, ΔF^*, 25°; H, ΔF^* 50°; I, ΔF^*, 77°; J, ΔF^*, 97.5°.

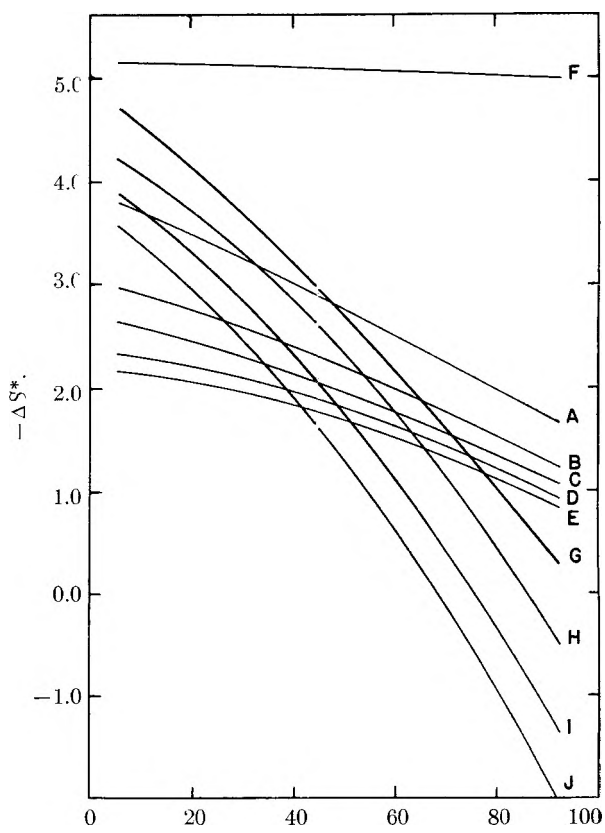

Fig. 6.—Entropy changes for the ammonium–hydrogen and thallous–hydrogen exchanges: A, 0°, NH_4–H; B, 25°, NH_4–H; C, 50°, NH_4–H; D, 77°, NH_4–H; E, 97.5°, NH_4–H; F, 0°, Tl–H; G, 25°, Tl–H; H, 50°, Tl–H; I, 77°, Tl–H; J, 97.5°, Tl–H.

desirable. Calculations indicate an ionization constant of the order of magnitude of five to ten. When the resin is predominantly in the salt form, the percentage of hydrogen existing in the undissociated form would be greater than when the resin is predominantly in the acid form, thus leading to smaller values of ΔF^* for lower hydrogen loadings. This second assumption would also explain the decrease in ΔF^* at constant resin composition with increasing temperature as most ionization constants decrease with increasing temperature.[11]

The negative values of ΔH^* are to be expected for these exchange reactions since the hydrogen ion is being diluted while the ammonium or thallous ion is being concentrated. One finds upon calculation of the heats of dilution for the nitrates,[12] that the dilution of nitric acid is an exothermic process while the dilution of the nitrate salts with the exception of lithium is an endothermic process. On the basis of the second assumption the smaller negative values of ΔH^* at low hydrogen loadings and high temperatures may be attributed to the absorption of energy for the ionization of some of the hydrogen associated with the resin when the exchange occurs.

The values of ΔF^0, ΔH^0 and ΔS^0 for the over-all ion-exchange process as represented by equation 1 have been calculated (Tables I and II) using equations 6–8. These functions for both exchange systems have the same arithmetic sign but are larger in magnitude than the corresponding functions for the sodium–hydrogen exchange.[5]

Values of ΔF and ΔH may be calculated for the dilution of solutions of ammonium nitrate and nitric acid approximating the concentration of ammonium or hydrogen ion in the resin phase to a concentration of 0.1 M. Although they are not so large in absolute magnitude, the differences between the free energy of dilution and enthalpy of dilution of ammonium nitrate and nitric acid have the same arithmetic sign as the values of ΔF° and ΔH° for the ammonium–hydrogen exchange. This gives some justification to the consideration of the ion-exchange process as being essentially a concentration of one ion with the simultaneous dilution of the second ion.

(11) H. S. Harned and B. B. Owen, "The Physical Chemistry of Electrolytic Solutions," Reinhold Publ. Corp., New York, N. Y., 1958, p. 755.

(12) F. R. Bichowsky and F. D. Rossini, "The Thermochemistry of Chemical Substances," Reinhold Publ. Corp., New York, N. Y., 1936, pp. 33, 34, 134, 142, 156, 166, 167, 169, 170.

THE EFFECT OF TEMPERATURE ON ION-EXCHANGE EQUILIBRIA. III. EXCHANGES INVOLVING SOME DIVALENT IONS

BY O. D. BONNER AND ROBERT R. PRUETT[1,2,3]

Department of Chemistry, University of South Carolina, Columbia, S. C.

Received January 30, 1959

Ion-exchange equilibria in seven systems involving divalent ions have been investigated over the temperature range 0 to 97.5° using sulfonic acid type (Dowex-50) resins. In all exchanges between two divalent ions, the equilibrium constant decreases with increasing temperature, with a resulting negative value for ΔH^0. This is apparently characteristic of exchanges between ions of the same valence type since for all exchanges between two univalent ions negative ΔH^0 values have also been observed. With the exception of the cupric–magnesium system, the values of ΔS^0 for all exchanges between two divalent ions are positive. For the magnesium–hydrogen exchanges ΔH^0 and ΔS^0 are positive. The algebraic signs of these functions are identical with those of the cupric–hydrogen system already reported.

One divalent ion, the cupric ion, was included in the first paper[4] of this series reporting preliminary investigation of the temperature dependence of ion-exchange equilibria. It was noted that the equilibrium constant for the sodium–hydrogen system (an exchange between two ions of the same valence) decreased with increasing temperature, while the equilibrium constant for the cupric–hydrogen system increased with increasing temperature. No exchange reactions between two divalent ions were included in this earlier investigation.

(1) These results were developed under a project sponsored by the United States Atomic Energy Commission.

(2) Part of the work described herein was included in a thesis submitted by Robert R. Pruett to the University of South Carolina in partial fulfillment of the requirements for the degree of Master of Science.

(3) The authors are indebted to Mr. L. A. Kitching, a Summer Research Associate supported by a grant from the National Science Foundation, for assistance with some of the analytical results reported herein.

(4) O. D. Bonner and L. L. Smith, THIS JOURNAL, **61**, 1614 (1957).

Experimental

The variation of the equilibrium quotient with temperature and resin composition of five additional ion-exchange systems involving divalent ions has been investigated. In two of these systems the per cent. divinylbenzene, or cross-linkage, of the resin has also been included as a variable. The method of attainment of equilibrium, temperature control and separation of resin and aqueous phases has been reported previously.[4] The concentrations of both ions in both the resin and aqueous phases were determined experimentally as described below.

(a) **Cupric–Zinc Exchange**—The total concentration of cupric plus zinc ion was determined[5] by complexiметric titration with a standard solution of the disodium salt of ethyenediaminetetraacetic acid (EDTA), PAN[6] serving as an indicator. Cupric ion was then determined by the customary iodometric titration and zinc ion was calculated by difference.

(b) **Cupric–Magnesium and Calcium–Cupric Exchanges**[6]—In both of these exchanges cupric ion was determined complexiметrically by titration with EDTA, in a solution acidified with acetic acid to a *p*H of 5, PAN serving as an

(5) H. Flaschka and H. Abdine, *Chemist Analyst*, **45**, 58 (1956).

(6) PAN is the abbreviation given the compound 1-(2-pyridylazo)-2-naphthol.

indicator. The total concentration was then determined by a similar titration in a solution buffered to a *p*H of 10 with ammonium nitrate and aqueous ammonia. The alkaline earth ion was then calculated by difference.

(c) **Lead-Calcium Exchanges.**—Lead ion was titrated complexiметrically in acidic solution and the total ion concentration was determined in alkaline solution as in the exchanges described above. It was necessary, however, to add a measured quantity of cupric ion before titration in order to obtain the necessary color change at the equivalence point.

(d) **Magnesium-Hydrogen Exchanges.**—The magnesium ion concentration was determined complexiметrically as described above. The hydrogen ion concentration was determined by titration with standard sodium hydroxide solution.

Discussion and Results

It is preferable for these systems involving divalent ions to consider the exchange reaction involving one equivalent rather than one mole of divalent ion. The equilibrium constants and the thermodynamic functions ΔF°, ΔH° and ΔS° for these exchanges may then be compared directly with the corresponding functions for exchanges involving univalent ions. These exchanges are therefore represented by the equations

$$^1/_2MX_2 + B\ Res = {}^1/_2M\ Res_2 + BX \qquad (1)$$

and

$$^1/_2MX_2 + {}^1/_2Q\ Res = {}^1/_2M\ Res_2 + {}^1/_2QX_2 \qquad (2)$$

where MX_2 and QX_2 are salts of divalent cations and BX is the salt of a univalent cation. The equilibrium quotients using the N to represent the molar fraction of the ion in the resin phase are

$$k_{1,2} = \frac{N^{1/2}_{M\ Res_2}\, m_{BX}}{N_{B\ Res}\, m^{1/2}_{MX_2}} \qquad (3)$$

and

$$k_{2,2} = \frac{N^{1/2}_{M\ Res_2}\, m^{1/2}_{QX_2}}{N^{1/2}_{Q\ Res_2}\, m^{1/2}_{MX_2}} \qquad (4)$$

The equilibrium constant for each exchange reaction is calculated from the equation[7]

(7) W. J. Argersinger, A. W. Davidson and O. D. Bonner, *Trans. Kans. Acad. Sci.*, **53**, 404 (1950).

$$\log K = \int_0^1 \log k\, dX \qquad (5)$$

where X is the equivalent fraction of the preferred ion in the resin phase. The activity coefficients of the aqueous electrolytes must be ignored in all calculations since they are not known over this temperature range. It is probable that all activity coefficient *ratios* do not differ too greatly from unity since for every exchange study solutions of an ionic strength of 0.1 were used.

In almost all of the isothermal exchange reactions between two univalent ions which have been studied, the equilibrium quotient or selectivity coefficient, k, has varied considerably with the percentage of each ion associated with the resin at equilibrium. In contrast to this behavior, the selectivity coefficient for many exchange systems involving two divalent ions is almost independent of resin composition. This non-dependence of the selectivity coefficient on resin composition is not always true as for example some of the exchanges reported previously of barium, calcium and strontium with cupric ion.[8] The values of k at any temperature for the five exchange reactions (Tables I-V), however, vary only a few per cent. over the entire range of resin composition and

(8) O. D. Bonner and F. L. Livingston, THIS JOURNAL, **60**, 530 (1956).

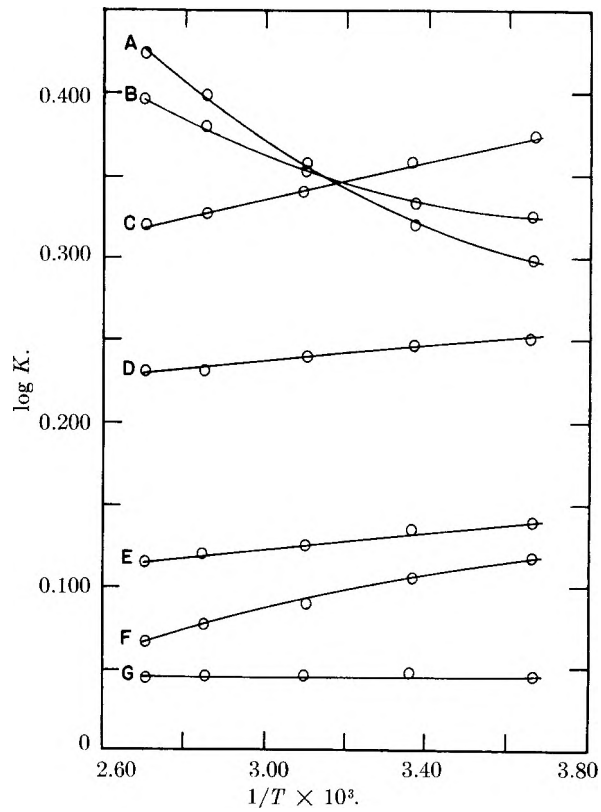

Fig. 1.—Temperature dependence of equilibrium constants: A, Mg-H, 16% DVB; B, Mg-H, 8% DVB; C, Pb-Ca, 16% DVB; D, Pb-Ca, 8% DVB; E, Ca-Cu, 8% DVB; F, Cu-Mg, 16% DVB; G, Cu-Zn, 16% DVB.

TABLE I

CUPRIC-ZINC EXCHANGE DATA ON 16% DVB DOWEX-50

Temp., °C.	K^{Cu}_{Zn}	ΔF^0, cal.	ΔH^0, cal.	ΔS^0, e.u.
0	1.11	−58	0	0.21
25	1.12	−68	0	.23
50	1.11	−68	0	.21
77	1.11	−73	0	.21
97.5	1.11	−78	0	.21

TABLE II

CUPRIC-MAGNESIUM EXCHANGE DATA ON 16% DVB DOWEX-50

Temp., °C.	K^{Cu}_{Mg}	ΔF^0, cal.	ΔH^0, cal.	ΔS^0, e.u.
0	1.31	−146	−169	−0.08
25	1.28	−145	−183	− .13
50	1.23	−135	−229	− .29
77	1.20	−127	−279	− .43
97.5	1.17	−113	−333	− .59

TABLE III

CALCIUM-CUPRIC EXCHANGE DATA ON 8% DVB DOWEX-50

Temp., °C.	K^{Ca}_{Cu}	ΔF^0, cal.	ΔH^0, cal.	ΔS^0, e.u.
0	1.38	−175	−116	0.22
25	1.36	−183	−118	.22
50	1.34	−188	−119	.21
77	1.32	−194	−120	.21
97.5	1.31	−198	−121	.21

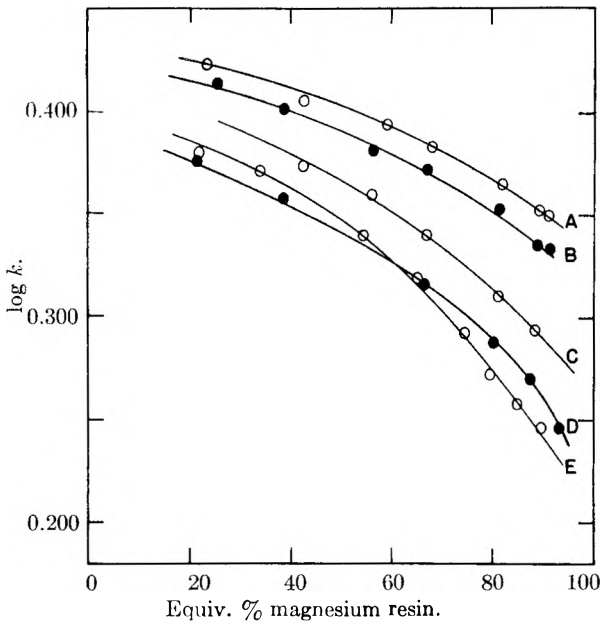

Fig. 2.—Magnesium–hydrogen exchange equilibrium data on 8% DVB Dowex 50: A, 97.5°; B, 77°; C, 50°; D, 25°; E, 0°.

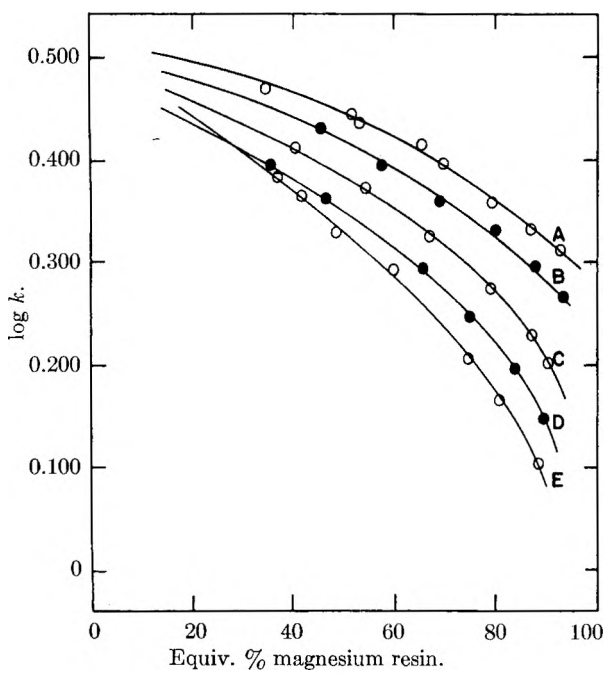

Fig. 3.—Magnesium–hydrogen exchange equilibrium data on 16% DVB Doxex 50: A, 97.5°; B, 77°; C, 50°; D, 25°; E, 0°.

therefore k at any resin composition is essentially equal to K, the equilibrium constant.

The cupric–zinc exchange is an exchange reaction between two very similar divalent ions. Both are transition elements and the fully swollen resin in both ionic forms contains approximately the same amount of water. The equilibrium constant for the exchange is near unity and is independent of temperature.

The cupric–magnesium, calcium–cupric and lead–calcium exchanges each represent an exchange reaction between an alkaline earth element ion and a transition element ion. Each of these reactions is exothermic, as are exchanges between univalent ions, but the values of ΔH^0 for these exchanges are not so great in absolute magnitude. This combination of smaller heat effect and free energy changes

Table IV

Lead–Calcium Exchange Data on 8% DVB Dowex-50

Temp., °C.	K_{Ca}^{Pb}	ΔF^0, cal.	ΔH^0, cal.	ΔS^0, e.u.
0	1.78	−313	− 84	0.84
25	1.77	−338	−115	.75
50	1.74	−356	−139	.67
77	1.71	−373	−146	.65
97.5	1.71	−395	−152	.65

Table V

Lead–Calcium Exchange Data on 16% DVB Dowex-50

Temp., °C.	K_{Ca}^{Pb}	ΔF^0, cal.	ΔH^0, cal.	ΔS^0, e.u.
0	2.37	−468	−286	0.67
25	2.28	−487	−269	.73
50	2.20	−505	−254	.78
77	2.13	−527	−238	.82
97.5	2.09	−544	−224	.86

Table VI

Magnesium–Hydrogen Exchange Data on 8% DVB Dowex-50

Temp., °C.	K_H^{Mg}	ΔF^0, cal.	ΔH^0, cal.	ΔS^0, e.u.
0	2.13	−410	101	1.87
25	2.15	−453	256	2.38
50	2.29	−532	445	3.02
77	2.42	−615	467	3.09
97.5	2.50	−673	485	3.12

Table VII

Magnesium–Hydrogen Exchange Data on 16% DVB Dowex-50

Temp., °C.	K_H^{Mg}	ΔF^0, cal.	ΔH^0, cal.	ΔS^0, e.u.
0	1.98	−370	284	2.39
25	2.10	−439	595	3.47
50	2.29	−531	723	3.88
77	2.51	−639	824	4.18
97.5	2.68	−726	897	4.38

Table VIII

Cupric–Hydrogen Exchange on 16% DVB Dowex-50
Comparison of Experimental and Calculated Values for Thermodynamic Functions

Temp., °C.	K_H^{Cu}	ΔF^0, cal.	ΔH^0, cal.	ΔS^0, e.u.
	Experimental Values			
0	2.56	−511	183	2.54
25	2.68	−586	471	3.54
50	2.90	−683	604	3.98
77	3.10	−788	613	4.00
97.5	3.27	−872	622	4.03
	Calculated Values[a]			
0	2.59	−516	115	2.31
25	2.69	−584	412	3.34
50	2.82	−666	494	3.59
77	3.01	−766	545	3.75
97.5	3.14	−839	564	3.79

[a] Calculated from data for the Cu–Mg and Mg–H exchanges.

of moderate magnitude result in calculated values of ΔS^0 which are positive for all exchanges which have been studied between divalent ions with the exception of the cupric–magnesium exchange. This is in contrast with exchanges between univalent ions where only negative ΔS^0 values have been observed. The lead–calcium exchange has been studied on two resins of 8 and 16% divinylbenzene content. The increased crosslinkage increases the selectivity of the resin as would be expected. The absolute value of ΔH^0 also increases but ΔS^0 does not change significantly.

The values of ΔF^0, ΔH^0 and ΔS^0 for the magnesium–hydrogen exchange on 16% DVB resin have the same algebraic sign as the values of these functions for the cupric–hydrogen exchange reported previously and are similar in magnitude to these values. The values of all of these functions are smaller for this exchange on the 8% DVB resin with the exception of the free energy changes at 0 and 25°. The selectivity of the 8% crosslinked resin is greater than that of the 16% resin at the lower temperatures. Plots of the logarithm of the equilibrium quotient as a function of resin composition (Figs. 1,2) show a crossing of the 0 and 25° curves for resins of both crosslinkages.

Values of the equilibrium constant and of the standard free energy, enthalpy and entropy changes for the cupric–magnesium and magnesium–hydrogen system on 16% DVB resin are reported in Tables II and VII. From these values one may calculate the corresponding quantities for the cupric–hydrogen exchange. A comparison of these calculated quantities with those reported previously is shown in Table VIII. The agreement at all temperatures is quite satisfactory, if consideration is given to the probability of greater experimental error in exchanges involving ions of different valence types such as the magnesium–hydrogen and cupric–hydrogen exchanges.

EFFECT OF POISONING ON THE INFRARED SPECTRUM OF CARBON MONOXIDE ADSORBED ON NICKEL[1]

By Carl W. Garland

Department of Chemistry and Spectroscopy Laboratory, Massachusetts Institute of Technology, Cambridge 39, Massachusetts

Received February 2, 1959

The infrared spectrum has been determined for CO adsorbed on both freshly-reduced nickel samples and on a series of nickel samples poisoned by preadsorption of CS_2. The nickel is supported on a high-area alumina and comprises 10% of the sample by weight. Spectra were recorded as a function of increasing coverage as CO was adsorbed.

I. Introduction

The spectrum of CO chemisorbed on supported nickel has been reported at full coverage and during desorption.[2] The work reported below is concerned with the effect of "poisoning" on the adsorption of CO as seen by changes in the infrared spectrum. The poisoning was accomplished by preadsorption of small amounts of CS_2. Carbon disulfide has several unshared electron pairs and should be strongly chemisorbed. The spectrum of adsorbed CO was studied as a function of coverage for stepwise addition of CO gas to samples of nickel supported on a high-area, non-porous alumina. Both freshly-reduced samples and a series of poisoned samples were investigated.

II. Experimental

The adsorption cell and modified Perkin–Elmer 12C infrared spectrometer used in this work have been described previously.[3]

A standard procedure was used in preparing all samples. Two grams of $Ni(NO_3)_2 \cdot 6H_2O$ was dissolved in 20 ml. of distilled water and 70 ml. of pure acetone. To this solution, 3.60 g. of high-area alumina (Alon C)[4] was added slowly, with shaking, to give a uniform suspension. This mixture was sprayed slowly through a very fine nozzle onto three 30 mm.-diam. CaF_2 plates, which were heated to about 75° on a hot plate. During the spraying, air was bubbled through the mixture to maintain a uniform suspension of Alon C and care was taken to obtain a uniform deposit on all three plates. Deposits of about 110 mg. per plate were obtained.

The cell was then assembled and the sample degassed at 10^{-3} mm. and 150° for 30 min. and then at 10^{-5} mm. and 300° for 30 min. more. Reduction was carried out by heating at 300° in 10 cm. pressure of hydrogen gas for one hour, pumping briefly and repeating the reduction for a second hour. The sample was then pumped at 10^{-6} mm. for 20 min. at 300° to remove most of the reduction products. A final reduction with hydrogen at 10 cm. pressure was carried out overnight (16 hours) at 300°. The sample was then degassed at 300° by pumping at 10^{-6} mm. for 3 hours and pumping continued while the sample cooled to room temperature. After reduction the deposit weighed about 80 mg. and contained 10% Ni by weight. This reduction procedure is similar to that used by Eischens, *et al.*[2,5]

The spectral region from 1400 to 2500 cm.$^{-1}$ was investigated using a CaF_2 prism. The background transmission was determined for each reduced sample prior to adsorption and found to be free of interfering bands. Due to the low transmission, slit widths of 0.25 to 0.40 mm. were used. Fortunately, band shapes were not sensitive to slit width for these samples.

III. Results

Four sets of samples were studied, each set consisting of the three plates that were prepared together in a single spraying. Different sets are designated by I-IV, and the three samples which make up a set by A, B, C. For each set, spectra

(1) This work was supported in part by the Office of Naval Research.

(2) R. P. Eischens, S. A. Francis and W. A. Pliskin, THIS JOURNAL, **60**, 194 (1956).

(3) A. C. Yang and C. W. Garland, *ibid.*, **61**, 1504 (1957).

(4) Alon C is a product of Godfrey L. Cabot, Inc., Boston 10, Mass. We wish to thank Mr. K. A. Loftman for providing a sample with a B. E. T. area of 90 m.^{2} g.$^{-1}$.

(5) R. P. Eischens and W. A. Pliskin, "Advances in Catalysis," Academic Press, Inc., New York, N. Y., Vol. 9, 1957, p. 662.

TABLE I

Sample no.	Slit width (mm.)	CS_2 added to cell (cc. at S.T.P.)	CO present in the cell (cc. at S.T.P.)	Frequency of bands obsd. ($cm.^{-1}$)[a]			
IA	0.34						
IIA	.24	0	0.11	...	2045	...	1910vb
IIIA	.45		.44	2075	~2045sh	1960	~1910sh
IVA	.27						
IIIB	.37	0.015	.11	...	2045	...	1930vb
			.44	2078	~2045sh	1955	~1930sh
IVB	.24	.020	.11	...	2042	...	1930vb
			.44	2082	~2045sh	1955	~1930sh
IIC	.23	.026	.11	2092	2050	...	1935vb
			.44	2087	~2050sh,w	1952	?
IIB	.22	.051	.11	2095	2050	...	~1935vb,w
			.44	2089	~2050sh,w	1950	?
IIIC	.43	.061	.11	2090	~2045?sh,w	1950b,w	...
			.44	2085	...	1950b,w	...
IC	.35	~ .073	.10	2094	~2050?sh,vw	...	...
			.40	2091	...	...	...
IB	.38	.16	.10	2091	...	...	...
			.40	2084	...	...	...

[a] sh = shoulder, b = broad, vb = very broad, w = weak, vw = very weak.

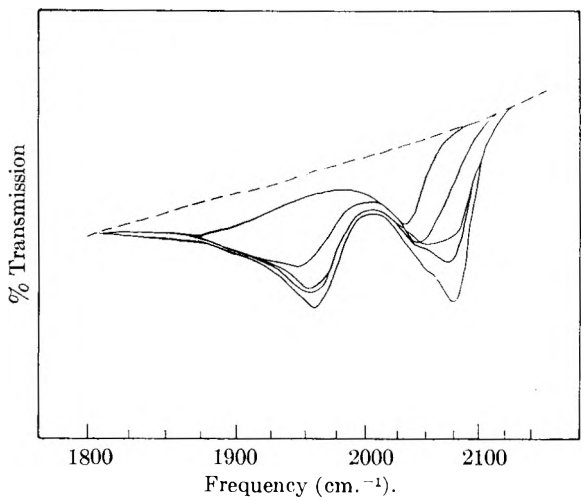

Fig. 1.—Spectra of CO chemisorbed on a freshly-reduced Ni sample (sample IIIA) for increasing coverages. The amount of CO present in the cell was 0.11, 0.22, 0.33, 0.44 and 0.83 cc. (S.T.P.), respectively.

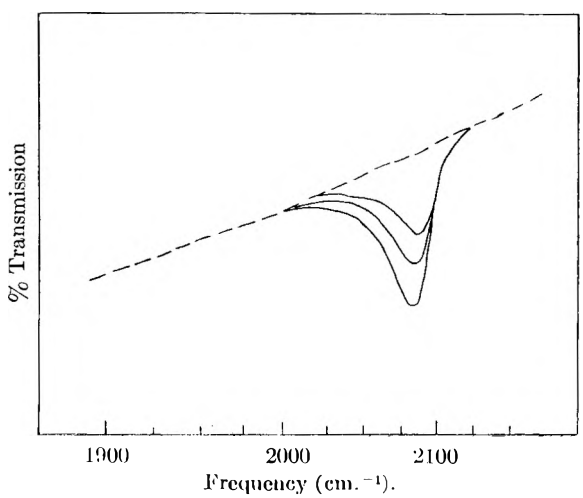

Fig. 2.—Spectra of CO chemisorbed on a heavily poisoned Ni sample (sample IB) for increasing coverages. The amount of CO present in the cell was 0.10, 0.20 and 0.40 cc. (S.T.P.), respectively.

were recorded for the stepwise addition of CO to one freshly-reduced sample (sample A). The other two samples (B and C) in the set were poisoned by the addition of CS_2 vapor prior to stepwise addition of CO. Spectra were always recorded both before and after this addition of CS_2 and no change was observed in the background. A summary of results for the samples studied is given in Table I. The table is arranged in order of increasing amount of CS_2 added prior to CO adsorption. As seen, there is a variation in the slit widths used, but CO adsorption on all the "A" samples gave very similar band contours and roughly the same band intensities when the same amount of CO gas had been added to the cell. Thus Table I is qualitatively arranged in order of increasing fraction of the surface poisoned. Equilibrium pressures were not measured and the amount of CO adsorbed at full coverage is not known. Judging from results obtained on other samples prepared in the same manner,[6] full coverage on a freshly-reduced sample is roughly 0.25 cc. (S.T.P.) of CO.

Unpoisoned Samples.—Figure 1 shows the spectra of adsorbed CO as a function of increasing coverage on sample IIIA and is typical of all the "A" samples. For small amounts of CO admitted to the cell, there are only two bands: one at 2045 $cm.^{-1}$ and a very broad band whose center is approximately at 1910 $cm.^{-1}$. As the amount of CO is increased these grow somewhat and two new bands develop at 2075 and 1960 $cm.^{-1}$ until they dominate the spectrum.

Samples IIIB and IVB.—For the two samples which are poisoned with the smallest amount of CS_2, the spectra of adsorbed CO is quite similar to that observed for unpoisoned samples. At low coverages of CO, the low frequency band appears to be centered at 1930 $cm.^{-1}$ but it is still very broad. As seen in Table I, there are some slight frequency shifts in the two bands prominent at high coverage. The band shapes vary with in-

(6) Work being carried out by Mr. John T. Yates, Chemistry Department, M. I. T.

creasing amount of CO in the same manner as for unpoisoned samples, but the intensities are somewhat reduced.

Samples IIC, IIB and IIIC.—For these samples, which are moderately poisoned, the spectra of adsorbed CO differ considerably from that observed on unpoisoned samples. Even at low coverages of CO, two bands appear in the region above 2000 cm.$^{-1}$: one at 2050 cm.$^{-1}$ as on unpoisoned samples and the other at about 2092 cm.$^{-1}$. As the amount of CS_2 poisoning is increased the 2050 cm.$^{-1}$ band becomes weaker and the 2092 cm.$^{-1}$ band stronger. In the region below 2000 cm.$^{-1}$, adsorbed CO bands are weaker, less broad, and grow less with addition of CO to the cell in comparison with the unpoisoned samples. In particular there is a loss of intensity below 1900 cm.$^{-1}$ as CS_2 poisoning is increased.

Samples IC and IB.—Figure 2 shows the spectra of adsorbed CO on sample IB, a heavily poisoned sample. Only one band appears at all coverages. This band is the same as the high-frequency band in samples IIC, IIB and IIIC. There are no bands in the region below 2000 cm.$^{-1}$. Results for sample IC are the same as those in Fig. 2 except that a very weak band at ~2050 cm.$^{-1}$ is present as a shoulder on the 2094 cm.$^{-1}$ band at low coverage.

Desorption of CO.—After the final CO addition, the cell was pumped at 10^{-6} mm. and room temperature. Spectra were recorded after 30 min. and again after 60 min. of pumping. The effect on unpoisoned samples was to reduce the intensity of the bands at 2075 and 1960 cm.$^{-1}$ while making very little change in the bands at 2045 and 1910 cm.$^{-1}$, in agreement with the results of Eischens, Francis and Pliskin.[2] For all samples, the 2045–2050 cm.$^{-1}$ band and the very broad low-frequency band (1910–1930 cm.$^{-1}$) changed little on pumping, while the other bands decreased appreciably. For sample IB, the most heavily poisoned sample, all the CO was desorbed after 30 minutes of pumping.

Spectra of CS_2 on Alon.—As noted above, none of the samples in Table I showed any change in the background after CS_2 was admitted to the cell. Other Alon-supported nickel samples were exposed to CS_2 vapor at an equilibrium pressure of ~1 mm. The only band observed was at 1520 cm.$^{-1}$ and it disappeared after a few hours of pumping at room temperature. In the region from 1400–2500 cm.$^{-1}$, the only intense infrared-active band of liquid CS_2 is the stretching vibration at 1520 cm.$^{-1}$. Thus this band is believed due to physically adsorbed CS_2 on the alumina present.

IV. Discussion

The spectra of CO shown in Fig. 1 for increasing coverages on a freshly reduced 10% Ni sample are in general agreement with those of Eischens, *et al.*,[2] for the desorption of CO from ~8% Ni samples. A comparison of band frequencies at full coverage shows excellent agreement for bands above 2000 cm.$^{-1}$; however, our low frequency bands occur at 1910 and 1960 cm.$^{-1}$ in contrast to 1850 and 1930 cm.$^{-1}$ reported in the previous work.[2] Bands in the region 2000 to 2100 cm.$^{-1}$ are due to a linear CO species and are not very sensitive to bond strength, sample treatment, or even to the transition metal used.[2,3] The bands lying below 2000 cm.$^{-1}$ are believed due to bridged CO species (*i.e.*, a CO bonded to two adjacent metal atoms) and are sensitive to bond strength[2] and sample treatment.[3] It seems likely that the differences in frequencies between the present results and those of Eischen, *et al.*, are due to differences in sample preparation.

Since small amounts of CS_2 have an appreciable effect on subsequently adsorbed CO, one can infer that this CS_2 is strongly held on the Ni surface rather than physically adsorbed on the Alon. However, no bands due to chemisorbed CS_2 were found even on samples having large amounts of CS_2 present. Perhaps any bands due to chemisorbed CS_2 are very weak, very broad or lie below 1400 cm.$^{-1}$. It is also possible that CS_2 decomposes on the nickel surface and poisons it in that way.

The effect of CS_2 poisoning on the CO bands above 2000 cm.$^{-1}$ (linear CO species) is to reduce the intensity of the 2045–2050 cm.$^{-1}$ band and to increase, relatively, the intensity of a band at about 2090 cm.$^{-1}$. The bands at 2045 or 2050 cm.$^{-1}$ are assigned to a strongly bonded linear CO species which is isolated from other surface species; thus it appears most strongly at low coverage on unpoisoned samples. The bands at 2075 to 2095 cm.$^{-1}$ are assigned to a more weakly held linear CO species which is sensitive to the environment of the bonding site involved. For unpoisoned samples, this species occurs only after the "isolated" CO species have been adsorbed (*i.e.*, only at high coverage); poisoning with CS_2 results in the appearance of this species at low coverages, which is to be expected. The infrared frequency for this species changes with poisoning since the influence of CO and CS_2 on the sites for adsorbing this weakly held CO species would be different.

The effect of CS_2 poisoning on the CO bands below 2000 cm.$^{-1}$ is to reduce the intensity in general and particularly that below 1900 cm.$^{-1}$. The very broad band at 1910 cm.$^{-1}$ is assigned to bridged CO species which are isolated. The band at 1960 or 1950 cm.$^{-1}$ is assigned to bridged CO species which are influenced by the presence of other CO species or CS_2, respectively, on the surface. The fact that the bands below 2000 cm.$^{-1}$ are greatly reduced or eliminated by moderate to strong CS_2 poisoning is in agreement with this assignment, since the preadsorption of CS_2 would eliminate adjacent sites which were able to adsorb bridged CO species.

Acknowledgment.—The author wishes to thank Dr. Andrew C. Yang, now at Air Force Cambridge Research Center, and Mr. Leslie Isaacs, M. I. T. Department of Chemistry, for preliminary investigations on this work.

KINETICS OF CHLORINE EXCHANGE BETWEEN HCl AND CHLOROACETIC ACID IN AQUEOUS SOLUTION[1]

BY R. A. KENNEY AND F. J. JOHNSTON

Contribution from the Department of Chemistry, University of Louisville, Louisville, Kentucky

Received February 2, 1959

In aqueous solutions containing HCl and $CH_2ClCOOH$, exchange of chlorine between the two species has been found to occur simultaneously with the hydrolysis of the latter. The rate of this exchange is first order with respect to each of the HCl and chloroacetic acid concentrations and may be adequately described by the expression rate = 0.95×10^{11} exp $[(-24{,}500 \pm 500)/RT](HCl)(CH_2ClCOOH)$ moles $l.^{-1}$ $sec.^{-1}$. The corresponding entropy of activation evaluated at 80° is −10.6 cal. $mole^{-1}$ $deg.^{-1}$ The simultaneous hydrolysis reaction followed a pseudo first-order type behavior with the rate = 2.11×10^9 exp $[(-24{,}800 \pm 800)/RT](CH_2ClCOOH)$ moles $l.^{-1}$ $sec.^{-1}$.

Introduction

In aqueous $CH_2ClCOOH$ solutions at elevated temperatures hydrolysis occurs with the production of Cl^- and $CH_2OHCOOH$. This reaction has been studied over a wide range of conditions by a number of investigators.[2-7] We have found, using Cl^{36}, that in the presence of HCl exchange of the chlorine in the chloroacetic acid with the chloride occurs simultaneously with the hydrolysis. This article reports the results of a kinetic study of the simultaneous exchange and hydrolysis reactions.

The mathematical treatment of isotopic exchange in such non-equilibrium systems has been clearly formulated by Luehr, Challenger and Masters.[8] A slightly modified version of their results as applied to the $CH_2ClCOOH$–HCl system is given below.

For the hydrolysis reaction

$$CH_2ClCOOH + HOH \longrightarrow CH_2OHCOOH + HCl$$

$$\frac{d(Cl^-)}{dt} = \frac{-d(CH_2ClCOOH)}{dt} = \alpha(t) \qquad (1)$$

Then

$$(Cl^-)_t = (Cl^-)_0 + \int_0^t \alpha(t)dt = a + \rho(t) \qquad (2)$$

and

$$(CH_2ClCOOH)_t = (CH_2ClCOOH)_0 - \int_0^t \alpha(t)dt = b - \rho(t) \qquad (3)$$

For the exchange reaction

$$CH_2ClCOOH + Cl^{-*} \rightleftharpoons CH_2Cl^*COOH + Cl^-$$

the exchange rate

$$R_x(t) = k_x(Cl^-)^m(CH_2ClCOOH)^n = k_x[a + \rho(t)]^m[b - \rho(t)]^n \qquad (4)$$

Then

$$\ln(1 - F_t) = -\int_0^t \frac{R_x(t)(a + b)}{[a + \rho(t)][b - \rho(t)]} = -k_x(a + B)\int_0^t [a + \rho(t)]^{m-1}[b - \rho(t)]^{n-1}\,dt \qquad (5)\ (6)$$

In this expression F_t is the ratio of specific activity of the chloroacetic acid at time t to that of total chlorine in the system at exchange equilibrium.

In the special case in which the exchange rate is first order with respect to each of the exchanging species, equation 6 reduces to

$$\ln(1 - F_t) = -k_x(a + b)t \qquad (7)$$

It is interesting to note that this expression is identical to that for a reaction of similar order in an equilibrium system.

Experimental

The chloroacetic acid used was reagent grade material fractionally crystallized twice from benzene. Prepared solutions were stored in the dark at 0°.

HCl solutions were "spiked" with H-Cl^{36} obtained from the Radioactive Isotope Sales Department at Oak Ridge National Laboratory.

Groups of reaction cells were prepared by first mixing the chloroacetic acid and HCl solutions and diluting to a predetermined volume, usually 200 cc. Ten-cc. aliquots were introduced into cleaned Pyrex reaction cells and thoroughly degassed by repeated thawing and freezing on a vacuum line. The cells were then sealed off and if not reacted immediately, stored in the dark at 0° until used. No hydrolysis or exchange was detectable under these conditions of storage for at least two weeks.

Reactions were carried out by immersing the cells in an oil thermostat controlled at 80 to ± 0.05° and at 110 to ± 0.10°. All cells were wrapped in aluminum foil during exposure to eliminate light catalyzed exchange or hydrolysis. Following reaction, the cells were rapidly cooled, opened, neutralized by titration with NaOH and titrated potentiometrically with $AgNO_3$. The solution was quickly filtered through sintered glass, the supernatant chloroacetic acid solution diluted and an aliquot taken for counting. Blank experiments showed that no exchange or hydrolysis was induced by this procedure.

Chloroacetic acid fractions were counted in RCL solution type Geiger tubes with an annular volume of 33 cc. Because the Cl^{36} β is not highly energetic (0.714 Mev.) and the wall thickness of such a tube is roughly 30 mg./cm.^{2}, counting efficiencies were quite low. We nevertheless felt the advantage of reproducibility made this method preferable to the several solid phase counting techniques for this radiation. Observed counting rates for the chloroacetic acid fractions of from 25 to 600 c./m. above background were obtained. These low counting rates required that extremely long counts had to be taken, in some cases as long as three hours. In all cases a sufficient number of counts was accumulated to achieve an expected standard deviation for the net counting rate of less than 2%.

The total counting rate for a cell in a given set was obtained directly by counting an aliquot of the original reactant mixture.

The fraction of equilibrium exchange at time t, F_t, was obtained from the expression

$$F_t = \frac{(\text{Specific activity of } CH_2ClCOOH)_t}{(\text{Specific activity of total chlorine})_{t=\infty}}$$

(1) This work was supported by a Frederick Gardner Cottrell Grant from the Research Corporation. This paper was abstracted from the Ph.D. thesis of Richard A. Kenney, University of Louisville, 1958.

(2) W. A. Drushel and G. S. Simpson, *J. Am. Chem. Soc.*, **39**, 2455 (1917).

(3) E. A. Moelwyn-Hughes, *J. Chem. Soc.*, 101 (1932).

(4) H. M. Dawson and E. R. Pycock, *ibid.*, 153 (1936).

(5) O. Reitz, *Z. physik. Chem.*, **A177**, 85 (1936).

(6) L. F. Berhenke and E. C. Britton, *Ind. Eng. Chem.*, **38**, 544 (1946).

(7) F. Kunze, *Monatsh.*, **79**, 254 (1948).

(8) C. P. Luehr, G. E. Challenger and B. J. Masters, *J. Am. Chem. Soc.*, **78**, 1314 (1956).

TABLE I

DATA SUMMARY FOR EXPERIMENTS AT 90.0°

$T = 363.2°$

t (hr.)	$(CH_2ClCOOH)$,[a] mole/l.	(HCl), mole/l.	Counts/min. in $CH_2ClCOOH$	F	k_h (hr.$^{-1}$)	k_x (l. mole^{-1} hr.$^{-1}$)
			Set I, 876 c./m.			
0.00	0.0405	0.0186	0	0	...	...
1.00	.0403	.0187	23	0.038	...	0.655
2.00	.0399	.0191	44	.074	...	.653
4.00	.0392	.0198	80	.138	...	.625
8.00	.0377	.0214	152	.271	0.829×10^{-2}	.671
21.00	.0335	.0257	271	.546	.912	.637
37.00	.0294	.0298	324	.743	.871	.625
			Set II, 896 c./m.			
0.00	0.1214	0.0186	0	0	...	...
1.00	.1212	.0188	68	0.088	...	.658
2.00	.1201	.0198	129	.168	...	.656
4.00	.1175	.0225	242	.322	0.854×10^{-2}	.694
9.00	.1126	.0274	407	.564	.836	.660
17.50	.1048	.0352	538	.802	.841	.661
32.00	.0935	.0465	529	.884	.815	.480[b]
			Set III, 873 c./m.			
0.00	0.0809	0.0186	0	0	...	...
1.00	.0807	.0188	47	0.067	...	0.697
4.00	.0777	.0219	161	.236	...	.676
17.00	.0697	.0298	405	.664	0.877×10^{-2}	.646
23.00	.0659	.0336	445	.772	.891	.646
32.00	.0617	.0378	471	.872	.848	.646
			Set V, 438 c./m.			
0.00	0.0405	0.0093	0	0	...	...
1.00	.0404	.0094	12	0.034	...	0.693
2.00	.0400	.0097	23	.065	...	.675
4.00	.0391	.0107	44	.128	0.861×10^{-2}	.689
8.00	.0374	.0124	77	.231	.993[b]	.661
21.00	.0336	.0161	149	.503	.880	.671
37.00	.0292	.0205	179	.696	.880	.647
			Set VI, 1775 c./m.			
0.00	0.0405	0.0362	0	0	...	...
1.00	.0404	.0363	48	.052	...	0.697
2.00	.0401	.0366	93	.095	...	.688
4.00	.0393	.0374	178	.198	...	.718
9.00	.0374	.0393	312	.365	0.882×10^{-2}	.658
17.00	.0350	.0416	461	.575	.848	.655
24.00	.0332	.0435	550	.725	.829	.703
32.00	.0312	.0455	553	.775	.815	.607

[a] Concentrations are quoted for 363.2°K. [b] These values were not included in the calculation of the average.

Results and Discussion

Reaction rate constants for exchange, k_x, were calculated using expression 7, *i.e.*

$$k_x = -\frac{2.303 \log (1 - F_t)}{(a + b)t}$$

Reaction rate constants for hydrolysis were calculated assuming a pseudo first-order process, *i.e.*

$$k_h = \frac{2.303}{t} \log \frac{b}{b - \rho(t)} \qquad (8)$$

Total chloroacetic acid concentrations were used in both expressions. The half-time for the exchange was much shorter than for the hydrolysis. Significant hydrolysis rate data were therefore usually obtained only after 20–30% exchange.

In Table I are summarized in detail our results at 90.0°. In Table II are listed average rate constants for exchange and hydrolysis for the several temperatures.

Under these experimental conditions the hydrolysis is adequately described by the pseudo first-order relationship. The consistency of the reaction rate constants for exchange over quite wide ranges of reactant concentrations indicates that this is a process first order with respect to the chloride concentration and to the total chloroacetic acid concentration. Our results suggest either that a negligible fraction of the chloroacetic acid is present in the dissociated form or that ionic and molecular forms exchange at essentially the same rate. Wright[9] has obtained the following relationship for the temperature dependence of the ionization constant for chloroacetic acid up to 40°.

(9) D. D. Wright, *J. Am. Chem. Soc.*, **56**, 314 (1934).

TABLE II

SUMMARY OF REACTION RATE CONSTANTS FOR EXCHANGE AND HYDROLYSIS

Temp., °K.	Set	$(CH_2Cl\text{-}COOH)_0$,[a] mole/l.	$(HCl)_0$,[a] mole/l.	k_h (hr.$^{-1}$)	k_x (l. mole^{-1} hr.$^{-1}$)
353.2	II	0.1222	0.0187	3.41×10^{-3}	0.232
	III	.0815	.0187	3.16	.235
	VI	.0408	.0374	2.95	.239
			Av.	3.17×10^{-3}	0.235
363.2	I	0.0405	0.0186	0.871×10^{-2}	0.644
	II	.1214	.0186	.837	.666
	III	.0809	.0186	.872	.662
	V	.0405	.0093	.874	.673
	VI	.0405	.0362	.843	.675
			Av.	0.859×10^{-2}	0.664
373.2	I	0.0402	0.0184	2.20×10^{-2}	1.63
	II	.1205	.0184	2.17	1.58
	III	.0803	.0184	2.14	1.61
	V	.0402	.0092	2.34	1.60
	VI	.0402	.0359	2.10	1.59
			Av.	2.19×10^{-2}	1.60
383.2	VIII	0.1038	0.0204	5.11×10^{-2}	3.67
	XI	0.0245	0.0190	5.35	3.66
			Av.	5.25×10^{-2}	3.67

[a] Concentrations are quoted for the temperatures of the reaction.

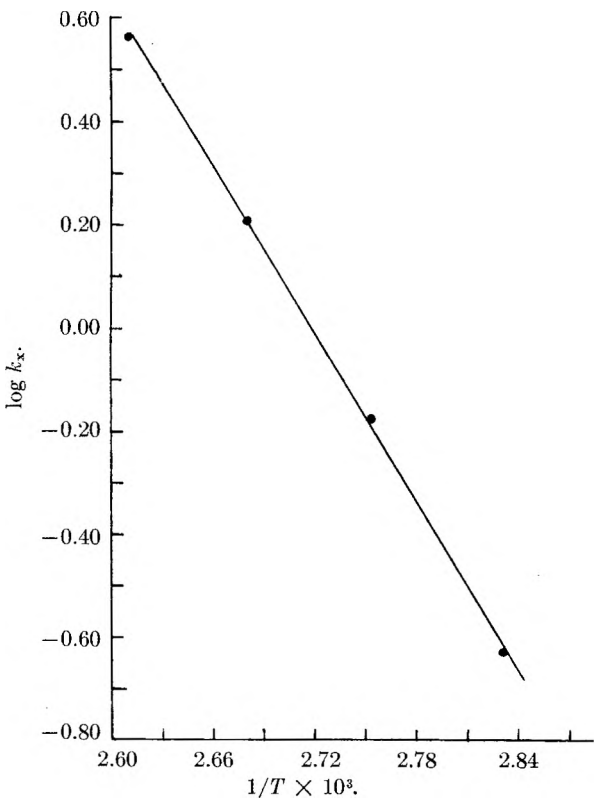

Fig. 1.—Plot of k_x *vs.* $1/T$ for the exchange reaction E_a = 24,500 ± 500 cal./mole.

$$\log K = -\frac{6669.53}{T} - 89.40736 \log T + 0.0523310T + 225.1390$$

Constants calculated using this equation were somewhat greater than those observed experimentally at the higher temperatures. We have, nevertheless, used this expression to estimate ionization constants at the temperatures of our experiments. It was estimated that the initial degree of dissociation of chloroacetic acid in our experiments varied from 3.1% (set II at 353.2°K.) to 1.7% (set VI at 373.2°K.). This, of course, decreases during a reaction because of the increasing ratio of HCl to chloroacetic acid. In order to evaluate the relative importance of the ionic species as a participant in the exchange, a limited number of experiments were performed at 80° in which the initial mixture was titrated to *p*H 7.5 with NaOH before reaction.[10] The results of these experiments are summarized in Table III.

TABLE III

353.2°K., 2020 c./m.

Exchange of Cl^- with CH_2ClCOO^- (Initial *p*H 7.5)

Time, hr.	(Cl^-), mole/l.	$(CH_2Cl\text{-}COO^-)$, mole/l.	Counts/min. in $CH_2Cl\text{-}COO^-$	F	k_x'
0	0.00899	0.1233	0	0	...
5.5	.0455	.0868	47.1	0.054	0.051
12.5	.0813	.0319	110.4	0.139	0.091

Apparent reaction rate constants, k_x', calculated according to equation 7 indicate a much slower exchange rate for the ionic species than for the undissociated acid. The suggested increase of this apparent constant with increasing acidity is also consistent with this conclusion.

No further experiments were performed to test the role of the ionic species in the hydrolysis reaction. The consistency of the reaction rate constant for hydrolysis suggests only that it is not markedly more important than that of the undissociated molecule. We have therefore assumed the rate constants listed in Table II to be characteristic of reaction by the undissociated molecule. Any error introduced into the rate constants by the use of the total chloroacetic acid concentrations in their calculation would then seem to be within the observed experimental variation.

The activation energy and frequency factor for the exchange reaction were evaluated in the usual way from a plot of log k_x *vs.* $1/T$ (Fig. 1). It was found that

$$k_x = 0.95 \times 10^{11} \exp[(-24{,}500 \pm 500)/RT] \text{ l. mole}^{-1} \text{ sec.}^{-1} \quad (9)$$

Figure 2 shows the corresponding plot for the hydrolysis rate constants from which

$$k_h = 2.11 \times 10^9 \exp[(-24{,}800 \pm 800)/RT] \text{ sec.}^{-1} \quad (10)$$

This rate constant, of course, includes the water concentration to an unknown exponent. Despite the slightly better fit of the hydrolysis constants to the logarithmic plot, a greater uncertainty has been ascribed to the Arrhenius activation energy for this reaction. This is a consequence of the somewhat larger expected deviation for the rate constant ratios.

Using the relationship[11] $k_r = (kT/h) \exp[\Delta S^{\ddagger}/R] \exp[-\Delta H^{\ddagger}/RT]$ with $\Delta H^{\ddagger} = E_a - RT$, $\Delta S^{\ddagger}$ for the exchange reaction was calculated to be −10.6

(10) These results were obtained by Mr. Kinziro Aizawa in this Laboratory and are used with his kind permission.

(11) A. A. Frost and R. G. Pearson, "Kinetics and Mechanism," John Wiley and Sons, Inc., New York, N. Y., 1953, p. 96.

cal. mole^{-1} deg.$^{-1}$. This evaluation was made for 80° and the standard state is one mole per liter.

A calculation of the frequency factor for the exchange was made using a simple gas phase collision rate expression, *i.e.*

$$A = \sigma_{12}^2 \left[8\pi kT \left(\frac{m_1 + m_2}{m_1 m_2} \right) \right]^{1/2}$$

σ_{12}, the collision dimeter, was estimated to be 4.5 Å. This estimate was based upon an ionic radius for chloride of 1.81 Å.[12] and upon a molecular radius of 2.7 Å. for chloroacetic acid. The latter value was obtained from the expression[13] $r = 0.66 \times 10^{-8} V_m^{1/3}$ in which V_m is the molar volume of chloroacetic acid. When expressed in comparable units, this calculated frequency factor is, at 353.2°K., 2.06×10^{11} l. mole^{-1} sec.$^{-1}$, a value in reasonable agreement with the experimental.

Our results indicate that the exchange takes place through a simple bimolecular displacement type reaction

$$Cl^{-*} + CH_2ClCOOH = CH_2Cl^*COOH + Cl^-$$

Dawson and Pycock[4] measured pseudo first-order constants for the hydrolysis at 25 and 45°. The rate constant corresponding to k_h, when expressed in the time unit we have used, was found by them to be 2.25×10^{-8} at 45° Equation 10 predicts that at this temperature, $k_h = 1.92 \times 10^{-8}$ sec.$^{-1}$. Our activation energy for hydrolysis, however, is considerably smaller than the 28,000 cal./mole calculated from their results at the two temperatures.

The similarity in our activation energies for exchange and hydrolysis may be fortuitous or it may suggest the interesting possibility of an activated complex involving an acid molecule, a chloride ion and one or more molecules of water. The complex may then decompose by two paths, replacement of chloride being the more probable.

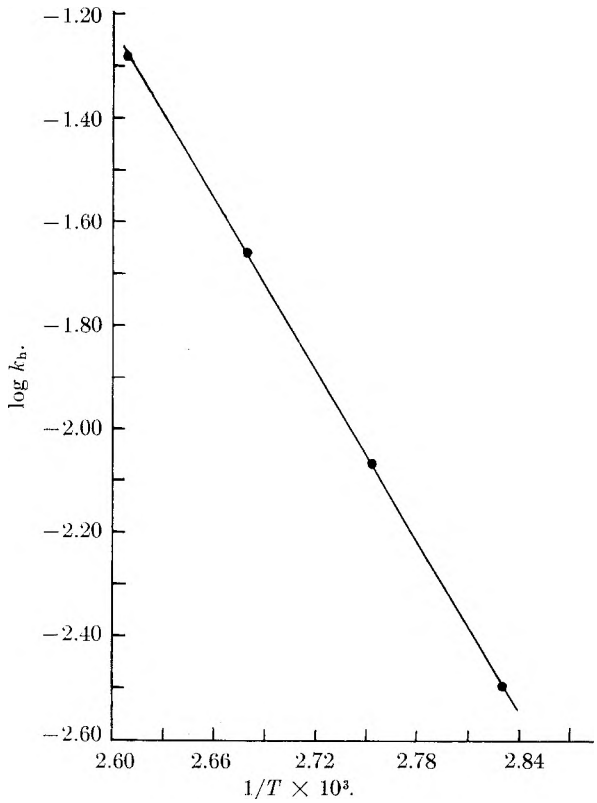

Fig. 2.—Plot of log k_h *vs.* $1/T$ for the hydrolysis reaction $E_a = 24{,}800 \pm 800$ cal./mole.

We wish to express our appreciation to the Research Corporation for a grant in support of this work.

(12) L. Pauling, "The Nature of the Chemical Bond," Cornell University Press, Ithaca, N. Y., 1948, p. 346.

(13) E. A. Moelwyn-Hughes, "The Kinetics of Reactions in Solutions," Oxford University Press, London, 1947, p. 7.

THE TEMPERATURE–INTERFACIAL TENSION STUDIES OF SOME ALKYLBENZENES AGAINST WATER

BY JOSEPH J. JASPER AND HELEN R. SEITZ

Department of Chemistry, Wayne State University, Detroit, Michigan

Received February 10, 1959

This is the third of a series of studies involving the thermodynamic properties of the interfacial region between a number of homologous series and water. The present paper included the four lower alkylbenzenes over the temperature range 19.45 to 79.30°. The least squares were applied to formulate empirical equations which express the interfacial tensions as functions of the temperature. These equations were employed to calculate the entropy, enthalpy and latent heat of formation per cm.^{2} of interface. The calculated results, together with the densities of the mutually saturated liquids and their interfacial tension values for four temperatures, are presented in tables.

The interfacial region between two relatively immiscible liquids consists of a transitional concentration gradient, the depth of which is determined by the magnitude of the intermolecular interaction between the unlike molecular species. Since this effect increases with increasing temperature, the mutual solubility of the two liquids increases, and it is obvious, therefore, that there must be an expansion of the transitional phase as the critical solution temperature is approached. As a consequence of this increasing solubility and concomitant increasing thickness of the transitional phase, it might be expected that the magnitude of the interfacial free surface energy would vary inversely with the temperature. The linear surface tension–temperature relations of liquid–gas surfaces are not realized, however, for liquid–liquid interfaces. Experimental evidence proves that the interfacial tension always decreases more rapidly than the temperature increases, giving curves

which are concave to the temperature axis. Two factors apparently are involved, namely, the influence of the kinetic activities of the molecules in the surface region and the increasing similarity of the contiguous phase. The effect of the former is probably similar to that in liquid–gas surfaces, namely, to descrease the interfacial tension linearly. The effect of the latter is superimposed upon the former, although this is generally not immediately evident at normal room temperatures. With increasing temperatures, however, the deviation from apparent linearity becomes more and more obvious. It appears evident, therefore, that the magnitude of the interfacial free surface energy is dependent upon the same forces which make the interface possible. These are, in turn, dependent upon the nature of the two molecular species between which the interface is established.

The long range objective of this series of interfacial tension studies is to determine how the same substituted groups, either electron accepting or releasing, influence this intensive interfacial property when substituted in a given compound or in different homologous series. In all cases, the arbitrarily chosen standard liquid is water.

This is the third of the series of studies, the first of which involved the halogenated benzenes,[1] and the second by the halogenated toluenes.[2]

In the present paper, the results of the study of four alkylbenzenes over a temperature range of 60° are presented. The interfacial tension data were applied to calculate the temperature variation of some thermodynamic properties of the liquid interfaces.

Experimental

Purification of the Compounds.—The best of their grades of toluene, ethylbenzene, *n*-propylbenzene and *n*-butylbenzene were obtained from Eastman Organic Chemicals Industries, and each was further purified by vacuum fractionation. For this purpose, a 15-inch column was employed which was packed with single-turn glass helices and equipped with a total reflux variable take-off head. In each case the middle third was collected for use in the experimental operations which followed. The refractive indexes of the purified compounds agreed with the values given in Beilstein to the fourth place of decimals.

Determination of the Densities.—It was highly important that the densities of the mutually saturated liquids be determined accurately, since they appear in the interfacial tension equation as explicit variables. To ensure accuracy, the densities were measured simultaneously with the corresponding interfacial tensions with the use of a modified form of the "type D" pycnometer described by Bauer.[3] Three pycnometers, each of which had a volume of 20 ml., were constructed as nearly identical in dimensions and shape as possible. These were calibrated and two of them reserved for the respective liquids, while the third was used as a counterpoise. The alkylbenzenes and water were saturated with each other by vigorously stirring quantities of each together and then allowing the two liquids to remain in contact at least 24 hours before they were used. The liquids were introduced into the pycnometers by means of a 30-ml. glass hypodermic syringe equipped with a 12-cm., 20-gauge, stainless steel needle which could be inserted into the capillary neck of the pycnometers to a depth of their total length. A constant volume of liquid was maintained in the pycnometer by adding or withdrawing small quantities, as the situation demanded, during the temperature variation of the experiments. The densities of the two mutually saturated liquids are shown in Table I, and these represent the average of four independent determinations.

TABLE I

THE DENSITIES OF THE MUTUALLY SATURATED LIQUID COMPOUNDS

Compound	Temp., °C.	Density, g./ml. Aqueous phase	Organic phase
Toluene	19.45	0.9968	0.8652
	40.50	.9906	.8457
	60.00	.9819	.8276
	79.30	.9710	.8090
Ethylbenzene	19.45	.9968	.8652
	40.50	.9906	.8469
	60.00	.9821	.8297
	79.30	.9712	.8122
n-Propylbenzene	19.45	.9968	.8583
	40.50	.9907	.8406
	60.00	.9829	.8243
	79.30	.9712	.8079
n-Butylbenzene	19.45	.9968	.8587
	40.50	.9906	.8417
	60.00	.9812	.8262
	79.30	.9703	.8104

To maintain a constant temperature during the various measurements, a specially designed glass-wool insulated water-bath was used. This was equipped with heat resistant plate glass windows and a covering of one-inch fiber board. Four thermoregulators were used at respective instrument settings of 20, 40, 60 and 80°, and these were used interchangeably, which greatly facilitated the rechecking of data at precisely the same temperature previously used. The stirring system was sufficiently efficient, and the thermoregulators sensitive enough, to maintain a temperature constant to 0.002° in the range 20–40°, and to 0.004° up to 80°. The actual temperatures were read from NBS certified thermometers having two-degree ranges and 0.01° scale divisions.

Determination of the Interfacial Tensions.—A modification of the drop-weight apparatus of Harkins and Brown was used in measuring the interfacial tensions. Drop volumes instead of drop weights were measured because of the greater experimental difficulties attending the latter. The apparatus assembly, and the exact procedure, have been described in a previous paper.[1] A series of interchangeable tips, having radii varying from 0.0785 to 0.44615 cm., and measuring pipets of different volumes, permitted measurement of a variety of liquids representing a large range of densities.

Preliminary experiments proved that the aqueous phase wet the surface of the tip and spread on it much more readily than the organic phase; hence the former was selected as the drop-forming liquid. Since the aqueous phase was in every case the more dense, it was necessary to arrange the tip in such a position that the drops could form vertically downward and subsequently become detached and coalesce into a homogeneous layer below the organic phase. The pipet and tip chosen to deliver the drops to the organic phase depended upon the density differential. For the toluene the pipet and tip selected delivered 18 to 24 drops; for ethylbenzene, 16 to 22 drops, for *n*-propylbenzene, 16 to 22 drops, and for *n*-butylbenzene, 18 to 21 drops. Twenty-four hours were required to make the measurements for each compound, and each measurement was repeated four times.

Results and Discussion

The equation used for calculating the interfacial tension values was that employed by Harkins and Cheng[5] and is given as

$$\gamma_i = vg(d_o - d_w)/2\pi rl'$$

(1) J. J. Jasper and T. D. Wood, THIS JOURNAL, **59**, 541 (1955).

(2) J. J. Jasper and Helen R. Seitz, *ibid.*, **62**, 1331 (1958).

(3) N. Bauer in "Physical Methods of Organic Chemistry," Vol. 1, Interscience Publishers, Inc., New York, N. Y., 1945, p. 79.

(4) W. D. Harkins and F. E. Brown, *J. Am. Chem. Soc.*, **41**, 499 (1919).

(5) W. D. Harkins and Y. C. Cheng, *ibid.*, **43**, 35 (1921).

where γ_i is the interfacial tension in ergs per cm.^{2}, v the drop volume in ml., d_0 the density of the organic phase, d_w the density of the aqueous phase, g the gravitational factor, r the radius of the tip in cm., and F the Harkins and Brown[4] correction factor.

To calculate the magnitude of the entropy of the interface s the latent heat l, and the enthalpy h, the two-dimensional form of the Clapeyron equation was used.[6] Each of these thermodynamic properties refer to unit area of the interface measured under isobaric and isothermal conditions. These, together with the interfacial tension values, are presented in Table II. Empirical equations, expressing the interfacial tension as a function of the temperature, were formulated for each of the liquid systems by the method of least squares. These were used to calculate the values of the interfacial tensions for the temperatures given in the table. The equations are

Toluene: $\gamma_i = 33.124 - 0.0120t - 0.000463t^2$
Ethylbenzene: $\gamma_i = 34.081 + 0.0033t - 0.000566t^2$
n-Propylbenzene: $\gamma_i = 35.464 - 0.00276t - 0.000436t^2$
n-Butylbenzene: $\gamma_i = 35.687 + 0.0190t - 0.000657t^2$

The form of the empirical equations indicate that the corresponding functions are monotonically decreasing with their concavity directed toward the temperature axes. This behavior appears to be typical of interfacial tension–temperature relations and has been observed in all such studies made in this Laboratory. From reference to Table II, it is to be noted that the entropies, latent heats and enthalpies of the interfaces all increase with the temperature. The latent heats of liquid–gas surfaces, likewise vary in this direction, but the entropies and enthalpies are, generally, relatively constant. Plots of these intensive interfacial properties as functions of the temperature show that these relations are linear but not parallel. With the exception of the *n*-propylbenzene–water system, the temperature rate of change of the entropies, latent heats and enthalpies increase with increasing molecular weight of the organic compounds. At 80°, the entropy and latent heat curves converge at respective values of 0.0865 and 30.55. The enthalpy curves converge at about 52°, giving an average value of 52.0 ergs. The temperature rate of increase of the latent heats are somewhat greater than that of the enthalpies, but this is to be expected if the interfacial free surface energies decrease more rapidly than the temperature increases. The table also shows that the interfacial tensions increase with increasing molecular weights of the compounds in the homologous series at all of the temperatures. This can also be expected, since the magnitude of the interfacial free surface energy is dependent upon the degree of dissimilarity between the molecular species in the contiguous phases. It can be concluded, therefore, that the thickness of the transitional phases must decrease as the molecular weight of the organic liquids increase.

TABLE II

INTERFACIAL TENSIONS, ENTROPIES, LATENT HEATS AND ENTHALPIES OF THE INTERFACES

Compound	Temp., °C.	γ_i	$-(d\gamma_i/dt)$	s	h
Toluene	20	32.70 ± 0.03	0.0305	8.95	41.65
	40	31.90 ± .03	.0490	15.34	47.24
	60	30.74 ± .03	.0676	22.52	53.26
	80	29.20 ± .02	.0861	30.41	59.61
Ethylbenzene	20	33.92 ± .02	.0193	5.68	39.60
	40	33.31 ± .02	.0420	13.15	46.46
	60	32.24 ± .09	.0646	21.52	53.76
	80	30.72 ± .07	.0873	30.83	61.55
n-Propylbenzene	20	35.24 ± .03	.0202	5.96	41.20
	40	34.66 ± .06	.0376	11.77	46.43
	60	33.73 ± .06	.0551	18.36	52.09
	80	32.46 ± .08	.0725	25.60	58.06
n-Butylbenzene	20	35.80 ± .03	.0073	2.14	37.94
	40	35.39 ± .03	.0335	10.49	45.88
	60	34.46 ± .02	.0598	19.92	54.38
	80	33.00 ± .06	.0861	30.41	63.41

Although the interfacial tensions of the *n*-propylbenzene–water system vary logically in accord with its position in the present homologous series, repeated experiments proved that the other thermodynamic properties do not. The reason for this is not immediately clear.

At 20°, the ratio of the entropies of the *n*-butyl-, *n*-ethyl- and methylbenzene systems, respectively, is approximately 1:3:4 while the corresponding molecular weight ratio is 1:0.8:0.7. Since the entropy is generally qualitatively described as a measure of the internal disorder of a system, it is interesting to note that, for the interfacial regions, the rate at which the entropy increases with the temperature in turn increases with the molecular weight of the organic molecules. This may be accounted for by assuming that, in addition to the kinetic activity of the organic molecules which always increases with the temperature, there is an intramolecular activity, such as that described by Adam,[7] which might become increasingly significant as the alkyl chain, attached to the benzene molecule, increases in length.

(6) W. D. Harkins, "The Physical Chemistry of Surface Films," Reinhold Publ. Corp., New York, N. Y., 1952, p. 6–8.

(7) N. K. Adam, "The Physics and Chemistry of Surfaces" Oxford University Press, 1941, p. 67.

PROPERTIES OF SOME RARE GAS CLATHRATE COMPOUNDS

BY P. H. LAHR AND H. L. WILLIAMS

Research Laboratory, Linde Company, Division of Union Carbide Corporation, Tonawanda, New York

Received February 11, 1959

The clathrate compounds, argon(hydroquinone)$_3$, argon(phenol)$_4$, krypton(phenol)$_4$ and xenon(phenol)$_3$ were prepared by the direct reaction of the rare gas with the solid organic compound. Heats of formation of the phenol clathrates were found to be −9.85, −8.97 and −8.8 kcal., respectively, per gram mole of argon, krypton and xenon. At room temperature the xenon–phenol clathrate is stable above 3 atm. abs., krypton–phenol above 20 atm., and argon–phenol above 136 atm. The rates of formation and decomposition of these compounds at room temperature are diffusion-controlled. The time required to form the phenol clathrate compounds increases in the same order as the reaction pressures and in reverse order of the sizes of the rare gas atoms. This suggests that compression of phenol slows down the diffusion of the rare gas through the solid structure.

Introduction

Compounds of the heavier rare gases with water, phenol and hydroquinone are classed as clathrate (cage) compounds. The exact cage structure and stoichiometry, the methods of preparation from the melt or from solution, and the heats of formation are known for most of these compounds.[1–6] Powell[4] has defined a clathrate as a compound "in which two (or more) components are associated without ordinary chemical union through the complete enclosure of one molecular kind by a suitable structure formed by the other." He writes further that "an imprisoning action is an essential factor . . ." Because the compounds named above as examples are known to lose gas at atmospheric pressure and temperature, it is generally recognized that the imprisoning action is incomplete.

The nature of this imprisoning action has been further explored by experiments reported herein on the clathrates of argon–phenol, krypton–phenol, xenon–phenol and argon-hydroquinone. In contrast to the previously described methods of preparation of the hydroquinone compound from argon and liquid or dissolved hydroquinone, solid hydroquinone was pressurized directly with argon in this work. Phenol–rare gas compounds also were prepared directly from solid host and gaseous guest. Nikitin[1] prepared the xenon–phenol compound by a similar method and observed that argon and krypton also entered phenol, but he employed mixtures of rare gas with catalytic amounts of hydrogen sulfide or started with seed crystals of xenon clathrate or hydrogen sulfide clathrate. His information on the argon and krypton compounds was sketchy.

Experimental results have been obtained which extend and supplement the existing data on rare gas clathrates. These results include new data on the pressures of formation of compounds of phenol with argon, krypton and xenon at several temperatures. They indicate that the ratio of argon and krypton to phenol may be 1 to 4 rather than 1 to 3 as predicted.[2] The relative rates of formation of argon, krypton and xenon compounds of phenol and of argon–hydroquinone clathrate from gas and solid were qualitatively compared.

(1) B. A. Nikitin, *Z. anorg. allgem. Chem.*, **227**, 81 (1936); *Compt. rend. acad. sci. URSS*, **24**, 562 (1939); **29**, 571 (1940); *Bull. Acad. Sci. USSR Div. Chem. Sci.*, 23 (1952).

(2) M. von Stackelberg, *Z. Electrochem.*, **62**, 123 (1958); *Rec. trav. chim.*, **75**, 902 (1956); *Naturwissenshaften*, **38**, 456 (1951); **39**, 20 (1952).

(3) M. von Stackelberg, *Z. Electrochem.*, **58**, 25 (1954).

(4) H. M. Powell, *Rec. trav. chim.*, **75**, 885 (1956); *J. Chem. Soc.*, 61 (1948); D. E. Palin and H. M. Powell, *ibid.*, 208 (1947); 571 (1948); 815 (1948); *Nature*, **156**, 334 (1945).

(5) R. E. Richards, *Proc. Roy. Soc. (London)*, **A223**, 238 (1954).

(6) J. H. Van der Waals and J. C. Platteeuw, *Rec. trav. chim.*, **75**, 912 (1956); J. H. Van der Waals, *Trans. Faraday Soc.*, **52**, 184 (1956); J. C. Platteeuw, *Rec. trav. chim.*, **77**, 403 (1958).

Apparatus and Materials.—The apparatus used to explore the reactions between rare gases and solid phenol and hydroquinone was chosen primarily to fit the pressures at which the tests were made. For pressures below 68 atm., the vessel used consisted of a quartz tube 4 mm. i.d. by 12 mm. o.d. and 25 cm. long. The tube was closed at the lower end and cemented at the open end with high-temperature Pyseal wax into a stainless steel fitting drilled to give several thousandths of an inch clearance around the quartz. This fitting was screwed directly into an Aminco gauge block containing a 1000 p.s.i. Ashcroft test gauge. The high-pressure system was connected through a Kovar seal to a glass vacuum manifold containing a 100-ml. gas buret, manometer, sample bulb, cold trap and McLeod gauge.

For pressures above 68 atm., experiments were carried out in a 50-ml. pressure vessel rated at 3500 atm. or a 300-ml. pressure vessel rated at 1000 atm. Compressibilities of solid phenol and hydroquinone were determined in a pellet press with $^1/_4$-in. pistons and in a 70-ton press with a cylinder containing $^3/_4$-in. pistons.

"Linde" rare gases and Baker reagent-grade organic chemicals were used as received. The phenol had a melting point of 40°.

Procedure and Results

A. Compounds of Rare Gases with Phenol. 1. Procedure.—Phenol clathrates of krypton and xenon were formed in the quartz vessel. A weighed quantity (1 to 2 g.) of phenol crystals was packed into the tube and held in place with a plug of Pyrex glass wool. After the apparatus had been evacuated the rare gas was metered from the buret into the tube where it was condensed at liquid nitrogen temperature. The tube and pressure gauge were then isolated and the system was allowed to warm to room temperature. The section of the tube containing phenol could be independently heated by a water-bath. The approximate gas-loading of the solid was determined by comparing the quantity of gas metered into the system with the corresponding quantity present at the same pressure when the phenol was absent.

Argon and phenol were combined by pressurizing 31.5 g. of phenol with argon in the 50-ml. pressure vessel. The vessel was then cooled to −50° and the pressure was lowered to atmospheric pressure by letting the excess argon escape. Argon remaining in the crystals was determined by warming the vessel and collecting the gas evolved.

2. Composition.—The maximum ratio of moles of gas per mole of phenol was smaller than the theoretical ratio of $^1/_3$ obtained by Stackelberg,[2] except for the xenon compound. The ratios obtained from experimental data are given in Table I.

3. Decomposition Pressures.—The decomposition pressures were determined at several temperatures. Data for krypton and xenon over phenol above 25° were arrived at from both above and below equilibrium pressure and are therefore equilibrium values. A logarithmic plot of p *vs.* the reciprocal decomposition temperature for experimental values is shown in Fig. 1. The values from Nikitin's data[1]

TABLE I

COMPOSITION OF PHENOL CLATHRATES

Gas	Mole ratio of gas to phenol as prepared: From gas + solid	From melt
Argon	1:4.1	....
Krypton	1:5.6	1:4.1
Xenon	1:3.0	1:3.0

for xenon are included. The agreement of Nikitin's data with the new data is rather good.

Decomposition pressures of the three compounds at room temperature increase in the order of decreasing atomic weight of the gases involved. The break in the xenon–phenol curve is due to the fact that above 40° the solid complex is in equilibrium with liquid rather than solid phenol. This decomposition with melting was followed visually in the quartz tube.

4. **Heat of Formation.**—Heats of formation estimated from the slope of the graph of $\log p$ *vs.* $1/T$ for the decomposition of the phenol compounds, using the Clausius–Clapeyron equation, are given in Table II.

TABLE II

HEAT OF FORMATION FROM CLAUSIUS–CLAPEYRON EQUATION

$$(\text{Guest})_g + n(\alpha\text{-Phenol})_s = [\text{Guest}_g(\beta\text{-Phenol})_n]_s{}^a$$

Gas	Found (kcal. g.-mole^{-1}) (0–40°)	Nikitin[1] (kcal. g.-mole^{-1}) (0°)
Argon	−9.85	....
Krypton	−8.97	....
Xenon	−8.8	−7.33

[a] α and β are used to distinguish between the normal and "clathrate" structure of phenol as described by von Stackelberg.[2]

The above values are all several kcal. more negative than the −5 to −6 kcal. heat of "solidification" of these gases estimated by Stackelberg.[3] The difference represents a finite binding energy for the reaction of solid guest with solid phenol. Nikitin's lower value for the xenon compound may be due to a small temperature dependence of the heat of reaction. As seen in the graph, Fig. 1, the slope of a line through Nikitin's values alone would be less than the slope of the line drawn through all the points.

One way to estimate the ratio of xenon to phenol in the phenol clathrate is to compare the heats of formation of Xe·n(phenol) below and above 40°. These should differ by the heat of fusion of the n-moles of phenol associated with each atom of xenon. Above 40° the heat of formation of solid compound from liquid phenol and xenon, based on the graph, is −18.4 kcal. The difference (18.4−8.8 kcal.) is 3.5 times the molar heat of fusion (2.735 kcal.) of phenol. Lowest equilibrium ratios obtained experimentally were 3 ±0.3. The correct formula is presumed to be xenon-(phenol)$_3$.

5. **Relative Reaction Rates.**—The over-all rates of heterogeneous reactions of this type depend on the rates of a number of processes, such as diffusion of gas into the bed of crystals, interaction with surface layers of the crystals and diffusion into the interior of the crystals. No attempt was made to determine these rates precisely. Qualitatively it was observed that a longer time was required to saturate the crystals than to remove the gas, or to regain an equilibrium decomposition pressure over the compound after the gas had been removed to slightly below the decomposition pressure. For example, most of the argon taken up by phenol during a period of several days was removed from the phenol clathrate at atmospheric pressure and temperature in 30 min. To regain an approximate equilibrium pressure following only a slight drop in pressure or change in temperature, 5 min. was required for xenon over phenol above 40°, 15 to 20 min. for xenon or krypton over phenol at 36 to 40°, and 2 to 5 hr. for argon, krypton or xenon over phenol at 25°.

The approach to equilibrium pressures for xenon over phenol at 25°, for example, was observed by suddenly lowering the pressure 0.3 to 0.6 atm. by release of xenon and recording the subsequent pressure rise as equilibrium was restored. The pressure was then raised an equivalent amount

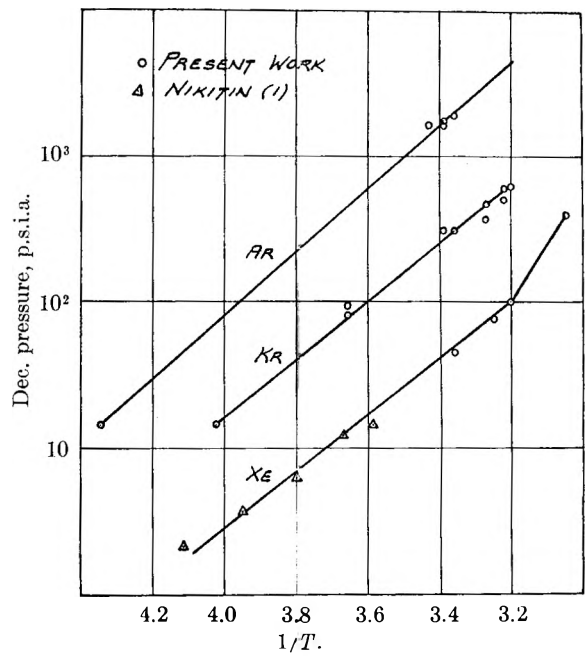

Fig. 1.—Decomposition pressure of phenol clathrates of argon, krypton and xenon *vs.* reciprocal temperature.

by a momentary fluctuation in the bath temperature in order to drive some gas out of the phenol. In both cases the pressure approached an equilibrium value asymptotically, with a 95% recovery of the pressure upset in 100 min.

To get 70% or more of saturation of phenol with gas at 25° with an excess pressure, 3 hr. was required for xenon, one day for krypton, and 7 to 10 days for argon. Although variables of excess pressure, crystal size (about 20 mesh per inch and larger) and packing density were not strictly controlled, the unexpected trend toward lower reaction rates for the smaller atoms is apparent. Table III gives experiments carried out with argon over phenol at 25° and illustrates the low reaction rate involved.

TABLE III

DIRECT FORMATION OF ARGON–PHENOL CLATHRATE AT 25°

Argon pressure, atm.	Time, hr.	Mole ratio, [Ar][PhOH]$^{-1}$	Av. rate of absorption [Ar][PhOH]$^{-1}$ hr.$^{-1}$
1800	16	1:8.3	0.0075
1600	18	1:11.5	.0048
480	65	1:6.05	.0026
475	42	1:6.65	.0036
250	200	1:4.53	.0011
340	240	1:4.1	.0010

A possible explanation for the lower rate of saturation of phenol with argon than with xenon is that the phenol is appreciably compressed at the higher argon pressure. Both the holes and the diffusion channels between the holes may be considerably smaller at 340 atm. than at 3 atm.

6. **Compression of Solid Phenol.**—Bridgman[7] found that phenol undergoes a reversible polymorphic transition with a 5–6% decrease in volume at 1500 atm. and room temperature. It was of interest to learn if this transition is affected by the presence of clathrated argon. Phenol (27.6 g. in a 50-ml. vessel) was charged with argon at 2000 atm. at room temperature and allowed to stand overnight. A small asymptotic drop in pressure signified adsorption of gas by phenol. As the argon was metered out of the pressure vessel, a leveling off of the pressure was noted at 1150 atm. A graph of pressure in the vessel *vs.* total volume of contained gas showed a shift in the curve at 1150 atm. corresponding to a 3.5% expansion of phenol and a consequent decrease in the free volume of the vessel. The argon present in the crystals apparently affected both the pressure and the volume change of this polymorphic transition. On the basis of data from

(7) P. W. Bridgman, *Proc. Am Acad. Arts Sci.*, **51**, 112 (1915.)

previous experiments carried out at this pressure overnight, the crystals contained about one molecule of argon to eight molecules of phenol. It is reasonable to suppose that the argon clathrate formed above the transition pressure differs from the compound formed below this pressure, although the data do not permit a separation of the factors of rate of formation and ultimate composition.

B. **Compound of Argon with Hydroquinone.**—1. **Preparation.**—Clathrate compounds of hydroquinone with argon (and other gases) have been reported in the literature.[4-6] Usually α-hydroquinone was melted or dissolved in a solvent and recrystallized under argon pressure to obtain the Ar(β-hydroquinone)$_3$ clathrate.

Pressurizing solid α-hydroquinone with argon was found to effect the same transformation. After pressurizing at 300 atm. or above for a day or longer, the pressure was released. The gas content of the solid was determined by dissolving the hydroquinone in alcohol, and the change from the α-form to the β-form was verified by X-ray diffraction. As indicated by the data in Table IV, the low rate of formation of the compound was relatively insensitive to changes in pressure above 300 atm.

TABLE IV

FORMATION OF ARGON–HYDROQUINONE CLATHRATE

Argon pressure, atm.	Time, hr.	Mole ratio [Ar] [Hq^{-1}]	Av. rate of absorption [Ar][Hq]$^{-1}$ hr.$^{-1}$	Remarks
9100	66	1:4.7	0.0032	Mixture of α- and β-forms
6100	88	1:3.5	.0033	Nearly pure β-forms
1000	100	1:4.1	.0024	.....
300	48	1:9.7	.0022	.....

2. **Decomposition.**—The hydroquinone–argon clathrate decomposed at a much lower rate at atmospheric pressure and room temperature than the compound of phenol with argon. The pattern of decay with time was typical for the diffusion of a gas from solid particles, since the logarithm of the volume of contained gas decreased asymptotically with time to a limiting slope. No change was observed in the relative intensity of α- and β-lines in the X-ray pattern of the crystals during the decay. The decompositon was followed for a time both by measuring the gas evolved from crystals of random size (20 to 150μ in diameter) and by X-ray fluorescence. For example, 15 g. of the compound containing 58 cc./g. of argon was found to contain 50 cc./g. in 24 hr., 46 cc./g. in 46 hr., 43 cc./g. in 70 hr., and 40 cc./g. in 144 hr.

3. **Effect of Pressure on the Structure.**—No polymorphic transitions were observed for α-hydroquinone at pressures up to 14,000 atm. Argon-loaded β-hydroquinone was compressed momentarily to 14,000 atm. without apparent loss of argon or change in structure.

C. **Organic Compounds Which Did Not React with Argon.**—A number of other organic compounds selected at random did not form compounds with argon. Urea is a relatively open-structured compound which undergoes a polymorphic phase transition with a decrease in volume at 5000 atm. Although other urea clathrates are known, no interaction of urea with argon was observed other than a slight gas solubility. Resorcinol, which is isomorphic with and less dense than hydroquinone, showed only a small gas solubility when pressurized to 2700 atm. in argon.

No reaction was detected when argon was compressed to 2700 atm. over pentaerythritol, amylodextrin, *m*-phenylenediamine, diphenylbenzidine, *p*-*t*-butylphenol, *p*,*p*-difluorobiphenyl, phenolphthalein, 1,8-diamino-naphthalene, diphenylamine, phenanthrene or 5-indanol. Although several of the above compounds showed evidence of some argon solubility, the amount of gas absorbed was too small for compound formation to be suspected.

Discussion of Results

The experimental results show that solid phenol reacts directly with argon, krypton or xenon to form "β-phenol" clathrate compounds. Similarly, α-hydroquinone reacts directly with argon to give the β-hydroquinone–argon clathrate compound. It is necessary in each case merely to apply a gas pressure that is above the decomposition pressure of the compound. The lower rate and ultimate mole ratio of reaction of phenol with argon or krypton than for xenon may be due to the decrease in volume of the spaces within the phenol crystal at the higher reaction pressures. The possibility cannot be ruled out, of course, that a 1 to 3 mole ratio for argon and krypton in phenol might have been obtained if more time had been allowed for the reaction to reach completion.

On decomposition, the "β-phenol" compounds revert to phenol and rare gas. The clathrate compound of argon–β-hydroquinone decomposes at a much lower rate than the phenol compound, and the β-structure is retained, at least during the initial stages of the decay. This phenomenon is explained by van der Waals and Platteeuw,[6] who regard the hydroquinone clathrate as a mixed crystal of filled and empty cages of hydroquinone.

The reversible reaction of liquid phenol plus xenon to give the solid clathrate is evidence of true compound formation, since solution of gas should lower the melting point of phenol, and the pressure applied was not sufficient to raise the melting point by the observed amount. This is related to the phenomenon that rare gas hydrates melt under pressure above 0°, whereas both pressure and dissolved gas would normally lower the freezing point of water.

No way was discovered to predict host compounds for rare gas guests on the basis of physical properties. There is no strict correlation between packing density or compressibility and clathrating ability. For example, resorcinol, which is less dense than its isomer, hydroquinone, did not form an argon clathrate. Ice, phenol and urea undergo polymorphic phase transitions with considerable contraction in volume at elevated pressures, whereas hydroquinone and resorcinol have only a normal compressibility below 14,000 atm. Urea and resorcinol do not form gas clathrates, at least by direct action of gas and organic solid.

The data are consistent with the accepted view that rare gas clathrates are true van der Waals compounds held together by a small energy of interaction within a unique cage configuration. In the region of temperatures and pressures for which the compound is stable, the energy of interaction of guest and host is sufficient to account for the thermodynamic stability of the compound. The temporary imprisoning action of the host at pressures below the decomposition pressure is to be pictured as a small potential energy barrier to diffusion of the guest atoms through the lattice of the host. The formation of the clathrates from solid host and gaseous guest and the decomposition of the solid clathrate appear to be diffusion-controlled processes.

Acknowledgment.—The authors wish to thank Dr. S. A. Stern and Dr. C. J. Ultee for some of the data used herein. We also thank Dr. W. G. Eversole and the Linde Company for permission to publish this paper.

TEMPERATURE DEPENDENCE OF THE REFRACTIVE INDEX INCREMENT OF POLYSTYRENE IN SOLUTION

BY J. H. O'MARA AND DONALD MCINTYRE

National Bureau of Standards, Washington, D. C.

Received February 11, 1959

The refractive index increments of polystyrene in cyclohexane and in toluene have been determined interferometrically as a function of temperature. The experimental results have been found to be in good agreement with calculations based on the Gladstone–Dale rule when the liquidus state curves for the refractive index and specific volume of polystyrene are extrapolated below the glass transition and then used to calculate the refractive index increment for temperatures below this transition.

Introduction

An accurate evaluation of the refractive index increment, dn/dc, of polymer solutions at various temperatures has become increasingly important for several reasons. The square of this quantity occurs in equations used to derive molecular weights and virial coefficients from light-scattering data. Experimental work is often conducted to test the predictions of polymer solution theories by determining the increase of the size of the molecule in a poor solvent while increasing the temperature. Also, an increasing amount of work is being conducted on new polymers at higher temperatures where the refractive increments have not been determined. Furthermore, many workers are using relative instruments to determine these increments, and the optical constants of these instruments are not easily established as a function of temperature.

The need to know the temperature dependence of dn/dc arose as a result of work to determine the virial coefficients of polystyrene in cyclohexane at different temperatures. Earlier experimental work[1] had indicated that there was no temperature variation, although a temperature dependence had been assumed and used by some investigators.[2,3] Table I lists some calculated (c) and measured (M) values obtained by the previously-mentioned investigators and also by Outer, Carr and Zimm.[4]

These somewhat divergent results led us to examine another solvent, toluene, in addition to cyclohexane, over a wider temperature range because of its higher boiling point and its better solvent power. Both of these solvents are easy to handle, can be obtained "pure" and have well known physical constants. In addition, they have a relatively large refractive index increment with polystyrene. Literature data on the temperature dependence of dn/dc for polystyrene–toluene are not available, although the actual dn/dc values reported in the literature vary from 0.118 to 0.108 at 436 mμ[5,6] and 0.108 to 0.104 at 546 mμ[4,6] wave length of light near room temperature. Actually these values are in relatively good agreement as compared with the values reported for systems[7] involving polar solvents and macromolecules.

(1) W. R. Krigbaum and D. K. Carpenter, THIS JOURNAL, **59**, 1166 (1955).

(2) H.-J. Cantow, *Z. physik. Chem. (Frankfurt)*, **7**, 58 (1956).

(3) N. T. Notley and P. J. W. Debye, *J. Polymer Sci.*, **17**, 99 (1955).

(4) P. Outer, C. I. Carr and B. H. Zimm, *J. Chem. Phys.*, **18**, 830 (1950).

(5) W. R. Krigbaum and D. K. Carpenter, *ibid.*, **24**, 1041 (1956).

(6) H. P. Frank and H. F. Mark, *J. Polymer Sci.*, **17**, 1 (1955).

(7) C. I. Jose and A. B. Biswas, *ibid.*, **27**, 575 (1958).

Experimental

Materials.—Two separate fractions of polystyrene[8] were used in this investigation. Fraction I was prepared by thermal initiation and had a molecular weight of 34,500. Fraction II was prepared by benzoyl peroxide initiation with the aid of a mercaptan transfer agent and had a molecular weight of 50,000. When the polymers were dried above the glass temperature for several hours they were found to contain less than 0.5% residual solvent from freeze drying.

The solvents used were ACS reagent-grade samples of cyclohexane and toluene. Before use they were fractionally distilled in columns packed with glass helices. The toluene was distilled over sodium. The refractive indices of both solvents as measured with a dipping refractometer at 30° checked with literature values.

Interferometer.—A Hilger Rayleigh Interferometer was used to determine the refractive index increment. The instrument had been modified so as to contain a special thermostatting compartment which could accommodate not only the usual cells but also some special all-glass fused cells used for volatile liquids. The cell used in the present investigation was a 1-cm. cell provided by Hilger[9] which had fused glass joints throughout. When in use, the cell was covered by glass plugs to prevent evaporation. Originally, a 1-cm. cell was used that had been cemented together with polyvinyl alcohol, but the results obtained with toluene in this cell were erratic, probably because of pick up of water by the toluene from the polyvinyl alcohol.

The monochromatic source of radiation was provided by an AH-3 mercury lamp manufactured by the General Electric Company. The monochromatic light was filtered by a Corning filter combination of No. 3484, 5120 and 4303 for the 546 mμ line and a combination of No. 3389 and 5113 for the 436 mμ line. The white light was furnished by a 100-watt projection bulb.

Technique.—The achromatic band shift can cause a problem with organic materials where the dispersion of the organic solute is markedly different from that of the glass compensating plates. This problem is easily resolved, however, if enough time and care are taken to work with sufficiently dilute solutions so that the shift of one band is drastic enough to cause severe changes in the calculated refractive index increment. Once the location of the true refractive index increment is known, the accuracy of the determination may easily and judiciously be increased. The accuracy of the measurement reported here is $\pm 2 \times 10^{-6}$ units of refractive index. In other routine work in these laboratories, the location is often made by means of a differential refractometer.

All solutions were prepared independently on a weight-percentage basis, and the concentration at each temperature was determined in grams per deciliter by multiplying the weight concentration by the density of the solvent at the temperature in question. The concentrations ranged from 0.05 to 0.6 g./dl. Three to five solutions were measured at each temperature.

In determining the temperature dependence of the dn/dc, the solvent and solutions were measured at one temperature, then the thermostat raised to a new temperature, and fresh samples of solvent and solutions measured. The temperatures in the cell were measured by means of a thermocouple. In one experiment the dn/dc of a 0.3 g./dl. solution

(8) D. McIntyre, J. H. O'Mara and B. C. Konouck, *J. Am. Chem. Soc.*, **81**, 3498 (1959).

(9) E. Grunwald and B. J. Berkowitz, *Anal. Chem.*, **29**, 124 (1957).

TABLE I

REFRACTIVE INDEX DATA FOR POLYSTYRENE–CYCLOHEXANE SOLUTIONS

Ref.	$(dn/dc)_{25^0}$	546 mμ light $(dn/dc)_{40^0}$	$(d/dt)(dn/dc)$	$(dn/dc)_{25^0}$	436 mμ light $(dn/dc)_{40^0}$	$(d/dt)(dn/dc)$
1	0.173(c)	0.173(M)	0(M)	0.183(c)	0.183(M)	0(M)
2	.1695(M)	.174(c)	2.8×10^{-4}(c)	.181(M)	.185(c)	3.0×10^{-4}(c)
3					.184(c) Av.	3.8×10^{-4}(c)
4		.179(c)				

of polystyrene in cyclohexane was determined from 30 to 55° after a separate determination of the solvent zero band position. The results in this case were identical with the others.

Results

Table II summarizes the data obtained on refractive index increments for both the 546 and 436 mμ wave lengths of light and for both fractions of polystyrene in cyclohexane and fraction I in toluene. The values for $d/dt(dn/dc)$ represent the least squares slope and its standard error. Figure 1

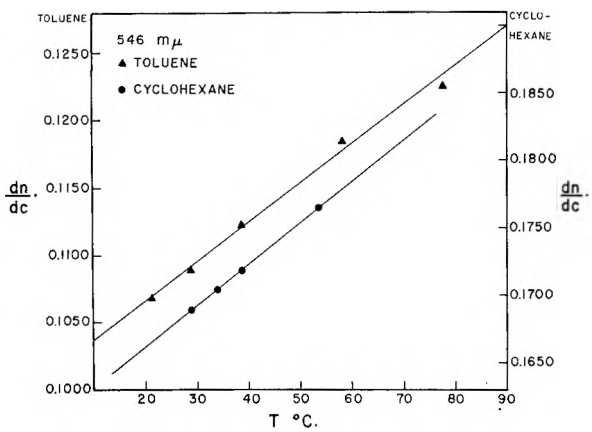

Fig. 1.—Refractive index increments at 546 mμ wave length of light for polystyrene fraction I in cyclohexane and in toluene at various temperatures.

shows these data in graphical form for fraction I in toluene and in cyclohexane for light of 546 mμ wavelength. From observations in this work using simple glass cell covers it appears that any measurements of the refractive index increments that are made without adequate closure of the compartments to prevent creep or volatilization should be viewed with skepticism. In addition, solvents that have been thoroughly dried during preparation can give very misleading results because they are prone to pick up water during the course of the measurements when the cells are not thoroughly closed.

Discussion

The specific refraction of the mixture of two liquids may be successfully represented in many cases by the sum of their respective specific refractivities.[10] The representation of the specific reactivity R of a material by the expression $(n - 1)/\rho$, where n and ρ are the refractive index and the density, respectively, is known as the Gladstone–Dale expression. If the summation of these refractivities is to be made on the basis of the volumes occupied, or mathematically on the basis of their weight fractions w, then the Gladstone–Dale rule for the refractivity of a mixture may be represented by the equation

(10) J. R. Partington, "An Advanced Treatise on Physical Chemistry," Vol. IV, Longman, Green and Co., London, 1953.

TABLE II

REFRACTIVE INDEX DATA FOR POLYSTYRENE SOLUTIONS

Polystyrene–Cyclohexane

Fraction		I		II
Light, mμ		546	436	546
	28.9°	0.1689	0.1798	0.1693
dn/dc	34.0	.1705	.1810	.1703
	38.6	.1719	.1823	.1715
	53.5	.1765	.1884	
$(d/dt)(dn/dc)$		$(3.08 \pm 0.04) \times 10^{-4}$	$(3.58 \pm 0.29) \times 10^{-4}$	2.3×10^{-4}

Polystyrene–Toluene

Fraction		I	
Light, mμ		546	436
	21.2°	0.1068	0.1109
dn/dc	28.9	.1089	.1126
	38.6	.1122	.1168
	58.0	.1185	.1242
	79.4	.1226	.1280
$(d/dt)(dn/dc)$		$(2.89 \pm 0.14) \times 10^{-4}$	$(3.21 \pm 0.25) \times 10^{-4}$

$$R = w_1R_1 + w_2R_2 \qquad (1)$$

If the specific volume v of a binary mixture is also considered to be an additive sum of the weighted specific volumes of its pure components, then an expression can be derived for the refractive index of the dilute solution in terms of the concentration of the solute species, c, as

$$n - 1 = (1 - c/\rho_2)\rho_1R_1 + cR_2 \qquad (2)$$

Since the refractivities are not functions of the concentration of the solute, the refractive index and its temperature variation may be expressed as in equations 3 and 4

$$dn/dc = R_2 - (\rho_1/\rho_2)R_1 = (n_2 - n_1)/\rho_2 \qquad (3)$$

$$(d/dt)(dn/dc) = v_2\, d(n_2 - n_1)/dt + (n_2 - n_1)(dv_2/dt) \qquad (4)$$

If (1) the data for the specific volume of polystyrene taken from Fox and Flory,[11] both above and below the glass transition temperature (~90°), (2) the refractive index data for polystyrene from Jenckel,[12] both above and below the glass transition temperature, for light of wave length 5890 Å; and (3) the data for the refractive index of cyclohexane and toluene from Timmermans[13] are used to calculate the dn/dc at 30° and the temperature dependence from equations 3 and 4, results are obtained that are shown in Table III, columns 1, 4, 5 and 8. The results listed as glassy values in the table were obtained by assuming that the true glassy state refractive index and specific volume values obtained from the data below the glass temperature were the correct ones to use in the above equations. The second set of values were derived from the assumption that the proper values to be used in these equations are from the liquidus, derived by extrapolating the

(11) T. G. Fox and P. J. Flory, *J. Appl. Phys.*, **21**, 581 (1950).

(12) E. Jenckel and R. Heusch, *Kolloid-Z.*, **130**, 89 (1953).

(13) J. Timmermans, "Physico-Chemical Constants of Pure Organic Compounds," Elsevier Publishing Co., New York, N. Y., 1950.

TABLE III

CALCULATED AND MEASURED VALUES OF dn/dc AND $(d/dt)(dn/dc)$ AT 30°

	Cyclohexane				Toluene			
	dn/dc			$(d/dt)(dn/dc)$	dn/dc			$(d/dt)(dn/dc)$
Column no.	1	2	3	4	5	6	7	8
Wave length, mμ	589	546	436	589	589	546	436	589
Glassy	0.159	0.162	0.174	4.2×10^{-4}	0.0931	0.0935	0.0976	4.14×10^{-4}
Extrapd.	.166	.170	.183	2.8×10^{-4}	.102	.1025	.1070	2.46×10^{-4}
Measured	...	.1693	.1800	.....	.....	.1096	.1134	.....

curve above the glass temperature to lower temperatures. This makes the calculation more closely approximate the mixing of two liquids.

Unfortunately, the light-scattering measurements are conducted at 546 and 436 mμ rather than at the sodium-D line, so that the measurements of dn/dc cannot be directly compared with the above calculations using Jenckel's data. The dispersion curve for glassy polystyrene has been given[14] and fits a Cauchy relation. Similarly the dispersion of the solvents is known so that the dn/dc for glassy polystyrene can be calculated directly. The dispersion effects would be expected to be similar both above and below the glass temperature since it is directly a function of the internal molecular structure; therefore, the values for the dispersion dn/dc of the extrapolated liquidus state of polystyrene may also be calculated. These values appear in columns 2, 3, 6 and 7 of Table III. The temperature dependence of the refractive index of polystyrene and the solvents changes very little with wave length so the calculated value at 589 mμ can be directly compared with the measured values in Table II.

The excellent agreement of the calculated and experimental values for the dn/dc using the polystyrene constants extrapolated from the liquidus state is indeed encouraging, although the calculated temperature dependence of dn/dc in blue light does not seem to fit the measured values regardless of the choice of state. However, it is to be re-emphasized that there is a sizable temperature dependence of dn/dc and it must be taken into account in experimental measurements performed at different temperatures.

(14) R. M. Boundy and R. F. Boyer, "Styrene, Its Polymers, Copolymers, and Derivatives," Reinhold Publ. Corp., New York, N. Y., 1952.

THERMODYNAMICS AND KINETICS OF THE REACTION OF MERCURIC SALTS WITH OLEFINS. PART I. THE REACTION WITH MERCURIC CHLORIDE

BY E. R. ALLEN, J. CARTLIDGE, M. M. TAYLOR AND C. F. H. TIPPER

Dept. of Inorganic and Physical Chem., The University, Liverpool, England

Received February 18, 1959

The equilibrium constant of the reaction $HgCl_2 + C_2H_4 + H_2O \rightleftharpoons ClHgC_2H_4OH + HCl$ has been measured at 25° approaching the equilibrium position from both sides. The values are in agreement within the experimental error. The constant has also been determined at other temperatures between 15 and 40° commencing with mercuric chloride and ethylene and thus the heat content and entropy changes of the reaction have been calculated. The kinetics do not correspond to a first-order reaction opposed by one of the second order. Added sodium chloride had a marked retarding effect. The results are discussed and it is considered that they lend strong support to the hypothesis that the reaction proceeds by an ionic mechanism.

Introduction

The interaction of mercuric salts with olefins has been studied for many years. Many mercurials have been prepared and their reactions studied, but relatively little work has been reported on the thermodynamics and kinetics of these systems and the mechanism of the processes involved is still not clear.[1] Sand and Breest[2] investigated the equilibrium (1) and obtained values of the equilibrium

$$HgCl_2 + C_2H_4 + H_2O \rightleftharpoons ClHgC_2H_4OH + HCl \quad (1)$$

constant approaching the equilibrium position from both sides. Their work has been criticized,[3] and certainly their method of calculating K is incorrect. However, this system is a relatively simple one, and so the physical chemistry of the reaction of mercuric chloride and simple olefins has been reinvestigated by more direct methods.

(1) J. Chatt, *Chem. Revs.*, **48**, 7 (1951).
(2) J. Sand and F. Breest, *Z. physik. Chem.*, **59**, 424 (1907).
(3) P. Brandt and O. Plum, *Acta Chem. Scand.*, **7**, 97 (1953).

Experimental

The uptake of ethylene or propylene by mercuric chloride solutions (volume 20 or 25 cc.) was followed at a constant pressure by conventional means. The 100-ml. reaction vessel was immersed in a thermostat, constant to ±0.1°, and shaken about 350 times per minute. The rate of absorption was independent of shaking rate. The air in the flask had previously been swept out by the olefin, and the volume absorbed was determined by means of a thermostated gas buret connected to the flask by wide capillary tubing and polythene tubing. Before an experiment the vessel was washed with concentrated nitric acid, distilled water and acetone, and dried over a flame. The solubility of the gas in water was determined in the same way. It was found in all the experiments that no uptake occurred until the solution was shaken.

The equilibrium was approached from the opposite direc-

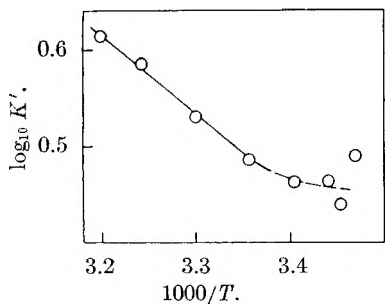

Fig. 1.—Variation of the equilibrium constant K' of the reaction $C_2H_4 + HgCl_2 + H_2O \rightleftharpoons ClHgC_2H_4OH + HCl$, with temperature.

tion in the following manner. Solutions of hydroxyethylmercuric chloride were prepared as described later. In an experiment the reaction vessel containing a solution was immersed in the thermostat, air displaced by ethylene and the flask shaken. When the solution was saturated with gas, a known amount of hydrogen chloride in a small volume (<1 ml.) of aqueous solution was added. On shaking ethylene was evolved, and the total volume given off was measured.

When solvents other than water were used, they were stored and transferred to the reaction flask under dry conditions.

Hydroxyethylmercuric chloride was prepared by the method of Aranda and Pastor.[4] The white solid melted at 153–154° (*cf.* 155°), but contained a small amount of impurity insoluble in water at room temperature. On addition of a large excess of hydrochloric acid only 95% of the theoretical amount of ethylene was evolved and the insoluble impurity still remained. Solutions of the compound were prepared directly as follows. From the volume of ethylene absorbed by an aqueous solution of mercuric chloride the amounts of HCl formed and of $HgCl_2$ unreacted were calculated. A quantity of sodium hydroxide equal to that required to neutralize exactly the HCl and precipitate the unreacted mercury as HgO, was added. The precipitate was filtered and washed. The whole solution plus washings were made up with water to a definite volume which contained a known amount of hydroxyethylmercuric chloride. The accuracy of this procedure was checked by addition of a large excess of HCl to one such solution. The theoretical volume of ethylene was given off.

An aqueous solution of mercuric chloride was shaken with ethylene until no more gas was absorbed, and the conductivity of the equilibrium mixture was measured by means of a conventional Wheatstone bridge apparatus. From the amount of olefin taken up the concentration of mercuric chloride left in solution and of hydrogen chloride formed was calculated and a mixture prepared containing these concentrations of chloride and acid. The conductivity of this mixture was the same within experimental error as that of the equilibrium mixture, indicating that the conductivity of an aqueous solution of hydroxyethylmercuric chloride is negligible.

All water was purified by distillation from a trace of potassium permanganate in an all-glass apparatus. Mercuric chloride, sodium chloride, hydrochloric and perchloric acids, methanol, ethyl acetate, acetic and trichloroacetic acids were of Analar quality. Sodium perchlorate was prepared from Analar sodium carbonate and acid. Analar piperidine and nitrobenzene were distilled in a stream of nitrogen before use, and *t*-butyl hydroperoxide was distilled under reduced pressure. Benzoyl peroxide was recrystallized from Analar chloroform and a sample of boron trifluoride etherate used directly. Nitrogen was taken from a cylinder, freed from oxygen by washing with alkaline hydrosulfite solution and dried with magnesium perchlorate. Cylinder ethylene and propylene were shown to contain no appreciable impurity by gas chromatography. However, the former was passed through 85% H_2SO_4, a trap at −78° and a drying tube successively.

Results

Thermodynamic.—The equilibrium constant for reaction 1 is easily calculated from the volume of gas at a known temperature and pressure taken up (allowing for the physical solubility in water) and the initial concentration of mercuric chloride, approaching the equilibrium position from the L.H.S., and from the initial concentrations of hydroxyethylmercuric chloride and HCl added and the volume of ethylene given off, approaching the equilibrium position from the R.H.S. Since water was the solvent Table I shows values of

$$K' = \frac{[ClHgC_2H_4OH]_e\,[HCl]_e}{[HgCl_2]_e\,[C_2H_4]_e}$$

under various conditions.

Irreproducible results were obtained when the pressure of ethylene was much below or above atmospheric due to difficulty in measuring the volume change, and it was not possible to investigate the variation of water concentration since suitable "inert" solvents, *e.g.*, acetone, to replace part of the water had high vapor pressures, causing expansion when shaking was started.

The individual values of K' are not very accurate since the volume of ethylene taken up or evolved was less than 20 ml., owing to the limited solubility of mercuric chloride and hydroxyethylmercuric chloride. Any error in this volume involves at least double the percentage error in K'. The accuracy of the experiments was less for the reaction of the addition compound and hydrochloric acid, owing to the number of operations necessary to prepare the aqueous solution of hydroxyethylmercuric chloride. Nevertheless the various values of K' at 25° agree quite well approaching the equilibrium position from both sides and at other temperatures for the $HgCl_2$–C_2H_4 reaction. The equilibrium may be displaced completely to one side or the other by the addition of excess base to the aqueous mercuric chloride solution or excess HCl to the solution of addition compound. Addition of sodium chloride to the mercuric chloride solution appeared to reduce K' somewhat, but the presence of sodium perchlorate had little or no effect. Addition to 0.066 *M* $HClO_4$ to 0.111 *M* $HgCl_2$ at 25° decreased the amount of ethylene taken up, but calculation of K' on the assumption that the acid concentration at equilibrium was given by $[HClO_4] + [HOC_2H_4HgCl]_e$ gave a value of 6.5. It was found that the addition of excess acetic acid to the aqueous solution of hydroxyethylmercuric chloride led to the evolution of only about 12% of the theoretical volume of ethylene, whereas all the olefin was given off when excess trichloroacetic acid was added.

The variation of K' with temperature is shown in Fig. 1. The results between 15 and 20° were rather erratic owing to the very long time necessary to attain equilibrium and the reduced solubility of the hydroxyethylmercuric chloride. However, above 25° at any rate the Van't Hoff isochore was a straight line from the slope of which the heat content change in the reaction was calculated to be +3790 cal. mole^{-1}. Taking into account the concentration of water the true value of the equilibrium constant K at 25° is 0.055 l. mole^{-1}.

$$\Delta G^0_{298} = -2.303RT \log K = +1720 \text{ cal. mole}^{-1}$$

and

(4) V. G. Aranda and O. S. Pastor, *Combustibles*, **10**, 183 (1950); *C. A.*, **46**, 423 (1952).

TABLE I

SECTION (a) VALUES OF THE EQUILIBRIUM CONSTANT K' OF THE REACTION OF MERCURIC CHLORIDE AND ETHYLENE IN AQUEOUS SOLUTION

Temp. °C.	Solubility of C_2H_4, mole/l.[a] × 10^3	Initial concn. $HgCl_2$, mole/l. × 10^2	Concn. additive mole/l.	Vol. C_2H_4 reacted per l. $HgCl_2$ soln. (ml. at S.T.P.)	K'	Average K'
15.2	4.7	6.2	.....	542	3.3	3.1
		11.3	.....	750	3.0	
		18.0	.....	989	3.0(5)	
16.4	4.6	11.8	.....	735	2.7(5)	
17.5	4.5	5.9	.....	497	2.9	
20.8	3.8	7.3	.....	526	2.9	2.9
		11.6	.....	679	2.8	
		13.3	.....	751	3.0	
25.0	3.1	5.6	.....	400	2.8	3.0(5)
		11.4	.....	628	3.0	
		11.8	.....	684	3.0	
		16.8	.....	820	3.3	
		17.6	0.0643 (HCl)	414	3.0	
		5.7	0.0101 (piperidine)	542	3.3	
		5.8	Excess piperidine	1200 (5.4×10^{-2} mole)	...	
		4.2	0.034 (NaCl)	314	2.3	
		4.2	0.12 ($NaClO_4$)	373	3.3	
30.0	2.7	4.7	.....	368	3.3	3.4
		11.2	.....	630	3.5	
		11.8	.....	645	3.4(5)	
		17.0	.....	802	3.5	
35.5	2.3	5.7	.....	425	4.1	3.8(5)
		8.8	.....	528	3.7(5)	
		11.9	.....	616	3.6	
		16.9	.....	785	4.0	
39.7	1.9	5.8(5)	.....	402	4.2	4.1
		11.8	.....	589	4.0	

SECTION (b) VALUES OF THE EQUILIBRIUM CONSTANT K' OF THE REACTION OF HYDROXYETHYLMERCURIC CHLORIDE AND HYDROGEN CHLORIDE IN AQUEOUS SOLUTION

Temp., °C.	Solubility of C_2H_4, mole/l. × 10^3	Initial concn. $ClHgC_2H_4OH$, mole/l. × 10^2	Initial concn. HCl, mole/l.	Vol. C_2H_4 given off per l. soln. (ml. at S.T.P.)	K'	Av. K'
25.0	3.1	1.27[b]	1.60	150	2.7	3.0
		1.42[b]	1.91	165	3.5	
		1.83[b]	1.92	228	2.3	
		1.88[b]	1.70	201	2.8	
		3.06[c]	3.92	444	3.4	
		4.92[c]	4.80	681	3.5	

[a] Mean of several determinations. [b] $ClHgC_2H_4OH$ prepared in solution. [c] Using solution of solid "complex"—concn. corrected for purity.

$$\Delta G^0_{298} = \Delta H^0 - T\Delta S^0$$

$$\therefore$$

$$\Delta S^0 = +7.0 \text{ cal. degree}^{-1} \text{ mole}^{-1}$$

The absorption of propylene by an aqueous solution of mercuric chloride also ceased before one mole per mole $HgCl_2$ was taken up. Values of the equilibrium constant

$$K'' = \frac{[HOC_3H_6HgCl]_e\,[HCl]_e}{[HgCl_2]_e\,[C_3H_6]_e}$$

were somewhat inconsistent [Table II] owing to the fact that, even at 40°, the addition compound tended to precipitate, the solubility being less than that of hydroxyethylmercuric chloride. It was thus difficult to obtain an "infinity" reading, owing to a slow drift, even by plotting values of the uptake at intervals during an experiment and extrapolating. However, the values of K'' do show that the equilibrium constant is not altered appreciably by changing from ethylene to propylene.

Kinetic.—Under the conditions of the experiments it might be supposed that the kinetics would correspond to those of a first-order reaction opposed by one of the second order. It can be shown quite simply[5] that for the equilibrium, $A \rightleftarrows B + C$, the velocity constant of the forward reaction is given by

$$k = \frac{2.303x_e}{t(2a - x_e)} \log\left(\frac{ax_e + x(a - x_e)}{a(x_e - x)}\right)$$

where a is the initial concentration of A and x and x_e the amounts of A reacted at time t and equilibrium. For the ethylene–mercuric chloride reaction, substituting for a, x_e and x

(5) S. Glasstone, "Textbook of Physical Chemistry," The Macmillan Co., New York, N. Y., 1940, p. 1051.

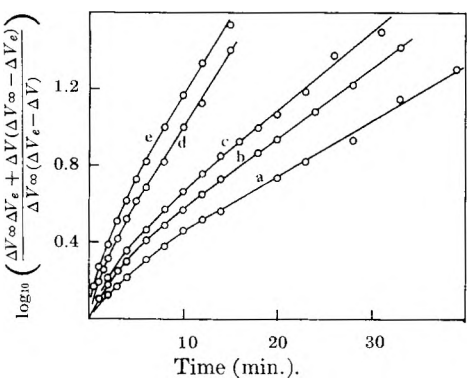

Fig. 2.—Kinetic plots of the rates of oxymercuration of ethylene with aqueous mercuric chloride on the assumption that a first-order reaction is opposed by one of the second order. a, b, and c, temp. 25.0°; concn. $HgCl_2$, 0.056, 0.114 and 0.168 *M*, respectively. d and e, temp. 39.7°; concn. $HgCl_2$, 0.0585 and 0.118 *M*, respectively.

TABLE II

VALUES OF THE EQUILIBRIUM CONSTANT *K''* OF THE REACTION OF MERCURIC CHLORIDE AND PROPENE IN AQUEOUS SOLUTION

Temp., °C.	Solubility of C_3H_6, mole/l. × 10^3	Initial concn. $HgCl_2$, mole/l. × 10^2	Vol. C_3H_6 reacted per l. $HgCl_2$ soln. (ml. at S.T.P.)	*K''*	Av. *K'*
25.0	3.7	3.34	340	3.4	3.3
		5.36	439	3.0[5]	
		7.34	560	3.5	
35.0	2.5	1.85	170	2.1	3.7
		3.45	314	3.8	
		3.84	358	4.6	
		4.72	412	4.7	
		5.36	394	3.4	
		5.72	470	4.9	
		6.85	394	2.4	
40.0	2.16	1.83	215	4.9	5.1
		1.85	224	5.4	
		3.25	313	4.9	

$$k = \frac{2.303\Delta V_e}{t(2\Delta V_\infty - \Delta V_c)} \log\left(\frac{\Delta V_\infty \Delta V_e + \Delta V(\Delta V_\infty - \Delta V_c)}{\Delta V_\infty(\Delta V_e - \Delta V)}\right)$$

where ΔV_∞ is the volume of ethylene corresponding to complete reaction, and ΔV and ΔV_e are the volumes taken up at time t and equilibrium. Thus a plot of the log term *versus* the time should be a straight line. The results at 25 and 39.7°, plotted in this way, are shown in Fig. 2. It can be seen that the lines are by no means straight, except possibly over the last 30% or so of the reaction before equilibrium was attained, the apparent value of k decreasing as the reaction proceeded. Even the value of k calculated from the slopes of the "straight" portions of the graphs varied as the initial concentration of mercuric chloride was increased at a constant temperature (at 25°, $k/2.303$ = 4.85, 5.11 and 5.36 × 10^{-3} min.$^{-1}$ with $[HgCl_2]_i$ = 5.6, 11.4 and 16.8 × 10^{-2} *M*, respectively; at 39.7° $k/2.303$ = 9.9 and 13.5 × 10^{-3} min.$^{-1}$ with $[HgCl_2]_i$ = 5.85 and 11.8 × 10^{-2} *M*, respectively). The temperature coefficient of k is low. It increases about 2.3 times between 25 and 39.7°, implying an apparent energy of activation of about 10 kcal. mole^{-1}. It was found that plots of log $(\Delta V_\infty - \Delta V)$ and log $(\Delta V_e - \Delta V)$ *versus* time were also curved.

Addition of sodium perchlorate or perchloric acid had little effect on the rate of reaction, but addition of sodium chloride reduced it greatly. At 25° with 0.042 *M* $HgCl_2$ $t_{1/2}$ was 9.3 min. without and 40 min. with 0.034 *M* NaCl present. In the presence of 0.71 *M* NaCl the reaction was too slow to measure.

When dissolved in ethyl acetate or nitrobenzene mercuric chloride did not react with ethylene. With methanol as solvent a very slow reaction occurred. Addition of water increased the rate and it is probable that, if the alcohol has been anhydrous—it actually contained 0.12 mole % H_2O,—no reaction would in fact have taken place. It has been reported that a solution of mercuric chloride in piperidine absorbs ethylene over a period of 48 hr. to give $C_5H_{10}NCH_2CH_2$-$HgCl$.[6] It was hoped to investigate the kinetics of this reaction, but with purified reagents no uptake of gas took place over 60 hr., even in the presence of 10 vol. % methanol. On addition of benzoyl peroxide, *t*-butyl hydroperoxide or boron trifluoride etherate (catalysts for mercuration), or when impure piperidine was used, a very slow reaction occurred, and a precipitate, probably piperidine hydrochloride as reported by the Russian workers, was formed. Addition of water, however, led to a rapid absorption of ethylene.

Discussion

The reaction of cyclohexane with mercuric chloride in "anhydrous" methanol is also very slow.[7] Brandt and Plum[3] have claimed that "very pure ethylene" prepared by the reaction of freshly distilled ethylene dibromide and zinc did not react with aqueous mercuric chloride, and they suggested that the results of Sand and Breest[2] were due to impurities in the ethylene as prepared by their method (from ethanol and concentrated sulfuric acid). The ethylene used in this work certainly contained no detectable impurities and consistent results were obtained. It can only be assumed that the apparatus used by Brandt and Plum was not capable of detecting the uptake of gas under their conditions.

The method for the calculation of equilibrium constants makes no assumption as to the mechanism of the forward or back reactions, the mercuric being considered as in two states either combined with the olefin or not. Thus the results in Table I confirm that the reaction of aqueous mercuric chloride with ethylene is indeed (1) and show that *K'* and *K''* (or *K*) are true thermodynamic equilibrium constants. The values of the heat content and entropy changes are therefore meaningful.

Sand and Breest[2] measured the increase in conductivity of an aqueous solution of mercuric chloride, due to the formation of HCl as the reaction with ethylene proceeded. Unfortunately it is difficult to connect this conductivity change with

(6) R. KR. Freidlina and N. S. Kochetkova, *Bull. Acad. Sci. U.S.S.R. Classe Sci. chim.*, 128 (1945).

(7) A. Rodgman, D. A. Shearer and G. F. Wright, *Can. J. Chem.*, **35**, 1377 (1957).

the equilibrium concentrations of reactants and products and thus their values of K' are not really significant. However, in order to approach the equilibrium position from the opposite direction they reacted an aqueous solution of hydroxyethylmercuric chloride with hydrochloric acid and measured the pressure of ethylene evolved. They incorrectly attempted to allow for the formation of $HgCl_3^-$ ions but it is easy to recalculate K' from their results, the values being 4.4 and 3.5 at 25°, assuming the solubility of ethylene given in Table I. In order, presumably, to simplify matters they used a saturated solution of complex containing excess solid and nearly all the HCl added (~85%) had reacted at equilibrium. Thus their values of K' cannot be very accurate. However, that of 3.5 is probably the better, since the concentration of acid added was double that in the first experiment, and it agrees quite well with the value of K' at 25° in Table I.

Rowland and Kluchesky[8] investigated the reaction of mercuric chloride with allylacetic acid and *o*-allylphenol in aqueous solution. They also took into account the concentrations of $HgCl_3^-$ and $HgCl_4^=$ ions, but recalculation of their few results showed that the value of K''', corresponding to K' and K'', agreed quite well approaching the equilibria from opposite directions, the average constants being 18.6 and 540, respectively, at room temperature. Thus both the mercurials are more stable toward decomposition by hydrochloric acid than those from olefins, the phenol compound being most stable, probably because of its ring structure.

Sand and Breest[2] also found that, as the reaction between ethylene, mercuric chloride and water proceeded to equilibrium, the apparent velocity constant decreased. The reaction is therefore not taking place in the simple way suggested by the stoichiometry. Chatt[1] has given an excellent discussion of the probable mechanisms of the formation and decomposition by acids of addition compounds of mercuric salts and unsaturated compounds. There seems to be a choice between two—one essentially molecular, favored by Wright[9] on the basis of his studies of methoxymercuration in non-aqueous solvents, and the other involving ions, supported by Chatt himself. Applied to mercuric chloride these are

$$HgCl_2 + H_2O \rightleftharpoons HOHgCl + H^+ + Cl^- \quad (1)$$

(A)

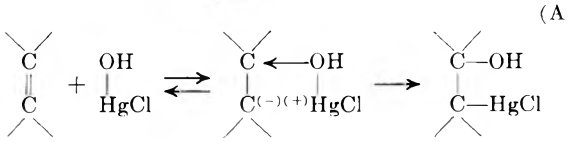

(2)

$$HgCl_2 \rightleftharpoons HgCl^+ + Cl^- \quad (3)$$

(B)

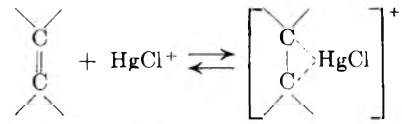

(4)

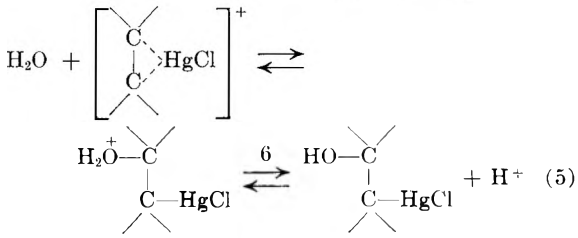

(5)

In a solution of mercuric chloride the relative proportion of positive ions is very small and decreases rapidly to virtually zero as excess chloride is added, $HgCl_3^-$ and $HgCl_4^=$ becoming the main species present.[10] The salt is also hydrolyzed to a slight extent according to equation 1.[10] Thus assuming the velocity constants of reactions 2 or 4 were high, the over-all rate of oxymercuration would be measurable as found experimentally. Also the autoretardation and retardation by added chloride is easily explained on either mechanism as having been due to the effect on the equilibria 1 or 3.

Nevertheless there are several strong objections to the molecular mechanism. For instance mercuric chloride did not react in solution unless water was present, though methoxymercuration by mercuric acetate in dry methanol takes place readily.[9] Despite reduced hydrolysis on the addition of perchloric acid, the rate of reaction with ethylene was not greatly altered. However, the main support for mechanism B is the fact that the system is thermodynamically reversible, which mechanism A is not. Even if it could be modified to correct for this the fact that the back reaction involved hydrogen and chloride ions, since the HCl must have been completely dissociated at such low concentrations, means that the oxymercuration must also have involved ions. The fact that there was a positive entropy change of formation of hydroxyethylmercuric chloride, despite the concurrent formation of hydrated hydrogen ions, suggests that the entropy of hydration of a $HgCl^+$ [or Hg^{++}] ion was being lost during the reaction.

The fact that the strength of the acid was important in the deoxymercuration further supports the ionic mechanism, the first stage being a proton transfer from an H_3O^+ ion to the basic oxygen atom of the non-ionic hydroxyethylmercuric chloride, *i.e.*, the reverse of stage 6. However, the efficiency of the trichloro-acetic acid might be partly accounted for if mercuric trichloroacetate was only weakly dissociated in aqueous solution. Thus perchloric acid although a strong acid was by no means as effective as HCl in decomposing the addition compound, probably because equilibrium 3 was not affected by ClO_4^- ions.

(8) R. L. Rowland and E. F. Kluchesky, *J. Am. Chem. Soc.*, **73**, 5490 (1951).

(9) *E.g.*, A. G. Brook and G. F. Wright, *Can. J. Research*, **B28**, 623 (1950).

(10) M. C. Sneed and R. C. Brasted, "Comprehensive Inorganic Chemistry," Vol. IV, D. Van Nostrand Co., New York, N. Y., 1955.

THE THERMODYNAMICS AND KINETICS OF THE REACTION OF MERCURIC SALTS WITH OLEFINS. PART II. THE REACTION WITH MERCURIC ACETATE AND PERCHLORATE

BY E. R. ALLEN, J. CARTLIDGE, M. M. TAYLOR AND C. F. H. TIPPER

Department of Inorganic and Physical Chemistry, The University, Liverpool, England

Received February 18, 1959

The reaction of aqueous mercuric perchlorate and acetate with ethylene and propylene is too rapid to measure with the apparatus used. Addition of pyridine retards the process. As pyridine is added the rate drops sharply to a minimum value at about two to four moles of pyridine per mole of mercuric salt, and then increases slightly. The fully retarded reaction is of the first order with respect to the mercuric concentration, and the rate increases linearly with ethylene pressure at around atmospheric. It seems probable that in aqueous solution an ionic mechanism similar to scheme B (Part I) is operative, and the retardation by pyridine is due to complex formation between various mercuric species and the base.

Introduction

Some physicochemical studies of oxymercuration by mercuric acetate and perchlorate have been reported. The methoxymercuration of cyclohexene by mercuric acetate in methanol solution is of the second order,[1] as is the deoxymercuration of compounds such as the α-2-methoxycyclohexylmercuric halides by hydrogen halides.[2] Brandt and Plum[3] have measured the very high rates of reaction of ethylene with aqueous mercuric perchlorate and nitrate by following the fall in pressure of the gas at a constant volume. This method does not allow the determination of low rates of reaction and is open to the objection that at low pressures of ethylene it is difficult to be sure that the solution is saturated. However they showed that an equilibrium was attained, though the constant (corresponding to K′, part I) was very high.

In Part I it is suggested that the reaction with mercuric chloride proceeds by an ionic mechanism, and the work described in this part was undertaken with a view to finding whether a similar mechanism was likely for oxymercurations with acetate and perchlorate.

Experimental

The apparatus used to measure the rate of uptake of ethylene or propylene has been described in Part I. The purity and purification of the water, sodium chloride, methanol, perchloric acid, acetic and trichloroacetic acids, nitrogen, ethylene and propylene has been described previously (Part I). Analar pyridine and acetic anhydride were distilled in a stream of nitrogen. Analar sodium acetate, potassium cyanide, ethyl cyanide, ethylamine, acrylonitrate, diethyl sulfide and ethyl hydrogen sulfide were used directly.

Mercuric oxide was precipitated from mercuric chloride solution by Analar sodium hydroxide in the presence of sodium chloride. Solutions of mercuric perchlorate were prepared by dissolving a known weight of or excess HgO in a known amount of perchloric acid (60%). On diluting to the required strength slight precipitation occurred in the absence of excess acid, and the mercury content of the solution was checked from time to time by titration with ammonium thiocyanate. Mercuric acetate was prepared by dissolving HgO in the minimum quantity of glacial acetic acid, or the commercial material was recrystallized from acetic acid. The crystals were filtered off, washed with Analar chloroform and stored over NaOH in a desiccator. The mercury content was determined by precipitation of HgO, dissolving this in nitric acid and titration with ammonium thiocyanate.

Hydroxyethylmercuric Perchlorate.—Two aqueous solutions of known concentrations of this compound were prepared by shaking different amounts of mercuric perchlorate with ethylene. The depressions of the freezing points of the solutions were measured with a Beckmann thermometer in the usual way. Assuming that the perchloric acid formed in equivalent amounts was completely dissociated the Van't Hoff factors for the hydroxyethylmercuric perchlorate were calculated to be 2.05 and 2.1.

Dipyridine-Mercuric Perchlorate.—Excess pyridine was added to a concentrated solution of aqueous mercuric perchlorate. Small needle-like colorless crystals were precipitated. These were filtered, washed with cold water, recrystallized from hot water, filtered and dried *in vacuo*. *Anal.* Calcd. for $C_{10}H_{10}N_2O_8Cl_2Hg$: Hg, 36.0; N, 5.02. Found: Hg, 34.9; N, 5.09. The dipyridine-mercuric perchlorate crystals were probably slightly contaminated with pyridine or pyridine perchlorate.

Results

The reaction of ethylene or propylene with solutions of mercuric acetate or perchlorate was too rapid to be measured with the apparatus used. With aqueous solutions of the two mercuric salts the uptake of gas is about 95% of the theoretical, assuming 1 mole per mole Hg^{++}, with the perchlorate even in the presence of 100-fold excess of perchloric acid. The rate was still not measurable with 0.094 *M* $Hg[OAc]_2$ in the presence of 0.88 *M* acetic acid, but the addition of 0.12 *M* sodium acetate slowed the reaction to a measurable though still high velocity. Solutions of mercuric acetate in dry acetic acid or methanol very rapidly absorbed olefin, but less than the theoretical amount. Addition of pyridine, ethyl cyanide or ethyl hydrogen sulfide did not retard the reaction in acetic acid. However, diethyl sulfide did reduce the rate but also the uptake, while a small amount of potassium cyanide caused complete inhibition. With a 0.012 *M* mercuric acetate solution in a 1:3 v./v. acetic acid–acetic anhydride mixture addition of trichloroacetic acid led to a reduction in uptake of ethylene from the theoretical. However, the amount of gas absorbed did not vary appreciably as the amount of acid was increased, though with the higher acid concentrations a slow evolution of ethylene occurred after equilibrium had apparently been established. Ethyl cyanide, diethyl sulfide, ethylamine and acrylonitrile were ineffective as retarders with mercuric perchlorate, but with aqueous solutions of both acetate and perchlorate addition of enough pyridine decreased the rate to measurable values, the uptake of ethylene or propylene not being appreciably altered, and it was decided to investigate the kinetics of these reactions.

(1) J. Romeyn and G. F. Wright, *J. Am. Chem. Soc.*, **69**, 697 (1947).

(2) O. W. Berg, W. P. Lay, A. Rodgman and G. F. Wright, *Can. J. Chem.*, **36**, 358 (1958).

(3) P. Brandt and O. Plum, *Acta Chem. Scand.*, **7**, 97 (1953).

In the presence of pyridine plots of log $[\Delta V_\infty - \Delta V_t]$ against time were straight lines to about 90% reaction (Fig. 1), ΔV_t and ΔV_∞ being the volumes of olefin absorbed at time t and at the end of the reaction, respectively, both corrected for the solubility of the gas. This means that the process is of the first order with respect to mercuric mercury. Usually the slopes of the lines are fairly reproducible (~10%) under the same conditions. The variation of the rate, represented by this slope, with the relative amounts of pyridine and mercuric salt is shown in Figs. 2 and 3. With mercuric acetate and ratios of pyridine to salt of around 2 and between 4 and 7 the results were erratic (Fig. 3). Whatever the reason for this it does not affect the general shape of the curves. As pyridine was added to the aqueous solution of mercuric salt the rate, which was very high, dropped rapidly to a shallow minimum, increasing again somewhat when a considerable excess of pyridine was present. Despite the general similarity between the curves in Figs. 2 and 3 there are significant differences in detail. With the perchlorate the decrease in rate to the minimum as the pyridine concentration was increased from zero was very sharp, much more so than with the acetate. However, this minimum rate was considerably smaller when the perchlorate solution did not contain excess perchloric acid, *i.e.*, the ratio ClO_4^-: Hg^{++} was 2 (curves b and e), or when the mercuric concentration was the highest used (curve a). In this case addition of pyridine caused a precipitation of the complex dipyridine–mercuric perchlorate, which, however, disappeared during the uptake of ethylene. Also the minimum rate occurred at different ratios pyridine: Hg^{++} depending on the amount of excess acid in the aqueous perchlorate. With propylene a precipitate presumably the addition compound was formed, if the amount of pyridine present was less than 3 times that of the mercuric perchlorate.

There appeared to be a linear variation of rate with ethylene pressure, and thus probably with ethylene concentration in the solution, both with aqueous acetate and perchlorate, although with the former the points are somewhat scattered (Fig. 4). However, the lines do not pass through the origin, and presumably the rate of reaction depended on a power of the ethylene concentration of greater than one at low pressures.

At 25° in the presence of 0.043 *M* NaCl the absorption of ethylene by a 0.024 *M* solution of mercuric perchlorate took place at a measurable speed and only 0.0156 mole of gas was taken up per l. of solution. The presence of 0.086 *M* NaCl inhibited the reaction completely. With 0.032 *M* perchlorate containing 0.096 *M* pyridine addition of 0.0079 *M* NaCl had no effect on the total uptake of ethylene (0.031 mole l. soln.), but addition of 0.030 *M* NaCl caused complete inhibition.

Attempts were made to isolate the addition compounds from mercuric perchlorate and ethylene in aqueous solution in the presence and absence of pyridine, but without success, gums being produced. However, if the reaction in the absence of pyridine was similar to that with mercuric chloride, *i.e.*, hydroxyethylmercuric perchlorate was formed,

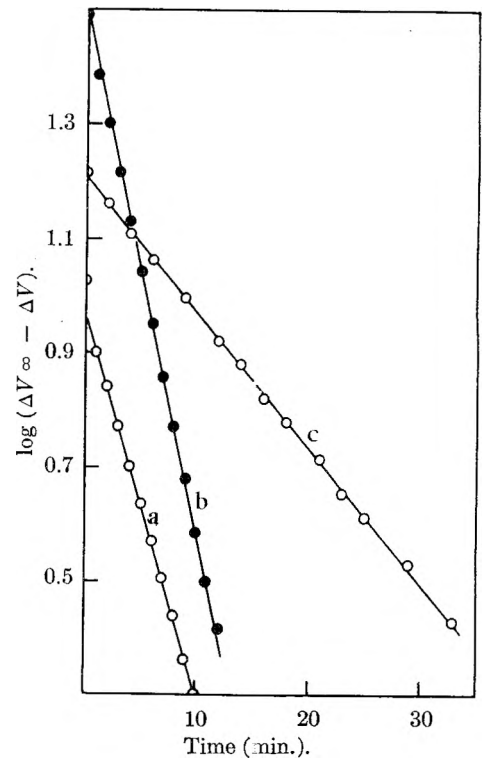

Fig. 1.—First-order plots of oxymercuration of ethylene in aqueous solution in the presence of pyridine; temp. 25.0°. (a) 20 ml. of 0.024 *M* mercuric perchlorate (ratio ClO_4^- to Hg^{++}, 3.4) + 0.11 *M* pyridine; (b) 20 ml. of 0.071 *M* mercuric acetate + 1.25 *M* pyridine; (c) 25 ml. of 0.026 *M* mercuric perchlorate (ratio ClO_4^- to Hg^{++}, 2.02) + 0.51 *M* pyridine.

then the depression of the freezing point of its aqueous solution indicated that it was completely dissociated as would be expected. Addition of pyridine to a concentrated perchlorate solution yielded crystals of $Hg[ClO_4]_2 \cdot 2C_5H_5N$. This complex did not melt up to 300°, showing its ionic character and was stable *in vacuo*.

Discussion

It seems necessary to postulate an ionic mechanism for the reaction of olefins with aqueous mercuric perchlorate since the salt is completely dissociated at low concentrations. This would account for the very high rate. Brandt and Plum[3] suggested a mechanism similar to scheme B (Part I), the mercuric species being $Hg^{++} \cdot 2H_2O$ since excess perchloric acid was present to prevent hydrolysis. They were able to reverse the reaction to a slight extent, but this must only occur under very acid conditions since it is necessary to transfer a proton to a positive ion.

Wright and his co-workers[4] have extensively investigated the oxymercuration of such compounds as cyclohexene by mercuric acetate mainly in methanol solution, and consider that a molecular mechanism similar to A (Part I) is operative. In aqueous solution mercuric acetate certainly hydrolyzes to a slight extent. However if the first step in the oxymercuration was

$$Hg[OAc]_2 + H_2O \rightleftarrows HOHgOAc + HOAc$$

(4) *E.g.*, A. G. Brook and G. F. Wright, *Can. J. Research*, **B28**, 623 (1950).

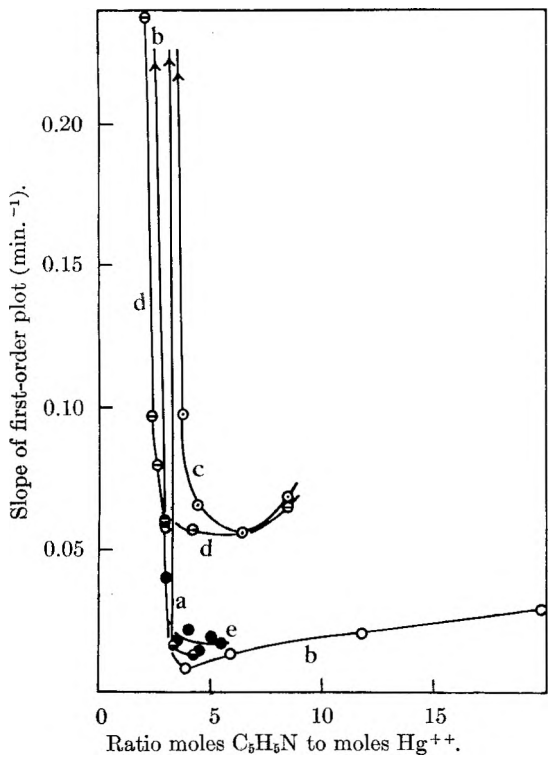

Fig. 2.—Variation of the rate of oxymercuration by aqueous mercuric perchlorate with amount of pyridine added; temp. 25.0°. Ethylene: (a) 0.074 *M* mercuric; ratio ClO_4^- to Hg^{++}, 3.35; to 0.42 min.$^{-1}$ at ratio of 3.0; (b) 0.026 *M* mercuric; ratio ClO_4^- to Hg^{++}, 2.02; to 0.73 min.$^{-1}$ at ratio of 2.0; (c) 0.025 *M* mercuric; ratio ClO_4^- to Hg^{++}, 3.39; to 0.96 min.$^{-1}$ at ratio of 3.0; (d) 0.0375 *M* mercuric; ratio ClO_4^- to Hg^{++}, 2.15. Propylene: (e) 0.026 *M* mercuric; ratio ClO_4^- to Hg^{++}, 2.01.

rather than

$$Hg[OAc]_2 \rightleftharpoons HgOAc^+ + OAc^-$$

then the rate of reaction with ethylene should be reduced by the addition of acetic acid, but not by the addition of sodium acetate. The reverse was actually the case, supporting the ionic mechanism with water as the solvent. The results of Wright, *et al.*,[2,4,5] do, however, give strong support to the molecular mechanism for oxymercuration and deoxymercuration by acids in non-aqueous solvents. In glacial acetic acid the reaction with ethylene is very rapid giving $AcOC_2H_4HgOAc$ quantitatively,[6] although it is likely that the ionization of mercuric acetate is not important. The results on the effect of trichloroacetic acid on the reaction in acetic acid–acetic anhydride mixtures indicate that it appeared to be reversible under these conditions, but not in the strict thermodynamic sense.

The retardation of oxymercurations by organic bases and sulfur compounds has been noted previously,[7] and indeed might be expected since many complexes of mercuric salts with these substances are known. As far as can be ascertained the complex dipyridine–mercuric perchlorate has not been

(5) A. Rodgman, D. A. Shearer and G. F. Wright, *Can. J. Chem.*, **35**, 1377 (1957).

(6) G. Hugel and J. Hibou, *Chemie e Ind.* Special No. 296 (1929); *C. A.*, **23**, 3899 (1929).

(7) J. Chatt, *Chem. Revs.*, **48**, 7 (1951).

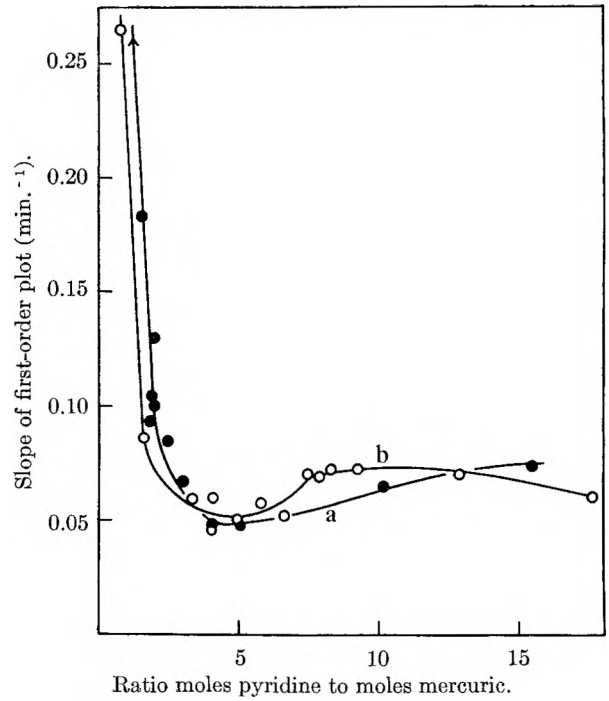

Fig. 3.—Variation of the rate of oxymercuration by aqueous mercuric acetate with amount of pyridine added; temp. 25.0°. (a) 0.035 *M* $Hg[OAc]_2$; (b) 0.071 *M* $Hg[OAc]_2$.

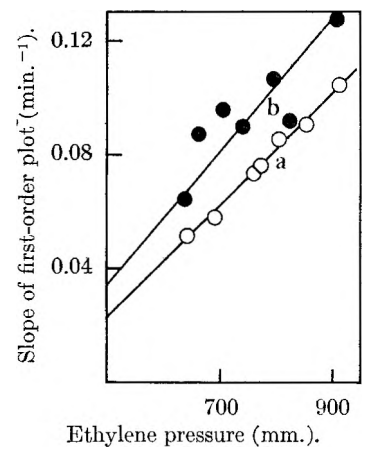

Fig. 4.—Variation of the rate of oxymercuration in aqueous solution in the presence of pyridine with the pressure of ethylene; temp. 25.0°. (b) 0.071 *M* mercuric acetate + 0.92 *M* pyridine; (a) 0.0375 *M* mercuric perchlorate (ratio ClO_4^- to Hg^{++}, 3.4) + 0.13 *M* pyridine (ord. − 0.02).

previously prepared, though similar ones *e.g.*, $Hg[NO_3]_2 \cdot 2C_5H_5N$ have been reported.[8] Although the over-all reactions occurring in the retarded oxymercurations are not completely clear, the results do allow a probable mechanism to be put forward. The kinetics are somewhat more complicated than for the unretarded oxymercurations.[1,3] In the experiments with aqueous mercuric perchlorate containing excess acid, if it is assumed that part of the pyridine added was removed by this excess, then the minimum in the rate occurred at a pyridine/mercuric ratio of about two. Since the minimum rates were about the same with the

(8) R. H. Wiley, J. L. Hartman and E. L. De Young, *J. Am. Chem. Soc.*, **74**, 3452 (1952).

acetate and the more dilute solutions of perchlorate, it is unlikely that a molecular mechanism was operative. It is more probable that the pyridine removed mercuric or $HgOAc^+$ ions as $Hg[C_5H_5N]_2^{++}$ *e.g.*

$$Hg^{++} + 2C_5H_5N \rightleftharpoons Hg[C_5H_5N]_2^{++}$$

$$K = \frac{(Hg[C_5H_5N]_2^{++})}{[Hg^{++}][C_5H_5N]^2}$$

If the free mercuric ion only took part in the oxymercuration, the rate of which was proportional to $[Hg^{++}] = [Hg[C_5H_5N]_2^{++})/K[C_5H_5N]^2$, then the retarded reaction would not have been of the first order with respect to mercuric over the whole range of pyridine/mercuric ratios and the rate constant would have fallen continuously with added pyridine. Thus it must be assumed that the complex ion $Hg[C_5H_5N]_2^{++}$ reacted slowly with the olefin, *e.g.*

$$Hg[C_5H_5N]_2^{++} + C_2H_4 + H_2O = HOC_2H_4Hg^+ + C_5H_5NH^+ + C_5H_5N$$

The slower fall in rate constant toward a minimum value with the acetate may have been due to the fact that the salt is only partly dissociated in solution. With solutions of mercuric perchlorate, which did not contain excess acid originally, however, the minimum rate was not only much smaller but also occurred at a higher relative concentration of base. Hydrolysis of mercuric ions occurs in perchlorate solutions in the absence of excess acid,[9] the main species formed being $Hg[OH]_2$ and the relative amount of $HgOH^+$ at equilibrium being small, and the addition of ammonia to dilute mercuric perchlorate gives a pale yellow precipitate of a basic complex of indefinite composition, *i.e.*, xHgO·$[1 - x](Hg[ClO_4]_2 \cdot 2NH_3)$.[10] Thus with pyridine it is probable that a similar basic complex was formed and reacted more slowly with the olefins than $Hg[C_5H_5N]_2^{++}$ did. The complete complex formation in this case must have required a higher relative concentration of pyridine. The increase in rate at high pyridine concentrations was probably due to the increased solubility of the olefin in the pyridine–water mixtures.

(9) S. Hietanen and L. G. Sillen, *Acta. Chem. Scand.*, **6**, 747 (1952).
(10) H. T. S. Britton and R. M. Wilson, *J. Chem. Soc.*, 1045 (1933).

THE HEAT CAPACITIES OF YTTRIUM OXIDE (Y_2O_3), LANTHANUM OXIDE (La_2O_3) AND NEODYMIUM OXIDE (Nd_2O_3) FROM 16 TO 300°K.[1]

BY HAROLD W. GOLDSTEIN, E. F. NEILSON, PATRICK N. WALSH AND DAVID WHITE

Contribution of the Cryogenic Laboratory, Department of Chemistry, The Ohio State University, Columbus, Ohio

Received February 19, 1959

The heat capacities of the sesquioxides of yttrium, lanthanum and neodymium have been determined in the temperature range 16 to 300°K. The entropies, enthalpies and free energy functions have been calculated from the heat capacity data and are tabulated for several temperatures. Yttrium oxide and lanthanum oxide exhibit typical sigmoidal heat capacity curves with no anomalies in the temperature range studied. The shape of the heat capacity curve for neodymium oxide is similar except that at the lowest temperature there is evidence for the existence of an anomaly. At 298.16°K. the entropies are 23.693 ± 0.07 and 30.580 ± 0.07 cal. mole^{-1} deg.$^{-1}$ for yttrium oxide and lanthanum oxide, respectively. For neodymium oxide $S_{298.16} - S_{16}$ is 33.607 cal. mole^{-1} deg.$^{-1}$. The free energy functions have been extended to 2500°K. by the use of some higher temperature heat capacity data available in the literature.

Introduction

The present study is part of a series of investigations being carried out in this Laboratory dealing with the thermodynamic properties of some rare earth oxides. Yttrium oxide has been included in these studies because of its similarity to these compounds.

The heat capacities of many of the rare earth oxides can be expected to exhibit anomalies that are presumably related to their magnetic behavior. The magnetic properties of many salts of the rare earth metals have been investigated[2] and these properties correlated with the electronic structure of the rare earth ions. Because of the structural similarity of the rare earth oxides, and the relatively small variations in molecular weight and lattice dimensions in this series[3] it seems reasonable to assume that the lattice heat capacities of all these compounds will be very similar, and that the major differences will be due to the magnetic contributions associated with the degenerate ground states of the lanthanide ions.

The total heat capacity of lanthanum oxide should be due entirely to lattice vibrations, as the La^{+3} ion has a $^1S_0$ ground state. Hence, the heat capacity of La_2O_3 may be used as an approximation for the lattice contribution to the heat capacities of the other rare earth oxides. Addition of the magnetic contribution characteristic of any other member of the series should yield a reasonable estimate for the total heat capacity of that oxide.

Of course, not all of the entropy, $R \ln (2J + 1)$, associated with the ground state degeneracy, will necessarily be developed at any given temperature. It was of interest, therefore, to study the heat capacity of neodymium oxide to determine the fraction of the magnetic entropy, resulting from the $^4I_{9/2}$ ground state, that is developed at room temperature.

Apparatus and Procedure

The equipment employed in this research and the procedure for the heat capacity measurements have been de-

(1) This work was supported by the Air Force Office of Scientific Research, Washington, D. C.
(2) J. H. Van Vleck, "The Theory of Electric and Magnetic Susceptibilities," Oxford University Press, London, 1932.
(3) W. Zachariasen, *Z. physik. Chem.*, **123**, 134 (1926).

scribed by Johnston and Kerr.[4] The temperatures reported are based on a thermodynamic temperature scale established by Rubin, Johnston and Altman.[5]

For all the rare earth heat capacity measurements, calorimeter "No. 3" was used. It is one of a group of seven calorimeters of identical design in use in this Laboratory. Although the calorimeter had been calibrated previously over the temperature range 16 to 300°K., the calibration was rechecked, before and after use, over the entire temperature range.

Immediately before filling the calorimeter, the samples were heated to constant weight in a platinum dish at 950° in air, to decompose any hydroxide or carbonate present. The transfer of the sample to the calorimeter was carried out in a dry box with a helium atmosphere. After the heat capacity measurements were completed the calorimeter was emptied in the dry box. Portions of the sample were taken from the top, middle and bottom of the calorimeter and heated to determine whether any contamination occurred during handling. In all cases these samples showed no weight change upon being heated for 24 hours at 950° in air.

Materials

Y_2O_3.—The yttrium oxide, obtained from the Lindsay Chemical Company, West Chicago, Illinois, had a reported purity of greater than 99.9%. Analysis of the sample showed these impurities: Gd_2O_3, less than 0.01%; Dy_2O_3, less than 0.01%; and Ho_2O_3, less than 0.02%.[6] A powder X-ray pattern of the heat treated material showed only the cubic, Mn_2O_3 type, sesquioxide structure.[7]

La_2O_3.—The lanthanum oxide, obtained from the Lindsay Chemical Company, had a reported purity of 99.997%. Analysis of the sample showed only 1.5 p.p.m. of Fe_2O_3 as impurity.[6] A powder X-ray pattern of the heat-treated material showed only the A-form sesquioxide structure.[6]

Nd_2O_3.—The neodymium oxide, obtained from the Lindsay Chemical Company, had a reported purity of 99.9%. Analysis of the sample showed as impurities: Pr_6O_{11}, less than 0.1%; Sm_2O_3, less than 0.1%.[6] A powder X-ray pattern of the heat-treated material showed only the A-form sesquioxide structure.[8]

Experimental Results

The heat capacity measurements were made using 60.8680 g. (0.26952 mole) of yttrium oxide, 98.9526 g. (0.30368 mole) of lanthanum oxide and 97.9633 g. (0.29109 mole) of neodymium oxide. The molecular weights were taken as 225.84, 325.84 and 336.54, respectively. The experimental heat capacities, expressed in terms of the defined thermochemical calorie, equal to 4.1840 absolute joules, are listed in Tables I, III and V. Values of the heat capacities at selected temperatures, read from smooth curves through the experimental points, together with derived thermodynamic functions, are given in Tables II, IV and VI, for yttrium oxide, lanthanum oxide and neodymium oxide, respectively. As evidence exists for an anomaly in the specific heat curve of neodymium oxide below 16°K., thermodynamic functions for this substance are given relative to 16°K.

The entropy of yttrium oxide at 298.16°K. is 23.693 cal. mole^{-1} deg.$^{-1}$, of which 0.112 cal. mole^{-1} deg.$^{-1}$ is contributed by extrapolation below 16°K. A Debye θ of 178 degrees, estimated from the lowest temperature heat capacities, was used for the extrapolation. The uncertainty in the entropy is estimated to be ± 0.07 cal. mole^{-1} deg.$^{-1}$, of which ± 0.02 cal. mole^{-1} deg.$^{-1}$ is due to the extrapolation

(4) H. L. Johnston and E. C. Kerr, *J. Am. Chem. Soc.*, **72**, 4733 (1950).

(5) T. Rubin, H. L. Johnston and H. Altman, *ibid.*, **73**, 3401 (1951).

(6) Analyses supplied by Lindsay Chemical Co.

(7) H. W. Swanson, R. K. Fuyat and G. M. Ugrinic, Natl. Bur. Standards Circ. 539, III, IV, 1953.

(8) T. M. Douglass, *Anal. Chem.*, **28**, 551 (1956).

TABLE I

HEAT CAPACITY OF YTTRIUM OXIDE

Mean T, °K.	C_p, cal. mole^{-1} deg.$^{-1}$	Mean T, °K.	C_p, cal. mole^{-1} deg.$^{-1}$
15.96	0.345	131.89	13.02
18.37	.367	138.96	13.85
20.45	.401	146.21	14.64
21.63	.453	153.27	15.39
23.87	.527	160.92	16.13
26.01	.583	166.50	16.64
30.85	.801	173.02	17.28
33.86	1.098	176.95	17.52
36.67	1.417	184.37	18.21
40.93	1.855	186.58	18.41
44.34	2.145	193.37	18.91
47.86	2.512	200.19	19.52
52.15	2.931	207.07	19.97
56.33	3.536	212.86	20.27
65.78	4.753	214.27	20.30
70.75	5.391	219.22	20.63
76.13	6.011	225.62	20.93
80.83	6.653	232.05	21.29
81.81	6.782	238.41	21.67
91.08	8.014	240.33	21.78
93.81	8.300	246.77	22.10
97.02	8.798	253.61	22.48
100.06	9.179	263.59	23.06
102.83	9.547	266.48	23.05
106.21	9.914	276.56	23.57
108.42	10.23	279.94	23.83
112.44	10.74	283.31	23.87
118.75	11.57	292.36	24.41
125.23	12.33	298.26	24.48

TABLE II

THERMODYNAMIC FUNCTIONS FOR YTTRIUM OXIDE

Temp., °K.	C_p, cal. mole^{-1} deg.$^{-1}$	S°, cal. mole^{-1} deg.$^{-1}$	$H^\circ - H_0^\circ$, cal. mole^{-1}	$-(F^\circ - H_0^\circ)/T$, cal. mole^{-1} deg.$^{-1}$
16	0.323	0.1120	1.342	0.02812
20	.405	.1928	2.796	.05300
30	.777	.4120	8.320	.1347
40	1.717	.7575	20.56	.2436
50	2.796	1.255	43.06	.3941
60	3.966	1.867	76.77	.5873
70	5.236	2.572	122.71	.8194
80	6.545	3.357	181.61	1.0867
90	7.854	4.204	252.88	1.3937
100	9.152	5.098	338.66	1.7117
120	11.66	6.991	547.07	2.4324
140	13.96	8.965	803.70	3.2240
160	16.03	10.966	1103.9	4.0666
180	17.86	12.963	1443.3	4.9443
200	19.37	14.925	1816.1	5.8447
220	20.64	16.833	2216.6	6.7573
240	21.75	18.677	2640.6	7.6742
260	22.77	20.459	3086.1	8.5895
280	23.70	22.181	3550.9	9.4992
298.16	24.50	23.693	3989.3	10.313
300	24.58	23.846	4033.7	10.400

below 16°K. The entropy of lanthanum oxide at 298.16°K. is 30.580 cal. mole^{-1} deg.$^{-1}$, of which 0.1535 cal. mole^{-1} deg.$^{-1}$ is contributed by extrapolation between 16°K., using a Debye θ of 160 degrees. The uncertainty in the entropy is estimated to be ± 0.07 cal. mole^{-1} deg.$^{-1}$, of which ± 0.02 cal.

TABLE III

HEAT CAPACITY OF LANTHANUM OXIDE

Mean T, °K.	C_p, cal. mole^{-1} deg.$^{-1}$	Mean T, °K.	C_p, cal. mole^{-1} deg.$^{-1}$
16.91	0.501	129.89	16.376
19.55	0.850	136.43	17.110
21.27	1.067	142.67	17.647
23.35	1.278	148.65	18.200
25.36	1.469	155.04	18.661
27.78	1.870	166.03	19.534
30.39	2.111	171.57	20.070
33.12	2.552	177.35	20.364
36.13	3.184	183.07	20.680
39.73	3.764	188.81	21.236
43.95	4.357	201.66	21.967
48.52	5.071	215.03	22.675
53.73	6.187	221.90	23.123
58.49	6.991	228.54	23.330
69.81	8.683	235.16	23.633
75.77	9.681	241.61	23.910
82.12	10.475	254.11	24.529
88.71	11.450	260.07	24.687
92.13	11.930	272.36	25.066
98.17	12.668	279.79	25.277
104.46	13.488	287.18	25.395
110.89	14.239	294.27	25.662
117.22	14.980	300.30	25.649
123.45	15.757		

TABLE IV

THERMODYNAMIC FUNCTIONS FOR LANTHANUM OXIDE

T, °K.	C_p, cal. mole^{-1} deg.$^{-1}$	S°, cal. mole^{-1} deg.$^{-1}$	$H^\circ - H_0^\circ$, cal. mole^{-1}	$-(F^\circ - H_0^\circ)/T$, cal. mole^{-1} deg.$^{-1}$
16	0.526	0.1535	1.838	0.03862
20	0.860	.3049	4.576	.07610
30	2.094	.8713	18.600	.2513
40	3.742	1.6920	47.525	.5039
50	5.480	2.7143	93.662	.8411
60	7.135	3.8612	156.82	1.2475
70	8.697	5.0794	236.05	1.7073
80	10.18	6.3390	330.54	2.2072
90	11.60	7.6209	439.51	2.7375
100	12.94	8.9131	562.28	3.2903
120	15.35	11.491	845.79	4.4427
140	17.39	14.016	1173.9	5.6310
160	19.08	16.451	1539.0	6.8322
180	20.57	18.787	1935.9	8.0320
200	21.86	21.022	2360.6	9.2190
220	22.91	23.157	2808.7	10.390
240	23.83	25.191	3276.3	11.540
260	24.61	27.130	3761.0	12.665
280	25.27	28.979	4260.0	13.765
298.16	25.79	30.580	4724.2	14.735
300	25.84	30.742	4771.2	14.838

mole^{-1} deg.$^{-1}$ is due to the extrapolation below 16°K. For neodymium oxide, $S_{298.16} - S_{16}$ is 33.607 cal. mole^{-1} deg.$^{-1}$.

Discussion

Yttrium oxide and lanthanum oxide show typical sigmoidal variations with temperature and exhibit no anomalies in the temperature range studied. The heat capacity of lanthanum oxide, however, at any given temperature, is greater than that of yttrium oxide. Although yttrium oxide is classified with the rare earth oxides, its heat capacity can be expected to be considerably lower than that of lanthanum oxide, owing to the large difference in molecular weight, if one assumes the heat capacity to result only from lattice vibrations. This is not the case when one compares the rare earth oxides, neodymia and lanthana. Due to the small difference in mass of these compounds and the similarity of

TABLE V

HEAT CAPACITY OF NEODYMIUM OXIDE

Mean T, °K.	C_p, cal. mole^{-1} deg.$^{-1}$	Mean T, °K.	C_p, cal. mole^{-1} deg.$^{-1}$
18.26	2.209	96.86	13.202
20.28	2.422	103.38	14.126
22.34	2.673	109.57	14.882
24.27	2.889	115.67	15.610
26.05	3.106	121.88	16.394
27.78	3.308	128.14	16.998
29.43	3.542	134.41	17.589
31.37	3.755	141.00	18.218
33.43	4.064	147.30	18.819
35.71	4.384	161.32	20.017
36.94	4.689	167.68	20.440
37.70	4.785	173.97	20.935
39.43	5.105	180.27	21.354
40.25	5.239	186.97	21.866
42.46	5.586	193.54	22.316
42.86	5.644	200.02	22.590
45.58	5.929	206.45	23.007
48.91	6.421	212.45	23.302
52.63	7.036	222.88	23.742
55.47	7.541	229.88	24.195
56.72	7.750	236.50	24.467
60.47	8.221	243.29	24.728
60.97	8.351	250.12	24.834
65.67	9.004	263.43	25.401
72.70	10.083	277.60	25.910
78.53	10.801	284.76	26.205
84.78	11.711	291.49	26.390
90.89	12.625	298.13	26.401

TABLE VI

THERMODYNAMIC FUNCTIONS FOR NEODYMIUM OXIDE

T, °K.	C_p, cal. mole^{-1} deg.$^{-1}$	$S_T - S_{16}$, cal. mole^{-1} deg.$^{-1}$	$H_T - H_{16}$, cal. mole^{-1}	$-(F_T - H_{16})/T$, cal. mole^{-1} deg.$^{-1}$
16	1.988			
20	2.394	0.4863	8.748	0.04890
30	3.619	1.6785	38.563	.3931
40	5.105	2.9186	82.024	.8680
50	6.680	4.2271	140.95	1.4081
60	8.202	5.5805	215.42	1.9902
70	9.666	6.9556	304.82	2.6010
80	11.07	8.3382	408.51	3.2318
90	12.44	9.7216	526.09	3.8762
100	13.74	11.100	657.06	4.5294
120	16.10	13.819	955.99	5.8524
140	18.14	16.458	1298.9	7.1801
160	19.88	18.997	1679.6	8.4995
180	21.37	21.426	2092.4	9.8016
200	22.65	23.746	2533.0	11.081
220	23.72	25.957	2997.0	12.334
240	24.58	28.058	3480.3	13.557
260	25.32	30.056	3979.4	14.751
280	26.01	31.958	4492.8	15.912
298.16	26.59	33.607	4970.9	16.935
300	26.65	33.774	5019.4	17.043

their crystal structures,[3] one should expect their lattice heat capacities to be nearly equal. The greater heat capacity exhibited by neodymium oxide at any given temperature can therefore be attributed to a magnetic effect associated with the presence of Nd^{+3} ions in the lattice. This is consistent with the observed paramagnetism of many salts of neodymium.[2]

Blomeke and Ziegler[9] have determined the heat capacities of neodymium oxide and lanthanum oxide between 30 and 900°. Their results suggest that even at the highest temperatures there is still a considerable magnetic contribution to the heat capacity of neodymium oxide.

Assuming that the lattice heat capacity of neodymium oxide is identical with that of lanthanum oxide, the magnetic contribution can be obtained by comparing the heat capacity differences at any temperature. This magnetic heat capacity is shown in Table VII. Unfortunately there exists no spec-

TABLE VII

MAGNETIC HEAT CAPACITY OF NEODYMIUM OXIDE

T, °K.	C_p, cal. mole^{-1} deg.$^{-1}$	T, °K.	C_p, cal. mole^{-1} deg.$^{-1}$
16	1.46	220	0.81
20	1.53	240	.75
30	1.53	260	.71
40	1.36	280	.74
50	1.20	300	.78
60	1.07	400	.81
70	0.97	500	1.12
80	.89	600	1.49
90	.84	700	1.83
100	.80	800	2.14
120	.75	900	2.43
140	.75	1000	2.72
160	.80	1100	3.02
180	.80	1200	3.29
200	.79		

troscopic data for neodymium oxide which can be used to compute the magnetic heat capacity. The absorption spectrum of the salt $Nd_2(SO_4)_3 \cdot 8H_2O$ has been observed by Spedding, Hamlin and Nutting.[10] Although the two observed electronic levels, 77 and 260 cm.$^{-1}$, are in agreement with the heat capacity data[11] (assuming the ground state of the Nd^{+3} ion is $^4I_{9/2}$) the situation in neodymium oxide can be expected to be considerably different. Not only are the electric fields in these two crystals quite different but the closer proximity of the Nd^{+3} ions in the oxide could give rise to large magnetic interactions at temperatures considerably above absolute zero. This might result in an increase in the heat capacity, as suggested by our data at the lowest temperatures.

If the ground state of the Nd^{+3} ion is $^4I_{9/2}$, then the magnetic entropy of neodymium oxide at high temperature is 9.16 cal. mole^{-1} deg.$^{-1}$. From the experimental data it is found that the magnetic contribution to the entropy between 16 and 298.16°K. is 3.17 cal. mole^{-1} deg.$^{-1}$. (The lattice entropy is assumed equal to that of lanthanum oxide.) Not only is this a small fraction of the total possible magnetic entropy but it is considerably less than the spin-only value ($2R \ln (2S + 1) = 5.50$ cal. mole^{-1} deg.$^{-1}$). The absolute magnetic entropy, however, may be considerably larger than 3.17 cal. mole^{-1} deg.$^{-1}$ when the entropy below 16°K. is taken into account.

In order to establish a reasonable estimate for the absolute entropy of neodymium oxide at 298.16°K., a comparison with the actinides has been made. In neptunium dioxide (possible ground state $^4I_{9/2}$) it has been found that the spin-only value of the magnetic entropy is attained at 95°K.[12] In uranium dioxide (possible ground state $^3H_4$) the spin-only value is attained at 73°K.[12] As a first approximation, it has been assumed that for neodymium oxide, ground state $^4I_{9/2}$, the spin-only value of the magnetic entropy is attained at 100°K. Combining this with the lattice contribution, the entropy of lanthanum oxide at this temperature, one obtains a value for the absolute entropy of neodymium oxide at 100°K. of 14.413 cal. mole^{-1} deg.$^{-1}$, which, when combined with the increase in the entropy between 100 and 298.16°K. calculated from the experimental data, gives 36.92 cal. mole^{-1} deg.$^{-1}$ for the entropy at 298.16°K.

The entropies and free energy functions of yttrium oxide, lanthanum oxide and neodymium oxide from 298.16 to 2500°K. are given in Table VIII. In the case of lanthanum oxide, these thermal functions were computed from the results of this research and that of Blomeke and Ziegler,[9] extrapolated to 2500°K. As no high temperature heat capacities have been reported for yttrium oxide, the low temperature data were extrapolated on the assumption that the temperature dependence of the heat capacity above 300°K. is identical with that of lanthanum oxide. In the case of neodymium oxide, a simple extrapolation cannot be employed to obtain the thermal functions at high temperatures. This is evident when one examines the data in Table VII. At the higher temperatures, it appears that a magnetic anomaly, possibly attributable to excitation to the $^4I_{11/2}$ state, may be developing. Although there is no information on the energy difference between the $^4I_{9/2}$ and the $^4I_{11/2}$ states of Nd^{+++} in crystalline Nd_2O_3, a value of 0.2 e.v. was assumed in order to estimate the heat capacity at 2500°K. (This is approximately the value found for dilute salts[13] and dilute solutions[14] of Nd^{+++} and should be considered only a first approximation.) Assuming the lattice heat capacity at 2500°K. to be that of La_2O_3, one finds the heat capacity of Nd_2O_3 at this temperature to be 37.00 cal. mole^{-1} deg.$^{-1}$. For the calculation of the thermal functions of Nd_2O_3 between 1200°K., the limit of the Blomeke and Ziegler data, and 2500°K., an arbitrary smooth curve was drawn linking the heat capacity data of the former with the value calculated at 2500°K., such that the heat capacities at 1500, 1800 and 2000°K. were 36.71, 36.89 and 36.85 cal. mole^{-1} deg.$^{-1}$, respectively.

(9) J. O. Blomeke and W. T. Ziegler, *J. Am. Chem. Soc.*, **73**, 5099 (1951).

(10) F. H. Spedding, H. F. Hamlin and G. C. Nutting, *J. Chem. Phys.*, **5**, 191 (1937).

(11) J. E. Ahlberg, E. R. Blanchard and W. O. Lundberg, *ibid.*, **5**, 552 (1937).

(12) D. W. Osborne and E. F. Westrum, Jr., *ibid.*, **21**, 1884 (1953).

(13) W. G. Penny and R. Schalpp, *Phys. Rev.*, **41**, 202 (1932).

(14) S. P. Keller and G. D. Pettit, *J. Chem. Phys.*, **30**, 434 (1959).

TABLE VIII

HIGH TEMPERATURE ENTROPIES AND FREE ENERGY FUNCTIONS

	Y_2O_3		La_2O_3		Nd_2O_3	
Temp., °K.	$S°$, cal. mole^{-1} deg.$^{-1}$	$-(F° - H_0°)/T$, cal. mole^{-1} deg.$^{-1}$	$S°$, cal. mole^{-1} deg.$^{-1}$	$-(F° - H_0°)/T$, cal. mole^{-1} deg.$^{-1}$	$S°$, cal. mole^{-1} deg.$^{-1}$	$-(F° - H_0°)/T$, cal. mole^{-1} deg.$^{-1}$
298.16	23.69	10.31	30.58	14.74	36.92	20.21
500	37.98	18.75	45.02	24.39	51.44	30.16
1000	59.04	34.15	66.08	40.49	73.80	46.94
1500	72.18	44.76	79.22	51.33	88.26	58.44
2000	82.00	52.89	89.04	59.58	98.86	67.28
2500	89.97	59.52	97.01	66.28	107.08	74 45

Acknowledgments.—The authors wish to acknowledge the assistance of Mr. Donald Flynn in some of the experiments and of Mr. John Farnham in carrying out preliminary measurements.

RADIOLYSIS OF METHANOL AND METHANOLIC SOLUTIONS BY Co^{60} γ-RAYS AND 1.95×10^6 VOLT VAN DE GRAAFF ELECTRONS[1]

BY NORMAN N. LICHTIN[2]

Contribution from the Department of Chemistry, Brookhaven National Laboratory, Upton, N. Y.

Received February 19, 1959

Yields of hydrogen, formaldehyde, ethylene glycol (determined by means of an improved procedure), methane and carbon monoxide per 100 e.v. of absorbed radiation obtained on irradiation of methanol are compared with values reported in the literature. The several sets of data are not in good agreement with each other. Initial study of the effects of several solutes suggests a variety of modes of intervention in the radiolytic process.

The radiolysis of methanol and methanolic solutions has been the subject of an increasing number of investigations.[3] Two recent reports[4,5] dealing with the action of Co^{60} γ-rays on pure dry methanol and on a variety of solutions in this solvent include extensive discussions of the mechanisms of the radiolytic processes. These two reports are not in good agreement with each other or with earlier work[3c] with respect to the *G*-yields of the principal products[3b] of radiolysis of pure methanol, H_2, CH_4, CO, CH_2O and $HOCH_2CH_2OH$, nor as to the effect of small amounts of water. Although the work described below does not provide a basis for mechanistic interpretation, it presents additional extensive data on the radiolysis of pure methanol. These data are not in complete accord with any one of the previously published reports.

The results of a preliminary survey of the yields of the five principal products obtained on radiolysis of solutions containing a wide variety of solutes are also reported and discussed.

Experimental

Methanol.—Mallinckrodt AR anhydrous grade material was employed. This was generally subjected to rectification by means of a 50 theoretical plate glass-helix packed column protected from atmospheric moisture; the first third of the distillate routinely was discarded. (The methanol employed in half of the Van de Graaff runs was not rectified. No systematic difference in results distinguished these runs from the other experiments.) Eastman 99.9% "Grignard Grade" magnesium (1 to 2 g./100 ml. methanol) was added and the flask containing the methanol then was attached *via* a ⅌ joint to a manifold used in drying and degassing the methanol and filling the radiation cells. After dissolution of the magnesium was complete, the methanolic $Mg(OCH_3)_2$ was refluxed for a minimum of three hours. Tubes containing silica gel and "Ascarite" protected the solution so long as H_2 was venting. Degassing was next accomplished by alternately pumping with a diffusion pump while the methanol was frozen in liquid nitrogen and permitting the methanol to warm to room temperature under autogenous pressure. A minimum of three such cycles was always employed. Each aliquot of dry degassed methanol was distilled at autogenous pressure through a trapping system into a radiation cell (chilled to −80°) which was attached to the manifold *via* a ⅌ joint. The cell then was sealed off at a constriction. Sample sizes were determined by weight. The density of methanol was taken as 0.790 in calculations.

Solutes and Preparation of Solutions.—Magnesium methoxide solution was prepared by distilling dry degassed methanol onto magnesium metal (Eastman "Grignard Grade") maintained at −80°. Dissolution of the metal did not appear to begin until the solvent warmed to room temperature. Hydrogen evolved into an isolated portion of the manifold and was removed rigorously by a degassing procedure like that described above. Water and heptaldehyde (Eastman "White Label") were introduced into cells equipped with stopcocks and were separately degassed in the usual way before the solvent was distilled in. Cells containing samples of benzoquinone (Eastman "Practical," recrystallized from ligroin and then sublimed) and maleic anhydride (Pfanstiehl, "Pure") were also equipped with stopcocks and were subjected to prolonged pumping while maintained at −80° before distilling in the solvent. Cells containing lithium chloride (Baker "Analyzed"), pyrogallol (Eastman "White Label"), anthracene (Eastman "Fluorescent Grade"), sulfuric acid (concd. B. and A., C.P.), $FeCl_3 \cdot 6H_2O$ (B. and A. "Reagent" grade) and boric oxide (B. and A. "purified grade") were subjected to prolonged pumping at room temperature. A trace of the anthracene and a substantial fraction of the ferric chloride (estimated as 10–20% of added solute) did not dissolve even after prolonged shaking at

(1) Research carried out under the auspices of the U. S. Atomic Energy Commission.

(2) Visiting Chemist at the Brookhaven National Laboratory, 1957–1958. Department of Chemistry, Boston University, Boston, Mass.

(3) (a) W. J. Skraba, J. C. Burr, Jr., and D. N. Hess, *J. Chem. Phys.*, **21**, 1296 (1953); (b) W. R. McDonell and A. S. Newton, *J. Am. Chem. Soc.*, **76**, 4651 (1954); (c) W. R. McDonell and S. Gordon, *J. Chem. Phys.*, **23**, 208 (1955); (d) W. R. McDonell, *ibid.*, **23**, 208 (1955); (e) G. Meshitsuka, K. Ouchi, K. Hirota and G. Kusumoto, *J. Chem. Soc. Japan*, **78**, 129 (1957).

(4) G. Meshitsuka and M. Burton, *Radiation Research*, **8**, 285 (1958).

(5) G. E. Adams and J. H. Baxendale, *J. Am. Chem. Soc.*, **80**, 4125 (1958).

room temperature. Methyl borate solution was prepared by dissolving the boric oxide in methanol which was distilled onto it in the usual way.

Radiation Cells.—Cells for irradiation in the Co^{60} source were fabricated of Pyrex glass. Each was provided with a breakoff seal and a side-arm equipped with a $\overline{\$}$ joint for attachment to the charging manifold. The sizes of the cells were adapted to the amount of methanol required to give convenient yields of gaseous products, namely, 12 to 70 ml. Free volume varied from 10 to 50% of cell volume.

The Van de Graaff cells, which also were made of Pyrex, were provided with glass-clad iron propellers for magnetic stirring, 0.01″ thick windows, breakoff seals and $\overline{\$}$ joint equipped side-arms.[6] Each cell was charged with about 30 ml. of methanol. Both types of cells were cleaned by a sequence that included soaking in a hot "acid bath" (concd. H_2SO_4 and HNO_3 at above 110°), rinsing with water, soaking in aqueous ammonia, and final thorough rinsing with water. All the cells were oven dried and, immediately before being filled, subjected to prolonged pumping at about 10^{-6} mm. The cells for γ-ray irradiation were thoroughly flamed while being pumped but the Van de Graaff cells were too delicate to permit this treatment.

Irradiations.—The cobalt source has been described in detail.[7] The dose rate was in the vicinity of 1.8×10^{16} e.v. ml.$^{-1}$ min.$^{-1}$. The temperature in the source was maintained at 20–25°.

The Van de Graaff electron accelerator was a High Voltage Engineering model capable of delivering 2×10^6 volts. The electron beam was operated at 1.95×10^6 volts and 0.7×10^{-7} to 1.5×10^{-7} ampere, corresponding to dose rates in the range 1.7×10^{18} to 3.7×10^{18} e.v. ml.$^{-1}$ min.$^{-1}$. Irradiations took place at ambient temperature without detectable warming. During irradiation cell contents were stirred at 1000 r.p.m. by a motor-driven external magnet.

Dosimetry.—The intensity of the cobalt source had been established previously by H. A. Schwarz by means of the acid $FeSO_4$ dosimeter. The dose rate in methanol was calculated by multiplying the rate in 0.8 *N* aqueous H_2SO_4 by the factor $0.790 \times (18.02/32.04)/1.021 \times (10/18)$, thus correcting for the difference in electron density in the two media.

Determination of dose for irradiations by Van de Graaff electrons presented an unexpected difficulty. *G*-values calculated from the total doses indicated by the current integrator were erratic and in poor agreement with the value for γ-ray irradiation; discrepancies ranged as high as 29%. These dose values have accordingly been discarded. Because of the constancy of G_{H_2} for γ-ray irradiation over the dose range of the Van de Graaff experiments, hydrogen production has been used as an internal dosimeter for the latter, using $G_{H_2} = 4.57$. This procedure assumes that the 100 to 200-fold greater dose *rate* characteristic of the Van de Graaff experiments does not alter this value. In any case, this dosimetry permits a comparison of *relative* yields of products to be made conveniently. This matter is discussed further in connection with the data.

Analysis of Gaseous Products.—After irradiation, each cell was sealed to a vacuum line provided with the equipment necessary for collecting and analyzing the gaseous products. The methanol was cooled to −80°, the breakoff tip was smashed with a glass-clad magnetic hammer and the gaseous products Toepler pumped through a trap immersed in liquid nitrogen into a McLeod bulb. In almost all the runs involving irradiation of pure methanol with γ-rays, and in half the Van de Graaff runs, the methanol was next subjected to bulb-to-bulb distillation after which Toepler pumping was repeated. In other runs bulb-to-bulb distillation was replaced by warming the methanol to room temperature and agitating it. No significant differences were observed between the results of these two procedures. The latter procedure was used for analysis of almost all runs involving solutes. After total gas yield had been measured in the McLeod bulb an aliquot was transferred to a Saunders–Taylor type manometric microcombustion apparatus[8] where H_2 was determined by combustion at 295° over CuO for 5 minutes and absorption of resulting water on $MgClO_4$, CO by absorption on "Ascarite" of the CO_2 produced in this combustion, and CH_4 by subsequent combustion over CuO at 510° for 20 minutes and absorption of water and CO_2 as before. The CuO-packed furnace usually was pumped for 1–18 hours at 190–260° before an analysis (or set of duplicate analyses) was carried out. Analysis of a few sets of duplicate aliquots indicated a precision of 0.2%, or better, in the determination of H_2. The precision of the CH_4 and CO analysis was, on a similar basis, 1 to 5% of the value determined. The reliability of the CO and CH_4 analyses is not properly indicated by this degree of precision, however. The excessive scatter is indicated by the data of Fig. 1. In view of this scatter and the fact that these analyses were not tested against known mixtures during the course of these experiments, analytical results for CO and CH_4 must be treated with caution. This uncertainty does not appear to apply to the analyses for hydrogen which composed more than 90% of the gaseous product.

Residual gas was assumed to be nitrogen. It normally constituted 0.5%, or less, of the gas.

Analysis for Formaldehyde and Ethylene Glycol.—After removal of gaseous products and, in some cases, sealing off a bulb containing a sample for determination of water (*vide infra*), air was admitted to the cell and the contents transferred to a glass stoppered volumetric flask which had been subjected to a cleaning procedure like that employed with the cells.

Formaldehyde was determined with chromotropic acid according to the procedure of Bricker and Johnson.[9] Matheson, Coleman and Bell "practical" grade chromotropic acid was purified by filtering a 10% aqueous solution. Such filtered solutions were stored in glass stoppered flasks for no more than 24 hours before use. A calibration curve was established with solutions prepared by dilution of formalin (General Chemical Co. "Reagent Grade") which had been analyzed shortly before use[10] by oxidation with alkaline H_2O_2.[11] Both methanolic and aqueous calibration solutions were employed. Aliquots of methanol and of water, respectively, were used as blanks. Data for these solutions were in good agreement. Beer's law was obeyed up to concentrations around 65 γ of CH_2O/ml. (O.D. = 0.65), with negative deviation of the optical density at higher concentrations. The method was used only for solutions in the range of adherence to Beer's law. In this range, molecules of CH_2O per ml. = $2.025 \times 10^{18} \times$ optical density. All analyses were carried out in duplicate, usually on 1-ml. aliquots of irradiated methanol. For doses smaller than 8×10^{18} e.v. ml.$^{-1}$, 2-ml. aliquots were also analyzed. For doses greater than 7×10^{19} e.v. ml.$^{-1}$, 1-ml. aliquots of suitably diluted solutions were employed. The average of the mean deviations of all duplicate analyses for irradiated pure methanol was 0.003 optical density units per ml. This corresponds to an uncertainty of about ±10% for the smallest dose and of less than ±4% for all doses greater than 7×10^{18} e.v. ml.$^{-1}$.

Ethylene glycol was determined by an adaptation of the method of Critchfield and Johnson[12] which employs the chromotropic acid method to estimate formaldehyde produced from glycol by the action of periodate. It was established in the present work, however, that periodate converts methanol into formaldehyde at a rate which is significant compared to its rate of attack on ethylene glycol when the ratio of concentrations, (MeOH)/(glycol), is in the range encountered in this work (roughly 1.7×10^3 to 3×10^5). It was necessary, therefore, to devise a procedure for the essentially quantitative removal of methanol before introducing periodate. Formaldehyde was simultaneously completely removed. Thus the determinations of glycol and formaldehyde reported here are completely independent of each other. The procedure described below was validated by showing that over a 50-fold concentration range standard solutions of ethylene glycol in water and in methanol yield the same results. These solutions were prepared from Eastman "White Label" ethylene glycol which was analyzed[10] by oxidation with periodic acid,[13] reduction of ex-

(6) These cells were adapted from the design of Saldick and Allen, *J. Chem. Phys.*, **22**, 438 (1954).

(7) H. A. Schwarz and A. O. Allen, *Nucleonics*, **12**, 58 (1954).

(8) *Cf.*, R. H. Schuler and C. T. Chmiel, *J. Am. Chem. Soc.*, **75**, 3792 (1953).

(9) C. E. Bricker and H. R. Johnson, *Ind. Eng. Chem., Anal. Ed.*, **17**, 400 (1945). Aliquots of irradiated methanol were analyzed directly without removing methanol.

(10) Analysis performed by J. K. Rowley.

(11) "Scott's Standard Methods of Chemical Analysis," D. Van Nostrand, Inc., 5th Ed., New York, N. Y., 1939, p. 2149.

(12) F. E. Critchfield and J. B. Johnson, *Anal. Chem.*, **29**, 797 (1957).

cess periodate with iodide and titration of iodine with arsenite.

The glycol analysis yields solutions of the chromotropic acid–formaldehyde derivative which obey Beer's law up to glycol concentrations equivalent to 90 γ of formaldehyde per ml. The ratio, O.D.:concn. of equivalent formaldehyde, determined from this calibration line is 6% smaller than the corresponding ratio determined from the formaldehyde calibration line. Apparently this small fraction of the ethylene glycol is oxidized to products other than formaldehyde. Thus $1.072 \times 10^{18} \times$ O.D. = molecules of glycol per ml. All analyses were run at least in duplicate. Sample sizes (or dilutions) were chosen so as to provide convenient quantities of glycol. The average of the mean deviations for all replicate analyses of irradiated pure methanol was 0.010 optical density units per ml. corresponding to an uncertainty of ±5% or less at doses above 7×10^{18} e.v. ml.$^{-1}$ and increasing to about 20% for the lowest dose employed. A description of the procedure is given.

Procedure for Determination of Ethylene Glycol.—To each of a series of 12-ml. graduated centrifuge tubes sealed to 14/20 female ⧩ joints is added an aliquot of unknown, an Alundum boiling chip and a small drop of concentrated hydrochloric acid.[14] A complete male 14/20 ⧩ joint is inserted and the "distillation unit" immersed in a boiling-water bath and heated almost to dryness. On cooling, the condensed vapors in the unit should yield a residual volume of 0.2 to 0.25 ml. The unit is rinsed down with 0.25 ml. of water with a hypodermic syringe and the contents made up to 1.2 ml. with benzene. Heating in the boiling water-bath is resumed until no more benzene distils out of the unit, the walls are washed down with 0.25 ml. of H_2O and, after drainage is complete, the male joint is removed. The tube is returned to the water-bath to complete removal of the benzene. The tube then is allowed to cool and drain and an excess of solid $NaHCO_3$ is added, followed by 0.1 ml. of 0.2 *F* HIO_4. The walls of the tube are rinsed with 0.25 ml. of H_2O and 25 minutes (at room temperature) is then permitted for reaction before adding 0.5 ml. of 1.0 *F* Na_2SO_3 to consume excess periodate. The resulting solution then is subjected to the usual conditions for determination of formaldehyde with chromotropic acid. Finally, a rapid stream of nitrogen is passed through the diluted developed dye solution for 40 minutes before adjusting its volume precisely.

All optical densities were determined at 570 γ with a model DU Beckman spectrophotometer using 10 mm. Corex cells and correcting for absorption by the cells. All optical densities were measured against blanks obtained by subjecting aliquots of methanol to the corresponding analytical procedure. In most cases, the methanol used as a blank had been subjected to the same purification sequence as the irradiated methanol.

In order to test the effects of solutes on the determination of glycol and formaldehyde, solutions, each of which was approximately 0.01 *F* in one of the solutes as well as of fixed concentration in formaldehyde and ethylene glycol (*ca.* 1×10^{-3} and 5×10^{-4} *F*, respectively), were analyzed. It was found that $MgSO_4$ (model for $Mg(OCH_3)_2$), maleic anhydride, LiCl and $FeCl_3 \cdot 6H_2O$ do not interfere significantly with the aldehyde determination whereas benzoquinone, anthracene, pyrogallol and heptaldehyde do. The situation is the same with respect to analysis for ethylene glycol except that heptaldehyde does not interfere.

Determination of Water, Borate and Hydroperoxide.—Determinations of water[10] content were carried out with the objective of establishing the efficacy of the drying procedure and of estimating the value of G_{H_2O}. Analyses were by an amperometric version of the Karl Fischer method. In order to exclude atmospheric moisture, aliquots of methanol, before or after irradiation, were transferred by distillation on the vacuum line or by direct pouring within the sealed cell, respectively, into thin walled bulbs which were attached by ⧩ joints to the appropriate cell or line. The necks of the bulbs were sealed off with the methanol held at −80°. The bulbs were broken under the surface of excess Karl Fischer reagent in a vessel closed to the atmosphere and the resulting current change related to the amount of water *via* a calibration curve. The results were too erratic to provide useful information on radiation yields of water. The analyses demonstrated, however, that, prior to irradiation, the methanol contained less than 0.001% of water.

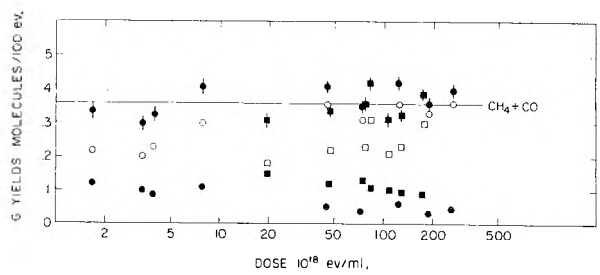

Fig. 1.—Yields of CO and CH_4 for irradiation of pure methanol: ●, ○ and ◐ represent G_{CO}, G_{CH_4} and the sum thereof, $G\Sigma$, respectively, for a given irradiation with γ-rays; ■, □ and ◧ represent the same quantities for a given irradiation with 1.95×10^6 volt electrons. The horizontal line represents the average value of $G\Sigma$.

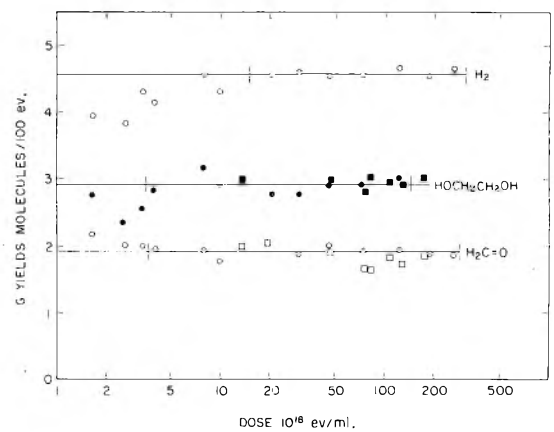

Fig. 2.—Yields of major products from irradiation of pure methanol: ○ and ● data for γ-rays; □ and ■ data for 1.95×10^6 volt Van de Graaff electrons. Horizontal lines are average values of yields obtained with γ-rays over the dose ranges indicated by vertical lines.

Information that methyl borate may influence the photolysis of methanol[15] instigated the determination of boron in samples of methanol which had been stored in a Pyrex flask for seven weeks as well as an experiment in which a methanolic solution of methyl borate was irradiated. No dissolved boron was detected upon analysis[16] by a procedure[16] capable of detecting 6×10^{16} atoms of boron per ml. (4×10^{-4} mole %).

Analysis for H_2O_2 plus CH_3OOH was carried out by a procedure[17] capable of detecting as little as 2.5×10^{15} molecules of peroxide per ml. None was detected in aliquots of solutions which had absorbed doses of 7.84×10^{18} e.v. ml.$^{-1}$ of γ-rays or 1.94×10^{19} and 10.7×10^{19} e.v. ml.$^{-1}$ of Van de Graaff electrons.

Stopcock Grease.—All stopcocks and ⧩ joints employed in this work were lubricated with Spectro Vac Type II grease.

Data

Hydrogen, Ethylene Glycol and Formaldehyde Yields from Pure Methanol.—Yields per 100 e.v. are plotted as a function of total dose in Fig. 2 for hydrogen, ethylene glycol and formaldehyde. G_{H_2} for γ-irradiation is constant for total doses in the range from 2×10^{19} e.v. ml.$^{-1}$ (6.5×10^{-3} % reaction) to 2.6×10^{20} e.v. ml.$^{-1}$ (8.8×10^{-2} % reaction). The apparent diminution in G_{H_2} at lower dose (down to 4.7×10^{-4} % reaction) seems

(13) I. M. Kolthoff and R. Belcher, "Volumetric Analysis," Vol. III, Interscience Publishers, New York, N. Y., 1957 p. 490.

(14) The acid is necessary to catalyze the formation of methylal which azeotropes with methanol. Formaldehyde may not be completely removed in the absence of acid.

(15) Private communication from A. O. Allen.

(16) W. T. Dible, E. T. Truog and K. C. Berger, *Anal. Chem.*, **26**, 418 (1954).

(17) *Cf.*, C. J. Hochanadel, THIS JOURNAL, **56**, 587 (1952).

TABLE I

YIELDS OF MAJOR PRODUCTS FROM IRRADIATION OF METHANOL WITH Co^{60} GAMMA-RAYS AND 1.95×10^6 VOLT ELECTRONS

Product	Radiation	G, molecules/100 e.v. This report[a]	Ref. 3c	Ref. 4	Ref. 5
H_2	γ-Ray	4.57 ± 0.08[b]	4.0[f]	5.39[h]	4.1[j]
H_2	Van de Graaff	(4.57)[c]			
$HOCH_2CH_2OH$	γ-Ray	2.91 ± 0.11[d]	3.0[g]	3.63[i]	3.1[k]
$HOCH_2CH_2OH$	Van de Graaff	$2.96 \pm .09$[e]			
$H_2C{=}O$	γ-Ray	$1.91 \pm .06$[e]	1.3[g]	1.84[i]	2.05[l]
$H_2C{=}O$	Van de Graaff	$1.84 \pm .12$[e]			

[a] Calculated by averaging data of Fig. 1 over indicated dose ranges. Uncertainties are standard deviations. Van de Graaff yields normalized to $G_{H_2} = 4.57$; *cf.* "Experimental." [b] 20.5 to 262 $\times 10^{18}$ e.v. ml.$^{-1}$. [c] 13.7 to 174 $\times 10^{18}$ e.v. ml.$^{-1}$. [d] 3.92 to 122.3 $\times 10^{18}$ e.v. ml.$^{-1}$. [e] 3.92 to 262 $\times 10^{18}$ e.v. ml.$^{-1}$. [f] 3.6 to 14.4 $\times 10^{18}$ e.v. ml.$^{-1}$. [g] 346 to 1728 $\times 10^{18}$ e.v. ml.$^{-1}$. [h] 4 to 400 $\times 10^{18}$ e.v. ml.$^{-1}$. [i] 400 $\times 10^{18}$ e.v. ml.$^{-1}$. [j] 1.6 to 8.8 $\times 10^{18}$ e.v. ml.$^{-1}$. [k] Extrapolated to zero dose from data over the range 5.5 to 20 $\times 10^{18}$ e.v. ml.$^{-1}$. For dose of 12 to 20 $\times 10^{18}$ e.v. ml.$^{-1}$. $G_{glycol} = 3.3$. [l] 6 to 16 $\times 10^{18}$ e.v. ml.$^{-1}$.

to be paralleled in the data of Adams and Baxendale[5] although these workers treated their data as indicating that G_{H_2} is independent of dose. Hydrogen yields observed in this low dose range are very nearly the same as those reported by Adams and Baxendale for virtually the same range. Caution must be exercised with respect to this apparent dose dependence of G_{H_2}. It should be noted, however, that, aided by variation in the amount of methanol irradiated, the precision of the analysis for H_2 does not depend significantly on the dose per ml. Average values of the essentially constant G-yields obtained in the higher dose region are presented in Table I along with published results of other workers. Neither the plateau value of G_{H_2} (4.57) nor the values characteristic of lower doses agree with that reported by Meshitsuka and Burton (5.39). Moreover the data of the latter workers do not indicate any dependence of G_{H_2} on dose at low dose values. McDonell and Gordon[3c] report a value of G_{H_2}, in substantial agreement with that reported by Adams and Baxendale. This is based on data for a range of total dose values similar to that employed by the latter workers. However, McDonell and Gordon did not report any variation of G_{H_2} with total dose in this range.[18]

The present data indicate that G_{glycol} is essentially constant to somewhat lower dose levels than is G_{H_2}. There is a suggestion of diminution in yield at the low end of the dose range but this is the least reliable portion of the data. The data of Adams and Baxendale are sufficiently suggestive of a similar dose dependence to lead these workers to treat the trend as real. The value of G_{glycol} found by these workers for doses of about 1–2 $\times$ 10^{19} e.v. ml.$^{-1}$ is about 13% higher than the plateau value of Fig. 1. Meshitsuka and Burton report an even higher value of G_{glycol} for a sample about 0.25% of which had been radiolyzed.

The present and two[4,5] of the older values of G_{CH_2O} are in reasonable accord and no dose dependence of this specific yield is apparent in any of the data. The significance of the low value of G_{CH_2O} reported by McDonell and Gordon is complicated by uncertainty as to the concentration of water in their methanol and the effect of any which may have been present (*vide infra*).

The values of G_{glycol} and G_{CH_2O} calculated from the data for Van de Graaff irradiations by using hydrogen yield as a measure of dose are in good accord with the corresponding yields from γ-irradiation as determined in this work. This tends to support the "dosimetry" employed but does not prove its validity. The data establish unequivocally, however, that *relative yields* of hydrogen, ethylene glycol and formaldehyde are the same for the two types of irradiation in spite of the hundredfold difference in dose rates.

CH_4 and CO Yields from Pure Methanol.—The scatter of G_{CO} and G_{CH_4} apparent in Fig. 1 prevents the detailed analysis of these quantities. It is clear, however, that the analytical difficulty lies in determination of the separate quantities; their sum, G_Σ, is much more constant. The average value of G_Σ is 0.36 with a standard deviation of 0.04. This can be taken as representing an upper limit for both G_{CO} and G_{CH_4}. There is no apparent trend in G_Σ with dose. Thus, a limited comparison of G_{CH_4} (and G_{CO}) with the results of other workers is possible.

There is very poor agreement among different workers as to G_{CH_4}. Thus, Adams and Baxendale report a slight negative dependence on dose of G_{CH_4} and a value, extrapolated to zero dose, of 1.23. Meshitsuka and Burton report the opposite sign of dose dependence and, ascribing this dependence to incomplete collection of methane in low dose runs, report a value of G_{CH_4} based on data of highest dose (400 $\times$ 10^{18} e.v. ml.$^{-1}$), namely, 0.54. Adams and Baxendale find G_{CO} to be 0.15 and independent of dose (up to about 2 $\times$ 10^{19} e.v. ml.$^{-1}$). Meshitsuka and Burton report G_{CO} as 0.11 over this dose range but observe a much lower value at 4 $\times$ 10^{20} e.v. ml.$^{-1}$. These two groups of workers analyzed gaseous products mass spectrometrically. McDonell and Gordon, who used a Saunders-Taylor type of manometric combustion analysis, report $G_{CH_4} = 0.24$ and $G_{CO} = 0.16$ for total doses of 3.6 to 14.4 $\times$ 10^{18} e.v. ml.$^{-1}$. The values of G_Σ are, respectively, 1.38 (A and B), 0.65 (M and B), 0.40 (M and G). The discrepancies are, at present, without explanation.

Peroxide Yields from Pure Methanol.—No peroxide was detected by the analytical procedure employed. This indicates that ($G_{H_2O_2} + G_{CH_3OOH}$) is less than 0.003.

Material Balance in Radiolysis Products from Pure Methanol.—In order to estimate material balance in the plateau region for hydrogen from

(18) These workers did not dry or otherwise purify the methanol they employed.

the data for γ-irradiations only, averaged values for G_{CO} and G_{CH_4} in this region have been arbitrarily employed; these are 0.045 and 0.34, respectively. Hence $G_{Red} = G_{H_2} + G_{CH_4} = 4.91$ and $G_{Ox} = G_{glycol} + G_{CH_2O} + 2G_{CO} = 4.91$. The precise agreement is entirely fortuitous. Any choice of G_{CO} and G_{CH_4} reasonably related to the data of Fig. 2 yields a good material balance, however. A certain degree of caution in accepting a good material balance as substantiating its individual components is suggested by the fact that Adams and Baxendale provide an excellent balance (5.33/5.30) based on a quite different distribution of terms.

Yields from Solutions in Methanol.—Data are summarized in Table II. It is seen, in agreement with the report of Meshitsuka and Burton and

TABLE II

YIELDS OF PRODUCTS FROM RADIOLYSIS OF METHANOLIC SOLUTIONS BY Co^{60} γ-RAYS[a]

Solute	Concn., mole l.$^{-1}$	G_{H_2}	G_{CH_4}	G_{CO}	G_{CH_2O}	$G_{C_2H_6O_2}$
Unknown[b]	...	3.44	0.25	0.11	1.06	3.00
H_2O	0.48[c]	3.61	.23	.09	1.29	3.00
$Mg(OCH_3)_2$	.0087	4.09	.28	.04	3.33	0.87
LiCl	.021	3.80	.27	.05	2.24	2.52
H_2SO_4	.0094	4.94	.25	.10	2.37	3.62
$FeCl_3 \cdot 6H_2O$[d]	< .0114	2.15	.13	.14	7.13	0.5
Quinone[e]	.0087	2.47	.12	.11	..	..
Heptaldehyde	.0104	3.86	.27	.10	..	2.29
Pyrogallol	.0088	4.09	.22	.09	..	..
Anthracene	.0082	2.60	.21	.10	..	..
Maleic anhydride[f]	.0081	3.57	.24	.11	2.35	0.94
Methyl borate[g]	.51	4.43	..	..	..	..

[a] Total doses were in the range 2.126×10^{19} to 2.412×10^{19} e.v. ml.$^{-1}$. [b] An aliquot from a bottle of Mallinckrodt AR methanol was degassed but was neither dried nor rectified before irradiaton. [c] 1.1% by weight. [d] This sample was contaminated with air equivalent to 2.32×10^{17} molecules of O_2 per ml. of methanol. [e] This sample was contaminated with air equivalent to 7.13×10^{17} molecules of O_2 per ml. of methanol. [f] This sample was contaminated with air equivalent to 2.25×10^{17} molecules of O_2 per ml. of methanol. [g] Values of $G_{CH_4} = 0.18$ and $G_{CO} = 0.04$ have been discarded because the CuO furnace was pumped at 600° before this analysis.

contrary to that of Adams and Baxendale, that G_{H_2} is substantially reduced in the presence of water. G_{CH_2O} is affected similarly. McDonell and Gordon[3c,18] agree with the present result in finding no effect of water on G_{glycol}. Their finding that G_{CH_2O} varies inversely with water concentration is qualitatively, but not quantitatively, in accord with the present observation. The four other solutes for which information was secured all have the opposite effect on G_{CH_2O}. The results with methanol which had been degassed but not otherwise purified[19] are similar to those obtained in the presence of water.

The results with benzoquinone and $FeCl_3 \cdot 6H_2O$ are similar but not identical to those reported by Adams and Baxendale. In view of the fact that a fivefold greater dose was used in the present work and of the presence of a small amount of oxygen in the samples, the differences do not merit discussion. To the extent that comparisons may be made in spite of differences in dose and concentration, sulfuric acid influences the radiolysis of almost dry methanol (~0.002 *M* in water added in the form of concentrated H_2SO_4) in a fashion qualitatively similar to the effect of sulfuric acid on methanol containing 3% of water.[5] It is the only substance tested which increases the yield of either hydrogen or glycol.

(19) This material was subjected to bulb-to-bulb distillation in the course of charging the radiation cell; some purification may have been effected thereby.

Discussion

These results emphasize that accurate information concerning the radiolysis of "pure" methanol is not easily obtained. Resolution of substantial discrepancies in the reported values of G_{CH_4} and G_{H_2} is needed. The several values for G_{glycol} are not in good agreement. There appears to be no agreement as to the effect of small amounts of water. Whether G_{H_2} and G_{glycol} do, in fact, diminish at very low dose remains to be substantiated. There are no data on G_{H_2O} for radiolysis by γ-rays. Under these circumstances chemical interpretation of the data for "pure" methanol is not justified.

It does not, of course, follow that equal difficulty is to be anticipated in securing reliable information for solutions containing efficient radical scavengers as solutes.[5] The behavior of aqueous systems suggests that such solutions should be more tractable.

Table II summarizes very limited data for solutions of well known radical scavengers (*e.g.*, $FeCl_3$ and benzoquinone) and also of solutes that may perhaps intervene in other ways in the radiolytic process.

Methyl borate appears to have a negligible effect on the hydrogen yield (and probably on the yields of CH_4 and CO as well). This datum, taken in conjunction with the failure to detect borate in methanol which had been in prolonged contact with Pyrex glass appears to eliminate methyl borate as a complicating factor in the radiolysis of liquid methanol. However, extensive evidence that borate does accumulate in anhydrous methanol upon exposure to Pyrex has been reported[20] along with observations concerning the profound influence of methyl borate on the photolysis of methanol in the gas phase. Since the latter is related to more efficient absorption of light by methyl borate, there is not necessarily any conflict between the data on photolysis and radiolysis. The disagreement as to attack of methanol on Pyrex is substantial and without explanation, however.

The effect of $Mg(OCH_3)_2$ is similar in a qualitative way to that observed with $FeCl_3 \cdot 6H_2O$. However, in the latter case two molecules of formaldehyde appear for each molecule of glycol that disappears whereas with $Mg(OCH_3)_2$ less than one molecule of formaldehyde (about 0.7) appears for each glycol molecule lost. An oxidation of CH_2OH radicals to $CH_2O + H^+$ such as that which has been suggested[5] to explain the action of Fe(III) clearly does not apply here. The result with $Mg(OCH_3)_2$ suggests promotion of a disproportionation process: "$2 \cdot CH_2OH$" → $CH_2O + CH_3OH$ (where no distinction is made between $\cdot CH_2OH$ and $CH_3O\cdot$). Lacking, as yet,

(20) R. F. Porter, THIS JOURNAL, **61**, 1260 (1957).

a knowledge of whether Mg(II) ion or methoxide anion (or possibly both) is the active species, more detailed speculation is not justified. Lithium chloride, at twice the concentration, but, if we assume complete dissociation, half the ionic strength has a smaller but analogous effect: somewhat less than one molecule of formaldehyde appears for each molecule of ethylene glycol lost. Whatever the mechanism by which these solutes intervene, it seems highly improbable that it involves oxidation of radicals.

If it is assumed that the value of G_{H_2} found for "pure" methanol in this work can be used for purposes of estimating solute effects, then both electrolytes (a base and a neutral salt) reduce hydrogen formation. Since it is not known as yet whether ionic strength or stoichiometric concentration is the proper measure of concentration, the data do not tell which is more effective. In view of the uncertainty in the determinations of G_{CO} and G_{CH_4} it can only be concluded that no drastic changes in these values are brought about by LiCl or $Mg(OCH_3)_2$ as G_Σ falls in the range of values found for "pure" methanol. Finally, the material balance is good only with $Mg(OCH_3)_2$ as a solute. There appears to be an undetected reduction product formed in the presence of LiCl. These initial results with solutions of "non-oxidizing" electrolytes are suggestive and extensive work in this area is planned.

Heptaldehyde (0.010 M) was employed as a conveniently handled model of formaldehyde. Hydrogen and glycol yields are diminished about equally by this solute while G_Σ is not affected. Since irradiation with a dose sufficient to produce 0.020 M formaldehyde yielded normal "plateau" values of G_{H_2} and G_{glycol} it appears that heptaldehyde is not a good model for formaldehyde.

Pyrogallol, a very effective scavenger for peroxy radicals, has a relatively small effect on G_{H_2}. Anthracene, which has a high "methyl affinity,"[21a] (although only 1/20th as large as that of benzoquinone[21b]) has about the same effect on G_{H_2} as does benzoquinone and probably is acting as a radical scavenger. Information of G_{CH_2O} and G_{glycol} in the presence of anthracene and quinone would be of great value in determining whether or not they operate by similar mechanisms, but this is, as yet, not available. Neither anthracene nor pyrogallol alters G_Σ sufficiently to treat the effect as real.

Maleic anhydride reduces glycol formation drastically with only a small increase in formaldehyde formation: only about 0.2 molecule of aldehyde appears per glycol molecule lost. The material balance remains fairly good, however. Perhaps some of the glycol is suppressed *via* formation of a product (or products) of addition of H· and ·CH_2OH or a precursor thereof to the olefinic link. Information on the fate of maleic anhydride would be useful in formulating a specific mechanistic hypothesis to account for its action. With maleic anhydride as solute, G_Σ is, again, unaffected. Only the radical scavengers benzoquinone and $FeCl_3 \cdot 6H_2O$ affect G_{CH_4} (or G_Σ) so substantially that, in spite of the analytical uncertainty, the effect can be accepted as real. A much larger diminution of G_{CH_4} by oxidizing scavengers has been reported and interpreted by Adams and Baxendale.[5]

In the presence of water or of sulfuric acid material balance appears to be poor: oxidation products appear to be in about 15 to 20% excess over reduction products. This observation is not in accord with the results which Adams and Baxendale report[5] for 97% methanol containing 0.05 M H_2SO_4, where they obtain fairly good material balance.

The evidence that the ratio G_{glycol}/G_{CH_2O} is influenced in a variety of ways by different solutes for which this information is available suggests that there are several modes of intervention by solutes and that this quantity may be a valuable guide to their mechanisms of action. It is hoped that analytical procedures can be developed to provide this information for other solutes.

Acknowledgment.—Many stimulating and informative discussions with Dr. A. O. Allen are herewith gratefully acknowledged. The author also wishes to express his appreciation of the advice and critical interest provided by Dr. H. A. Schwarz and of the extensive aid provided by Dr. J. K. Rowley in connection with some of the analytical determinations carried out in the course of this work.

(21) (a) M. Levy and M. Szwarc, *J. Am. Chem. Soc.*, **77**, 1949 (1955); (b) A. Rembaum and M. Szwarc, *ibid.*, **77**, 4468 (1955).

THE PREPARATION OF URANIUM MONOCARBIDE AND ITS HEAT OF FORMATION[1]

BY JOHN D. FARR, ELMER J. HUBER, JR., EARL L. HEAD AND CHARLES E. HOLLEY, JR.

Contribution from the University of California, Los Alamos Scientific Laboratory, Los Alamos, New Mexico

Received February 21, 1959

The preparation of uranium monocarbide, UC, by direct combination of the elements is described. Its heat of formation was found by combustion calorimetry to be $\Delta H^0_{298°K.} = -21.0 \pm 1.0$ kcal./mole. The combustion experiments were done with UC–UO_2 mixtures in order that the final uranium oxide formed would be stoichiometric U_3O_8.

Introduction

The uranium carbides are of considerable interest in connection with the technology of nuclear reactors. Uranium monocarbide has been known for some time.[2] This paper reports a method of preparing this compound by direct combination of the elements and an experimental determination of its heat of formation.

The Preparation of Uranium Monocarbide.—High purity uranium metal, depleted of U-235, was used. The surface oxide layer was removed with dilute nitric acid, and the metal was then washed and dried and given a preliminary arc-melting for outgassing and removal of any volatile impurities. Oxygen and nitrogen are soluble in the UC lattice and care had to be taken to exclude them from the reaction.

The AUC graphite from the National Carbon Company was outgassed at 2000° *in vacuo* before use.

The arc furnace was of water-cooled copper construction. It had a movable cathode with a tungsten tip. Pickup of either copper or tungsten by the sample was found to be negligible. The furnace could be evacuated by an oil diffusion pump backed by a mechanical pump to approximately 10^{-5} mm. The power for melting of samples came from a 34.5 kw. welding generator of the rectifier type. A high frequency unit was used to initiate the arc.

The UC was prepared by placing the uranium metal and the necessary graphite on the copper hearth and closing the furnace. After evacuation of the system, tank argon was admitted to a pressure approximately 8–10 cm. below the ambient atmospheric pressure. Next, a button of zirconium metal was melted in the arc furnace as a getter for the impurities in the argon. The uranium was then melted in contact with the graphite to form the carbide. This piece of carbide, after cooling, was turned over on the hearth by means of the movable cathode without opening the furnace to the atmosphere. What was previously the bottom side of the sample could now be melted. This procedure was repeated until the carbide had been melted on both sides a total of three times. The product was a shiny, brittle, metallic-appearing button which analyzed 95.36% U, 4.61% C, 0.008% O, 0.005% H and 0.015% Si, other impurities being negligible. This corresponds to 95.99% UC, 3.47% U metal, 0.13% UO, 0.40% UH_3 and 0.015% Si. All percentages given are weight percentages. That the excess uranium was present as metal was shown metallographically and by X-rays. If more graphite was used in an attempt to convert all the uranium to UC, then a UC_2 phase was found in the product as an impurity. The lattice constant of the UC was found to be $a = 4.9554 \pm 0.0003$ Å.

The Heat of Formation of Uranium Monocarbide.—The heat of formation of uranium monocarbide was determined indirectly from measurements of its heat of combustion in oxygen. From these measurements, ΔH was calculated for the reaction

$$3UC + 7O_2 = U_3O_8 + 3CO_2 \qquad (1)$$

and, since the heats of formation of U_3O_8 and CO_2 are known, the heat of formation of UC was found.

From preliminary experiments it was determined that when UC was burned by itself a fused oxide was formed which was not stoichiometric U_3O_8. But when UC was mixed with several times its weight of UO_2 and the mixture burned, the resulting oxide had not fused and was stoichiometric U_3O_8. This behavior is similar to that observed in the combustion of uranium metal.[3]

The calorimeter and general procedure, which involved the determination of the heat evolved from the simultaneous combustion of weighed amounts of uranium monocarbide and uranium dioxide in a bomb calorimeter at a known initial pressure of oxygen, have been described.[4] The energy equivalent of the calorimeter was 9988.0 ± 3.3 joules/°C. as determined by the combustion of standard benzoic acid. The uncertainty interval for the calorimetric measurements is taken as twice the standard deviation of the mean.

The powdered carbide was mixed with powdered dioxide and burned in a thoria dish supported on a platinum platform in the combustion bomb. Ignition was by means of a 0.010 in. diameter uranium wire as a fuse, which in turn was ignited electrically.

The uranium monocarbide, after being ground to a powder in an "inert" atmosphere box contained 95.38% U, 4.52% C, 0.085% O, 0.005% H and 0.015% Si. Apparently some oxidation took place during grinding. It was assumed that the carbon was all present as UC, the oxygen as UO, the hydrogen as UH_3, the silicon as elemental Si, and the excess uranium as U metal. The silicon was probably present as uranium silicide, but thermal data are lacking on this compound and the amount of silicon was so small that negligible error was introduced by assuming it to be present as free silicon. The oxygen was assumed to be present as UO because it is believed that UC stabilizes UO.[5] On these assumptions the actual composition of the powdered uranium monocarbide was thus 94.11% UC, 4.125% U, 1.35% UO, 0.40% UH_3 and 0.015% Si.

The uranium dioxide had the formula $UO_{2.014}$. Its heat of combustion under the conditions of the experiment was determined separately.

The solid combustion product was a dark, slightly sintered mass of uranium oxide which was easily powdered. It was analyzed by heating to constant weight in oxygen at 750° and noting any change in weight. The exit gases were passed through ab-

(1) This work was done under the auspices of the Atomic Energy Commission.

(2) See J. J. Katz and G. T. Seaborg, "The Chemistry of the Actinide Elements," John Wiley and Sons, Inc., New York, N. Y., 1957, p. 148, for a recent review of the uranium-carbon system.

(3) E. J. Huber, Jr., C. E. Holley, Jr., and E. H. Meierkord, *J. Am. Chem. Soc.*, **74**, 3406 (1952).

(4) C. E. Holley, Jr., and E. J. Huber, Jr., *ibid.*, **73**, 5577 (1951).

(5) R. E. Rundle, N. C. Baenziger, A. S. Wilson and R. A. McDonald, *ibid.*, **70**, 99 (1948).

TABLE I

THE HEAT OF COMBUSTION OF UC

Mass UC, g.	Mass UO_2, g.	Mass U, mg.	Energy equiv., j./°C.	ΔT, °C.	Firing energy, j.	Energy from UO_2, j.	Energy from UC, j./g.	Dev.
1.2090	19.5640	73.3	10016.2	1.4915	5.6	7487.5	5856.7	20.2
1.0601	18.4404	64.3	10015.8	1.3578	4.8	7057.5	5864.3	12.6
1.2808	17.4359	72.9	10015.7	1.4513	4.8	6673.0	5851.5	25.4
0.9844	15.4431	74.5	10015.0	1.2064	4.9	5910.4	5887.2	10.3
0.9749	14.4102	76.2	10014.6	1.1601	5.6	5515.1	5864.6	12.3
1.0241	14.9250	73.7	10014.8	1.2097	5.0	5712.1	5888.5	11.6
1.1436	15.3697	76.0	10015.0	1.2983	5.3	5882.3	5890.3	13.4
0.9578	14.8057	66.3	10014.8	1.1633	4.9	5666.4	5897.3	20.4
1.0562	14.7218	72.6	10014.8	1.2189	5.1	5634.3	5875.5	1.4
1.0182	14.4235	67.6	10014.7	1.1845	4.9	5520.2	5893.0	16.1
					Av.		5876.9	14.4
					2 × standard dev.			10.5

sorption tubes to determine water and carbon dioxide. These amounted to about 5 and about 1 mg., respectively, and are believed to be present because of adsorption. These amounts are negligible unless the carbon dioxide was due to unburned UC in the combustion products. No correction was made for this possibility. The results confirmed the formula of the product oxide as U_3O_8.

Ten runs were made. The results are presented in Table I. The average initial temperature of the runs was 25.05°. The initial volume of the bomb was 350 ml. The initial oxygen pressure was 25 atm.

The heat of combustion of UC under the particular experimental conditions is thus 5876.9 ± 10.5 joules/g.

In order to find the heat of formation of UC, corrections must be made to a constant pressure process from a constant volume process. And, because an appreciable fraction of the heat from the actual process carried out came from UO_2, in addition to that from the UC, it was necessary to correct the total reaction in the bomb to constant pressure and then subtract the contribution of the UO_2 and the impurities to arrive at ΔH_{298} for the combustion reaction (eq. 1).[6] After ΔH for reaction (1) was so found, this value was combined with the heats of formation of U_3O_8 and CO_2 to give the heat of formation of UC, $\Delta H_f = -87.9 \pm 4.2$ kjoules/mole.[7,8] In defined calories this is -21.0 ± 1.0 kcal./mole. There are no previous experimental values for comparison. Estimates have been made by Brewer of -43 kcal./mole[9] and by Krikorian and Brewer of -28 kcal./mole.[10]

Acknowledgments.—The authors wish to acknowledge the valuable assistance of D. Pavone, metallographic analysis, F. H. Ellinger, X-ray analysis, and M. E. Smith, E. Van Kooten and O. Kriege, chemical analysis.

(6) In the conversion to a constant pressure process $(\partial\Delta E/\partial P)_{298}$ for oxygen was taken as -6.51 joules/atm./mole [F. D. Rossini and M. Frandsen, *J. Research Natl. Bur. Standards*, **9**, 733 (1932)] and for carbon dioxide as -28.5 joules/atm./mole (W. N. Hubbard, D. W. Scott and Guy Waddington, "Experimental Thermochemistry," F. D. Rossini, Editor, Interscience Publishers, Inc., New York, N. Y., 1956, p. 101.)

In the correction for the impurities, ΔH_f for UO was taken as half the value for UO_2. This value is uncertain, but the fact that UO has not been prepared in bulk indicates that it is probably not appreciably more stable than UO_2. For UH_3, ΔH_f was taken as -126.9 kcal./mole and for SiO_2 as -205 kcal./mole.

The heat of the reaction $3UO_{2.014} + 0.979\ O_2$ (1 atm.) = U_3O_8 was calculated from separate measurements of the heat of combustion of this particular batch of uranium dioxide and found to be -313.05 ± 0.31 kjoule/mole.

(7) The heat of formation of U_3O_8 was recalculated from the data in ref. 3 as -3567.6 ± 6.7 kjoules/mole and the heat of formation of CO_2 was taken as -393.51 ± 0.04 kjoules/mole (NBS Circular 500).

(8) The uncertainty includes the uncertainty in the calorimetric measurements on the UC–UO_2 mixtures and on the energy equivalent, both expressed as twice the standard deviation, the recalculated uncertainty in the heat of formation of U_3O_8, estimated values for the uncertainties in the heats of formation of CO_2, UO, UH_3 and SiO_2, and estimated values for uncertainties in the amounts of oxygen, hydrogen and silicon impurities in the UC, all combined according to standard methods for the propagation of errors.

(9) Leo Brewer, *et al.*, "The Thermodynamic Properties and Equilibria at High Temperatures of Uranium Halides, Oxides, Nitrides and Carbides." University of California Radiation Laboratory Report BC-82 (MDDC-1543) Sept. 1945.

(10) O. H. Krikorian, "High Temperatures Studies. Part II. Thermodynamic Properties of the Carbides," University of California Radiation Laboratory Report UCRL-2888, April 1955.

SALT EFFECTS IN THE RACEMIZATION OF A BIPHENYL HAVING ANIONIC BARRIER GROUPS[1]

BY J. E. LEFFLER AND B. M. GRAYBILL

Contribution from the Department of Chemistry, Florida State University, Tallahassee, Florida

Received February 21, 1959

The rates and activation parameters for the racemization of the salts of 2,2′-dimethoxy-6,6′-dicarboxydiphenyl depend on the solvent and on the concentration of added salts. Salts added to the aqueous solution decelerate the reaction by as much as a factor of 3.5, while the addition of organic solvents can cause a deceleration of a factor of ten or more. This is in contrast to the acceleration reported previously for the racemization of *o*-(2-dimethylaminophenyl)-phenyltrimethylammonium ion under the same conditions. In both reactions the added salts or solvent components lower the enthalpy and entropy of activation, but the rate effects in the reaction reported earlier are enthalpy-controlled, while those in the present reaction are entropy-controlled.

Salt and Concentration Effects in Water.—The racemization of the ion I is decelerated by an increase in the concentration of its disodium salt or by the presence of added salts. The reduction in rate is

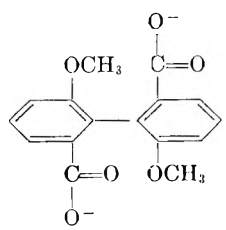

I

entropy-controlled and amounts in some cases to a factor of 3.5, while the activation enthalpies and entropies are generally lowered by the added salt, by as much as 3.6 kcal./mole and 11.6 cal./mole-deg. Metal ions have an effect which appears to increase with decreasing size or increasing charge of the ion. However, very large cations (detergents) are approximately as effective as lithium or sodium ions. Detergent anions do not appear to have any marked effect.

The behavior of the dicarboxylate ion I is quite different from that of the cationic biphenyl II reported earlier[1b,c]. Salts and organic solvent components added to aqueous solutions of II were found to accelerate, rather than decelerate

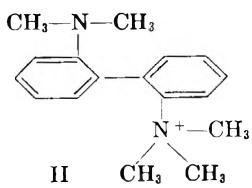

II

the racemization. The cationic biphenyl II also differs in that large ions were found to have a greater effect than small ones. Furthermore, the charge type of the ions added was found to be relatively less important than in the case of the present biphenyl. The single point of resemblance in behavior between the two biphenyls is that the added salts or solvent components in both cases lower the enthalpy and entropy of activation with respect to that in pure water. The difference in direction of the effect on the rates is due to the fact that the previously reported reaction is enthalpy-controlled rather than entropy-controlled.

The salt effects in the racemization of I can be explained in terms of a stronger association between the added cation and the ground state of I, than between the added cation and the transition state of I. In the case of the biphenyl II, the reverse was postulated; the transition state was considered to be de-solvated and hence able to interact more strongly with the associated anion. We would like to suggest two reasons for the difference in behavior of the two biphenyls. The first is that the ion pair formed by the ground state of I with a cation is a chelate, or at least that it is stabilized relative to transition state ion pairs because of the lesser distance between the carboxylate groups. The second possibility is that the transition state for the racemization of I may be vibrationally less excited, and therefore less desolvated than the transition state for the racemization of II.

TABLE I

THE EFFECT OF CONCENTRATION ON THE RACEMIZATION OF THE DISODIUM SALT OF 2,2′-DIMETHOXY-6,6′-DICARBOXYBIPHENYL IN WATER

Biphenyl concn., mole/l.	$k \times 10^5$, sec.$^{-1}$[b] 100°	79.4°	$\Delta H^{\pm}$, kcal./mole[a]	$\Delta S^{\pm}$, cal./mole-deg.
0.0055	14.05	1.83	24.99 ± 0.08	−14.22 ± 0.22
.0070	13.8	1.80	25.29 ± .09	−13.45 ± .23
.0134	13.3	1.77	24.72 ± .10	−15.03 ± .28
.0228	13.2	1.75	24.95 ± .11	−14.43 ± .32
.0339	12.9	1.73	24.83 ± .15	−14.66 ± .41
.0662	12.0	1.61	24.85 ± .07	−14.90 ± .20
.103	11.2	1.50	24.78 ± .06	−15.22 ± .22
.005[c]	14.3	1.94	24.38 ± .07	−15.85 ± .21
.005[d]	14.3	1.84	25.23 ± .06	−13.55 ± .16

[a] For the significance of the error figures and methods of calculation see reference 1c. [b] Mean rate constants. [c] The dipotassium salt. [d] The ditetramethylammonium salt.

Models indicate that a chelate structure for the ion-pair made from the ground state conformation of I is sterically quite reasonable. The ring formed by the chelation is a large one, but the ready formation of large rings by aromatic compounds is not unusual,[2] since rigid molecules lose comparatively less entropy by ring closure than do flexible ones.

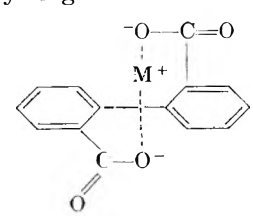

The chelate ion-pair

The role of the metal ion in the proposed chelate

(1) (a) Based on the doctoral dissertation of B. M. G. and presented in part at the Symposium "Solvent Effects and Reaction Mechanisms," Queen Mary College, London, July 1957. For previous papers of this series, see: (b) W. H. Graham and J. E. Leffler, THIS JOURNAL, **63**, 1274 (1959) and (c) J. E. Leffler and W. H. Graham, *ibid.*, **63**, 87 (1959).

TABLE II

THE EFFECT OF ADDED SALTS ON THE RACEMIZATION OF THE DISODIUM SALT OF 2,2′-DIMETHOXY-6,6′-DICARBOXYBIPHENYL IN WATER

Added substance and its concn., mole/l.[a]		$k \times 10^5$, sec.$^{-1}$[b] 100°	79.4°	$\Delta H^{\ddagger}$, kcal./mole[c]	$\Delta S^{\ddagger}$, cal./mole-deg.
None		14.05	1.83	24.99 ± .08	−14.22 ± .22
NaOH	0.0148	14.05	1.83	24.99 ± 0.08	−14.22 ± 0.22
	.0302	13.5	1.77	25.11 ± .06	−13.95 ± .16
	.0500	12.3	1.69	24.46 ± .10	−15.90 ± .27
	.0811	12.1	1.65	24.57 ± .10	−15.62 ± .26
	.1800	11.5	1.56	24.45 ± .11	−16.05 ± .31
	.3134	10.9	1.49	24.78 ± .08	−15.22 ± .22
NaCl	.2	11.3	1.59	24.24 ± .05	−16.64 ± .12
	.5	8.93	1.27	24.04 ± .13	−17.64 ± .37
	.75	8.48	1.16	24.56 ± .12	−16.36 ± .33
	1.0	7.71	1.04	24.80 ± .10	−15.91 ± .27
LiCl	0.075	11.4	1.49	25.18 ± .18	−14.12 ± .33
	.20	8.31	1.10	24.96 ± .11	−15.32 ± .32
	.74	5.50	0.75	24.62 ± .09	−17.05 ± .24
	1.00	4.30	0.65	23.25 ± .08	−21.23 ± .23
$BaCl_2$	0.01	7.37	1.19	22.50 ± .12	−22.17 ± .32
	.02	6.27	1.00	22.65 ± .10	−22.08 ± .27
	.05	5.16	0.906	21.40 ± .10	−25.83 ± .28
	.10	4.01	0.596	23.73 ± .15	−20.03 ± .43
$MgCl_2$	.01	6.97	1.17	22.01 ± .14	−23.58 ± .36
KCl	1.0	8.26	1.18	24.07 ± .10	−17.72 ± .27
NaBr	0.2	11.45	1.53	24.88 ± .12	−14.91 ± .35
NaOAc	.2	11.2	1.53	24.56 ± .10	−15.81 ± .26
Sodium tosylate	.2	10.8	1.50	24.35 ± .05	−16.44 ± .14
$(CH_3)_4N^+Cl^-$	1.0	14.3	1.91	24.88 ± .10	−14.46 ± .27
$C_6H_5N^+(CH_3)_3Cl^-$	1.0	13.85	1.85	24.91 ± .11	−14.46 ± .30
Polydiallyldimethylammonium bromide, 26 g./l.		14.4	1.89	25.19 ± .08	−13.61 ± .22
Sodium lauryl sulfate, 0.11 *M*		13.05	1.80	.....	.....
Dodecyltrimethylammonium chloride, 0.2 *M*		11.75	1.69	23.99 ± .10	−17.23 ± .28
Cetyltrimethylammonium chloride, 0.2 *M*		8.53	1.19	24.32 ± .15	−17.00 ± .43

[a] The concentration of the disodium salt of 2,2′-dimethoxy-6,6′-dicarboxybiphenyl is approximately 0.005 mole/l. [b] Mean rate constants. [c] For the methods of calculation and the significance of the error figures, see reference 1c.

is somewhat like that of a hydrogen atom in a hydrogen bond.[3] Partial neutralization to the monocarboxylate ion (Table III) does in fact have an effect on the rates similar to that of added salts, although the deceleration might also be expected as a result of the loss of the intraionic repulsion of the two carboxylate groups.

TABLE III

THE RACEMIZATION OF THE MONOSODIUM SALT OF 2,2′-DIMETHOXY-6,6′-DICARBOXYBIPHENYL IN WATER

Conditions	$k \times 10^5$, sec.$^{-1}$[a] 100°	79.4°	$\Delta H^{\ddagger}$, kcal./mole[b]	$\Delta S^{\ddagger}$, cal./mole-deg.
The acid plus NaOH, both 0.014 *M*	2.73	0.433	22.71 ± 0.11	−23.57 ± 0.32
The disodium salt, 0.005 *M*, plus NH_4Cl, 1.0 *M*	3.77	0.739	20.01 ± .10	−30.16 ± .27

[a] Mean rate constants. [b] For methods of calculation and significance of error figures, see ref. 1c.

The decreased entropies of activation for the ion-pairs can be explained if the ion pair dissociates in the activation process and if both of the ions thus formed are considerably more solvated than the ion-pair. Solvation of the dicarboxylate transition state will be favored if the activation energy for this racemization is largely potential rather than kinetic. An indication that this might indeed be the case is the fact that trinitrobenzene accelerates the racemization of the related dimethyl ester. The formation of π-complexes is favored by coplanarity and conjugation in the substrate and would seem to be difficult in a molecule having free internal rotation.[4] Evidence suggesting conjugation between the two rings in the transition state is the acceleration produced by the substitution X = CH_3O^- in the biphenyl III.[5]

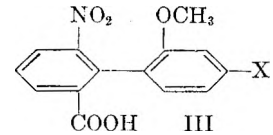

III

(2) Tri-*o*-thymotide is an example. W. Baker, B. Gilbert and W. D. Ollis, *J. Chem. Soc.*, 1443 (1952); A. C. D. Newman and E. M. Powell, *ibid.*, 3747 (1952)

(3) Spectroscopic evidence indicates the existence of intermolecular lithium bonds. A. Rodionov, D. Shigorin, T. Talelaeva and K. Kocheskoe, *Izvestia Akad. Nauk S.S.S.R., Otdel. Chim.*, 120 (1957).

(4) Hindered biphenyls (in the ground state) do not form complexes with TNB. C. E. Castro, L. J. Andrews and R. M. Keefer, *J. Am. Chem. Soc.*, **80**, 2322 (1958).

(5) W. E. Hanford and R. Adams, *ibid.*, **57**, 1592 (1935). See also M. Calvin, *J. Org. Chem.*, **4**, 256 (1939) and F. W. Cagle and H. Eyring, *J. Am. Chem. Soc.*, **73**, 5628 (1951).

The Enthalpy–Entropy Relationships in the Salt Solutions.[6]—As the concentration of added salt is increased the reaction rate continues to decrease, but the enthalpy and entropy of activation pass through a minimum. However, the net effect is always a lowering of the enthalpy and entropy with respect to that of water. Figure 1 shows the behavior of the activation parameters with varying concentrations of sodium chloride.

The Effect of Organic Solvent Components.—Addition of alcohols or acetone to aqueous solutions of the dicarboxylate salt decelerates the reaction and decreases the enthalpy and entropy of activation (Table IV and Fig. 2). Factors that might be expected to cause the deceleration are an increase in ion association and a medium effect on the intramolecular repulsion of the two carboxylate ion groups. The interpretation is complicated,

TABLE IV

THE EFFECT OF ORGANIC SOLVENT COMPONENTS ON THE RACEMIZATION OF THE DICARBOXYLATE SALT IN AQUEOUS MIXTURES

Solvent, wt. % of organic component		$k \times 10^6$, sec.$^{-1}$[a] 100°	79.4°	$\Delta H^{\ddagger}$, kcal./mole[b]	$\Delta S^{\ddagger}$, cal./mole-deg.
CH_3OH[c]	0.0	13.8	1.80	25.29 ± 0.09	−12.45 ± 0.23
	25.4	12.95	1.80	24.41 ± .10	−15.91 ± .28
	53.4	12.2	1.79	23.68 ± .07	−18.00 ± .20
	73.1	9.16	1.62	21.35 ± .12	−24.80 ± .30
	82.0	5.66	1.15	19.51 ± .10	−30.71 ± .26
	93.7	3.15	0.714	18.15 ± .16	−35.5 ± .40
	100	1.43	0.289	19.67 ± .06	−33.00 ± .16
EtOH[d]	0.0	14.3	1.84	25.23 ± .06	−13.55 ± .16
	26.6	13.6	1.80	25.01 ± .10	−14.22 ± .28
	52.2	12.0	1.76	23.70 ± .07	−17.97 ± .21
EtOH[e]	100	~ .15	~ .039	.....	.....
Acetone[f]	0.0	14.05	1.83	24.99 ± .08	−14.22 ± .22
	12.9	12.12	1.70	24.32 ± .09	−16.30 ± .23
	24.9	9.57	1.35	24.28 ± .10	−16.88 ± .26
	52.7	5.42	0.812	23.47 ± .11	−20.16 ± .29

[a] Mean rate constants. [b] For the method of calculation and the significance of the error figures, see ref. 1c. [c] The disodium salt at 0.008 *M*. [d] The bis-tetramethylammonium salt at 0.007 *M*. [e] The sodium salt at 0.009 *M*. [f] The disodium salt at 0.005 *M*.

however, by the probability that the dicarboxylate ion partly solvolyzes to monocarboxylate ion in the more organic media. For example, in the case of phthalic acid there is a change in second ionization constant of three *pK* units as the solvent is changed from water to 80% ethanol.[7] Whatever the mechanism, the solvent effect is quite a large one. In 93.7% methanol the enthalpy of activation is reduced by 7 kcal./mole and the entropy of activation by 23 cal./mole-degree. The rate is reduced by more than a factor of four. In pure methanol the enthalpy and entropy have risen somewhat over the values for 93.7% methanol, but the rate at 100° is only about one-tenth that in water. It should be noted (Table III) that the monosodium salt racemizes at about one-fourth the rate of the disodium salt, both in water.

For the rate studies in aqueous ethanol it was necessary to use the bis-tetramethylammonium salt rather than the sodium salt and to limit the solvents to the more aqueous mixtures, because the

(6) For a general discussion of enthalpy–entropy relationships see J. E. Leffler, *J. Org. Chem.*, **20**, 1202 (1955).

(7) M. Mizutani, *Z. physik. Chem.*, **118**, 318 (1925).

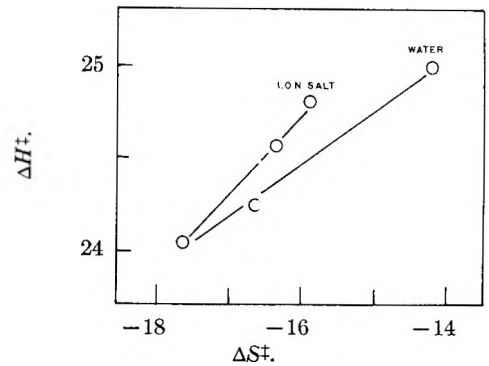

Fig. 1.—Effect of added NaCl on the activation parameters for the racemization of the disodium salt in water.

partly racemized disodium salt tended to precipitate. This particular difficulty was not encountered with the disodium salt in absolute ethanol. However a troublesome yellow discoloration eventually developed in that solvent, and the approximate rates obtained were so extremely slow (about 1/70) compared to the reaction is water that we suspect the formation of aggregates of some kind even though no precipitation occurred.[8]

Experimental

Synthesis of 2,2′-Dimethoxy-6,6′-dicarboxybiphenyl.—The synthetic scheme outlined below proved to be more convenient and gave better over-all yields than that previously reported.[8]

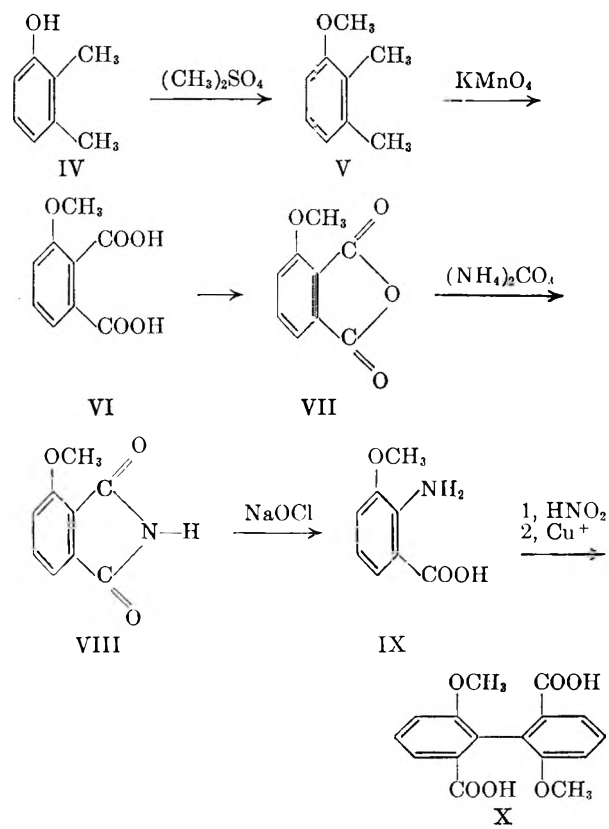

(8) In spite of several repetitions of the experiment we were unable to reproduce the much higher rate reported in the literature. The solutions were made by dissolving the acid in a slight excess of a freshly prepared solution of sodium in ethanol. *Cf.* W. Stanley, E. McMahan and R. Adams, *J. Am. Chem. Soc.*, **55**, 706 (1933).

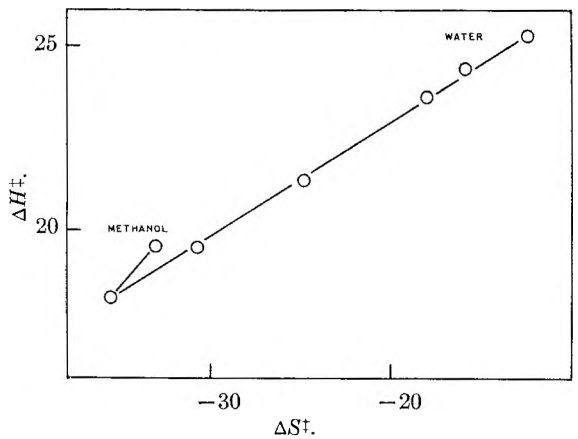

Fig. 2.—Effect of methanol on the activation parameters for the racemization of the disodium salt in water.

2,3-Dimethylanisole (V).—The phenol (89 g., 0.73 mole) and NaOH (30 g., 0.73 mole) are stirred in 200 cc. of water while dimethyl sulfate (46 g., 0.37 mole) is added during about one-half hour. After two hours of heating on the steam-bath, an additional 46 g. of dimethyl sulfate is added slowly and the mixture allowed to reflux for 15 hr. Alkali is added periodically in sufficient amount to keep the reaction basic. After cooling, the upper layer is extracted with ether, washed with alkali, dried over $CaCl_2$ and vacuum distilled; b.p. 90° at 20 mm.; yield 70 g.

3-Methoxyphthalic Acid (VI).—à la King.[9]

3-Methoxyphthalic Anhydride (VII).—The mixture of KCl and 3-methoxyphthalic acid obtained in the oxidation step is refluxed for 5 minutes in 45 cc. of acetic anhydride, filtered to remove KCl, refluxed an additional 2 hours and allowed to cool. The anhydride is then removed by filtration and washed with acetic acid. Additional product is obtained by adding ice-water to the filtrate; yield 13 g. from 20 g. of 2,3-dimethylanisole, m.p. 160–161°.

3-Methyoxyphthalimide (VIII).—The anhydride (50 g.) is fused with 60 g. of ammonium carbonate at about 220°. The heating and occasional stirring are continued until no more vapor is evolved and the melt is quiescent. The product, crystallized from methanol, melts at 219–221°; yield 45 g. (90%).

2-Amino-2-methoxybenzoic Acid (IX).—A 1.0 *N* solution of NaOCl is prepared by dissolving 35 g. of Cl_2 in one l. of cold 10% aqueous NaOH. To 50 g. of the 3-methoxyphthalimide (0.28 mole) dissolved in 200 cc. of 10% NaOH is added 800 cc. of the NaOCl solution. The solution is then heated to about 70° for 45 minutes, the color changing from yellow to red-brown. The solution is then cooled, precisely neutralized with moderately concentrated H_2SO_4 and cooled in ice. The first crop of crude brown crystals is removed and the filtrate extracted with ethyl acetate. The precipitated and the extracted fractions are combined and crystallized from aqueous ethanol; yield 28 g. (60%), light brown needles, m.p. 169–171°, not depressed by a sample made by reduction of 3-methoxy-2-nitrobenzoic acid.

2,2′-Dimethoxy-6,6′-dicarboxybiphenyl.—The following method was found to be quite superior to the Ullman reaction.

(9) H. King, *J. Chem. Soc.*, 1157 (1939).

The 2-amino-3-methoxybenzoic acid (5 g., 0.03 mole) is ground in a mortar with 15 cc. of H_2O and 10 cc. of concd. HCl, the suspension cooled to 0–5°, and to it is added a solution of 2.9 g. (0.04 mole) of $NaNO_2$ in 35 cc. of H_2O during 15 to 20 minutes. The resulting diazonium salt solution is filtered if necessary and kept below 5° until used.

The reducing agent is prepared from 15 g. (0.06 mole) of $CuSO_4 \cdot 5H_2O$ in 50 cc. of H_2O and 25 cc. of 28% ammonium hydroxide. This solution is cooled to 10° and treated (stirring) with a fresh, cold solution consisting of 4.25 g. (0.06 mole) of $H_2NOH \cdot HCl$ in 15 cc. of H_2O plus 9 cc. of 6 *N* NaOH. A gas is evolved and the color changes immediately from dark to light blue.

The diazonium salt solution is introduced, with stirring, below the surface of the reducing solution during about 20 minutes and the mixture stirred in its ice-bath for an additional 10–15 minutes. The solution is then boiled while 30 cc. of concd. HCl is carefully added. The diphenic acid, which precipitates from the cooled solution, is treated with charcoal in $NaHCO_3$ solution and recrystallized from 85 cc. of 95% ethanol; yield 2.8 g. (67%), m.p. 300–302°. It is important to use pure amino acid as the starting material.

Resolution of the 2,2′-Dimethoxy-6,6′-dicarboxydiphenyl.—The procedure of Adams[8] and Turner[10] gives the less soluble quinine salt, m.p. 176–177° (from acetone), $[\alpha]^{27}D$ +119.5° and the more soluble salt, m.p. 90–100° $[\alpha]^{27}D$ −56.7°.

A mixture of the less soluble salt (3 g.) and 40 cc. of 5% NaOH is ground in a mortar, shaken vigorously and extracted with four 15-cc. portions of cold $CHCl_3$ to remove the quinine. Acidification precipitates the *l*-acid as a white, spongy mass which after drying melts at 293–295°, $[\alpha]^{28}D$ −109°. It may be clarified if necessary by treatment with charcoal in acetone. The *d*-acid, similarly prepared, melts at 295–297°, $[\alpha]^{25}D$ +104°.

Solutions for the Kinetic Experiments.—The disodium salt solutions of the 2,2′-dimethoxy-6,6′-diphenic acid are prepared by adding a 5% excess of standard NaOH solution to the acid and diluting to a diphenate ion concentration of 0.005 *M*. For the kinetic procedure, see reference 1c.

Error Analysis.—Based on a conservative estimate of ±0.003° as the maximum error in the average of the twelve readings of the optical rotation at each point, the expected error in an individual rate constant is about ±2%. The tabulated rate constants are mean values computed from three or more individual rate constants. The expected errors in $\Delta H^{\ddagger}$ and $\Delta S^{\ddagger}$ for a *single* pair of rate constants are ±0.3 kcal./mole and ±0.9 cal./mole degree. The tabulated activation parameters should be considerably better than that since they are the result of least squares calculations using all of the rate constants (six or more points). The tabulated measures of precision have the form of probable errors and are a by-product of the least squares calculation. Although the number of points involved is too small for the individual error quantities to have much meaning, their average value for any given series of related solvents is probably a fair indication of the precision. The values for aqueous solutions seem to be about ±0.1 kcal./mole and ±0.3 cal./mole-deg. For a discussion of the shape of the error contour in the $\Delta H^{\ddagger}$, $\Delta S^{\ddagger}$ plane, see reference 1c.

Acknowledgments.—This investigation was supported in part by the Office of Ordnance Research, U. S. Army and by a Tennessee Eastman Company fellowship held by B. M. G.

(10) E. E. Turner, *ibid.*, 2348 (1928).

SOLVENT EFFECTS IN THE RACEMIZATION OF 2,2′-DIMETHOXY-6,6′-DICARBOXYDIPHENYL AND ITS DERIVATIVES[1a]

BY B. M. GRAYBILL[1b] AND J. E. LEFFLER[1c]

Contribution from the Department of Chemistry, Florida State University, Tallchassee, Florida

Received February 21, 1959

The racemization of 2,2′-dimethoxydiphenyl with carboxyl, ester or amide groups in the 6,6′-positions is subject to medium effects both on the reaction rates and on the activation parameters. The effect of a change in solvent on the rate constants can be as much as a factor of five, the effect on the enthalpy of activation as much as 9 kcal./mole, and the effect on the entropy of activation as much as 21 cal./mole-degree.

The racemization of the sodium salt of 2,2′-dimethoxy-6,6′-dicarboxydiphenyl has been found to be decelerated by salts or organic solvent components added to the aqueous solution.[2] The present paper is an extension of that work to derivatives of the biphenyl in which the barrier groups and the solvent are non-ionic but possess varying degrees of ability as donors or acceptors of hydrogen bonds. The acid, the dimethyl ester and the diamide (I–III) have been racemized in an extensive series of solvents at two temperatures.

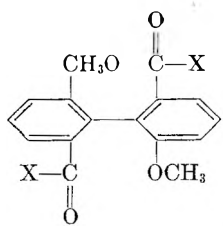

I, X = OH
II, X = OCH_3
III, X = NH_2

Solvent Effects in the Racemization of the Acid.—The rates and activation parameters for the racemization of *o,o′*-dimethoxydiphenic acid (I) have been determined in a series of 24 solvents (Table I). The solvent effects are quite complicated. The enthalpy and entropy are roughly correlated with each other, to the extent that the spread in rates is much less than it would otherwise be. However, the sequence of decreasing rates does not correspond to the sequence of decreasing or increasing activation parameters. Excluding the solvent N,N-dimethylethanolamine, the range in rate constants is about a factor of four, while $\Delta H^{\ddagger}$ and $\Delta S^{\ddagger}$ vary by 3.3 kcal. and 8 cal./mole-deg., respectively. There is some tendency for the reaction to be faster in the more polar solvents, although there is no correlation with macroscopic parameters such as the dielectric constant. Benzene added to methanol decelerates the reaction, while water accelerates it. Solubility limited the amount of water that could be added, but the acceleration is less than that produced by water in the case of the disodium salt[2]; in both cases the more aqueous solutions have the higher activation enthalpies and the less negative activation entropies. The relationship between the activation enthalpy and entropy for the methanol–benzene mixtures is N-shaped.

Within the series of pure alcohols, the order of decreasing rates is methanol>ethanol>trifluoroethanol > ethylene glycol > benzyl alcohol > isopropyl alcohol>*t*-butyl alcohol>>N,N-dimethylethanolamine. The latter solvent is unique in having a negative sign for the rotation of the *d*-acid. The rate in that solvent is somewhat slower even than that of the mono-sodium salt in water[2]; the activation energy is a little lower, but the activation entropy is very much more negative. The activation parameters for the racemization of the acid in N,N-dimethylethanolamine also deviate widely from the roughly linear relationship between the activation parameters in the other solvents. The activation entropy for the racemization of the disodium salt in pure methanol is also very large and negative.[2]

Racemization of the Acid in an Asymmetric Environment.—The *dl*-acid does not show any spontaneous resolution on heating in D-2-methyl-1-butanol; hence the rates of racemization of the

TABLE I

RACEMIZATION OF 2,2′-DIMETHOXY-6,6′-DICARBOXYDIPHENYL[a] IN VARIOUS SOLVENTS

Solvent	$k \times 10^5$, sec.$^{-1}$[b] 100°	79.4°	$\Delta H^{\ddagger}$, kcal./mole[c]	$\Delta S^{\ddagger}$, cal./mole-deg.[c]
Methanol	16.55	2.52	23.24 ± 0.06	−18.58 ± 0.17
Acetic acid	16.0	2.21	24.41 ± .12	−15.51 ± .34
Acetone	15.4	2.03	25.07 ± .13	−13.81 ± .36
Ethanol	15.0	2.18	23.88 ± .11	−17.06 ± .30
Trifluoroethanol	14.3	2.16	23.39 ± .10	−18.46 ± .28
Acetonitrile	14.1	1.95	24.45 ± .11	−15.63 ± .31
Dimethylformamide	13.8	1.81	25.12 ± .11	−13.91 ± .31
Ethylene glycol	13.6	1.78	25.14 ± .12	−13.87 ± .34
Benzyl alcohol	12.2	1.76	23.85 ± .10	−17.55 ± .26
Isopropyl alcohol	10.5	1.57	23.50 ± .11	−18.77 ± .30
Dimethylsulfoxide	10.4	1.25	26.17 ± .10	−11.65 ± .27
Tetrahydrofuran	8.99	1.32	23.72 ± .14	−18.51 ± .38
Pyridine	8.43	1.15	24.66 ± .11	−16.11 ± .30
1,2-Dimethoxyethane	7.60	1.04	24.65 ± .07	−16.34 ± .20
t-Butyl alcohol	5.93	0.709	26.31 ± .11	−12.37 ± .31
Dioxane	5.00	0.653	25.15 ± .07	−15.85 ± .20
N,N-dimethylethanolamine	0.91	1.52	22.14 ± .27	−27.29 ± .73
Methanol–benzene, wt. % benzene				
27.0	14.3	2.21	22.98 ± .11	−19.57 ± .29
52.7	12.7	1.89	23.52 ± .11	−18.36 ± .30
65.0	11.4	1.73	23.40 ± .11	−18.90 ± .32
76.9	9.67	1.40	23.87 ± .13	−17.95 ± .36
88.6	8.50	1.20	24.23 ± .11	−17.25 ± .30
Methanol–water, wt. % methanol				
70.3	18.5	2.6	24.14 ± .09	−15.93 ± .25
44.1	19.5	2.68	24.55 ± .08	−14.74 ± .21

[a] Diphenic acid concentration 0.013 *M*. [b] Mean rate constants. [c] For the significance of the probable error figures and the method of calculation, see J. E. Leffler and W. H. Graham, THIS JOURNAL, **63**, 687 (1959).

(1) (a) Presented in part at the Symposium "Solvent Effects and Reaction Mechanisms," Queen Mary College, London, July 1957; (b) Based on the doctoral dissertation of B. M. G. (c) To whom requests for reprints should be sent.

(2) J. E. Leffler and B. M. Graybill, THIS JOURNAL, **63**, 1457 (1959).

d- and *l*-isomers in this solvent must be the same. The interaction between the acid and alcohol is therefore not very stereospecific.

Solvent Effects in the Racemization of the Dimethyl Ester.—The dimethyl ester II has been racemized in 23 solvents and in the presence of HCl, sodium tetraphenylborate and trinitrobenzene (Table II). The rates vary by about a factor of two, and the activation enthalpy and entropy have ranges of 2.1 kcal./mole and 4.4 cal./mole-degree, respectively. The higher enthalpies of activation tend to be associated with the less negative entropies of activation. The more polar solvents, in which the rates at 100° range from 12.9×10^{-6} to 15.6×10^{-6} sec.$^{-1}$, give activation parameters falling on a single isokinetic line or linear enthalpy–entropy relationship.[3] However, the solvents in which the rates are in the range 12.9×10^{-6} to 8.28×10^{-6} sec.$^{-1}$ deviate from the relationship by having higher enthalpies of activation. The least polar of these solvents, for example, benzene, dioxane and carbon tetrachloride, in which the reaction is slowest, tend to give points about 0.4 kcal. above the isokinetic line. The racemization of the acid (Table I) also gives some points falling on the *same* isokinetic line, and the points representing activation parameters for the solvents in which the racemization of the acid is slow again fall above the line.

It is interesting to note that five solvents (methanol, acetic acid, acetone, ethanol and dimethylformamide) give points on the isokinetic line for *both* the ester and the acid. Of these five solvents, dimethylformamide gives the slowest reaction for the acid and the fastest for the ester, while methanol is fastest for the acid and slowest for the ester.[5] That is to say, in spite of a general tendency for both the ester and the acid to racemize more rapidly in polar solvents, within a restricted group of solvents the racemization of the acid is slowest in solvents which are hydrogen-bond acceptors and the racemization of the ester is slowest in solvents which are hydrogen-bond donors. This suggests that hydrogen bonding between the ground state of the biphenyl and the solvent may be an important factor influencing the racemization rate. The ester racemizes much more slowly in trifluoroethanol than in ethanol, whereas the acid racemizes at about the same rate in both solvents.

Symmetrical trinitrobenzene added to a chloroform solution of the ester accelerates the racemization. The acceleration by 0.23 *M* TNB amounts to about 13 to 16%, and is accompanied by a lowering of the entropy of activation. Although the effect is small it is in the expected direction. A hindered biphenyl in its ground state will not form pi-complexes[4] but a planar transition state might well do so, especially if it does not possess very much kinetic energy. Such a relatively static transition state is reasonable if the delocalization energy due to conjugation between the rings actually produces a metastable intermediate; in that case the transition state can be regarded as consisting of *moderately* excited vibrational levels of the intermediate rather than *highly* excited vibrational levels of the ground state.

Solvent Effects in the Racemization of the Diamide III.—The racemization of the diamide III is considerably slower than that of the other derivatives and the rates have been measured at higher temperatures (Table III). The number of solvents studied was limited by the solubility of the diamide. It is almost insoluble in benzene, carbon tetrachloride and dioxane, and only slightly soluble in isopropyl alcohol, *t*-butyl alcohol, ethylene glycol and chloroform. The range in rate constants at the temperatures used is about a factor of five, but the variation in the activation parameters is remarkable: about 9 kcal./mole and 21 cal./mole-degree. The variation in rate constant as the solvent is changed would be extremely large if it were not for the high degree of correlation between the enthalpies and entropies of activation (Fig. 1).

As in the case of the acid and the ester, the five solvents acetic acid, methanol, ethanol, acetone and dimethylformamide give activation parameters falling at least roughly on an isokinetic line. The isokinetic temperature, or slope of the $\Delta H^{\ddagger}$, $\Delta S^{\ddagger}$ relationship is about 120° or 20° higher than that for the ester and acid. The order of increasing rate for the racemization of the diamide in this

TABLE II

RACEMIZATION OF THE DIMETHYL ESTER OF 2,2′-DIMETHOXY-6,6′-DICARBOXYDIPHENYL[a] IN VARIOUS SOLVENTS

Solvent	$k \times 10^6$, sec.$^{-1}$[b] 100°	79.4°	$\Delta H^{\ddagger}$, kcal./mole[c]	$\Delta S^{\ddagger}$, cal./mole-deg.[c]
Dimethylformamide	15.6	2.19	24.25 ± 0.08	−16.00 ± 0.22
Nitrobenzene	14.9	2.03	24.65 ± .10	−14.99 ± .26
Benzonitrile	14.5	2.00	24.53 ± .11	−15.37 ± .31
Isopropyl alcohol	14.4	2.02	24.30 ± .13	−16.02 ± .35
Dimethyl sulfoxide	14.3	1.92	24.86 ± .06	−14.53 ± .18
Acetone	14.2	2.00	24.21 ± .11	−16.27 ± .31
Ethanol	14.0	1.95	24.41 ± .08	−15.76 ± .22
t-Butyl alcohol	13.7	2.07	23.32 ± .11	−18.73 ± .31
H_2O 30 wt. % Methanol 70 wt. %	13.8	1.97	24.11 ± .12	−16.59 ± .32
Methanol	13.7	1.94	24.12 ± .10	−16.58 ± .27
Acetic acid	13.6	1.91	24.26 ± .09	−16.24 ± .26
Propionitrile	12.9	1.86	23.98 ± .14	−17.07 ± .37
Ethylene glycol	12.9	1.81	24.30 ± .07	−16.23 ± .18
Pyridine	11.5	1.60	24.35 ± .15	−16.34 ± 41
1,2-Dimethoxyethane	11.3	1.64	23.86 ± .12	−17.68 ± .34
Trifluoroethanol	10.8	1.50	24.41 ± .11	−16.28 ± .29
Acetonitrile	10.4	1.42	24.63 ± .11	−15.80 ± .31
Anisole	10.2	1.41	24.45 ± .10	−16.28 ± .26
Chlorobenzene	9.87	1.32	24.81 ± .13	−15.40 ± .36
Benzene	9.45	1.31	24.40 ± .11	−16.57 ± .30
Dioxane	9.14	1.19	25.25 ± .12	−14.38 ± .33
Chloroform	8.63	1.16	24.77 ± .08	−15.76 ± .21
Carbon tetrachloride	8.28	1.12	24.62 ± .12	−16.25 ± .32
Methanol, satd. with HCl plus 0.11 *M* sodium tetraphenylborate	13.01	1.86	24.08 ± .11	−16.79 ± .30
	13.94	1.99	24.07 ± .16	−16.68 ± .45
Chloroform plus				
0.012 *M* TNB[d]	8.60	1.18	24.56 ± .11	−16.33 ± .31
0.14 *M* TNB	8.90	1.22	24.60 ± .06	−16.17 ± .16
0.23 *M* TNB	9.72	1.35	24.40 ± .13	−16.52 ± .35
Acetonitrile plus				
0.07 *M* TNF[e]	10.6	1.46	24.60 ± .17	−15.80 ± .46

[a] Concentration of the ester 0.013 *M*. [b] Mean rate constants. [c] For the significance of the probable error figures and the method of calculation, see J. E. Leffler and W. H. Graham, THIS JOURNAL, **63**, 687 (1959). [d] 1,3,5-Trinitrobenzene. [e] Tetranitrofluorenone.

(3) J. E. Leffler, *J. Org. Chem.*, **20**, 1202 (1955).

(4) C. E. Castro, L. J. Andrews and R. M. Keefer, *J. Am. Chem. Soc.*, **80**, 2322 (1958).

TABLE III

RACEMIZATION OF THE DIAMIDE OF 2,2′-DIMETHOXY-6,6′-DICARBOXYDIPHENYL[a] IN VARIOUS SOLVENTS

Solvent	$k \times 10^5$, sec.$^{-1}$[b] 108.9°	90.5°	$\Delta H^{\ddagger}$, kcal./mole[c]	$\Delta S^{\ddagger}$, cal./mole-deg.[c]
Acetic acid	20.3	4.60	21.49 ± 0.21	−28.81 ± 0.57
Methanol	16.8	2.73	26.51 ± .13	−16.04 ± .36
Ethanol	15.6	2.44	27.12 ± .33	−14.61 ± .88
Acetone	7.73	0.958	30.59 ± .14	− 6.91 ± .37
Dimethylformamide	7.68	1.49	23.90 ± .21	−24.45 ± .55
Acetonitrile	7.11	1.27	25.07 ± .26	−21.53 ± .69
Dimethyl sulfoxide	5.41	0.950	25.33 ± .39	−21.40 ± 1.0
52.6% benzene, 47.4% methanol[d]	14.1	2.25	26.79 ± .08	−15.68 ± .31
69% benzene, 31% methanol[d]	13.5	2.15	26.89 ± .12	−15.49 ± .31
55.9% water, 44.1% methanol[d]	27.9	4.24	27.53 ± .24	−12.37 ± .63

[a] Concentration of the diamine 0.02 *M*. [b] Mean rate constants. [c] For the method of calculation and the significance of probable error figures, see J. E. Leffler and W. H. Graham, THIS JOURNAL, 63, 687 (1959). [d] Weight per cent.

series of five solvents is almost the same as that for the acid and the reverse of that for the ester, suggesting that the ability of the amide hydrogen atoms to form hydrogen bonds is an important factor.[5] There also seems to be some correlation between the rate and the polarity of the medium, since, as is also the case for the acid and the ester, dilution of a methanolic solution with benzene decelerates the reaction while dilution with water accelerates it.

The most drastic medium effect on the racemization of the diamide is the effect of its own crystal lattice. Thus, the *l*-diamide has a characteristic melting point, 227–228°, but quickly resolidifies and remelts at 270–271°, the melting point of the *dl*-diamide.[6] In any fluid medium above 200° the diamide would racemize instantaneously.

Experimental

The *d*- and *l*-2,2′-dimethoxy-6,6′-dicarboxydiphenyls were made as described in the previous paper of this series.[2] The purification of the solvents and the details of the kinetic measurements have also been reported previously.[7]

Dimethyl Ester of 2,2′-Dimethoxy-6,6′-dicarboxydiphenyl.—To 25 cc. of 50% aqueous KOH and 80 cc. of ether cooled to 5° is added 7 g. (0.068 mole) of N-nitrosomethylurea with shaking. The diazomethane and about two-thirds of the ether are distilled over into a receiver containing 4.0 g. of the optically active acid and 40 cc. of ether. The acid and ethereal diazomethane are allowed to stand until all of the acid has dissolved and the yellow color is gone. Filtration and removal of the ether gives the dimethyl ester which is recrystallized from methanol–water to 3.9 g. of fine white needles, m.p. 100–101°, $[\alpha]^{25}D$ +152° (acetone), +134° (methanol). The racemic dimethyl ester melts at 134–136°.

Diamide of 2,2′-Dimethoxy-6,6′-dicarboxydiphenyl.—The *l*-diamide[6] after recrystallization from ethyl acetate melts at 227–228° but quickly resolidifies and remelts at 270–271°.

Anal. Found: C, 63.71; H, 5.46. Calcd.: C, 63.99; H, 5.37. $[\alpha]^{24}D$ −79° (methanol), −69° (acetic acid).

Asymmetric Environment Experiments.—The *dl*- acid, 0.15 g., is diluted to 20 cc. with D-2-methyl-1-butanol, filtered, the rotation measured and the solution heated for 70 hours at 100°. Initial polarimeter reading 167.0992° at 24.2°; final reading 167.0950° at 24.3°.

Error Analysis.—For a discussion of the expected errors and the tabulated measures of precision see references 2 and 7. The precision of the data for the acid and ester is comparable to that of the data for the salts and agrees with the expected error. The data for the diamide are somewhat less precise than expected on the basis of the known sources of error; however, the times of heating were longer and the temperatures higher than in the case of the acid and the ester.

Acknowledgment.—This investigation was supported in part by the Office of Ordnance Research, U. S. Army and by a Tennessee Eastman Company fellowship held by B. M. G.

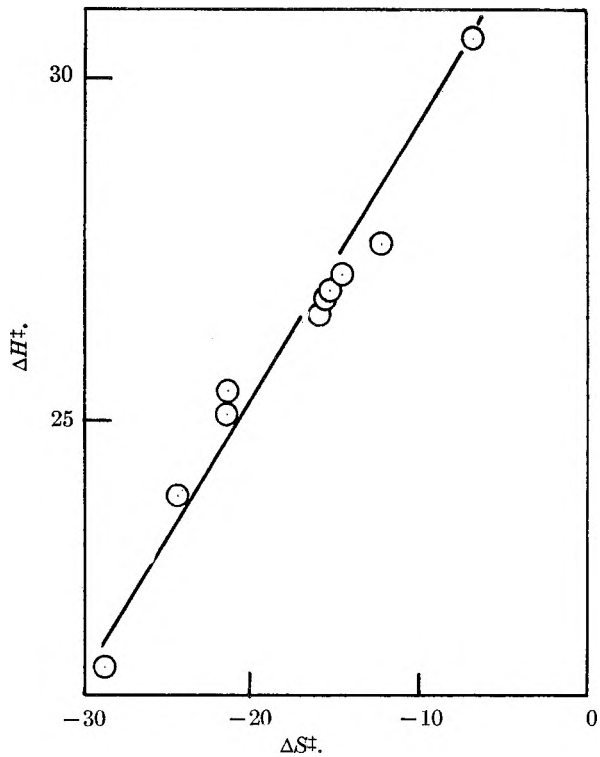

Fig. 1.—The correlation between the activation parameters for the racemization of the diamide in various solvents.

(5) These rates do not fall in the same order as the enthalpies of activation because the working temperature is so close to the approximate isokinetic temperature that the differences in rate are largely the result of deviations from a perfect isokinetic relationship.

(6) W. Stanley, E. McMahan and R. Adams, *J. Am. Chem. Soc.*, **55**, 706 (1933).

(7) J. E. Leffler and W. H. Graham, THIS JOURNAL, **63**, 687 (1959); W. H. Graham and J. E. Leffler, *ibid.*, **63**, 1274 (1959).

ON THE EQUILIBRIUM CONSTANT FOR LOOSELY BOUND MOLECULES

BY DOYLE BRITTON

School of Chemistry, University of Minnesota, Minneapolis 14, Minn.

Received February 23, 1959

Bunker and Davidson, and Stogryn and Hirschfelder have recently described calculations of the equilibrium constant for loosely bound molecules using the methods of classical statistical mechanics. Alternative approximate methods of calculating this equilibrium constant using quantum mechanical partition functions for the species involved are described here.

In a recent paper,[1] Bunker and Davidson have proposed a theory to account for the observed rates of atom recombination reactions. The reaction in question is

$$X + X + M \longrightarrow X_2 + M \qquad (1)$$

$$\frac{d(X_2)}{dt} = k_R(M)(X)^2 \qquad (2)$$

Equation 2 defines the rate constant for recombination. The theory describes the dependence of k_R upon the temperature and upon the third body, M. The essential features of the theory are that intermediate molecules, MX, are formed from the third body molecules and the atoms in question, that these molecules are present in their equilibrium concentration, and that the equilibrium constant for the formation of these molecules can be calculated by the methods of classical statistical mechanics. Alternative approximate methods of calculating this equilibrium constant using quantum mechanical partition functions for the species involved are described here.[2]

The equilibrium constant for the formation of MX

$$M + X \rightleftharpoons MX \qquad K = \frac{(MX)}{(M)(X)} \qquad (3)$$

is given by the expression

$$K = \frac{Q_{MX}}{Q_M Q_X} e^{\epsilon_0/kT} \qquad (4)$$

where Q is the partition function of the species in question and ϵ_0 is the binding energy of the molecule MX. If it is assumed that M is a monatomic species, then the partition functions Q_M and Q_X involve only translational states. For the partition function Q_{MX}, rotation and vibration must also be considered. It is in the evaluation of Q_{MX} that the three approximations differ.

First Approximation: Rigid Rotor, Harmonic Oscillator.—The translational partition function is

$$Q_t = \left(\frac{2\pi mkT}{h^2}\right)^{3/2} \text{molecules/cc.} \qquad (5)$$

The rotational partition function for a rigid rotor is usually written

$$Q_r = \sum_{K=0}^{\infty} (2K + 1)e^{-K(K+1)\epsilon_r/kT} \qquad (6)$$

If ϵ_r is small compared to kT, as is true here, then the sum may be replaced by an integral.

$$Q_r = \int_{K=0}^{\infty} (2K + 1)e^{-K(K+1)\epsilon_r/kT} = \frac{kT}{\epsilon_r} \qquad (7)$$

To allow for the possibility of homonuclear molecules, Q_r as given in equation 7 should be divided by the symmetry number of the molecule σ. However, it should be noted that the rotational quantum number K cannot increase indefinitely since it is unreasonable to allow the rotational energy to be greater than the binding energy for MX.[3] This means that there is a maximum value of K, given by

$$K_m(K_m + 1)\epsilon_r = \epsilon_0 \qquad (8)$$

Using the value of K as an upper limit to the integral in equation 7 yields the correct expression[4] (in which the symmetry number has been included).

$$Q_r = \frac{kT}{\sigma\epsilon_r}(1 - e^{-\epsilon_0/kT}) \qquad (9)$$

The vibrational partition function for a harmonic oscillator is

$$Q_v = \sum_{v=0}^{\infty} e^{-\epsilon_v(v+1/2)/kT} \qquad (10)$$

which can be summed directly to give

$$Q_v = \frac{e^{-\epsilon_v/2kT}}{1 - e^{-\epsilon_v/kT}} \qquad (11)$$

Again, however, the quantum number v cannot increase indefinitely. There is a maximum value given by

$$\epsilon_v(v_m + 1/2) = \epsilon_0 \qquad (12)$$

If this upper limit is placed on the sum in 10, then

$$Q_v = \frac{e^{-\epsilon_v/2kt} - e^{-(\epsilon_0+\epsilon_v)/kT}}{1 - e^{-\epsilon_v/kT}} \qquad (13)$$

If ϵ_v is small compared to ϵ_0 and kT, then

$$Q_v \cong \frac{kT}{\epsilon_v}(1 - e^{-\epsilon_0/kT}) \qquad (14)$$

In order to evaluate equation 4 for the equilibrium constant, we need to know ϵ_0, ϵ_r and ϵ_v. The first of these can be obtained from virial coefficient data[1,5] which also give the distance of closest ap-

(1) D. L. Bunker and N. Davidson, *J. Am. Chem. Soc.*, **80**, 5090 (1958).

(2) This problem has also been considered by D. E. Stogryn and J. O. Hirschfelder ("The Contribution of Bound, Metastable and Free Molecules to the Second Virial Coefficient," WIS-ONR-32a, N7onr-28511, 4 November 1958) who have carried out a more complete calculation by the methods of classical statistical mechanics. The first two approximations given here more closely parallel the treatment of Bunker and Davidson; the third, that of Stogryn and Hirschfelder. I would like to thank Dr. Hirschfelder for making his work available to me.

(3) This corresponds to the crucial assumption of Bunker and Davidson that the integral over phase space should include only those parts of momentum space which correspond to a bound molecule.

(4) In the cases usually encountered $\epsilon_0 >> kT$ so that the term in parentheses is equal to unity. This is not the case here, however.

(5) J. O. Hirschfelder, C. F. Curtiss and R. B. Bird, "Molecular Theory of Gases and Liquids," John Wiley and Sons, New York, 1954, pp. 1110–1112.

proach, r_s. (Both ϵ_0 and r_s were obtained assuming a Lennard-Jones potential function describes the interaction between M and X.) The quantum of rotational energy

$$\epsilon_r = \frac{\hbar^2}{2\mu r_0^2} \tag{15}$$

where μ is the reduced mass of the molecule and r_0 (which is equal to $2^{1/6}r_s$) is the equilibrium internuclear distance. Rather than use the Lennard-Jones function, it is more convenient to use a Morse potential function

$$\epsilon(r) = \epsilon_0[1 - e^{\alpha(1-r/r_0)}]^2 \tag{16}$$

where α is a parameter which determines the shape of the curve. The Morse curve can be adjusted to be roughly the same shape as the Lennard-Jones by choosing a suitable value of α. If the behavior of the molecule is described by a Morse function, then[6]

$$\epsilon_v = 2\alpha(\epsilon_0\epsilon_r)^{1/2} \tag{17}$$

The results in equations 5, 9 and 14 can now be substituted into equation 4

$$K = \frac{1}{\sigma}\left(\frac{h^2}{2\pi\mu kT}\right)^{3/2}\frac{(kT)^2}{\epsilon_r\epsilon_v}(1 - e^{-\epsilon_0/kT})^2\, e^{\epsilon_0/kT} \tag{18}$$

This can be simplified further if the exponentials are expanded into series and the various series are combined.

$$K = \frac{4\pi^{3/2}}{\sigma\alpha} r_0^3 \left(\frac{\epsilon_0}{kT}\right)^{3/2}\left[1 + 0\left(\frac{\epsilon_0}{kT}\right) + \frac{1}{12}\left(\frac{\epsilon_0}{kT}\right)^2 \cdots\right] \tag{19}$$

This may be compared with the result of Bunker and Davidson[1]

$$K = \frac{8\pi^{1/2}}{3\sigma} r_s^3 \left(\frac{\epsilon_0}{kT}\right)^{3/2}\left[1 - \frac{4}{15}\left(\frac{\epsilon_0}{kT}\right) \cdots\right] \tag{20}$$

Since $r_0^3 = 2^{1/2}r_s^3$, the terms outside the series are the same if $\alpha = 3\pi/\sqrt{2} = 6.67$. For comparison: if α is evaluated by matching the curvature of the Morse curve at r_0 to that of the Lennard-Jones at r_0, then $\alpha = 6$; if α is evaluated by making the Morse potential have a value of ϵ_0 at $r = r_s$, then $\alpha = \ln^2/(1 - 2^{-1/6}) = 6.38$. It can be seen that both expressions show the same temperature dependence at high temperatures and have about the same absolute value. At temperatures where $\epsilon_0 \sim kT$, equation 19 gives a poor picture of the temperature dependence.

The separation of the vibrational and rotational parts of the partition function involves two approximations.[7] The first of these is the familiar one that the energy can be expressed as a sum of terms involving the rotational quantum number only and terms involving the vibrational quantum number only, and that there are no cross terms. This is discussed more fully in the third part of this paper. The second, which is considered in both of the other parts, is that the limits to be taken in summing the separated partition functions are independent. This is clearly not true and is at first glance a poor assumption since at high vibrational levels we are clearly counting too many rotational states. A rough estimate would be that Q_r is too large by a factor of two. However, this is balanced, somewhat, by another approximation, that the vibrational energy levels are evenly spaced. If the Morse function is used, the correct distribution of vibrational states is[8]

$$\epsilon(v) = \epsilon_v(v + 1/2) - \frac{\epsilon_v^2}{4\epsilon_0}(v + 1/2)^2 \tag{21}$$

This leads to just twice as many levels as the harmonic oscillator does, so that Q_v is underestimated by a factor of two if the vibrational excitation is essentially complete, as is the case in these weak complexes. At high temperatures the partition function for vibration and rotation depends only upon the total number of states available to the molecule, while at lower temperatures the distribution of these states also matters. It is therefore reasonable that the derivation described here gives an answer which is close to correct at high temperatures and which is poor at low temperatures.

The above arguments as well as those that follow also apply to complexes between molecules if one assumes that the complexes are loose enough so that the two molecules are free to rotate within the complex. In this case all the internal parts of the partition functions of the separated molecules will also appear in the partition function of the complex and will cancel out.

Second Approximation: Rigid Rotor, Morse Oscillator.—In this approximation it will be assumed that the rotational energy levels are those of the rigid rotor, the vibrational levels are those for a molecule that is described by the Morse potential function, and that the total internal energy cannot exceed the binding energy for the molecule. This last restriction means that the rotational and vibrational partition functions may not be summed independently. As usual the sum over the rotational states is approximated by an integral.

$$Q_{rv} = \frac{1}{\sigma}\sum_{v=0}^{v_m}\left[e^{-1/kT\left[\epsilon_v(v+1/2) - \frac{\epsilon_v^2}{\epsilon_0}(v+1/2)^2\right]}\int_{K=0}^{K_m} e^{-\frac{\epsilon_r}{kT}K(K+1)}(2K+1)\,dK\right] \tag{22}$$

The upper limits indicated are given by

$$v_m = 2\frac{\epsilon_0}{\epsilon_v} - \frac{1}{2} \tag{23a}$$

$$K_m(K_m + 1) = \frac{1}{\epsilon_r}\left[\epsilon_0 - \epsilon_v(v + 1/2) + \frac{\epsilon_v^2}{4}(v + 1/2)^2\right] \tag{23b}$$

The integral in equation 22 can be evaluated exactly. The resulting summation can be performed by expanding the exponentials in power series and summing the individual terms. The result is

$$Q_{rv} = \frac{2\epsilon_0^2}{3\sigma\epsilon_r\epsilon_v}\left[1 - 0.700\frac{\epsilon_0}{kT} + 0.271\left(\frac{\epsilon_0}{kT}\right)^2 - 0.074\left(\frac{\epsilon_0}{kT}\right)^3 \cdots\right] \tag{24}$$

Each of the coefficients in this power series should be a finite power series in ϵ_v/ϵ_0. The constant terms are those given, the terms in ϵ_v/ϵ_0 are all exactly zero and the terms in $(\epsilon_v/\epsilon_0)^2$ and higher only contribute a per cent. or so and are omitted.[9]

(6) A. G. Gaydon, "Dissociation Energies," Dover Publications, Inc., New York, N. Y., 1950, p. 29.

(7) I would like to thank Professor N. Davidson for a clarifying discussion on this point and also for some good advice.

(8) G. Herzberg, "Spectra of Diatomic Molecules," 2nd Ed., D. Van Nostrand Co., Inc., New York, N. Y., 1950, p. 101.

If the value of Q_{rv} just obtained is used to evaluate the equilibrium constant, then

$$K = \frac{8\pi^{3/2}}{3\sigma\alpha} r_0^3 \left(\frac{\epsilon_0}{kT}\right)^{3/2} \left[1 + 0.300 \frac{\epsilon_0}{kT} + 0.071 \left(\frac{\epsilon_0}{kT}\right)^2 + 0.014 \left(\frac{\epsilon_0}{kT}\right)^3 \ldots\right] \quad (25)$$

This may be compared with equations 19 and 20, and with the result of Stogryn and Hirschfelder[2]

$$K = \frac{128}{45\sigma} \pi^{1/2} r_e^3 \left(\frac{\epsilon_0}{kT}\right)^{3/2} \left[1 + 0.254 \frac{\epsilon_0}{kT} + 0.057 \left(\frac{\epsilon_0}{kT}\right)^2 + 0.011 \left(\frac{\epsilon_0}{kT}\right)^3 \ldots\right] \quad (26)$$

The leading term in equation 25, which corresponds to the high temperature limit, is about 25% smaller than the result of Bunker and Davidson, and about 30% smaller than the result of Stogryn and Hirschfelder. The power series which gives the change in the temperature dependence at lower temperatures is about the same as both of their results.

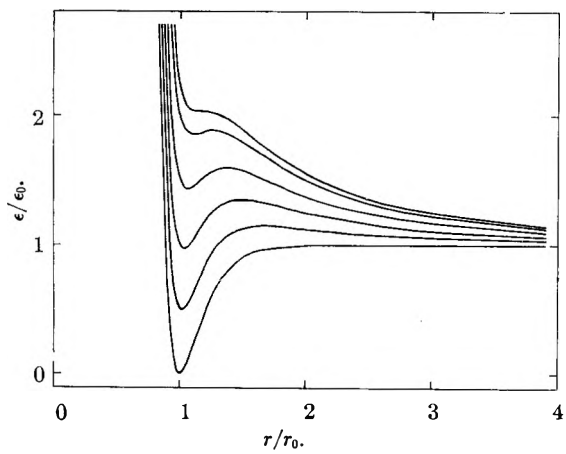

Fig. 1.—The Morse potential function plus the centrifugal potential for various rotational states. From the bottom the values of $\epsilon_r K(K+1)/\epsilon_0$ are 0, 1/2, 1, 3/2, 2 and 2.215. The last is the highest rotational state for which the potential function shows a minimum.

Third Approximation: The Potential Function of the Molecule Given by the Morse Potential Plus a Centrifugal Potential.—As Stogryn and Hirschfelder have pointed out,[2] a calculation of an equilibrium constant of this nature should be based on a potential function which includes the centrifugal potential for all rotational levels above the ground level. If this were included with the Morse potential given in equation 16, the proper potential function for the Kth level[10] would be

$$\epsilon(r,K) = \epsilon_0[1 - e^{\alpha(1-r/r_0)}]^2 + \frac{\epsilon_r K(K+1)}{(r/r_0)^2} \quad (27)$$

This potential function is pictured in Fig. 1 for a Morse potential with $\alpha = 6$, and for various values of K. As inspection of this figure will show, the inclusion of the centrifugal potential gives rise to the possibility of metastable molecules; that is, molecules with total internal energy greater than ϵ_0 but which can only dissociate by leakage through the barrier caused by the centrifugal potential. Stogryn and Hirschfelder have obtained equilibrium constants for both the bound and metastable molecules by integrals over classical phase space. Similar calculations will be made here in terms of the quantum mechanical partition functions.

The wave equation has been solved for a molecule with the potential energy given by equation 27 by Morse,[11] who assumed that r remained constant at r_0 in the second term in the potential energy expression, and by Pekeris[12] who obtained a more exact solution in the neighborhood of the minimum of the potential. Both of these results give the energy of the molecule as having the following relationship to the quantum numbers K and v.

$$\epsilon = \epsilon_v(v + 1/2) - \frac{\epsilon_v^2}{4\epsilon_0}(v + 1/2)^2 - \gamma \frac{\epsilon_v \epsilon_r}{\epsilon_0}(v + 1/2) K(K+1) + \frac{\epsilon_r}{\epsilon_0} K(K+1) - \delta \frac{\epsilon_r^2}{\epsilon_0} K^2(K+1)^2 \quad (28)$$

Morse found $\gamma = 1/2$ and Pekeris found $\gamma = 3(\alpha+1)/2\alpha^2 = 5/24$ for $\alpha = 6$. Both found $\delta = 1/\alpha_2 = 1/36$. In the calculation given here, $\gamma = 2/5$ and $\delta = 1/30$ will be used, for reasons which will be developed below.

In Fig. 2 the values of the maxima and minima in the potential energy curves of Fig. 1 have been plotted as a function of $\epsilon_r K(K+1)/\epsilon_0$. The value of the energy at the minimum should be given by equation 28 with $(v + 1/2)$ set equal to zero. The fit here at high energies is much improved if $\delta = 1/30$ is used rather than $\delta = 1/36$. For the ground rotational level, the maximum value of the vibrational quantum number v occurs at the point where $\partial\epsilon/\partial v = 0$. If this same criterion is chosen to find the maximum value of v for excited rotational levels, and this is a convenient but purely arbitrary choice to make, then $\gamma = 2/5$ gives

$$(v_{max} + 1/2)\epsilon_v = 2\epsilon_0 - \frac{4}{5}\epsilon_r K(K+1) \quad (29)$$

which, when substituted back into equation 28, gives a good approximation to the position of the maxima, as Fig. 2 shows. It should be noted that this choice for the upper limit of v gives the maximum possible number of vibrational levels.

The partition function that we wish to evaluate is

$$Q_{rv} = \sum_v \sum_K (2K+1) e^{-\epsilon(v,K)/kT} \quad (30)$$

where $\epsilon(v,K)$ is given by equation 28. This is evaluated by completely expanding the exponential, replacing the sum over K by an integral, integrating between limits which depend upon v, and finally summing the individual terms of the expansion over v.[9] These sums are tedious to obtain, the more so as the exponent of ϵ_0/kT becomes larger, but there are no unusual features involved in the summations so the details will be omitted here and only the final answers given.

(9) If the sum over rotational states is replaced by an integral, as in equation 22, then the order of the summation and integration must be considered. The order given is correct. If the summation over v is performed first (with the appropriate changes in the limits) then errors of the order of ϵ_v/ϵ_0 are introduced in each of the coefficients in the series.

(10) The Kth level is that level where the square of the total angular momentum due to the rotation of the molecule equals $K(K+1)\hbar^2$. The energy must be determined for this state by solving the radial wave equation.

(11) P. M. Morse, *Phys. Rev.*, **34**, 57 (1929).

(12) C. L. Pekeris, *ibid.*, **45**, 98 (1934).

Equation 30 has been evaluated first over all energy levels where $\epsilon \leq \epsilon_0$. This corresponds to the bound molecule and gives

$$Q_{rv} = \frac{0.910\epsilon_0^2}{\sigma\epsilon_r\epsilon_v}\left[1 - 0.735\frac{\epsilon_0}{kT} + 0.292\left(\frac{\epsilon_0}{kT}\right)^2 + 0.082\left(\frac{\epsilon_0}{kT}\right)^3 \ldots\right] \quad (31)$$

This in turn gives

$$K = \frac{3.376}{\sigma} r_0^3 \left(\frac{\epsilon_0}{kT}\right)^{3/2}\left[1 + 0.265\frac{\epsilon_0}{kT} + 0.057\left(\frac{\epsilon_0}{kT}\right)^2 + 0.009\left(\frac{\epsilon_0}{kT}\right)^3 \ldots\right] \quad (32)$$

These are both assuming $\alpha = 6, \gamma = 2/5, \delta = 1/30$, and with each coefficient evaluated to about 1% accuracy. The individual coefficients should be finite power series in ϵ_v/ϵ_0 but the first power terms are all zero and the higher terms have been omitted as contributing 1% or less to the total. Equations 24 and 25, which were special cases of this solution with $\gamma = \delta = 0$, gave about the same result. The leading term in equation 32 agrees to within about 1% with that of Bunker and Davidson (equation 20), and is about 6% less than that of Stogryn and Hirschfelder (equation 26). The series are almost identical.[13]

Equation 30 also has been evaluated over all energy levels with energy greater than ϵ_0 but less than the height of the centrifugal barrier, that is, over the region in Fig. 2 indicated as the metastable region.

$$Q_{rv}^m = \frac{1.590\epsilon_0^2}{\sigma\epsilon_r\epsilon_v}\left[1 - 1.359\frac{\epsilon_0}{kT} + 0.965\left(\frac{\epsilon_0}{kT}\right)^2 - 0.475\left(\frac{\epsilon_0}{kT}\right)^3 \ldots\right] \quad (33)$$

$$K^m = \frac{5.892}{\sigma} r_0^3 \left(\frac{\epsilon_0}{kT}\right)^{3/2}\left[1 - 0.369\frac{\epsilon_0}{kT} + 0.106\left(\frac{\epsilon_0}{kT}\right)^2 + 0.023\left(\frac{\epsilon_0}{kT}\right)^3 \ldots\right] \quad (34)$$

This may be compared with the result of Stogryn and Hirschfelder

$$K^m = \frac{1.016}{\sigma}\pi^{1/2} r_a^3 \left(\frac{\epsilon_0}{kT}\right)^{3/2}\left[1 - 0.190\left(\frac{\epsilon_0}{kT}\right) + 0.032\left(\frac{\epsilon_0}{kT}\right)^3 - 0.005\left(\frac{\epsilon_0}{kT}\right)^3 \ldots\right] \quad (35)$$

In calculating K^m the assumption was made here that the energy levels for the metastable molecules were given by the same equation that gave the energy levels for the bound molecules, and that there was no leakage through the barrier to dissociation. If these assumptions are made, it appears intuitively correct that the partition function for vibration and rotation should have the same temperature dependence at high temperatures as the partition function for the bound molecules, since in both cases the partition function approaches the total number of vibrational–rotational states. This is the result that was obtained, and at the high temperature limit the equilibrium constant for the formation of metastable molecules is slightly greater than that for stable molecules. The relative importance of the metastable molecules decreases at lower temperatures. This is essentially the same result as that of Stogryn and Hirschfelder except that the numerical agreement is much worse than was the case with the equilibrium constant for the bound molecules.

(13) It should be mentioned that Stogryn and Hirschfelder give the coefficients for the first eight terms in this series and also for the first eight terms in the series for the metastable molecules.

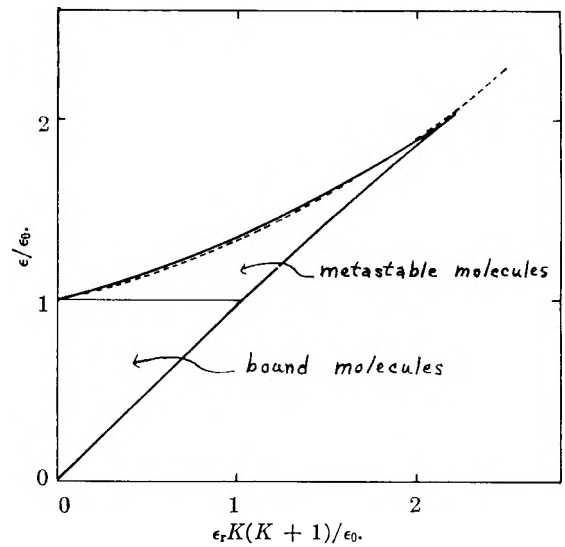

Fig. 2.—The region of summation for the vibrational–rotational partition function: heavy line, limits as given by the potential curves in Fig. 1; dashed line, limits given by equation 28 with $\gamma = 2/5$ and $\delta = 1/30$. Light line, boundary between the region of bound molecules and that of metastable molecules.

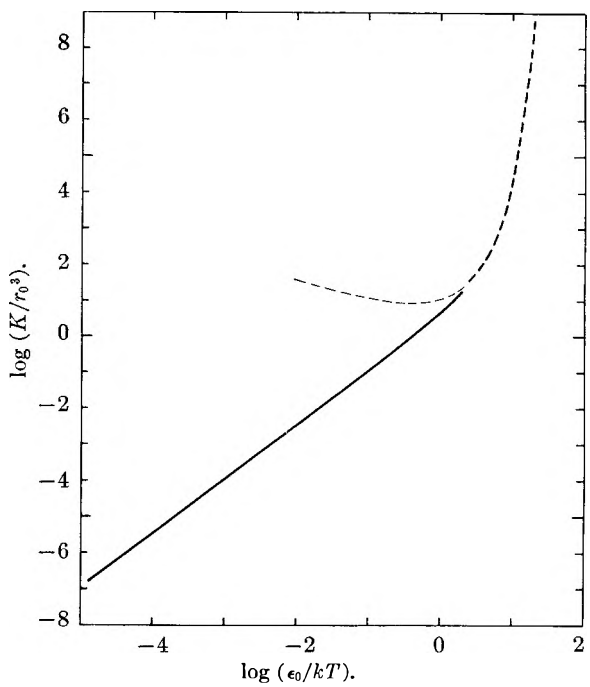

Fig. 3.—The equilibrium constant for bound molecules as a function of temperature: solid line, value at high temperatures given by equation 32; dashed line, value at low temperatures given by equation 36.

Further Discussion.—The calculations made above for the bound molecules all agree quite well with the results of the classical statistical mechanical derivations at temperatures where $\epsilon_0 < kT$, and have the advantage that they use functions which are in general more familiar. There is one additional advantage in this approach which appears when an attempt is made to carry out similar calculations which will be good at lower temperatures.

If $\epsilon_0 < kT$, then the high rotational and vibrational states become unimportant, and the upper limits for the sums can be taken as infinite with very little error. In this case, the expressions for the partition functions are the usual ones, given in equations 7 and 11, and the equilibrium constant is

$$K = \frac{2}{3\sigma}\pi^{3/2} r_0^3 \left(\frac{\epsilon_0}{kT}\right)^{1/2} \frac{\epsilon_v}{\epsilon_0} \left(\frac{e^{(\epsilon_0-\epsilon_v/2)/kT}}{1-e^{-\epsilon_v/kT}}\right) \quad (36)$$

where this has been put in a form to resemble equations 19, 25 and 32. Figure 3 shows K as calculated by equation 32 displayed with K as calculated by equation 36. It can be seen that they join quite smoothly in the neighborhood of $\epsilon_0 = kT$.

Acknowledgments.—I wish to thank Professors Z Z. Hugus and Rufus Lumry for helpful discussions. This work was sponsored in part by the Office of Ordnance Research, U. S. Army.

THE GAS PHASE FLUORINATION OF HYDROGEN–METHANE MIXTURES

BY P. D. MERCER AND H. O. PRITCHARD

Chemistry Department, University of Manchester, Manchester 13

Received February 25, 1959

A study of the reaction between fluorine gas and hydrogen–methane mixtures has been made over a temperature range from 25–150° in both inconel and quartz reaction vessels. The kinetics are complicated by surface effects but may reasonably be interpreted in terms of a chain mechanism in which the rate-determining steps are $F + H_2 \rightarrow HF + H$ (1) and $F + CH_4 \rightarrow HF + CH_3$ (2) with $E_1 - E_2 \approx 0.5 \pm 0.2$ kcal./mole.

The fluorination of a hydrocarbon such as methane may be expected to take place by one of two mechanisms. The first, which is analogous to the chlorination and bromination reactions, may be represented by the scheme

$$F_2 \longrightarrow F + F \quad (1)$$
$$F + CH_4 \longrightarrow HF + CH_3 \quad (2)$$
$$CH_2 + F_2 \longrightarrow CH_3F + F \quad (3), \text{ etc.}$$

Steps 2 and 3 are both highly exothermic and should have small or zero activation energies. Because of the extreme reactivity of fluorine and because of the uncertainty over chain ending mechanisms at the walls and by impurities, such a reaction is most conveniently studied, not in isolation, but in competition with another similar fluorination. The second possibility, which was considered unlikely, arises because the process

$$CH_4 + F_2 \longrightarrow CH_2 + 2HF \quad (4)$$

is exothermic; our evidence will show that it does not seem to be important.

Experimental

In planning the experiment, it was thought desirable to guard against any possibility of ignition (perhaps wall-catalyzed) upon mixing the fluorine with the hydrocarbon mixture. The apparatus was therefore designed so that the final reactant mixture should consist of about 1 mm. of F_2, 3 mm. of H_2, 3 mm. of CH_4 and 350 mm. of inert gas (N_2 or CO_2). The arrangement of the metal reaction vessel is shown diagrammatically in Fig. 1. C_1 and C_2 represent two cylindrical inconel chambers of 150-ml. capacity each; one end of C_1 was fitted with a transparent polychlorotrifluoroethylene (Kel-F) window and a light-tight shutter. V_1, V_2, V_3 and V_4 represent needle valves, V_3 carrying a suitable connection for attachment to the vacuum system and V_4 carrying one suitable for connection to the fluorine generator. The volume C_3 consisted of a steel cylinder of about 1-ml. capacity, fitted with a piston P which could sweep the contents of C_3 through V_2.

An individual run was performed in the following manner. A mixture of H_2 and CH_4 was made up and led into the reaction vessel *via* V_3, giving a total pressure in C_1 of about 0.5–1.0 cm.; V_1 was closed and the contents of C_2 only were pumped into a sample tube to provide a standard against which to compare the reaction products. Volume C_2 was filled to approximately 1 atm. with CO_2 and V_2 closed. The system was then attached to the fluorine cell and C_3 was flushed out with F_2 (free of HF[1]) for about 30 minutes, when V_3 and V_4 were closed; the fluorine was compressed into C_2 using the piston, and V_2 again closed. After coming to the thermostat temperature, V_1 was momentarily opened to allow the CO_2–F_2 mixture to expand into C_1 and the reaction was initiated by illumination with a medium pressure mercury lamp. After a period of 0.5 to 2 hours, the vessel was reattached to the vacuum system and the contents of C_2 and C_3 were pumped away; the contents of C_1 were then pumped through absorption tubes containing NaF pellets and $CaCl_2$–KI mixture (to remove, respectively, HF and any unused F_2), through a liquid nitrogen trap (to remove CO_2, fluorocarbons and any I_2), the remaining H_2–CH_4 mixture being pumped into a second sample tube (taking care to avoid differential pumping).[1] The relative rate of reaction of fluorine with hydrogen and methane was found by a direct comparison of the initial and final mixtures on a mass-spectrometer. Provision was also made for fractional distillation of the contents of the liquid nitrogen trap in order to find the nature of the fluorinated products.

In later experiments, a Pyrex system with a quartz reaction volume was constructed on the same principles (except that the transference of F_2 from C_3 to C_2 was effected by expansion only) with the three sections separable from each other; the stopcocks and joints were lubricated with Kel-F vacuum grease without any undesirable effects.

Results

Experiments in the Metal Reaction Vessel.—These may be divided into two phases, the earlier one where the reaction occurred spontaneously in the dark, and the later one where photo-initiation was necessary.

Phase 1.—Initially, qualitative experiments were performed to find out the nature of the reaction products between F_2 and CH_4. The first run gave mainly CH_3F with some CH_2F_2, but after about six runs, the product of fluorination of methane was almost completely C_2F_6; the products from the intervening runs revealed a steady transition from the expected to the unexpected behavior (among the products being CF_3H, CF_4, C_2F_4, $C_2F_4H_2$ and C_2F_5H in varying proportions). All subsequent runs gave the same reaction product, *i.e.*, C_2F_6 despite a threefold variation in the pressure of each component of the reaction mixture. The addition of oxygen to the reaction mixture had no effect and in some quantitative experiments, the relative rates

(1) It should be noted that electrolytic fluorine always contains some oxygen, and there is no convenient method of separation.

of consumption of H_2 and CH_4 were quite irreproducible. Clearly this is a surface reaction (*cf.*, the production of some C_2Cl_6 in the fluid-bed chlorination of methane) and it was eventually stopped by aging the reaction vessel with fluorine.

Phase 2.—In these reactions the fluorination was initiated using a medium pressure mercury lamp; the fact that neither a tungsten lamp nor a high pressure mercury lamp would cause the reaction to occur, although their output overlaps the tail of the fluorine absorption spectrum, implies that the chain-length of the reaction scheme 1, 2, 3, etc., is very short. The products of the photochemical fluorination of methane were about 65% CH_3F, 30% CH_2F_2,[2] and some CHF_3 and CF_4 in that order; in addition, there were traces (<1%) of fluorine derivatives of C_3 and C_4 alkanes (which could be eliminated on aging the vessel immediately beforehand with fluorine) and oxygen containing materials (from the O_2 impurity in the fluorine). When the reaction vessel was in this inert condition, no reaction occurred at 60° in the dark, although at 100° there was a reaction between hydrogen and fluorine, indicating the onset of a thermal reaction.

In four quantitative experiments at 34°, with initial H_2/CH_4 ratios varied over the range 2:1 to 1:2, and the percentage consumption of reactants varying between 5 and 90%, relative rate constants k_2/k_1 (assuming reactions 1 and 2 are rate determining) were satisfactorily reproducible at 2.37 ± 0.07. Two satisfactory experiments were performed at 54°, but thereafter the vessel walls began to absorb fluorine rapidly, leaks appeared due to corrosion of the silver-soldered joints, and the metal vessel was discarded in favor of the quartz one.

Experiments in the Quartz Reaction Vessel.—Although no reaction was found to occur in the dark at −80 and −35°, all reactions above 18° proceeded spontaneously, although quite slowly, going to completion over a period of several hours. The rate of reaction (as indicated by the over-all rate of consumption of the H_2–CH_4 mixture) was affected by two factors: irradiation with the medium pressure mercury lamp increased the rate by a factor of about 2.5, whereas the removal of HF from the reaction mixture by sodium fluoride brought about a reduction by a factor of 3; this reduction was independent of the amount of sodium fluoride used. However, the relative rate constants obtained were independent of these variations and of variation in the initial concentrations of H_2, CH_4, F_2 and CO_2, the average of ten runs at 25° being $k_2/k_1 = 2.45 \pm 0.20$. The fluorinated reaction products were very similar to those obtained from the experiments in the metal vessel.

A number of experiments were successfully carried out at 50 and 100°, at which temperature the spontaneous reaction went to completion in less than 1.5 hours. Again, independence of the rate ratios on the various factors was observed. At 150°, the rate of consumption of fluorine decreased markedly, although the rate ratio had a reasonable value; however, further runs gave much lower values for k_2/k_1, and on reverting to 25°, a similar observation was made: the rate of consumption of fluorine was very much less than usual, as was also the value of k_2/k_1, but after six more runs, both had returned to their normal values.

(2) This ratio of CH_3F to CH_2F_2 would suggest that CH_3F is rather more readily fluorinated than is CH_4 itself.

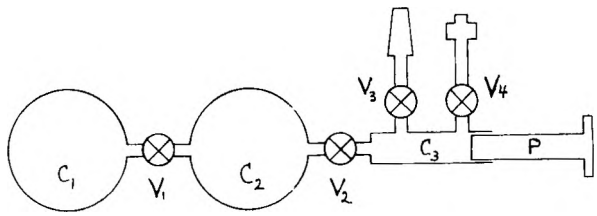

Fig. 1.—Schematic diagram of the metal reaction system.

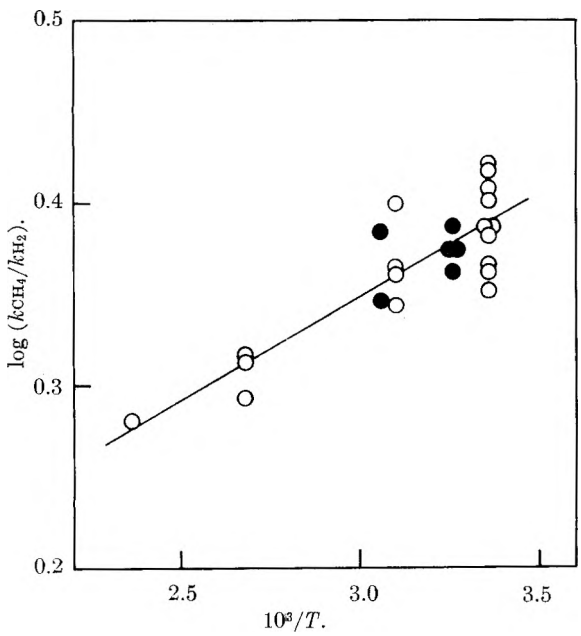

Fig. 2.—●, experiments in the metal reaction vessel; ○, experiments in the quartz reaction vessel.

Assuming that the fluorination of the H_2–CH_4 mixtures takes place by the chain mechanism involving reactions 1, 2, 3, etc., the values of k_2/k_1 from both sets of experiments are plotted in Arrhenius form in Fig. 2, giving $k_2/k_1 \approx 1.05e^{(0.5 \pm 0.2)/RT}$; this small difference in activation energy between reactions 1 and 2 is very reasonable in view of the fact that both individual activation energies were expected to be quite small. However, before accepting this quantity as a true activation energy difference, a little needs to be said about the assumption that the above reactions are the correct ones. The fact that in the metal vessel the reaction would only proceed photochemically is most important, as it demonstrates that fluorine atoms are involved (since fluorine is the only component of the reactant mixture which can be affected by radiation from a medium pressure mercury lamp); the conclusion that the chains involved are very short would be consistent with the rapid removal of fluorine atoms by the walls or the oxygen impurity. The coincidence of the results from the metal and quartz vessels suggests that we are studying the same reaction in each case, although the initiation processes are different. This conclusion is reinforced by the observation that in the quartz vessel

the ratios of k_2/k_1 are unaffected by the presence of additional photochemical initiation. Hence, it would appear that short chains involving fluorine atoms can be initiated on the quartz surface; it is apparent that hydrogen fluoride plays some part in this process, and that the thermal history of the quartz surface is also relevant. Our interpretation of these experiments is further supported by the fact that the calculated ratio k_2/k_1 is independent of fluorine, hydrogen, methane or inert gas pressure, and percentage consumption of the reactants. Furthermore, we can exclude the reaction 4, at least below 60° on the grounds that no reaction took place in the metal vessel in the absence of ultraviolet irradiation, and, judging from the general behavior in the quartz system, we can probably exclude it over the whole temperature range studied, *i.e.*, up to 150°.

DIMERIZATION OF GASEOUS BUTADIENE—EQUILIBRIUM STUDY[1]

BY GEORGE J. JANZ AND MICHAEL A. DE CRESCENTE[2]

Department of Chemistry, Rensselaer Polytechnic Institute, Troy, New York

Received February 24, 1959

The reaction equilibrium for the dimerization of butadiene and the depolymerization of vinylcyclohexene has been studied in the temperature range from 630–700°K. The results are evaluated in the light of equilibrium calculations from thermodynamic data and reaction velocity constants for this system. The close agreement between the entropy change for this reaction at 600°K. and the entropy of activation for the dimerization suggests a highly circumscribed transition state rather similar in structure to the cyclic product in this process.

Comparatively few experimental studies on reaction equilibria in the homogeneous gas phase have been made. The rate of the gas phase cyclization of butadiene to vinylcyclohexene

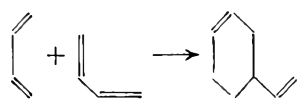

(1)

in the temperature range of 200–400° is well established.[3,4] The reaction may be interpreted as a Diels–Alder type process occurring in the gas phase, *i.e.*, uninfluenced by solvent effects. A comparison of the thermodynamically predicted reaction equilibria with values calculated from the rate equations for dimerization[3,4] and depolymerization[5] has also been reported.[6,7] The marked disagreement between the values of the reaction equilibria predicted from thermodynamic data and the rate constants suggested a need for further work. While from the estimated free energy change for the reaction equilibrium at 400°, −9.6 kcal./mole, rather complete conversions of the diene to vinylcyclohexene would be predicted at reaction equilibrium, modern analytical methods such as gas chromatography made an experimental study of the process still seem feasible. The present communication reports the results of some experimental equilibrium measurements in the gas phase at temperatures up to 400° and further theoretical considerations on this fundamental gas phase dienes reaction.

(1) Abstracted in part from a thesis submitted by M. A. De Crescente in partial fulfillment of the requirements for the degree of Doctor of Philosophy, Rensselaer Polytechnic Institute, June, 1958.

(2) Union Carbide Corporation Fellow in Chemistry, 1956–1958.

(3) D. Rowley and H. Steiner, *Disc. Faraday Soc.*, **10**, 198 (1951).

(4) G. B. Kistiakowsky and W. W. Ransom, *J. Chem. Phys.*, **7**, 723 (1939).

(5) T. F. Doumani, R. F. Deering and H. C. McKinnis, *Ind. Eng. Chem.*, **39**, 89 (1947).

(6) N. E. Duncan and G. J. Janz, *J. Chem. Phys.*, **20**, 1644 (1952).

(7) G. J. Janz, "Estimation of Thermodynamic Properties for Organic Compounds," Academic Press, Inc., New York, N. Y., 1958, p. 115. 122.

Experimental

Butadiene (1,3-) was a C.P. grade subjected to two simple low temperature distillations before use. It was stored at −78° in 500-cc. glass ampoules fitted with 14/35 standard taper joints and pressure stopcocks. Before use, the butadiene was degassed several times by the conventional manner to remove last traces of dissolved air.

The experimental assembly for the high temperature gas phase equilibrium measurements was a hermetically sealed constant volume system. Butadiene was allowed to expand into the evacuated system to fill the 5-liter calibrated reaction volume to a pre-determined pressure. For this purpose, the flask was connected to the manifold through a side arm in place of one of the ampoules. By chilling a side arm trap on the reaction flask to −195°, the diene was frozen out while the reaction flask was sealed off with a torch. The flask was placed in the furnace and sealed into the system with the magnetically controlled hammer above the breaker seal.

To study the depolymerization, a measured amount of redistilled and degassed vinylcyclohexene was introduced into the side arm trap of the reaction flask using a rubber serum cap and hypodermic syringe and an auxiliary inlet to the side arm trap. Otherwise, the procedure was as above.

The temperature of the furnace was controlled to ±1° by a Brown recording potentiometer. After the reaction period, the breaker seal was ruptured and the contents were rapidly expanded into an ampoule which had been chilled to −195°. Condensation in the manifold was prevented by maintaining the temperature electrically at approx. 130°. The reaction vessel was then sealed off with a torch to isolate the high temperature zone from the system.

Analyses of the products proceeded by conventional low temperature distillation techniques. Gas chromatography was used to check the identity of the products, and the amounts were quantitatively determined by direct weighing or pressure measurements. Some of the run conditions, data and results over the temperature range, 360–430°, are summarized in Table I.

At 400° and higher, some hydrogen and methane in equal amounts, and a liquid product in which cyclohexane, benzene, cyclohexene, ethylbenzene and styrene were identified as well as vinylcyclohexene were obtained. The amounts of butadiene and vinylcyclohexene in these mixtures, as found by chromatographic analyses, were used for the calculation of the equilibrium data.

At no time was carbonization of the reaction vessel observed in this work. With reference to the data which are collected in Table I, certain observations are possible. At 666°K. and reaction times greater than 40 minutes, the experimental ΔF does reach a constant value (*i.e.*, -9.7 ± 0.2

TABLE I

BUTADIENE–VINYLCYCLOHEXENE—EQUILIBRIUM EXPERIMENTS

Input Temp. (°K.)	Press. (atm.)	Moles	Time (min.)	Recovery (moles × 10³) C_4H_6	C_8H_{12}	K_p (× 10⁻³)	$-\Delta F°$ (kcal. mole⁻¹)
698	0.930	0.0918	62	8.86	40.8	0.178	8.0
690	.936	.0875	31	2.70	38.8	.498	8.5
688	.975	.0914	30	2.33	41.4	.715	9.0
626	.907	.0935	46	16.2	33.8	.013	3.1
666	.866	.0840	40	3.68	39.7	.262	7.4
666	.939	.0910	81	1.18	25.3	1.77	9.9
669	.923	.0906	60	1.42	31.9	1.55	9.8
666	.927	.0898	70	1.58	26.9	1.04	9.4
668	.613	.0601	70	1.80	16.8	0.513	8.3
667	.639	.0618	90	0.55	15.0	4.84	11.2
670	.647	.0632	90	1.54	16.8	0.696	8.8
667	.654	.0633	91	0.80	15.7	2.36	10.3
626	.932	.0974	180	.56	39.5	13.0	11.8
645	.977	.0978	139	.82	36.5	5.48	11.0
656	.933	.0932	128	.89	25.0	3.14	10.5
676[a]	4.18	.0474	68	.76	41.8	3.69	11.0
658[a]	4.10	.0471	171	1.02	41.0	7.12	11.3
639[a]	3.27	.0401	156	0.59	32.7	7.84	11.4

[a] Depolymerization experiments.

kcal./mole). The experimental ΔF at a constant temperature is independent of the initial pressure of the reactants, although the reproducibility of the results at lower initial pressures is far less satisfactory. In view of the rather small amounts of diene remaining at reaction equilibrium, the greater scatter in the low pressure experiments reflects the limitations of such experimental studies; the agreement is all that could be expected. That the value of ΔF observed is an equilibrium value was demonstrated by the depolymerization experiments in which vinylcyclohexene was used as the initial reactant.

Comparison of the values predicted by the thermodynamic method and the values calculated from reaction rate data leaves little doubt that the present experimental values confirm the thermodynamic values. The fact that reaction equilibrium data can be predicted more accurately by the thermodynamic method where precise data are available than by experimental measurements, especially in the gas phase at moderately high temperatures, is clearly illustrated by these results.

Discussion

The method of group equations[7,8] may be used to estimate the thermodynamic properties for a compound quite precisely providing the thermodynamic properties of the parent compounds are accurately known and the corrections arising from differences in symmetry factors and internal rotations are observed. The free energies of formation for vinylcyclohexene were thus estimated by the group equation

$$\Delta F_f^0 \text{ [vinylcyclohexene]} = \Delta F_f^0 \text{ [styrene]} + \Delta F_f^0 \text{ [cyclohexane–benzene]} + RT \ln 3 \quad (2)$$

using the data for styrene, cyclohexene and benzene,[8] and where the factor $RT \ln 3$ brings about a balance in the contributions due to the symmetry factors. The hindered internal rotation in vinylcyclohexene was assumed equal to that in styrene in this estimate. The results together with the data for butadiene,[8] and the equilibrium free energy changes for the dimerization reaction

$$2(\text{Butadiene}) \underset{k_r}{\overset{k_f}{\rightleftharpoons}} \text{Vinylcyclohexene} \quad (1)$$

are summarized in Table II. These values are recommended for calculations to those reported by Duncan and Janz[6] since in the earlier work, the more approximate method of group contributions with no corrections for symmetry factors was used (*e.g.*, at 1000°K., the earlier estimate is 2.8 kcal./mole too low).

The values predicted from the rate data (Table II) were calculated from the expressions for the dimerization of butadiene[3]

$$k_f = 1.38 \times 10^{11} e^{-(26,800/RT)} \text{ cc. mole}^{-1} \text{ sec.} \quad (690\text{–}925°\text{K.})$$

and the depolymerization of vinylcyclohexene[4]

$$k_r = 2.35 \times 10^{8} e^{-(36,000/RT)} \text{ sec.}^{-1} \quad (783\text{–}977°\text{K.})$$

and the well known relation between the equilibrium and reaction rate constants

$$K_p = \frac{k_f}{2k_r}(RT)^{-1} \quad (3)$$

where the subscripts refer to the forward and reverse processes (equation 1), R is the gas constant in l.-atm./deg. mole, and the factor 2 refers both rate processes to one gram mole of butadiene in the equilibrium expression. Inspection of the calculations by Duncan and Janz[6] shows that these factors were not taken into account so that the earlier results are of qualitative rather than quantitative significance only.

The experimental results of the present study agree well with the limits of the experimental work with the thermodynamically predicted values for the equilibrium free energy changes. The cause for the disagreement of the results predicted from the reaction velocity studies lies most probably in the expression for the rate of depolymerization of vinylcyclohexene as discussed elsewhere.[6] The frequency factor and activation energy for the depolymerization[5] seem unusually low for homogeneous thermal dissociation processes.

The heat and entropy changes for the dimerization at 25° and 1 atm. are −35.40 kcal. and −43.01 e.u., respectively, as calculated from the recent value for heat of formation of vinylcyclohexene,[9] 17.26 kcal./mole, an estimated value for the entropy of vinylcyclohexene, 90.23 e.u., and the current values for butadiene.[8] The same basic group equation as in the preceding calculations was used for entropy but with the factor from symmetry considerations now $-R \ln 3$. The above value may be compared with the values 89.6, 90.3, 88.3 and 86.7 e.u. as estimated by Kistiakowsky and Ransom[4] using cyclohexane, methylcyclohexane, cyclohexene and ethylcyclohexane as "parents" and the more approximate procedures of simple group contributions.

A comparison of the value of entropy of reaction with the values for the entropies of activation observed experimentally[4] for the dimerization reaction of butadiene at 600°K. is of interest. The entropy of activation $\Delta S^{\ddagger}$ for the dimerization of butadiene, calculated from the value of non-exponential A factor, $10^{9.46 \pm 0.18}$ cm.³/g. mole sec., found in the kinetic measurements[4] at 600°K. is

(8) F. D. Rossini and Associates, Eds.; "Selected Values of Physical and Thermodynamic Properties of Hydrocarbons and Related Compounds," Carnegie Press, Pittsburgh, Pa., 1953.

(9) F. W. Maron and E. J. Prosen, Nat. Bur. Stds. Report 2037, Washington, D. C., 1952.

TABLE II

THERMODYNAMICS OF THE BUTADIENE–VINYLCYCLOHEXENE EQUILIBRIUM

T (°K.)	298.1	300	400	500	600	700	800	900	1000
	(a) Free energies of formation (kcal./mole)								
Butadiene[a]	36.01	36.07	39.46	43.05	46.78	50.60	54.48	58.40	62.36
Vinylcyclohexene	46.18	46.07	57.20	68.82	80.70	92.76	104.92	117.17	129.43
	(b) Equilibrium free energy changes (kcal./mole)								
Thermodynamic data	−25.84	−26.07	−21.72	−17.28	−12.86	− 8.44	−4.04	0.37	4.71
Reaction rate[b] data	.....	.....	.....	.....	(− 3.2)	(− 1.9)	−0.6	0.7	2.0

[a] See ref. 8. [b] Values in brackets are extrapolated values.

−18.3 e.u. per g. mole per cc. if the transmission coefficient is assumed to be unity. The entropy of reaction ΔS for this process at 600°K. may be computed from the value for butadiene,[8] 84.36 e.u., and vinylcyclohexane, 124.75 e.u., both at 1 atmosphere, using the Sackur Tetrode equation to correct these values to volume concentration units. The above value for vinylcyclohexene was calculated by the method of group equations. This computation gives, as the entropy change for the dimerization of butadiene at 600°K., the value of −21.2 e.u./per cc. per g. mole of butadiene. Whereas the calculations based on statistical thermodynamics for the entropies of activation assuming both linear and a cyclic transition state complexes were not sufficiently free from assumptions to distinguish conclusively between the two possibilities,[10] the close agreement above between the entropy change for the reaction and entropy of activation makes the assumption of a highly circumscribed transition state, rather similar in structure to the product molecule, *i.e.*, cyclic, a very probable one. The question still remains open whether the transition state in this process is a diradical or simply a polarized molecular state.

Acknowledgments.—One of us (G.J.J.) wishes to thank Hervey H. Voge, Emeryville, Calif., and Yukio Mikawa, Tokyo, Japan, for directing attention to the need for revision and correction of the earlier calculations.

(10) A. Wassermann, *J. Chem. Soc.*, 612 (1942).

VOLUME EFFECTS ON MIXING IN THE LIQUID Bi–BiI_3 SYSTEM[1]

BY F. J. KENESHEA, JR., AND DANIEL CUBICCIOTTI

Stanford Research Institute, Menlo Park, California

Received February 26, 1959

Volume effects on mixing in the liquid Bi–BiI_3 system have been determined by measurements of the density as a function of temperature. The total volume of the system decreases on mixing. The partial molar volume of BiI_3 differs only slightly from the molar volume of the pure salt while the partial molar volume of the bismuth is much less than the molar volume of pure bismuth. These volume effects are analogous to the changes found previously for the bismuth–chloride and bismuth–bromide systems and are interpreted in terms of the same model of an interstitial type of solution. The experimental values in all three halide systems are in fair agreement with an expression derived from the model which relates the partial molar volume of the bismuth with the halide ion radius.

Introduction

In an effort to gain some knowledge concerning the nature of metal–salt solutions we have previously studied the volume effects in the Bi–$BiCl_3$ and the Bi–$BiBr_3$ systems.[2] As a continuation of this work we have measured the volume changes in the Bi–BiI_3 system. Bismuth has been shown[3] to exhibit appreciable solubility in BiI_3, analogous to the Bi–$BiCl_3$ and Bi–$BiBr_3$ systems. There is some evidence for the formation of solid BiI. In the temperature range 406–500° and up to about 50 mole % bismuth, one liquid phase is obtained. Solutions of Bi–BiI_3 in this range have been investigated in the present study.

(1) This work was made possible by the financial support of the Research Division of the United States Atomic Energy Commission.

(2) F. J. Keneshea, Jr., and D. Cubicciotti, THIS JOURNAL, **62**, 843 (1958); **63**, 1112 (1959).

(3) (a) L. Marino and R. Becarelli, *Atti Accad. Lincei*, **21** [5], 695 (1912); (b) H. S. Van Klooster, *Z. anorg. Chem.*, **80**, 104 (1913); (c) G. G. Urazov and M. A. Sokolova, *Akad. Nauk. SSSR., Inst. Obshch. Neorg. Khim., Sektor Fiz-Khim. Anal., Izvest.*, **25**, 117 (1954).

Experimental

As in the previous experiments, the densities of the liquid Bi–BiI_3 mixtures were determined by a pycnometric method. In general, the procedures were the same as those used for the chloride and bromide experiments.[2]

The BiI_3 was prepared by reaction of reagent grade Bi_2O_3 with aqueous HI followed by evaporation of the water under a nitrogen stream. The crude BiI_3 thus obtained was distilled twice under a stream of dry N_2. The product from the second distillation was ground in a mortar and stored in a desiccator. Two separate preparations of BiI_3 were made. They gave bismuth analyses of 35.32 and 35.20% compared to the theoretical amount for bismuth of 35.44%. As it had previously been found in vapor pressure measurements on the Bi-BiI_3 system[4] that BiI_3 tends to decompose to yield free I_2 when heated, it was thought that a small amount of free I_2 might be present in the distilled BiI_3. To test for the presence of any free I_2, duplicate samples of BiI_3 were dissolved under a nitrogen atmosphere in oxygen-free KI solution acidified with HCl and immediately titrated with $Na_2S_2O_3$ solution. The results showed less than 0.03% I_2 to be present in the BiI_3. The melting point of the BiI_3 used ranged from 405.9 to 406.6°.[4]

(4) D. Cubicciotti and F. J. Keneshea, Jr., THIS JOURNAL, **63**, 295 (1959).

In the experiment successive portions of the BiI_3 were melted under N_2 in a weighed pycnometer. When the proper volume was obtained the pycnometer and contents were again weighed and the weight of the BiI_3 obtained by difference. A weighed amount of bismuth was then added and the pycnometer was sealed under vacuum. The density measurements were then made as in previous experiments.[2]

Results

The densities of seven Bi–BiI_3 solutions, ranging in composition from pure BiI_3 to 0.34 mole fraction of bismuth, are shown as a function of temperature in Fig. 1. The least squares equations obtained from the data are given in Table I. From the

TABLE I

DENSITY EQUATIONS FOR Bi–BiI_3 MIXTURES

Mole fraction Bi	$\rho = a - bt$ (g./cc.) a	$b \times 10^3$	Standard error, g./cc.	Exptl. temp. range, °C.
0[a]	5.558	2.22	0.003	425–492
0.0190	5.523	2.09	.002	434–494
.0450	5.597	2.16	.002	423–489
.0927	5.664	2.10	.001	452–490
.1708	5.761	2.02	.002	436–494
.2313	5.821	1.85	.002	420–494
.3443	6.013	1.72	.002	414–494

[a] Two different preparations of pure BiI_3 were measured and the average density taken. In the range of temperatures investigated the samples differed by less than 0.3% in their densities. (Both data are plotted in Fig. 1.)

experimental densities the molar volumes were calculated and plotted as a function of composition for temperatures of 420, 460 and 500°. From these curves the partial molar volumes were calculated as previously described[2] and are listed in Table II for several compositions.

TABLE II

PARTIAL MOLAR VOLUMES IN Bi–BiI_3 MIXTURES

Mole fraction Bi	$\bar{V}_{BiI_3}$, cc. 420°	460°	500°
0	127.9 ± 0.1	130.0 ± 0.1	132.7 ± 0.1
0.10 to 0.20	127.0 ± .2	129.6 ± .2	132.0 ± .2
0.30	125.0 ± .8	127.0 ± .8	129.5 ± .8
	$\bar{V}_{Bi}$, cc.		
0	2 ± 3	1 ± 3	−5 ± 3
0.10 to 0.20	8.8 ± 2.8	5.9 ± 2.8	5.2 ± 2.8
0.30	13.3 ± 2.2	13.1 ± 2.2	11.5 ± 2.2
1.00	21.22 ± 0.02	21.33 ± 0.02	21.45 ± 0.02

As in the chloride and bromide systems, a decrease in the total volume occurs when bismuth is mixed with BiI_3. This decrease amounts to about 6% at a bismuth mole fraction of 0.35 and a temperature of 500°, which is about the same decrease found in the bromide system at a bismuth mole fraction of 0.4 and a temperature of 400°.

The partial molar volumes in the iodide system exhibit the same behavior as in the other halide systems. The partial molar volume of BiI_3, $\bar{V}_{BiI_3}$, varies by only 2% up to 0.3 mole fraction of bismuth, indicating that the BiI_3 behaves almost ideally in this composition range. The partial molar volume of BiI_3 increases with increasing temperature (Table II). The partial molar volume of bismuth, $\bar{V}_{Bi}$, in dilute solutions is much less than the molar volume of pure bismuth and approaches the value for bismuth with increasing concentration. For a given concentration, $\bar{V}_{Bi}$ decreases with increasing temperature and in very dilute solutions becomes negative at higher temperatures. This trend toward negative values of $\bar{V}_{Bi}$ was noticed also for the chloride and bromide systems.

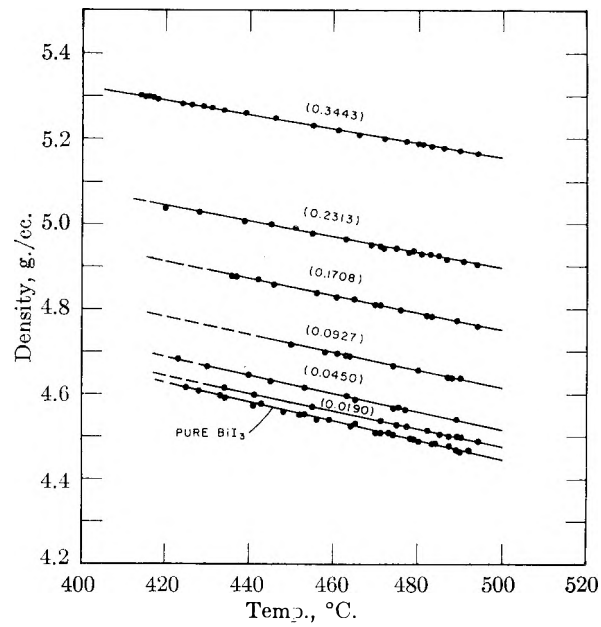

Fig. 1.—Density of Bi–BiI_3 mixtures. Numbers on curves indicate mole fraction Bi.

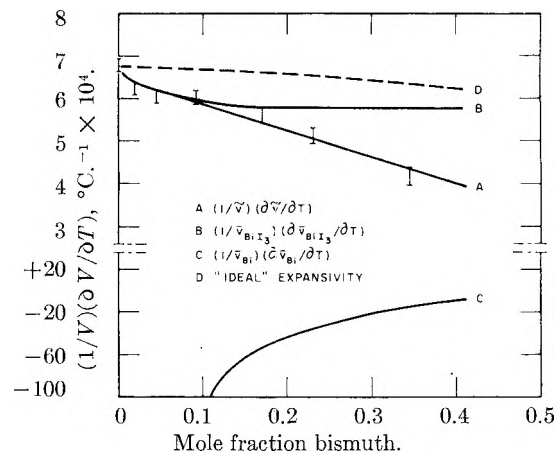

Fig. 2.—Expansivity of Bi–BiI_3 mixtures at 500°.

The expansivity, $1/V(\partial V/\partial T)$, of the iodide solutions also shows the same general behavior as the chloride and bromide solutions. The tota expansivity, $1/\bar{V}(\partial \bar{V}/\partial T)$ (Fig. 2) show negative deviations from the ideal value. This negative deviation is again due to the behavior of the bismuth in the solution as can be seen from the contributions of the bismuth and BiI_3 expansivities, $1/\bar{V}(\partial \bar{V}/\partial T)$, to the total expansivity in Fig. 2. These curves indicate that the BiI_3 expansivity in the solution is fairly constant, reflecting the almost ideal behavior of the BiI_3, while the bismuth expansivity is negative, due to the decrease of $\bar{V}_{Bi}$ with increasing temperature. The expressions relating the various expansivities have been developed in previous reports.[2]

Discussion

Since the results found for the iodide system are similar to those of the other halide systems, the model previously suggested is also applied here. In this model the bismuth species from the added bismuth metal enter empty octahedral holes in the liquid halide quasi-lattice. Thus, there is a net decrease in volume on mixing bismuth with the bismuth halide because the bismuth occupies holes already present in the salt. With an increase in temperature the lattice expands and allows the added bismuth to be more readily accommodated; hence there is a decrease in $\bar{V}_{Bi}$ with an increase in temperature.

At bismuth concentrations approaching zero the very small and negative values for $\bar{V}_{Bi}$ suggest that the added bismuth enters an empty hole and also causes a contraction of the bismuth and halogen species in the vicinity of the hole. At higher concentrations, where the added bismuth enters holes which are very near one another, it might be expected that this contraction would be essentially cancelled because of competition for the same surrounding halides. In this case, the volume effects are due mainly to the changes produced by inserting the added bismuth into the empty octahedral holes. Thus the volume change is roughly the difference between the volume of the bismuth species added to a hole and the volume of the hole. For a mole of added bismuth this may be expressed by the equation

$$\bar{V}_{Bi} = V^*_{Bi} - V_{hole} \qquad (1)$$

where $\bar{V}_{Bi}$ is the partial molar volume of bismuth in cc., V^*_{Bi} is the volume in cc. of a mole of added bismuth species, without specifying the nature of these species and V_{hole} is the volume in cc. of a mole of empty octahedral holes. Equation 1 holds only for $V^*_{Bi} > V_{hole}$; if $V^*_{Bi} < V_{hole}$ then $\bar{V}_{Bi}$ should be zero for the simple model used here. The volume of a hole can be approximated by the volume of a sphere which can be accommodated by the hole, assuming contact of the halide ions, *i.e.*, $4/3\pi \cdot (\sqrt{2}\cdot 1)^3 r_x^3$ A.^{3} per hole or $0.179 r_x^3$ cc. per mole of holes, where r_x is the radius of the halide ion in A. Equation 1 then becomes

$$\bar{V}_{Bi} = V^*_{Bi} - 0.179 r_x^3 \qquad (2)$$

In the range of concentrations where equation 2 is expected to hold both V^*_{Bi} and r_x (at constant temperature) may be assumed to be independent of x_{Bi}, the mole fraction of bismuth, and from equation 2 we find that $(\partial \bar{V}_{Bi}/\partial x_{Bi})_T = 0$. Experimentally, $\partial \bar{V}_{Bi}/\partial x_{Bi} = 0$ in all three halide solutions at bismuth mole fractions of 0.1 to 0.2. For these concentrations it is possible to fit a straight line with a slope equal to 0.179 to the experimental data when $\bar{V}_{Bi}$ is plotted *vs.* r_x^3 (using Pauling's crystal radii[5]), in agreement with the relationship shown in equation 2. The agreement is well within experimental error, both at 400 and at 250°. (The data for the iodide system were obtained by linear extrapolation of the experimental densities (Table I), a super-cooled liquid being assumed at 250°.)

Extrapolation of the curve for 250° discussed above yields a value for V^*_{Bi} in equation 2 of about 16 cc., which is rather close to the value of 14.2 cc. that one would calculate for V^*_{Bi} if the added bismuth species were atoms (taking $r_{Bi} = 1.78$ A.).[2] However, roughly the same value would be possible for V^*_{Bi} if the added bismuth reacts with the solvent to yield a monohalide (*e.g.*, Bi + $^1/_2$ BiI_3 = 3/2 BiI), with Bi^+ instead of atoms entering the holes. In this case the volume change associated with a mole of Bi^+ would be smaller than that of bismuth atoms (since $r_{Bi^+} < r_{Bi}$) but there is also a volume increase due to the change of $^1/_2$ mole of Bi^{+3} to Bi^+.

It has been suggested[6] that for the Bi–$BiCl_3$ system, results of cryoscopic[7] and vapor pressure[8] measurements may be interpreted in terms of the formation of an ideal solution of $BiCl_3$ and Bi_4Cl_4. In view of the more recent value for the heat of fusion of $BiCl_3$[9] a better interpretation would be the formation of Bi_2Cl_2 instead of the tetramer. It is of interest to calculate, from the known molar volume of these solutions,[2] the apparent molar volume of the Bi_2Cl_2

$$\phi_{Bi_2Cl_2} = \bar{V}/x_{Bi_2Cl_2} - (x_{BiCl_3}/x_{Bi_2Cl_2})\bar{V}_{BiCl_3}$$

where x = mole fraction. At 250° this volume varies from −9 cc. at $x_{Bi_2Cl_2} = 0.039 (x_{Bi} = 0.050)$ to 5 cc. at $x_{Bi_2Cl_2} = 0.177 (x_{Bi} = 0.200)$. (The corresponding values for Bi_2Br_2(250°) are −21 and 1 cc.; for Bi_2I_2(420°) they are −34 and −10 cc.) At higher temperatures ϕ is smaller. For an ideal solution the apparent volume of each component should be constant and equal to the molar volume of the pure component. The large change in ϕ and the small, even negative, values calculated for this quantity thus do not appear to be consistent with the assumption of an ideal mixture of bismuth trihalide and dimeric bismuth monohalide.

Acknowledgments.—The authors are indebted to Dr. C. M. Kelley for many helpful discussions and to Mr. W. Robbins for assistance in the experimental work.

(5) L. Pauling, "Nature of the Chemical Bond," Cornell Univ. Press, Ithaca, N. Y., 1948. p. 346.

(6) J. D. Corbett, THIS JOURNAL, **62**, 1149 (1958).

(7) S. W. Mayer, S. J. Yosim and A. J. Darnell, Abstracts of Papers, ACS Meeting, New York, N. Y., Sept. 1957, Abstract No. 71, p. 28S.

(8) D. Cubicciotti, F. J. Keneshea, Jr., and C. M. Kelley, THIS JOURNAL, **62**, 463 (1958).

(9) L. E. Topol and S. W. Mayer, Abstracts of Papers, ACS Meeting, Chicago, Ill., Sept. 1958, Abstract No. 29, p. 14S.

THE ADSORPTION OF AROMATIC AMINES AT THE INTERFACE: MERCURY-AQUEOUS ACID SOLUTION

BY E. BLOMGREN AND J. O'M. BOCKRIS

John Harrison Laboratory of Chemistry, University of Pennsylvania, Philadelphia, Penna.

Received February 26, 1959

Electrocapillary studies have been made of aniline, *o*-toluidine, 2,3-dimethylaniline, 2,6-dimethylaniline, pyridine and quinoline at a series of concentrations in 0.1 *N* aqueous HCl. The Gibbs surface excess (Γ_A) varies little with potential over a range of about 1 volt. The charge at the interface (q_s) is little affected by the adsorption of the amines. There is a small degree of adsorption of RNH_2 molecules at negative potentials and high concentrations. The surface coverage (θ) by an amine on Hg parallels the corrosion inhibiting effect of the substance at iron. The electrocapillary thermodynamics of the system $RNH_3^+ \rightleftarrows RNH_2 + H^+$ is deduced. The substances are adsorbed predominantly as RNH_3^+ ions, lying flat upon the electrode surface, and the principal adsorption forces arise from a π-bond orbital interaction with the Hg. The adsorption isotherms indicate strong repulsion in the adsorbed layer and this is interpreted in terms of coulombic and dispersive interaction potentials between the adsorbed ions. The absence of a significant experimental dependence of q_s upon θ is consistent with a thermodynamic treatment of the dependence of the free energy of adsorption upon potential. The zeta potential (φ_2) is shifted in a positive direction in the presence of the amines, bringing about a repulsion of H_3O^+ and an attraction of Cl^- over the whole potential range. The standard free energy of adsorption at zero surface coverage per unit area of adsorbed molecule remains constant. The results imply that the inhibition characteristics of aromatic amines in acid solution arise primarily from their partial coverage of the electrode surface, resulting from the adsorption forces connected with the conjugate bonds in the aromatic nucleus.

Study of the adsorption of organic substances at metal-solution interfaces has been rare. Gouy[1] determined electrocapillary curves on Hg in the presence of many substances but at only one concentration. By assuming proportionality between surface tension depression ($\Delta\gamma$) and surface excess (Γ) Butler[2] developed relations between Γ, the electrode potential (e), and properties of the adsorbed molecule, *e.g.*, its polarizability, using Gouy's data. Frumkin[3] studied the adsorption of neutral organic substances and developed a semi-empirical theory for the variation of Γ with e. Individual electrocapillary curves for solutions of tetraalkyl ammonium ions have been given by Frumkin.[4] Conway, Bockris and Lovrecek[5] determined the adsorption of certain alkaloids from electrocapillary measurements and developed from this data model concepts concerning the adsorption of large ions in the double layer. The electrocapillary method was also used by Parsons and Devanathan[6] to study the adsorption of methanol at Hg and the structure of the double layer in aqueous methanolic solutions of HCl; and Devanathan and Peries[7] determined the ionic constituents of the double layer in solutions of specifically adsorbed inorganic salts.

Other workers[8-11] have applied measurements of a.c. impedance for the study of the adsorption of organic compounds on Hg. Whereas this method yields information on the *kinetics*[10] of the adsorption of the compounds, determination of Γ from capacitance data is dependent upon non-thermodynamic assumptions, *e.g.*, a proportionality between Γ and the change of the differential capacity of the double layer, ΔC.

The sparse earlier work has been limited to the study of adsorption of *neutral* organic species; no information seems available concerning the degree of adsorption of organic ions as a function of potential and particularly of the structure of the organic groups. However, it is just this type of experimental work which provides the clearest diagnostic information on the structural arrangement of the adsorbed layer and on the intermolecular forces which bring about adsorption.

There is here described a study of the adsorption of a number of aromatic amines on Hg in aq. HCl, in which $[RNH_3^+]/[RNH_2] > 10^3$.

To such a system, Gibbs' equation may be applied so

$$d\gamma = q_s dE - \Gamma_{H_3O^+}\, d\bar{\mu}_{H_3O^+} - \Gamma_{Cl^-} d\bar{\mu}_{Cl^-} - \Gamma_{RNH_3^+}\, d\bar{\mu}_{RNH_3^+} - \Gamma_{RNH_2} d\mu_{RNH_2} = q_s dE - \Gamma_{H_3O^+} d\mu_{H_3O^+} - \Gamma_{Cl^-} d\mu_{Cl^-} - \Gamma_{RNH_3^+} d\mu_{RNH_3^+} - \Gamma_{RNH_2} d\mu_{RNH_2} \quad (1)$$

E is the potential of the mercury with respect to a reference electrode, the potential of which is assumed not to vary with the composition of the solution; q_s is the charge on the solution side of the interface.

Now

$$d\mu_{H_3O^+} + d\mu_{Cl^-} = d\mu_{HCl} \quad (2)$$

$$d\mu_{H_3O^+} + d\mu_{RNH_2} = d\mu_{RNH_3^+} \quad (3)$$

If E_H is the potential of the mercury with respect to a hydrogen electrode in the aqueous HCl–amine solution

$$dE = dE_H + \frac{1}{F}\, d\mu_{H_3O^+} \quad (4)$$

Furthermore

$$q_s = F(\Gamma_{H_3O^+} + \Gamma_{RNH_3^+} - \Gamma_{Cl^-}) \quad (5)$$

From 1–5

$$d\gamma = q_s dE_H - (\Gamma_{RNH_3^+} + \Gamma_{RNH_2}) d\mu_{RNH_2} - \Gamma_{Cl^-} d\mu_{HCl} \quad (6)$$

(1) G. Gouy, *Ann. chim. phys.*, [7], **29**, 145 (1903); [8], **8**, 291 (1906); [8], **9**, 75 (1906); *Ann. phys.*, [9], **6**, 5 (1916); [9] **7**, 129 (1917).

(2) J. A. V. Butler, *Proc. Roy. Soc. (London)*, **A122**, 399 (1929).

(3) A. Frumkin, *Z. Physik*, **35**, 792 (1926).

(4) A. Frumkin, *Ergebn. exakt. Naturwiss.*, **7**, 235 (1928).

(5) B. E. Conway, J. O'M. Bockris and B. Lovrecek, *CITCE Proc.*, **6**, 207 (1955).

(6) R. Parsons and M. A. V. Devanathan, *Trans. Faraday Soc.*, **49**, 673 (1953).

(7) M. A. V. Devanathan and P. Peries, *ibid.*, **50**, 1236 (1954).

(8) V. I. Melik-Gaikazyan, *Zhur. Fiz. Khim.*, **26**, 560, 1184 (1952).

(9) R. S. Hansen, R. E. Minturn and D. A. Hickson, THIS JOURNAL, **60**, 1185 (1956); **61**, 953 (1957).

(10) W. Lorentz and F. Möckel, *Z. Elektrochem.*, **60**, 507, 939 (1946); W. Lorentz, *ibid.*, **62**, 192 (1958).

(11) I. R. Miller and D. C. Grahame, *J. Am. Chem. Soc.*, **78**, 3577 (1956); **79**, 3006 (1957).

Hence

$$\left(\frac{\partial\gamma}{\partial E_H}\right)_{\mu HCl,\mu RNH_2} = q_s \quad (7)$$

$$\left(\frac{\partial\gamma}{\partial\mu_{RNH_2}}\right)_{E_H,\mu HCl} = -(\Gamma_{RNH_3^+} + \Gamma_{RNH_2}) \quad (8)$$

$$\left(\frac{\partial\gamma}{\partial\mu_{HCl}}\right)_{E_H,\mu RNH_2} = -\Gamma_{Cl^-} \quad (9)$$

From the entities determined by means of equations 7–9 two additional entities of interest are derivable

$$F(\Gamma_{H_3O^+} - \Gamma_{RNH_2}) = q_s - F(\Gamma_{RNH_3^+} + \Gamma_{RNH_2}) + F\Gamma_{Cl^-} \quad (10)$$

and

$$q_+ = F(\Gamma_{H_3O^+} + \Gamma_{RNH_3^+}) = q_s + F\Gamma_{Cl^-} \quad (11)$$

where q_+ represents the charge due to the total surface excess of positive ions in the double layer.

Equation 8 shows that only the *sum* of $\Gamma_{RNH_3^+}$ and Γ_{RNH_2} can be determined (this is in the following denoted Γ_A). The thermodynamic analysis provides only the *difference* between $\Gamma_{H_3O^+}$ and Γ_{RNH_2}.

Experimental

The electrocapillarometer has been described.[5,6] It comprised three compartments, one containing the capillary, one a reference hydrogen electrode and one an auxiliary electrode. The compartments were separated by glass stopcocks provided with water seals which permitted sealing without the use of contaminating greases. The capillary was made from As-free Pyrex glass. It was 0.05 cm. i.d., and tapered off to 10^{-3} cm. i.d. It was inserted in the cell through a ground glass joint and sealed to a glass reservoir, containing mercury. The reservoir was connected to a system containing dry N_2. By increasing the pressure thereof and observing the lower end of the capillary through a microscope (magnification: 60×), the meniscus was brought to a position 0.005 cm. above the top of the capillary. The total pressure required to bring the meniscus to its position was obtained as the sum of the N_2 pressure (read on a manometer) plus the height of the mercury column in the capillary and was corrected for the part of the Hg column below the surface of the solution. All readings were made with a cathetometer to an accuracy of 0.1 mm. The precision of the pressure measurement was 1 in 2,500. The meniscus was renewed before each measurement by expelling a mercury drop from the capillary; because of the small volume of the drops the height of the mercury column in the capillary was read only before and after measurement of an electrocapillary curve.

Potentials were applied to the mercury in the capillary and the auxiliary electrode by means of a potentiometer circuit fed from a battery. The potential of the mercury *versus* the hydrogen electrode was measured to an accuracy of 5×10^{-4} volt using a potentiometer with an input impedance of 10^{12} ohms.

The capillarometer was calibrated by measuring the surface tension of mercury in pure 0.1 *N* aq. HCl, using the value of 425.7 dyne cm.$^{-1}$ for $E_{e.c.m.}$ as standard.[12] The surface tension values were determined for every 50 millivolt over the whole potential range (*ca.* −900 to +400 mv.), except near the electrocapillary maximum, where the intervals were 15 millivolts. The solutions were deoxygenated and the measurements were carried out in an atmosphere of purified[13] hydrogen.

At the beginning of an experiment a pure HCl solution was introduced in the cell and an electrocapillary curve taken with the solution in both the reference and capillary compartment. The values thus obtained agreed within 0.2 dyne cm.$^{-1}$ with those earlier published.[5,6,14] A purified (*vide infra*) solution of RNH_3Cl was added to the HCl solution in the capillary compartment, and the electrocapillary curve determined after each addition. The highest concentration of RNH_3Cl amounted to 0.10 of the HCl concentration. All measurements were made at 25 ± 2°. To avoid poisoning of the hydrogen electrode, the stopcock between the capillary and the reference compartment was closed before the addition of amine.

The water used was purified by distillation over $KMnO_4$ and KOH in an He atmosphere, refluxed in purified H_2 and distilled directly into the cell; the specific conductivity of this water originally in the cell was less than 5×10^{-7} mho cm.$^{-1}$. The HCl solutions were prepared from conductance water and gaseous HCl obtained from KCl and redistilled H_2SO_4 as described.[13] The mercury was purified as described,[15] and before the addition of amines the HCl solutions were pre-electrolyzed for 12–18 hours at a mercury cathode with a current density of 10^{-4} amp. cm.$^{-2}$.

Merck A. R. aniline and pyridine, Eastman *o*-toluidine, 2,6-dimethylaniline and quinoline (synthetic) were redistilled *in vacuo*, collecting only a small part of the middle fraction. The redistilled base was added to an HCl solution, prepared as described above, the amine hydrochlorides recrystallized twice and diluted to desired concentration with conductivity water. For 2,3-dimethylaniline, Eastman's 2,3-DMA·HCl was used, and recrystallized four times. The preparation, recrystallization and dilution operations were carried out in an all glass apparatus in a purified H_2 atmosphere; the solutions were forced into the cell by means of hydrogen pressure. The concentrations of the amines were determined spectrophotometrically (to ±1%) using the absorption maxima at *ca.* 2600 Å. Between each experiment the cell and preparation vessels were very carefully cleaned with concd. H_2SO_4 + HNO_3 and washed with conductivity water.

Stable surface tension values[16] were obtained except in the presence of 2,3-DMA and quinoline, where γ decreased by 0.1–0.2 dyne cm.$^{-1}$ per minute immediately after the renewal of the meniscus; at quinoline the measurements had also to be restricted to $E_H > -500$ mv. for the evolution of hydrogen made the formation of a stable meniscus impossible at more negative potentials. The decrease of γ with time was particularly noticeable in the vicinity of the e.c.m. and decreased in rate with prolonged time; values of Γ_A and q_s evaluated from the instantaneous values and those obtained from the values observed after 10–15 minutes were found to differ by *ca.* 10%. The surface tension values were independent of the direction in which the curves were taken; repetition of determinations gave values agreeing to within 0.5 dyne cm.$^{-1}$ in 0.1 *N* HCl, and within 1 dyne cm.$^{-1}$ at $c_{HCl} < 0.1$ *N*.

The electrocapillary curves were drawn on a large scale and q_s determined graphically from the slopes. Values of Γ_A were obtained from the slopes of $\Delta\gamma$ − log $c_{RNH_3^+}$ curves. From equation 9, Γ_{Cl^-} follows from the slopes of $\Delta\gamma$ − μ_{HCl} curves for constant a_A. Surface tension values for constant ratios $c_{RNH_3^+}:c_{HCl}$ were thus interpolated from measurements at various concentrations of RNH_3Cl and HCl and plotted as function of μ_{HCl}, using the values of $f_{\pm HCl}$ given by Harned and Owen[18]; the slope of the curves was determined graphically.

Errors

(a) Reproducibility in the Evaluation of Results.—(1) q_s. This was about 2% (referred to a level of 10 μcoulombs) as determined by comparison of results of independent co-workers.

(2) Γ.—This was about 10% in respect to

(12) S. R. Craxford, Dissertation, Oxford, 1936.

(13) N. Pentland, J. O'M. Bockris and E. Sheldon, *J. Electrochem. Soc.*, **104**, 182 (1957).

(14) S. Jofa and A. Frumkin, *Acta physicochim. U. R. S. S.*, **10**, 473 (1939).

(15) G. A. Hulett and H. D. Minchin, *Phys. Rev.*, **21**, 388 (1905); **33**, 307 (1911).

(16) Experiment indicates that the reduction of aromatic amines in aqueous solution does not occur in the potential range here used. Experimental confirmation of the previous work[17] was carried out, except for quinoline, in which a catalytic wave was observed at potentials more negative than about 500 mv. with respect to the potential of the H_2 electrode in the same solution.

(17) I. M. Kolthoff and J. J. Lingane, "Polarography," Interscience Publishers, New York, N. Y., 2nd ed., Vol. 2, 1952, p. 769.

(18) H. S. Harned and B. B. Owen, "The Physical Chemistry of Electrolytic Solutions," Reinhold Publ., New York, N. Y., 3rd ed., 1958.

experimental determinations carried out by independent co-workers.

(b) Errors Inherent in Experimental Conditions.—The experimental conditions in the presence of RNH_3Cl differed from those demanded by electrocapillary thermodynamics in two respects:

(i) The hydrogen electrode was not present in the same solution as the capillary but remained in the original HCl solution. The potential of the mercury *vs.* the hydrogen electrode thus differed from the ideal value by an amount corresponding to the difference in H_3O^+ concentration between the two solutions. The value of q_s in (7) was hence obtained for a somewhat different value of E_H than if the H_3O^+ concentration had been identical in both solutions. Furthermore, the constancy of E_H in formulas 8 and 9 is not exactly fulfilled.

(ii) The value of a_{HCl} decreases as a result of the addition of the RNH_3Cl to the solution. Hence the constancy of μ_{HCl} in (7) and (8) is not exactly fulfilled. Correspondingly, the value of Γ_{Cl^-} in (9) is obtained for a slightly different value of μ_{HCl} than if the H_3O^+ concentration had remained unchanged.

The errors due to (i)–(ii) can be expressed as

$$dX = \frac{\partial X}{\partial E_H} dE_H + \frac{\partial X}{\partial \mu_{HCl}} d\mu_{HCl} = \Delta' X + \Delta'' X \quad (12)$$

where X represents either q_s, $F\Gamma_{Cl^-}$ or $F\Gamma_A$.

Since the concentration of the added RNH_3Cl solution was identical to the original concentration of the HCl solution ($c_{0,HCl}$), the concentration of H_3O^+ ions in the capillary compartment decreases by an amount identical to $c_{RNH_3^+}$ in the final solution, *i.e.*, becomes $c_{0,HCl} - c_{RNH_3^+}$, whereas the Cl^- concentration remained unchanged. The value of dE_H is thus $0.059 \log (1 - c_{RNH_3^+}/c_{0,HCl})$.

Neglecting the changes in activity coefficients during the small change of H_3O^+, the second term in (12) becomes

$$\frac{1}{2} \frac{\partial X}{\partial \log c_{0,HCl}} d \log (1 - c_{RNH_3^+}/c_{0,HCl}) \quad (13)$$

The errors are evaluated below for the maximum value of $[RNH_3^+]/[HCl] = 0.1$ and without attention to sign. Hence $dE_H = 2.7$ mv. and d log $(1 - c_{RNH_3^+}/c_{0,HCl}) = 0.046$.

In calculating $\Delta' q_s$ it is observed that the first differential quotient in (12) is identical to the differential capacitance C of the mercury–solution interface. Since $C < 40\ \mu$ Farad. cm.$^{-2}$, one finds ($dE = 2.7$ mv.) $\Delta' q_s = 0.1\ \mu$coul. cm.$^{-2}$.

For $F\Gamma_A$ the first differential quotient in (12) did not exceed 5 μcoul. cm.$^{-2}$ per 100 millivolt (except at the extreme ends of the potential interval). Also for $F\Gamma_{Cl^-}$ the first differential quotient in (12) was less than 5 μcoul. cm.$^{-2}$ per 100 mv. Hence, $\Delta' F\Gamma_A = \Delta' F\Gamma_{Cl^-} = 0.1\ \mu$coul. cm.$^{-2}$.

The differential quotient in (13) for q_s was ≤ 5 μcoul. cm.$^{-2}$ per log c_{HCl} unit. Hence, $\Delta'' q_s = 0.2\ \mu$coul. cm.$^{-2}$.

For $F\Gamma_{Cl^-}$ and $F\Gamma_A$ the differential quotient in (13) did not exceed 20 μcoul. cm.$^{-2}$ per log c_{HCl} unit. Hence, $\Delta'' F\Gamma_A = \Delta'' F\Gamma_{Cl} = 0.5\ \mu$coul. cm.$^{-2}$.

Assuming that the inherent errors possess the same sign, one obtains for the total inherent error

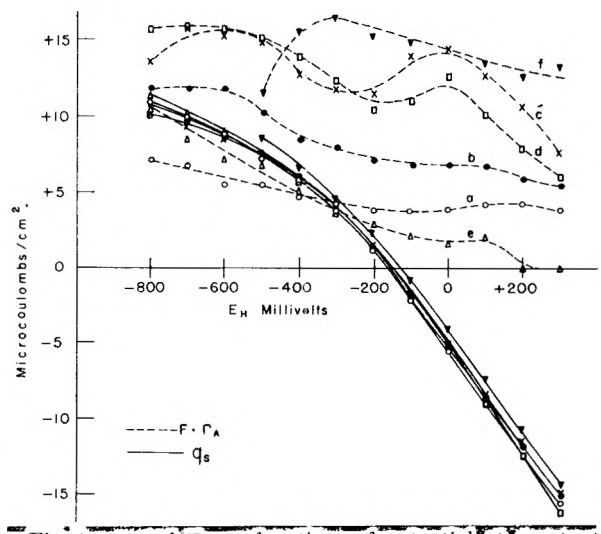

Fig. 1.—q_s and $F\Gamma_A$ as functions of potential at constant concentration: (a) aniline; (b) *o*-toluidine; (c) 2,3-dimethylaniline; (d) 2,6-dimethylaniline; (e) pyridine; (f) quinoline. $c_{RNH_3^+} = 5 \times 10^{-3}$ mole l.$^{-1}$; $c_{HCl} = 0.1$ mole l.$^{-1}$.

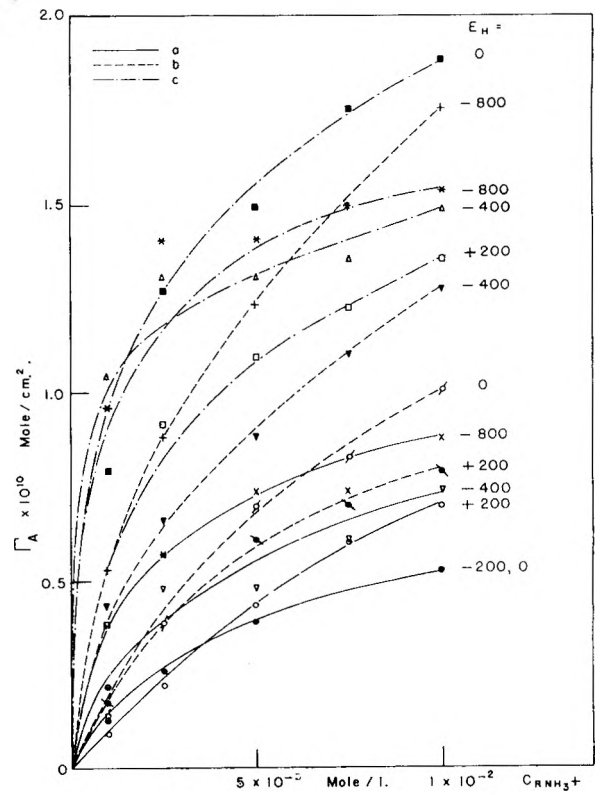

Fig. 2.—Γ_A as a function of $c_{RNH_3^+}$ at constant potentials and $c_{HCl} = 0.1\ N$: (a) aniline; (b) *o*-toluidine; (c) 2,3-dimethylaniline. (Potentials stated on figure).

$dq_s = \pm 0.5\ \mu$coul. cm.$^{-2}$
$d F\Gamma_{Cl} = \pm 0.6\ \mu$coul. cm.$^{-2}$
$d F\Gamma_A = \pm 0.6\ \mu$coul. cm.$^{-2}$
$d F(\Gamma_{H_3O^+} - \Gamma_{RNH_2}) = \pm 1.5\ \mu$coul. cm.$^{-2}$
$dq_+ \pm 0.9\ \mu$coul. cm.$^{-2}$

These evaluations concern maximum probable systematic errors. Their significance to the absolute values clearly depends upon the magnitude of these. As an order of magnitude statement, the inherent errors in $F\Gamma$ and q values are 1 μcoul.

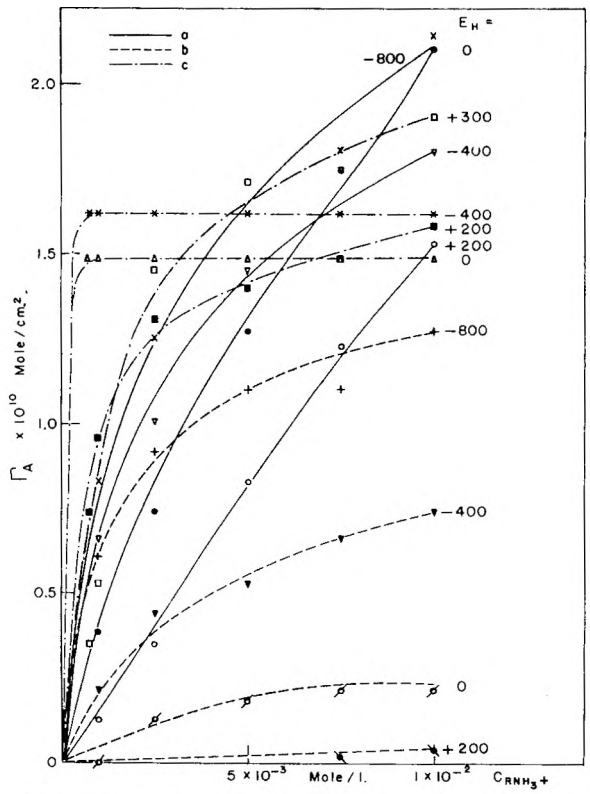

Fig. 3.—Γ_A as a function of $c_{RNH_3^+}$ at constant potentials and c_{HCL} = 0.1 N: (a) 2,6-dimethylaniline; (b) pyridine; (c) quinoline. (Potentials stated on figure.)

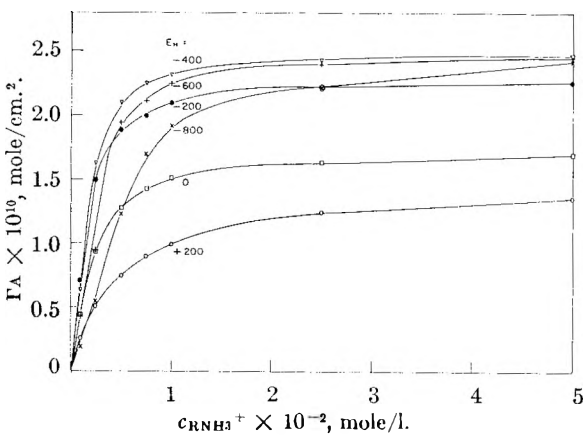

Fig. 4.—Γ_A as a function of $c_{RNH_3^+}$ for 2,6-dimethylaniline at constant potentials and c_{HCl} = 1.2 N. (Determined by Mrs. C. Jesch).

cm.$^{-2}$ and the mean order of magnitude of these quantities is about 7 μcoul. cm.$^{-2}$, *i.e.*, the systematic error has a mean order of magnitude of some 15%.

Results

From the measurements on pure HCl solutions the values of q_s, $\Gamma_{H_3O^+}$ and Γ_{Cl^-} were evaluated for 1.0, 0.1 and 0.01N HCl and found to be consistent within the evaluated error limits with those of Parsons and Devanathan.[6]

Fig. 1 shows q_s and Γ_A as functions of potential for a single concentration. It is observed that Γ_A has a tendency towards a maximum on the negative branch of the e.c.m. and decreases gradually toward positive potentials, in certain systems showing a maximum at intermediate positive potentials. Γ_A values on the positive branch for all substances except pyridine and quinoline were of the same order as those on the negative branch.

The adsorption of aromatic amines produces only minor changes in the total charge on the interface.

Figures 2 and 3 give adsorption isotherms in 0.1 N HCl. Figure 4 gives adsorption in 1.2 N HCl.

Figures 2 and 3 indicate that the adsorption of the aromatic amines (for the same potential and concentration of HCl and RNH_3^+) increases on the negative branch in the order aniline < *o*-toluidine < 2,3-dimethylaniline ≤ 2,6-dimethylaniline < quinoline, whereas on the positive branch the order between aniline and pyridine is reversed.

Table I gives values of $E_{e.c.m.}$.

TABLE I

VALUES OF $E_{e.c.m.}$ IN 0.1 N HCl IN PRESENCE OF AROMATIC AMINES

($E_{c.c.m.}$, 0.1 N HCl = 185 mv.)

Substance	$E_{e.c.m.}$ (mv.) $c_{RNH_3^+}$ 1 × 10⁻³	5 × 10⁻³	1 × 10⁻²
Aniline	−172	−165	−160
o-Toluidine	−170	−162	−155
2,3-Dimethylaniline	−162	−156	−150
2,6-Dimethylaniline	−170	−160	−150
Pyridine	−165	−150	−145
Quinoline	−135	−130	−123

The components of charge in the double layer in the presence of 2,6-DMA at various RNH_3 and HCl concentrations have been worked out. An example of the calculated values is given in Fig. 5. The adsorbate exerts the following effects on the double layer: (1) Γ_{Cl^-} increases considerably over its value in pure HCl and assumes positive values on the negative branch; (2) The positive values of $\Gamma_{H_3O^+}$ on the negative branch in pure HCl are replaced by negative values of $\Gamma_{H_3O^+} - \Gamma_{RNH_2}$. (3) The values of q_+ increase considerably over F-$\Gamma_{H_3O^+}$ for pure HCl and approach $F\Gamma_A$.

Discussion

(1) The Mechanism of the Adsorption of Aromatic Amines on Mercury.—The adsorption of aromatic amines on Hg is distinguished from that of neutral molecules[2,3,9] and NR_4^+ ions,[4] by the relatively small variation of Γ_A with potential. Coulombic forces cannot be responsible for the adsorption of the organic cations on the positive branch. A mechanism of their adsorption *via* an intermediate of specifically adsorbed chloride ions is excluded by the results of measurements of the adsorption of 2.6-DMA on Hg from aqueous $HClO_4$[19a] which show that adsorption on the positive branch is not less than that in HCl, although $\Gamma_{Cl^-} >> \Gamma_{ClO_4^-}$.[19b] Nor are aliphatic amines significantly adsorbed on the positive branch in 0.1 N HCl.[19a] The adsorption of aminium ions on the positive branch must hence be ascribed to effects connected with the aromatic nucleus. Thus, Gerovich[20] found that aromatic hy-

(19) (a) E. Blomgren, J. O'M. Bockris and C. Jesch, unpublished; (b) D. C. Grahame, M. A. Poth and J. I. Cummings, *J. Am. Chem. Soc.*, **74**, 4422 (1952).

(20) M. A. Gerovich, *Doklady Akad. Nauk S.S.S.R.*, **105**, 1278 (1955).

drocarbons, and, in general, hydrocarbons containing conjugate double bonds, adsorb on Hg at potentials positive to that of the e.c.m. and are desorbed toward negative potentials. The adsorption forces on the positive branch must arise from an interaction of the π-electrons of the conjugate double bonds with the metal, and consequently, the adsorption must be with the benzene rings parallel to the Hg surface. The smaller variation of Γ_A with potential for aromatic aminium ions over the whole potential range examined compared with that for other cations, is hence to be interpreted in terms of the effect of π-electron interaction (effective principally on the positive branch), and coulombic forces (effective on the negative branch).

The more rapid increase of Γ_A with increasingly negative potential for pyridine compared with that for aniline derivatives, and the practically complete absence of adsorption of pyridine at positive potentials, is in accordance with this view. The positive charge on the N atom causes a reduction of the electron density of the π-orbitals in the pyridine nucleus, as evidenced by the smaller tendency of pyridine to nuclear substitutions with electron absorbing agents and greater reactivity with electron donating agents.[21] Since the π-electron forces are weaker, coulombic forces will predominate, and the forces bringing about the adsorption of pyridine become similar to those effecting the adsorption of the tetraalkyl ammonium ions.

Comparison of results given in Figs. 2, 3, and 4 with those calculated for monolayer adsorption for the planar configuration (Table II) support a *planar* model for the adsorption of the amines, for the maximum Γ_A observed is much less than Γ_{max} for planar adsorption in 0.1 *N* HCl and accedes to the calculated Γ_{max} (planar) value at saturation for the negative branch at higher concentrations.

In evaluations of Γ_A from (8), the activity coefficient, f_A^s of the aminium ions in solution has been assumed to be 1 at all concentrations. Thus, using $a = 6$ Å., $\log f_A^s = -0.10$ for RNH_3^+ in 0.1 *N* HCl is calculated from the extended version of the Debye-Hückel theory.

The following facts observed, *e.g.*, for 2,6-DMA, indicate that the aromatic amines dissolved in aqueous HCl are adsorbed on Hg predominantly as RNH_3^+ ions.

(a) **The q_+ Values.**—The values of q_+ observed in the presence of the adsorbate are interpretable either as a result of a predominant adsorption of RNH_3^+ ions or as an increase in the surface excess of H_3O^+ ions over that present when the interface is in contact with aqueous HCl solution (0.1 *N*) in the absence of aminium ions. If the enhanced q_+ values were due to an increase in H_3O^+ ions in the diffuse part of the double layer, the potential of the outer Helmholtz plane, φ_2, would possess negative values[22] above those which it would in the corresponding pure HCl solution. However, it is seen in Fig. 5 that for the system 2,6-DMA in 0.1 *N* HCl the value of Γ_{Cl^-} remains positive even at potentials highly negative with respect to the potential of the e.c.m. This behavior, which is found to be repeated in all systems examined, is inconsistent with specific adsorption of Cl^- but is consistent with a positive φ_2 value (on the negative branch) which then indicates that the specifically adsorbed entity is RNH_3^+, rather than RNH_2, and that the increased q_+ observed is due to this, and not to increased H_3O^+ adsorption.

(21) C. R. Noller, "Chemistry of Organic Compounds," W. B. Saunders Co., Philadelphia, Pa., 2nd ed., 1957.

(22) D. C. Grahame, *Chem. Revs.*, **41**, 441 (1947).

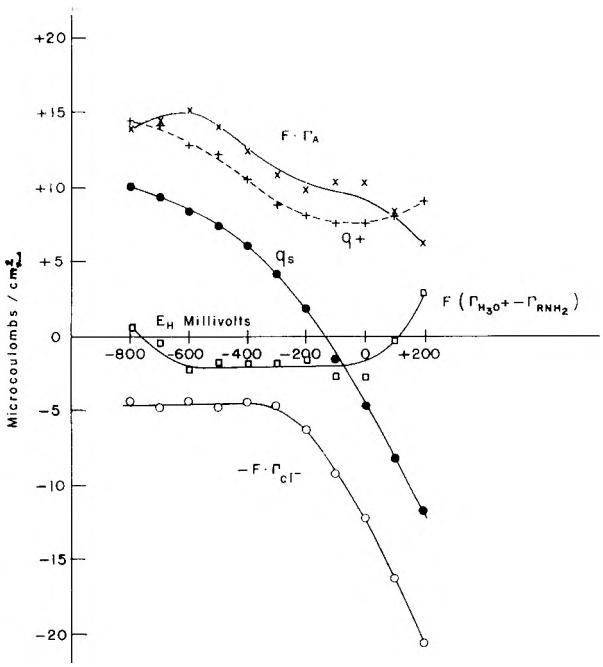

Fig. 5.—Example of components of charge in the double layer as a function of potential: 2,6-Dimethylaniline in 0.1 *N* HCl. $c_{RNH_3^+} = 0.004$ mole $l.^{-1}$.

TABLE II

PROJECTED SURFACE AREA (*S*) AND MAXIMUM ADSORPTION (Γ_{max}) OF AROMATIC AMINES CALCULATED FROM MOLECULAR DIMENSIONS

Substance	*S*(Å.)² Planar	*S*(Å.)² Perpend.	$\Gamma_{max} \times 10^{10}$ (mole cm.$^{-2}$) Planar	$\Gamma_{max} \times 10^{10}$ (mole cm.$^{-2}$) Perpend.
Aniline	50	19	3.4	8.8
o-Toluidine	56	22	3.0	7.4
2,3-Dimethylaniline	62	22	2.7	7.4
2,6-Dimethylaniline	64	26	2.6	6.4
Pyridine	40	19	4.3	8.8
Quinoline	60	25	2.8	6.5

(b) **The Composition of the Double Layer at the E.c.m.**—The total adsorption of amine species, diminished by Γ_{RNH_2} (*vide infra*), is roughly equal to Γ_{Cl^-} at the e.c.m. for several concentrations of HCl and amine (*cf.* Fig. 5) and this suggests that the adsorbate consists of RNH_3Cl in the vicinity of this potential.

(c) **The Approximate Identity of q_+ and $F\Gamma_A$ at High Positive Potentials.**—This is shown as an example in Fig. 5 and is clearly consistent with RNH_3^+ as the predominant amine-adsorbing species.

(2) **Isotherm for the Adsorption of Aromatic Amines on Mercury.**—The adsorption of neutral organic substances on Hg has been found[3,9] to deviate from Langmuir's adsorption isotherm, a fact which has been interpreted in terms of Temkin's adsorption isotherm. It can be shown, however, that Temkin's isotherm is applicable primarily if

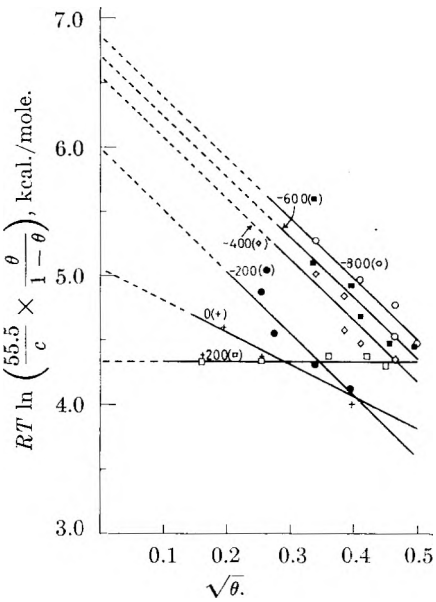

Fig. 6.—Deviations from Langmuir isotherm for aniline in 0.1 N HCl at constant potentials. (Potentials stated on figure.)

only short range interactions between the adsorbed particles influence the dependence of the heat of adsorption on coverage.

Because of the indications that the adsorbed species is ionic a more general discussion will be given.

If the adsorption of A is considered to be ideal (in the sense of zero interaction between the adsorbed particles), no activity coefficient appears in the expression for $\bar{\mu}_A{}^a$, which may then be written

$$\bar{\mu}_A{}^a = \bar{\mu}_A{}^{0,a} + RT \ln \theta \qquad (14)$$

where $\bar{\mu}_A{}^a$ is the electrochemical potential of the adsorbed entity A, $\bar{\mu}_A{}^{0,a}$ is the standard electrochemical potential referred to a standard state of unit surface mole fraction, and θ is the fraction of the surface covered with A.

For water adsorbed on the electrode, and for conditions such that specific adsorption of other substances than water and amine is negligible

$$\mu_{H_2O}{}^a = \mu_{H_2O}{}^{0,a} + RT \ln (1 - \theta) \qquad (15)$$

where $\mu_{H_2O}{}^a$ is the chemical potential of the adsorbed water and $\mu_{H_2O}{}^{0,a}$ is the standard chemical potential H_2O referred to a surface mole fraction of unity.

Correspondingly, for A and H_2O in the solution

$$\bar{\mu}_A{}^s = \bar{\mu}_A{}^{0,s} + RT \ln a_A{}^s \qquad (16)$$

where $\bar{\mu}_A{}^s$ is the electrochemical potential of A in solution and $\bar{\mu}_A{}^{0,s}$ is the standard electrochemical potential of amine referred to unit mole fraction; and

$$\bar{\mu}_{H_2O}{}^s = \mu_{H_2O}{}^{0,s} + RT \ln a_{H_2O}{}^s \qquad (17)$$

where $\mu_{H_2O}{}^s$ is the chemical potential of water in solution and $\mu_{H_2O}{}^{0,s}$ is the standard chemical potential of water referred to a standard state of unit mole fraction of water in solution.

Now, since

$$\bar{\mu}_A{}^a - \mu_{H_2O}{}^a = \mu_A{}^s - \mu_{H_2O}{}^s \qquad (18)$$

and denoting the difference in standard electrochemical free energy of adsorption of adsorbate and water by $\Delta\bar{G}_0$

$$\Delta\bar{G}_0 = (\bar{\mu}_A{}^{0,a} - \bar{\mu}_A{}^{0,s}) - (\mu_{H_2O}{}^{0,a} - \mu_{H_2O}{}^{0,s}) \qquad (19)$$

then

$$\frac{\theta}{1-\theta} = f_A{}^a \frac{c_A}{55.5} e^{-\Delta G_0/RT} \qquad (20)$$

where c_A is the concentration of A in the solution in mole $l.^{-1}$.

For $f_A{}^s = 1$ equation 20 is equivalent to a Langmuir isotherm. It indicates that $RT \ln (55.5/c_A \times \theta/1 - \theta) = \Delta\bar{G}_0$ and should be independent of θ. This relation has been applied to the data, as shown, *e.g.*, in Fig. 6. Strong systematic deviations of $\Delta\bar{G}_0$ from constancy are seen to occur; this behavior is characteristic of all the examined material over the negative branch.

The deviations from the Langmuir isotherm (20) can be interpreted by introducing into (14) the activity coefficient $f_A{}^a$ for A in the adsorbed state, and referring $\bar{\mu}_A{}^{0,a}$ to infinite dilution of A on the surface by selecting $f_A{}^a = 1$ for $\theta = 0$. Then

$$RT \ln f_A{}^a = U_{AA} \qquad (21)$$

where U_{AA} is the interaction energy per mole of the adsorbed species. If the average distance between the adsorbed centers is r, then, accounting for coulombic and dispersive potentials

$$U_{AA} = N \left(\frac{e_0{}^2}{\varepsilon_s r} - \frac{3}{4} \frac{h\nu\alpha^2}{\varepsilon_0} \frac{1}{r^6}\right) \qquad (22)$$

where ε_s is the static dielectric constant of water in the adsorbed layer, ε_0 is the electronic dielectric constant of the solvent, ν is a characteristic frequency of the electronic oscillators in the adsorbate molecules, and α is the electronic polarizability of the adsorbate.

Introducing

$$r = \sqrt{S/\theta} \qquad (23)$$

$$\alpha = R^3 \qquad (24)$$

and using

$$\pi R^2 = S \qquad (25)$$

where R is the "radius" of the aminium ions

$$\frac{\theta}{1-\theta} = f_A{}^s \frac{c_A}{55.5} \exp\left[-\frac{1}{RT}\left(\Delta\bar{G}_0{}^0 + \frac{Ne_0{}^2}{\varepsilon_s S^{1/2}} \cdot \theta^{1/2} - \frac{3}{4\pi^3} \frac{Nh\nu}{\varepsilon_0} \theta^3\right)\right] \qquad (26)$$

where $\Delta\bar{G}_0$ is the value of $\Delta\bar{G}_0$ corresponding to $\theta = 0$, *i.e.*, is by definition a constant at all values of θ.

This value can be identified with the extrapolated value of $RT \ln (55.5/c_A \times \theta/1 - \theta)$ (*i.e.*, $-\Delta\bar{G}_0$) for $\theta = 0 (U_{AA} = 0)$. By comparing this value with the actual values of $RT \ln (55.5/c_A \times \theta/1 - \theta)$ at any given θ the experimental U_{AA} can be obtained from the equation $U_{AA} = \Delta\bar{G}_0 - \Delta\bar{G}_0{}^0$. The theoretically calculated U_{AA}, namely, the second term in the exponential of (26), is compared with the experimental value in Fig. 7 for $\varepsilon_s = 9.7$. Equation 26 is therefore consistent with the experimental isotherm for aniline, where the interaction forces causing deviation from the Langmuir isotherm are consequently almost entirely coulombic. Similar agreement between (26) and the experimental isotherms is obtained for the other substances examined on the negative branch for $\theta < 0.25$ using $\varepsilon_s = 9\text{-}10$.[23]

(23) That this is a reasonable order of the value of the effective dielectric constant of the water which presumably separates the adsorbed aminium ions is confirmed by comparison with the value of

Equation 26 shows that at high θ values the $RT \ln (55.5/c_A \times \theta/1 - \theta) - \sqrt{\theta}$ plot should pass through a minimum. This forecast behavior is experimentally observed at $\theta \geq 0.2$ on the negative branch, as shown in Fig. 8 for a typical example. The θ at which minimum is expected on the basis of equation 26 is evaluated from $\partial U_{AA}/\partial\theta = 0$ and found to be $\theta = 0.55$ for the parameters $\epsilon_s = 10$, $h\nu = E_{ion} = 10$ e. v., $S = 60$ Å.^{2} (*cf.* Fig. 9 compared with the experimental value of 0.42 from Fig. 8.

This reasonable and quasiquantitative interpretation of the deviations of the isotherms from ideality applies to the negative branch. On the positive branch the behavior conforms more closely to that of a Langmuir isotherm, as seen in Figs. 6 and 8 for $E_H = 0$ and $+200$ mv. Thus, on the positive branch, the coulombic interactions between the adsorbed particles appear to be reduced. It can be seen from Fig. 5, however, that strong specific adsorption of Cl^- occurs at these positive potentials, the Cl^- ions being in excess of RNH_3^+ ions. It seems reasonable to suggest that the Cl^- ions reduce the coulombic repulsion between the adsorbed organic cations, forming dipoles essentially equivalent to RNH_3^+ Cl^-. Some dispersive interaction remains, and in agreement with this $RT \ln (55.5/c_A \times \theta/1 - \theta)$ on the positive branch commences to become more positive at high θ values (Fig. 10).

The fact that the deviations from a Langmuir isotherm appear to be reasonably interpretable in terms of largely ionic respulsion between the adsorbed particles supports the conclusion the adsorbed layer consists of RNH_3^+ rather than RNH_2 molecules.

(3) The Total Charge of the Interface in the Presence of Aromatic Amines.—The change in q_s as a result of the adsorption of a substance A may be thermodynamically related to the variation of Γ_A with potential, from equations 7 and 8, according to which

$$\left(\frac{\partial q_s}{\partial \mu_A^s}\right)_{E_H} = -\left(\frac{\partial \Gamma_A}{\partial E_H}\right)_{\mu_A} \qquad (27)$$

A numerical calculation shows that the order of the observed changes in q_s for aromatic amines are in accordance with (27). Equation 27 can be transformed to

$$\left(\frac{\partial q_s}{\partial \Gamma_A}\right)_{E_H} = \left(\frac{\partial \mu_A^s}{\partial E_H}\right)_{\Gamma_A} \qquad (28)$$

From (26) one obtains

$$\left(\frac{\partial \mu_A^s}{\partial E_H}\right)_{\Gamma_A} = \left(\frac{RT\,\partial \ln c_A}{\partial E_H}\right)_{\Gamma_A} = \left(\frac{\partial \Delta \bar{G}_0^0}{\partial E_H}\right)_{\Gamma_A} \qquad (29)$$

and hence

$$\left(\frac{\partial q_s}{\partial \Gamma_A}\right)_{E_H} = \left(\frac{\partial \Delta \bar{G}_0^0}{\partial E_H}\right)_{\Gamma_A} \qquad (30)$$

Assuming for simplicity $(\partial \Delta \bar{G}_0^0/\partial E_H)_{\Gamma_A}$ to be constant ($= k$) and integrating (30)

$$q_{s,0} - q_{s,A} = -k\Gamma_A \qquad (31)$$

where $q_{s,0}$ is the charge on the solution side of the interface at any given value of E_H for $\Gamma_A = 0$, *i.e.*, in pure HCl; and $q_{s,A}$ is the corresponding value of the charge at E_H in a solution containing A, the concentration of which corresponds to the value Γ_A.

Values of $k\Gamma_A$ may be calculated for chosen val-

about 6 obtained, *e.g.*, in electrostatic calculations of field effects on the dissociation constants of benzoic acids.[24]

(24) G. Kortüm, "Lehrbuch der Elektrochemie," Weinheim, 1957, p. 335.

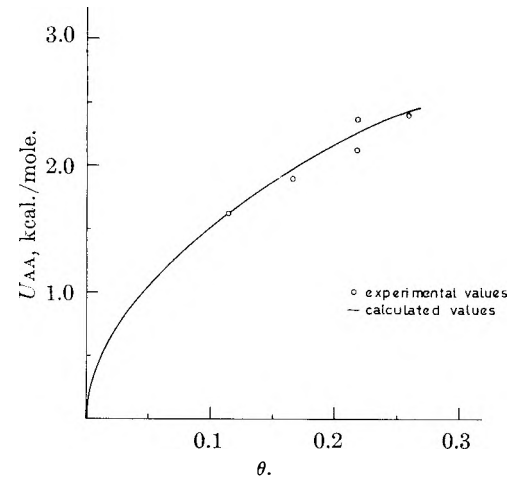

Fig. 7.—Comparison of calculated and experimental interaction energies for aniline in 0.1 N HCl. $E_H = -800$ mv.

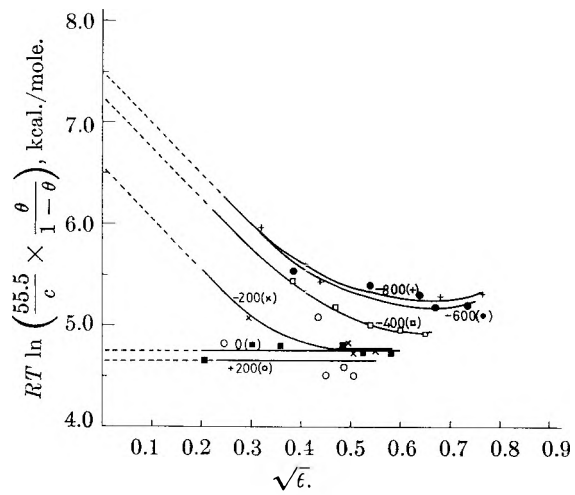

Fig. 8.—Deviations from Langmuir isotherm for *o*-toluidine in 0.1 N HCl at constant potentials. (Potentials stated on figure.)

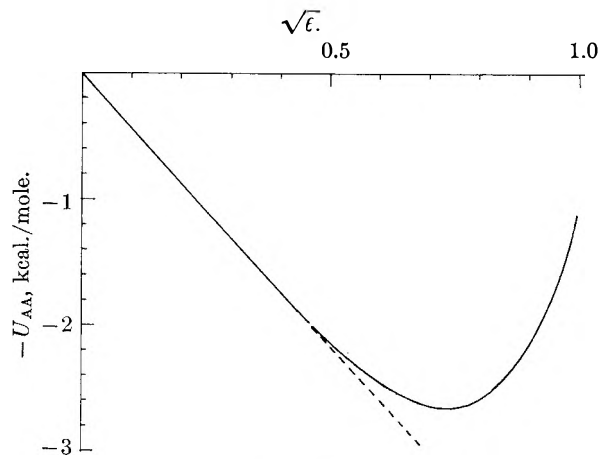

Fig. 9.—Theoretical values of interaction energies for aromatic amines as a function of $\sqrt{\theta}$. Parameters: $\epsilon_s = 10$, $E_{ion} = 10$ e.v., $S = 60$ Å.^{2}.

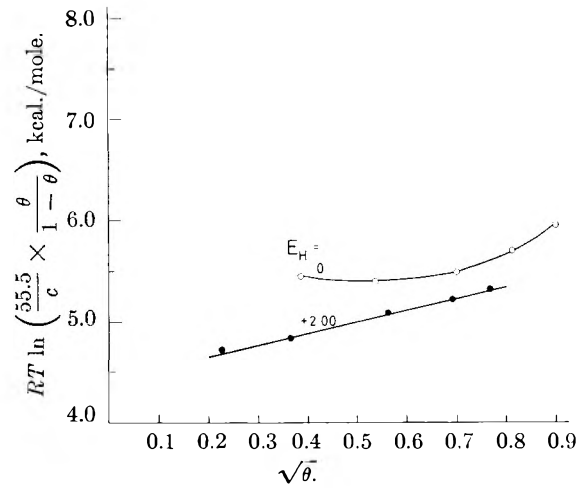

Fig. 10.—Deviations from Langmuir isotherm for 2,6-dimethylaniline in 0.1 N HCl at constant potentials. E_H = 0, +200 mv.

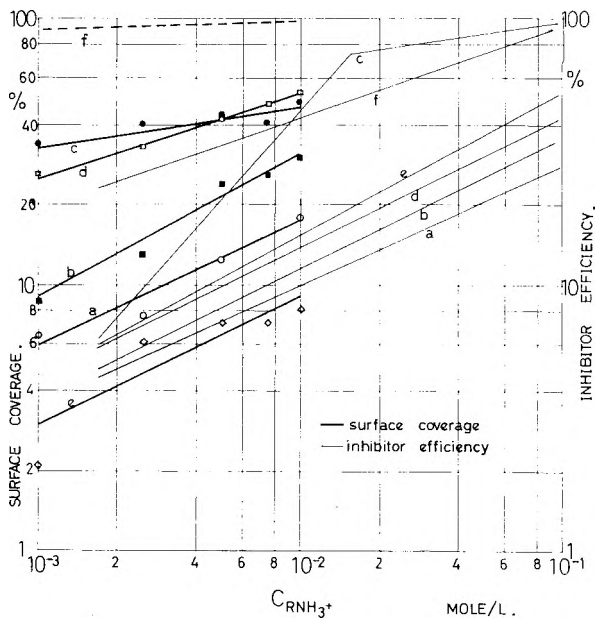

Fig. 11.—Surface coverage on Hg in 0.1 N HCl at e.c.m. and corrosion inhibiting efficiency at mild steel in 1 N H_2SO_4 as functions of concentration: (a) aniline; (b) o-toluidine; (c) 2,3-dimethylaniline; (d) 2,6-dimethylaniline; (e) pyridine; (f) quinoline.

ues of E_H and solution concentrations. Thus, k, defined by (30) and (31), can be obtained, from $\Delta\bar{G}_0^0$ at various potentials, given, *e.g.*, in Fig. 6; and Γ_A is selected for any potential in the range of potentials for which k is approximatly constant, and for a given concentration. On the negative branch and for aniline, one finds $k \sim 3$ kcal. mole^{-1} volt^{-1}. However, Γ_A has the order of 1×10^{-10} mole cm.$^{-2}$, and hence, from these values and equation 31, $q_{s,0} - q_{s,A} \sim 1$ μcoul. cm.$^{-2}$. Hence, even for the more adsorbable substances examined, the calculated change of q_s brought about by adsorbing the aminium ions is about the same as the experimental. Thus, the fact that q_s, as given, *e.g.*, in Fig. 5, differs (at first surprisingly) very little compared with that for the adsorption of HCl at corresponding concentration is consistent with the thermodynamics of the interface.

(4) Composition of the Double Layer in the Presence of 2,6-DMA.—From Fig. 5 it is seen that the value of $F(\Gamma_{H_3O^+} - \Gamma_{RNH_2})$ over the whole potential range with the exception of extremely positive and extremely negative potentials is between about -1 and -3 μcoul. cm.$^{-2}$ at $c_{RNH_3^+} = 0.004$ mole l.$^{-1}$. It can be shown from diffuse double layer theory[22] that the value of $F\Gamma_{H_3O^+}$ for the maximum repulsion of H_3O^+ ions at the HCl concentration of 0.1 N is -1.9 μcoul. cm.$^{-2}$. It is therefore reasonable to suppose that, under the conditions stated, a negligible amount of RNH_2 is adsorbed in the double layer. At $c_{RNH_3^+} = 0.01$ mole l.$^{-1}$, $F(\Gamma_{H_3O^+} - \Gamma_{RNH_2})$ exceeds the value corresponding to the limiting repulsion of H_3O^+ ions by up to about 3 μcoul. cm.$^{-2}$. At $c_{RNH_3^+} = 0.001$ mole l.$^{-1}$ the values of $(\Gamma_{H_3O^+} - \Gamma_{RNH_2})$ are positive on both the positive and negative branch but lower than $\Gamma_{H_3O^+}$ for pure HCl, which suggests that the smaller surface coverage of RNH_3^+ causes a smaller displacement of φ_2 toward positive values than at the higher concentrations of the amine.

The values of Γ_{Cl^-} on the negative branch for $c_{RNH_3^+} = 0.004$ and 0.01 mole l.$^{-1}$ and 0.1 N HCl correspond to $\varphi_2 \sim +0.060$ volt; on the positive branch Γ_{Cl^-} surpasses its values in pure HCl by an amount corresponding approximately to the value of $\varphi_2 \sim +0.06$ volt. The conditions at the higher concentrations of RNH_3^+ are hence consistent with a displacement of φ_2 to positive values over the whole potential range, resulting in an electrostatic repulsion of H_3O^+ ions and a corresponding electrostatic attraction of Cl^- ions into the diffuse double layer.

In summary, the structure of the double layer in the presence of 2,6-DMA is consistent with the following model. The amine is adsorbed predominantly as RNH_3^+ ions and causes a change of φ_2 to less negative values than those in pure HCl. At a coverage of RNH_3^+ ions $\geq 50\%$, this results in positive values of φ_2 and thereby an electrostatic repulsion of H_3O^+ ions and attraction of Cl^- ions over the whole potential range. At higher RNH_3^+ concentrations, a small amount of RNH_2 is adsorbed, except at highly positive potentials.

(5) The Standard Electrochemical Free Energy of Adsorption of Aromatic Amines on Mercury.—Values of $\Delta\bar{G}_0^0$ for $E_H = E_{e.c.m.}$ are given in Table III. ΔG_0^0 is of the same order for the aromatic amines as for the adsorption of neutral organic molecules at mercury.[9] $\Delta\bar{G}_0^0$ increases roughly proportionally to the surface area of the molecules. Thus, the adsorption energy per surface unit remains essentially constant for mononuclear aromatic amines.

(6) The Mechanism of Corrosion Inhibition.—The following conclusions arise from Fig. 11.

(1) With the exception of pyridine the inhibitory effect[25] for the corrosion of mild steel in 1N H_2SO_4 and the degree of adsorption on mercury at the e.c.m. increase essentially in the same order for the substances examined. Only minor differences exist, *e.g.*, the adsorption on Hg is approximately the same for 2,3-DMA and 2,6-DMA, whereas the former isomer is a better inhibitor than the latter.

(25) (a) C. A. Mann, B. E. Lauer and C. T. Hultin, *Ind. Eng. Chem.*, **28**, 1048 (1936); (b) B. E. Lauer, Thesis, Univ. of Minnesota, 1929.

(2) With increasing concentration, the increase of effectiveness of inhibition parallels an increase in surface coverage. For the same concentration the percentage surface coverage on Hg and the percentage inhibition do not differ by more than a factor of five for any of the substances examined.

An earlier examination[26] of the suppressing effect of aromatic amines on polarographic maxima gave a result analogous to (1), but the suppression was found to occur at *ca.* 10^2 times lower concentration than the inhibition[27] thus making the applicability of such data to evaluation of the mechanism of corrosion inhibition significantly less direct than that obtained from the degree of adsorption studies reported here, where the solution concentration of the adsorber is in the same range as that for the inhibitor.

TABLE III

$\Delta\bar{G}_0^0$ FOR ABSORPTION ON Hg IN 0.1 *N* HCl AT e.c.m.

Substance	$-\Delta\bar{G}_0^0$, kcal. mole^{-1}	$-\Delta\bar{G}_0^0/S$ kcal. mole^{-1} Å.$^{-2}$
Aniline	6.0	0.120
o-Toluidine	6.6	.118
2,3-Dimethylaniline	8.3	.133
2,6-Dimethylaniline	8.1	.126
Pyridine	5.2	.130

The results of Fig. 11 present the closest correlation hitherto recorded between the inhibiting effect and another physical property of a group of substances. This suggests adsorption studies on Hg as an appropriate method for determining the effective range of concentration for substances capable of inhibiting corrosion, for the screening of such compounds, investigation of structural group effects among them and studies of the basic phenomena involved in effects of adsorbed substances on the kinetics of electrode reactions.

Figure 11 represents the first *direct* evidence for the usually *assumed* model that aromatic amines in acid solutions bring about inhibition of certain electrode reactions on iron by effects following upon their *adsorption* at the electrode–solution interface. It suggests that the following factors are involved in such inhibition.

(a) **Molecular Weight.**—The known increase of corrosion inhibiting effect at Fe with molecular weight parallels the increase of adsorption on Hg with molecular dimensions (*cf.* Table III). This suggests that the observed dependence of inhibitor efficiency upon molecular weight for Fe follows an increase of adsorption following upon the increase of the molecular dimensions of the inhibitor.

(b) **Orientation of Molecules on the Electrode Surface.**—The *planar* orientation of adsorbed aromatic amines, established for Hg in the present work, clearly increases inhibition effects per molecule of adsorbed inhibitor. It is probably always an important feature of inhibition effects by aromatic substances.[28]

(c) **Dependence of Adsorption on Potential.**—The small variation of adsorption with potential (Fig. 1) will probably also be found for aromatic amines on solid metals, a supposition consistent with the fact that aromatic amines are effective on metals with widely different corrosion potentials (Al, Fe, Sn).[25a]

(d) **Character of Adsorbed Species.**—It has been suggested by Hackermann, *et al.*,[29a-c] that amine type inhibitors are adsorbed from acid solution essentially as free amine molecules in which the amine group forms a dative link with the metal. The present results suggest a noticeable adsorption of free amine molecules on Hg only at high RNH_3^+ concentrations and limited essentially to the negative branch of the electrocapillary curve. In the absence of relevant data on the potential of the e.c.m. at Fe in acid solutions,[29c,30] it is not possible to decide if the mixed potential of iron corroding in acid solutions is in the potential range in which an adsorption of RNH_2 may take place on Hg. Decisive evidence about the role of free amine adsorption in corrosion inhibition could be obtained by comparison of the inhibiting properties of phenyl substituted quaternary ammonium ions with their adsorption on Hg; a parallel between the inhibiting effect of such ions and their adsorption on Hg would not support free amine hypothesis.

(e) **Effect on the Diffuse Part of the Double Layer.**—Bockris and Conway[31] observed that the overpotential of hydrogen evolution on Fe at a given c.d. in the presence of aromatic amines increases in essentially the same order as does the inhibiting effect of the substances and concluded that reduction in the rate of cathodic reaction plays an essential role in the mechanism of the inhibition of H_2 evolution corrosion by aromatic amines in acid solutions. This conclusion is supported by the present results which indicate a change in φ_2 leading to a reduction of the H_3O^+ ion concentration at the outer Helmholtz plane. The change in φ_2, and the resultant H_3O^+ reduction, extends over nearly the whole potential range at sufficiently high surface coverages of the adsorbate, and would therefore be effective in retarding the rate of the hydrogen evolution reaction not only in the more negative potential region at which hydrogen is evolved under a net cathodic current but also at the corrosion potential for Fe (*cf.* Kaesche and Hackermann's results on the retardation of the hydrogen evolution reaction at the corrosion potential of Fe, brought about by aromatic amine inhibitors).

(f) **Corrosion Inhibition and Surface Coverage.**—The parallelism between the adsorption of aromatic amines on Hg and their effect in reducing the rate of corrosion of Fe suggests that (in the absence of highly active groups, *e.g.*, CN or S, which appear at present to cause inhibiting effects at very low surface coverages) inhibition by aromatic amines increases roughly linearly with coverage.

(26) H. C. Gatos, *J. Electrochem. Soc.*, **101**, 433 (1954).

(27) The present adsorption studies hence show that aromatic amines exert their suppressing effect on polarographic maxima at a surface coverage of *ca.* 0.1%.

(28) B. E. Conway, R. G. Barradas and T. Zawidski, THIS JOURNAL, **62**, 676 (1958).

(29) (a) N. Hackermann and A. C. Makrides, *Ind. Eng. Chem.*, **46**, 523 (1954); (b) N. Hackermann, *Trans. N. Y. Acad. Sci.*, [2] **17**, 7 (1954); (c) H. Kaesche and N. Hackermann, *J. Electrochem. Soc.*, **105**, 191 (1958).

(30) A. Frumkin, *Z. Elektrochem.*, **59**, 807 (1955).

(31) J. O'M. Bockris and B. E. Conway, THIS JOURNAL, **53**, 527 (1949).

Implications concerning the mechanism of corrosion inhibition of Fe can, of course, only be made here on the *assumption* that a similarity exists between the mechanism of adsorption of the aromatic amines on Hg and on Fe, supported by the parallelisms shown in Fig. 11. On this basis, it appears that the most necessary structural property of an inhibitor of the aromatic amine type in acid solution is simply that of a high degree of adsorbability and that specific attachments to "active centers" on the electrode surface are not of primary importance. The degree of adsorbability on Hg appears to depend mainly upon the degree of conjugation of the molecules. These considerations of the molecular structure required by an inhibitor must clearly be balanced against other secondary features, *e.g.*, solubility.

Acknowledgments.—The authors' thanks are due to E. I. du Pont de Nemours and Company, Inc., and to the Esso Research and Engineering Company, who individually gave financial support for different portions of this work. The authors wish to express their appreciation to Professor A. R. Day and Dr. F. Brutcher for discussion of electronic aspects of organic structures. Their thanks are also due to Mrs. Maire Blomgren and to Mrs. Catherine Jesch for assistance in the experimental work.

THERMAL DISSOCIATION OF TiI_2

BY D. M. HARRIS, M. L. NIELSEN AND GORDON B. SKINNER

Research and Engineering Division, Monsanto Chemical Company, Dayton, Ohio

Received March 2, 1959

The principal reaction of the Ti–I system at 1723 °K. and pressures of 3 to 15 mm. is $TiI_2(g) = Ti(s) + 2I(g)$. Under these conditions $K_p = 8.2 \times 10^{-2}$ atm.; $\Delta F^\circ = 8.6 \pm 0.6$ kcal./mole. The calculated heat of reaction is 49 ± 4 kcal./mole based on a calculated molar entropy of 101 ± 2 e.u. for titanium diiodide gas at 1723 °K.

Introduction

Thermodynamic data have been published for the titanium iodides only in the range 750 to 902 °K.[1] The present work was undertaken to obtain thermodynamic data at a higher (1723 °K.) temperature, at which titanium metal can be deposited. Other investigators have done qualitative work in this temperature range.[2–4]

Experimental

Materials.—Titanium tubing was obtained from the Superior Tube Company. Titanium rod, obtained from the same source, was turned on a lathe to prepare 0.005 inch thick metal turnings. Titanium diiodide was made by heating TiI_4 or I_2 with a 10-fold excess of titanium metal at 550°.[5]

Apparatus and Procedure.—Equilibrium mixtures of TiI_4, lower iodides and titanium metal for 1723°K. and two different pressures were obtained by vaporizing the lower iodides in the presence of titanium turnings. The resulting mixtures were swept into a collection zone and analyzed to obtain the titanium-to-iodine ratios.

The apparatus consisted of a 0.75 inch by 8.5 inch long titanium tube closed at one end, surrounded by a quartz tube (37 mm. o.d.). The quartz tube was connected to a vacuum source and auxiliary equipment for maintaining a controlled pressure over the range 1 to 25 mm. (± 0.1 mm.). For a run, about 0.8 g. of TiI_2 was charged into a small titanium holder and placed in the bottom of the larger titanium tube. The larger tube was filled with titanium turnings and the tube covered by a cap having an $^1/_8$ inch hole in the center. The cap prevented heat loss by radiation from that end of the tube.

The capped end of the tube was heated first by an induction coil 8 inches in length to bring the metal to the desired temperature. The coil was then gradually lowered to vaporize the iodide. There was, of course, a severe temperature gradient in the bottom half of the tube, so that the bottom end was hundreds of degrees cooler than the top part. The rate of evaporation of iodide could be controlled by adjusting the position of the induction coil relative to the tube, by use of a screw mechanism to give smooth, accurate positioning. During the operation, a stream (about 36 ml./min. at S.T.P.) of argon purified by gettering with titanium at 900–1000°[6] was swept past the titanium tube to transport the mixture of iodine and iodides issuing from the tube into a Dry Ice-cooled collection trap. The progress of the reaction could be followed visually by watching the build-up of deposit in the Dry Ice trap, and the flow of reaction products being swept along in the tube leading to the trap. The time at which reaction started was noted for each run, and the position of the induction coil was adjusted from time to time to give a roughly constant rate of product evolution throughout each experiment. Finally, the products in the trap were dissolved by treatment with 0.5 *M* H_2SO_4 to dissolve the iodides, followed by ethanol to dissolve free iodine. The combined acid–ethanol solution was analyzed for total iodine and titanium.

To determine whether the iodine-to-titanium ratios were equilibrium values, the rate of vaporization of the iodide was varied. Table I lists the average rate of flow of vapors over the hot titanium turnings, in cc./sec.

It is important to note that the total volume of the titanium tube was about 40 cc., while the total volume of vapors liberated (calculated as $TiI_2 + I$ as discussed below) was of the order of thousands of cc. It is clear then that the argon originally filling the tube was swept out by the first few per cent. of vapors evolved. Moreover, all of the vapors emerged through a hole of about 0.08 sq. cm. area with a flow velocity varying between 14 and 300 cm./sec., which seems high enough to prevent diffusion of argon back into the tube during the experiment. While the total volume of the titanium tube was about 40 cc., only the top third was at the uniform 1723°K. temperature, so the residence time of vapors in the hot zone varied between 0.5 and 12 seconds.

Since direct measurement of the reaction temperature during the dissociation was not convenient, the oscillator settings were calibrated in terms of the tube temperature. This was done by heating the tube containing titanium turnings in the absence of iodides and measuring the temperature by means of a calibrated optical pyrometer sighted on the turnings through the hole in the cap. During this operation the pressure and rates of flow of purified argon were the same as for actual runs. The settings were reproducible to within

(1) A. Herczog and L. Pidgeon, *Can. J. Chem.*, **34**, 1687 (1956).

(2) O. Runnalls and L. Pidgeon, *J. Metals*, **4**, 843 (1952).

(3) A. Loonam (to Chilean Nitrate Sales Corporation), U. S. 2,694,652 (Nov. 16, 1954)

(4) A. Loonam (to Chilean Nitrate Sales Corporation), U. S. 2,694,653 (Nov. 16, 1954).

(5) J. Fast, *Rec. trav. chim.*, **58**, 174 (1939).

(6) M. Mallett, *Ind. Eng. Chem.*, **42**, 2095 (1950).

TABLE I

SUMMARY OF EXPERIMENTAL DATA AND CALCULATIONS, TEMPERATURE = 1723 °K.

Experiment no.	1	2	3	4	5
Pressure, mm.	15.1	15.2	15.1	3.4	3.4
Total TiI_2 charged, g.	1.9	0.8	0.7	0.9	0.8
Total wt. evaporated, g.	0.0358	0.313	0.667	0.223	0.161
Total reaction time, sec.	1,500	2,300	1,200	5,000	4,500
Total vol. of gas, cc.	1,640	14,200	29,300	51,800	37,800
Rate of flow of gas, cc./sec.	1.1	6.2	24.4	10.4	8.4
I/Ti atomic ratio	6.96	6.60	5.53	20.4	23.4
$K_p \times 10^2$ for reaction $TiI_2(g) = Ti(s) + 2I(g)$	8.2	7.5		7.8	9.1
$K_p \times 10^4$ for reaction $TiI_3(g) = Ti(s) + 3I(g)$	10.0	8.7		3.1	3.7
$K_p \times 10^6$ for reaction $TiI_4(g) = Ti(s) + 4I(g)$	9.7	7.7		1.2	1.5

±5 °K. For purposes of calculation, the error was assumed to be ± 10°.

In order to establish that black body temperatures were being read, a portion of the titanium turnings was replaced by a titanium block with a hole 1/8 inch by 3/4 inch to sight on with the optical pyrometer. The temperature reading was unaffected by this substitution.

Measurements were made at 1723 and 1420 °K.; only the data for the higher temperature are reported since data obtained at 1420 °K. were not reproducible, presumably owing to inability to obtain equilibrium mixtures.

Results and Discussion

The experimental results are summarized in Table I. Since the lowest I/Ti ratio was 5.53, it is clear that some titanium deposited on the titanium turnings in all experiments. In run 3, with the fastest flow rate, equilibrium does not seem to have been reached, but in runs 1 and 2 the substantial difference in flow rate caused no significant change in composition. A flow rate of about 10 cc./sec., corresponding to a residence time of just over a second, seems slow enough to give equilibrium data within the accuracy of our analyses at 1723°K. At lower temperatures, of course, a longer time would be required.

To determine which titanium iodide is the major species under these conditions, the equilibrium constants may be calculated. If TiI_2 is the major species, then equilibrium (a) will govern the composition, (since there is no appreciable amount of undissociated I_2 under these conditions), with corresponding equations for TiI_3 and TiI_4. Since the calculated equilibrium constants (see Table I) are nearly constant for equation (a) and not for the others, TiI_2 is indicated as the major titanium species in the vapor phase.

$$TiI_2(g) = Ti(s) + 2I(g) \qquad (a)$$

The free energy of reaction (a), as calculated from the average value of the equilibrium constant, 8.2×10^{-2} atm. at 1723°K. is 8.6 ± 0.6 kcal./mole. The estimate of error is based on a ± 10° uncertainty in temperature, and ± 10% equilibrium composition. This free energy value is in rough agreement with the value of 21 ± about 15 kcal./mole calculated from Brewer's tables.[7]

As stated in the Experimental Section, attempts to obtain satisfactory data at temperatures other than 1723°K. failed. Therefore, the molar entropy of $TiI_2(g)$, 101 ± 2 e.u. at 1723 °K., was calculated using estimated molecular dimensions and vibrational frequencies of TableII.

TABLE II

ESTIMATED MOLECULAR DIMENSIONS AND VIBRATIONAL FREQUENCIES FOR TiI_2

Iodine–titanium–iodine angle, degree	110
Iodine–titanium distance, Å.	2.50
Vibrational frequencies,[a] cm.$^{-1}$	
1	320
2	130
3	340

[a] An error of 30% in vibrational frequencies will give rise to an error of ±2.3 entropy units in the molar entropy of TiI_2.

Because of its unused pair of "valence" electrons, the TiI_2 molecule is probably bent, as are H_2O, SO_2 and Cl_2O, which have somewhat similar electronic configurations.[8]

The average bond angle of these bent molecules is about 110°. Pilcher and H. A. Skinner have also assumed that $TiCl_2$ is a bent molecule with the slightly larger Cl–Ti–Cl angle of 120°.[9] For the Ti–I distance we have assumed a covalent bond. Since the Ti–Cl distance in $TiCl_4$ is 2.18 Å.[10] and the covalent radius of iodine is about 0.34 Å. larger than that of chlorine,[11] the distance of 2.50 Å. seems reasonable. If the TiI_2 molecule were ionic, the Ti–I distance would be 2.84 Å., according to Pauling's tables, but this seems rather unlikely. Even as "ionic" a molecule as NaCl has a bond distance of only 2.51 Å. in the vapor state,[12] whereas the sum of Pauling's ionic radii is 2.76 Å., and Herzberg lists many other halides and oxides where the same effect is observed. In estimating the vibrational frequencies, the known frequencies of $TiCl_4$,[13] $TiBr_4$[13] and $TiCl$[12] were used, along with informa-

(7) L. Brewer, "The Chemistry and Metallurgy of Miscellaneous Materials: Thermodynamics," McGraw-Hill Book Co., Inc., New York, N. Y., 1950, pp. 60–275.

(8) G. Herzberg, "Infrared and Raman Spectra of Polyatomic Molecules," D. Van Nostrand Co., New York, N. Y., 1945.

(9) G. Pilcher and H. A. Skinner, *J. Inorg. Nuclear Chem.*, **7**, 8 (1958).

(10) M. W. Lister and L. E. Sutton, *Trans. Faraday Soc.*, **37**, 393 (1941).

(11) L. Pauling, "The Nature of the Chemical Bond," Cornell University Press, Ithaca, N. Y., 1940.

(12) G. Herzberg, "Molecular Spectra and Molecular Structure. I. Diatomic Molecules," Prentice-Hall, Inc., New York, N. Y., 1939.

(13) M. L. Delwaulle and F. Francois, *Compt. rend.*, **220**, 173 (1945); *J. phys. radium*, **7**, 15, 53 (1946).

tion on bent triatomic molecules given by Herzberg.[8] The estimates of the vibrational frequencies introduces the largest uncertainty into the entropy calculation. An error of 30% in the frequencies will give rise to an error of ±2.3 entropy units at 1723 °K.

The ΔS of reaction (a), 23.4 e.u., was then calculated using the published entropies of titanium and iodine.[14] The heat of reaction, then, is 8.6 + (1723 × 23.4)/1000 or 49 ± 4 kcal./mole.

(14) National Bureau of Standards, Selected Values of Chemical Thermodynamic Properties, Series III (1952–54).

THE SURFACE PROPERTIES OF LIQUID LEAD IN CONTACT WITH URANIUM DIOXIDE

BY D. H. BRADHURST AND A. S. BUCHANAN

Chemistry Department, University of Melbourne, Australia

Received March 10, 1959

The sessile drop technique has been used to measure surface tensions and contact angles of liquid lead on uranium dioxide surfaces. The influence on these properties of the metallic solute bismuth and the non-metallic solutes oxygen, sulfur, selenium and tellurium has been investigated. Oxygen is clearly the most effective in reducing the surface tension and contact angle of the molten lead.

Introduction

The present study forms part of an investigation on the stability of suspensions of uranium dioxide in liquid metals. As a preliminary approach to this problem it was decided to investigate the wetting of uranium dioxide by lead, and for this purpose the sessile drop technique of Humenik and Kingery[1,2] appeared admirably suited, since both contact angle of the liquid with the solid, and the surface tension of the former could be measured in the one experiment. Abrahams, Carlson and Flotow[3] have used this method for an investigation of the sodium–potassium alloy–uranium dioxide system. The sessile drop method has been adapted to the requirements of the lead–uranium dioxide system, and the influence of variables such as the constitution of the liquid, the stoichiometry of the uranium dioxide, and its density; nature and pressure of the surrounding atmosphere, and the temperature, have been investigated.

Experimental

The apparatus consisted of a 6″ by 1″ dia. molybdenum tube furnace, heated by induction and enclosed within a water-cooled Pyrex glass or silica tube. This tube was equipped with optical flats at each end, enabling the sessile drop and uranium dioxide plaque to be photographed under any desired conditions. The induction heater was of the radiofrequency type and enabled temperatures of greater than 1500° to be maintained indefinitely. The temperature was measured using a Cambridge optical pyrometer, and a Cu–advance alloy thermocouple, the latter checked in each run against the melting point of lead.

A vacuum line was connected to the furnace tube, and evacuated by a mercury diffusion pump and backing pump, giving a pressure of about 10^{-6} mm. Purified argon, carbon monoxide or hydrogen atmospheres could be introduced through a purification line consisting of a liquid oxygen trap, sodium–potassium alloy trap and two P_2O_5 drying columns.

A magnified image of the sessile drop and uranium dioxide plaque was focussed on to a photographic plate by an f4.5, 8″ focal length lens and microscopic eyepiece, mounted on an optical bench. Using an exposure of 60 seconds at f23, very sharp images were obtained. Measurements of drop dimensions and contact angle were made on traced enlargements (magnification 30 times) of these plates, and using Dorsey's[4] method of calculation, surface tensions could be reproducibly determined to within ±2%, and contact angles to within ±2°. Figure 1 shows that the measurements taken for calculation of surface tension are independent of the over-all height of the drop and its angle of contact with the plaque surface, and may be precisely determined. The equation used was

$$T = gdr^2(0.05200/f - 0.1227 + 0.0481f)$$

where

T = surface tension, dyne. cm.$^{-1}$
f = $y/r - 0.4142$
g = acceleration due to gravity, cm. sec.$^{-2}$
d = density of the lead, g. cm.$^{-3}$
r = radius of drop, cm.
y = distance from drop apex to the point of intersection of the two 45° tangents.

Lead samples (99.999%, supplied by the Metallurgy Department, University of Melbourne) were prepared in cylindrical pellet form (3.5 by 6.5 mm.) using a stainless steel punch. The lower surface of the pellet so obtained was hemispherical, ensuring a uniform advancing angle of contact on melting. The lead surface was scraped clean with a stainless steel blade before each pellet was made, after which ivory tipped forceps were used for handling. The extent of oxidation during handling was negligible. The pellet was weighed, then reweighed in the cases where surface active agents had been added. The additives were confined in a small hole drilled in the surface of the pellet and concentrations in the range 0.003 to 0.05 molal with respect to PbX (X = O, S, Se, Te) were used.

Uranium dioxide plaques were prepared by igniting "Baker's Analyzed" uranyl acetate at 1100° in air, then completely reducing the U_3O_8 formed to brown $UO_{2.00}$ in purified hydrogen at 900°. A weighed sample of this product was heated in air for 10 minutes at 200° during which time the composition was altered to $UO_{2.13}$. This non-stoichiometric oxide sinters more readily than $UO_{2.00}$,[5] and plaques of density 8.5 to 9.3 were obtained by cold pressing at 100,000 p.s.i. and sintering at 1400–1500° in dynamic vacuum of approximately 10^{-3} mm. For the study of the effect of plaque density on surface tension and contact angle, specially prepared samples of uranium dioxide of density 10.8 were obtained from the Industrial Group, U. K. Atomic Energy Authority.

The plaque surfaces were ground flat and lightly polished on a silicon carbide stone, then reduced to stoichiometric UO_2 prior to each run as described above. The plaque and preweighed pellet were inserted into the molybdenum susceptor of the induction furnace and levelled horizontally and

(1) M. Humenik and W. D. Kingery, THIS JOURNAL, **57**, 359 (1953).

(2) W. D. Kingery, USAEC report, NYO-3144.

(3) B. M. Abrahams, R. D. Carlson and H. E. Flotow, USAEC report, NESC-104, 1957.

(4) N. E. Dorsey, *J. Wash. Acad. Sci.*, **18**, 505 (1928).

(5) P. Murray, E. P. Rodgers and A. E. Williams, AERE report, M/R-893, 1952.

longitudinally with the aid of a cathetometer. The furnace was evacuated and then heated to a temperature of 750°, to assist degassing. Photographs were taken at 700, 750, 600 and 500° and were spaced at intervals of 30, 45, 50 and 60 minutes, respectively.

Photomicrographs of the plaque surface and features of the lead surface, were taken when necessary at the completion of a run and the solidified drop was checked for uniform diameter.

Results

The initial work was concerned with the measurement of surface tension of lead–bismuth alloys as a function of composition, and Fig. 2. shows the isotherm obtained for 700°. The relationship appears to be linear as was also found for the Fe–Ni system at higher temperatures.[2] An interesting result which emerged from this work was evidence for the sensitivity of both surface tension and contact angle of lead towards oxygen present as dissolved oxide. Figure 3 shows two contact angle *vs.* composition curves obtained in atmospheres of hydrogen and cylinder argon, respectively. The cylinder argon used at the time contained some oxygen, as shown by the blackening of the UO_2 surface surrounding the solidified drop, and the appearance of microcrystalline tetragonal lead oxide on the lead surface after solidification.[6] In hydrogen at 700°, uranium dioxide would be present as $UO_{2.00}$ and any PbO would be reduced to lead. The lower contact angle with the argon atmosphere was almost certainly due to oxygen dissolved in the liquid phase, the effect obviously being much less for bismuth than for lead. Subsequent work on the addition of lead oxide to the liquid lead has confirmed this explanation. Furthermore, an order of surface activity has been established for lead oxide, lead sulfide, lead selenide and lead telluride dissolved in liquid lead. Figure 4 shows the surface tension isotherms for these solutes, while Table I gives the order of surface activity and indicates clearly the unique position of oxygen as a solute.

TABLE I

System	Maximum reduction in surface tension % at 750°, dyne cm.$^{-1}$	Work of adhesion in contact with $UO_{2.00}$, dyne cm.$^{-1}$
Pure Pb		61.4
PbO + Pb	22.2	198.0
PbS + Pb	7.0	137.0
PbSe + Pb	5.0	132.0
PbTe + Pb	2.5	133.0

Oxygen present in non-stoichiometric forms of uranium dioxide in the range $UO_{2.00}$ to $UO_{2.67}$ was converted to lead oxide by the molten lead, and produced similar depressions in surface tension and contact angle to those obtained by direct additions of lead oxide.

Surface tension and contact angle were found to be independent of the density of the uranium dioxide plaque, identical values being obtained for plaques of density 6.5, 9.3 and 10.8.

Discussion

The surface activity of the solute elements has been shown to be in the order O>>S>Se≃Te (Table I and Fig. 4). The considerable effect of the first member of this series in lowering the surface free energy of liquid lead indicates an appreciable excess concentration of solute species in the surface of the liquid, and moreover, the entities in the surface must have a significantly lower field of force than that operating between the atoms of the liquid lead. This suggests that the PbO dissolved in the lead has an appreciable covalent character in its bonding. In additional support of this view is the fact that the solubility of oxygen in lead is relatively low (Table II), and furthermore it has been observed in the present experiments that PbO comes out of solution in the liquid lead when the temperature is reduced; its solubility must therefore be quite inappreciable at low temperatures.

(6) D. H. Bradhurst and A. S. Buchanan, to be published.

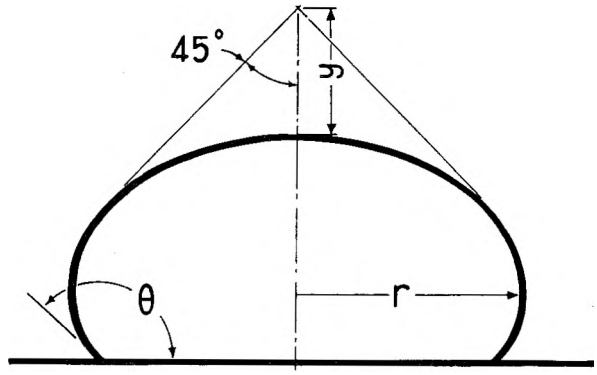

Fig. 1.—Profile of a typical sessile drop showing the measurements made for calculation of surface tension.

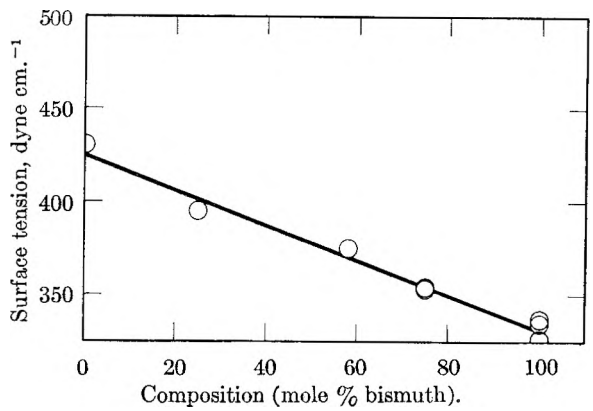

Fig. 2.—Surface tension *vs.* composition isotherm for lead-bismuth alloys at 700°.

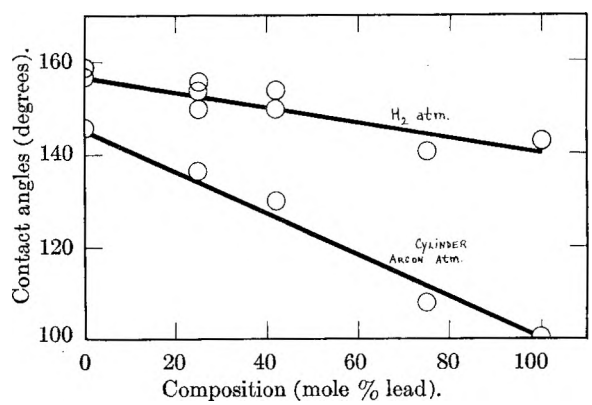

Fig. 3.—Two contact angle *vs.* composition curves of different slopes for lead-bismuth alloys in hydrogen and cylinder argon atmospheres.

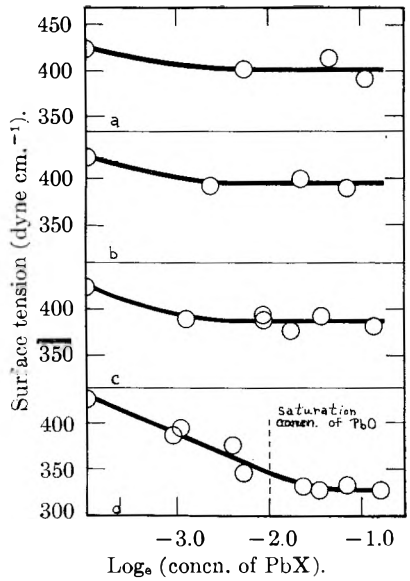

Fig. 4.—Surface tension *vs.* concentration isotherms for lead containing solutes (a) PbTe, (b) PbSe, (c) PbS, (d) PbO, at 750°. Note that the maximum depression in surface tension in (d) corresponds approximately to the saturation concentration of PbO at this temperature.

TABLE II

Solute	Solubility in liquid lead at 750°, wt. %[7,8]
O	0.20
S	0.46
Se	2.5
Te	10.8

The order of surface activity described above does not appear to be the same in all metals, *e.g.*, in liquid iron, the order is O<S<Se>>Te.[9]

It may be noted from Fig. 4 that the maximum lowering of surface tension of lead with oxygen as a solute coincides approximately with the saturation concentration[7] of the solution at the experimental temperature. If indeed the surface activity of oxygen dissolved in liquid lead is associated with appreciable covalent character of the bonding in PbO, then it is surprising that the other members of the solute series S, Se, Te, display so little surface activity since the larger ions $S^{=}$, $Se^{=}$, $Te^{=}$, should be more readily polarized by Pb^{++}, giving enhanced covalent character to the bonding. Even if the solute species consisted largely of independent ions S″, Se″, Te″, the considerable size of these entities should mean that they are difficult to accomodate within the bulk of the liquid lead and should therefore exhibit surface activity (Table III).

TABLE III

Species	Radius, Å. Covalent	Radius, Å. Ionic (X″)	Ionization potential[10] for loss of 1 electron (e.v.)
Oxygen	0.74	1.4	13.61
Sulfur	1.04	1.8	10.36
Selenium	1.17	1.98	9.75
Tellurium	1.37	2.2	8.96
Lead (Pb^{++})		1.2	

The relative lack of surface activity of the solutes S, Se, Te, appears to be associated with increasing metallic character, particularly in the case of the latter two. This leads to enhanced solubility (Table II) with less tendency to form a surface layer in the liquid. We have observed in the present experiments that PbS, PbSe and PbTe dissolve very rapidly in the liquid lead, and moreover, do not come out of solution appreciably when the lead is cooled, in comparison to PbO as a solute (although Greenwood[11] has observed the formation of very small PbS crystals on a solidified lead surface, using a magnification of 900 times).

The metallic character of selenium and tellurium particularly in the molten state[12] is undoubted, the elements both existing in a metallic form which exhibits slight electronic conductivity and appreciable photoconductivity, indicating ready excitation of electrons to the conduction bands (*cf.* ionization energies in Table III). Furthermore, the compounds PbS, PbSe and PbTe all exhibit electronic conductivity, the electronic mobilities being PbS 640, PbSe 1400 and PbTe 2100 cm.^{2}/volt sec. and associated with this is the metallic appearance of these compounds. It is likely therefore that the solutes S, Se and Te are readily accommodated in the bulk of the liquid lead, existing either as a solution of neutral atoms, or more probably, with some transfer of electrons to the conduction bands of the liquid metal. It may be noted in this respect that the covalent radii of Se and Te in particular are close to the radius of Pb^{++}.

As the works of adhesion indicate (Table I), the solute oxygen is the most effective in enhancing the wetting of UO_2 by liquid lead, but this effect is not considerable until quite high temperatures are attained. There is therefore some advantage in having traces of oxygen in liquid lead where wetting of oxide surfaces is desired.

This work was supported by a grant from the Australian Atomic Energy Commission, and forms part of a program of work on the surface chemistry of liquid metal systems.

(7) F. D. Richardson and L. E. Webb, *Trasn. Inst. Min. and Met.*, **64**, 529 (1955).

(8) M. Hansen, "Constitution of Binary Alloys," McGraw-Hill Book Co., Inc., New York, N. Y., 2nd ed., 1958, pp. 1099–1112.

(9) W. D. Kingery, THIS JOURNAL, **62**, 878 (1958).

(10) Landolt and Börnstein, "Zahlwerte und Funktionen aus Chemie," Vol. 1, Part 1, pp. 211–212.

(11) J. N. Greenwood and H. W. Worner, *J. Inst. Metals*, **66**, 435 (1939).

(12) W. Klemm, *Proc. Chem. Soc.*, 329 (1958).

I. PHOTOLYSIS OF LOW MOLECULAR WEIGHT OXYGEN COMPOUNDS IN THE FAR ULTRAVIOLET REGION[1]

BY ANNA J. HARRISON AND JUDITH S. LAKE[2]

Contribution from the Carr Laboratory of Mount Holyoke College, South Hadley, Mass.

Received March 11, 1958

A preliminary survey has been made of the far ultraviolet vapor phase photolysis of several low molecular weight alcohols, ethers, ketones and acetaldehyde by identifying the far ultraviolet absorption bands which appear during the process of irradiation. Although the reaction mechanism would be expected to be complex, most of the products which were detectable fit into comparatively simple patterns. Probable primary processes are discussed.

Pitts[3] has recently pointed out both the importance of, and the experimental difficulties of, extending photolysis studies into the far ultraviolet. The present study gives some of the qualitative information which should aid in the planning of significant quantitative experiments.

This investigation started with two compounds, diethyl ether and ethanol, which do not absorb below 50,000 cm.$^{-1}$. No work has been reported on the photolysis of pure diethyl ether and there is only one article on ethanol vapor. In an attempt to distinguish between primary products and secondary products, the problem was expanded to include an investigation of the identified products. By this time the prediction of detectable products had become surprisingly accurate and a number of compounds were investigated to test the generalization which had become apparent.

Experimental

The equipment[4] consisted of the source, a reaction vessel and a vacuum spectrograph. All optical parts were either calcium or lithium fluoride and a nitrogen atmosphere was maintained in the spaces between the three sections of the equipment. The source, a hydrogen discharge lamp, gave a continuum throughout the visible and ultraviolet to 59,700 cm.$^{-1}$ and beyond that a closely spaced line spectrum which was cut off at about 66,000 cm.$^{-1}$ by the particular window used on the lamp. The reaction vessel, which was a 32.5 cm. Pyrex tube, 1.4 cm. in diameter, was contained in a vapor handling system such that a study could be made of either flowing or static vapor samples. Ilford Q 1 and Q 3 spectrographic plates were used.

The combination of lamp intensity, dispersion of the instrument and plate response necessitated an exposure time of 2–3 minutes. All measurements were therefore a kind of integrated record of the compounds present in the absorption tube during a 2 or 3 minute irradiation period. In the photolysis studies, static vapor samples were irradiated for a total time ranging up to a maximum of 21 minutes. The pressures of the initial vapor samples in the absorption tube ranged from 10^{-2} to 1 mm. of mercury.

Six exposures were recorded on each photographic plate. For any one plate these exposures were selected from some combination of the following: (1) the flowing vapor at a known pressure, (2) the initial irradiation period of the static vapor sample at the same pressure, (3) later periods of irradiation of the same static vapor sample, and (4) a series of time calibration exposures. The first gave the truest picture of the spectrum of the compound being studied and in all cases was free from evidence of photochemical reactions taking place. The second showed the emerging pattern which was followed in later exposures. Time calibration exposures, which were made through the evacuated absorption tube, served as a check on the transmission of the cell windows and also as a basis for estimating relative concentrations.

Results

The microphotometer records of each successive exposure recorded the decrease in absorption of the reactant and at the same time the increase in absorption of the photodecomposition products. See Fig. 1. As the photolysis proceeded, the characteristic narrow bands of the reactant receded toward the general continuum of broad bands and the characteristic narrow bands of the products rose above the general absorption curve.

A number of patterns of reaction were observed. Frequently the spectrum of a product appeared readily during the initial period of irradiation but increased only slightly on continued irradiation. In some cases one product appeared during the initial period while another product, which had an equivalent extinction coefficient, required more prolonged irradiation. All narrow bands which appeared during the photolyses have been identified.

Since this method of analysis is extremely insensitive for those compounds having either structureless broad bands or low intensity narrow bands, the experimental results emphasize certain compounds and minimize others. In order to keep the results in perspective, the spectra of a number of compounds have been summarized in Table I, for the region 2000-1500 Å., (50,000-66,000 cm.$^{-1}$). The aldehydes and ketones also have low intensity absorption bands in the near ultraviolet region and 2,3-butanedione also absorbs in the visible region. Unless a footnote is given, the description is based upon measurements which have been made in this Laboratory. In general the method is particularly sensitive for detecting those compounds which have π-bands but quite intensitive for saturated compounds.

Rough approximations using known or estimated extinction coefficients indicate that during the time of observation, not more than 50% of the reactant disappeared and that the products observed account for 10–50% of the reacting molecules. The experimental results are summarized below. Diethyl ether: ethylene, acetaldehyde and formaldehyde were all produced in significant quantities. See Fig. 1. Dimethyl ether: formaldehyde was produced in significant quantity. On longer exposure a small quantity of ethylene and acetaldehyde were also produced. The appearance of acetaldehyde was more apparent at higher pressures of the ether va-

(1) The spectrographic research program in this Laboratory has received financial support from the Esso Research and Engineering Company and the National Science Foundation (NSF-G752). This research was supported in part by a grant from the Petroleum Research Fund administered by the American Chemical Society. Grateful acknowledgment is hereby made to the donors of this fund.

(2) Sinclair Fellow, 1956–1957.

(3) J. N. Pitts, *J. Chem. Ed.*, **34**, 112 (1957).

(4) A. J. Harrison, C. L. Gaddis and E. M. Coffin, *J. Chem. Phys.*, **18**, 221 (1950).

TABLE I

FAR ULTRAVIOLET SPECTRA OF THE COMPOUNDS

Compounds	Regions of absorption max. (cm.$^{-1}$ × 10^{-3})	Max. molar extinction coefficient (× 10^{-3})	Spectral character
Water	60	1.5	Broad, structureless
Alkyl alcohols	55	0.1	Broad, structureless
	62–66	1	Some structure
Alkyl ethers	52–56	2–3	Pattern of small blunt bands
	57–63	4	Some structure
Formaldehyde	57	18	Sharp
	64	23	Sharp
Acetaldehyde	55–60	13	Three main pairs of bands
	60–64	24	Diffuse bands
Propionaldehyde	54–55		Sharp, narrow
	55–58		Low intensity
	59–60		Intense, diffuse
Acetone	50–55	10	3 main sets of bands
	60–65	10	Several bands
2-Butanone	51–55		Diffuse, similar to acetone
	58–60		Intense, diffuse
2-Pentanone	51–55		Similar to 2-butanone
	58–60		
2,3-Butanedione	57–59		Broad, structureless
2,5-Hexanedione	52–55		Similar to other monoketones
	55–60		Broad, intense
Ketene[5]	55–59		Several sharp bands
	61–64		Several diffuse bands
Ethylene[6]	57–61	16	6 bands
Carbon monoxide[7]	50–60		Low intensity
Hydrogen and satd. hydrocarbons			Transparent

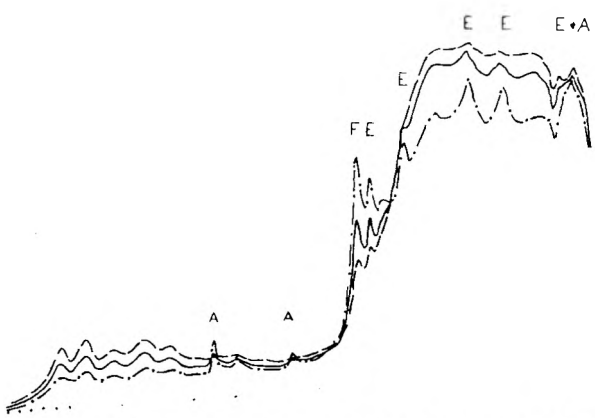

Fig. 1.—Microphotometer record showing the photolysis of diethyl ether, at an initial pressure of 0.19 mm. of mercury. Record: — —, the initial 3 min. exposure of the static vapor sample; ———, the second 3 min. exposure; — · —, the sixth 3 min. exposure; . . ., a 3 min. exposure through the evacuated absorption tube. Bands marked A are due to acetaldehyde, F to formaldehyde and E to ethylene. Note that some photolysis occurred during the initial 3 min. exposure.

(5) W. C. Price, J. P. Teegan and A. D. Walsh, *J. Chem. Soc.*, 920 (1951).

por. Ethanol: ethylene, acetaldehyde and formaldehyde were all produced in significant quantities. Methanol: formaldehyde was produced in significant quantity. Acetaldehyde could also be detected but in relatively smaller quantity. 1-Propanol: ethylene, propionaldehyde and formaldehyde were all produced in significant quantities. 2-Methyl-2-propanol: acetone was very readily produced. A much smaller quantity of ketene appeared as the irradiation was continued. Acetaldehyde: ketene and acetone were produced. The rate of disappearance of acetaldehyde was rapid but the quantity of acetone produced was small in comparison to the quantity of acetaldehyde decomposed. Since the extinction coefficients for ketene are not known, it is not possible to estimate quantities, but they appeared to be small. Acetone: ketene was the only detectable product. The quantity produced was much greater than that produced in the photolysis of acetaldehyde. 2-Butanone: ethylene and ketene were produced in significant quantities, and acetaldehyde may have been produced. If it was, the quantity was so small that its identification cannot be considered as definite. 2-Pentanone: ethylene, ketene and acetone were all produced in significant quantities. 2,3-Butanedione: ethylene, ketene and acetone were produced, but the quantities were very small in comparison to the quantity of reactant decomposed. 2,5-Hexanedione: ethylene, ketene and acetone were all produced in significant quantities.

Discussion

Generalizations.—Most of the observed products can be summarized by three empirical rules. In stating these, there is no intent to imply the mechanism by which the products are formed. They simply give an easy way of summarizing a number of details. The photolysis of all the compounds which had two adjacent carbon atoms, other than a carbonyl carbon atom, led to the formation of ethylene

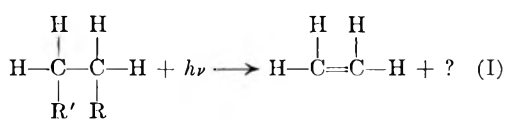

(I)

where R′ may be a hydroxy group, an alkoxy group or a carbonyl group and R may be a hydrogen, an alkyl group or a group containing a carbonyl group. The photolysis of alcohols and ethers led to the formation of aldehydes or ketones

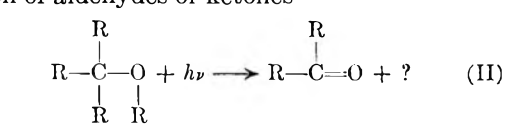

(II)

where R may be a hydrogen atom or an alkyl group. Acetaldehyde and all of the ketones reacted to form ketene

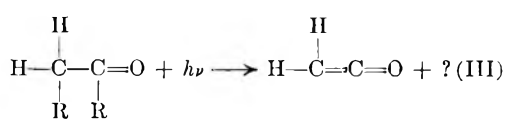

(III)

(6) V. J. Hammond and W. C. Price, *Trans. Faraday Soc.*, **51**, 605 (1955).

(7) D. N. Read, *Phys. Rev.*, **46**, 571 (1934).

where R is a hydrogen atom, an alkyl group or a more complicated group which may contain a second carbonyl group.

The above three statements include all of the observed products with the exception of acetaldehyde from dimethyl ether$^+$ and methanol*; ethylene from dimethyl ether$^+$ and 2,3-butanedione*; acetone from acetaldehyde*, 2-pentanone, 2,3-butanedione* and 2,5-hexanedione; and ketene from 2-methyl-2-propanol$^+$.[8]

The generalizations may reflect the fundamental nature of the process. On the other hand they may be the consequence of the selectivity of the method of detection.

Although the present study can give no direct information as to the formation of carbon monoxide, its formation is so probable that a fourth reaction should be added to the above list.

$$\mathrm{R{-}\underset{\displaystyle R}{\overset{\displaystyle |}{C}}{=}O} + h\nu \longrightarrow CO + ? \qquad (IV)$$

Compounds which do not absorb below 50,000 cm.$^{-1}$: the region of 50,000–60,000 cm.$^{-1}$ corresponds to 143–189 kcal. per mole. These energies are sufficient to break any bond in the molecule or to break two bonds providing the energy is properly distributed. If transfer of energy by collision is neglected, probable types of primary reaction are

$$\text{Reactant} + h\nu \longrightarrow R' + R'' \qquad (1)$$

where R′ and R″ are two radicals which result from breaking any bond in the molecule

$$\text{Reactant} + h\nu \longrightarrow R' + M + R'' \qquad (2)$$

where R′ and R″ are two radicals which are formed by breaking two single bonds and M is a molecule which in its ground state contains a new π-bond. and

$$\text{Reactant} + h\nu \longrightarrow M_1 + M_2 \qquad (3)$$

where M_1 and M_2 are stable molecules, one of which contains a new π-bond. For any one reactant several primary processes of any one of these three types could conceivably take place.

Since the free radicals produced by process (1) have unusually high energies, the rate of decomposition would be much greater than that usually observed and the rate of combination reactions which are not followed by decomposition would be much less than that which is usually encountered. Process (1) followed by the decomposition of one radical, $R'' \rightarrow M + R'''$, approaches process (2) as the life time of R″ approaches zero. This two step process will be designated as (2′).

The low pressure of the sample would have tended to favor decomposition reactions in the vapor phase and reactions at the wall. The small diameter of this reaction vessel would also tend to accentuate the latter.

The same principal products were detected in the photolysis of an alcohol and the corresponding ether: ethanol and diethyl ether gave ethylene (see empirical rule I), acetaldehyde and formaldehyde (see empirical rule II); methanol and dimethyl ether gave formaldehyde (II) and smaller quantitites of acetaldehyde. Using radiation up to 55,000 cm.$^{-1}$. Patat and Hoch[9] obtained acetaldehyde and hydrogen as the photolysis products of ethanol vapor, and formaldehyde and hydrogen as photolysis products of methanol vapor. On the basis of a parahydrogen method of detecting hydrogen atoms they concluded that intramolecular reactions were involved (process 3). In an attempt to determine whether the ethylene and formaldehyde found in the present work were due to the second electronic transition of ethanol, an oxygen filter was introduced to cut off the region of the second band. The rate of photolysis was decreased but in so far as it is possible to tell by inspection the relative quantities of the three products were not changed.

Since the ethylene and acetaldehyde formed in the photolysis of the dimethyl ether did not appear until a rather high concentration of formaldehyde had been produced, it seems probable that these products are the result of a free radical mechanism which involves formaldehyde. This also seems to be true for the formation of acetaldehyde from methanol. In both cases, the quantity of formaldehyde seemed to approach a maximum value during the irradiation.

1-Propanol reacted in a similar manner to give ethylene (I), propionaldehyde (II) and formaldehyde (II). It would be interesting to know whether the ethylene contains carbons 1 and 2, or 2 and 3. Not enough is known about the spectrum of propylene to conclude that it was not produced.

2-Methyl-2-propanol.—Since the ketene most probably resulted from the photolysis of acetone, the direct photolysis of this tertiary alcohol seems to have followed the usual pattern—the single product, acetone (II), being the result of the symmetry of the alcohol. The spectrum of 2-methyl-1-propene has too little structure to determine its presence or absence as a product.

Compounds which also absorb below 50,000 cm.$^{-1}$: for a substance which has four absorption bands with extinction coefficients of 10, 100, 1000 and 10,000, the relative number of molecules undergoing the four transitions, in an infinitely thin sample, would be approximately 1, 10, 100 and 1000, respectively. Strictly speaking, oscillator strengths should be compared, the light source should be of uniform intensity at the four wave lengths and the quantity of material in the light path should be small enough to not drastically reduce the light intensity For an infinitely thick sample, where all of the light at these wave lengths is absorbed, the relative number of molecules undergoing the four transitions would be approximately 1, 1, 1 and 1. Many of the compounds studied have molar extinction coefficients of the order of 10 or less below 50,000 cm.$^{-1}$, as compared to coefficients of the order of 10^2 to 10^4 in the far ultraviolet. This, coupled with the small quantity of material in the light path, minimized the number of electronic transitions produced by the low frequency region of the source. Unless fluorescence was markedly different in the two regions, the observed photolysis was therefore due for the most part to the

(8) Of these, products marked * were found in relatively small amounts; products marked $^+$ appeared only on prolonged irradiation and in small amounts.

(9) F. Patat and H. Hoch, *Z. Elektrochem.*, **41**, 494 (1935).

high frequency portion of the source band. Although many of the observed products are also produced in the near ultraviolet by well known mechanisms, the authors are inclined to believe that the same processes are not necessarily involved in the far ultraviolet region.

Acetaldehyde.[10]—The relatively small amounts of detectable products may be due to the formation of methane and carbon monoxide (IV, 3). This intramolecular reaction has been shown to be increasingly important at higher frequencies in the near ultraviolet. The small quantity of acetone probably indicates that a free radical mechanism is also involved. The relative quantity of ketene is too high to have resulted from the photolysis of acetone. Any number of mechanisms could account for the ketene: a free radical reaction or any one of processes 2, 2′ or 3. Formaldehyde and 2,3-butanedione were not detected. The first is significant since formaldehyde has such a characteristic pattern of high intensity absorption bands. On the basis of the literature, it had been expected that 2,3-butanedione[11] could have been detected but preliminary measurements in this Laboratory indicated that this compound does not have intense narrow absorption bands and it is doubtful that it could have been detected. It is also doubtful if it would have been produced under the existing energy conditions.

Acetone.[10,12]—The near ultraviolet photolysis of acetone proceeds entirely by a free radical mechanism which is largely initiated by dissociation to give methyl and acetyl radicals. On the basis of the increased yield of hydrogen obtained by Manning[13] using an aluminum spark and fluorite windows, dissociation to hydrogen and acetonyl radicals is believed to be increasingly important at higher wave numbers. However, Howe and Noyes[14] found no hydrogen at low pressures and 1900 Å. and concluded that decomposition proceeded almost entirely by an intramolecular dissociation to ethane and carbon monoxide (IV, 3). It is probably significant that 2-butanone, 2,5-hexanedione and acetaldehyde were not detected in the present work. The spectra of the first two are similar to that of acetone but the maxima fall at different wave lengths and any appreciable concentration of either should have been detected. The absence of acetaldehyde probably eliminates one means of formation of ketene: the disproportionation of two acetyl radicals. The intramolecular reaction of Howe and Noyes[14] is consistent with the relative low concentration of detectable products.

(10) The photolysis of acetaldehyde has been extensively studied in the near ultraviolet. Only one reference is given below. E. W. R. Steacie, "Atomic and Free Radical Reactions," Vol. I, Reinhold Publ. Corp., New York, N. Y., 1954.

(11) V. R. Ells, *J. Am. Chem. Soc.*, **60**, 1864 (1938).

(12) The photolysis of acetone has been extensively studied in the near ultraviolet. Only one reference is given below. W. A. Noyes, Jr., G. B. Porter and J. E. Jolley, *Chem. Revs.*, **56**, 49 (1956).

(13) W. M. Manning, *J. Am. Chem. Soc.*, **56**, 2589 (1934).

(14) J. P. Howe and W. A. Noyes, Jr., *ibid.*, **58**, 1404 (1936).

Since the situation becomes so complex and consequently even more speculative only a few comments are made about the higher molecular weight ketones.

2-Butanone.—The formation of ethylene is in keeping with (I) but the absence of a significant quantity of acetaldehyde indicates that the reaction did not proceed by 3. It is doubtful that the ethylene was formed by the photolysis of ketene since ethylene was not detected as a product in the photolysis of either acetone or acetaldehyde. In both of the latter a comparable quantity of ketene was produced.

2-Pentanone.—The formation of ethylene (I) and acetone is consistent with the near ultraviolet intramolecular reactions 3 of aldehydes and ketones which contain a γ-carbon atom.[1]

2,5-Hexanedione.—The rate of photolysis and the quantities of detectable products were similar to that of 2-pentanone. Ethylene is consistent with (I) but acetone is an anomaly unless a combination of (I) and (IV) is considered, possibly as a single intramolecular reaction.

2,3-Butanedione.—On the basis of iodine inhibited vapor phase studies in the near ultraviolet, Bell and Blacet[15] suggested that, in addition to the free radical mechanism, some acetone and carbon monoxide were formed by an intramolecular process (IV, 3) and that this process became increasingly significant at higher wave numbers The rapid photolysis and the small quantities of detectable products obtained in the present work may indicate that other intramolecular processes, such as a direct decomposition to ethane and carbon monoxide, are involved. The formation of ethylene is not consistent with either the free radical mechanisms[10] proposed for the near ultraviolet, or the results obtained with other compounds in the far ultraviolet where two adjacent carbon atoms other than the carbonyl carbon seem to have been a necessary condition for the formation of ethylene. Its presence here suggests a unique reaction of the conjugated system or an impurity in the sample. The latter seems improbable since all of the samples were fractionated in a Fenske column, the boiling point checked well with the reported value and a gas chromatogaphic analysis indicated a single component.

At this preliminary stage in the investigation, no conclusions can be drawn but it seems probable that processes 2, 2′ and 3, particularly 2 and 2′ are more important in this region than in the near ultraviolet. An effort should be made to extend the work. More restricted energy sources are possible although high intensity monochromatic sources are not available. By combining mass spectrometer and gas chromatographic analyses with a quantitative study of absorption spectra it should be possible to obtain the quantitative data necessary to establish the mechanisms involved.

(15) W. E. Bell and F. E. Blacet, *ibid.*, **76**, 5332 (1954).

THE KINETICS OF THE REACTION BETWEEN PU(IV) AND U(IV)[1]

BY T. W. NEWTON

University of California, Los Alamos Scientific Laboratory, Los Alamos, New Mexico

Received March 13, 1959

The kinetics of the reaction between Pu(IV) and U(IV) have been studied in perchlorate media. The rate law indicates that the activated complex is formed from water, U^{+4} and Pu^{+4} with the prior loss of two hydrogen ions. Minor paths involving other activated complexes appear unlikely. The thermodynamic quantities of activation in 2 *M* $HClO_4$ solutions at 25° were found to be $\Delta F^{\ddagger} = 15.4$ kcal./mole, $\Delta H^{\ddagger} = 24.3$ kcal./mole and $\Delta S^{\ddagger} = 30.1$ e.u. The relation between the kinetics of this reaction and similar ones is discussed. It was found that the presence of small amounts of H_2SO_4 greatly increases the rate of the reaction.

Introduction

A review of the oxidation–reduction kinetics of the ions of uranium, neptunium and plutonium showed that an important factor in determining the entropy of an activated complex is its total charge.[2] The purpose of the present paper is to provide further kinetic data in support of this conclusion and to aid in the identification of the other factors which influence the entropies of activated complexes.

The reaction between Pu(IV) and U(IV) is between ions which, in acid solution, are predominantly charged +4. Two other reactions of this type have been reported, the disproportionation of Pu(IV)[3] and the reaction between Ce(IV) and U(IV).[4] The disproportionation reaction was not studied as a function of temperature in perchlorate solutions; so an estimate of the entropy of the activated complex cannot be made.

The present work also extends knowledge of the chemistry of uranium and plutonium solutions; the kinetics of the reduction of Pu(VI) by U(IV) have already been reported.[5]

Experimental Part

Reagents.—Pu(III) stock solutions were prepared by the dissolution of weighed amounts of pure plutonium metal in standardized concentrated $HClO_4$ and dilution to the desired final concentrations. Sometimes a small amount of insoluble residue was observed; so the solutions were filtered. These solutions were used within eight hours of preparation in order to minimize the effects of α-particle self oxidation.

$K_2Cr_2O_7$ solutions were prepared from analytical reagent grade material and were analyzed before use. This was done by addition of an aliquot to excess standard U(IV) solution and titration of the excess with standard ceric sulfate solution.

A U(IV) stock solution was prepared by the electrolytic reduction of a $UO_2(ClO_4)_2$ solution with a mercury cathode. The $UO_2(ClO_4)_2$ solution was made by dissolution of pure U_3O_8 in hot concentrated $HClO_4$. The U(IV) solution was assayed for total uranium by reduction with zinc amalgam, air oxidation and titration with standard ceric sulfate solution. The hydrogen ion concentration was determined by titration with standard NaOH after the uranium was removed with an ion-exchange resin column. Correction was made for the hydrogen ion released by the column. The U(IV) solutions for the individual runs were prepared by appropriate dilution of the stock solution and were analyzed before use by titration with standard ceric sulfate solution.

The $HClO_4$ solutions were prepared by the dilution of concentrated acid and were standardized by titration. The concentrated acid was analytical reagent grade and was further purified by boiling at atmospheric pressure and again under reduced pressure.

Solutions of $LiClO_4$ and $NaClO_4$ were prepared by neutralization of the appropriate analytical reagent grade carbonate with $HClO_4$, boiling out the CO_2 and crystallization from water, three times for the $LiClO_4$ and two times for the $NaClO_4$. The solutions were analyzed by titration of the effluent from a cation-exchange column originally in the hydrogen form.

The water used in the preparation of all the solutions was doubly distilled; the second distillation was from alkaline $KMnO_4$ in an all Pyrex still.

Procedure.—Appropriate amounts of Pu(III) and Cr(VI) solutions were mixed in one of the compartments of a two chambered absorption cell. The amount of Cr(VI) was usually chosen so that about half the Pu(III) was oxidized to Pu(IV). Auxiliary experiments showed that only negligible amounts of Pu(VI) are formed under these conditions. U(IV) solution and the appropriate mixture of salt and acid solutions were placed in the other compartment. The two chambered cell had a 10 cm. light path and was arranged so that in a vertical position the two portions of solution could be kept separate during temperature equilibration in a thermostat. After mixing the two portions, the cell was placed in the cell holder in the spectrophotometer. This holder contained water which was in direct contact with the cell and was thermostated by water pumped from the thermostat. With this arrangement it was possible to maintain the temperature to within 0.2° even at 2.5°. The spectrophotometer was the Cary Recording Spectrophotometer, Model 14, No. 5.

The extent of reaction was followed by measuring the light absorption at 4695A where Pu(IV) absorbs much more strongly than the other species present. The determination of the concentration of Pu(IV) from the absorbance values involves the quantity $\epsilon_1 - \epsilon_2 + {}^1/_2(\epsilon_3 - \epsilon_4)$ where ϵ_1, ϵ_2, ϵ_3 and ϵ_4 refer to the molar absorptivities of Pu(IV), Pu(III), U(IV) and U(VI), respectively. Rather than determine all of the individual values separately, the required combination was determined from measurements on appropriate solutions made by mixing Pu(III), U(IV) and Cr(VI).

The concentration units employed in this paper are moles per liter at 23°. The actual concentrations will be different at different temperatures, for example being about 1% greater at 2.8°.

Catalytic Impurities.—The possibility that catalytic impurities were present in the various solutions was examined. All solutions except some of the Pu(III) solutions were found to be essentially free of catalysts.

Runs were made in which the ordinary $HClO_4$ stock was compared with some which had been prepared by vacuum distillation. The observed rate constants were the same within the experimental error. The ordinary $LiClO_4$ stock was compared with some prepared by electrolysis as previously described,[5] again the rate constants were essentially identical.

Two experiments were performed which showed that doubling the initial concentration of total uranium changed the apparent second-order rate constants by 1.5% or less. In addition, runs designed to compare a stock solution made from UCl_4 with the ordinary U(IV) stock gave rate constants which agreed within 3%. An auxiliary experiment showed that the small amount of chloride introduced with the UCl_4 had no effect.

The lack of catalyst in the $K_2Cr_2O_7$ stock solution was shown by reducing some quantitatively with U(IV) and observing that the resulting Cr(III) solution had no effect on the reaction rate. Thus a rate run made with three

(1) This work was done under the auspices of the U. S. Atomic Energy Commission.

(2) T. W. Newton and S. W. Rabideau, *J. Phys. Chem.*, **63**, 365 (1959).

(3) S. W. Rabideau, *J. Am. Chem. Soc.*, **75**, 798 (1953).

(4) F. B. Baker, *et al.*, *J. Phys. Chem.*, **63**, in press (1959).

(5) T. W. Newton, *ibid.*, **62**, 943 (1958).

times the usual Cr(III) concentration gave a rate constant only 1.5% greater than a similar run without excess chromium. This result also showed that Cr(III) does not appear in the rate law.

Runs which had the same concentrations of acid, salt, U(IV) and Pu(IV) but differing concentrations of total plutonium gave different apparent second-order rate constants. The rate constants were found to be essentially a linear function of the total plutonium concentration; see Table I. When two different preparations of plutonium metal were compared, the rate constants extrapolated to zero plutonium were the same although the slopes differed by a factor of nearly two. Since it has been shown (see further) that very small amounts of sulfate can catalyze the reaction it is not unlikely that trace contamination of the plutonium metal by sulfur, or some other sustance which yields an ion capable of complexing Pu(IV), is the catalyst. The presence of this catalyst makes it impossible to be sure that Pu(III) itself does not appear in the rate law.

TABLE I

EXAMPLE OF THE EFFECT OF TOTAL Pu ON THE APPARENT SECOND-ORDER RATE CONSTANTS

Initial concentrations, $[HClO_4] = 0.50\ M$, $[LiClO_4] = 1.50\ M$, $[Pu(IV)] = 2.14 \times 10^{-3}\ M$ and $[U(IV)] = 1.08 \times 10^{-3}\ M$. Temperature, 2.8°.

$[Pu(III)] + [Pu(IV)]$, $M \times 10^3$	k' (obsd.), M^{-1} min.$^{-1}$	k (calcd.[a]) M^{-1} min.$^{-1}$
0	..	514
3.22	523	528
6.44	547	542
9.66	562	556
12.87	564	569

[a] Calculated from $k' = 514.3 + 4.278 \times 10^3\{[Pu(III)] + [Pu(IV)]\}$.

However, all the quantitative conclusions in this paper are based on extrapolated rate constants and so refer to the Pu(III) independent part of the rate law even if terms involving Pu(III) are present.

Results and Discussion

Stoichiometry.—The pertinent oxidation potentials indicate that when Pu(IV) and U(IV) are mixed the over-all reaction is

$$2Pu(IV) + U(IV) = 2Pu(III) + U(VI) \qquad (1)$$

The possibility of additional induced oxidation of U(IV) by oxygen or by perchlorate ion was investigated and found to be negligible. This was done as follows. A definite amount of Cr(VI) (as $K_2Cr_2O_7$ solution) was added to an excess of Pu(III) oxidizing part of it to Pu(IV).[6] A sample of U(IV), insufficient to reduce all of the Pu(IV) was added and the reaction allowed to go to completion. The same amounts of the same reagents were then mixed in a different order: the Cr(VI) was added to the U(IV) oxidizing all of it to U(VI), then the Pu(III) was added, reducing the excess Cr(VI). The absorbances of these two solutions were then determined at 4695 Å. where Pu(IV) absorbs relatively strongly. The values agreed within 0.6% indicating that the final compositions of the two solutions were essentially the same. Thus the U(IV) reduced the same number of equivalents of Pu(IV) as of Cr(VI). Since analytical experience indicates that the reaction between Cr(VI) and U(IV) is stoichiometric, it has been concluded that the Pu(IV) + U(IV) reaction is stoichiometric also.

The Rate Law.—The rate was found to be first order in each of the reactants, Pu(IV) and U(IV); that is, when all other concentrations were essentially constant the rate is given by $-d[Pu(IV)]/dt = k'[Pu(IV)]\,[U(IV)]\ M$ min.$^{-1}$, where k' is the apparent second-order rate constant and the quantities in brackets are concentrations. This was shown by the linearity of plots of $\{\log [U(IV)] - \log [Pu(VI)]\}$ *versus* time or of plots of $Pu(VI)^{-1}$ *versus* time where the equivalent concentrations of the two reactants were essentially equal. The data shown in Table II are from a typical rate run and indicate

TABLE II

DATA FROM TYPICAL RATE RUN SHOWING THE ADHERENCE TO A SECOND-ORDER RATE LAW

2.5°C. Initial concentrations: $[HClO_4] = 0.4\ M$; $[LiClO_4] = 1.6\ M$; $[Pu(IV)] = 2.06 \times 10^{-3}\ M$ and $[U(IV)] = 1.05 \times 10^{-3}\ M$.

Time, min.	Obsd. absorbance[a]	Pu(IV),[b] $M \times 10^3$	Calcd. absorbance[c]
0.5	1.068	1.452	1.067
1.0	0.850	1.107	0.853
1.5	.713	0.890	.714
2.0	.623	.748	.624
2.5	.557	.644	.557
3.0	.507	.565	.508
3.5	.469	.505	.468
4.0	.437	.454	.436
4.5	.411	.413	.410
5.0	.388	.376	.388
6.0	.354	.323	.353

[a] Or optical density. [b] Calculated from the observed absorbance. [c] Calculated from the best straight line through $[Pu(IV)]^{-1}$ *vs.* time.

that the reaction follows a second-order rate law at least as far as 84% completion. Further confirmation of the order with respect to U(IV) was obtained when it was found that the apparent second-order rate constant was essentially unchanged when the U(IV) concentration was varied by a factor of 2.5. That the product U(VI) does not appear in the rate law was shown by the fact that the apparent second-order rate constant did not change when the initial U(VI) concentration was varied by a factor of four. As mentioned in the section on catalytic impurities, it cannot be stated with certainty that the other product, Pu(III), does not enter the rate law. If it does enter, it is in the form of an additional term, $k''[Pu(III)]\,[Pu(VI)]\,[U(VI)]$. It has already been mentioned that the Cr(III), which is introduced when Pu(III) is oxidized to Pu(IV), has no effect on the rate.

The rate was found to be influenced strongly by the hydrogen ion concentration, depending inversely on the square of the concentration. The rate law was then formulated as

$$-d[Pu(IV)]/dt = k[Pu^{+4}][U^{+4}]\,[H^+]^{-2}\ M \text{ min.}^{-1} \qquad (2)$$

which is written in terms of the principal species present in the solution. Since $[Pu^{+4}] = [Pu(IV)]\,[H^+]([H^+] + K_{Pu})^{-1}$ and $[U^{+4}] = [U(IV)][H^+]([H^+] + K_U)^{-1}$ the rate constant k in equation 2 given by $k = k'([H^+] + K_{Pu})([H^+] + K_U)$ where k' is the apparent second-order rate constant, and K_{Pu} and K_U are the hydrolysis quotients for Pu(IV) and U(IV), respectively. Table III lists values of k' as a function of $[H^+]$ at 2.6°; values for k were calculated assuming $K_{Pu} = 0.021$ and $K_U = 0.005$. These values for the hydrolysis

(6) S. W. Rabideau and J. F. Lemons, *J. Am. Chem. Soc.*, **73**, 2895 (1951), have shown that this reaction is stoichiometric.

quotients were obtained by extrapolating the data of Rabideau[7] for plutonium and the data of Kraus and Nelson[8] for uranium. The values of k are essentially constant indicating that the rate law given in equation 2 is correct. The values listed in Table III were not extrapolated to zero plutonium and are thus a little high since they include a small contribution from the catalytic path.

TABLE III

THE EFFECT OF HYDROGEN ION CONCENTRATION ON THE REACTION IN $HClO_4$–$LiClO_4$ SOLUTIONS AT $\mu = 2.05 \pm 0.01$ M AND $2.6 \pm 0.2°$

Initial concentrations				
$HClO_4$, M	Pu(IV), $M \times 10^3$	U(IV), $M \times 10^3$	k', M^{-1} min.$^{-1}$	k, M min.$^{-1}$[a]
2.00	2.15	5.78	35.8	145
2.00	2.14	2.18	36.9	150
2.00	2.13	5.56	37.1	150
1.80	2.15	5.78	44.4	146
1.60	2.15	5.78	55.3	144
1.60	2.14	4.16	53.7	139
1.40	2.14	4.16	69.9	138
1.20	2.14	4.16	95.0	138
1.20	2.14	3.09	92.6	136
1.00	2.14	3.09	134.6	138
0.80	2.14	3.09	206.6	137
.80	2.06	2.11	206	136
.60	2.06	2.11	365	137
.50	2.13	2.18	532	140
.50	2.14	2.15	523	138
.40	2.06	2.11	813	139

[a] Calculated using $k = k'([H^+] + 0.021)([H^+] + 0.005)$.

To show that the presence of a catalytic path does not affect the conclusion with respect to the rate law, three series of runs with varying total plutonium concentrations were made at 2.8° and $\mu = 2$ in solutions 2.00 M in $HClO_4$ and in solutions 0.50 M in $HClO_4$. In the 2.00 M acid solutions the extrapolated k values were 139.4 ± 3.1 M min.$^{-1}$ and 138.9 ± 3.2 M min.$^{-1}$; in the 0.50 M acid solution the corresponding value was 135.3 ± 1.7 M min.$^{-1}$. These values agree within their probable errors (the uncertainties given); hence k is independent of the hydrogen ion concentration within the experimental error.

The rate law given by equation 2 indicates that the activated complex in the rate-determining reaction is formed from water, Pu^{+4} and U^{+4} with the prior loss of two hydrogen ions. The over-all reaction, given without regard to H^+ or H_2O by equation 1, consumes two Pu^{+4} ions and forms UO_2^{+2}; therefore it must actually consist of two consecutive reactions which are probably

$$Pu^{+4} + U^{+4} + 2H_2O = Pu^{+3} + UO_2^+ + 4H^+ \quad (3)$$

which is rate determining, followed by

$$Pu^{+4} + UO_2^+ = Pu^{+3} + UO_2^{+2} \quad (4)$$

or by

$$2UO_2^+ + 4H^+ = UO_2^{+2} + U^{+4} + 2H_2O \quad (5)$$

Reactions 4 and 5 cannot both be important, for if they were the over-all rate would not be first order in both Pu(IV) and U(IV). This is because Pu(IV) is reduced in reaction 4 but not in reaction 5.[9] It seems quite likely that reaction 5 is relatively unimportant since it involves the breaking of a U–O bond and reaction 4 does not. When this assumption is made, the over-all rate is twice the rate of reaction 3.

A mechanism for reaction 3 which is consistent with the $[H^+]^{-2}$ in the rate law would picture the collision of $PuOH^{+3}$ with UOH^{+3}, and/or a collision of $Pu(OH)_2^{+2}$ with U^{+4}, and/or a collision of Pu^{+4} with $U(OH)_2^{+2}$, where the various hydrolyzed species were formed in rapid equilibrium reactions prior to the oxidation–reduction reaction. These three possibilities are kinetically indistinguishable but a distinction among them is unimportant in terms of the absolute reaction rate theory which assumes that the "initial reactants are always in equilibrium with the activated complexes."[10] According to this theory the rate depends on the properties of the activated complex and not on the details of how it was formed. We prefer, then, to ignore any intermediates which are in equilibrium with the principal reactant species and to describe the kinetics of the rate-determining reaction by a net activation process which is written in terms of the principal species. In the present case this is

$$Pu^{+4} + U^{+4} + H_2O = (Pu{\cdot}O{\cdot}U^{+6})^{\ddagger} + 2H^+ \quad (6)$$

where the symbol $(Pu{\cdot}O{\cdot}U^{+6})^{\ddagger}$ stands for the activated complex.

Temperature Dependence.—The temperature dependence was determined from rate constants measured in solutions 2.00 M in $HClO_4$ and extrapolated to zero total plutonium. Values for k, defined by equation 2, were calculated from the observed apparent second-order rate constants using the appropriate values of K_{Pu} and K_U The results of these experiments and calculations are shown in Table IV.

TABLE IV

THE EFFECT OF TEMPERATURE ON THE REACTION IN 2.00 M $HClO_4$, $\mu = 2.025 \pm 0.01$ M

Temp., °C.	k M^{-1} min.$^{-1}$	K_{Pu},[a] M	K_U,[b] M	k, M min.$^{-1}$	k (calcd.)[c], M^{-1} min.$^{-1}$
29.8	1861	0.071	0.032	7831	1899
20.3	526.5	.048	.017	2175	506.4
10.4	113	.031	.009	461	115.3
2.8	34.35	.021	.005	139.2	34.3

[a] Obtained by extrapolating the data of Rabideau.[7] [b] Obtained by extrapolating the data of Kraus and Nelson.[8] [c] Calculated from $k' = (2.0 + K_{Pu})^{-1}(2.0 + K_U)^{-1}\ 7.74 \times 10^{21} \exp(-24930/RT)\ M^{-1}$ min.$^{-1}$.

A plot of log k *vs.* $1/T$ was found to be a good straight line. The method of least squares was used to determine best values for the slope and intercept and the uncertainties in these quantities. The logarithmic form of the Arrhenius equation describing the data was thus found to be

$$\log k = (21.8887 \pm 0.4144) - (24{,}930 \pm 560)(2.303\ RT)^{-1}$$

where the units of k are M min.$^{-1}$ and of R are cal. deg.$^{-1}$ mole^{-1} and the uncertainties are twice the standard deviations. This indicates that the

(7) S. W. Rabideau, *J. Am. Chem. Soc.*, **79**, 3675 (1957).

(8) K. A. Kraus and F. Nelson, *ibid.*, **72**, 3901 (1950); **77**, 3721 (1955).

(9) See reference 5, footnote 10 for a discussion of a similar case.

(10) S. Glasstone, K. Laidler and H. Eyring, "The Theory of Rate Processes." McGraw-Hill Book Co., New York, N. Y., 1941, p. 185.

experimental activation energy is 24.93 ± 0.56 kcal./mole.

Thermodynamic Quantities of Activation.—The quantities of $\Delta F^{\ddagger}$, $\Delta H^{\ddagger}$ and $\Delta S^{\ddagger}$ which are associated with the net activation process, equation 6, were calculated according to absolute reaction rate theory[11] under the assumption that the observed rate is twice the rate of reaction 3. The results at 25° were $\Delta F^{\ddagger}$ = 15.36 kcal./mole, $\Delta H^{\ddagger}$ = 24.34 ± 0.56 kcal./mole and $\Delta S^{\ddagger}$ = 30.11 ± 1.9 e.u.

In Table V these results are compared with those for other reactions for which the charge on the activated complex is +6. Except where indicated the values were taken from Table I of reference 2. As in that paper, the quantity $S^{\ddagger}_{complex}$ is the formal ionic entropy of the activated complex calculated from $\Delta S^{\ddagger}$ using the standard entropies of the ordinary species present. It is seen that although the $\Delta H^{\ddagger}$ values range from 9.5 to 24.3 kcal./mole and the $\Delta S^{\ddagger}$ values range from −13 to +30 e.u., the values for $S^{\ddagger}_{complex}$ range only between −116 and −126 e.u.

TABLE V

THERMODYNAMIC QUANTITIES OF ACTIVATION, 25°

Net activation process	$\Delta F^{\ddagger}$, kcal./mole	$\Delta H^{\ddagger}$, kcal./mole	$\Delta S^{\ddagger}$, e.u.	$S^{\ddagger}$ complex, e.u.
[a] $Pu^{+4} + U^{+4} + H_2O =$ $(Pu{\cdot}O{\cdot}U^{+6})^{\ddagger} + 2H^{+}$	15.4	24.3	30.1	−118
[b] $CeOH^{+3} + U^{+4} =$ $(Ce{\cdot}O{\cdot}U^{+6})^{\ddagger} + H^{+}$	12.2	13.9	6.2	−116
[c] $Fe^{+3} + U^{+4} + H_2O =$ $(Fe{\cdot}OH{\cdot}U^{+6})^{\ddagger} + H^{+}$	16.8	21.4	15.5	−118
[d] $Pu^{+4} + Ti^{+3} + H_2O =$ $(Ti{\cdot}OH{\cdot}Pu^{+6})^{\ddagger} + H^{+}$	15.0	16.7	5.8	−126
[e] $Pu^{+4} + Pu^{+3} + H_2O =$ $(Pu{\cdot}OH{\cdot}Pu^{+6})^{\ddagger} + H^{+}$	13.3	9.5	−13	−120

[a] This work. μ = 2. [b] F. B. Baker as tabulated in ref. 2, μ = 2. [c] R. H. Betts as tabulated in ref. 2, μ = 1. [d] S. W. Rabideau and R. J. Kline, THIS JOURNAL, **63**, 1502 (1959). [e] T. K. Keenan as tabulated in ref. 2, μ = 2.

It is interesting to note that for the three reactions in which U^{+4} is oxidized, the rate is higher (smaller $\Delta F^{\ddagger}$) the better the oxidizing agent. In fact, a plot of $\Delta F^{\ddagger}$ *vs.* the standard potential of the oxidizing agent is nearly linear.

Ionic Strength and Medium Effects.—The approximate effect of varying the ionic strength was determined in a short series of experiments in which the $HClO_4$ concentration was varied without the addition of salt. The results are given in Table VI. The rates were not extrapolated to zero total plutonium so the rate constants are probably all high by about 7%.

TABLE VI

EFFECT OF $HClO_4$ ON THE RATE AT 2.6° WITHOUT ADDED SALT

μ	$HClO_4$, M	k, M^{-1} min.$^{-1}$	K_{Pu},[a] M	K_U[a], M	k, M min.$^{-1}$
0.472	0.429	494.4	0.033	0.008	100
1.66	1.61	48.8	.022	.005	128
2.06	2.00	36.7	.021	.005	149

[a] Ionic strength effect on the hydrolysis constants estimated using the Debye–Hückel expression with $\hat{a}$ = 7.5 Å.

The effect of substituting $NaClO_4$ for $LiClO_4$ was determined at 2.6° in 0.5 M $HClO_4$ solutions with μ = 2. Extrapolation to zero total plutonium gave k = 134.7 ± 0.9 M min.$^{-1}$ which is in good agreement with 135.3 ± 1.7 M min.$^{-1}$ which was found in $LiClO_4$ solutions.

The Effect of H_2SO_4.—Preliminary experiments showed that small amounts of H_2SO_4 greatly accelerate the reaction. This is shown by the data in Table VII.

TABLE VII

EFFECT OF H_2SO_4 ON THE APPARENT SECOND-ORDER RATE CONSTANT IN 2 M $HClO_4$ SOLUTIONS AT 2.8°

Initial concentrations: $[Pu(IV)] = 2.14 \times 10^{-3}$ M and $[U(IV)] = 2.18 \times 10^{-2}$ M

H_2SO_4, $M \times 10^3$	HSO_4^-,[a] $M \times 10^3$	k' (initial obsd.) M^{-1} min.$^{-1}$	k' (calcd.)[b]
0	0	37	37
0.50	0.224	396	401
1.00	.461	847	826
2.00	.967	1782	1794

[a] Calculated assuming $[H^+][SO_4^{=}]/[HSO_4^-] = 0.38$ M and $[H^+][USO_4^{+2}][HSO_4^-]^{-1}[U^{+4}]^{-1} = [H^+][PuSO_4^{+2}][HSO_4^-]^{-1}[Pu^{+4}]^{-1} = 506$. [b] Calculated from the expression: $k' = (37 + 153 \times 10^4[HSO_4^-] + 135 \times 10^7[HSO_4^-]^2)(1 + 253[HSO_4^-])^{-2}$.

The effect of H_2SO_4 is most simply interpreted under the assumption of three parallel paths involving zero, one and two sulfate groups in the activated complexes. Thus at constant hydrogen ion concentration

$$-d[Pu(IV)]/dt = [U^{+4}][Pu^{+4}](k_0 + k_1[HSO_4^-] + k_2[HSO_4^-]^2)$$

which is written in terms of the principal species. To put this expression in terms of the stoichiometric concentrations, values for the acid dissociation quotient of bisulfate and the association quotients of $PuSO_4^{+2}$ and USO_4^{+2} are needed at 2.8° in solutions with μ = 2. The first of these quantities may be estimated with sufficient accuracy to be 0.38 M.[12] The work of Day, *et al.*,[13] may be extrapolated to give $K'_U = [H^+][USO_4^{+2}][HSO_4^-]^{-1}[U^{+4}]^{-1} = 506$ at μ = 2 and 2.8°. The corresponding quotient for plutonium, K'_{Pu}, has not been determined so we will assume provisionally that it is the same as for uranium. Using these values for the equilibrium quotients, HSO_4^- concentrations were calculated and k_0, k_1 and k_2 were determined graphically. $k' = (k_0 + k_1[HSO_4^-] + k_2[HSO_4^-]^2)(1 + K_U'[HSO_4^-]/[H^+])^{-1}(1 + K_{Pu}'[HSO_4^-]/[H^+])^{-1} = (37 + 153 \times 10^4[HSO_4^-] + 135 \times 10^7[HSO_4^-]^2)(1 + 253[HSO_4^-])^{-2}$. This expression was used for the calculated values in Table VII; it is seen that these assumptions reproduce the observed values very well. However, other values also are satisfactory. For example, if it is assumed that K_{Pu}' = 316 which is equal to the extrapolated value for the association quotient of $NpSO_4^{+2}$ [14] the values for k_1 and k_2 are slightly different from the ones given above and the calculated and observed k' values are in as good agreement as before.

(11) Reference 10, pages 195–199.

(12) This is a guess based on the results of E. Eichler and S. W. Rabideau, *J. Am. Chem. Soc.*, **77**, 5501 (1955).

(13) R. A. Day, Jr., R. N. Wilhite and F. D. Hamilton, *ibid.*, **77**, 3180 (1955).

(14) J. C. Sullivan and J. C. Hindman, *ibid.*, **76**, 5931 (1954).

This large effect on the rate due to HSO_4^- is to be contrasted with the effect of Cl^-. It was mentioned above that small amounts of Cl^- have no effect; a further experiment in which the chloride concentration was 0.35 *M* in 2 *M* acid solution showed a rate increase of only 45%.

Acknowledgments.—The author wishes to acknowledge the help of F. B. Baker in performing some of the preliminary experiments. He also wishes to acknowledge helpful discussions with Dr. C. E. Holley, Jr., and especially with Dr. J. F. Lemons, under whose general direction this work was done.

FLOCCULATION-DEFLOCCULATION IN AGITATED SUSPENSIONS.[1] I. CARBON AND FERRIC OXIDE IN WATER

BY IRVING REICH[2] AND ROBERT D. VOLD

Department of Chemistry, University of Southern California, Los Angeles 7, California

Received March 18, 1959

The degree of flocculation of aqueous suspensions of ferric oxide and carbon was studied as a function of concentration and of time and intensity of agitation. Average floc sizes were determined from turbidity measurements. The average floc size always increased with increasing concentration and with decreasing speed of agitation. In unagitated suspensions, average floc size remained almost constant for long periods, the suspension being in a pseudo-stable state. In agitated suspensions, floc formation and destruction resembles a reversible chemical reaction, with the level of agitation playing a role similar to that of temperature in molecular reactions. For particles larger than about one micron, thermal motion of the particles is unimportant compared to even mild agitation as the governing factor in floc formation and destruction. Simple statistical reasoning leads to principles governing steady-state dispersion in agitated suspensions.

Introduction

This study was undertaken as the initial step in an investigation of the effect of deflocculation on soil redeposition during detergency. It has often been assumed that the ability of a detergent to deflocculate and suspend a powdered soil affords a measure of its detergent power. Hence there have been numerous investigations of the degree of flocculation of powdered solids in detergent solutions.[3-9] The usual procedure has been to agitate the powder with the detergent solution in some arbitrary manner, then to allow the suspension to stand undisturbed for a period of time and measure the amount of powder which has sedimented out.

There does not seem to have been any systematic study of the effects of agitation and of suspensoid concentration on degree of flocculation, although these factors must be of great importance. Greatest interest attaches to flocculation in suspensions which are undergoing agitation, since the degree of flocculation of an unagitated suspension is not an inherent property of the system but depends on its history and especially on its past agitation. In an agitated suspension, the degree of flocculation must depend on the balance between floc formation and floc destruction. The rate of formation, which depends on rate of collisions between particles, will vary with both agitation and concentration, while the rate of destruction will depend on agitation.

The object of the present work was to determine the effects of concentration and agitation on aqueous suspensions of two simple "soils," ferric oxide and carbon.

Experimental[10]

Materials.—The ferric oxide was reagent grade material (General Chemical Division, Allied Chemical and Dye corporation). The carbon was Sterling NS carbon black (Godfrey L. Cabot) and was extracted with benzene followed by acetone to remove all oils and tarry matter. Distilled water was used throughout the work reported.

Apparatus.—Suspensions were agitated in a Waring Blendor whose blade speed could be varied from 1000 to 12,000 r.p.m. by means of a variable transformer. Speed was observed and controlled by stroboscopic illumination of a pin inserted in the bottom of the motor shaft. In all experiments, 500 cc. of suspension was agitated in the quart-sized blender jar and maintained at 30 ± 2° throughout the run.

Turbidities of suspensions were read in a Klett–Summerson photoelectric colorimeter, employing the blue filter KS-42 which passes light from 4000 to 4500 Å. with maximum transmission at 4200 Å. The less opaque suspensions were read in standard Klett–Summerson cells which resemble test-tubes and have an effective light path of 1.25 cm. The more opaque suspensions were read in a special cell with an effective light path of 0.07 cm. This special cell consisted of a regular Klett–Summerson cell with a slightly smaller tube centered inside it. The suspension was placed in the outer tube and the inner tube was then lowered, so that the suspension occupied the space between.

Turbidities are expressed as "specific readings," these being defined as R/C for the standard cell and 18.0 R/C for the special cell, where R is the instrument reading and C is the concentration of suspended solid in grams/liter. The factor 18 is employed because the special cell has a light path $^1/_{18}$ that of the standard cell.

Since the instrument readings are logarithmic, the specific reading as defined above is an extinction coefficient. It is an intrinsic measure of the turbidity of the suspension and should be independent of the cell used or the concentration of the dispersed material, provided the Beer–Lambert law is followed. The instrument was set to read zero when the cells were filled with water, so that the turbidity readings would refer only to the suspended solid.

(1) Presented at National Meetings of the American Chemical Society, Atlantic City, 1956, and Los Angeles, 1953.

(2) Lever Brothers Research Center, 45 River Road, Edgewater, New Jersey.

(3) P. H. Fall, THIS JOURNAL, **31**, 801 (1927).

(4) F. D. Snell, *Ind. Eng. Chem.*, **25**, 162 (1933).

(5) L. Greiner and R. D. Vold, THIS JOURNAL, **53**, 67 (1949).

(6) J. W. McBain, R. S. Harborne and A. M. King, *J. Soc. Chem. Ind.*, **42**, 373T (1923).

(7) R. D. Vold and C. C. Konecny, THIS JOURNAL, **53**, 1262 (1949).

(8) I. Reich and F. D. Snell, *J. Soc. Chem. Ind.*, **68**, 98 (1949).

(9) A. M. Mankowich, *Ind. Eng. Chem.*, **44**, 1151 (1952).

(10) More detailed description of experimental methods as well as complete tabulations of results are in the Ph.D. dissertation of Irving Reich, 1956, available in microfilm from the Library of the University of Southern California, Los Angeles 7, California.

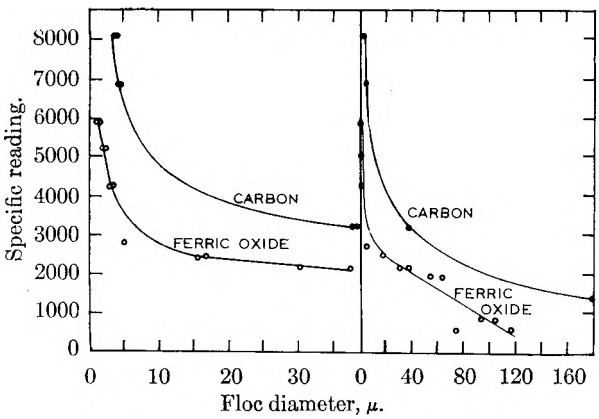

Fig. 1.—Calibration curves of specific reading as a function of average floc diameter. Specific reading is the turbidity of the suspension defined as $272/Cl \ln I_0/I$, where C is concentration in grams per liter, l is light path in cm., and I_0 and I are intensities of incident and transmitted light.

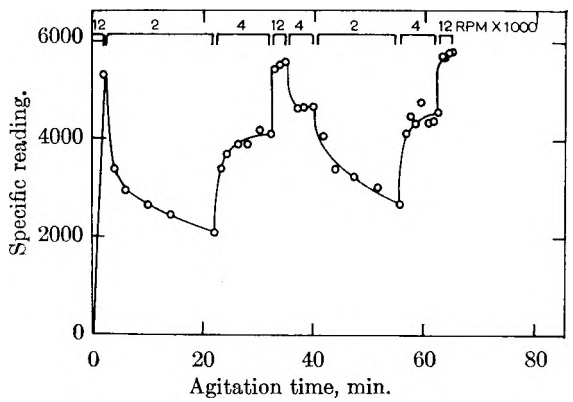

Fig. 2.—Variation of turbidity of 0.1% ferric oxide suspension agitated in blender at 30°.

Preliminary Studies.—Measurement of turbidities of India ink and potassium dichromate solution in both cells at various dilutions confirmed applicability of the Beer–Lambert law. Specific readings remained constant within 1% over the range of instrument scale readings from 50 to 500.

In preliminary experiments, suspensions of carbon and of ferric oxide were agitated continuously, small samples being withdrawn for turbidity reading during the agitation. It was found that the degree of flocculation in the sample did not change appreciably upon withdrawal and transfer to the cell, provided the sample was removed and transferred slowly without undue agitation. However very coarse suspensions were an exception; they gave erratic readings which depended on the details of the sampling method. Such suspensions were coarse enough so that the flocs were readily visible to the naked eye. They had specific readings well below 1000 for ferric oxide and well below 2000 for carbon.

It was found that suspensions could be diluted without undergoing any change in specific reading provided they were mixed very gently with the diluent water. It follows that the average floc size of the suspension is not changed when the suspension is diluted unless sufficient agitation is provided to disrupt or join flocs together.

Estimation of Average Floc Size.—If the flocs were homogeneous opaque spherical particles which merely blocked out the light striking them, it would be possible to calculate average floc size from the turbidity of the suspension. However this treatment was found to be grossly inaccurate for particles having the small size and the irregular, loose structure of the flocs studied here. It was found possible, however, to use the turbidity reading as a measure of average floc size by photomicrographing suspensions, measuring floc sizes and preparing calibration curves of average floc size *versus* specific reading.

A series of suspensions of carbon and ferric oxide was prepared covering wide ranges of floc size. The average floc size could be controlled by varying the concentration and agitation of the suspension. Suspensions were read for turbidity and were photomicrographed.[10] The Martin's diameters[11] of the flocs in each photomicrograph were measured, and the volume-weighted average diameter was calculated, applying the usual formula $D = \Sigma n_i d_i^4 / \Sigma n_i d_i^3$ where n_i is the number of flocs with diameter d_1. D is also the weight-average diameter if floc density is independent of floc size.

Figure 1 shows specific readings of carbon and ferric oxide suspensions plotted against average floc sizes. The left portion of the figure covers the finer suspensions on an expanded scale. Over the dispersion range covered, specific reading increases with decreasing floc size. Obviously this relationship could reverse itself in the region of particle size below about 0.2 μ, but this is irrelevant for the present investigation.

Although the microscopic measurements were not capable of very great accuracy, due to the extreme irregularity and the fragility of the flocs, the calibration curves were satisfactory for the present study, since the changes in floc size which were measured were enormous.

Systematic Study of Flocculation and Deflocculation.—Suspensions were agitated in the blender at a fixed speed, while small samples were removed periodically for turbidity measurement. Usually agitation was held constant until the turbidity approached a constant value. The blender speed was then altered, and a series of readings was taken at the new speed. Speeds were increased and decreased several times to determine whether the flocculation was reversible.

Figures 2 and 3 show data obtained for 0.1% and 0.4% suspensions of ferric oxide. Each time the agitation rate was increased, the specific reading increased rapidly at first, then more slowly, approaching a constant value. Similarly, when the agitation rate was decreased, the specific reading fell rapidly at first, then more slowly. Here also a constant value was approached, although in the experiments covered by these figures the agitation was not always continued long enough to demonstrate this.

Dispersion was not always completely reversible. When the rate of agitation was altered and then brought back to its initial value, the earlier specific

(11) G. Herdon, "Small Particle Statistics," Elsevier, Houston, 1953, p. 440.

reading was always approximated but not necessarily duplicated exactly.

The following average floc diameters (microns) were obtained at steady state in suspensions of ferric oxide at various rates of agitation

Concn. of ferric oxide, %	Blender speed, r.p.m. 1000	2000	4000	5000	12000
0.1			3		1.7
.2	90	45	4	2.2	
.4		95	56	12	
.6		110	100		

The values were determined by taking average steady-state specific readings for the ferric oxide suspensions agitated at different rates and determining the floc diameters with the aid of the calibration curves shown in Fig. 1. It is obvious that the degree of flocculation depends very much on concentration as well as on agitation. A variation of over fifty-fold in average floc diameter was obtained over the fairly limited ranges of concentration and agitation studied. This, of course, means a variation of some 125,000-fold in number of flocs.

Similar studies were carried out on suspensions of carbon in water at concentrations of 0.005, 0.02 and 0.1%. Flocculation behavior followed the same principles as that of ferric oxide, except that there was somewhat greater tendency toward irreversible flocculation for the more dilute carbon suspensions. The 0.1% suspension (Fig. 4) appears to have undergone strong irreversible flocculation during the first few minutes of agitation; thereafter it showed excellent reversibility.

Average steady-state floc diameters (μ) of carbon were

Concn., of carbon, %	Blender speed, r.p.m. 1000	4000	8000	12000
0.005			3	
.02	78	48		12
.1	>200	>200	155	110

Here also, flocculation increases markedly with increasing concentration and with decreasing intensity of agitation. However at any given concentration and agitation, carbon flocculates much more extensively than ferric oxide.

A broader study of the effect of concentration was conducted by agitating suspensions of ferric oxide over the concentration range of 0.002 to 0.5%. The ferric oxide was first agitated in the blender for 3 minutes at 0.4% concentration to break up dry flocs. It was then diluted to various concentrations and the suspensions were agitated gently for 9 hours by rotating 200-cc. portions at 41 r.p.m. in pint Mason jars in an Atlas Launder-O-Meter at 30°. During this period of agitation, all suspensions reached a steady state.

The profound effect of concentration is shown in Fig. 5. The extremes in specific reading were 4000 and 600, corresponding to average floc diameters of 3.5 and 110 μ.

Throughout these studies it was observed repeatedly that agitation of suspensions could be halted for periods of up to several hours without appreciable change in specific reading taking place. The only requirement for this was that the period

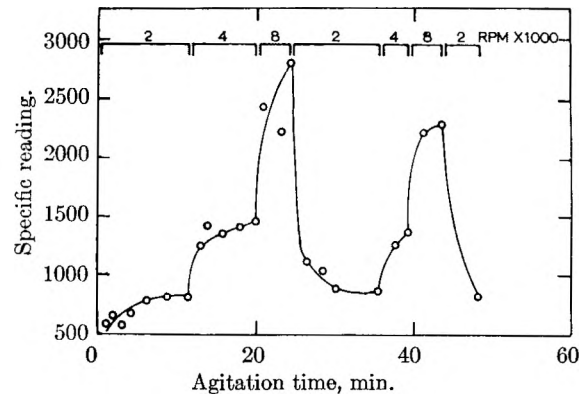

Fig. 3.—Variation of turbidity of 0.4% ferric oxide suspension agitated in blender at 30°.

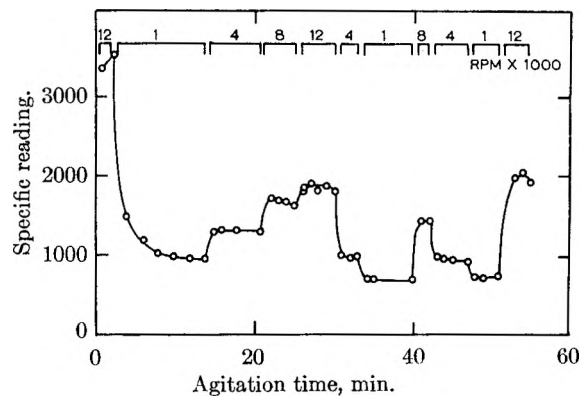

Fig. 4.—Variation of turbidity of 0.1% carbon agitated in blender at 30°.

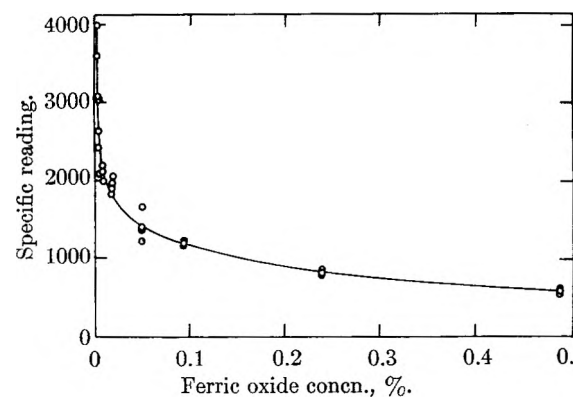

Fig. 5.—Variation of specific reading with concentration of ferric oxide suspensions. All suspensions agitated 9 hours in Launder-Ometer at 30°.

of no agitation be short enough so that little sedimentation occurred. A rapidly-agitated suspension is, in effect, "frozen" in a highly deflocculated form if agitation is suddenly halted. If this suspension is subsequently agitated at low speed, its degree of flocculation increases.

Discussion

The most significant result of this investigation is the demonstration of the great importance of concentration and agitation in governing the degree of flocculation of a suspension. These factors are just as important, and as amenable to scientific treatment, as the more familiar factors of interparticle attraction, double-layer repulsion

etc. Agitation, in particular, plays a role analogous to the role played by temperature in governing chemical reactions.

It will be helpful to the discussion to define an "ideal" suspension whose flocculation will obey simple laws. The ideal suspension will be defined as follows. (A) The suspended particles are spherical. (B) Forces of attraction and repulsion between particles are uniform over the surface of each sphere and are alike for all spheres. (C) Forces of attraction between particles do not change with time. (This eliminates such phenomena as progressive adsorption of desorption of a solute, progressive solvation, etc.) (D) The force–distance curves obtained when two particles are brought together and then separated are identical, regardless of how long the two particles remain in contact. (This rules out Ostwald ripening or other effects which might form permanent bonds.) (E) The particles are sufficiently large so that Brownian motion will not cause an appreciable fraction of them to collide during the period of observation. (F) The particles and flocs are sufficiently small so that no appreciable creaming or settling occurs during the period of observation.

Items A-D are intended to eliminate the possibility of irreversible flocculation or deflocculation. Items E and F eliminate Brownian motion and gravitational motion as factors causing buildup or disruption of flocs, leaving mechanical agitation as the sole kinetic factor.

The following behavior would be expected of such an ideal suspension.

(1) Under continuous agitation at a constant intensity, the suspension will approach a fixed and definite floc-size distribution. The degree of flocculation approached depends on the concentration, composition and agitational intensity, but does not depend on the history of the system.

(2) The more intense the agitation, the smaller will be the average floc size which is approached. This will hold because the maximum stable floc size decreases as the intensity of agitation increases. The cross-sectional area, and hence the resistance to splitting, of a floc increases as the square of floc diameter, whereas the disruptive force due to a shear field increases as the cube of floc diameter.

(3) If average floc size is increasing in a suspension under constant agitation, then the slower the agitation, the slower will be the rate at which the appropriate average floc size will be approached. This follows from the low frequency of collisions at slow agitational intensity.

(4) An unagitated system will maintain its initial floc-size distribution unchanged. This is simply the extreme case of rule 3. Such a suspension is analogous to a chemical system which has been "frozen" and is apparently stable although actually far from its equilibrium state.

(5) At any given intensity of agitation, the average floc size which is approached will increase with increasing concentration of particles. This follows from simple statistical reasoning similar to that which underlies the law of mass action. Increased concentration favors formation of large flocs more than it favors formation of small ones.

(6) The rate of decrease of floc size by agitation is independent of concentration. This follows from the fact that disruption of the floes is due to the shear field and not to collision between flocs. Hence the lifetime of a floc in a disruptive shear field will not depend on the number of flocs or particles present.

(7) If average floc size is increasing in a suspension under constant agitation, then the lower the concentration, the slower will be the rate at which the appropriate average floc size will be approached. This follows from the low frequency of collisions in dilute suspensions.

The data obtained in this investigation followed the foregoing rules quite well. This is true despite the palpable departure of the carbon and ferric oxide from the requirements for ideal suspensions. Although some irreversible changes did occur, the suspensions showed a remarkable degree of reversibility.

The particles in these suspensions are analogous to molecules undergoing reversible association, except that they move under the influence of agitation rather than thermal motion. Davies[12] and Kalinske[13] have shown that particles suspended in a turbulent fluid behave in some ways like a gas. They undergo diffusion and they exhibit an osmotic pressure.

The description of flocculation as a reversible process governed by agitation has been stated by Mason[14] who studied the flocculation of cellulose fibers in a laminar flow field. He states that one would expect "a dynamic equilibrium to be established between floc formation and floc destruction. One would further expect the rate of establishment of equilibrium to increase and the position of equilibrium to shift in the direction of higher dispersion as the shear rate increases. By analogy, shear rate in fiber flocculation is comparable to the temperature in a chemical reaction."

It is helpful to consider under what circumstances the flocculation behavior of a suspension will be governed primarily by agitation rather than by thermal motion of the particles (item E in the description of an ideal suspension). It is obvious that, since all particles have the same thermal energy regardless of size, velocity of thermal motion will become negligible for very large particles as compared with even minor or accidental convection currents in the liquid. For very small particles, however, thermal motion will cause far more collisions between particles than even vigorous agitation. The time required for half of the particles in a suspension to collide by Brownian motion is given[15,16] by the equation

$$t = \frac{1}{4\pi DRn_0} \qquad (1)$$

where n_0 is the number of particles per unit volume at the outset, D is the diffusion constant of the particles, and R is the distance of approach (be-

(12) R. W. Davies, *J. Appl. Phys.*, **23**, 941 (1952).

(13) A. A. Kalinske in "Fluid Mechanics and Statistical Methods in Engineering," U. of Pennsylvania Press, Philadelphia, 1941.

(14) S. G. Mason, *Pulp & Paper Mag. Canada*, **49**, No. 13, 99 (1948).

(15) M. von Smoluchowski, *Physik. Z.*, **17**, 557, 585 (1916).

(16) M. von Smoluchowski, *Z. physik. Chem.*, **92**, 129, 155 (1917).

tween centers) at which adhesion occurs. If we take R as the diameter of a particle and substitute for D its equivalent from Einstein's diffusion equation, we obtain

$$t = \frac{3\eta}{4kTn_0} \qquad (2)$$

where η is the viscosity of the liquid, k is the Boltzmann constant, and T is the absolute temperature.

Let us apply equation 2 to a 0.1% suspension of ferric oxide. If the particles are 0.1 μ in diameter, t will be 0.4 second, and flocculation by Brownian motion will proceed rapidly. But if the particles are 1 μ in diameter, t will be 400 seconds, and if they are 10 μ in diameter, t will be 111 hours. In the last case, Brownian motion will not cause appreciable flocculation for many hours.

Von Smoluchowski[16] and Tuorila[17] showed that for small particles collisions caused by agitation are few compared to collisions caused by Brownian motion, but that for large particles the situation is reversed. The equation derived was

$$\frac{J}{I} = \frac{\eta R^3(du/dz)}{2kT} \qquad (3)$$

where J is the probability of collision due to motion in a laminar flow field of shear gradient du/dz, I is the probability of collision due to Brownian motion, η is the viscosity of the liquid, and R is the distance of approach at which adhesion occurs. Again let us take R as the particle diameter. Assume that a 0.1% suspension of ferric oxide is agitated in a rather mild flow field, such that $du/dz = 100$ sec.$^{-1}$. Then if the particles are 0.1 μ in diameter, J/I will be 1/100. However for particles 1 μ in diameter it will be 10/1 and for particles 10 μ in diameter it will be 10,000/1. This shows clearly the transition, at about 1-μ particle size, between the region of colloidal dispersions, where Brownian motion is predominant, and the region of suspensions, where agitation is predominant in governing flocculation.

Insofar as deflocculation is concerned, thermal motion is always ineffective since the binding forces between flocculated particles are much greater than 3/2 kT. That is why lyophobic colloidal systems are inherently unstable, as Verwey and Overbeek have noted.[18] In the complete absence of agitation, flocs would grow indefinitely in any dispersion whose particles liberate free energy upon adhesion. However when flocs become large enough, they will be disrupted by even mild agitation due to thermal convection currents in the liquid. Hence in practice, a steady state with finite average floc size is always reached. This is in contrast to the classical theory which sets no limit to the size of flocs formed by lyophobic dispersions. If the individual particles are of colloidal size, flocculation will proceed initially by Brownian-motion collisions, following the classical equations of von Smoluchowski. After the flocs have grown to about one micron or larger, agitation will become the dominant factor and a steady-state distribution will be approached. The system will have changed from a classical sol to a suspension, entering a realm in which new principles apply.

The rules set forth above for ideal suspensions appear to apply quite well to the practical dispersions studied, despite the non-ideality of the particles. These rules should be of general value in controlling and predicting behavior of suspensions. In particular there does not seem to have been general recognition of the extreme importance of concentration as a factor controlling degree of dispersion. Deflocculation may be greatly facilitated by dilution of a suspension before agitation. On the other hand, flocculation and settling may be promoted by adding additional solid particles to a suspension. Suspensions can be flocculated more effectively by gentle agitation than by leaving them undisturbed. Indeed, there must be an optimum intensity of agitation required to obtain any desired degree of flocculation. Agitation more intense than the optimum will drive the system toward a steady state which is too disperse, while agitation less intense than the optimum will flocculate the particles more slowly than would optimum agitation.

Careful study of suspensions should be of as much theoretical value as the more familiar studies of sol flocculation. A suspension may be considered to be a stable, well-defined system, provided agitation is properly controlled and has been maintained at a constant value long enough for the system to have reached its steady state. The general principles noted above for ideal suspensions can be given mathematical form if the nature of the agitation is capable of mathematical description. This will be most feasible for the extreme cases of highly ordered and highly random agitation.

The authors wish to express their appreciation to the Lever Brothers Company for a research grant to one of them (I R.) which made this work possible.

(17) P. Tuorila, *Kolloidchem. Beih.*, **24**, 1 (1927).

(18) E. J. W. Verwey and J. Th. Overbeek, "The Theory of the Stability of Lyophobic Colloids," Elsevier Press, New York, N. Y., 1948, p. 186.

THE KINETICS OF THE REACTION BETWEEN PLUTONIUM(VI) AND TITANIUM(III) IN PERCHLORATE SOLUTION[1]

BY S. W. RABIDEAU AND R. J. KLINE

Contribution from the University of California, Los Alamos Scientific Laboratory, Los Alamos, New Mexico

Received March 20, 1959

The kinetics of the reaction between Pu(VI) and Ti(III) has been studied as functions of temperature and acidity using spectrophotometric methods. Since the reductions of Pu(VI) and Pu(IV) by Ti(III) are measurable, whereas the reduction of Pu(V) is very rapid, the data were treated as competitive consecutive second-order reactions. The rate law written in terms of the rate of disappearance of Pu(VI) is $-d[Pu(VI)]/dt = k_1[Pu(VI)][Ti(III)][H^+]^{-1}$. The inverse first power of the hydrogen ion concentration in the rate law suggests that the slow step may consist of the reaction, $PuO_2^{++} + TiOH^{++} \rightarrow PuO_2^{+} + TiO^{++} + H^+$. With values of the specific rate constant for the reaction between Pu(IV) and Ti(III) obtained from independent experiments, the spectrophotometric data were coded for the IBM-704 computer and the calculation was made using an iterative procedure to evaluate the specific rate constant for the reaction between Pu(VI) and Ti(III). At 25° in molar perchloric acid, the rate constant for the Pu(VI)–Ti(III) reaction was found to be 108 sec.$^{-1}$. The reduction of perchlorate ion by Ti(III) has been considered, and it has been shown that reductions of Pu(VI) and Pu(IV) by Ti(III) are not catalyzed by chloride ion. The thermodynamic quantities for the activation process written in terms of the principal species are $\Delta F^{\ddagger} = 14.7 \pm 0.01$ kcal./mole, $\Delta H^{\ddagger} = 10.3 \pm 0.4$ kcal./mole and $\Delta S^{\ddagger} = -14.7 \pm 1.3$ e.u.

Introduction

Rapid reductions of the plutonyl ion can be followed spectrophotometrically with high precision at plutonium concentrations as low as 10^{-4} *M* because of the relatively large molar absorptivity of the plutonyl ion (*ca.* 550 M^{-1} cm.$^{-1}$) at 8304 Å. using the Cary Model 14 Spectrophotometer. As part of continuing research on the effect of size and charge type upon the thermodynamic quantities of activation for oxidation–reduction reactions of plutonium, the kinetics of the reaction between Pu(VI) and Ti(III) has been studied. In the reduction of Pu(VI) with Ti(III) it is necessary to consider the reactions

$$Pu(VI) + Ti(III) \xrightarrow{k_1} Pu(V) + Ti(IV) \quad (1)$$

$$Pu(V) + Ti(III) \xrightarrow{k_2} Pu(IV) + Ti(IV) \quad (2)$$

$$Pu(IV) + Ti(III) \xrightarrow{k_3} Pu(III) + Ti(IV) \quad (3)$$

In exploratory experiments, it was found that the reactions of Pu(VI) and Pu(IV) with Ti(III) occurred at measurable rates; however, the reduction of Pu(V) as shown in equation 2 was too rapid to measure. Thus, considering equation 2 fast in comparison with (1) and (3), it is possible to consider this system as a competitive consecutive second-order reaction system, that is

$$Pu(VI) + 2Ti(III) \xrightarrow{k_1} Pu(IV) + 2Ti(IV) \quad (4)$$

$$Pu(IV) + Ti(III) \xrightarrow{k_3} Pu(III) + Ti(IV) \quad (5)$$

Frost and Schwemer[2] have considered a system somewhat analogous to the present work, and the differential rate equations were derived for the special case of stoichiometrically equivalent amounts of the reactants. Since Ti(III) reacts with perchlorate ion as a side reaction, it was not practical to use predetermined concentrations of reductant in the present rate experiments.

Experimental

Plutonium(VI) was prepared from an especially selected lot of high purity metal by removal of the oxide film, dissolution of the metal in the appropriate weighed quantity of boiled and standardized Baker and Adamson reagent grade 71% perchloric acid, and oxidation with ozone. The titanium(III) perchlorate stock solution was prepared by the dissolution in hydrochloric acid of a sample of titanium hydride obtained from Metal Hydrides, Inc., Beverly, Mass. The stock solution was filtered and stored under an atmosphere of helium. Prior to use in the reaction with Pu(VI), a portion of the stock solution was added to a deaerated perchloric acid solution which was then placed in a thermostat. Periodically samples of the Ti(III) were removed and quenched in solutions of cerium(IV) sulfate. The cerium(IV) sulfate solutions were analyzed with the Model 14 Cary Spectrophotometer at 25° at a wave length of 4390 Å. With the use of cerium(IV) sulfate solutions standardized against U. S. Bureau of Standards As_2O_3, sample 83a, it was found that the molar absorptivity at this wave length is 191.1 ± 0.3 M^{-1} cm.$^{-1}$ Pseudo first-order plots of log[Ti(III)] *versus* time gave straight lines which permitted the titanium(III) perchlorate concentration used in the experiment to be determined.

All solutions were prepared with distilled water which had been redistilled from alkaline permanganate in an all-Pyrex apparatus. Sodium perchlorate was obtained by the neutralization of C.P. sodium carbonate with perchloric acid and double recrystallization of the salt. The perchloric acid was standardized by weight against Baker Analyzed Grade mercuric oxide.

In each determination of the rate constant for the reaction between Pu(VI) and Ti(III), the molar absorptivity of PuO_2^{++} was determined in the solution environment and at the temperature to be used in the kinetic experiment. No correction was required for absorption by the Ti(III) or Ti(IV) or by the plutonium species produced during the course of the reaction, since these concentrations were in the 10^{-4} *M* range and their molar absorptivities are small.

Weighed quantities of a diluted plutonium(VI) perchlorate stock solution, together with the appropriate amounts of acid and salt, were placed in one leg of a double chambered ten cm. spectrophotometric absorption cell. After flushing the cell with nitrogen, a known volume of diluted Ti(III) stock solution was added to the second leg of the absorption cell. The solutions were brought to temperature in a water thermostat, mixed quickly, and placed in the cell compartment of the spectrophotometer. With circulating water, the temperature of the bath-water in the cell compartment was maintained at ±0.2°. The first readings were obtained within 20 to 25 seconds after the start of mixing.

The experimental observations consisted of the determination of the concentration of PuO_2^{++} as a function of time through use of the strong absorption peak at 8304 Å. measured with the Cary Model 14 Recording Spectrophotometer. The initial titanium(III) perchlorate concentration was known, and the concentration of this species as a function of time was computed from the observed change in the concentration of PuO_2^{++} plus a small correction for the reaction of Ti(III) with the Pu(IV) formed. The specific

(1) This work was done under the auspices of the U. S. Atomic Energy Commission.

(2) A. A. Frost and W. C. Schwemer, *J. Am. Chem. Soc.*, **74**, 1268 (1952).

rate constants for the reaction between Pu(IV) and Ti(III) have been determined[3] from independent work. Under the conditions of the present work, the reaction between Pu(III) and Pu(VI) has been found to be negligible.

Stoichiometry.—Since it was found that a solution of PuO_2^+, prepared by the reaction of Pu(III) and PuO_2^{++}, was reduced to Pu(IV) by Ti(III) within the time of mixing, the initial approximation of the titanium(III) perchlorate concentration was considered to be the original concentration less twice the change in the concentration of PuO_2^{++}. The linearity of second-order plots to 30 to 40% completion supports this stoichiometry. Further, in experiments at 10° in which approximately equal molar quantities of Ti(III) and PuO_2^{++} were used, the ratio of the change in the titanium to the change in the plutonium concentrations at the time of essential completion of the reaction closely approximated 2.00. This result indicates that under the conditions of the experiments, the essential reduction process was the conversion of PuO_2^{++} to Pu(IV). In experiments at 25°, the ratio of change of Ti(III) concentration to that of PuO_2^{++} was somewhat greater, indicating that a significant amount of Pu(IV) had been reduced at the time of complete reaction of the Ti(III).

Results and Discussion

Theoretical.—The difficulties inherent in the use of initial slopes in the evaluation of specific rate constants in kinetic studies have been stated by Ingold.[4] However, in the case of some fairly rapid reactions, it may be difficult to improve upon the values of the rate constants derived from initial slopes. In the present work, the kinetic data were first analyzed with the assumption that reaction 4 alone need be considered. The values of k_1 were then obtained in the usual way from plots of log $\{[Ti(III)]/[Pu(VI)] \times [Pu(VI) - x]/[Ti(III) - 2x]\}$ *versus* time, where x is the change in the Pu(VI) concentration at any time, t. Although in all instances initially linear plots were obtained in this way, departure from linearity occurred sooner when k_1 and k_3 were relatively large. (See equations 6 and 7). It was interpreted that the deviation from a straight line relation arose chiefly from the fact that the reduction of Pu(IV) by Ti(III) is not negligible.

Using in part the notation of earlier work,[2] the following derivation develops an expression for the calculation of k_1 which takes into consideration the amount of Ti(III) lost through the reaction with Pu(IV). If equations 4 and 5 are rewritten

$$B + 2A \xrightarrow{k_1} C + 2E \quad (6)$$

$$C + A \xrightarrow{k_3} D + E \quad (7)$$

then from stoichiometry considerations

$$C = (A - A_0) + 3(B_0 - B) \quad (8)$$

where A, B, C, D and E represent the molar concentrations of Ti(III), Pu(VI), Pu(IV), Pu(III) and Ti(IV), respectively, and the subscript zero corresponds to initial concentrations. The rate equation in terms of the disappearance of A can be written

$$-dA/dt = 2k_1AB + k_3AC \quad (9)$$

$$= 2k_1AB + k_3A[(A - A_0) + 3(B_0 - B)] \quad (10)$$

A simplification in the mathematical treatment is achieved through the use of the substitutions

$$K = k_3/k_1 \qquad \tau = 2k_1B_0t \quad (11)$$

$$\alpha = A/A_0 \qquad d\tau = 2k_1B_0\,dt$$

$$\beta = B/B_0$$

Dividing equation 10 by $2k_1A_0B_0$ and simplifying, we obtain

$$d\alpha/d\tau = [(3K/2) - 1]\alpha\beta - [(3/2) - A_0/2B_0]K\alpha - (KA_0\alpha^2/2B_0) \quad (12)$$

Then, making the further substitutions

$$a = [(3/2) - A_0/2B_0] \quad (13)$$

$$b = A_0/2B_0$$

equation 12 becomes

$$d\alpha/d\tau = [(3K/2) - 1]\alpha\beta - aK\alpha - bK\alpha^2 \quad (14)$$

Since the rate equation in terms of the rate of disappearance of B is

$$-dB/dt = k_1AB \quad (15)$$

then it follows that

$$-d\beta/d\tau = b\alpha\beta \quad (16)$$

and also

$$-d\alpha/d\beta = (3K - 2)/2B - aK/b\beta - K\alpha/\beta \quad (17)$$

Multiplying equation 17 by β^{-K} and integrating, we find that

$$\alpha = [(3K - 2)\beta/2b(K - 1)] - a/b + c\beta^K \quad (18)$$

where c is the constant of integration and has the value

$$c = 1 + a/b - (3K - 2)/2b(K - 1) \quad (19)$$

since $\alpha = 1$ when $\beta = 1$. Substituting the value of c in equation 18, gives

$$d\beta/d\tau = (3K - 2)\beta^2(\beta^{K-1} - 1)/2(K - 1) - 3\beta^{K+1}/2 + a\beta \quad (20)$$

Finally, transposing and inserting the limits of integration

$$\int_0^\tau d\tau = \int_1^\beta \frac{d\beta}{(3K - 2)\beta^2(\beta^{K-1} - 1)/2(K - 1) - 3\beta^{K+1}/2 + a\beta} \quad (21)$$

Values of τ as functions of β, and consequently as functions of time, have been graphically evaluated by plotting 1/denominator of equation 21 *versus* β. The preliminary values of k_1 for use in the computation of K were obtained from initial slopes of second-order rate plots assuming no loss of Ti(III) through reaction 5. The values of k_3 used with k_1 in the evaluation of K at various acidities and temperatures were obtained experimentally from independent measurements. The manual graphical integration procedure was tedious inasmuch as iterations were required to obtain the best value of K, and hence of k_1. Consequently, the integral expression in equation 21 was programmed for the IBM-704 computer. A comparison was made between the areas evaluated manually and by computer methods. The areas were found to be in excellent agreement.

Input data for the IBM-704 consisted of initial reactant concentrations and optical density readings of the plutonium–titanium solutions at a wave length of 8304 Å. Readings were taken at one second intervals from the strip chart recording with the use of a transparent plastic template which had lines carefully ruled on it to provide divisions corresponding to this time unit. The integration was performed with the computer coded to make use of the

(3) S. W. Rabideau and R. J. Kline, THIS JOURNAL, to be published.
(4) C. K. Ingold, *J. Chem. Soc.*, 2170 (1931).

trapezoidal rule. The optical density values for the period between the time of mixing and the first recorded trace on the spectrophotometer were computed from the value of k_1 derived from the initial slope plot and the known initial concentrations of reactants assuming second-order rate behavior. These points were used to evaluate the integral over the limits of integration used. With the IBM-704 computer, iterations were performed until the difference between successive values of K were less than 0.1%. In most of the τ *versus* time plots, the line was constrained to go through the origin; however in those cases in which the least squares line was not required to go through the origin, it was found that the intercept was very small. All the values of k_1 were derived from slopes of lines restricted to pass through the origin as theoretically required. Included in the computer program was the evaluation of the least squares slope of the τ *versus* time plots.

In an effort to determine the influence of the value of k_3 upon the result obtained for k_1, various k_3 results were fed into the calculation, otherwise using the same experimental data. It was found that k_1 was not very sensitive to the value chosen for k_3. The use of a k_3 value which differed from the experimentally determined value by about 10% resulted in a change of k_1 of only 0.1%.

Arbitrarily, it was decided to use data up to 40% completion of the reaction in the computation of the values of k_1. However, tests were made to determine the influence of using data obtained at greater percentages of reaction. For the reaction at 2.2° in 0.25 M $HClO_4$–1.75 M $NaClO_4$, a difference of 1.8% in the values of k_1 was noted when experimentally obtained results up to 40 and 63% completion were used. It is known that at the higher extents of reaction a greater contribution toward the decrease in the concentration of PuO_2^{++} is made by the Pu(III)–Pu(VI) reaction.

As discussed in the experimental section of this paper, it is observed that the reduction of PuO_2^+ by Ti(III) is fast in comparison with the rate of reduction of PuO_2^{++}. This result is somewhat unexpected in view of the slowness observed in the reduction of PuO_2^+ by vanadium(III) perchlorate.[5] Further, it has become customary to consider that reactions involving the making or breaking of metal–oxygen bonds are slower than those reactions involving an electron transfer, *e.g.*, the disproportionation reactions of Pu(IV) or Pu(V) are slower than the Pu(III)–Pu(VI) reaction. However, in the present work, the low total plutonium ion concentration precludes the disappearance of appreciable quantities of PuO_2^+ by the disproportionation path, and the change in the concentration of Ti(III) indicates that it is involved in the reduction. It is not clear why the reduction of PuO_2^+ by Ti(III) should be much more rapid than the reduction of PuO_2^{++}.

Hydrogen Ion Dependence.—In Table I are given the results of a study of the hydrogen ion concentration dependence of the reaction between Pu(VI) and Ti(III) at 2.5°. The ionic strength was maintained at two by the addition of appropriate quantities of anhydrous sodium perchlorate. The uncertainty of the mean value of the product $k_1[H^+]$ is given as twice the standard deviation of the mean. Within the limits of uncertainty it appears that the rate of the reaction between Pu(VI) and Ti(III) is given by the rate expression $-d[Pu(VI)]/dt = k_1[Pu(VI)][Ti(III)][H^+]^{-1}$. A possible mechanism suggested by this result for the rate-determining step is

$$PuO_2^{++} + TiOH^{++} \xrightarrow{k_1} PuO_2^{+} + TiO^{++} + H^+ \quad (22)$$

TABLE I

HYDROGEN ION CONCENTRATION DEPENDENCE OF RATE CONSTANT FOR THE Pu(VI)-Ti(III) REACTION IN PERCHLORATE SOLUTIONS OF IONIC STRENGTH TWO AT 2.5°

$[H^+]$, M	k_1, M^{-1} sec.$^{-1}$	$k_1[H^+]$, sec.$^{-1}$	$[H^+]$, M	k_1, M^{-1} sec.$^{-1}$	$k_1[H^+]$, sec.$^{-1}$
2.00	12.6	25.2	0.50	56.2	28.1
	11.3	22.6		60.6	30.3
	12.6	25.2		57.4	28.7
	12.5	25.0	0.25	113	28.2
1.00	22.2	22.2		113	28.2
	21.0	21.0		114	28.5
	21.8	21.8		109	27.2
	22.3	22.3			
	24.2	24.2		Mean	25.5 ± 1.4

Temperature Dependence.—Measurements of the temperature coefficient of the specific rate constant for the reaction between Pu(VI) and Ti(III) have been made in molar perchloric acid solutions. The results are given in Table II.

TABLE II

TEMPERATURE DEPENDENCE OF Pu(VI)-Ti(III) REACTION IN MOLAR PERCHLORIC ACID SOLUTIONS OF UNIT IONIC STRENGTH

t, °C.	$1/T \times 10^3$	k_1, M^{-1} sec.$^{-1}$	t, °C.	$1/T \times 10^3$	k_1, M^{-1} sec.$^{-1}$
2.5	3.628	23.1	15.5	3.464	56.0
		23.1			56.8
		22.0			56.8
5.8	3.585	29.5			57.3
		29.6			59.1
		31.2	20.0	3.411	81.8
		32.5			78.0
		31.8			76.5
10.2	3.529	42.7	25.0	3.354	108
		43.8			108
		42.4			103
					112

With the expressions of the transition state theory,[6] values of the free energy, heat and entropy of activation were computed using the data of Table II. The values are found to $\Delta F^{\ddagger} = 14.7 \pm 0.01$ kcal./mole, $\Delta H^{\ddagger} = 10.3 \pm 0.4$ kcal./mole and $\Delta S^{\ddagger} = -14.7 \pm 1.3$ e.u. for the reaction between Pu(VI) and Ti(III) in terms of the principal species, *i.e.*, $PuO_2^{++} + Ti^{+++} + H_2O \rightarrow (PuO_2 \cdot Ti \cdot OH)^{+4} + H^+$.

Effect of Chloride Ion.—Inasmuch as it is impossible to carry out an investigation of the reaction between Pu(VI) and Ti(III) in perchlorate solution in the absence of Cl^- because of the reduc-

(5) S. W. Rabideau, THIS JOURNAL, **62**, 414 (1958).

(6) S. Glasstone, K. Laidler and H. Eyring, "The Theory of Rate Processes," McGraw-Hill Book Co., Inc., New York, N. Y., 1941, p. 417.

tion of perchlorate by Ti(III), it was of interest to determine whether an increased Cl^- concentration altered the observed rate of reaction. A solution of 1 M $HClO_4$ was made 0.02 M in Cl^-, and the specific rate constant for the Pu(VI)–Ti(III) reaction was determined at 10.2° in this medium. A value of 45.0 M^{-1} sec.$^{-1}$ was obtained which is in good agreement with the value of k_1 determined at this temperature in 1 M $HClO_4$ with a total Cl^- concentration of about 0.002 M. (See Table II.)

Ionic Strength Effect.—From measurements of the value of k_1 at 2.5° in molar perchloric acid and at ionic strengths of 1.00 and 2.00 it was observed that k_1 was little altered by this change in ionic strength. This is in contrast to the effect of ionic strength on the reduction of Pu(IV) by Ti(III).[3] In this reaction the value of k_1 nearly doubled as the ionic strength was increased from 1 to 2.

Acknowledgments.—It is a pleasure to express our appreciation to Dr. J. F. Lemons for valuable discussions and interest in this work and to Drs. D. T. Cromer and A. H. Zeltmann for their assistance in the calculations.

HEAT CAPACITY OF Na_2O_2 AT HIGH TEMPERATURES[1]

BY M. S. CHANDRASEKHARAIAH, R. T. GRIMLEY AND JOHN L. MARGRAVE

Department of Chemistry, University of Wisconsin, Madison 6, Wisconsin

Received March 28, 1959

Samples of Na_2O_2 contained in gold capsules have been studied in a drop-type calorimeter from 375 to 869°K. The heat content is given by $(H_T - H_{298}) = 16.7T + 7.8 \times 10^{-3}T^2 - 5642$ cal. mole^{-1} [298° < T°K. < 869°]. A transition at 510 ± 10° has a heat of 1280 cal. mole^{-1}. The melting point of Na_2O_2 is higher than 869°K.

Very little high temperature thermodynamic data for sodium peroxide have been available. Two papers,[2,3] give the heat capacity and entropy of sodium peroxide up to 100°. This calorimetric measurement was undertaken in order to obtain enthalpy and heat capacity data at higher temperatures.

The apparatus is similar in design to one described by Southard[4] and the details of construction are given elsewhere.[5] A platinum-wound furnace was used to heat the sample and was maintained at constant power by a constant voltage regulator. The constant temperature oil-bath was maintained constant to ±0.002°. The calorimeter resistance thermometer was a transposed bridge arrangement of two copper and two manganin resistances, and the change in the temperature of the calorimeter was measured in terms of the change in the resistance of this arrangement. An electrical calibration experiment yielded the factor for converting the observed change in resistance to heat content of the sample.

Sodium peroxide was obtained from the Niagara Falls Laboratory of the du Pont Company and was analyzed by standard methods. The result of the analysis indicated: sodium peroxide, 98.3%; sodium carbonate, 1.5%; sodium oxide (by difference), 0.2%. X-Ray diffraction indicated no other phases present, and no solid solutions were indicated in either original or quenched samples.

Experimental Procedures

A weighed quantity (9.6537 g.) of the sample was transferred into a gold capsule, which was then sealed tight and welded. Except for welding, the rest of the operation was done inside a dry box. The enthalpy of the empty gold capsule above 298°K. was determined at different temperatures using the calorimeter assembly. This capsule plus the sample was then heated in the furnace to a measured temperature and dropped into the copper calorimeter. The rise in temperature of this calorimeter was measured on a resistance thermometer with a White Double Potentiometer.

Results and Discussion

Enthalpy differences of the empty gold capsule were measured from 100 to 800° at 100° intervals. The results fit the analytic function

$$(H_T - H_{298})_{\text{capsule}} = 0.4341T + 2.463 \times 10^{-3}T^2 - 131 \text{ cal.}$$

where $(H_T - H_{298})$ is the enthalpy difference for the capsule between room temperature and the temperature T,° K. in calories. This equation was employed for computing the heat transferred by the capsule as distinguished from the total heat transferred to the calorimeter in cooling the sample and the capsule from the furnace temperature to the final calorimeter temperature. Table I contains the experimental results, and Table II presents the molar heat content, entropy and free energy functions at selected temperatures as calculated from the data.

In calculating the enthalpy differences for sodium peroxide, corrections for the contributions from sodium carbonate and from sodium monoxide were made. Heat capacity data for sodium oxide were taken from the thesis of Grimley[5] and for sodium carbonate, data were taken from Popov and Ginzberg.[6] Entropies were calculated from these enthalpy data using the method of Kelley.[7]

Equations for the entropy and enthalpy differences for sodium peroxide as a function of temperature have been derived by the method of Shomate[8] to fit the experimental data with an uncertainty of ±1% between 298.15 and 869° K., if the heat of transition is included for temperatures above 783°K.

(1) Presented before the 134th meeting of the American Chemical Society, Chicago, Illinois, September 8, 1958.

(2) S. S. Todd, *J. Am. Chem. Soc.*, **75**, 1229 (1953).

(3) A. M. Vedeneev and S. M. Shuratov, *Zhur. Fiz. Khim.*, **25**, 837 (1951).

(4) J. C. Southard, *J. Am. Chem. Soc.*, **63**, 3142 (1941).

(5) R. T. Grimley, Ph.D. Thesis, University of Wisconsin, 1958.

(6) M. M. Popov and D. M. Ginzberg, *J. Gen. Chem.* (*U.S.S.R.*), **26**, 1103 (1956).

(7) K. K. Kelley, Bulletin No. 476, U. S. Bureau of Mines, 1949.

(8) C. H. Shomate, THIS JOURNAL, **58**, 368 (1954).

$H_T - H_{298.15} = 16.7T + 7.8 \times 10^{-3} T^2 - 5642$ cal. mole^{-1}

$S_T - S_{298.15} = 38.5 \log (T/298.15) + 15.6 \times 10^{-3} (T - 298.15)$ e.u.

$C_p = 16.7 + 15.6 \times 10^{-3}) T$, cal. mole^{-1} degree^{-1}

TABLE I

EXPERIMENTAL VALUES OF ENTHALPIES, ENTROPIES AND FREE ENERGY FUNCTIONS FOR Na_2O_2

Temp., °K.	$(H^0_T - H^0_{298})$, cal. mole^{-1}	$(S^0_T - S^0_{298})$, cal. mole^{-1} deg.$^{-1}$	$-(F^0_T - H^0_{298})/T$, cal. mole^{-1} deg.$^{-1}$
375.4	1712	5.01	23.10
472.9	4021	10.46	24.61
573.3	6525	15.27	26.54
672.9	9184	19.52	28.52
722.3	10527	21.43	29.51
739.6	10890	21.91	29.84
769.5	11733	23.04	30.44
794.0	13747	25.62	30.96
822.2	14640	26.70	31.54
869.2	15803	28.07	32.54

A discontinuity was observed in the heat content between 773 and 793°K. indicating some kind of transition. Rode and Gol'der[9] suggested that sodium peroxide melts at 510° based on differential thermal analysis. The transition was observed to be reversible. The heat of transition (1280 cal./mole) calculated from the experimental results seems too small to be the heat of fusion. The capsule was opened inside a dry box after it had been heated to 869°K. and no apparent melting of the sample was found.

(9) T. V. Rode and G. A. Gol'der, *Izvest. Akad. Nauk S.S.R. Otdel. Khim. Nauk*, **3**, 299 (1956).

TABLE II

ENTHALPIES, ENTROPIES AND FREE ENERGY FUNCTIONS FOR Na_2O_2 (COMPUTED FROM ENTHALPY EQUATION)

Temp., °K.	$(H^0_T - H^0_{298})$, cal. mole^{-1}	S^0_T,[a] cal. mole^{-1} deg.$^{-1}$	$-(F^0_T - H^0_{298})/T$ (Table II),[a] cal. mole^{-1} deg.$^{-1}$
298.15	0	22.65	22.65
400	2286	29.16	23.44
500	4658	34.43	25.11
600	7186	39.05	27.07
700	9870	43.17	29.07
800	13990	48.63	31.14
869	16040	51.03	32.57

[a] $S^0_{298.15} = 22.65$, taken from ref. 2.

A solid–solid transition has been reported by Föppl from X-ray studies of Na_2O_2.[10] Recent high temperature X-ray studies by Tallman and Margrave[11] have established a crystal transition at 510 ± 10°.

Acknowledgment.—The authors wish to acknowledge the support of the Callery Chemical Company, the U. S. Air Force, and the Wisconsin Alumni Research Foundation for high temperature calorimetric studies. The Na_2O_2 was generously provided by Dr. A. S. Bjornson of the Niagara Falls Laboratory of E. I. du Pont de Nemours and Company.

(10) H. Föppl, *Z. anorg. allgem. Chem.*, **291**, 12 (1957).

(11) R. L. Tallman and J. L. Margrave, unpublished work, University of Wisconsin, 1958.

THERMAL DIFFUSION IN METHANE–*n*-BUTANE MIXTURES IN THE CRITICAL REGION

BY W. M. RUTHERFORD AND J. G. ROOF

Shell Development Company, Exploration and Production Research Division, Houston, Texas

Received April 10, 1959

Thermal diffusion measurements have been made on the methane–*n*-butane system at two compositions, 0.40 and 0.49 mole fraction methane, in the pressure range from 1400 to 3000 lb./in.^{2}. These measurements have been carried out in a single-stage apparatus at temperatures of 115, 160, 190, 220 and 250°F. The experimental conditions fall in the liquid and critical regions of the mixture. The thermodynamics of irreversible processes predicts that, if the net heat of transport is essentially constant, the thermal diffusion factor α is inversely proportional to $x_1(\partial\mu_1/\partial\mu_1)$, where μ_1 is the chemical potential and x_1 is the mole fraction of component 1. In order to examine this relationship, values of $x_1(\partial\mu_1/\partial x_1)$ were calculated from the Benedict–Webb–Rubin equation of state. It was found that the experimentally determined values of α exhibited essentially the same dependence on temperature and pressure as the function $2000/x_1(\partial\mu_1\partial x_1)$, where the factor 2000 has units of cal./mole.

Introduction

Although the phenomenon of thermal diffusion has been known for many years, experimental data on compressed systems are meager. Precise thermal diffusion measurements for compressed hydrocarbon systems are of considerable theoretical interest, particularly near the critical state. Previous investigators have studied thermal diffusion in the critical region by means of the thermal diffusion column[1–4]; however, no binary hydrocarbon pairs have been studied.

This paper presents the results of thermal diffusion measurements on the methane–*n*-butane system in the critical region. We have used steady-state thermodynamics to interpret the thermal diffusion behavior of this system, and we shall demonstrate the strong dependence of the thermal diffusion factor on the composition derivative of the chemical potential.

Phenomenological Theory

In this paper, we shall use the thermal diffusion

(1) N. C. Pierce, R. B. Duffield and H. G. Drickamer, *J. Chem. Phys.*, **18**, 950 (1950).

(2) E. B. Giller, R. B. Duffield and H. G. Drickamer, *ibid.*, **18**, 1027 (1950).

(3) W. L. Robb and H. G. Drickamer, *ibid.*, **18**, 1380 (1950).

(4) F. E. Caskey and H. G. Drickamer, *ibid.*, **21**, 153 (1953).

factor α as defined by the following equation for the mass flux of one component of a binary mixture subjected to a temperature gradient

$$J_1 = -D_{12}\frac{M_1\rho}{\bar{M}}\left(\text{grad } x_1 - \frac{\alpha x_1 x_2}{T}\text{grad } T\right) \quad (1)$$

where D_{12} is the ordinary diffusion coefficient, J_1 is the mass flux, ρ is the density, x_1 and x_2 are the mole fractions of components 1 and 2, and T is the absolute temperature. M_1 is the molecular weight of 1, and $\bar{M}$ is $x_1M_1 + x_2M_2$.

At the steady state ($J_1 = 0$), the above expression can be integrated to give

$$\alpha = \frac{\ln\left[(x_1/x_2)_h/(x_1/x_2)_c\right]}{\ln\left(T_h/T_c\right)} = \frac{\ln q_\infty}{\ln\left(T_h/T_c\right)} \quad (2)$$

where the subscripts h and c refer to the hot and cold boundaries, respectively, and q_∞ is the steady-state separation.

In the strictest sense, the above integration is valid only if α is independent of temperature and composition. It is easy to show, however, that extremely large temperature and composition coefficients are necessary to cause a significant error in values of the thermal diffusion factor calculated by means of equation 2.

Thermodynamic Theory

Ordinary thermodynamic methods are inadequate for the treatment of steady-state, non-equilibrium processes such as thermal diffusion. It is possible, however, to treat such phenomena by means of the thermodynamics of the steady state, the methods of which have been described by De Groot[5] and others.[6,7]

In steady-state thermodynamics, the assumption is made that fluxes of heat and matter are linearly related to thermodynamic forces. For instance, we may write the following flux equations for an n-component system subjected to a temperature gradient

$$\frac{J_i}{M_i} = \sum_{k=1}^{n} L_{ik}\mathbf{X}_k + L_{iu}\mathbf{X}_u \quad (3)$$

$$J_q = \sum_{k=1}^{n} L_{uk}\mathbf{X}_k + L_{uu}\mathbf{X}_u$$

J_i/M_i is the molecular flux of component i; J_q is the reduced heat flow, which is defined as the total heat flow less the enthalpy transported with the molecular flux. The $\mathbf{X}_k$ are the thermodynamic forces related to flow of matter in isothermal diffusion, and $\mathbf{X}_u$ is the force involved in heat conduction.

L_{ik}, L_{iu}, L_{uk} and L_{uu} are phenomenological coefficients which are related by the Onsager[8,9] reciprocal relations

$$L_{ik} = L_{ki},\ L_{iu} = L_{ui} \quad (4)$$

The forces must be chosen to satisfy the relationship

$$T\sigma = \sum_{i=1}^{n}\frac{J_i}{M_i}\cdot\mathbf{X}_i + J_q\cdot\mathbf{X}_u \quad (5)$$

where σ is the rate of entropy generation in the process, and T is the absolute temperature. For the case under discussion, these forces are

$$\mathbf{X}_k = -(\text{grad } \mu_k)_T \quad (6)$$

$$\mathbf{X}_u = -\frac{1}{T}\text{grad } T \quad (7)$$

where μ_k is the chemical potential of component k.

Equations 3, 4, 6 and 7 can be used in the manner outlined by De Groot[5] to arrive at the following expression for the thermal diffusion factor in a binary system

$$\alpha = \frac{-Q_1^{**}}{x_1(\partial\mu_1/\partial x_1)} \quad (8)$$

Q_1^{**}, the net heat of transport, is the heat transported at uniform temperature per mole of moving molecules of type 1 less the enthalpy transport. If different conventions are used for such quantities as the flux of matter or the flux of heat, somewhat different expressions for α result. Such expressions are equivalent and can be readily transformed to equation 8.

Apparatus and Procedure

Two types of single-stage apparatus are commonly used for experimental study of thermal diffusion in fluids. These are the open cell and the two-chamber cell. The open cell is the simpler type in principle. In such a cell, fluid is confined between two parallel surfaces, one hot and one cold, thereby achieving an essentially uniform temperature gradient. The resulting steady-state concentration gradient can be determined by removing successive layers of fluid for analysis or by optical means. Absolute values of the thermal diffusion factor can be determined for most systems from measurements with such a cell.

The two-chamber cell consists of two well-mixed reservoirs maintained at different temperatures and connected by a porous diaphragm or by a capillary tube. In this configuration, the diffusional processes take place in microscopic pores where convection is easily inhibited; in addition, the presence of the reservoirs permits easy removal of samples for analysis. A two-chamber cell is convenient for high-pressure operation; however, uncertainty as to the effective temperature difference in such a cell makes calibration necessary for best results.

In this investigation, thermal diffusion measurements were made in a two-chamber, magnetically stirred, thermal diffusion cell suitable for pressures to 8000 lb./in.^{2} and temperatures to 300°F. The cell was a small pressure vessel divided into two chambers by means of a porous diaphragm. The vessel, machined from type 302 stainless steel, was 3.75 inches in outside diameter. The interior of the cell was 1.5 inches in length and had a diameter of 1.5 inches.

The cold chamber of the cell was attached to one of the vessel heads (Fig. 1). This chamber was formed by a Teflon cup with a stainless steel liner for internal support. A porcelain filter disk (Selas microporous porcelain No. 02) which served as the diaphragm was held against the open end of the cup by a stainless steel sleeve screwed onto the vessel head. The remainder of the vessel was the hot chamber.

Each chamber contained a small, magnetically operated, iron stirrer for the purpose of maintaining uniform temperature and composition. A sample tube and a mercury inlet were provided on each side. These were made from stainless steel hypodermic tubing, 0.032-inch o.d. by 0.020-inch i.d., introduced through the heads of the cell and sealed with steel ferrules.

The thermocouple wells were hypodermic tubing welded shut at one end and sealed into the head in the same manner as the other tubes. The iron–constantan thermocouples were made of No. 36 B & S gauge wire with soldered junctions. Testing of these thermocouples indicated that the temperature-sensitive area was confined to a region extend-

(5) S. R. de Groot, "Thermodynamics of Irreversible Processes," Interscience Publishers, New York, N. Y., 1951.

(6) K. G. Denbigh, "The Thermodynamics of the Steady State," John Wiley and Sons, New York, N. Y., 1951.

(7) I. Prigogine, Thesis, L'Universite Libre de Bruxelles, 1947.

(8) L. Onsager, *Phys. Rev.*, **37**, 405 (1931).

(9) L. Onsager, *ibid.*, **38**, 2265 (1931).

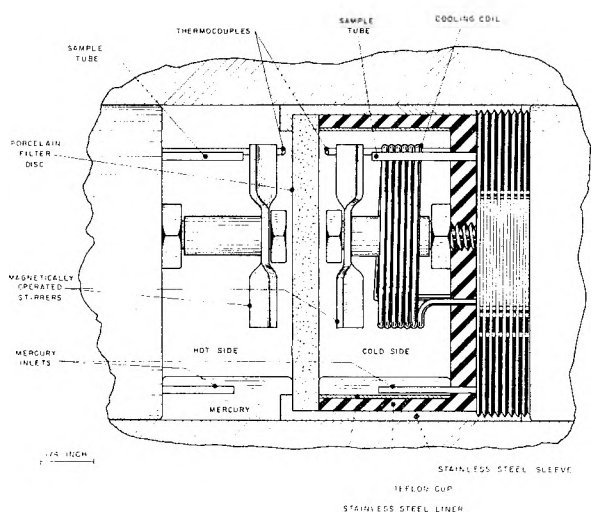

Fig. 1.—Details of the thermal diffusion cell.

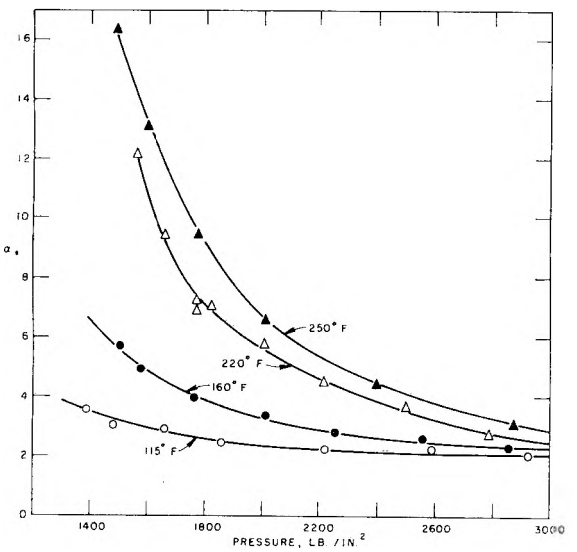

Fig. 2.—Thermal diffusion factor in the methane–*n*-butane system at 0.40 mole fraction methane.

ing not more than 3 to 4 mm. from the tip. E.m.f. of the thermocouples was measured on a Rubicon potentiometer to ±1 microvolt relative to a 0.00° cold junction. The thermocouples were calibrated against ASTM thermometers.

A temperature difference between the chambers was created by circulating liquid through a coil of hypodermic tubing placed in the cold chamber. The inlet tube to the coil was brought through the vessel head and sealed with a Teflon and textolite gland to minimize heat transfer from the head to the tube. The outlet tube was brought through and sealed with a steel ferrule. An oil-bath was provided to regulate the temperature of the pressurized water which was used as a coolant.

Direct cooling of one chamber is superior to electrical heating when mixtures are being studied near the two-phase boundary, since the hot-side temperature cannot go above the ambient temperature of the cell. Heat input, furthermore, is through the relatively large wall area of the hot chamber, and the wall temperature is fairly close to the bulk fluid temperature, thereby minimizing the risk of forming two phases.

The cell was mounted horizontally in a constant-temperature air-bath in such a position that a magnetron magnet could be rotated around it to activate the internal stirrers. Sample and mercury lines from the cell were connected through a system of valves to the various facilities for filling, mercury injection, analysis and pressure measurement.

Pressure in the cell was measured by means of a 0- to 3000-lb./in.² Heise bourdon gauge connected to the mercury line. This gauge was calibrated periodically against a deadweight gauge and was readable to ±1 lb./in.²

A Zeiss gas interferometer with a 25-cm. path length was used to determine the composition differences between samples taken from the hot and cold chambers of the cell. The interferometer was used in conjunction with a system for handling the gas samples. With the 25-cm. chambers, the interferometer had a range of about 20 mole % in the methane–*n*-butane system at atmospheric pressure. Precision of the measurement of the difference in composition was approximately 0.02 mole %, based on experience with the instrument.

Operation of the cell was started by filling the cell with the fluid mixture (methane–*n*-butane), checking the concentration and bringing the coolant and air-baths to the proper temperatures. When the cooling fluid was admitted to the cell, the temperature difference of 10 to 20°F. was created almost immediately; and after the pressure was set by adding or removing mercury, a run was considered to have begun. After an experiment had run for sufficient time to reach the steady state within the required accuracy (usually 1 to 3 days), the sample lines were purged and samples were displaced at constant pressure from first one chamber and then the other by injecting mercury into the bottom of the chamber being sampled. As the samples were displaced, they were flashed through sampling valves into the corresponding evacuated chambers of the interferometer, where the difference in refractive index, and hence the difference in composition, was read directly. Duplicate samples were always taken, and the order of sampling was reversed for the second analysis to average any error arising from the sequence of sampling.

Although the amount of mercury that entered each chamber during the course of an analysis was small (about 2 ml.) in relation to the cell volume of about 30 ml., there were indications that the presence of too much mercury distorted the cell temperature distribution. Thus, to prepare the apparatus for the next run, it was necessary to displace the injected mercury with some of the starting mixture.

Since a partial separation existed in the cell following a run, subsequent runs could be of much shorter duration. No run, however, was allowed to proceed for less than 24 hours.

The methane–*n*-butane mixtures used in this investigation were made up volumetrically from Phillips research grade hydrocarbons. The methane was certified to contain not more than 0.005 mole fraction impurities, and the *n*-butane was certified to contain not more than 0.001 mole fraction impurities.

Phillips pure grade *n*-heptane (0.99 mole fraction *n*-heptane) and *n*-propyl iodide (BP 100-102°) from Matheson, Coleman and Bell Inc. were used to prepare the calibration mixtures. All chemicals were used as received.

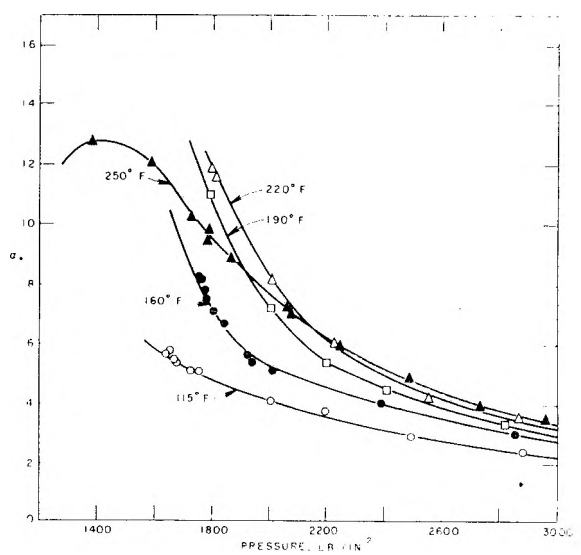

Fig. 3.—Thermal diffusion factor in the methane–*n*-butane system at 0.49 mole fraction methane.

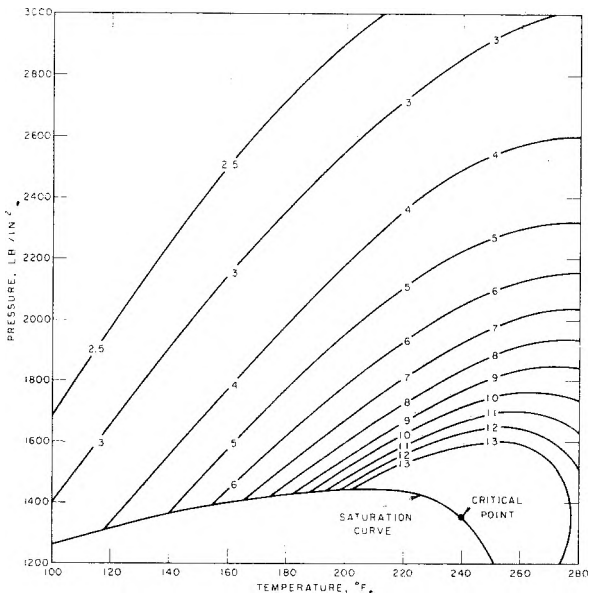

Fig. 4.—Lines of constant α in the methane–*n*-butane system at 0.40 mole fraction methane.

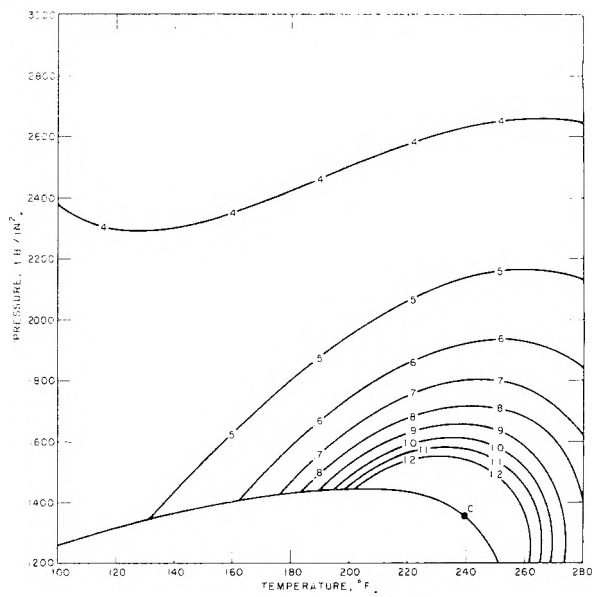

Fig. 5.—Lines of constant $2000/x_1(\partial\mu_1/\partial x_1)$ in the methane–*n*-butane system at 0.40 mole fraction methane.

TABLE I

THERMAL DIFFUSION FACTORS IN THE METHANE–*n*-BUTANE SYSTEM AT 0.40 MOLE FRACTION METHANE

Mean temp., °F.	Pressure, lb./in.²	Thermal diffusion factor, α
115.3	1385	3.56
114.9	1480	3.06
115.2	1659	2.92
114.7	1855	2.47
114.3	2218	2.24
115.5	2590	2.24
115.7	2925	2.06
160.5	1503	5.70
160.7	1575	4.96
160.9	1760	3.98
160.5	2010	3.38
160.6	2253	2.82
160.7	2558	2.60
161.1	2855	2.30
220.3	1560	12.19
220.5	1657	9.43
220.6	1767	6.95
219.8	1769	7.26
220.2	1820	7.07
220.3	2002	5.78
220.5	2215	4.49
220.7	2500	3.67
220.0	2790	2.76
249.7	1485	16.33
250.0	1592	13.11
249.9	1775	9.45
250.5	2007	6.62
250.4	2393	4.45
250.6	2872	3.12

Results

The thermal diffusion cell was calibrated with an equimolar mixture of *n*-propyl iodide and *n*-heptane; this mixture has been run on an absolute basis in an open cell by Drickamer and co-workers.[10] The thermal diffusion factor α for this system, as measured in our apparatus, was 2.0 ± 0.1 at 150 lb./in.² and 112°F.[11] This is to be compared to the value of 2.3 ± 0.1 at atmospheric pressure and 80°F. reported by Drickamer. Since the effect of temperature is small and the effect of pressure is negligible for this system, it appears that the results obtained with this cell are about 15% low. This is very satisfactory agreement for comparison between measurements made with a two-chamber cell and measurements made with an open cell.

After calibration, measurements of the thermal diffusion factor were made on the methane–*n*-butane system at two compositions, 0.40 and 0.49 mole fraction methane, in the pressure range from 1400 to 3000 lb./in.² These measurements were carried out at temperatures of 115, 160, 220 and 250°F. An additional isotherm at 190°F. was included in the measurements at 0.49 mole fraction methane.

The results[12] of these experiments are presented in Tables I and II and are plotted in Fig. 2 and 3. The values of α reported here are the experimental values calculated according to equation 2 and multiplied by 1.15 to account for the instrument error indicated by the calibration.

Because of the necessity of avoiding conditions which could create two phases at any point in the cell, a minimum experimental pressure existed for given values of temperature and composition. The presence of temperature and concentration gradients in the apparatus required that this pressure be somewhat above the saturation pressure at average cell conditions.

Reproducibility of the experimental values of α is very good, considering the small separations involved in a single-stage apparatus. An uncertainty

(10) E. L. Dougherty and H. G. Drickamer, THIS JOURNAL, **59**, 443 (1955).

(11) α is defined as positive when *n*-heptane concentrates at the hot wall.

(12) α is defined as positive when methane concentrates at the hot wall.

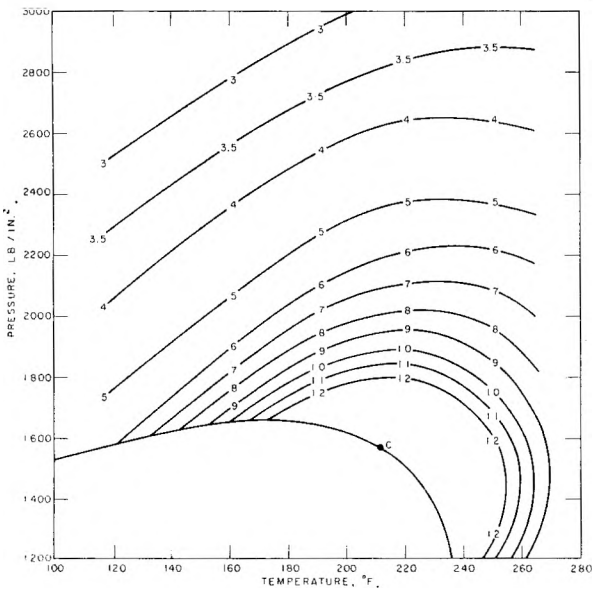

Fig. 6.—Lines of constant α in the methane–n-butane system at 0.49 mole fraction methane.

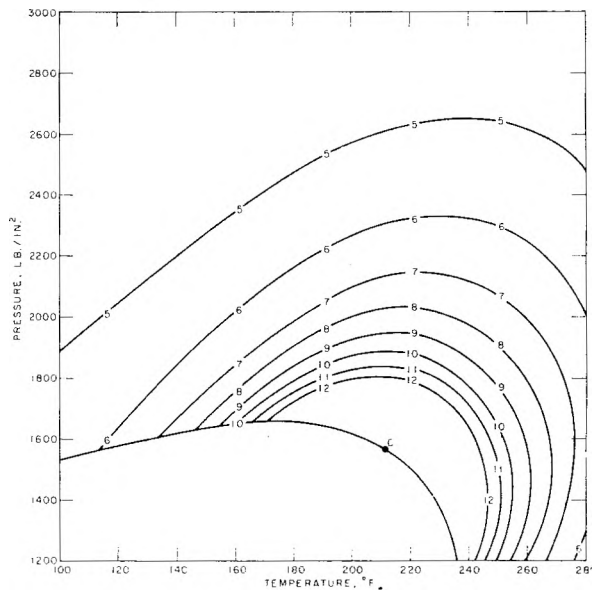

Fig. 7.—Lines of constant $2000/x_1(\partial\mu_1/\partial x_1)$ in the methane–n-butane system at 0.49 mole fraction methane.

TABLE II

THERMAL DIFFUSION FACTORS IN THE METHANE–n-BUTANE SYSTEM AT 0.49 MOLE FRACTION METHANE

Mean temp., °F.	Pressure, lb./in.²	Thermal diffusion factor, α
114.6	1640	5.60
114.3	1653	5.70
112.9	1670	5.41
114.1	1677	5.35
116.1	1725	5.06
116.4	1728	5.06
115.1	1754	5.03
114.8	2007	4.05
114.8	2198	3.69
115.1	2495	2.83
115.5	2880	2.31
158.9	1754	8.23
160.9	1767	8.19
160.6	1775	7.79
160.7	1780	7.49
158.7	1805	7.07
160.1	1845	6.63
160.9	1925	5.57
161.3	1940	5.32
159.7	2010	5.06
161.3	2390	3.98
160.5	2855	2.96
190.2	1789	10.97
190.4	2005	7.12
190.4	2200	5.37
190.4	2410	4.44
190.5	2820	3.22
219.3	1795	11.91
218.6	1810	11.64
221.6	2005	8.14
220.7	2225	5.96
221.5	2552	4.16
220.5	2865	3.47
249.1	1380	12.79
249.1	1588	12.10
249.8	1725	10.25
250.4	1780	9.45
250.2	1785	9.83
249.4	1862	8.88
250.2	2060	7.21
250.6	2075	7.05
249.0	2238	5.92
248.8	2486	4.86
248.8	2731	3.88
249.0	2955	3.42

in the absolute values of α is present because of inherent limitations in the calibration method.

Discussion

When the experimental data of the preceding section are presented as lines of constant α on a pressure–temperature plot (Fig. 4 and 6), it is quite evident that the most significant feature of the data is the rapid increase of α in the neighborhood of the critical point. This behavior is easily analyzed by means of equation 8. At the critical point (or at the critical solution temperature of a liquid mixture), the factor $x_1(\partial\mu_1/\partial x_1)$ goes to zero. Since the net heat of transport Q^{**} can be expected to retain a non-zero value, it is evident that the thermal diffusion factor becomes infinitely large as the critical point is approached. Such behavior for liquid mixtures near the critical solution temperature has been described by Thomaes[13] and by Tichacek and Drickamer.[14]

The Benedict–Webb–Rubin empirical equation for the fugacity of one component in a binary system can be differentiated to give an internally self-consistent set of values of $\partial\mu_1/\partial x_1$ for the methane–butane system.[15,16] (Partial volumetric data

(13) G. Thomaes, *J. Chem. Phys.*, **25**, 32 (1956).

(14) L. J. Tichacek and H. G. Drickamer, THIS JOURNAL, **60**, 820 (1956).

(15) M. Benedict, G. B. Webb and L. C. Rubin, *J. Chem. Phys.*, **10**, 747 (1942).

(16) M. Benedict, G. B. Webb and L. C. Rubin, *ibid.*, **8**, 334 (1940).

exist for this system,[17] from which $\partial\mu_1/\partial x_1$ can be calculated; however, the precision proved not good enough to give consistent values.) Such values have been calculated with the assistance of an electronic digital computer. Figures 5 and 7 show lines of constant $2000/x_1(\partial\mu_1/\partial x_1)$ on pressure-temperature plots for the two mixtures. (The factor 2000 has units of cal./mole.) Choice of the factor 2000, which corresponds to $-Q_1^{**}$ in equation 8, is rather arbitrary. This number was chosen to give reasonable correspondence with the experimental values of α. Neither the accuracy of the calculated $x_1(\partial\mu_1/\partial x_1)$ values nor the assumption of constancy of Q_1^{**} was sufficiently good to justify intensive efforts to arrive at the best possible value of that quantity.

From examination of Fig. 2 through 7, however, it is readily apparent that the function $2000/x_1 \cdot (\partial\mu_1/\partial x_1)$ duplicates every qualitative feature of the thermal diffusion data at both compositions. The quantitative differences between this function and the experimental values of the thermal diffusion factor could easily be the result of variations in Q_1^{**}, the net heat of transport, and of inaccuracies in the calculated values of $x_1(\partial\mu_1/\partial x_1)$.

(17) B. H. Sage and W. N. Lacey, "Thermodynamic Properties of the Lighter Paraffin Hydrocarbons and Nitrogen," Amer. Petroleum Inst., New York, N. Y., 1950.

SALTING-OUT CHROMATOGRAPHY. V. SPECIAL RESINS

By Gloria D. Manalo, A. Breyer, Joseph Sherma and Wm. Rieman III

Ralph G. Wright Chemical Laboratory, Rutgers, The State University, New Brunswick, New Jersey

Received April 14, 1959

Partly sulfonated, crosslinked polymers of styrene absorb organic non-electrolytes from aqueous solutions more tenaciously than do the fully sulfonated cation-exchange resins. Similarly, anion-exchange resins with less than the usual amount of quaternary ammonium groups generally absorb organic non-electrolytes more tenaciously than the usual anion exchangers. Resins with quaternary ammonium groups containing ethyl, propyl and butyl groups in place of the usual N-methyl groups were also studied.

Salting-out chromatography is the separation of water-soluble organic non-electrolytes by elution through ion-exchange resins with aqueous salt solutions as the eluents. The best resins for this purpose are the sulfonated crosslinked polystyrene (a strong-acid cation exchanger) and the analogous polymer with the $-CH_2N(CH_3)_3^+$ group in place of the sulfonate group (a strong-base anion exchanger). The use of an aqueous solution of an appropriate salt as eluent makes the separation much more efficient than when water is used as the eluent. This has been demonstrated in the separation of alcohols,[1,2] amines,[3] ethers[4] and carbonyl compounds.[5]

This paper reports an investigation of the behavior of unusual ion-exchange resins as the stationary phase in the elutions of organic non-electrolytes with water and aqueous salt solutions as eluents. The resins were (1) partly sulfonated or partly quaternized crosslinked polystyrenes, *i.e.*, cation- and anion-exchange resins of less than the usual exchange capacity, and (2) anion-exchange resins containing three ethyl, *n*-propyl or *n*-butyl groups attached to the nitrogen atom instead of the usual methyl groups.

Experimental

Resins and Reagents.—The special resins were prepared for this study by The Dow Chemical Company. They were crosslinked with nominal 8% divinylbenzene. The sulfonate groups of the cation exchangers and the quaternary nitrogen groups of the anion exchangers were randomly distributed among the benzene rings of the resin. The mesh size, except where noted, was 200 to 400. Except for the low capacity and the change in the N-alkyl groups, these resins are analogous to Dowex 50-X8 and Dowex 1-X8.

All common reagents were of the best grade available and did not require further purification.

The exchange capacities of the resins were determined as follows: chromatographic tubes of internal cross-sectional area of 3.90 cm.^{2} were filled to depths of 10 to 15 cm. with the resin, either HR or RCl. Sodium chloride (for HR) or nitrate (for RCl), about 1 *M*, was passed through the column at a rate of about 0.8 cm. per minute until the hydrogen or chloride ions, respectively, were completely displaced. For resins of capacity of 2 meq. per g. or more, one liter or less sufficed; but larger volumes, sometimes up to 4 liters, were required for the resins of lower capacity because of the slow exchange rate. The hydrogen or chloride ion was determined in an aliquot of each effluent by titration with sodium hydroxide or silver nitrate to find the total exchange capacity of the column. Then the resins were converted, still in the column, to their original forms; and the determination was repeated. Finally, the resins were reconverted to the original forms, rinsed free of interstitial electrolytes, removed from the columns, dried to constant weight at 62° under vacuum (10 to 12 hours) and weighed.

The interstitial volumes of the resin columns were determined with polyphosphate (for the cation exchangers) and polysoap (for the anion exchangers) as described elsewhere.[6]

Elutions.—Samples of 0.05 to 0.1 mmole of alcohol or ketone were eluted through resin columns, about 20 cm. in length and 3.9 cm.^{2} in cross-sectional area, with water or standard solutions of ammonium sulfate as eluents. The resins were in the ammonium or sulfate form. Small fractions of the eluate were collected; the organic compound in each was determined as previously described.[5,7,8] Elution graphs were plotted from these data. The distribution ratio *C*, defined as the quantity of organic solute in the resin of any plate divided by the quantity in the interstitial solution of the same plate at equilibrium, was calculated from the equation[9]

(1) R. Sargent and W. Rieman, *J. Org. Chem.*, **21**, 594 (1956).
(2) R. Sargent and W. Rieman, This Journal, **61**, 354 (1957).
(3) R. Sargent and W. Rieman, *Anal. Chim. Acta*, **17**, 408 (1957).
(4) R. Sargent and W. Rieman, *ibid.*, **18**, 197 (1958).
(5) A. Breyer and W. Rieman, *ibid.*, **18**, 204 (1958).
(6) G. D. Manalo, R. Turse and W. Rieman, *ibid.*, in press.
(7) R. Sargent and W. Rieman, *ibid.*, **14**, 381 (1956).
(8) R. Sargent and W. Rieman, This Journal, **60**, 1370 (1956).
(9) W. Rieman and R. Sargent, "Ion Exchange" in "Physical Methods of Chemical Analysis," Vol. IV, edited by W. G. Berl, Academic Press, New York, N. Y., 1959, in press.

TABLE I

PROPERTIES OF LOW-CAPACITY RESINS

Capacity,[b] meq./g.	G. H_2O / g. dry resin[b]	Rel. interstitial vol.	Glycerol C_0	Glycerol k	Ethylene glycol C_0	Ethylene glycol k	Methanol C_0	Methanol k	Propanone C_0	Propanone k	Butanone C_0	Butanone k	Pentanone-2 C_0	Pentanone-2 k
Cation-exchange resins														
5.2	1.09	0.36	0.52	0.12	0.69	0.13	0.80	0.15	1.0	0.31	1.4	0.40	2.0	0.48
3.02	0.85	.38	.64	.11	.83	.13	.98	.16	2.9	.32	7.1	.37	20	
2.03	.56	.36	.54	.12	.74	.14	1.0	.16	4.7		21		31	
0.76	.32	.37	[a]		[a]		0.68	.18	4.2		19		30	
.56	.30	.39	[a]		[a]		.65		4.0		16		28	
.38	.21	.39	[a]		[a]		[a]		1.9		7.1			
.32	.19	.38	[a]		[a]		[a]		0.92		1.4		2.8	
.03	.20	.39	[a]		[a]		[a]		1.4		6.2			
.00	.00		[a]		[a]		[a]		0.37		0.26		0.26	
Anion-exchange resins														
3.55	0.82	0.41	0.34	0.14	0.55	0.13	0.56	0.16	0.69	0.32	1.3	0.40	2.5	0.45
2.35[c]	.72	.49	[a]		.35	.13	.49	.15	1.1	.29	2.0	.37	4.5	.42
1.15	.34	.37	[a]		.39	.17	.65	.17	1.8	.33	5.4	.39	17	.52

[a] Too small for measurement. [b] Determined on the hydrogen and chloride forms. [c] 100–200 mesh.

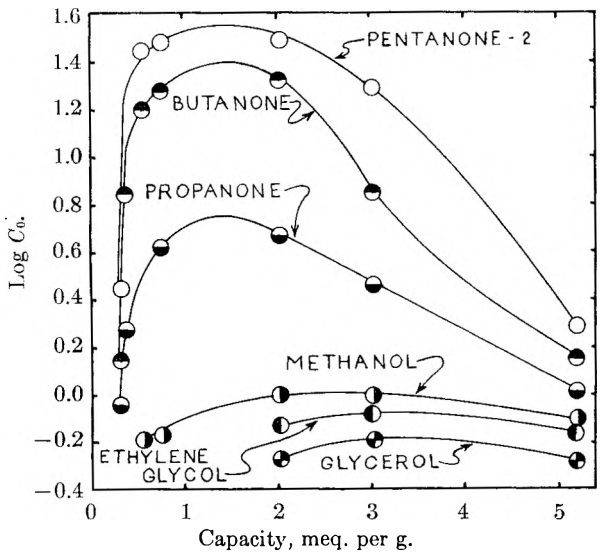

Fig. 1.—Effect of the capacity of sulfonated polystyrenes on the distribution ratios of organic solutes.

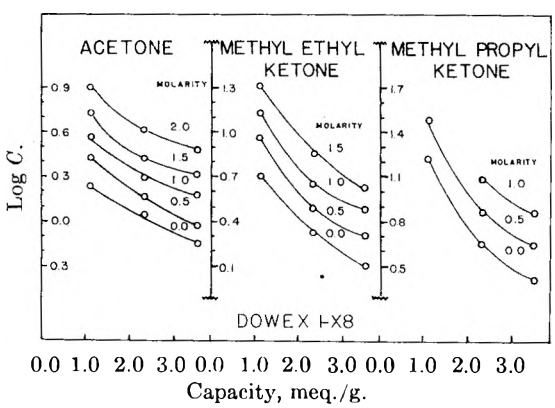

Fig. 2.—Effect of the capacity of anion-exchange resins and of the concentration of ammonium sulfate eluent on the distribution ratios C of three ketones.

$$U^* = CV + V \qquad (1)$$

where U^* is the volume of effluent collected at the peak of the elution graph and V is the interstitial volume of the column.

Results and Discussion

Resins of Low Capacity.—Columns 1 and 2 of Table I reveal a marked decrease in the absorption of water as the capacity of the cation exchangers is decreased. On the other hand, the interstitial volume of these resins is constant within the experimental error. The anion exchangers also exhibit a decrease in water absorption with decreasing capacity. The relative interstitial volume of the anion-exchange resin of capacity 2.35 is surprisingly large.

For any given resin and organic solute, plots of log C *vs.* M, the molarity of the ammonium sulfate, are linear, as has been observed with resins of normal capacity.[2,4,5] From such plots the parameters of eq. 2 were evaluated. C_0 denotes the distribution ratio with water as eluent. Table I reveals that k is almost constant from one resin to another. This is also true of the usual resins with 8% or more of divinylbenzene.[2,4,5]

$$\log C = \log C_0 + kM \qquad (2)$$

On the other hand, the data indicate that the following relationships exist between the values of C_0 and the capacity.

(1) Decreases in the capacity of the cation-exchange resins below the usual value cause the C_0 values to rise to a maximum and then fall (Fig. 1). There is some evidence (Table I) that further decreases in the capacity from 0.3 meq. per g. to zero cause another rise in the value of C_0. However, this may be due to the very large experimental difficulties encountered with resins of very low capacity (see below).

(2) Decreases in the capacity of anion-exchange resins from the usual value of 3.55 to 1.15 also cause an increase in the C values of the ketones, both with water and with solutions of ammonium sulfate as eluents (Fig. 2).

(3) The position of the maximum on the abscissa is influenced by the nature of the organic solute; the very hydrophylic compounds give maxima at larger capacities than do the less hydrophilic solutes.

(4) The nature of the organic compound in-

TABLE II

PROPERTIES OF ANION-EXCHANGE RESINS WITH VARIOUS *n*-ALKYL GROUPS

N-Alkyl group	Capacity, meq./g.	% quaternization	V/V_b	Values of C_0 of organic compounds Glycerol	Ethylene glycol	Methanol	Butanone	Pentanone-2
CH_3	3.55	61	0.41	0.34	0.55	0.56	1.3	2.5
C_2H_5	2.45	43	.39	.54	.67	.88	1.8	3.5
n-C_3H_7	1.59	27	.42	.35	.43	.66	2.3	5.4
n-C_4H_9	1.52	27	.43	.31	.39	.63	2.8	8.4

fluences markedly the magnitude of the rise of log C_0 on decreasing the capacity. The rise for pentanone is almost double that for the more hydrophilic acetone. The very hydrophilic alcobols give very flat maxima on the cation exchangers; on the anion exchangers, they reverse the usual trend and exhibit minima.

(5) In general, the difference in log C_0 values for any two organic compounds is greater for cation exchangers of low capacities than for the fully sulfonated resins. Since this Δ log C_0 is a measure of the separability, the partly sulfonated resins seem to be better for this purpose than the usual resins. The same can be said of the anion exchangers except for the most hydrophilic compounds.

Another consideration, however, limits the usefulness of low-capacity resins in separations. The decrease in capacity entails decreased imbibition of water (swelling) and hence restricts the diffusion of solutes within the resin. This in turn retards the approach toward sorption equilibrium and may cause tailing graphs. With flow rates of 0.4 cm. per minute, the organic solutes studied in this investigation yielded symmetrical graphs with resins of capacity greater than 2 meq. per g.

The factors that favor the sorption by an ion-exchange resin of an organic compound from aqueous solution are the following[10]: (1) the simple dissolution of the organic compound in the internal solution of the resin, (2) van der Waals forces of attraction between the hydrocarbon part of the solute and the hydrocarbon part of the resin, and (3) attraction of the fixed and counterions of the resin for the dipoles of the organic solute. Since the fixed and counterions of the resin are essentially dissolved in the internal water, they also exert a salting-out effect on the organic compound, tending to diminish the sorption.

As the capacity is decreased from the usual value, the first and third of the foregoing factors are diminished, whereas the second is increased. The interplay of these factors gives rise to the maximum. With the first decreases in capacity, the increase in the van der Waals forces overbalances the decrease in the other two; this is especially true of the more hydrophobic organic solutes. With further decreases in capacity, the paucity of water inside the resin is probably the major cause of the decrease in sorption. In addition, the diffusion of the solute into the shrunken resin is hampered so that adsorption on the surface of the resin beads eventually becomes the major type of sorption. Since the specific surface is small, adsorption can occur to only a very limited extent.

Anion-exchange Resins with Various N-Alkyl Groups.—The data for these resins are summarized in Table II. The salting-out constants k checked the values in Table I within the experimental error and are not recorded in Table II.

The decrease in capacity with increasing weight of the alkyl group is due not only to the increasing weight of the monomeric unit but also to the generally lesser quaternization of the product. The percentages quaternized were calculated on the assumptions[11] (1) that these special resins were prepared by the quaternization of chloromethylated polystyrene resin in which the chloromethyl groups were attached to 61% of the benzene rings and (2) that those chloromethyl groups which were not quaternized were converted to hydroxymethyl groups. The following equations[12] relating the capacity of the resins with the fractional quaternization were derived for the resins with N-ethyl, N-propyl and N-butyl groups, respectively.

$$Q = 1000F/[106 \times 0.39 + 136(0.61 - F) + 256F]$$
$$Q = 1000F/[106 \times 0.39 + 136(0.61 - F) + 298F]$$
$$Q = 1000F/[106 \times 0.39 + 136(0.61 - F) + 340F]$$

Q denotes the exchange capacity of the resin in milliequivalents per g.; F denotes the fraction of benzene rings quaternized; 106, 136, 256, 298 and 340 are the molecular weights of the average hydrocarbon monomer, the monomer with $-CH_2OH$, and those with triethyl-, tri-n-propyl- and tri-n-butylammonium groups, respectively.

The relative interstitial volumes, determined with polysoap,[6] are constant within the experimental error.

The C_0 values of the more hydrophilic solutes (the alcohols) rise with the change from N-methyl to N-ethyl and then fall as the N-alkyl group is further increased in size. With the more hydrophobic solutes (the ketones), the rise in C_0 is steady with the increase in the size of the N-alkyl group, at least within the range studied.

A better interpretation of the effect of the N-alkyl group is obtained by comparing the C_0 values of the special resins with those of low-capacity Dowex 1-X8 with the same percentage quaternization. This is shown in Table III. Here Q^* denotes the capacity of Dowex 1-X8 with the same percentage quaternization as the respective special resin. C_0^* is the C_0 of the organic compound on the low-capacity Dowex 1-X8 (read from graphs similar to those of Fig. 1).

From this table, it is seen that the substitution of higher alkyl groups for the methyl group of low-capacity Dowex 1-X8 causes first a rise in the value of C_0/C_0^* and then a decrease in the case of the

(10) D. Reichenberg and W. F. Wall, *J. Chem. Soc.*, 3364 (1956).

(11) R. E. Anderson, private communication.

(12) Analogous equations have been derived by A. Breyer, thesis, Rutgers, The State University, New Brunswick, N. J., 1958.

TABLE III

COMPARISON OF C_0 VALUES OF N-ALKYL RESINS WITH THOSE OF DOWEX 1-X8 OF THE SAME PERCENTAGE QUATERNIZATION

N-Alkyl group	% quaternized	Q^*	Ethylene glycol C_0^*	Ethylene glycol C_0/C_0^*	Methanol C_0^*	Methanol C_0/C_0^*	Butanone C_0^*	Butanone C_0/C_0^*	Pentanone-2 C_0^*	Pentanone-2 C_0/C_0^*
CH_3	61	3.55	0.55	1.0	0.56	1.0	1.3	1.0	2 5	1.0
C_2H_5	43	2.83	.42	1.6	.51	1.7	1.6	1.1	3 3	1.1
n-C_3H_7	27	2.00	.33	1.3	.49	1.3	2.4	0.96	5.7	0.95
n-C_4H_9	27	2.00	.33	1.2	.49	1.3	2.4	1.2	5.7	1.5

hydrophilic alcohols. With the less hydrophilic pentanone, the value of C_0/C_0^* rises somewhat erratically with increasing size of the N-alkyl. This is probably due to the greater van der Waals forces with the resins of large N-alkyl groups.

Acknowledgments.—The authors express their gratitude to The Dow Chemical Company for generous financial support of this investigation and for the preparation of the special resins. The receipt from U. P. Strauss of the polysoap used in the determination of the interstitial volumes is also gratefully acknowledged.

THE RATE OF REACTION OF HYDROGEN WITH THORIUM[1]

BY D. T. PETERSON AND D. G. WESTLAKE

Institute for Atomic Research and Department of Chemistry, Iowa State College, Ames, Iowa

Received April 22, 1959

The reaction between thorium and hydrogen, which produced a surface layer of thorium dihydride, was shown to follow the parabolic rate law. At pressures slightly greater than the dissociation pressure of the dihydride, the absorption rate was very dependent on the pressure, but at higher pressures the pressure dependency was less pronounced. Increasing the temperature accentuated the pressure dependency of the absorption rate at the higher pressures. The temperature dependence of the absorption rate satisfied an Arrhenius type equation at temperatures below 550° when the pressure was held constant at 120 mm. The activation energy for diffusion was found to be about 19.6 kcal. The absorption rate was the same for annealed thorium of two purity levels and for cold-swaged thorium.

Introduction

Thorium reacts with hydrogen to form ThH_2 and Th_4H_{15}. These compounds are intermediates in one process for preparing thorium metal powder and may have some use in nuclear reactions. The formation of a thorium hydride phase seems to be involved in the corrosion of thorium by aqueous media. However, no systematic study of the rate of reaction of hydrogen with thorium has been reported.

The reaction between thorium and hydrogen would be governed by different rate-controlling processes depending on whether the hydrogen pressure was above or below the dissociation pressure of thorium dihydride. If the hydrogen pressure was above the dissociation pressure of the dihydride, the metal would acquire a dihydride layer through which the hydrogen must diffuse. If the dihydride layer were adherent and protective, the parabolic rate law would be expected. If the hydride layer were non-protective, a linear reaction rate would be observed. If the hydrogen pressure was below the dissociation pressure of the dihydride, absorption would occur by the solution of hydrogen in thorium and the rate would depend on diffusion into the metal if surface reactions were not rate controlling. In this investigation, the reaction rates were determined over a temperature range from 350 to 700° at pressures from slightly above the dissociation pressure of the dihydride up to 400 mm., but below the pressure range in which Th_4H_{15} is stable.

(1) Contribution No. 743. Work was performed in the Ames Laboratory of the U. S. Atomic Energy Commission.

Experimental

Thorium prepared by different methods and of two purity levels was used. The crystal bar thorium was prepared at the Ames Laboratory from calcium-reduced Ames thorium. Ames thorium was prepared by reducing ThF_4 with calcium. This metal was melted in a BeO crucible under vacuum and cast into a graphite mold. The analyses are shown in Table I. Carbon was determined by combustion and nitrogen by the Kjeldahl method. The oxygen in Ames thorium was determined by weighing the hydrochloric acid in soluble residue as thorium oxide, whereas the oxygen in the crystal bar thorium was determined by vacuum fusion. All other elements were determined spectrographically.

TABLE I

ANALYSIS OF THORIUM METAL

Element	Crystal bar Th, p.p.m.	Ames Th, p.p.m.
C	145	410
N	70	70
O	60	1300
Fe	20	130
Mn	..	20
Cr	20	20
Ni	20	20
Al	50	40
Ca	25	50
Mg	..	20
Si	..	55
Be	..	170
Hardness	35 Dph	69 Dph

The thorium was swaged into rods and vacuum annealed at 800° for one hour. Cylindrical specimens, approximately 6.5 mm. in diameter and 3.5 mm. long, were machined after the chuck and the cutting tool of the lathe had been cleaned with trichloro-ethylene. Immediately after the specimens had been washed in trichloroethylene and rinsed in acetone, they

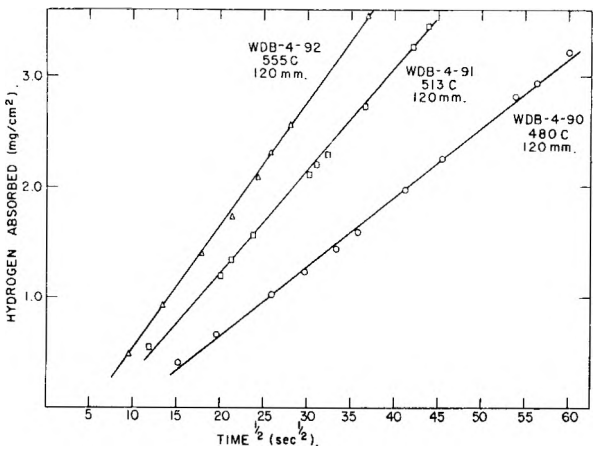

Fig. 1.—Amount of hydrogen absorbed *vs.* square root of time.

were inserted into the loading tree of the reaction apparatus.

The thorium samples were inserted into a furnace tube at constant temperature and under constant hydrogen pressure. The apparatus was evacuated with a mercury diffusion pump and degassed until a static vacuum of less than 1 $\times 10^{-5}$ mm. was maintained after the stopcock to the diffusion pump was closed. The furnace tube was enclosed in a stainless steel tube which was 10 cm. long. This provided a zone 7.5 cm. long in which the temperature was constant to within 2° and in which the sample was centered. The temperature was measured by a thermocouple between the stainless steel cylinder and the furnace tube.

The pressure in the system during degassing was measured with a cold cathode gauge. Purified hydrogen was generated by heating uranium hydride to about 400° and was stored in the pressure regulator. This device was a modification of that described by Belle, *et al.*,[2] and maintained a constant pressure of hydrogen in the sample tube. Hydrogen was allowed to enter the system to the desired pressure, and a specimen was pushed into the sample tube. The reaction rate was observed by measuring the quantity of hydrogen drawn from the pressure regulator at known times. Liquid nitrogen cold traps were used to prevent mercury from the manometer, diffusion pump and pressure regulator from reaching the furnace tube.

Results and Discussion

The absorption of hydrogen by thorium followed the parabolic rate law. Typical absorption curves are shown in Fig. 1. The failure of these curves to pass through the origin was due to the time required for the sample to reach the temperature of the furnace. No induction period was observed and the samples began to react with hydrogen as soon as they entered the furnace, but the constant parabolic rate was not obtained until the temperature of the sample reached the furnace temperature. The reaction rate was measured until between 10 and 30% of the thorium sample had reacted to form the dihydride. The reaction rate was not followed to completion since some deviation from the parabolic rate law would be expected when the thickness of the hydride layer became great enough to reduce significantly the thorium–thorium hydride interface area and change the gradient at the corners of the sample. However, this deviation would not be due to a change in the rate-controlling process.

The parabolic rate constant is related to the diffusion coefficient and the concentration gradient of hydrogen in the hydride layer. The parabolic rate law can be expressed as $m = kt^{1/2}$ where m = weight of H_2 absorbed per sq. cm. of surface, k = rate constant and t = time. The flux through the gas–solid interface, J, is dm/dt and if Fick's first law applies, $J = -D\,(\partial c/\partial x) = {}^1/_2\,kt^{-1/2}$. The concentration gradient in the direction of the flux is $-(C_s = C_i)/\Delta x = -\Delta C/\Delta x$ if the gradient is constant through the surface layer. C_s is the hydrogen concentration of the hydride at the gas–hydride surface, C_i is the hydrogen concentration at the metal–hydride interface and Δx is the thickness of the hydride layer. As nearly all of the hydrogen remained in the hydride phase, $\Delta x = Km$ where K is the volume of ThH_2 which contains one mg. of hydrogen. Consequently

$$\frac{\Delta C}{\Delta x} = \frac{\Delta C}{Kkt^{1/2}} \text{ and } -D\,\frac{\Delta C}{Kkt^{1/2}} = {}^1/_2kt^{-1/2}$$

Solving for the rate constant gives $k^2 = 2D\Delta C/K$.

The hydrogen pressure dependence of the reaction rate arises from the change in ΔC as the hydrogen concentration at the gas interface increases with pressure. At 550° and below, the reaction rate was nearly independent of pressure above 100 mm. The values of k^2 at several temperatures are plotted in Fig. 2 against the difference between the hydro-

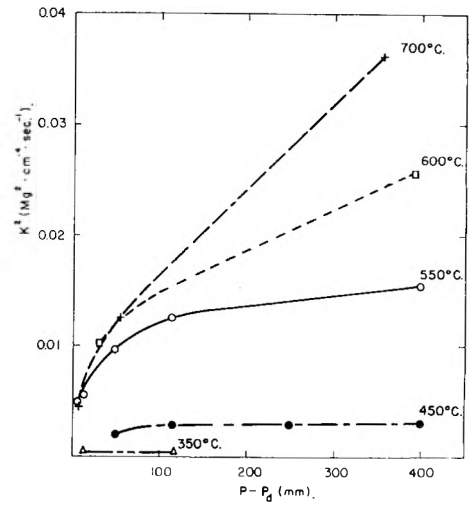

Fig. 2.—Parabolic rate constant squared *vs.* the pressure difference across the hydride layer.

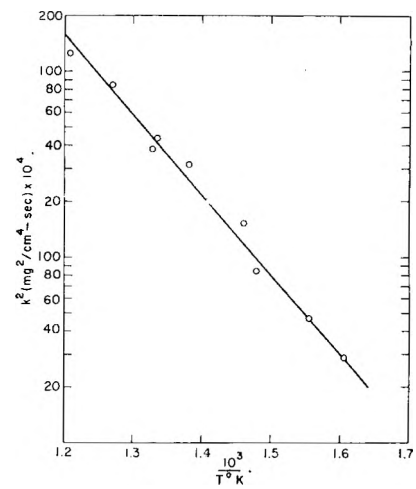

Fig. 3.—Log k^2 *vs.* $1/T$ at 120 mm. hydrogen pressure.

(2) J. Belle, B. B. Cleland and M. W. Mallett, *J. Electrochem. Soc.*, **101**, 211 (1954).

gen pressure over the sample and the dissociation pressure at the metal–hydride interface. The latter pressure was obtained from the pressure–composition data of Mallet and Campbell.[3] These curves must pass through the origin because the reaction must cease when the pressure of hydrogen over the sample is equal to the dissociation pressure of thorium dihydride. The pressure dependence of the reaction increased with increasing temperature. This behavior might be predicted from the hydrogen pressure–composition isotherms since the composition of the hydride phase changes more with pressure as the temperature increases.

The diffusion constant often follows an Arrhenius type equation $D = D_0\ e^{-\Delta H/RT}$. As the pressure dependence of the composition of thorium hydride was not known, the reaction rate could not be measured at constant concentration difference across the hydride layer to determine the temperature dependence of the rate. However, log k^2 was plotted in Fig. 3 against the reciprocal temperature for runs at a constant pressure of 120 mm. The apparent energy of activation obtained from this curve was 19.6 kcal. This value may be slightly larger than the activation energy for diffusion if the concentration difference increased over this temperature range.

The rate of reaction of Ames thorium was the same as that of crystal bar thorium. The difference in purity was not important in this reaction. Cold swaged samples of crystal bar thorium also gave the same reaction rate as annealed samples under comparable conditions. An appreciable induction time and a linear rate of reaction of hydrogen with thorium was reported by Straetz and Draley.[4] The linear rate was undoubtedly due to formation of Th_4H_{16} which is stable at one atmosphere hydrogen pressure over most of the temperature range of their study. With careful handling of the specimens and thorough outgassing of the system, no induction time was detected in the present investigation. The induction period was probably caused by a thin film of contamination.

(3) M. W. Mallett and I. E. Campbell, *J. Am. Chem. Soc.*, **73**, 4850 (1951).

(4) R. P. Straetz and J. E. Draley, "A Study of the Reaction Rate between Thorium and Purified Hydrogen," U. S. Atomic Energy Commission Report CT-3045, 9145.

NOTES

DECOMPOSITION OF ZINC OXIDE BY ZINC VAPOR

By Walter J. Moore and E. L. Williams

Chemical Laboratory, Indiana University, Bloomington, Indiana

Received February 5, 1959

In 1889 Morse and White[1] reported that the oxides of zinc and cadmium dissociated in the presences of the respective metals. They placed some zinc oxide and zinc in the end of a horizontal tube divided by a small dam. The tube was evacuated and heated. Just after the fusion of the zinc, they were able to collect some oxygen. The zinc evaporated and condensed beyond the dam, but as soon as some zinc collected there, the zinc oxide evaporated again and condensed further along the tube. After all the zinc had distilled, no more of the zinc oxide was found to evaporate.

We have made some quantitative measurements of the rate of evaporation of zinc oxide in flowing streams of oxygen, nitrogen, and zinc vapor in nitrogen. Three single crystals of zinc oxide (from 10 to 30 mg. each) were mounted in the ends of 1-cm. lengths of quartz capillary tubing, which were placed in a lavite holder inside a resistance furnace regulated to ±2°. The crystals were close to the mid-point of the furnace cross-section and mid-way from the ends of the furnace. One end was open and the other served as the entry for the flowing gases. The crystals were removed at intervals and weighed to determine their changes in weight. The results shown in Table I are the means of two or three quite concordant runs.

These data show that the rate of evaporation of ZnO in a stream of Zn vapor is about 100 times that in a stream of N_2 under the conditions cited at 1030°. The weight losses in O_2 and N_2 were so small that their apparent differences are not much outside the range of experimental uncertainty, but in the case of zinc vapor a greatly enhanced rate is clearly evident.

Table I

Evaporation Rates of Zinc Oxide

Gas flowing	Time, hr.	Flow rate, mmoles/min.	Temp., °C.	Rate of evaporation of ZnO, μg./hr.	Calcd. equilibrium rate
O_2	30	3.1	980	2.2 ± 1.1	0.03
O_2	46	6.5	980	2.2 ± 1.0	0.065
O_2	67	3.1	1100	3.5 ± 2.3	1.5
N_2	185	4.0	1030	1.1 ± 0.0	110
Zn	52	0.6	1030	120 ± 10	10^{-7}

The standard free energy change for the reaction

$$ZnO(c) = Zn(g) + 1/2\ O_2(g)$$

is $\Delta G^0 = -114640 + 51.65T$ (cal.).[2] Hence we can estimate the equilibrium constant $K_p = P_{Zn}P_{O_2}^{1/2}$. If we assume that the flowing gas is completely saturated with the equilibrium concentrations of zinc and oxygen, we estimate the evaporation rates given in the last column of Table I. The rate in N_2 is only about 1% of the equilibrium rate, the rate in O_2 at the highest temperature is still somewhat above the equilibrium value, but the rate in zinc is about 10^9 times the equilibrium value.

The first hypothesis that would serve to explain the enhanced decomposition of ZnO in Zn vapor would be the occurrence of a volatile suboxide of

(1) H. N. Morse and J. White, Jr., *Am. Chem. J.*, **11**, 258 (1889).

(2) J. A. Kitchener and S. Ignatowicz, *Trans. Faraday Soc.*, **47**, 1278 (1951).

zinc, such as Zn_2O. Inghram and Drowart[3] examined mass spectrometrically the products from a Knudsen cell containing a mixture of Zn and ZnO at temperatures from 1200 to 1400°K., but detected no lower oxide of zinc.

We are therefore inclined to explain the fast evaporation of ZnO by Zn vapor as a true catalytic effect on the rate of decomposition of the solid oxide. The reactions concerned in flowing Zn and O_2 may well be

$$*ZnO(c) + Zn(g) \longrightarrow ZnO(g) + *Zn(g) \quad (1)$$
$$ZnO(c) + O_2*(g) \longrightarrow ZnO*(g) + O_2(g) \quad (2)$$

Reaction 2 is likely to have a higher activation energy than reaction 1 since it involves the breaking of the strong O–O bond, whereas when a Zn atom from the gas phase strikes the ZnO surface it can readily remove an O atom by a reaction with low activation energy. This is a curious and unusual type of catalysis which involves the catalysis of a physical change (vaporization) by a chemical reaction, the exchange process at the surface. The subsequent reaction would be either precipitation of ZnO or

$$2\,ZnO \longrightarrow 2\,Zn + O_2 \quad (3)$$

(3) M. C. Inghram and J. Drowart, private communication.

SPECTROSCOPIC EVIDENCE OF TRIPHENYLMETHYL CATIONS ON A CRACKING CATALYST

BY HECTOR RUBALCAVA[1]

Union Oil Company of California, Research Department, Brea, California

Received February 16, 1959

This communication is a preliminary report of spectroscopic and chemical observations of the formation of triphenylmethyl cations on a silica–alumina catalyst from the reaction between the catalyst and triphenylmethanol. The sequence of infrared spectra shown are of a disc[2,3] of compressed, finely powdered silica–alumina (approximately 40 mg./cm.^{2} thickness) in which triphenylmethanol has been dispersed. The sequence shows the development of an absorption band at 7.32 μ as the dehydration of the disc, by evacuation at pressures of the order of 10 μ Hg at 25°, progresses in an "*in situ*" cell. Essentially the same changes were observed when the disc was dried by passing dry air over it. The appearance and growth of the band were accompanied by the appearance and intensification of a yellow color in the disc. Exposure of the disc to the air in the room caused both the yellow color and the absorption band to disappear. The changes were reversible.

Sharp and Sheppard[4] have discussed recently the infrared spectrum of the triphenylmethyl cation and show in their spectra that one of the strongest absorption bands of the ion falls at about 7.4 μ (*ca.* 1360 cm.$^{-1}$). Although triphenylmethanol does have weak absorption bands in the region we examined, they are, as can be seen in the first curve of Fig. 1, too weak to be seen under the conditions used in our experiments.

(1) Department of Chemistry, University College, Dublin, Ireland.

(2) R. H. Lindquist and D. G. Rea, paper presented before the Physical and Inorganic Division of the American Chemical Society, September, 1957.

(3) Personal communication, Dr. W. A. Pliskin.

(4) D. W. A. Sharp and N. Sheppard, *J. Chem. Soc.*, 674 (1957).

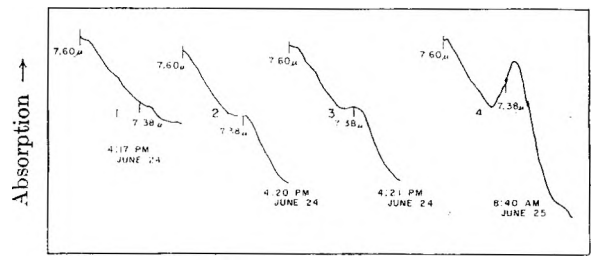

Fig. 1.—Sequence of spectra showing the growth of the triphenylmethyl cation band at 7.32 μ upon catalyst dehydration.

The yellow color of the triphenylmethyl cation in several different media, *e.g.*, in polar solvents such as acetone and acetonitrile, or as the crystalline perchlorate, is mentioned in ref. 3. We find that an intense yellow color appears immediately upon mixing moderately dry, powdered silica–alumina catalyst with a solution of triphenylmethanol in benzene or isooctane. If the experiment is performed with an alcoholic solution, the color does not appear until the resulting mixture is dried. The mixtures of catalyst and triphenylmethanol may be dried by gentle heating, or by the above-mentioned means. Storage of the mixture over a desiccant preserves the color. The color disappears upon contact with water, alcohol or moist air, and will re-appear after subsequent drying.

These facts are consistent with the reaction

$$(C_6H_5)_3COH + HOX \rightleftharpoons (C_6H_5)_3C^+OX^- + H_2O$$

HOX represents the catalyst acid and OX^- the anion. The reaction

$$(C_6H_5)_3CX + MX_n \rightleftharpoons (C_6H_5)_3C^+MX^-_{n+1}$$

is well known.[4] The spectra were obtained with a modified Beckman IR-2A spectrophotometer with a NaCl prism. The triphenylmethanol was Eastman-Kodak White Label grade, and the catalyst was Houdry type M-46.

Further work on this system is under way.

Invaluable discussions with Mr. R. C. Hansford and Dr. F. C. Seubold are acknowledged gratefully.

THE DOUBLE BOND ISOMERIZATION OF OLEFINS BY HYDROGEN ATOMS[1] AT −195°

BY MILTON D. SCHEER AND RALPH KLEIN[2]

National Bureau of Standards, Washington, D. C.

Received March 3, 1959

It has been established that the primary process in the reaction of hydrogen atoms with 1-olefins is addition to the terminal carbon to form a second-

(1) This research was performed under the National Bureau of Standards Free Radicals Research Program, supported by the Department of the Army.

(2) Guest Scientist, Olin-Mathieson Chemical Corp.

ary alkyl radical.[3-5] The subsequent reactions have not been elucidated in detail, although radical disproportionation and recombination undoubtedly occur. The major difficulty in the study of these systems is that there are several low activation energy, highly exothermic reactions which may and probably do occur simultaneously. The result is a variety of products particularly in the case of the higher olefins.

The reaction between hydrogen atoms and some condensed 1-olefins has been shown to occur at $-195°$[5,6] Under these conditions, atomic cracking reactions[7] were found to be absent (methane is not formed as a reaction product), so that the reaction system is considerably simplified. Further, large differences in reaction rate among the various olefins are found. 1-Butene at $-195°$ undergoes rapid reaction with hydrogen atoms while 2-butene under the same conditions is inert. If in the reaction between 1-butene and hydrogen atoms the double bond is shifted, 2-butene should accumulate in the products. This does occur, as we have reported previously.[6] Two possible disproportionation reactions resulting in a double bond shift are

$$2CH_3CH_2\dot{C}HCH_3 \longrightarrow CH_3(CH_2)_2CH_3 + CH_3CH{=}CHCH_3 \quad (1)$$

$$\dot{H} + CH_3CH_2\dot{C}HCH_3 \longrightarrow H_2 + CH_3CH{=}CHCH_3 \quad (2)$$

Reaction 2 may be established by using deuterium instead of hydrogen atoms. The accumulation of HD in the gas constitutes proof of (2). The exposure of solid isobutane at $-195°$ to deuterium atoms did not yield any HD. Since the tertiary hydrogen in isobutane was not abstracted under these conditions, the formation of HD by reactions other than (2) is unlikely.

TABLE I

TUNGSTEN RIBBON TEMPERATURE, 1600°; EXPOSURE TIME, 30 SECONDS; INITIAL D_2, 50μl. AT $-195°$

Olefin	HD/D_2[a]
Propylene	0.0
1-Butene	.2
3-Methyl-1-butene	.9

[a] Corrected for the H_2 formed as a result of isotope equilibration on tungsten ribbon.

Table I gives the HD formed as a result of irradiating propylene, 1-butene and 3-methyl-1-butene with deuterium atoms at $-195°$. Hydrogen abstraction from propyl radicals by deuterium atoms does not take place at $-195°$. However, the warmed-up products of the reaction D + $CH_3CH{=}CH_2$ showed the presence of propane-d_1.[6] Whether the reaction

$$2CH_3\dot{C}HCH_2D \longrightarrow CH_2{=}CHCH_2D + CH_3CH_2CH_2D$$

occurred at $-195°$ or during warm-up has not been established. The relative rates of abstraction of the hydrogen alpha to the free spin site of the alkyl radical are in the order tertiary > secondary > primary. The rate of double bond isomerization occurring by this mechanism is thus consistent with bond strength considerations.

(3) W. J. Moore, Jr., and L. A. Wall, *J. Chem. Phys.*, **17**, 1325 (1949).

(4) J. N. Bradley, H. W. Melville and J. C. Robb, *Proc. Roy. Soc. (London)*, **236**, 339 (1956).

(5) R. Klein and M. D. Scheer, *J. Am. Chem. Soc.*, **80**, 1007 (1958).

(6) R. Klein and M. D. Scheer, THIS JOURNAL, **62**, 1011 (1958).

(7) B. de B. Darwent and E. W. R. Steacie, *J. Chem. Phys.*, **13**, 563 (1945).

THE RATE OF OXIDATION OF I^- TO HYPOIODITE ION BY HYPOCHLORITE ION

BY YUAN-TSAN CHIA AND ROBERT E. CONNICK

Received January 31, 1959

In studying the behavior of iodine in the +1 oxidation state in alkaline solution,[1] it was convenient to prepare IO^- solutions by the oxidation of iodide ion by hypochlorite ion. Under most of our conditions this reaction appeared to be instantaneous as judged by spectrophotometric observations; however, at high hydroxide and low iodide concentrations at least part of the change from the hypochlorite spectrum to the hypoiodite spectrum occurred at a detectable rate. A fast mixing technique was then applied to make the reaction more readily measurable.

The net reaction was shown to be

$$I^- + ClO^- \rightleftharpoons IO^- + Cl^- \quad (1)$$

by studying the stoichiometry spectrophotometrically at varying ratios of I^- to ClO^-.[1] For interpreting the rate data the rate constant k' was defined

$$+\frac{d(IO^-)}{dt} = k'(I^-)(ClO^-) \quad (2)$$

where parentheses indicate concentrations in moles per liter. In Table I are given values of k' at a variety of experimental conditions. It is seen that the rate is first order in (I^-) and (ClO^-), a result also borne out by the time dependence of the individual runs. In the last column is the rate constant k which incorporates an inverse hydroxide dependence

$$\frac{d(IO^-)}{dt} = \frac{k(I^-)(ClO^-)}{(OH^-)} \quad (3)$$

TABLE I

RATE DATA FOR OXIDATION OF I^- BY IO^-

Temp. 25°, ionic strength 1.00 *M*

$(ClO^-) \times 10^3$, *M*	$(I^-) \times 10^3$, *M*	(OH^-), *M*	(Cl^-), *M*	k', M^{-1} sec.$^{-1}$	k, sec.$^{-1}$
4.00	2.00	1.00	0.004	60.3 ± 5	60.3 ± 5
2.00	4.00	1.00	0.002	62.7 ± 5	62.7 ± 5
2.00	2.00	1.00	.002	60.6 ± 5	60.6 ± 5
2.00	2.00	0.500	.502	116 ± 10	58.0 ± 5
2.00	2.00	0.250	.752	234 ± 20	58.5 ± 5

The hypoiodite formed is itself unstable with respect to disproportionation to iodate and iodide. Under the conditions chosen for the present study this latter reaction was much slower than the oxidation of iodide by hypochlorite and could be neglected in interpreting the data.

Discussion.—Anbar and Taube[2] have presented two possible mechanisms for the reaction of halide

(1) Y.-t. Chia, Thesis, University of California, Berkeley, June, 1958; University of California Radiation Laboratory Report UCRL-8311, June 2, 1958.

(2) M. Anbar and H. Taube, *J. Am. Chem. Soc.*, **80**, 1073 (1958).

ions with hypohalite ions: $X^- + YO^- = XO^- + Y^-$, when the form of the rate law is that found in the present study (equation 2). In the first mechanism the halide ion attacks the oxygen of the hypohalous acid. For our case the steps would be

$$ClO^- + H_2O \rightleftharpoons HOCl + OH^- \quad \text{rapid equil.}$$
$$I^- + HOCl \longrightarrow HOI + Cl^- \quad \text{rate determining}$$
$$HOI + OH^- \rightleftharpoons IO^- + H_2O \quad \text{rapid}$$

In the second mechanism the halide ion attacks the halogen of the hypohalous acid to yield the halogen molecule, which subsequently hydrolyzes to yield HOX and Y^-

$$ClO^- + H_2O \rightleftharpoons HOCl + OH^- \quad \text{rapid equil.}$$
$$I^- + HOCl \longrightarrow ICl + OH^- \quad \text{rate detn.}$$
$$ICl + OH^- \rightleftharpoons IOH + Cl^- \quad \text{rapid}$$
$$IOH + OH^- \rightleftharpoons IO^- + H_2O \quad \text{rapid}$$

Using the unpublished experimental results of Anbar and Rein they concluded that the exchange of bromine between Br^- and HOBr proceeds by attack of the Br^- on the oxygen of HOBr, corresponding to the first mechanism. No conclusion could be drawn about the exchange of chlorine between Cl^- and HOCl. From a comparison of several rate constants they reached the tentative conclusion that the reaction between Br^- and ClO^-, with rate law analogous to equation 3,[3] goes by the first mechanism also. From the above results no definite extrapolation can be made to the I^-–ClO^- reaction, although the first mechanism would seem more likely.

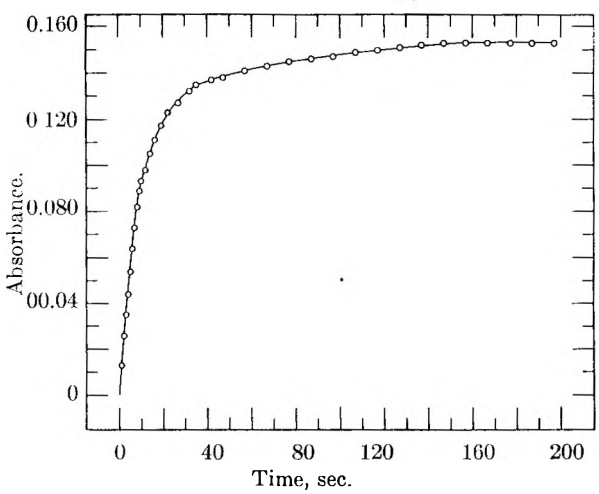

Fig. 1.—The absorbance–time curve for the third experiment of Table I.

Experimental

The reaction was followed spectrophotometrically on a Cary recording spectrophotometer. The rapid mixing was accomplished by injection with a hypodermic syringe, following the method developed by Stern and DuBois[4] and later applied by Below.[5] The 2.15 cm. absorption cell was that used by Below. Eight ml. of solution with the desired hydroxide and hypochlorite concentrations were placed in the cell and the absorption recorded on the chart. Iodide solution containing the same hydroxide concentration as that in the cell was introduced into a hypodermic syringe through a No. 16 needle. The syringe was filled to the 2-ml. mark with care being taken to avoid bubbles. With the Cary spectrophotometer recording at 400.6 mμ, the syringe was quickly emptied manually with the tip of the needle just below the surface. The measurement of absorbance was carried on as a function of time at the fixed wave length.

Zero time was taken as the point at which the absorbance on the spectrophotometer chart began to rise. Other times were calculated from the running speed of the chart. A typical set of points (third experiment of Table I) read from the chart is shown in Fig. 1 where the absorbance is plotted against the time in seconds. Slopes read from such plots yielded values of $d(IO^-)/dt$ for calculation of k' by equation 2. The molar absorptivity of IO^- and ClO^- at 400.6 mμ are 38.5 and 0.510, respectively.[1] Since the exact time of mixing (~1 sec.) was not known, the zero time was somewhat uncertain. The use of derivatives eliminated the need for zero time in the treatment of the data.

The syringe was lubricated carefully with a small amount of Kel-F No. 90 grease in the part above the 2.5-ml. mark. Too thin a layer gave rise to bubble formation. A qualitative test showed that the attack of the stainless steel needle by hypochlorite was unimportant. No effect was found on reversing the order of mixing by injecting hypochlorite into iodide.

In the hydroxide dependence experiments the ionic strength was held constant by the addition of sodium chloride.

(3) L. Farkas, M. Lewin and R. Block, *J. Am. Chem. Soc.*, **71**, 1988 (1949).

(4) K. G. Stern and D. DuBois, *J. Biol. Chem.*, **116**, 575 (1936).

(5) J. F. Below, Jr., University of California Radiation Laboratory Report UCRL-3011, June, 1955

THE DIFFERENTIAL THERMAL ANALYSIS OF PERCHLORATES. III. THE SYSTEM $LiClO_4$–NH_4ClO_4

BY MEYER M. MARKOWITZ AND ROBERT F. HARRIS

Foote Mineral Company, Research and Development Laboratories Berwyn, Pennsylvania

Received March 23, 1959

A previous study[1] had shown the utility of anhydrous lithium perchlorate as a component in phase investigations of ansolvous perchlorate systems. As an extension of this earlier work, a substantial portion of the system $LiClO_4$–NH_4ClO_4 has now been elucidated up to liquidus temperatures consistent with the thermal stability of ammonium perchlorate. These results are of interest in that a phase diagram involving the thermally relatively unstable ammonium perchlorate has been constructed, and that at 200° the rate of thermal decomposition of this salt in admixture with lithium perchlorate may be qualitatively related to the composition of the mixture.

Experimental Procedures

The experimental arrangement for carrying out the differential thermal analyses (d.t.a.) at a linear heating rate of 5° per minute has been described previously.[1] All liquidus temperatures were obtained by visual observations and were measured with a calibrated mercury-in-glass thermometer. Dry nitrogen gas was passed over the sample during each d.t.a. run and liquidus determination to avoid moisture absorption from the atmosphere.

The preparation of anhydrous lithium perchlorate has already been detailed.[1] Analysis of product by precipitation of nitron perchlorate: ClO_4^-, 94.1 (calcd. 93.5). Reagent grade ammonium perchlorate, dried at 105° for two hours was analyzed for ammonia content by distillation with sodium hydroxide solution. Analysis of product: NH_3, 14.37 (calcd. 14.49).

The Thermal Behavior of the Components.—Lithium perchlorate showed but one reversible break during any d.t.a. run up to about 260° and this was attributed to fusion at 247°.[1] Ammonium perchlorate on the other hand does not fuse but does undergo a reversible crystallographic transi-

(1) M. M. Markowitz, THIS JOURNAL, **62**, 827 (1958).

tion from the rhombic to cubic structure at about 240°.[2] Some decomposition of the pure salt was noted in this temperature region.

The System $LiClO_4$–NH_4ClO_4.—The salt mixtures of Table I were prepared and repeatedly subjected to d.t.a. and to visual determinations of the liquidus temperatures.

TABLE I

THE SYSTEM $LiClO_4$–NH_4ClO_4

$LiClO_4$, mole %	Eutectic temp., °C.	Transition temp., °C.	Liquidus temp., °C.
100.0	..	..	247
95.0	182	..	243
90.0	181	..	227
85.0	182	..	222
80.0	179	..	210
75.0	181	..	198
70.0	182	..	185
69.5	182	..	182 (eutectic)
69.0	182	..	183
68.0	182	..	184
65.0	182	..	188
60.0	184	..	217
55.0	182	244	..
50.0	178	242	..
45.0	180	239	..
40.0	180	239	..
30.0	180	239	..
20.0	180	239	..
10.0	181	239	..
0.0	..	240	..

Liquidus temperatures for samples containing more than 40 mole% ammonium perchlorate could not be obtained because of rapid decomposition of this salt as the temperature was raised. Decomposition of samples containing less than 40 mole % ammonium perchlorate was found, however, to be negligible in view of the ammonium perchlorate recoveries of 98.5, 98.9, 97.8 and 99.7% determined for samples initially containing 90, 80, 70 and 60 mole % lithium perchlorate, respectively. The persistence of the crystallographic transition characteristic of ammonium perchlorate throughout the ensuing composition range (55–0 mole % lithium perchlorate) indicates no complex interaction between the two components in this system. Accordingly, a plot of the data of Table I, given as Fig. 1, shows the system to be of the simple eutectic type with the eutectic at 69.5 mole % $LiClO_4$ and 182°.

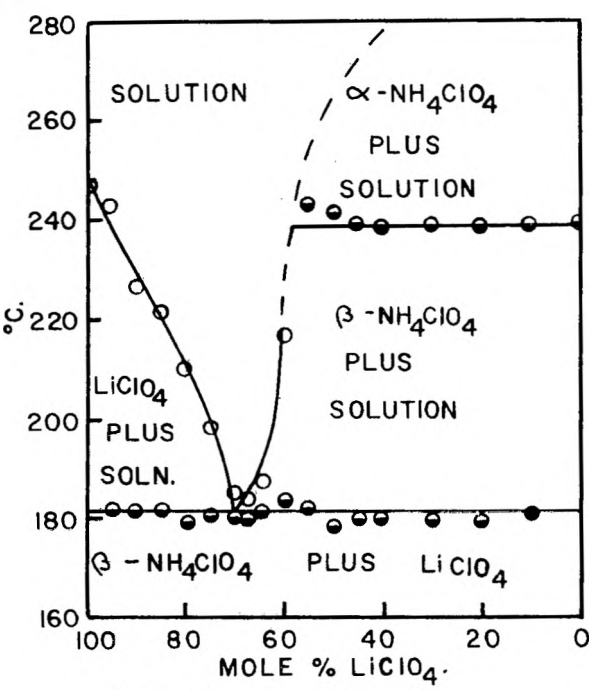

Fig. 1.—The system $LiClO_4$–NH_4ClO_4.

The Thermal Behavior of Mixtures of Lithium Perchlorate and Ammonium Perchlorate at 200°.—It was frequently noted during d.t.a. that salt mixtures containing lithium perchlorate in excess of the eutectic composition appeared to be thermally more stable than those mixtures containing ammonium perchlorate in excess of the eutectic composition. Thus, the former compositions did not fume at as low temperatures as the latter. To ascertain whether there was any specific effect of lithium perchlorate on the thermal decomposition of ammonium perchlorate, mixtures of the salts were prepared, fused at about 200° for a short period, ground, weighed and then maintained in a vented oven at 200° for 16 hours, followed by reweighing of the samples. Two-gram quantities of each mixture were used. The average results for four series of tests are given in Table II.

TABLE II

THE THERMAL DECOMPOSITION OF NH_4ClO_4 IN $LiClO_4$–NH_4ClO_4 MIXTURES AFTER 16 HOURS AT 200°

$LiClO_4$, mole %	Wt. % loss of available NH_4ClO_4	$LiClO_4$, mole %	Wt. % loss o available NH_4ClO_4
90.0	1.3	40.0	82
80.0	1.5	30.0	80
70.0	0.9	20.0	83
69.5 (eutectic)	0.3	10.0	89
60.0	82	0.0	30
50.0	70		

Chemical analyses of one group of mixtures after the heating period showed the samples to correspond to an average of 32.2 weight % NH_4ClO_4 (starting composition, 32.6 weight % NH_4ClO_4) and the pure ammonium perchlorate to correspond to 99.6 weight % NH_4ClO_4. The 30 weight % loss found for pure ammonium perchlorate is consistent with the stoppage of decomposition after 28–30% as reported by Bircumshaw, *et al.*,[3-5] This was found for ammonium perchlorate heated at 200–300° under high vacuum or at atmospheric pressure in a stream of nitrogen gas. The observed weight loss for pure ammonium perchlorate in the present work can in all likelihood be attributed primarily to decomposition rather than sublimation. Bircumshaw demonstrated that even at 260° scarcely any sublimation occurs at atmospheric pressure with passage of nitrogen gas over the sample of ammonium perchlorate.

The data in Table II would appear to delineate two modes of decomposition of ammonium perchlorate, depending on the composition of the original binary mixture. Where solid lithium perchlorate or clear solution persists, the decomposition reaction must be represented by equation I, NH_4ClO_4 (solution) → products. Reaction I is characterized by a different set of kinetic parameters from reaction II, NH_4ClO_4 (solid) → products, occurring when solid ammonium perchlorate is in contact with the solution. Undoubtedly reaction II proceeds at a more rapid rate than reaction I. As reaction II progresses, two factors may then actually give rise to an increased rate of decomposition. Decomposition products may accumulate in the liquid phase catalyzing reactions I and II simultaneously, and then solely reaction I after all the solid ammonium perchlorate has been decomposed. Temperature fluctuations within the oven and consequently within the test sample may also give rise to a periodic solution and recrystallization of the solid ammonium perchlorate. This would exert the solvent or "rejuvenation" effect originally proposed by Bircumshaw to account for the resumption of decomposition of the solid ammonium perchlorate residues remaining after the initial decomposition had proceeded to the extent of about 30 weight %.

(2) D. Vorlaender and E. Kaascht, *Ber.*, **56**, 1157 (1923).

(3) L. L. Bircumshaw in "Chemistry of the Solid State," edited by W. E. Garner, Academic Press, New York, N. Y., 1955, pp. 247–249.

(4) L. L. Bircumshaw and B. H. Newman, *Proc. Roy. Soc.*, (*London*), **227A**, 115, 228 (1954).

(5) L. L. Bircumshaw and T. R. Phillips, *J. Chem. Soc.*, 1741 (1957).

Acknowledgment.—This work was reported under Contract AF 33(616)-6057 with Wright Air Development Center. Their permission to publish is gratefully acknowledged.

THE HEAT OF VAPORIZATION AND VAPOR PRESSURE OF CARBON TETRACHLORIDE; THE ENTROPY FROM CALORIMETRIC DATA

By D. L. Hildenbrand and R. A. McDonald

Thermal Laboratory, The Dow Chemical Company, Midland, Michigan

Received February 2, 1959

Calculated values of the thermodynamic properties of the highly halogenated methanes are somewhat uncertain because the large vibrational contribution makes it important that the frequencies be known rather accurately. In addition, it is necessary to include significant corrections for vibrational anharmonicity, the data for which are seldom available. This is particularly true of carbon tetrachloride. For these reasons, it is important that the calculated thermodynamic properties be checked against accurate calorimetric vapor heat capacity and entropy data. It is the purpose of this note to summarize the best available calorimetric entropy data for carbon tetrachloride by combining newly measured heat of vaporization and vapor pressure data with available low temperature heat capacity data.

Hicks, Hooley and Stephenson[1] have reported low temperature thermal data for CCl_4 covering the range 17 to 298°K. Their results appear to be the most reliable and complete of a number of low temperature investigations. The recently reported liquid heat capacity data of Harrison and Moelwyn-Hughes[2] agree with those of Hicks, Hooley and Stephenson[1] within the 0.5% accuracy claimed by the former authors. Based on $\int C_p d \ln T$, Hicks, Hooley and Stephenson[1] have reported the entropy of liquid CCl_4 at 25° as 51.25 ± 0.15 cal. mole^{-1} deg.$^{-1}$. However, there appears to be a serious error in the extrapolation of the heat capacity below 18°K. Hicks, Hooley and Stephenson[1] made the extrapolation using a Debye function with $\theta = 148°$ and 15.4 degrees of freedom, obtaining an entropy of 1.39 cal. mole^{-1} deg.$^{-1}$ at 18°K. Experience in this Laboratory has shown that the empirical use of Debye functions with large numbers of degrees of freedom leads to significantly lower heat capacities and entropies than would be obtained with a Debye function of three degrees freedom plus the appropriate number of Einstein functions. This latter combination of functions is believed to give an extrapolation that is more acceptable from a fundamental view, since it allows three Debye degrees of freedom to account for the lattice contribution and makes up for internal vibrational degrees of freedom with Einstein functions. Aside from this, however, the extrapolation of H., H. and S. fits only the first three C_p values and above 20°K. it diverges rapidly from the experimental points. On the other hand, a Debye function (three degrees freedom) with $\theta = 70°$ together with four einstein functions each with $\theta = 98°$ gives an excellent fit over the range 17 to 32°K. and leads to an entropy of 1.805 cal. mole^{-1} deg.$^{-1}$ at 18°K. This latter extrapolation has been adopted for the entropy calculation and, when combined with the graphical integration of H., H. and S., gives an entropy of 51.67 ± 0.15 cal. mole^{-1} deg.$^{-1}$ for liquid CCl_4 at 25°.

The entropy of ideal gaseous CCl_4 can be evaluated from the above data and the heat of vaporization and vapor pressure data reported here. The calculation is summarized in Table I. The Berthelot equation and the critical constants given by Kobe and Lynn[3] ($T_c = 556.4$°K., $P_c = 45.0$ atm.) were used in evaluating the gas imperfection correction.

Table I

The Entropy of Carbon Tetrachloride, Cal. Mole^{-1} Deg.$^{-1}$

Satd. liquid, 298.15°K.	51.67 ± 0.15
Vaporization, 7746/298.15	25.980
Gas imperfection	0.036
Compression, R ln (114.2/760)	−3.766
Ideal gas, 298.15°K.	73.92 ± 0.20

For comparison with our calorimetric value, the most reliable calculated entropy appears to be that given by Albright, Galegar and Innes,[4] which is based on the infrared data of Plyler and Benedict,[5] the Raman measurements of Claassen[6] and includes a semi-empirical anharmonicity correction. The anharmonicity correction was obtained by correlation with the calculated and observed gas heat capacities of CCl_2F_2, and is considered to be only an approximation. Interpolation in the tables of Albright, Galegar and Innes[4] gives an entropy of 74.12 cal. mole^{-1} deg.$^{-1}$ at 298.15°K., which agrees with the calorimetric value within experimental error. The calculated value is probably uncertain by about 0.1 cal. mole^{-1} deg.$^{-1}$. Gelles and Pitzer[7] give a calculated entropy of 73.94 cal. mole^{-1} deg.$^{-1}$ at 298.15°K., in good agreement with the calorimetric value, but their value is based on only the infrared measurements of Plyler and Benedict[5] and does not include an anharmonicity correction. Accurate vapor heat capacity measurements would be very helpful in further reducing uncertainties in the calculated thermodynamic properties.

Experimental

Material.—Commercial carbon tetrachloride was purified by fractional distillation. A center cut was found to have a purity of 99.96 mole % by freezing curve analysis.

Heat of Vaporization.—The heat of vaporization of CCl_4 at 25° was measured using a newly constructed calorimeter that will be described in detail in a later publication. Briefly,

(1) J. F. G. Hicks, J. G. Hooley and C. C. Stephenson, *J. Am. Chem. Soc.*, **66**, 1064 (1944).

(2) D. Harrison and E. A. Moelwyn-Hughes, *Proc. Roy. Soc. (London)*, **A239**, 230 (1957).

(3) K. A. Kobe and R. E. Lynn, *Chem. Revs.*, **52**, 117 (1953).

(4) L. F. Albright, W. C. Galegar and K. K. Innes, *J. Am. Chem. Soc.*, **76**, 6017 (1954).

(5) E. K. Plyler and W. S. Benedict, *J. Research Natl. Bur. Standards*, **47**, 202 (1951).

(6) H. H. Claassen, *J. Chem. Phys.*, **22**, 50 (1954).

(7) E. Gelles and K. S. Pitzer, *J. Am. Chem. Soc.*, **75**, 5259 (1953).

the system consisted of a calorimeter vessel with glass exit tube mounted within a conventional adiabatic shield assembly and insulated by vacuum. The adiabatic control system is the same as that used on the low temperature calorimeter in this Laboratory.[8] The cylindrical sample container was constructed of copper and was fitted with a central re-entrant well containing a platinum resistance thermometer (R_0 = 91 ohms), an internal heater wrapped around the base of the thermometer well and a system of 40 radial heat transfer vanes. The heater was wrapped over only the lower one-fourth of the thermometer well so as to avoid superheating the vapor leaving the calorimeter. All parts of the sample container were nickel-plated before assembly. The calorimeter had a volume of 60 cm.^{3}

The temperature of the vapor leaving the calorimeter was measured with a chromel–constantan thermocouple attached to the short platinum exit tube soldered to the calorimeter top and could be maintained constant within 0.05° by manipulation of a throttle valve in the exit line. The exit line was provided with electrical heating where necessary in order to prevent condensation. Material vaporized was condensed in liquid nitrogen cooled glass bulbs and weighed. Corrections were applied for the heat effect corresponding to small changes in the temperature of the calorimeter and for the heat required to vaporize material replacing the liquid withdrawn from the calorimeter. As a check on the operation of the calorimeter, the heat of vaporization of a sample of high purity benzene was measured at several temperatures and compared with the accurate results of Osborne and Ginnings[9] and Waddington and Douslin.[10] The results of seven vaporization experiments over the range 20 to 60° all agreed with the accepted values to within 0.1%, the average difference being 0.04%. Varying the rate of vaporization produced no observable effect.

The measurements on CCl_4 are summarized in Table II. Uncertainties in the experimental value should not exceed 0.1%.

TABLE II

THE HEAT OF VAPORIZATION OF CARBON TETRACHLORIDE AT 25°, CAL. MOLE^{-1}

t, °C.	G., vaporized	Rate g. min.$^{-1}$	ΔH	$\Delta H_{25}°$
24.17	8.3406	0.278	7757	7747
24.68	8.3857	.279	7746	7742
24.58	5.2625	.175	7754	7749

Accepted value = 7746 ± 5

For comparison purposes, the heat of vaporization at 25° was calculated from the exact Clapeyron equation, using the Antoine vapor pressure equation given below and the Berthelot equation to obtain the vapor volume. The value thus calculated is 7730 cal. mole^{-1}, in reasonable agreement with the experimental value of 7746 cal. mole^{-1}. This would indicate that the use of the Berthelot equation to obtain the gas imperfection correction is reasonable.

Vapor Pressure.—Measurements of the vapor pressure were made using a twin ebulliometer system, with water as the reference substance. Pressures were determined from the measured boiling temperatures and the known vapor pressure of water.[9] The experimental points are given in Table III.

TABLE III

THE VAPOR PRESSURE OF CARBON TETRACHLORIDE

t, °C.	P(obsd.) mm.	P(obsd.) − P(calcd.) mm.
19.88	90.60	−0.03
36.93	189.10	+ .29
56.16	387.97	− .59
75.28	727.30	+ .20
76.16	747.70	+ .75
76.87	763.03	− .24
77.71	782.83	− .11
(76.73)	(760.00)	....

The constants in the Antoine equation

$$\log P(\text{mm.}) = 6.89406 - 1219.58/(t + 227.16)$$

were obtained by a least squares treatment. Values calculated from the above equation are compared with the experimental points in Table III.[11]

(8) D. L. Hildebrand, W. R. Kramer, R. A. McDonald and D. R. Stull, *J. Am. Chem. Soc.*, **80**, 4129 (1958).

(9) N. S. Osborne and D. C. Ginnings, *J. Research Natl. Bur. Standards*, **39**, 453 (1947).

(10) G. Waddington and D. R. Douslin, *J. Am. Chem. Soc.*, **69**, 2275 (1947).

(11) N. S. Osborne, H. F. Stimson and D. C. Ginnings, *J. Research Natl. Bur. Standards*, **23**, 261 (1939).

THE HEAT OF FORMATION OF METHYL NITRATE

BY JAMES D. RAY[1] AND R. A. OGG, JR.

Contribution from the Department of Chemistry, Stanford University, California

Received February 9, 1959

Recent interest in the kinetics of reactions involving methyl nitrate led the authors to a calorimetric investigation of the gas phase heat of the reaction between nitrogen pentoxide and methyl nitrite to form an equilibrium mixture of nitrogen dioxide and dinitrogen tetroxide plus methyl nitrate.

Preliminary studies by infrared analysis showed that the products of the reaction of equal pressures of reactants represented quantitative conversion with no evidence of side reactions. The reaction was found to be extremely rapid.

Materials.—Methyl nitrite was prepared by the reaction given in "Organic Syntheses."[2] The reaction was carried out in a vacuum system. The product was purified by condensation on anhydrous potassium carbonate and by distilling repeatedly from Dry Ice to liquid nitrogen temperatures. An infrared spectrum of the product showed no bands of possible impurities such as nitric acid, nitrogen dioxide or methyl nitrate. Nitrogen pentoxide of at least 99.9% purity was prepared as previously described.[3]

Apparatus and Experimental Procedure.—The calorimeter employed has been described previously.[3] It contained a 275-ml. gas reaction bottle. The heat capacity of the entire calorimeter including the chlorobenzene liquid was 168.4 ± 1.1 cal./deg. In the present study, after following the initial temperature drift, 75 mm. pressure of nitrogen pentoxide was admitted to the calorimeter bottle. This was as high a pressure as could be used with no question as to absence of a liquid phase forming from the products. One-half minute later, methyl nitrite was admitted quickly to a final pressure of 248 mm., which corresponded to a 69.5 mm. excess. It was shown by Yoffe and Gray[4] that the nitrogen dioxide product does not react with this excess of methyl nitrite. The temperature drift was then again followed. The final temperature was 25°. The system was thermostated at the mean reaction temperature. The observed temperature rise (average of 4 determinations) was 0.070 ± 0.002°. The equilibrium pressures of nitrogen dioxide and dinitrogen tetroxide present in the calorimeter bottle after the reaction were 57.0 and 46.5 mm., respectively. The stoichiometric equation for the reaction with the standard heat of formation of each compound from the elements written below each respective term is

$$\begin{array}{ccccc} 1.000\ N_2O_5 & + & 1.000\ CH_3ONO & = & \\ +3.17 & & -16.27 & & \\ 0.620\ N_2O_4 & & + 0.760\ NO_2 & + & 1.000\ CH_3ONO_2 \\ +0.620 \times 2.239 & & +760 \times 7.964 & & \Delta H_f(CH_3ONO_2) \end{array}$$

(1) Department of Chemistry, University of Minnesota, Minneapolis 14, Minn.

(2) W. H. Hartung and F. Crossley, "Organic Syntheses," Coll. Vol. II, A. H. Blatt, editor, John Wiley and Sons, Inc., New York, N. Y., 1943, p. 363.

(3) R. A. Ogg, Jr., and J. D. Ray, THIS JOURNAL, **61**, 1087 (1957).

(4) A. D. Yoffe and P. Gray, *J. Chem. Soc.*, 1412 (1951).

The enthalpy change for the reaction is

$$\Delta H = \Delta H_f(CH_3ONO_2) + 20.537$$

The measured heat evolution in kcal. per mole of methyl nitrate formed is given by

$$\Delta Q = \frac{\text{(calorimeter constant)}}{\text{(moles of } CH_3ONO_2\text{)}} \text{(temp. rise)} = \frac{(0.1684)(0.070)}{(0.00111)} = -10.620$$

This measured heat evolution is equal to the change in internal energy of the reaction plus an additional heat evolution due to the expansion of the two gases into the bottle. Thus

$$\Delta Q = \Delta E - (n_{N_2O_5} + n_{CH_3ONO_2})RT$$
$$\Delta Q = \Delta H - 1.958 \text{ kcal./mole}$$
$$-10.620 = \Delta Q = \Delta H_f(CH_3ONO_2) + 20.537 - 1.958 \text{ kcal./mole}$$

The heat of formation of methyl nitrate from the elements at 25° as the hypothetical gas at 1 atmosphere pressure is

$$\Delta H_f(CH_3ONO_2) = -29.2 \pm 0.3 \text{ kcal./mole (exothermic)}$$

The thermodynamic data used in the above calculations are given in Table I below. All values refer to the gases at 25° and 1 atmosphere pressure.

TABLE I

SUMMARY OF THERMODYNAMIC DATA USED IN THIS PAPER

	NO_2	N_2O_4	N_2O_5	CH_3ONO	CH_3ONO_2
$H^\circ_{298.16}$	7.964[5]	2.239[5]	3.17[3]	−16.27[6]	−29.2
$S^\circ_{298.16}$	57.47[5]	72.73[5]	82[8]	67.84[6]	80.97[7]

The thermal data for methyl nitrite in Table I based on the equilibrium between gaseous methyl nitrite, hydrogen chloride, methyl alcohol and nitrosyl chloride which was studied by Leermakers and Ramsperger[6] have been recalculated on the basis of the more modern value for the heat of formation of hydrogen chloride given by Rossini, Wagman, Evans, Levine and Jaffe,[9] and the thermodynamic data of nitrosyl chloride given by Beeson and Yost.[10] The recalculated entropy for methyl nitrite, 67.84, is to be compared with that for nitromethane, 63.82. It is to be expected that the lower symmetry and, as shown by Piette, *et al.*,[11] and D'Or and Tarte[12] the coexistence of approximately equal amounts of *cis* and *trans* isomers of methyl nitrite should result in an entropy higher by about three entropy units than that of nitromethane, whereas the entropy given in the original paper was only 0.58 e.u. higher. Thus, the direction of the correction is as should be expected.

Discussion of Results

The value for the heat of formation of methyl nitrate found in this paper, −29.2 ± 0.3 kcal./mole, may be compared to that found from the heat of explosion of the liquid as observed by Whittaker, Wheeler and Pike.[13] This value, combined with the heat of vaporization given by McKinley-McKee and Moelwyn-Hughes[14] gives for the heat of formation of gaseous methyl nitrate from the elements at 25° and one atmosphere pressure, −29.4 ± 0.8 kcal./mole, in excellent agreement with the value found in this paper from a completely different reaction involving gaseous instead of liquid methyl nitrate.

Of interest in kinetic studies, thermal data for reactions (1) and (2) were calculated.

$$CH_3ONO + 1/2\ O_2 = CH_3ONO_2$$
$$\Delta H = -12.93 \text{ kcal.}, K_{298} = 3.62 \times 10^7 \text{ atm.}^{-1/2} \quad (1)$$
$$CH_3ONO + NO_2 = CH_3ONO_2 + NO$$
$$\Delta H = +0.706 \text{ kcal.}, K_{298} = 6.17 \quad (2)$$

The enthalpy change for reaction 1 may be compared to the value −10.3 kcal. for the analogous reaction of the ethyl homologs. Since in the course of an hour, no nitric oxide band could be observed in the infrared spectrum of a mixture of methyl nitrite and nitrogen dioxide, it is concluded that reaction 2 is not active in the reaction between nitrogen pentoxide and methyl nitrite.

The present thermodynamic data are compatible with the assignment of *cis-trans* isomerism to the double methyl proton nuclear magnetic responance spectrum reported by Piette, Ray and Ogg[11] for methyl nitrite. The N^{14} resonance spectrum (to be displayed in a subsequent publication) is extremely broad ($\Delta W_{1/2}$ = 200 p.p.m. at 2.88 megacycles). The dynamic process involved in the rotational isomerism is expected to cause this great enhancement of the electric quadrupole relaxation of the N^{14} nucleus.

Acknowledgments.—This research was supported in part by the National Science Foundation, by a research grant (No. H-2339) from the National Heart Institute, Public Health Service, and by the Petroleum Research Fund administered by the American Chemical Society.

(5) W. F. Giauque and J. D. Kemp, *J. Chem. Phys.*, **6**, 40 (1938).

(6) J. A. Leermakers and J. C. Ramsperger, *J. Am. Chem. Soc.*, **54**, 1837 (1932).

(7) P. Gray and P. L. Smith, *J. Chem. Soc.*, 2380 (1953).

(8) K. K. Kelley, U. S. Bur. Mines Bull., **477**, 1948.

(9) F. D. Rossini, D. D. Wagman, W. H. Evans, S. Levine, I. Jaffe, "Selected Values of Chemical Thermodynamic Properties," Circular 500, U. S. Bur. Standards (1952).

(10) C. M. Beeson and D. M. Yost, *J. Chem. Phys.*, **7**, 44 (1939).

(11) L. H. Piette, J. D. Ray and R. A. Ogg, Jr., *ibid.*, **26**, 1341 (1957).

(12) L. D'Or and P. Tarte, *ibid.*, **19**, 1064 (1951).

(13) H. Whittaker, W. H. Wheeler and H. H. M. Pike, *J. Inst. Fuel*, **20**, 137 (1947).

(14) J. S. McKinley-McKee and E. A. Moelwyn-Hughes, *Trans. Faraday Soc.*, **48**, 247 (1952).

THE THERMAL DECOMPOSITION OF SOLID SILVER METHYL AND SILVER ETHYL[1]

BY B. S. RABINOVITCH, DONALD H. DILLS AND N. R. LARSON

Department of Chemistry, University of Washington, Seattle, Washington

Received February 14, 1959

This work was undertaken to investigate the potentialities of silver alkyls as low temperature gas phase sources of alkyl radicals according to the reaction, Solid (I) = Solid (II) + Gas. Semerano[2] studied the decomposition of silver alkyls below 0°. On heating wet (under alcohol) or moist silver methyl precipitate it decomposed to ethane and silver. Silver ethyl was reported to yield butane, ethylene and ethane. Semerano suggested the use of these compounds as sources of alkyl radicals. Bawn and Whitby[3] studied the decomposition of dissolved silver methyl and proposed that the decomposition proceeded through methyl radicals, although objection has been made to this interpretation.[3] Support for free radical mechanisms has been found in the decomposition of silver

(1) This work was supported by the Office of Naval Research.

(2) G. Semerano and L. Riccoboni, *Ber.*, **74B**, 1089 (1941); G. Semerano, L. Riccoboni and F. Callegari, *ibid.*, **74B**, 1297 (1941).

(3) C. E. H. Bawn and F. J. Whitby, *Disc. Faraday Soc.*, **2**, 288 (1947), *et seq.*

phenyl in solution,[4] and of silver isobutenyl precipitate under alcohol.[5]

In the present study, the decomposition of the dry alkyls has been investigated. The work proved more difficult than anticipated and the results (reproducibility, nature of samples, etc.) leave something to be desired. Certain aspects of interest appear worthy of report.

Experimental

Lead tetramethyl and lead tetraethyl were purified by distillation. The reactor consisted of a cylindrical tube 50 cc. in volume, fitted with a taper joint at the top and having a short tubular (area 0.75 cm.^{2}) extension with flat bottom at the lower extremity.

Twenty ml. of 1.2% silver nitrate methanol solution and 0.06 g. of lead tetramethyl in 15 ml. of methanol were cooled to −78° in a dry box. The solutions were mixed in the reactor which was then stoppered, and the yellow silver methyl precipitate was centrifuged at −78°. The precipitate deposited as a thin layer on the flat bottom of the reactor well. The methanol was siphoned off, 10 ml. of dimethyl ether at −78° was added and the precipitate stirred with a rod. The suspension was again centrifuged at −78°. All operations were performed under nitrogen. Seven washings removed methanol sufficiently to allow the reactor (with the well at −78°) to be evacuated below 10^{-3} mm. by pumping (3–15 hours). In this process the silver methyl wafer (~0.1 mm. thick) curled and cracked a little.

Red-brown silver ethyl was prepared in like manner.

To initiate decomposition, the −78° bath was replaced by a thermostat so that the reactor well and silver alkyl wafer were submerged. Temperature was constant to within 0.1°. Decomposition was followed by pressure change. Gas products were analyzed on a Consolidated 21-102 mass spectrograph.

Results and Discussion

Products of Decomposition.—Mass spectrographic analysis of the gas product (after warming the residue to room temperature) from silver methyl showed ethane, with 12% dimethyl ether, 1% methanol and some water. Although the original precipitate was pumped extensively at −78°, several mm. vapor of methanol, and some dimethyl ether and water were always left. Most of the methanol and water entered the gas phase only after warming the residue. Analysis of the silver residue showed ~13% $AgNO_3$; no lead was found. With silver ethyl, the product gas was butane, with possible small amounts of ethane and ethylene; the silver residue contained ~7% $AgNO_3$.

X-Ray diffraction patterns of the residue were identical with those of bulk silver powder, even when the residue was kept at reaction temperature. The sharpness of the pattern lines suggested particle diameter between 10^{-5} to 10^{-3} cm. No success was had in obtaining silver alkyl patterns.

The decomposition of silver ethyl was conveniently measurable at slightly lower temperature (> −38°) than for silver methyl (> − 30°). Excessive heating in both cases gave rise to explosions or occasional deflagration.

Form of the Decomposition Rate Curve.—For both silver methyl and silver ethyl, after an initial (2–15% reaction) rapid pressure increase accompanied by some browning (and followed sometimes by a short induction period), the rate of pressure increase was constant and changed quite sharply to zero near 100% decomposition. On the average, the rate was constant over the middle 80% decomposition and, neglecting the initial rapid pressure rise, was "zero order" over more than 90% of the reaction. Early work with a sample of lead tetramethyl from the Ethyl Corporation, used without any additional purification, gave rise to sigmoid decomposition pressure curves. These were never found using the compound prepared and purified by us, although an occasional run might bend a little from a straight line.[6] The rate of decomposition (slope) was not reproducible with different preparations of silver alkyl and varied several fold.

Cooling.—Interruption of reaction by freezing to −80° did not affect the subsequent decomposition rate on returning to the reaction temperature.

Addends.—Nitric oxide, oxygen, dimethyl ether or methanol gas, added during the middle of a run, were without effect on the rate. Preparations of silver methyl where excess silver nitrate or silver powder were added showed no apparent effect. Removal of gas products at a certain point during a run did not affect the subsequent rate.

Effect of Temperature.—Since rates were not reproducible between different samples, experiments were done in which, during the constant portion of the rate behavior, the initial temperature was raised 3–5° (and then sometimes lowered again), or the initial temperature was lowered (and then sometimes raised). Activation energies for both alkyls ranged around 35 ± 12 kcal. The occurrence of such large activation energies at the low temperatures employed signifies an abnormally large frequency factor. There was some indication that the heating–cooling cycle ($T_1 \rightarrow T_2 \rightarrow T_1$) was not reversible and that the final rate on reversion to T_1 was less than the original.

Remarks.—The decomposition of both alkyls evidently occurs by similar mechanisms. An adequate account must be compatible with the observed rate behavior and high frequency factor. Solid reactions have been customarily attributed to reaction at constant surface area, while high frequency factors have been attributed to layer or mosaic block decomposition.[6] In this case, the extreme range of reaction for which the constant rate holds would demand that the precipitate particles be monodisperse, while the decomposition of mosaic block or layers might be expected to lead to explosion in this exothermic reaction. Any process involving the propagation of a constant number of reactive sites would account for the rate behavior.

The initial rapid pressure rise was at least in part due to solvent release on warming to reaction temperature. In any case, the occurrence (sometimes) of a later short induction period signifies that the initial process is not directly related to the main process.

The lack of effect of nitric oxide and oxygen shows that free radicals do not enter the gas phase and that free radicals as such are not present in the solid.

Acknowledgment.—We thank Professor E. C.

(4) J. E. Spice and W. Twist, *J. Chem. Soc.*, 3319 (1956).

(5) F. Glockling, *ibid.*, 716 (1955).

(6) *Cf.* W. E. Garner, "Chemistry of the Solid State," Butterworth Scientific Publications, London, 1955; see p. 233, Fig. Ia and shape of lead azide curves.

Lingafelter for his kind coöperation in the use of the X-ray diffraction equipment and for an estimate of particle size. We thank the Ethyl Corporation for a gift of chemicals.

THERMODYNAMICS OF THE DISPROPORTIONATION OF TITANIUM TRIBROMIDE

By Elton H. Hall and John M. Blocher, Jr.

Contribution from Battelle Memorial Institute, Columbus, Ohio

Received August 29, 1958

As a means of obtaining the thermodynamic properties of $TiBr_2$ from published data for $TiBr_4$ and $TiBr_3$, the disproportionation equilibrium (1) has been studied

$$2TiBr_3(s) = TiBr_4(g) + TiBr_2(s) \qquad (1)$$

The partial pressure of $TiBr_4(g)$ was found to vary with the composition of the solid phase at constant temperature indicating that solid solubility occurs between $TiBr_3$ and $TiBr_2$. In fact, the variation was so much greater than in the corresponding $TiCl_3$ disproportionation[1-3] that the effects of solid solubility could not be neglected.

When the magnitude of the task of defining this system became apparent, it was decided that the results would not justify the expense, and the work was concluded. However incomplete, the data lead to a value for the heat of formation of $TiBr_2$ which is thought to be the best currently available.

Experimental

Titanium tribromide was prepared by reduction of distilled $TiBr_4$ with iodide-process titanium, and sublimation under the equilibrium pressure of $TiBr_4$. Chemical analysis of one such sample gave Ti, 16.9% and Br, 83.6%, corresponding to $TiBr_{2.97}$. The deviation from $TiBr_3$ is within the uncertainty of the analysis. For the purpose of later calculations, the composition $TiBr_3$ was assumed.

The pressures were measured with a null-indicating quartz Bourdon gage heated in an air-bath thermostat (±0.4°). After the pressure data were obtained over $TiBr_3$, a Willard valve[4] was opened and some $TiBr_4$ was pumped into a demountable cold trap. The composition of the residual solid phase was calculated from the original weight of the $TiBr_3$ and the weight of $TiBr_4$ removed. Pressure data then were observed on the new composition. In this manner, the data of Fig. 1 were obtained at five different compositions ranging from $TiBr_3$ to $TiBr_{2.65}$. In addition, measurements were made on a sample of uncertain composition near $TiBr_2$ which was prepared by the reduction of $TiBr_4$ with excess titanium. Since $TiBr_3$ is slightly volatile in the temperature range employed, the observed total pressure must be corrected to obtain the partial pressure of $TiBr_4(g)$. In order to make this correction, preliminary data were obtained[5] for the vapor pressure of $TiBr_3$ which may be represented by the equation

$$\log P_{mm} = -8930/T + 11.6 \qquad (2)$$

While this equation must be considered tentative, it is adequate for the present purpose since the correction amounts to a small fraction of the total pressure.

Discussion

Since the activities of $TiBr_3$ and $TiBr_2$ in the solid phase are not available, the equilibrium constant cannot be calculated directly from the observed $TiBr_4$ pressure at a given composition. Therefore, an alternative treatment was employed.

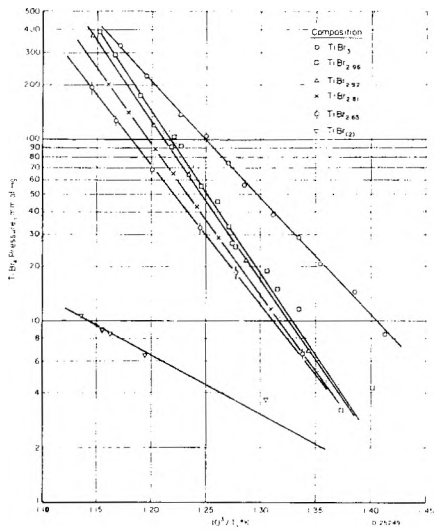

Fig. 1.—Disproportionation pressure of $TiBr_3$.

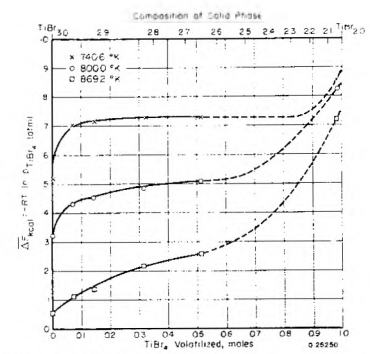

Fig. 2.—Partial molal free-energy isotherms.

The free energy change for converting 2 moles of $TiBr_3(s)$ to 1 mole of $TiBr_2(s)$ and 1 mole of $TiBr_4(g, 1\ atm.)$ is, by definition, the standard free-energy change, ΔF^0_1, for reaction 1. If no solid solubility existed, the equilibrium pressure, P_{TiBr_4}, would remain constant with composition as defined by $\Delta F^0_1 = -RT \ln P_{TiBr_4}$. With solid solution present, P_{TiBr_4} varies with the composition of the solid phase, and $dF/dN = \Delta\bar{F} = -RT \ln P_{TiBr_4}$, where dF is the free energy change for removal of dN mole of $TiBr_4$ at equilibrium and compressing it to 1 atm. As $TiBr_4$ is removed incrementally in converting the solid phase from 2 moles of $TiBr_3(s)$ to 1 mole of $TiBr_2$

$$\int_0^1 \Delta\bar{F}\, dN = \Delta F^0_1$$

since the difference in free energies of the initial and final states of the system must be equal regardless of the path taken.

Except for the points at the uncertain composition near $TiBr_2$, the available data are limited to the $TiBr_3$ side of the system. Therefore, in compensating for this deficiency, the estimated standard entropy change for reaction 1 was used to establish the shape of the $\Delta\bar{F}$ curves. The entropies are given in Table I together with the heat capacities used for extrapolation.

(1) G. B. Skinner and R. A. Ruehrwein, This Journal, **59**, 113 (1955).

(2) M. Farber and A. J. Darnell, *ibid.*, **59**, 156 (1955).

(3) B. S. Sanderson and G. E. MacWood, *ibid.*, **60**, 316 (1956).

(4) J. Willard, *J. Am. Chem. Soc.*, **57**, 2328 (1935).

(5) The $TiBr_3$ vapor pressure determinations were made by Neil D. Veigel, of Battelle, by the transpiration technique.

TABLE I

HEAT CAPACITIES AND ENTROPIES OF TITANIUM BROMIDES

(Values in parentheses are estimated)

	$TiBr_4(g)$	$TiBr_3(s)$	$TiBr_2(s)$
$C^0_{p298.2}$	24.0[a]	(24.8)[b]	(18.6)[c]
$S^0_{298.2}$	95.02[a]	43.4[b]	(30)[d]

For eq. 1: $\Delta C_p = -7.0$ cal./mole/deg.,[e] $\Delta S_{298.2} = 38.2$ e.u.

[a] Calculated from spectroscopic data of M. Delwaulle and F. Francois, *Compt. rend.*, 220, 173 (1945). [b] Reference 7. [c] The C_p value for $TiBr_3$ is 0.2 cal./g. atom lower than the Kopps law value. Subtraction of this amount from the Kopps law value for $TiBr_2$ gives 18.6 [d] L. Brewer, L. A. Bromley, P. W. Gilles and N. H. Lofgren, National Nuclear Energy Series, Vol. IV-19B, L. L. Quill, Editor, McGraw-Hill Book Co., New York, N. Y., 1950. Calculation from Latimer's tables, *J. Am. Chem. Soc.*, **73**, 1480 (1951), gives 31.6 e.u. [e] The ΔC_p value was taken to be constant in the temperature range 298 to 800°K.

Figure 2 gives isotherms calculated from the experimental data of Fig. 1 at 740, 800 and 869°K. In obtaining the final form of the data, Fig. 2, the areas under similar curves were measured and plotted as $\Delta F^0_1/T$ against $1/T$ to obtain ΔH^0_1 as the slope and ΔS^0_1 as the intercept. The shapes of the curves then were adjusted in the uncertain region and the process repeated to obtain the best approximation to the estimated $\Delta S^0_{800} = 31.3$ e.u. The final result was

$$\Delta H^0_{800} = 31.3 \text{ kcal./mole}$$
$$\Delta H^0_{298.2} = 34.8 \text{ kcal./mole}$$
$$\Delta S^0_{800} = 32.3 \text{ e.u.}$$
$$\Delta S^0_{298.2} = 39.2 \text{ e.u.}$$

To lower ΔS^0_{800} by another entropy unit for better agreement would require what appeared to be an inordinate distortion of the ΔF curves on the $TiBr_2$ side of the system. Moreover, the higher ΔS^0_{800} value is favored if equal weights are given to Latimer's and Brewer's entropy estimates for $TiBr_2(s)$, from which $\Delta S^0_{800} = 32.1$ e.u. is predicted. It should be noted that the assumption that a two-phase region extends from $TiBr_{2.5}$ to $TiBr_2$ gives $\Delta S^0_{800} = 38.2$ e.u. which is prohibitively high. Therefore, the above values are adopted as being the most consistent.

In view of the uncertainties in the data and the long extrapolation to 25° with the approximative assumption of a constant ΔC_p, an over-all uncertainty of ±3 kcal. is attached to heats of formation calculated from the above data.

The value $\Delta H^0_{298.2} = 34.8 \pm 3$ kcal./mole may be combined with the heat of formation of $TiBr_4(s)$, -147.4 ± 1.1 kcal./mole of Nelson, *et al.*,[6] the heat of formation of $TiBr_3$, -130.6 ± 1.2 kcal./mole of Hall and Blocher,[7] and the heats of vaporization and fusion of $TiBr_4$ (13.22 kcal./mole of Hall, *et al.*,[8] and 3.08 of Kelley,[9] respectively), at 298.2°K. to give the heat of formation of $TiBr_2(s)$

$$Br_2(l) + Ti(\alpha) = TiBr_2(s)$$
$$\Delta H^0_{298.2} = -95.3 \pm 3 \text{ kcal./mole}$$

which confirms the -95 ± 10 kcal. estimate of Brewer.[10]

It would be of interest to study the solid phases of this disproportionation reaction by high-temperature X-ray diffraction and more careful equilibrium pressure measurements. A two-phase region appears to exist between $TiBr_{2.9}$, and $TiBr_{2.25}$ at 740.6°K. which has almost disappeared at 800°K. At 869.2°K., solid solubility appears to be continuous. Thus, for the composition $TiBr_{2.65}$, a break would be predicted in the log P curve for the phase change between 740.6° and 800°K., *i.e.*, between $10^3/T = 1.35$ and 1.25 of Fig. 1. The present data do not justify a conclusion in this regard.

(6) R. A. Nelson, W. H. Johnson and E. J. Prosen, National Bureau of Standards, Report No. 4607 (November, 1955).

(7) Elton H. Hall and John M. Blocher, Jr., *J. Electrochem. Soc.*, **105**, 40 (1958).

(8) E. H. Hall, J. M. Blocher, Jr., and I. E. Campbell, *ibid.*, **105**, 271 (1958).

(9) K. K. Kelley, Quarterly Status Report to Office of Naval Research from U. S. Bureau of Mines, Report NRO 37-054 (October to December, 1955).

(10) L. Brewer, L. A. Bromley, P. W. Gilles and N. H. Lofgren, "National Nuclear Energy Series," Vol. IV-19B, L. L. Quill, Ed., McGraw-Hill Book Co., New York, N. Y., 1950.

THE PHOTOÖXIDATION OF ISOPROPYL IODIDE[1]

BY G. R. MCMILLAN[2]

Department of Chemistry, The University of Rochester, Rochester, New York

Received January 6, 1959

Recent work[3] has given some information about the mechanism of the photochemical decomposition of isopropyl iodide vapor. The present study represents an extension of this work to gain information about the reactions of the isopropyl radical with oxygen. The photoöxidation of isopropyl iodide has been investigated by Emschwiller,[4] who reported acetone among the products of the vapor and liquid phase reaction. Other products detected in the liquid system were carbon dioxide, propylene, possibly carbon monoxide and a viscous oil.

Experimental

The apparatus, a conventional vacuum line free of stopcocks, and the isopropyl iodide were the same as that used in the previous study.[3] Oxygen was prepared by heating reagent grade potassium permanganate and dried by passage through a series of traps cooled in liquid nitrogen.

The light source was a British Thomson–Houston ME/D mercury lamp. The lines at 3130 Å. were isolated by a filter

TABLE I

PHOTOLYSIS OF ISOPROPYL IODIDE IN THE PRESENCE OF OXYGEN

T = 35°; pressure of isopropyl iodide = 36 mm; Pyrex filter; rates in molecules/ml./sec. × 10^{-11}

Time, min.	I_a rel.	P_{O_2} av., μ	R_{O_2}	$R_{i\text{-}C_3H_7OH}$	$R_{(CH_3)_2CO}$	$R_{C_3H_6}$	R_{CO_2}	$R_{C_2H_6}$
10	1.0	1323	339	355	271	157	25	34
20	0.35	1316	186	108	30	50	9	9
20	.35	1339	170	119	57	55	2	9
60	.12	1376	61	77	24	25	4	2

(1) This research was supported in part by Contract AF18(600)1528 with the United States Air Force through the Air Force Office of Scientific Research of the Air Research and Development Command. Reproduction in whole or in part is permitted for any purpose by the United States Government.

(2) Chemical Division, Research and Development Laboratories, Celanese Corporation of America, Clarkwood, Texas.

(3) G. R. McMillan and W. A. Noyes, Jr., *J. Am. Chem. Soc.*, **80**, 2108 (1958).

(4) G. Emschwiller, *Compt. rend.*, **192**, 799 (1931); *Ann. chim.*, **17**, [10], 413 (1932).

TABLE II

PHOTOLYSIS OF ISOPROPYL IODIDE IN THE PRESENCE OF OXYGEN

$T = 35°$; $\lambda = 3130$ Å.; pressure of isopropyl iodide = 36 mm.

Time, min.	I_a, quanta/ml./sec. $\times 10^{-12}$	P_{O_2} ave. μ	Φ_{O_2}	$\Phi_{i\text{-}C_3H_7OH}$	$\Phi_{(CH_3)_2CO}$	$\Phi_{C_3H_6}$	Φ_{CO_2}	$\Phi_{C_3H_8}$
35	18.3	493	0.09	..	..	0.09	0.006	0.003
60	18.3	445	.17	..	..	.09	.006	.003
60	18.3	430	.18	..	..	.09	.005	.001
91	18.3	1660	.30	..	..	.11	.008	.003
61	18.3	441	.16	..	..	..	..	.
306	2.3	399	.41	..	..	.22	.10	.02
36	15.2	390	.49[c]	0.41	0.20	.13	.03	.01
36	14.6	423	.48[c]	.43	.16	.14	.03	.01
60	13.9	1396	.16[d]	.34	.14	.11	.02	.003
300	1.6	1405	.83	.62	.26	.22	.09	.02
60	13.9	1407	.30	.37	.05	.13	.02	.003
240	1.6	1249	.94	.61	.14	..	...	...

[a] Quantum yields referred to quantum yield of unity for carbon monoxide production from diethyl ketone at 110°. [b] Blanks indicate no analysis was made. [c] The mercury pools in the cell connecting tubing were cleaned by heating prior to these experiments. [d] Air was admitted to the cell, then three days of pumping preceded this experiment.

composed of a solution of 105 g./l. of $NiSO_4 \cdot 6H_2O$ and 30 g./l. of $CoSO_4 \cdot 7H_2O$, both in a 5 cm. optical path, together with a 3 mm. thickness of Corning Glass 9863 and 1 mm. of Pyrex. In a few experiments, a thickness of 5 mm. of Pyrex was used to remove all light of wave length less than 2900 Å. Light intensity was varied by the use of screens.

Quantum yields were based on the production of carbon monoxide from the photolysis of diethyl ketone at 110°.

The cylindrical quartz cell had a volume of 144 ml. and the volume of the cell, stirrer and connecting tubing was 438 ml. Mixing by the magnetically driven stirrer was begun 45 minutes before the start of the photolysis.

The oxygen pressure in the cell was held roughly constant by use of the dosing technique described by Porter.[5]

At the end of a photolysis, residual oxygen was pumped away and measured with all products and excess isopropyl iodide condensed in a trap cooled with liquid nitrogen. A fraction volatile at −130° was removed and analyzed with the mass spectrometer. Other products and unreacted isopropyl iodide were condensed into the gas sample valve of a Perkin–Elmer Model 154-B Vapor Fractometer and chromatographed on the A column provided with the instrument. Two product peaks were observed. The products were trapped out and analyzed with the mass spectrometer.

Results

The fraction of products not condensed at −130° contained only propylene, propane and carbon dioxide. The "liquid" products were isopropyl alcohol and acetone. Gas chromatograms of this fraction showed no acetaldehyde, water, methanol nor methyl iodide. After one photolysis, the contents of the reaction cell condensable at −130° were distilled into a tube containing a small amount of saturated potassium iodide solution. No liberation of iodine, an indication of the presence of peroxides, was noted. Considerable quantities of an iodide of mercury condensed outside the cell.

Strong heating of the cell and connecting tubing after a series of experiments resulted in the evolution of only traces of gas not condensed at liquid nitrogen temperature, indicating that mercuric oxide is not a major product of the oxidation.

The results are given in Tables I and II.

Discussion

The suppression of propane formation by oxygen is consistent with the known rapid reactivity of alkyl radicals with oxygen. In the earlier study[3] the rates of the reactions

$$\text{iso-}C_3H_7 + I_2 = \text{iso-}C_3H_7I + I \quad (1)$$

$$\text{iso-}C_3H_7 + \text{iso-}C_3H_7I = C_3H_6 + C_3H_8 + I \quad (2)$$

were compared, and in experiments using 3130 Å. radiation, k_1/k_2 was found to be approximately 500. A comparison of (2) with the rate of

$$\text{iso-}C_3H_7 + O_2 = \text{iso-}C_3H_7O_2 \quad (3)$$

may be made using the quantum yields of propane obtained in the oxygen free system and the data in Table II. The value of k_3/k_2 found is the order of 1000. Since the scatter is considerable, no great significance can be assigned to this estimate, but it is apparent by comparing with k_1/k_2 that isopropyl radicals react with oxygen and with iodine at comparable rates.

At 20° and a total pressure of 50 mm., Christie[6] found the ratio corresponding to k_1/k_3 for methyl radicals to be 170. This difference in rate constant was attributed largely to the third order nature of the methyl–oxygen reaction. In a complex radical such as isopropyl, no such tendency toward third-order kinetics would be expected at the pressure used in this investigation, and k_1 might not differ greatly from k_3.

The data give some evidence that a large fraction of the isopropyl radicals reach the walls and there react with iodine as in the oxygen free system. Quantum yields of oxygen consumed are low, and along with the quantum yield of propylene, increase with an increase in oxygen pressure. All yields increase as the light intensity is decreased, due probably to the greater availability of mercury in the cell at lower intensities to remove iodine. The increase in the carbon dioxide yield, however, seems too large to be accounted for in this manner. The ability of diffusion to the walls to compete with reaction with oxygen may be due to a low steric factor of the latter reaction, as suggested by Satterfield and Reid.[7]

Some possibilities for the fate of the isopropylperoxy radical may be discussed. Hydroperoxides

(5) G. B. Porter, *J. Am. Chem. Soc.*, **79**, 1878 (1957).

(6) M. A. Christie, *Proc. Roy. Soc.* (*London*), **A244**, 411 (1958).

(7) C. N. Satterfield and R. C. Reid, THIS JOURNAL, **59**, 283 (1955).

could not be detected, nor could mercuric oxide, the product of the reaction of isopropyl hydroperoxide with mercury.[8] Furthermore, such a hydroperoxide formed by abstraction of hydrogen could not be the main precursor of isopropyl alcohol in this system, since every abstraction from isopropyl iodide has been shown to result in propylene formation.[3] The present results show the yield of isopropyl alcohol to be about three times that of propylene.

The same reasoning leads to the conclusion that the alcohol cannot be formed entirely by abstraction by isopropoxy radicals. No decomposition products of this radical were detected, and it may not be present in this system.

The acetone and isopropyl alcohol can be explained partially by means of

$$2\text{iso-}C_3H_7O_2 = \text{iso-}C_3H_7OH + CH_3COCH_3 + O_2 \quad (4)$$

a step similar to that suggested for the interaction of α-phenethylperoxy radicals.[9] This requires that part of the acetone be converted into unidentifiable products, a possibility consistent with the erratic yields observed.

Acknowledgment.—The author wishes to thank Dr. W. Albert Noyes, Jr., for encouragement and guidance in this work.

(8) N. V. Fok and A. B. Nalbandyan, *Dok. Akad. Nauk, SSSR*, **86**, 589 (1952); N. R. C. TT-396.

(9) G. A. Russell, *J. Am. Chem. Soc.*, **79**, 3871 (1957).

COMPOSITION OF THE SOLID PHASE IN THE $Na_5P_3O_{10}$–$CaCl_2$–H_2O SYSTEM

BY W. J. DIAMOND[1] AND J. E. GROVE

Received January 14, 1959

Quimby[2] published the phase equilibrium diagram for the Ca^{++}–sodium tripolyphosphate system in aqueous solution as determined by Gray and Lemmerman. Moisture contents of the precipitates were reported and some conclusions were drawn as to sodium concentration in the precipitates. Bonneman-Bemia[3] reported a salt, $NaCa_2P_3O_{10}\cdot 4H_2O$, as the product of reaction of equimolar quantities of $Na_5P_3O_{10}$ and $CaCl_2$ at room temperature. Quimby[2] also suggested the possibility of a basic precipitate, $Ca_3(P_3O_{10})(OH)\cdot 5H_2O$. The experiments reported herein were designed to determine the ratio of Ca^{++} to $(P_3O_{10})^{-3}$ in these precipitates by a combination of gravimetric and radiometric techniques.

Experimental

0.008 *M* sodium tripolyphosphate stock solution was prepared by dissolving the recrystallized powder in distilled water. This high purity product (96.24% $Na_5P_3O_{10}$)[4] was supplied by Westvaco Mineral Products Division of Food Machinery and Chemicals Corporation. The radioactive calcium chloride solution (0.01 *M*) was prepared by dissolving Fisher U.S.P. $CaCl_2\cdot 2H_2O$ in distilled water and adding radioactive Ca-45 as the chloride (Union Carbide Nuclear Company's Ca-45-P-2).

(1) Brunswick-Balke-Collender Company, Muskegon, Michigan.

(2) O. T. Quimby, THIS JOURNAL, **58**, 603 (1954).

(3) P. Bonneman-Bemia, *Ann. Chem.*, **16**, 395 (1941).

(4) L. E. Netherton, A. R. Wreath and D. N. Bernhard, *Anal. Chem.*, **27**, 800 (1955).

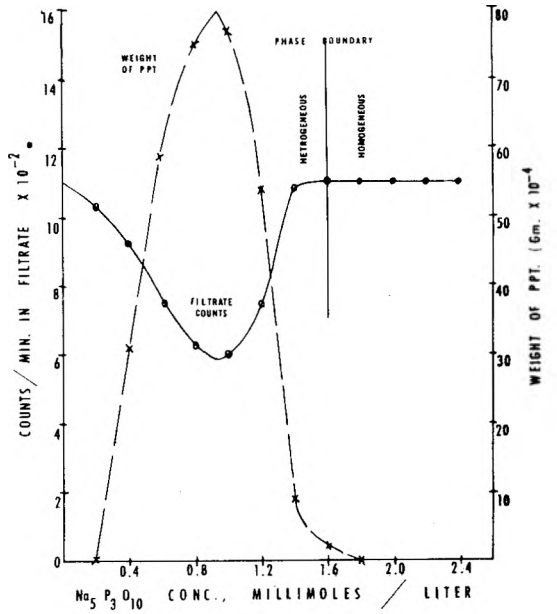

Fig. 1.

Two hundred-ml. samples of solutions 0.002 *M* in $CaCl_2$ and 0.0002 to 0.0018 *M* in $Na_5P_3O_{10}$ were made up and mixed for 5 minutes at 25 ± 1.1°. Previous experiments had established that equilibrium was essentially established in less than 5 min.[5] Three 50 lambda samples were withdrawn by micro pipet and deposited on aluminum planchets. These were dried and counted for radioactivity with a Nuclear Chicago Ultrascaler 192.

Fifty ml. of the solution was passed twice through a dried and weighed 0.45 Millipore filter disk supported on the standard Millipore filtration equipment with vacuum system. The filter disk was removed, dried for 1 hour at 50°, placed in a desiccator for one hour and reweighed. These conditions were found to be adequate to obtain a constant weight precipitate. Three 50 lambda samples of filtrate were deposited on planchets, dried and counted for radioactivity.

Results

Data are plotted in Fig. 1. The weights of precipitate reported are for the 50-ml. samples which were filtered. The filtrate counts are the average of three samples corrected for background. In all samples, count on the initial mixture was 1130 ± 30 counts/minute (95% confidence limits for any single determination). Consistency of this value over the range of tripolyphosphate concentration used indicates that self-absorption of the soft β-emission was small and in any case constant. Therefore, the ratio of filtrate counts to initial counts can be utilized for calculation of Ca^{++} concentration in the filtrate and the precipitate.

The phase boundary shown in Fig. 1 was determined by a Fisher Nefluorophotometer and correlates reasonably well with the weight of precipitate and radioactivity data.

Discussion

If a single solid phase is assumed, the reaction taking place may be supposed to be represented by the equation

$$x\text{Ca}^{++} + y(\text{P}_3\text{O}_{10})^{-5} + z\text{H}_2\text{O} \rightleftharpoons \text{Ca}_x(\text{P}_3\text{O}_{10})_y\cdot z\text{H}_2\text{O}\downarrow \quad (1)$$

since Quimby[2] has shown that the precipitate

(5) W. J. Diamond, THIS JOURNAL, **63**, 123 (1959).

contains no sodium except at concentrations near the phase boundary. For convenience the water is regarded as water of hydration, although it is recognized that the time and temperature of drying do not necessarily eliminate all absorbed moisture.

The ratio x/y (Table I) is calculated from

$$x/y = \frac{\text{wt. of Ca in ppt.}}{\text{wt. of } P_3O_{10} \text{ in ppt.}} \times \frac{\text{(mol. wt. } P_3O_{10})}{\text{at. wt. Ca}} \quad (2)$$

$$= \frac{\text{wt. of Ca in ppt.}}{\text{wt. of ppt.} \dfrac{(100 - \%\ H_2O)}{100} - \text{wt. Ca in ppt.}} \times \frac{\text{(mol. wt. } P_3O_{10})}{\text{at. wt. Ca}} \quad (3)$$

TABLE I

$Na_5P_3O_{10}$ concn., mmoles/l.	Wt. of ppt., g.	Wt. of Ca in ppt., g.	% H_2O	x/y
0.2	0	....	..	..
.4	0.0124	0.0029	20.3	2.57
.6	.0236	.0053	20.3	2.45
.8	.0300	.0069	20.3	2.53
1.0	.0308	.0075	16.2	2.57
1.2	.0216	.0053	16.2	2.61
1.4	.0036	.0005	16.2	1.27
1.6	.0008	....	..	..
1.8	0	....	..	..

% H_2O was determined for 4 samples in each of the water percentage ranges defined by Quimby. The averages of these values were assigned to the samples above.

These calculations yield a ratio x/y constant within experimental error, in the range from 0.4 to 1.2 mmoles/l. of sodium tripolyphosphate. The data for $Na_5P_3O_{10}$ concentrations greater than 1.2 mmoles/l. do not conform to this ratio, as would be expected, because of the known presence of sodium in the precipitates.[2]

With $x/y = 2.5$, the simplest whole number ratio of Ca to P_3O_{10} is 5:2 and the simplest (empirical) formula with 20% H_2O is $Ca_5(P_3O_{10})_2 \cdot 10H_2O$.

Using LaPine atomic models, the only molecule which could be constructed with the simplest ratio was

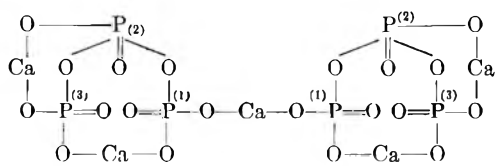

The transition from the above molecule to the chelate $(CaP_3O_{10})^{-3}$ could be explained in terms of simple chelation of both the ring Ca between the 1 and 3 phosphorus and the Ca joining the 1,1-phosphorus by additional sodium tripolyphosphate.

$$Ca_5(P_3O_{10})_2 + 3Na_5P_3O_{10} \rightleftharpoons 5Na_3CaP_3O_{10} \quad (4)$$

The presence of sodium in the precipitates near the phase boundary[2] was not examined but could be explained easily by postulating intermediate reactions as shown by the equations

$$Ca_5(P_3O_{10})_2 + Na_5P_3O_{10} \rightleftharpoons Na_2Ca_4(P_3O_{10})_2 \downarrow + Na_3CaP_3O_{10} \quad (5)$$

and

$$Na_2Ca_4(P_3O_{10})_2 + Na_5P_3O_{10} \rightleftharpoons Na_4Ca_3(P_3O_{10})_2 \downarrow + Na_3CaP_3O_{10} \quad (6)$$

The uniformity of the Ca/P_3O_{10} ratio in the range of 0.4 to 1.2 mmoles/l. of $Na_5P_3O_{10}$ is contrary to the finding of Quimby and would appear to indicate a uniform chemical composition in this range. However, in Fig. 1, the tripolyphosphate concentration for optimum weight of precipitate approximately corresponds to that reported by Quimby as separating the amorphous precipitates with 20–21% water and the crystalline precipitates with 16–17% water.

Conclusions

A constant ratio of 2.55 for Ca/P_3O_{10} was found for the precipitates formed by the reaction of solutions containing 2 mmoles/l. of $CaCl_2$ with solutions containing 0.4 to 1.2 mmoles of sodium tripolyphosphate/liter at 25°. The empirical formula $Ca_5(P_3O_{10})_2$ would satisfy this ratio.

DIFFUSION OF ALLYL CHLORIDE IN POLYVINYL ACETATE AT 40°

BY AKIRA KISHIMOTO AND KINYA MATSUMOTO

Physical Chemistry Laboratory, Department of Fisheries, University of Kyoto, Maizuru, Japan

Received January 16, 1959

It is often reported that integral diffusion coefficients D of systems of organic vapor and polymer (amorphous or primarily amorphous) above their glass transition temperatures increase exponentially with increasing penetrant concentration C. These coefficients at the limit of $C = 0$ are quantities of great physical interest which are expected to be eventually correlated with polymer–solvent interactions; and they are generally determined by extrapolating the observed exponential relation (which gives a straight line on a log $\bar{D}$ *vs.* C plot) graphically down to zero concentration. Recently, Meares[1] made accurate measurements of D for the system polyvinyl acetate (PVAc) and allyl chloride at 40° by using the steady-state method and compared his results with those obtained for the same system by Kokes and Long[2] who used the transient-state method (measurements of rates of sorption and desorption). He found that his values of $\bar{D}$ not only showed a marked deviation from the exponential concentration dependence which the data of Kokes and Long had obeyed, but also gave at zero concentration a value which was about one-half of that extrapolated from the results of the latter authors. The considerable difference in the magnitude of $\bar{D}$ as well as its concentration dependence found by these investigators may not be unexpected because the temperature used was not sufficiently above the glass transition point of the polymer (28–30°). At such a temperature the macro-Brownian motion of the polymer chains is not yet so rapid and active that the time effect as discussed by Crank and Park[3] may be involved in transient-state measurements; steady-state measurements are apparently free

(1) P. Meares, *J. Polymer Sci.*, **27**, 391 (1958).
(2) R. J. Kokes and F. A. Long, *J. Am. Chem. Soc.*, **75**, 6142 (1953).
(3) J. Crank and G. S. Park, *Trans. Faraday Soc.*, **47**, 1072 (1951).

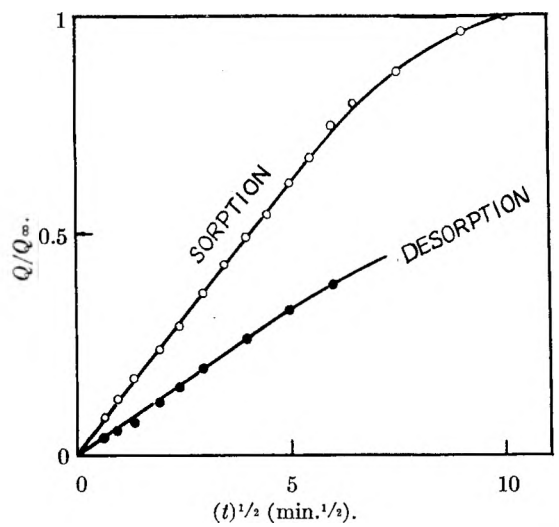

Fig. 1.—Sorption and desorption curves for allyl chloride in polyvinyl acetate at 40°. Allyl chloride vapor pressure = 130 mm.; equilibrium concentration Q_∞ = 4.60 × 10^{-2} g./g.; film thickness = 1.90 × 10^{-3} cm.

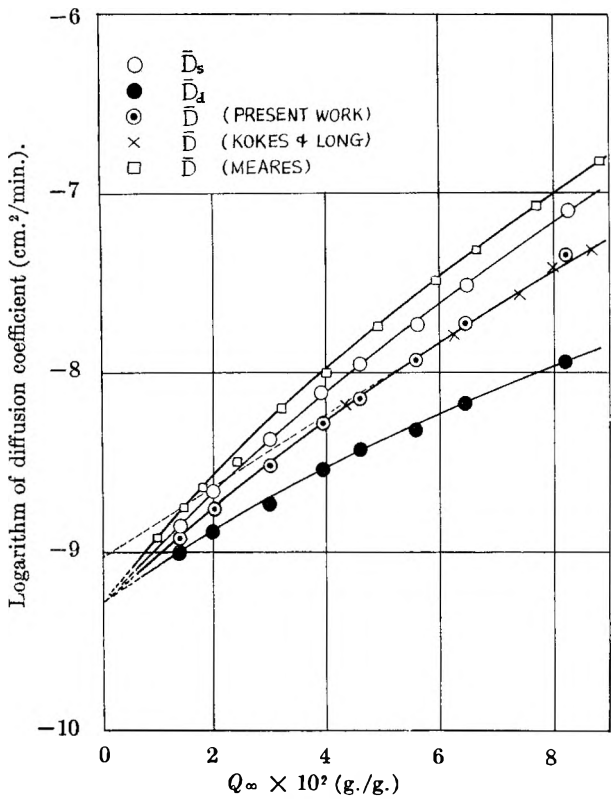

Fig. 2.—Concentration dependences of integral diffusion coefficients $\bar{D}$, $\bar{D}_s$ and $\bar{D}_d$.

from such an effect, because they deal with the state of a polymer in which all chain molecules are fully relaxed. Although it is very unlikely, as Meares mentioned, the fact that the molecular weights of the samples used might have been responsible for the difference between the data by the two methods is a subject of further consideration. The most interesting point is the discrepancy found for the values of $\bar{D}$ at zero concentration. As expected by Meares, the $\bar{D}$ values at zero concentration determined from the steady-state and transient-state methods should agree with each other, at least provided the temperature of the system is above its glass transition temperature. This is because the time effect, if any, should disappear at the limit of zero concentration where swelling or deswelling of the polymer accompanied with the sorption or desorption of the vapor is apparently negligible.

The present work was undertaken to obtain information which may aid to clarify this point.

Experimental

The PVAc which we had used in our previous study[4] of stress relaxation in swollen polymers also was employed for the present work. Its viscosity-average molecular weight was 3.5 × 10^5. The films for the sorption measurements were prepared in exactly the same manner as described previously.[4] The allyl chloride used as penetrant was dried over calcium sulfate and fractionally distilled. The sorption apparatus and the procedure for its actual uses were similar to those given elsewhere.[4] All measurements were made at 40 ± 0.1°. External pressures of allyl chloride in the sorption tube were kept constant to within ±1 mm. during each experiment.

Results and Discussion

Figure 1 shows typical plots of absorption and desorption runs. Here Q is the amount of allyl chloride absorbed or desorbed per gram of dry PVAc for a time t from the start of either a sorption or desorption run, and Q_∞ is the value of Q at sorption equilibrium. Both sorption and desorption plots are linear in the region of small value of $(t)^{1/2}$ and concave against the abscissa for large $(t)^{1/2}$. This indicates that the diffusion process of allyl chloride in PVAc at 40° is of the Fickian type. The initial slope of the sorption plot is larger than that of the desorption one. It was found that not only these initial slopes themselves but also their difference increased with increasing Q_∞. These facts imply that the diffusion coefficient D of the system PVAc and allyl chloride at 40° is an increasing function of penetrant concentration C in the range studied here.

The initial diffusion coefficients for sorption and desorption, denoted by $\bar{D}_s$ and $\bar{D}_d$, respectively, are defined by the relations

$$(Q/Q_\infty)_{sorp} = 4(\bar{D}_s)^{1/2}(t)^{1/2}/(\pi)^{1/2}X \qquad (1)$$
$$(Q/Q_\infty)_{desorp} = 4(\bar{D}_d)^{1/2}(t)^{1/2}/(\pi)^{1/2}X$$

where X is the thickness of the sample film. Thus $\bar{D}_s$ and $\bar{D}_d$ are evaluated from the initial slopes of the curves of the type shown in Fig. 1. The integral diffusion coefficient $\bar{D}$ of the system is defined by

$$\bar{D} = (1/C)\int_0^C D(C)\,dC \qquad (2)$$

where $D(C)$ is the (mutual) diffusion coefficient of the system as a function of C. Crank[5] has shown that to a good approximation $\bar{D}$ is given by the arithmetic mean of $\bar{D}_s$ and $\bar{D}_d$. Thus

$$\bar{D} = (1/2)\,(\bar{D}_s + \bar{D}_d) \qquad (3)$$

The error involved in this approximation is immaterial for the purpose of the present discussion.

Values of $\bar{D}_s$, $\bar{D}_d$ and $\bar{D}$ were computed from all data obtained, and are plotted semi-logarithmically

(4) H. Fujita and A. Kishimoto. *J. Polymer Sci.*, **28**, 547 (1958).

(5) J. Crank, "The Mathematics of Diffusion," Clarendon Press, Oxford, 1956.

against Q_∞ in Fig. 2. In this graph are included the $\bar{D}$ values obtained by Kokes and Long[2] from their transient-state measurements (crosses) and those by Meares[1] from his steady-state measurements (squares). It should be noted that the steady-state method yields the integral diffusion coefficient without such an approximation involved in equation 3.

It is seen from Fig. 2 that in the concentration range where comparison can be made, our $\bar{D}$ values agree satisfactorily with those of Kokes and Long. So far as the behavior in this concentration range is concerned, it appears that the data follow a straight line, *i.e.*, that $\bar{D}$ increases exponentially with increasing concentration. Thus, as Kokes and Long did, we might extrapolate this straight line down to zero concentration and find a value of 9.5×10^{-10} cm.^{2}/min. for $D(0)$; as easily shown from equation 2, the limiting value of $\bar{D}$ for $C = 0$ is equal to $D(0)$. However, as Fig. 2 shows clearly, our data start to deviate downward from the straight line at a value of Q_∞ of about 4.0×10^{-2} g./g. and eventually appear to converge to a value 5.4×10^{-10} cm.^{2}/min. at the limit of zero concentration. Meares' data from steady-state measurements, though consistently higher than those from our transient-state measurements over the range studied, show a concentration dependence quite similar to ours and can be extrapolated to give a $D(0)$ value which agrees with that from the present measurements. Thus it is seen that (1), as Meares has expected, both transient-state and steady-state measurements lead to the same value for $D(0)$, provided the system is above its glass transition temperature, (2) the exponential concentration dependence of $\bar{D}$ applies only in the region of rather high concentrations and may not be extrapolated to evaluate $D(0)$ unless it does hold down to sufficiently low concentrations, and (3) the divergence between $\bar{D}$ values from the steady-state and transient-state methods is not the one due to the difference in molecular weights of the samples used but must be associated with the difference in molecular mechanisms related to the respective methods. Because the temperature studied is not far above the glass transition point of the pure polymer, the time effect[3] associated with the retarded segmental reorientation during the process of sorption or desorption is the most plausible reason for the observed divergence of the transient-state data and the steady-state ones. However, it should be emphasized that all the sorption and desorption curves observed in this study were Fickian within the limits of experimental error. It is apparent that further study needs to be done in order to explore this point.

In connection with the result (2) we shall show in forthcoming papers that plots of the type illustrated in Fig. 2 are of rather general nature for systems of amorphous polymer and organic solvent above their glass transition temperatures. It will be shown that, with increasing temperature above the glass transition point of the given polymer, the downward curvature of the plot of log $\bar{D}$ and against Q_∞ becomes less noticeable and eventually the exponential concentration dependence of $\bar{D}$ holds over the complete region of low concentrations.

Part of this investigation was supported by a grant from the Ministry of Education of the Government of Japan. We are indebted to Professor Hiroshi Fujita for his guidance in the course of this work.

THE RATE OF DIMERIZATION OF ALLOÖCIMENE[1]

BY J. ERSKINE HAWKINS AND ROBERT E. FUGUITT

Department of Chemistry, University of Florida, Gainesville, Florida

Received January 23, 1959

In an earlier publication[2] the various reactions taking place when α-pinene is thermally isomerized in the liquid phase have been elucidated. Subsequently, the rates of the simultaneous reactions taking place, namely, the racemization of α-pinene, the conversion to dipentene and the formation of alloöcimene, were reported.[3] In the first paper it was shown that alloöcimene dimerizes and forms an equilibrium mixture containing about 90% dimer when the reaction is carried out at approximately 200°. An excellent summary, including references, of the thermal isomerization of α- and β-pinenes is presented by Frost and Pearson.[4]

The present work was conducted in order to supply additional information concerning the rates of formation of the various products which result when α-pinene is thermally isomerized.

By analyzing samples of the product when alloöcimene was heated for known lengths of time, at fixed temperatures, it was possible to calculate the rate of the dimerization of alloöcimene.

Experimental

Purification of Alloöcimene.—Impure alloöcimene[5] was purified and had the physical properties described previously.[2]

The method of heating the samples of alloöcimene and analyzing the products was essentially the same as previously reported.[2]

It was necessary, in some cases, to take into account the rate of heating of the liquid after the tube was placed in the constant temperature bath. This correction was arrived at by placing 16 g. of alloöcimene in a sealed tube with a thermometer enclosed and observing the temperature at various time intervals. Based on this information, the starting time for the reaction was taken as four minutes after the tubes were inserted in the bath. An extra 250 watt heater was turned on during this period in order to counteract the cooling of the oil by the tube. No correction appeared to be necessary for the cooling rate as the temperature dropped so rapidly that no appreciable reaction occurred after removal from the bath.

Since the reaction proved to be second order, the rate constant involves a concentration unit. It was therefore necessary to know the density of alloöcimene at the temperatures at which the reaction was measured. To determine this, 35 ml. of alloöcimene was placed in a tube of 1 cm. inside diameter and sealed. The levels of the ocimene at 204.5 and at 25° were marked. After the tube was opened and the

(1) Presented at the 131st Meeting of the American Chemical Society, Miami, Florida, April, 1957.

(2) R. E. Fuguitt and J. E. Hawkins, *J. Am. Chem. Soc.*, **67**, 242 (1945).

(3) R. E. Fuguitt and J. E. Hawkins, *ibid.*, **69**, 319 (1947).

(4) A. A. Frost and R. G. Pearson, "Kinetics and Mechanism," John Wiley and Sons, Inc., New York, N. Y., 1953, pp. 318–325.

(5) Furnished through the courtesy of the Naval Store Research Laboratory, U.S.D.A., Olustee, Florida, and the Naval Stores Division, The Glidden Company, Jacksonville, Florida.

liquid removed, the increase in volume was found to be 19% by determining the weight of water in the tube when filled to each mark. Since the alloöcimene has a d^{25}_4 of 0.805 it follows that $d^{204.5}_4$ 0.805/1.19 = 0.68 g. per ml. By interpolation $d^{189.5}_4$ was estimated to be 0.69 g. per ml.

Calculations, Results and Discussion

The dimer produced appeared to be more homogeneous than the similar product obtained by the thermal isomerization of α-pinene.[2] It is quite possible that some pyronenes formed during the course of the reaction but apparently in too small quantities to affect the calculated values of the rate constants. This is to be expected[6] inasmuch as the monomeric cyclization products occur to an appreciable extent only at temperatures at least one hundred degrees above those used in the present study. In the present investigation the b.p. of the dimer was 173–176° (9 mm.) and the n^{25}D 1.5208–1.5212 compared to 120–175° (8 mm.) and n^{25}D 1.5171–1.5194 for the product from α-pinene. The reaction is

$$2A \underset{k_5}{\overset{k_4}{\rightleftharpoons}} D \qquad (1)$$

where A represents a mole of alloöcimene and D represents a mole of the dimer.

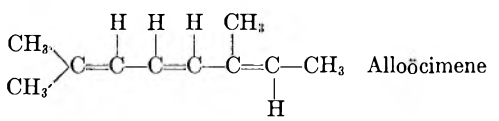

The rate equation may be written as

$$\frac{dx}{dt} = k_4(a - x)^2 - k_5 x/2 \qquad (2)$$

where a is the initial concentration of alloöcimene, M, x is the number of moles per liter of the alloocimene reacting in time t, and k_4 and k_5 are the specific reaction rate constants for the forward and reverse reactions, respectively. By applying the relation between the rate constants of a reversible reaction and the equilibrium constant, equation 2 upon integration and evaluation of the integration constant results in

$$k_4 = \frac{2.303}{t} \times \frac{q}{a^2 - q^2} \log \frac{q(a^2 - xq)}{a^2(q - x)} \qquad (3)$$

At 204.5° the initial concentration of alloocimene, $a = d \times 1000/\text{mole wt.} = 680/136 = 5.0$ moles per liter.

At 189.5°, $a = 690/136 = 5.07 = 5.1$ moles per liter.

The number of moles per liter of alloöcimene reacted at equilibrium, $q = x$ (fraction of alloocimene reacted). It was shown[2] previously that 89% of the alloöcimene had reacted at equilibrium at 189.5°. Thus, $q = 5.07(0.89) = 4.5$ moles per liter. Also it was shown previously at 204.5° that 88% of the alloöcimene had reacted at equilibrium. Hence at 204.5°, $q = 5.0 \times (0.88) = 4.4$ moles per liter.

The calculation of k_4 by equation 3 may be illustrated with the data for tube no. 54, which yielded 64% dimer when heated at 189.5° for 408 minutes. Since the units in the log term cancel, fractions may be substituted directly into this part of the equation, where $a = 1.0$, $q = 0.89$, and $x = 0.64$. Hence

$$k_4 = \frac{2.303}{408} \times \frac{4.5}{(5.1)^2 - (4.5)^2} \log \frac{0.89[1.0 - 0.89(0.64)]}{1.0(0.89 - 0.64)} \qquad (4)$$

$k_4 = 8.1 \times 10^{-4}$ l. mole^{-1} min.$^{-1}$. The data at 189.5 and 204.5° are listed in Tables I and II respectively.

Table I

Reversible Polymerization of Alloöcimene

Temp. = 189.5°, $a = 5.1\ M$, $q = 4.5\ M$

Tube no.	Time heated, min.	Alloocimene recovered, n^{22}D	Wt. mixture, g.	Wt. polymer, g.	% Polymer	$k_4 \times 10^4$, l./mole min.
50	108	1.5416	15.8	5.4	34	9.1
51	108	1.5417	16.6	5.3	32	7.9
52	254	1.5415	15.9	8.5	54	8.5
53	254	1.5419	15.9	8.4	53	8.3
54	408	1.5411	16.3	10.4	64	8.1
55	408	1.5415	16.1	10.4	65	8.5
56	720	1.5396	16.4	12.4	76	8.7
57	720	1.5410	16.3	12.3	76	8.7
58	1020	1.5412	32.0	25.6	80	7.8
59	1020	1.5412	32.0	25.6	80	7.8
60	1440	1.5388	16.3	13.7	84	8.1
61	1440	1.5410	16.4	13.9	85	8.9
					Av. =	8.4
					Av. dev. =	0.35
					% av. dev. =	4.2

Table II

Reversible Polymerization of Alloöcimene

Temp. = 204.5°, $a = 5.0\ M$, $q = 4.4\ M$

Tube no.	Time heated, min.	Alloocimene recovered, n^{25}D	Wt. mixture, g.	Wt. polymer, g.	% Polymer	$k_4 \times 10^4$, l./mole min.
68	50	1.5419	13.7	4.4	32	19
69	50	1.5418	14.9	4.9	33	20
70	130	1.5415	12.9	7.0	54	18
71	130	1.5420	13.6	7.4	54	18
72	185	1.5413	15.4	10.0	65	22
73	185	1.5411	15.5	9.7	63	19
74	285	1.5389	14.4	10.2	71	18
75	285	1.5395	14.9	10.4	70	17
76	395	1.5393	15.3	11.5	75	16.5
77	395	1.5400	14.4	10.8	75	16.5
78	640	1.5360	14.9	12.0	81	15.7
79	640	1.5374	15.4	12.4	81	15.7
80	3480	1.5263	13.6	11.9	87.5	
81	5700	1.5360	14.4	12.5	87	
					Av. =	18
					Av. dev. =	1.4
					% av. dev. =	7.7

The results indicate that the reaction is a reversible bimolecular association.

It was proposed earlier[2] that the dimerization resulted from a Diels–Alder type reaction. Other Diels–Alder reactions have been reported to be reversible bimolecular ones.[7]

To calculate the equilibrium constant K of the reaction it was necessary to evaluate the concentra-

(6) T. R. Savich and L. A. Goldblatt, *J. Am. Chem. Soc.*, **67**, 2027 (1945).

(7) The Faraday Society, "Reaction Kinetics," Gurney and Jackson, London, 1937, pp. 129–137.

tion of the alloöcimene and the dimer at equilibrium at 189.5 and 204.5°. The density of the equilibrium mixture at 25°, was 0.875 g. per ml. At 204.5°, its density was found to be 0.74 g. per ml. The densities at these latter temperatures were determined by the same procedure described in the case of alloöcimene.

At 189.5°

$$K = \frac{[\text{Dimer}]}{[\text{Alloöcimene}]^2} = \frac{0.89(0.75)1000}{272} \Big/ \left[\frac{0.11(0.75)1000}{136}\right]^2 = 6.7 \text{ l./mole}$$

$$k_5 = \frac{k_4}{K} = \frac{8.4 \times 10^{-4}}{6.7} = 1.25 \times 10^{-4} \text{ min.}^{-1}$$

At 204.5°, $K = \frac{0.88(0.74)1000}{272} \Big/ \left[\frac{0.12(0.74)1000}{136}\right]^2 =$ 5.6 l./mole

$$k_5 = \frac{18 \times 10^{-4}}{5.6} = 3.2 \times 10^{-4} \text{ min.}^{-1}$$

The energies of activation for the forward and reverse reactions and the heat of the reaction were calculated from the values of k_4, k_5 and K at the two temperatures. These values are listed in Table III.

TABLE III

Reaction	ΔH (cal. mole^{-1} deg.$^{-1}$)	ΔE_{act} (cal. mole^{-1} deg.$^{-1}$)	ΔS_{act} (e.u.)
2 Alloöcimene → Dimer	−5300	22,000	−13.6
Dimer → 2 Alloöcimene	+5300	28,000	− 2.5

The entropies of activation for the forward and reverse reactions were estimated by solving these equations for ΔS_a.

$$k = \frac{RT}{Nh} e^{-\Delta H_a/RT} e^{\Delta S_a/R}$$

where k is k_4 or k_5 as the case may be. These values also are listed in Table III.

THE B^{11} NUCLEAR MAGNETIC RESONANCE CHEMICAL SHIFTS AND SPIN COUPLING VALUES FOR VARIOUS COMPOUNDS

BY THOMAS P. ONAK, HERBERT LANDESMAN, ROBERT E. WILLIAMS AND I. SHAPIRO[1]

Research Laboratory, Olin Mathieson Chemical Corporation, Pasadena, California

Received February 24, 1959

The B^{11} nuclear magnetic resonance spectra of a variety of boron containing compounds have been obtained with a Varian V-4300 high resolution n.m.r. spectrometer operating at 12.83 Mc.; the chemical shifts and spin–spin coupling values[2] are given in Table I. Boron trifluoride ethyl etherate has been selected as the zero reference[4] because of the sharp resonance line as well as the

(1) Box 24231, Los Angeles 24, California.

(2) In addition to spin–spin coupling values of boron to hydrogen, the boron-deuterium coupling value of $DB(OCH_3)_2$ was obtained (see Table). Other deuterated boron compounds (ref. 3) fail to exhibit the B–D coupling due to broad resonance lines which overlap.

(3) (a) R. E. Williams and I. Shapiro, *J. Chem. Phys.*, **29**, 677 (1958); (b) T. Onak, H. Landesman and I. Shapiro, THIS JOURNAL, **62**, 1605 (1958).

(4) W. C. Dickinson, *Phys. Rev.*, **81**, 717 (1951).

TABLE I

B^{11} N.M.R. CHEMICAL SHIFTS AND SPIN COUPLING VALUES

Compound	δ^a	J, c./s.
B_5H_8I (apex boron) (CS_2 soln.)	55.0[b]	.....
B_5H_{11} (apex boron)[c]	53.5	170 (BH) ± 5
B_6H_9 (apex boron)	51.8	173 (BH) ± 5
B_6H_{10} (apex boron)[d]	51.2	182 (BH) ± 5
B_4H_{10} (BH)[e]	40.0	154 (BH) ± 5
$NaBH_4$ (aq. soln.)	38.7	82 (BH_4)[f] ± 3
$LiBH_4$ (ether soln.)	38.2	75 (BH_4) ± 3
B_5H_8Br (apex boron) (CS_2 soln.)	36.4	.....
$B_{10}H_{14}$ (2,4 pos.) (CS_2 soln.)	34.9	158 (BH) ± 5
$(CH_3)_2HNBH_3$ (benzene soln.)	15.1	91 (BH_3) ± 3
B_5H_9 (base borons)	12.5	160 (BH) ± 1
B_5H_8Br (base borons) (CS_2 soln.)	12.5	161 (BH) ± 5
B_5H_8I (base borons) (CS_2 soln.)	11.8	160 (BH) ± 5
$C_5H_5NBH_3$ (pure liquid)[g]	11.5	96 (BH_3) ± 3
$(CH_3)_3NBH_3$ (benzene soln.)	9.1	101 (BH_3) ± 3
$NaB(C_6H_5)_4$ (aq. soln.)	8.2	.....
B_4H_{10} (BH_2)[e]	6.5	123 (BH_2) ± 3
BI_3 (liquid melt)	5.5	.....
B_6H_{11} (base B–H)[c]	2.3 est.	133 (BH) est.
$NaBF_4$ (aq. soln.)	2.3	.....
BF_3·piperidine (CS_2 soln.)[h]	2.3	.....
NH_4BF_4 (aq. soln.)	1.8	.....
BF_3·hexamethylenetetramine	1.4	.....
$BF_3{\cdot}O(n\text{-}C_4H_9)_2$	0.0	.....
$BF_3{\cdot}O(C_2H_5)_2$	0.0	.....
HBF_4 (50% aq. soln.)	−0.1	.....
$BF_3{\cdot}P(C_6H_5)_3$ ($CHCl_3$ soln.)	−0.4	.....
$BF_3{\cdot}S(C_2H_4\text{-}C_6H_5)_2$ ($CHCl_3$ soln.)	− .5	.....
$B_{10}H_{14}$ (5,7,8,10 pos.) (CS_2 soln.)	− .5 est.	141 (BH) est.
Tetraacetyl diborate ($CHCl_3$ soln.)	−1.1 ± 1.0	.....
$NaBO_2$ ($B(OH)_4^-$) (aq. soln.)	−1.3	.....
NaB_3O_8 (aq. soln.) (see text)	−1.3 ± 1.0	.....
B_6H_{11} (base BH_2)[c]	−2.9 est.	130 (BH_2) est.
$LiB(OCH_3)_4$ (methanol soln.)	−2.9	.....
$NaBO_3$ (aq. soln.)	−5.5	.....
$K_2B_4O_7$ (aq. soln.)	−7.5 ± 1.0	.....
$HBCl_2{\cdot}O(C_2H_5)_2$	−7.9	152 (BH) ± 5
$DBCl_2{\cdot}O(C_2H_5)_2$	−8.0	? (BD)[i]
$Na_2B_4O_7$ (aq. soln.)	−8.9	.....
BF_3 (gas)	−9.4 ± 1.0	.....
$(NH_4)_2B_4O_7$ (aq. soln.)	−10.3	.....
$BCl_3{\cdot}O(C_2H_5)_2$ (ether soln.)	−10.5	.....
$N(CH_2CH_2O)_3B$ (aq. soln.)[j]	−10.7	.....
$B_{10}H_{14}$ (1,3,6,9 pos.) (CS_2 soln.)	−12.4 est.	138 (BH) est.
KB_5O_8 (aq. soln.)	−13.0	.....
Tri-*o*-chlorophenyl borate (ether soln.)	−13.7 ± 2.0	.....
NaB_3O_8 (aq. soln.) (see text)	−14.4 ± 1.0	.....
B_6H_{10} (base borons)[d]	−15.0	160 (BH) ± 5
Tri-*o*-cresyl borate (ether soln.)	−15.0 ± 1.0	.....
B_2H_6 (gas)[k]	−16.6	128 (BH_2) ± 4
Methyl metaborate (benzene soln.)	−17.3	.....
n-Butyl metaborate (benzene soln.)	−17.5	.....
$B(OCH_2CH{=}CH_2)_3$	−17.5	.....
$B(OCH_3)_3$	−18.1[l]	.....
$B(OC_2H_5)_3$	−18.1	.....
$B(OH)_3$ (aq. soln.)	−18.8 ± 1.0	.....
$B(OC_2H_5)_2Cl$	−23.3 ± 1.0	.....
$HB(OCH_3)_2$	−26.1	141 (BH) ± 5
$DB(OCH_3)_2$	−26.7	24 (BD) ± 4
$B(OH)_2(n\text{-}C_8H_{19})$ (ether soln.)	−29.3 ± 1.0	.....
$B(OC_2H_5)Cl_2$	−32.5 ± 1.0	.....
$B_2H_2O_3$[m]	−33.6 ± 3.0	169 (BH) ± 5
BBr_3	−40.1[l]	.....
BCl_3	−47.7[l]	.....
$B(C_2H_5)_3$	−85 ± 1.0	.....

[a] $\delta = (H_s - H_r)/H_r \times 10^6$; estimated deviation ±0.5 unit unless otherwise noted. Pentaborane-9 was used as a secondary standard; spacings were measured with respect to the low field doublet (160 c./s.). [b] This is at slightly higher field than that portrayed by R. Schaeffer, J. N. Shoolery and R. Jones (ref. 11). [c] R. E. Williams, S. G. Gibbins and I. Shapiro, *J. Chem. Phys.*, **30**, 320 (1959). [d] R. E. Williams, S. G. Gibbins and I. Shapiro, *ibid.*, **30**, 333 (1959). [e] R. E. Williams, S. G. Gibbins and I. Shapiro, Abstracts of the 135th Meeting of the American Chemical Society, Boston, Mass., April 1959, 38M. [f] Agrees with J-value given by R. Ogg, *J. Chem. Phys.*, **22**, 1933 (1954). [g] In benzene $\delta = 12.3$, $J = 98$. [h] In neohexane $\delta = 1.8$. [i] Line width smears B–

D spin–spin coupling (ref. 3). [j] Triethanolamine borate (ref. 5) in chloroform $\delta = -11.2$. [k] R. Ogg, (Table I, footnote *f*) report $J = 125$; see also J. N. Shoolery, *Faraday Soc. Disc.*, **19**, 215 (1955). [l] Dickinson (ref. 4) reports δ-values: $B(OCH_3)_3$, −18; BBr_3, −44; BCl_3, −46 [m] J. F. Ditter and I. Shapiro, *J. Am. Chem. Soc.*, **81**, 1022 (1959).

ready availability of the etherate. The compounds were studied as liquids or in solution. Where the line width of the B^{11} resonance was broadened by the viscosity of the solution, an inert solvent was added to reduce the viscosity, narrow the line width and thus obtain a measurable signal. Solvent effects upon the chemical shifts of B^{11} resonance spectra appear to be negligible at 12.83 Mc. except in those cases where a definite chemical reaction has occurred. Therefore, chemical shift values for boron compounds can be regarded as characteristic empirical constants for identification purposes. In addition, it is possible to deduce from these values information about the bonds within the molecules studied.

Within a series of planar boron compounds a general shift to higher field occurs with increasing double bond character between boron and its adjacent atoms. Triethylboron, positioned at lowest field, represents the only compound in Table I which cannot have more than a sextet of electrons around the boron atom. The atoms adjacent to the boron in the remaining trisubstituted compounds are capable of contributing electrons to the boron, thus enhancing the double bond character and approaching an octet of electrons around the boron atom.

The tetravalent and trivalent chemical shift regions can be subdivided further on the basis of individual inductive effects of the atoms directly bonded to boron since non-adjacent atoms have little effect on the shielding. For example, chemical shift values from Table I indicate that three oxygens bonded to trivalent boron occur approximately in the region $\delta -14$ to -19. An exception is triethanolamine borate,[5] which, when compared to other alkyl borates, is found at higher field. This shift is interpreted as increased shielding around the boron atom due to some B–N bonding, thus increasing the tetrahedral character and number of bonding electrons around the boron atom (see above). Another exception is the occurrence of the tetraacetyl diborate resonance line at higher field ($\delta - 1.1$) than expected for a boron bonded to three oxygens. The tetraacetyl diborate resonance line would be expected to occur at slightly lower field than the alkyl borates if only an inductive effect were operating. However, tetraacetyl diborate may undergo chelation to give either four-membered or six-membered rings,[6] which would increase the tetrahedral character (see above) and the shielding of the boron atoms. It is observed that the tetraacetyl diborate resonance line ($\delta - 1.1$) occurs in the region characteristic of the tetrahedral boron atom bonded to four oxygen atoms (*e.g.*, $B(OH)_4^-$, $\delta - 1.3$; $LiB(OCH_3)_4$, $\delta - 2.9$).

(5) 2,8,9-Trioxa-5-aza-1-borabicyclo[3.3.3]undecane in the oxa-aza-bora system of nomenclature.

(6) L. A. Duncanson, W. Gerrard, M. F. Lappert, H. Pyszora and R. Shafferman, *J. Chem. Soc.*, 3652 (1958).

The few series of boron compounds listed in Table I are essentially in agreement with the polar bond theory which requires that shifts become more negative as the electronegativity of the substituents increases. A trend toward lower field with increased electronegativity of the atom bonded to boron is noted in the trihalide series BI_3, BBr_3 and BCl_3.[7,8] Increased ionic character of BF_3[4,9,10] may be responsible for its deviation from this pattern. The inductive effect of the halides upon the B^{11} chemical shifts is again evidenced in the substituted pentaboranes[11] where the apex boron of bromopentaborane is at lower field than the apex boron of iodopentaborane.

The chemical shift values of certain tetravalent boron ions are in the order $BH_4^- > B(C_6H_5)_4^- > B(OCH_3)_4^-$. Similar trends are observed in the substituted phosphorus compounds, *viz.*, $PH_3 > P(C_6H_5)_3 > P(OCH_3)_3$,[8d] and in the methyl proton spectra of the related carbon compounds, *viz.*, $CH_4 > CH_3\text{-}C_6H_5 > CH_3\text{-}OR$.[12] The relative shielding by the adjacent elements is $H > C_{aromatic} > O$ which is inversely proportional to the electronegativity of the adjacent atoms as expected.

Structural information about borates in solution is suggested by the following observations: two peaks are seen in the spectrum of an aqueous solution of sodium pentaborate in contrast to one peak in an aqueous solution of potassium pentaborate. A synthetic solution prepared from sodium hydroxide and boric acid with the sodium pentaborate B/Na ratio also produces two peaks. Addition of acid to the sodium pentaborate solution decreases the intensity of the high field peak ($\delta - 1.3$) while shifting the low field peak at $\delta - 14.4$ to $\delta - 18.8$ (boric acid). Addition of small amounts of base to the pentaborate solution also decreases the intensity of the high field peak ($\delta - 1.3$) but shifts the low field peak ($\delta - 14.4$) to higher field. These observations would indicate that the low field peak which shifts with acid and base additions represents an equilibrium mixture of trivalent boric acid and tetravalent monoborate ion[13]; the appearance and disappearance of the high field peak shows another borate species is present, possibly pentaborate or tetraborate ion. A solution of potassium pentaborate, on the other hand, has only one peak which shifts to higher field with addition of base. Low solubility of an intermediate potassium polyborate may explain the lack of a high field peak such as was present in the sodium pentaborate spectrum.

Addition of mannitol to boric acid ($\delta - 18.8$)

(7) The chemical shift of BCl_3 was found in the same position in both liquid and vapor phase.

(8) For similar shifts in other element halides see: (a) P. C. Lauterbur, *J. Chem. Phys.*, **26**, 217 (1957); (b) C. H. Holm, *ibid.*, **26**, 707 (1957); (c) N. Muller, P. C. Lauterbur and J. Goldenson, *J. Am. Chem. Soc.*, **78**, 3557 (1956); (d) J. R. Van Wazer, C. F. Callis, J. N. Shoolery and R. C. Jones, *ibid.*, **78**, 5715 (1956).

(9) Linus Pauling, "The Nature of the Chemical Bond," Cornell Univ. Press, Ithaca, N. Y., 1948, second edition, p. 239.

(10) R. A. Ogg, Stanford Univ., Technical Research Report, MCC-1023-TR-120, January, 1955.

(11) R. Schaeffer, J. N. Shoolery and R. Jones, *J. Am. Chem. Soc.*, **80**, 2670 (1958).

(12) N. F. Chamberlain, *Anal. Chem.*, **31**, 56 (1959).

(13) Peter H. Kemp, "The Chemistry of Borates," W. S. Cowell Ltd., Butter Market, Ipswich, 1956, pp. 55–64.

did not shift the resonance line, but addition of excess alkali to this solution shifted the resonance line to $\delta - 7$. These observations are in agreement with equilibrium constants[14,15] for this system which indicate that only in basic solution is appreciable mannitol–boric acid complex present.

Nuclear magnetic resonance B^{11} chemical shifts also may be used to identify products and monitor the course of reactions without removing the materials from the reaction medium. For example, BCl_2OEt ($\delta - 32.5$) in contact with ether quickly disproportionates[16,17] to $BCl_3{:}OEt_2$ ($\delta - 10.5$) and $BCl(OEt)_2$ ($\delta - 23.3$) both of which are detected by n.m.r. In addition, the subsequent slow cleavage of $BCl_3{:}OEt_2$ is observed by the intensity decrease at $\delta - 10.5$ and intensity increase at $\delta - 23.3$.

(14) A. Deutsch and S. Osoling, *J. Am. Chem. Soc.*, **71**, 1637 (1949).
(15) S. D. Ross and A. J. Catotti, *ibid.*, **71**, 3563 (1949).
(16) H. Ramser and E. Wiberg, *Ber.*, **63**, 1136 (1930).
(17) E. Wiberg and W. Sutterlin, *Z. anorg. allgem. Chem.*, **202**, 21 (1931).

THE DENATURATION OF PEPSIN. V. THE ELECTROSTATIC FREE ENERGY OF NATIVE AND DENATURED PEPSIN[1]

BY HAROLD EDELHOCH[2]

Contribution from the Department of Pathology and Oncology, Kansas University Medical School, Kansas City, Kansas

Received March 13, 1959

It has been shown by viscosity, sedimentation and diffusion measurements that denatured pepsin has a much less compact structure than native pepsin.[3] In this report, this difference in structure is shown to markedly affect the electrostatic free energy of native and denatured pepsin.

Methods.—A stock solution was prepared by dissolving native pepsin (Worthington Biochemical Corp.) in 0.001 *M* NaCl (*p*H ~3.5) and then carefully adjusting, at 0°, with dilute base to *p*H 6.65. This solution is quite stable at 24°, the temperature of the experiments.

Denatured pepsin solutions were obtained by raising the *p*H of the stock solution from 6.65 to 9.60 with base and then reacidifying to *p*H 6.65. Pepsin solutions were titrated with small volumes of concentrated solutions of salt in order to keep the total volume approximately constant. The *p*H was read after each addition of salt. Other procedural details have been reported elsewhere.[3,4]

Results and Discussion

In Fig. 1 is reported the effects of NaCl on the *p*H of native and denatured pepsin as well as the influence of $BaCl_2$ on the *p*H of native pepsin.

The difference in behavior of native and denatured pepsin to NaCl was rather striking. The origin of these differences must be related to the structure of the two forms of pepsin since their composition was identical. Moreover, the net negative charge of denatured pepsin at *p*H 6.65 was greater than that of the native enzyme by at least the number of carboxyl hydrogen-bonded groups (5 or 6) which are lost on denaturation.[4] The larger charge should therefore increase the electrostatic effects if other parameters are unaffected.

(1) Supported in part by an Institutional Grant from the American Cancer Society and by Grants No. C-1974 and RG 4690 of the National Institutes of Health.
(2) National Institutes of Health, Bethesda, Md.
(3) H. Edelhoch, *J. Am. Chem. Soc.*, **79**, 6100 (1957).
(4) H. Edelhoch, *ibid.*, **80**, 6640 (1958).

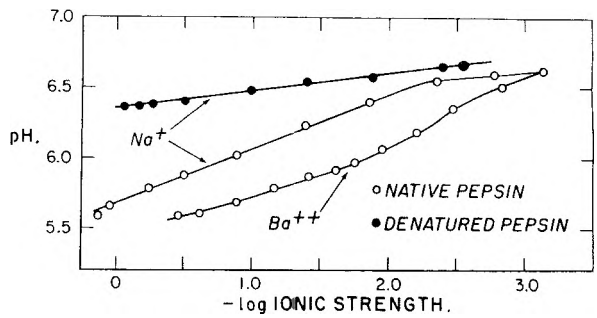

Fig. 1.—The effect of NaCl on the *p*H of solutions of native and denatured pepsin effect of $BaCl_2$ on the *p*H of native pepsin; pepsin concentration = 5 mg./ml.

The theoretical expression derived by Linderstrøm-Lang[5] has been found to fit satisfactorily the titration curves of numerous proteins. It was assumed that all the members of each type of dissociable group possessed the same intrinsic dissociation constant pK_0 and that all charged groups were uniformly distributed on the surface of a sphere and that there were no interactions amongst these groups other than electrostatic. The relation may be written as

$$p\mathrm{H} - \log \frac{r_i}{n_i - r_i} = (pK_0)_i - 0.868\omega Z \qquad (1)$$

where n_i is the total number of each type of dissociable group and r_i is the number dissociated at a particular *p*H value. Z is the net charge on the protein and ω is related to the electrostatic work required to remove a proton from a molecule possessing a charge of Z. The dependence of ω on ionic strength and the radius is given in eq. 2

$$\omega = \frac{N\epsilon^2}{2DkTR}\left(1 - \frac{\kappa R}{1 + \kappa A}\right) \qquad (2)$$

where R is the radius of the sphere, κ, the reciprocal Debye radius, A, the exclusion radius, D, the dielectric constant, k, the Boltzmann constant, ϵ, the protonic charge and T the absolute temperature.

A minimum value of R equal to 22 Å. may be calculated from the molecular weight of pepsin (35,000) and an assumed partial specific volume of 0.75. An effective radius may also be calculated from the intrinsic viscosity (0.033)[3] by the Einstein equation $[\eta] = 10\pi N R_e^3/3M$. A value of $R_e \cong 26$ Å. was obtained in this way. This larger value is due to protein hydration or lack of spherical symmetry in native pepsin. Most likely both effects contribute in some degree.

When ω was calculated from equation 2 at various ionic strengths of NaCl and then plotted against the corresponding experimental value of *p*H, a linear relationship was observed above ~0.01 $\Gamma/2$ as seen in Fig. 2. The points increasingly deviated from a straight line as the ionic strength decreased below this value. When the pepsin gegenion concentration was included in the low ionic strength solutions, the discrepancy was reduced somewhat as shown by the arrows in Fig. 2.[6]

(5) K. Linderstrøm-Lang, *Compt. rend. trav. Lab. Carlsberg*, **15**, No. 7 (1924).
(6) We need not concern ourselves greatly about the very low ionic strength data since the contribution of the charged protein-ion has been neglected and even more important, it is doubtful whether the theory is

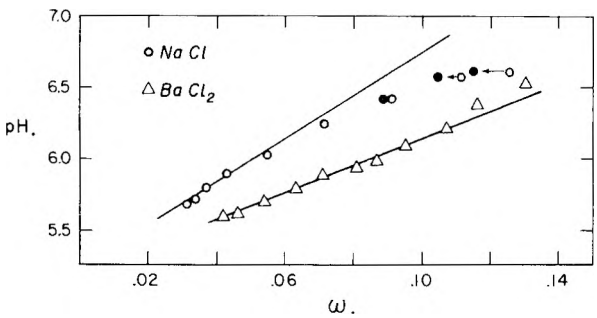

Fig. 2.—The data of Fig. 1 plotted according to electrostatic theory; see equations 1 and 2 in text for significance of notations.

When Z was evaluated by the application of equation 1, a value of ~15 was obtained from the slope of the straight line. That this value is reasonable may be demonstrated by making use of the analytical data of Van Vunakis and Herriott.[7] If we assume that all of the ionizable groups of pepsin are charged at pH 6.65, then the net charge due to hydrogen ion equilibria, is 31, since there are approximately 37 carboxyl groups and 6 basic amino acids (as well as 1 terminal carboxyl and amino group). This figure should be reduced by the number of carboxyl groups not titrated at this pH in native pepsin. In addition Carr[8] has shown that about 5 Na^+ ions are bound to pepsin at pH 7.5.[9] The combined influence of both of these factors should reduce the net charge to below 20. Due to a number of approximations that are made when equation 1 is used in this way, this kind of experiment cannot be expected to yield quantitative parameters. Nevertheless, the slope does appear to give a reasonable value for the charge considering the limitations of both theory and experiment.

The relatively small dependence of pH on NaCl concentration found with denatured pepsin reveals the marked decrease in the electrostatic free energy which results from the disorganization of the compact structure of native pepsin. Since Z is larger in denatured pepsin than in the native enzyme at pH 6.65,[4] then ω must be smaller and consequently R (effective) is considerably greater. The individual charged groups, therefore, now behave as if almost isolated from each other in denatured pepsin. This behavior is in accord with the large configurational changes that occur in pepsin concurrently with denaturation.[3]

Equation 1 does not strictly apply to the $BaCl_2$ data either, since Ba^{++} is also bound. A slope of 10 was computed from the linear relationship between ω and pH. The data (Fig. 2) fall on a line covering a greater range of ionic strength than observed with NaCl. The smaller slope found with $BaCl_2$ is presumably due to stronger binding and the larger valence of Ba^{++} ions. Carr[10] has reported that appreciable amounts of Mg^{++} and Ca^{++} are bound to pepsin at pH 7.5.

(10) C. W. Carr and K. R. Woods, *Arch. Biochem. Biophys.*, **55**, 1 (1955); C. W. Carr, *ibid.*, **46**, 424 (1953).

valid at the high electrical fields existing when the protein charge is large and but little salt is present.

(7) H. Van Vunakis and R. M. Herriott, *Biochim. Biophys. Acta*, **23**, 600 (1957).

(8) C. W. Carr, *Arch. Biochem. Biophys.*, **62**, 476 (1956).

(9) It is not clear whether the pepsin Carr employed at pH 7.5 was native or denatured. At very low ionic strengths pepsin can be quite stable at this pH.

ELECTRICAL CONDUCTIVITIES OF KCl-KBr SOLID SOLUTIONS[1,2]

BY JOHN E. AMBROSE AND W. E. WALLACE

Contribution No. 1039 from the Department of Chemistry, University of Pittsburgh, Pittsburgh 13, Penna.

Received April 15, 1959

In 1956 when the present work was initiated there appeared to be fairly convincing evidence to indicate that vacancies in KCl–KBr solid solutions were abnormally abundant. The evidence for this derived from a comparison[3] of densities measured by Tammann and Krings[4] with values computed from the unit cell determinations of Oberlies.[5] The former were found to be smaller by as much as 2% for some compositions, indicating a vacancy concentration for the solutions roughly 100 times that of the pure components.

If the vacancies were indeed this abundant, it appeared that their presence should affect physical properties of the system other than the density. In particular, the solutions should exhibit good electrical conductivity compared with the pure salts since conductivity in the alkali halides occurs by a motion of vacancies. Moreover, such a large population of vacancies should substantially augment the entropy of the system. The existence of an excess entropy in the KCl–KBr system was confirmed[6] by entropy of formation measurements in this Laboratory several years ago. The entropies of formation were found to be greatly in excess of that expected from theory,[7] even exceeding the entropy of random mixing. However, when an attempt[6] was made to account quantitatively for the excess entropy in terms of the presumed vacancy concentration, it was unsuccessful. This suggested that the extra entropy stemmed from another source and furthermore cast doubt on the validity of the data of Tammann and Krings and Oberlies. Accordingly it seemed desirable to redetermine the densities and unit cell dimensions for KCl–KBr solid solutions and at the same time to begin measurements of their electrical conductivities. Results of the redeterminations, which were quickly concluded and have already been published,[8] were at variance with the results of the earlier work in that they did not indicate an abnormal population of vacancies. The present

(1) This work was assisted by the U. S. Atomic Energy Commission.

(2) From a thesis submitted by John E. Ambrose to the Graduate Faculty of the University of Pittsburgh in partial fulfillment of the requirements for the M.S. degree.

(3) W. E. Wallace and R. A. Flinn, *Nature*, **72**, 681 (1953).

(4) G. Tammann and W. Krings, *Z. anorg. Chem.*, **130**, 229 (1923).

(5) F. Oberlies, *Ann. Physik*, **87**, 238 (1928).

(6) W. H. McCoy and W. E. Wallace, *J. Am. Chem. Soc.*, **78**, 5995 (1956).

(7) J. A. Wasastjerna, *Soc. Sci. Fennica, Commentationes Phys.-Math.* [XV], **3**, 1 (1949); V. Hovi, *ibid.*, [XV] **12**, 1 (1950).

(8) J. S. Wollam and W. E. Wallace, THIS JOURNAL, **60**, 1654 (1956).

paper contains the results of the electrical conductivity determinations.

Experimental Details

The solid solutions were prepared by fusing together high purity salts in a platinum crucible. The melt was strongly chilled so as to solidify the material rapidly. The solid was then ground to a fine powder and remelted in platinum. Upon slow cooling of this melt large single crystals formed. A suitable crystal was removed, ground to a regular shape and then its dimensions were measured with a micrometer. For the conductivity measurements the sample was clamped between a pair of aluminum rods through which connection was made with the rest of the measuring circuit. Contact resistance was minimized by evaporating a gold film onto the faces of the crystal[9] which touched the aluminum bars. To protect the sample from possible contamination by the aluminum, platinum foil was inserted between the rods and the sample.

The measuring circuit employed was similar in principle to that used by Mapother, Crooks and Maurer.[10] A mechanical switching arrangement supplied a d.c. pulse to the sample of approximately 0.1 sec. duration. The conductivity was measured by observing the deflection of a ballistic galvanometer in the circuit. The procedure followed was to observe first the deflection when the sample was pulsed. Then the sample was replaced in the circuit by a precision high resistance variable resistor. The resistor was adjusted until the deflection matched that produced when the sample was in the circuit. This was taken to be the resistance of the sample. The resistivity, computed from the measured resistance and known geometry of the sample, was found to be independent of the direction of the current and of the amount of charge transported through the sample.

With each composition studied the procedure followed was first to increase the temperature slowly to 500 to 550° and then maintain a constant temperature until equilibrium was established. Resistance of the sample was measured at intervals of about ½ hr. until a time-independent conductivity was indicated. Then the temperature was reduced 15 to 20° and the procedure repeated.

Results and Discussion of Results

Measurements were made on the two pure salts and three solutions. The data for even temperatures are given in Table I. The temperature range covered was extended downward to the limit of the experimental procedure in use since the main interest in the work was to obtain information concerning the vacancy population at or near room temperature. No attempts were made to extend the measurements up toward the vicinity of the melting point. When the raw data are plotted, they are found to exhibit the usual dependence[11] of conductivity on temperature, a kink occurring in the plot with the steeper slope on the high temperature side of the kink. The kinks are found at temperatures ranging from 450 to 475°.

The data in Table I show that the conductivity of the solutions in all cases is comparable in magnitude with that for the pure components. Such differences as exist easily could be attributed to a varying mobility rather than a changing number of carriers. Thus, the conductivity measurements support the conclusions derived from the density redetermination. They give no indication of an abnormal population of vacancies. It must be realized, however, that establishment of the carrier concentration from the measured conductivities must await a direct determination of their mobility, by a suitable tracer diffusion experiment or the like.

TABLE I

THE ELECTRICAL CONDUCTIVITIES OF KCl–KBr SOLID SOLUTIONS

	Conductivity, ohm^{-1} cm.$^{-1}$ × 10^6				
Temp., °C.	Pure KCl	Pure KBr	20 mole % KBr 80 mole % KCl	50 mole % KBr 50 mole % KCl	80 mole % KBr 20 mole % KCl
400	0.0322	0.0122	0.0148	0.00634	0.00813
420	.0449	.0204	.0237	.0113	.0145
440	.0617	.0327	.0363	.0193	.0248
460	.0891	.0519	.0552	.0337	.0417
480	.149	.0922	.0955	.0653	.0804
500	.241	.178	.172	.122	.150
520	.382	.339	.304	.222	.276
540	.603	.624	.525	.391	.485

TABLE II

VALUES OF B IN THE EQUATION $\sigma = \sigma_0 \exp(-B/T)$

	$B \times 10^{-3}$			
	Temp. above kink		Temp. below kink	
	This work	Jost	This work	Jost
KCl	14	23.5	8	11.5
KBr	19	23	12	11.5
20 mole % KBr	17	..	11	..
50 mole % KBr	19	..	14	..
80 mole % KBr	19	..	14	..

Plots of the data indicate an exponential dependence of conductivity on temperature of the form $\sigma = \sigma_0 \exp(-B/T)$. In Table II are listed values of B for the five compositions studied together with values taken from the compilation by Jost[11] for the pure salts, data being given for the regions above and below the kink. The values of B for KBr are in reasonable agreement with those tabulated by Jost, the differences being about what one might reasonably expect from independent determinations. The discrepancies in the case of KCl are somewhat puzzling. They are considerably larger than had been anticipated. The consistency of the conductivity data obtained in the present study for KCl is such that one would have expected a reliable value for B. At present the cause of the deviations is not known. It is to be noted, however, that despite the discrepancy in slope the actual measured conductivities are in satisfactory agreement with literature values. The values listed for KCl in Table I fall between the values found in the careful studies of Phipps and Partridge[12] and Lehfeldt.[13]

(9) Thanks are due Mr. C. H. T. Wilkens of the Mellon Institute for applying the gold coating.

(10) D. Mapother, H. N. Crooks and R. Maurer, *J. Chem. Phys.*, **18**, 1231 (1950).

(11) W. Jost, "Diffusion in Solids, Liquids and Gases," Academic Press, Inc., New York, N. Y., 1952, p. 179.

(12) T. E. Phipps and E. F. Partridge, *J. Am. Chem. Soc.*, **51**, 1331 (1929).

(13) W. Lehfeldt, *Z. Physik*, **85**, 717 (1933).

ACIDS AND BASES. XI. REACTIONS OF BORATES AND BORON ACETATE AS LEWIS ACIDS[1]

BY SAVERIO ZUFFANTI, RICHARD T. OLIVER AND W. F. LUDER

Contribution from the Department of Chemistry, Northeastern University, Boston, Mass.

Received February 27, 1959

In the preceding paper of this series[2] evidence was presented that both stannous chloride and

antimony tribromide behave as secondary acids[3] toward piperidine in dimethylformamide. Continuing this investigation of the manner in which various substances behave as acids according to the electronic theory of acids and bases, the work reported in this paper provides examples of the first three of Lewis' phenomenological criteria. Also, in the behavior of boron acetate an interesting contrast with that of antimony tribromide, as reported in the preceding paper,[2] has been noted.

Experimental

All the boron compounds (as listed in Table I) were supplied at no cost by the American Potash & Chemical Corporation, Los Angeles 54, California. Further purification of these compounds was unnecessary for the purposes of this investigation. However, because they are all reactive toward moisture they were opened and handled in a large dry-box filled with nitrogen.

(a) **Effect of Borates and Boron Acetate on Indicators.**—The first of the Lewis criteria tested was the effect of the compounds upon more than twenty indicators in benzonitrile, using piperidine as the base to establish the basic color of the indicator as described in a previous paper.[4] The boron compounds that were soluble in benzonitrile gave typically acid colors with these indicators. Most of the colors were the same as those observed in water solutions of hydrogen acids. These experiments were repeated with six of the indicators using methanol as the solvent. All of the boron compounds were soluble in methanol, and exhibited the acid colors of the indicators.

In these experiments the piperidine and the solvents were dried over suitable drying agents, refluxed and distilled. The solutions were made up in the dry-box.

(b) **Neutralization and Displacement.**—The other two criteria considered, neutralization and displacement reactions, were investigated by letting the boron compounds react in methanol with the base, sodium methoxide, according to the procedure described by Fritz.[5] Although several indicators, including thymol blue and azo violet, were tried, phenolphthalein gave the best reproducibility. Usually, at least four runs were made which checked within three parts per thousand. The results are summarized in Table I.

Results

The second column of Table I gives the molarity of each acid solution calculated from the weight of each sample dissolved in methanol. The third column gives the normality of each acid solution as obtained in the titrations with sodium methoxide. Considering that the acids were used as obtained without further purification, the agreement is sufficiently close to indicate that each molecule of borate is reacting with one methoxide ion.

Thus these reactions illustrate the first of the Lewis criteria, the neutralization of a primary acid.

(1) Abstracted from a thesis submitted by Richard T. Oliver to the faculty of Northeastern University in partial fulfillment of the requirements for the M.S. degree, June, 1955.

(2) W. F. Luder and L. S. Hamilton, THIS JOURNAL, **60**, 1470 (1956).

(3) W. F. Luder and S. Zuffanti, "The Electronic Theory of Acids and Bases," John Wiley and Sons, Inc., New York, N. Y., 1946.

(4) R. B. Rice, S. Zuffanti and W. F. Luder, *Anal. Chem.*, **24**, 1022 (1952).

(5) J. S. Fritz, "Acid-Base Titrations in Nonaqueous Solvents," G. Frederick Smith Chemical Co., Columbus, Ohio, 1952.

TABLE I

NEUTRALIZATION AND DISPLACEMENT REACTIONS OF BORON COMPOUNDS AS ACIDS REACTING WITH SODIUM METHOXIDE IN METHANOL USING PHENOLPHTHALEIN AS THE INDICATOR

Acid	Molarity by wt.	Normality by titration	Equiv per mole
Tri-(*n*-dodecyl) borate	0.0912	0.0909	1
Tri-(methylamyl) borate	.00970	.01020	1
Tri-(tetrahydrofurfuryl) borate	.1044	.1022	1
Tri-(2-ethylhexyl) borate	.1070	.1034	1
Tri-(*n*-butyl) borate	.1214	.1184	1
Boron acetate	.1041	.4008	4

According to the theory the base donates a share in a lone pair of electrons to the vacant orbital in the acid, forming a coördinate covalent bond between the two

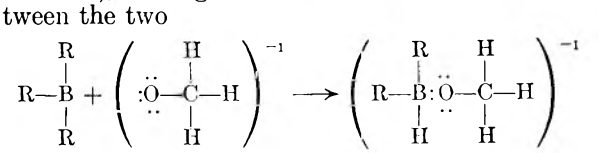

(primary acid) (base)

However, the last pair of concentration values in Table I shows that one molecule of boron acetate reacts with *four* methoxide ions. This behavior apparently involves the third of the Lewis criteria, displacement. The acetate ion is a much weaker base than the methoxide ion and the other radicals in the borates. Therefore, the methoxide ion besides adding to the vacant orbital in the boron atom can also displace the three acetate ions[6]

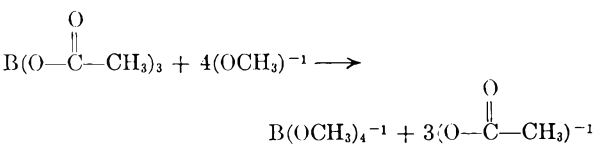

The contrast between this reaction and one reported in the preceding paper[2]

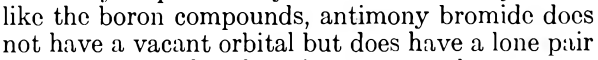

is readily explained by the Lewis theory. Unlike the boron compounds, antimony bromide does not have a vacant orbital but does have a lone pair of electrons. Therefore, it can act only as a secondary acid in reactions with bases that displace a maximum of three bromide ions.

The second of the Lewis criteria illustrated by this investigation, as mentioned above, was the observation of typically acid colors produced by the effect of the boron compounds on a large number of indicators.

(6) Two points may be of interest. First, no time-lag was noted in this titration (nor in the others). Second, the acetate ion (for example, in sodium acetate) is not a strong enough base to give phenolphthalein its basic color in methanol.

5946